*This document is the intellectual property of the fib – International Federation for Structural Concrete. All rights reserved.*
*This PDF of fib Bulletin 86 is intended for use and/or distribution solely within fib National Member Groups.*

fib CEB-FIP

Bulletin 86

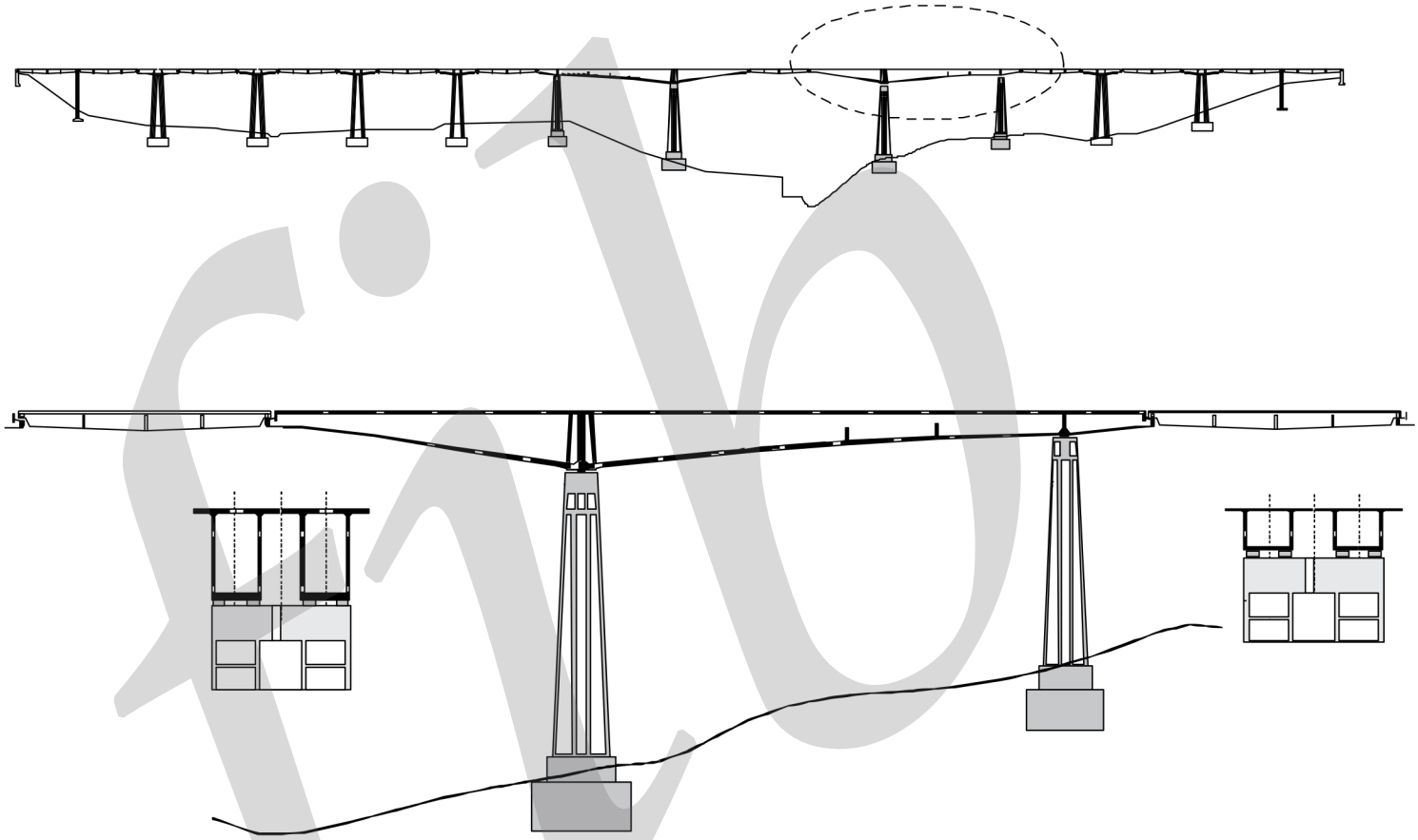

# Safety and performance concepts

## Reliability assessment of concrete structures

Guide to good practice

*This document is the intellectual property of the fib – International Federation for Structural Concrete. All rights reserved.*
*This PDF of fib Bulletin 86 is intended for use and/or distribution solely within fib National Member Groups.*

fib CEB-FIP

Bulletin 86

# Safety and performance concepts

## Reliability assessment of concrete structures

Guide to good practice

Task Group 2.8

August 2018

*This document is the intellectual property of the fib – International Federation for Structural Concrete. All rights reserved.*
*This PDF of fib Bulletin 86 is intended for use and/or distribution solely within fib National Member Groups.*

# Approval for this bulletin

Subject to priorities defined by the Technical Council and the Presidium, the results of the *fib*'s work in commissions and task groups are published in a continuously numbered series of technical publications called *bulletins*. The following categories are used:

| **Category**: | **Approval by**: |
|---|---|
| Technical report | Task group and chairpersons of the commission |
| State-of-the-art report | Commission |
| Manual / Guide to good practice / Recommendation | Technical Council |
| Model code | General Assembly |

Any publication not having met the above requirements will be clearly identified as a preliminary draft.

*fib* Bulletin 86 was approved as a guide to good practice by the technical council of the *fib* in Cape Town, November 2016.

Cover image: Sensitivity of the 1st modal shape of a cantilever beam with respect to a degraded cross section, gamma distribution of a stochastic material property, and sensitivity matrix of material parameters.

© Fédération internationale du béton (*fib*), 2018

Although the International Federation for Structural Concrete / Fédération internationale du béton (*fib*) does its best to ensure that all the information presented in this publication is accurate, no liability or responsibility of any kind, including liability for negligence, is accepted in this respect by the organisation, its members, employees or agents.

All rights reserved. No part of this publication may be reproduced, modified, translated, stored in a retrieval system or transmitted in any form or by any means - electronically, mechanically, through photocopying, recording or otherwise - without prior written permission from the *fib*.

ISSN 1562-3610
ISBN 978-2-88394-126-7
Proofreading by Gordon Clark. Layout by Marie Reymond (*fib*).
Printed by DCC Document Competence Center Siegmar Kästl e.K., Germany

*This document is the intellectual property of the fib – International Federation for Structural Concrete. All rights reserved.*
*This PDF of fib Bulletin 86 is intended for use and/or distribution solely within fib National Member Groups.*

# Acknowledgements

The report "Safety and performance concepts – Reliability assessment of concrete structures" was drafted by fib Commission 2 "Safety and performance concepts":

**Authors:**

**Luc Taerwe (Convener/Editor)**
Ghent University, Belgium

**Konrad Bergmeister (Co-Convener/Co-Editor)**
Universität für Bodenkultur, Vienna, Austria

**Alfred Strauss (Technical Secretary)**
Universität für Bodenkultur, Vienna, Austria

**José Manuel Antón Corrales**
E.T.S. de Ing. Agronomos, Madrid, Spain

**Jose Campos e Matos**
Uni. Minho, Porto, Portugal

**André de Chefdebien**
LB7 Saint Pierre des Corps, France

**Carl-Alexander Graubner**
Technische Hochschule Darmstadt, Germany

**S. G. Joglekar**
STUP Consultants, India

**Asterios Lolios**
Democritus University of Thrace, Greece

**David Meager**
Worley, Perth, Australia

**Drahomir Novak**
Techn. Univ. of Brno, Czech Republic

**Dirk Proske**
Univ. Bodenkultur, Vienna, Austria

**Daniel Straub**
TU München, Germany

**Bretislav Teplý**
Brno University of Technology, Czech Republic

**Konrad Zilch**
TU Munich, Germany

**Christian Bucher**
TU Wien, Austria

**Vladimír Cervenka**
Cervenka Consulting, Czech Republic

**Dan M. Frangopol**
Lehigh University, USA

**Simon Hoffmann**
Mageba, Bülach, Switzerland

**David Lehky**
Techn. Univ. Brno, Czech Republic

**Johannes Maier**
Hochschule Zurich-Winterthur, Switzerland

**Ainars Paeglitis**
Riga Techn. Univ., Latvia

**Markus Petschacher**
Petschacher Consulting, Austria

**Antonino Recupero**
R&S Engineering, Italy

**Motoyuki Suzuki**
Tohoku University, Sendai, Japan

**Roman Wendner**
Univ. Bodenkultur, Vienna, Austria

**Additional Contributors**

**Sergio Alcocer**
Institute of Engineering, UNAM, Mexico

**Jaime Fernández Gómez**
Intemac, Spain

**Ulrich Santa**
Autobrennero, Trento, Italy

**José Calavera**
Intemac, Spain

**Andrzej Nowak**
Univ. of Nebraska, USA

Full address details of Task Group members may be found in the *fib* Directory or through the online services on *fib*'s website, www.fib-international.org.

*This document is the intellectual property of the fib – International Federation for Structural Concrete. All rights reserved.*
*This PDF of fib Bulletin 86 is intended for use and/or distribution solely within fib National Member Groups.*

# Foreword

Concrete structures have been built for more than 100 years. At first, reinforced concrete was used for buildings and bridges, even for those with large spans. Lack of methods for structural analysis led to conservative and reliable design. Application of prestressed concrete started in the 40s and strongly developed in the 60s. The spans of bridges and other structures like halls, industrial structures, stands, etc. grew significantly larger. At that time, the knowledge of material behaviour, durability and overall structural performance was substantially less developed than it is today. In many countries statically determined systems with a fragile behavior were designed for cast in situ as well as precast structures. Lack of redundancy resulted in a low level of robustness in structural systems. In addition, the technical level of individual technologies (e.g. grouting of prestressed cables) was lower than it is today. The number of concrete structures, including prestressed ones, is extremely high. Over time and with increased loading, the necessity of maintaining safety and performance parameters is impossible without careful maintenance, smaller interventions, strengthening and even larger reconstructions. Although some claim that unsatisfactory structures should be replaced by new ones, it is often impossible, as authorities, in general, have only limited resources. Most structures have to remain in service, probably even longer than initially expected.

In order to keep the existing concrete structures in an acceptable condition, the development of methods for monitoring, inspection and assessment, structural identification, nonlinear analysis, life cycle evaluation and safety and prediction of the future behaviour, etc. is necessary. The scatter of individual input parameters must be considered as a whole. This requires probabilistic approaches to individual partial problems and to the overall analysis. The members of the *fib* Task Group 2.8 "Safety and performance concepts" wrote, on the basis of the actual knowledge and experience, a comprehensive document that provides crucial knowledge for existing structures, which is also applicable to new structures. This guide to good practice is divided into 10 basic chapters dealing with individual issues that are critical for activities associated with preferably existing concrete structures.

Bulletin 86 starts with the specification of the performance-based requirements during the entire lifecycle. The risk issues are described in chapter two. An extensive part is devoted to structural reliability, including practical engineering approaches and reliability assessment of existing structures. Safety concepts for design consider the lifetime of structures and summarise safety formats from simple partial safety factors to develop approaches suitable for application in sophisticated, probabilistic, non-linear analyses. Testing for design and the determination of design values from the tests is an extremely important issue. This is especially true for the evaluation of existing structures. Inspection and monitoring of existing structures are essential for maintenance, for the prediction of remaining service life and for the planning of interventions. Chapter nine presents probabilistically-based models for material degradation processes. Finally, case studies are presented in chapter ten. The results of the concrete structures monitoring as well as their application for assessment and prediction of their future behaviour are shown. The risk analysis of highway bridges was based on extensive monitoring and numerical evaluation programs. Case studies perfectly illustrate the application of the methods presented in the Bulletin.

*This document is the intellectual property of the fib – International Federation for Structural Concrete. All rights reserved.*
*This PDF of fib Bulletin 86 is intended for use and/or distribution solely within fib National Member Groups.*

The information provided in this guide is very useful for practitioners and scientists. It provides the reader with general procedures, from the specification of requirements, monitoring, assessment to the prediction of the structures' lifecycles. However, one must have a sufficiently large amount of experimental and other data (e.g. construction experience) in order to use these methods correctly. This data finally allows for a statistical evaluation. As it is shown in case studies, extensive monitoring programs are necessary. The publication of this guide and other documents developed within the *fib* will hopefully help convince the authorities responsible for safe and fluent traffic on bridges and other structures that the costs spent in monitoring are first rather small, and second, they will repay in the form of a serious assessment providing necessary information for decision about maintenance and future of important structures.

Jan L. Vítek

Chair of *fib* Commission 2 "Analysis and Design"

*This document is the intellectual property of the fib – International Federation for Structural Concrete. All rights reserved.*
*This PDF of fib Bulletin 86 is intended for use and/or distribution solely within fib National Member Groups.*

# Preface

The overall motivation of Commission 2 is based on the fact that structural systems are typically designed to stay in service for at least several decades. This implies that proper attention must be given to structural performance under various actions, both man-made and environmental, to the methodology of structural analysis and assessment, to material properties, to the inverse identification and monitoring of structural resistance among others. The main focus is on existing structures, such as concrete buildings and bridges.

Commission 2 considers itself responsible for the active support of the topic "safety and performance concepts of concrete structures" and for the active support of associated commissions. It comprises gathering and providing new technologies and techniques by considering both fundamental research and practical issues in the area of the aforementioned topic.

The aim of Commission 2 is to provide a comprehensive overview of the theoretical and practical developments in the areas of structural safety, serviceability and reliability, to promote understanding of advanced methodology including probabilistic methods, inverse analyses techniques, monitoring methods, and to encourage application of these methods to improve structural performance and minimize life-cycle cost.

The area of Commission 2's technical work and interest are:

- Performance-Based Design Requirements Ensuring the Life Cycle
- General Principles for the Reliability Assessment of Structures
- Fundamental Methods of Structural Reliability
- Safety Formats
- Testing for Assessment and Design
- Inspection and Monitoring
- Maintenance of Structures
- Structural Identification Methods
- Probabilistic based Models for Material Degradation Processes
- Case Studies

New research findings, methodological skills and reliability based models and design methods were developed and matured within the following important research projects:

- AdMaS UP – Advanced Materials, Structures and Technologies" - „National Sustainability Programme I" (Novák, Lehký, Teplý)
- SARAStrukturelle Analyse und Zuverlässigkeitsbewertung. Supported by Ingenieurteam Bergmeister, Italien (Bergmeister)
- Zustandsüberwachung von Ingenieurkonstruktionen. Supported by Autostrada del Brennero S.P.A., Via Berlino 10, 38100 Trento, Italien (Bergmeister)
- Sicherheits- und Zuverlässigkeitsanalyse von dreidimensionalen Strukturen Supported by Autostrada del Brennero S.P.A., Via Berlino 10, 38100 Trento, Italien (Bergmeister, Strauss)

*This document is the intellectual property of the fib – International Federation for Structural Concrete. All rights reserved.*
*This PDF of fib Bulletin 86 is intended for use and/or distribution solely within fib National Member Groups.*

- Optimierung des Lebenszyklus von Bauwerken durch Monitoring. Supported by FFG - Österreichische Forschungsförderungsgesellschaft, Bereich 1: Forschungsförderung Wirtschaft (FFF) (Bergmeister, Strauss)

- Integrale Strukturanalyse (MAI/B). Supported by BERNARD Ingenieure ZT-GmbH (Strauss)

- Risikobasierte Lebenszyklusbewertung (RLACS). Supported by Europäische Kommission / European Commission, Rue de la Loi, Brussels, Europäische Union (Bergmeister, Strauss)

- Inspektions und Lebenszyklusbewertungs System für Bogenbrücken (ILATAS) Supported by FFG - Forschungsförderungsgesellschaft (Strauss)

- ILATAS - Inspektions- und Lebensbeurteilungsanalyse (ILATAS). Supported by FFG - Forschungsförderungsgesellschaft (Strauss)

- Comprehensive Infrastructure Life-Cycle Assessment (CILIA). Supported by FFG - Forschungsförderungsgesellschaft (Strauss)

- Strukturanalyse Gossensass-Brücke (SAG). Supported by Autostrada del Brennero S.P.A. (Strauss)

- Lebenszeitbewertung ermüdungsgefährdeter Stahlbetontragwerke, MSLeB (MSLeB) Supported by ZIT Zentrum für Innovation und Technologie GmbH (Strauss)

- Monitoring basierte Analyse der Gleis Tragwerke Interaktion, MAGIT (MAGIT ) Supported by FFG - Forschungsförderungsgesellschaft (Strauss)

The *fib* documents already published which cover probabilistic performance-based seismic design (*fib* Bulletin 68) and durability design (*fib* Bulletin 34) as well as MC 2010 are partially covering related topics.

This Bulletin should be considered as a general document and has a strong relationship with the recently established *fib* activities.

| | |
|---|---|
| COM1 Concrete structures | M. Moussard /A. van der Horst |
| COM2 Analysis and design | J. Vítek / O. Bayrak |
| COM3 Existing concrete structures | S. Matthews / G. Mancini |
| COM4 Concrete and concrete technology | F. Dehn / T.A. Martius-Hammer |
| COM5 Reinforcements | T. Neff / L. Krauser |
| COM6 Prefabrication | S. Maas / W. Derkowski / L. Sennour |
| COM7 Sustainability | P. Hájek / T. Noguchi |
| COM8 Durability | F. Papworth / L. Linger |
| COM9 Dissemination of knowledge | G. Balázs / J. Walraven |
| COM10 Model Codes | G. Clark / A. Kasuga |

This state of the art report should help scientists and practitioners to understand the mechanical and physical behaviour of existing concrete structures and should promote more robust structural design.

The final editing of this document has been performed by Alfred Strauss, Konrad Bergmeister, David Lehky, Drahomir Novak and Jan Podrouzek.

| **Alfred Strauss** | **Luc Taerwe** | **Konrad Bergmeister** |
|---|---|---|
| Technical Secretary | Convener | Co-Convener |

*This document is the intellectual property of the fib – International Federation for Structural Concrete. All rights reserved.*
*This PDF of fib Bulletin 86 is intended for use and/or distribution solely within fib National Member Groups.*

## Acknowledgement

We appreciate very much the effort of all authors of the individual chapters to carry out the most recent know how and for reflecting their personal experience and scientific points of view. Special thanks are given to the reviewers Michael N. Fardis and Steinar Helland and to Michael Schwenn for the final editing.

## Motivation and background

Structural systems are designed to stay in service for at least several decades. This implies proper maintenance concepts that proper care must be taken to ensure their safety and serviceability in the presence of deterioration as well as changing conditions of utilization.

Over the past years, it became clear that unfortunately both deterioration as well as increasing traffic loads put severe constraints on the operating conditions of bridge structures. Without proper maintenance, the evolution of resistance and load would decrease the structural performance. Therefore, the main task of this Commission is to deal with reliability aspects that are specifically related to concrete structures and associated degradation processes.

In addition, more detailed information on the resistance and on the action side is required in order to quantify statistically the life cycle. Therefore continuous monitoring and information about time-dependent performance of structures and materials are needed.

## Scope and objective of technical work

The objective of *fib* Task Group 2.8 is to provide a guide to good practice of structural safety, serviceability and reliability, to promote understanding of advanced methodology including probabilistic methods, and encourage application of these methods, to improve structural performance and minimize life-cycle cost. In particular, the areas of interest are:

(a) Safety concepts for new and existing concrete structures (Safety of structures and infrastructure systems, general principles on risk assessment for building and infrastructure systems, reliability assessment of existing structures, safety factors)

Objective: Analysis of the current state of the safety concepts for new structures and existing structures, proposals for good practice design of safety concepts considering monitoring techniques, quality control procedures. Basic documents are: JCSS background documents, Eurocode documents, recently performed research activities from Commission 2 members and other researchers;

(b) Identification of system parameters on the basis of measured structural response

- Sensitivity factor based approaches
- Neural network based approaches
- Direct stiffness approaches
- Risk based inspection approaches

*This document is the intellectual property of the fib – International Federation for Structural Concrete. All rights reserved.*
*This PDF of fib Bulletin 86 is intended for use and/or distribution solely within fib National Member Groups.*

Objective: Investigation and assessment of methodologies for the identification of system parameters using inverse numerical and analytical methods based on measured structural responses.

## Contributors

In addition to the work carried out by the members of *fib* Task Group 2.8, the following members have participated in the development of the content of this bulletin "Safety and performance concepts Reliability assessment of concrete structures" during the past years. The members at time of completion of the final draft are given below.

**Performance-based design requirements ensuring the life- cycle**

Konrad Bergmeister

**Risk issues**

Konrad Bergmeister, Luc Taerwe

**Methods for structural reliability**

Konrad Bergmeister, Thomas Braml, Christian Bucher, Michael Faber, Manfred Keuser, Dirk Proske, Alfred Strauss

**Safety concepts for design**

Alfred Ahrens, Konrad Bergmeister, Thomas Braml, Vladimir Cervenka, Manfred Keuser, Peter Mark, Dirk Proske, Radomir Pukl, Alfred Strauss

**Testing for Assessment and Design**

Konrad Bergmeister, Simon Hoffmann, Anton Rieder, Ulrich Santa, Alfred Strauss, Roman Wendner

**Inspection and Monitoring**

Konrad Bergmeister, Dan Frangopol, Sunyong Kim, Markus Petschacher, Ulrich Santa, Daniel Straub, Alfred Strauss, Roman Wendner

**Life cycle performance**

Dan Frangopol M., Okasha Nader M.

**Structural identification methods**

Bergmeister Konrad, Hoffmann Simon, Lehky David, Novak Drahomir, Strauss Alfred, Wendner Roman

**Probabilistic based Models for Material Degradation Processes**

Teplý Břetislav, Vořechovská Dita, Chromá Markéta

Case studies – applications

Bergmeister Konrad, Eichinger-Vill Eva-Maria, Hoffmann Simon, Lehky David, Liolios, A., Novak Drahomir, Penka Erwin, Proske Dirk, Pukl Radomir, Strauss Alfred, Wendner Roman, Zilch Konrad

This document is the intellectual property of the fib – International Federation for Structural Concrete. All rights reserved.
This PDF of fib Bulletin 86 is intended for use and/or distribution solely within fib National Member Groups.

# Contents

Foreword i
Preface iii
1. Performance-based design requirements ensuring the life-cycle 1
1.1 Introduction 1
1.2 Component safety 2
1.3 Structural system safety 2
1.4 Life-cycle & time dependent reliability 2
1.5 Serviceability 3
1.6 Durability 3
1.7 Fatigue 4
1.8 Structural redundancy, robustness and progressive collapse 4
1.9 Resiliency 7
1.10 Network reliability 7
2. Risk issues 8
2.1 General overview of risk categories 8
2.2 Normative references 10
2.3 Terms and definitions 10
2.4 General framework of risk assessment for structures 12
2.5 Risk assessment -dire impact on the functioning of a community 13
2.6 Risk assessment - system identification 14
2.7 Risk estimation - evaluation 14
3. Methods of structural reliability 21
3.1 Main principles and methods 21
3.1.1 General 21
3.1.2 Probability theory 22
3.1.3 Structural reliability 27
3.1.4 Application example: Collapse of a plane frame 34
3.2 Reliability methods in engineering practice 37
3.2.1 Stages of the safety concept 37
3.2.2 Failure probability and reliability index 38
3.2.3 Partial safety factors for engineering practice 40
3.3 Reliability assessment of existing structures 41
3.3.1 General aspects 41
3.3.2 Assessment decision process 42

This document is the intellectual property of the fib – International Federation for Structural Concrete. All rights reserved.
This PDF of fib Bulletin 86 is intended for use and/or distribution solely within fib National Member Groups.

3.3.3 Decision tree 43
3.3.4 Probabilistic modelling 44
3.3.5 Limit state functions for assessment 44
3.3.6 Evaluation of benefits and consequences 45
3.3.7 Updating of probabilities 45
3.3.8 Updating of random variables 46
3.3.9 Engineering aspects 47
4. Safety concepts for design 52
4.1 Lifetime orientated design and remaining lifetime 52
4.1.1 Introduction 52
4.1.2 Design concepts 53
4.1.3 Remaining lifetime 54
4.2 Safety factor formats 55
4.2.1 Introduction 55
4.2.2 Global safety factors 55
4.2.3 Partial safety factors 56
4.2.4 Proof loading 64
4.3 Safety formats for non-linear analysis 65
4.3.1 Introduction 65
4.3.2 Safety formats 66
4.3.3 Methods of global safety verification 68
4.3.4 Partial factor method 70
4.3.5 Nonlinear analysis 71
4.3.6 Examples of application 71
4.3.7 Concluding remarks 74
5. Testing for assessment and design 75
5.1 Testing for design 75
5.1.1 Design and planning 75
5.1.2 Derivation of design values 76
5.1.3 Outlier test 76
5.1.4 Design values 77
5.1.5 Direct determination of design values 80
5.1.6 Probabilistic-based assessment of sampling 94
5.2 Stochastic models for design 98
5.2.1 Stochastic models for the resistance of structural engineering 98
6. Inspection and monitoring 104
6.1 Introduction 104
6.2 Inspection framework for maintenance of structures 105

This document is the intellectual property of the fib – International Federation for Structural Concrete. All rights reserved.
This PDF of fib Bulletin 86 is intended for use and/or distribution solely within fib National Member Groups.

6.2.1 General remarks 105
6.2.2 Hierarchical structure of databases 105
6.3 Structural monitoring 106
6.3.1 General remarks 106
6.3.2 Introduction 107
6.3.3 Principles of monitoring structures 107
6.3.4 Monitoring associated model updating 110
6.3.5 Sensors for monitoring systems: A brief review 111
6.3.6 Cost models for monitoring systems 117
6.3.7 Strategies for inspection and monitoring 117
6.3.8 Model uncertainties resulting from the structural inspection 120
6.4 Monitoring based reliability assessment 124
6.4.1 General remarks 124
6.4.2 Introduction 124
6.4.3 Design of monitoring systems 124
6.4.4 Acceptance by attributes 124
6.4.5 Acceptance by variables 126
6.4.6 Extreme value distributions for monitoring based predictions 127
6.4.7 Reliability assessment based on monitoring information 132
6.5 Monitoring based performance indicators 135
6.5.1 Code specific given limit states and associated monitored quantities 136
6.5.2 Properties of monitoring systems and associated sensors 136
6.5.3 Optimizing monitoring systems and sensor properties with respect to performance indicators 137
6.5.4 Definition of monitoring based performance indicators 137
6.5.5 Advanced monitoring system 137
6.6 Risk based inspections 138
6.6.1 General remarks 138
6.6.2 Introduction 138
6.6.3 Risk based inspection planning for structures 139
6.6.4 Optimization of inspection strategies 141
6.6.5 Example on deterioration using Risk Based Inspection (RBI) modelling 143
6.6.6 Generic approaches to risk based inspection (RBI) 146
6.6.7 System effects in risk based inspection 147
6.6.8 Conclusions 148
7. Life cycle performance 150
7.1 General 150
7.2 Prediction of life-cycle performance 150

This document is the intellectual property of the fib – International Federation for Structural Concrete. All rights reserved.
This PDF of fib Bulletin 86 is intended for use and/or distribution solely within fib National Member Groups.

7.2.1 Point-in-time reliability 151
7.2.2 Unavailability 152
7.3 Optimization of maintenance 153
7.3.1 Introduction 153
7.3.2 Types of maintenance actions 158
7.3.3 Optimization of essential maintenance 160
7.3.4 Optimization of preventive maintenance 162
7.3.5 Optimization of combined maintenance 165
8. Structural identification and prediction methods 167
8.1 Introduction 167
8.2 State of the art 169
8.2.1 Methods based on changes of basic modal parameters 170
8.2.2 Methods based on updating of structural parameters 174
8.3 Identification method based on artificial neural network 176
8.3.1 Introduction 176
8.3.2 Latin Hypercube Sampling statistical simulation 177
8.3.3 Statistical correlation 178
8.3.4 Sensitivity analysis 178
8.3.5 Artificial neural networks 179
8.3.6 Basic concept of the identification method 180
8.3.7 Software tools 181
8.4 Direct stiffness identification method 182
8.4.1 Introduction 182
8.4.2 Elements of a monitoring and system-identification system (MIS) 183
8.4.3 Structural model 184
8.4.4 System identification 185
8.4.5 Direct stiffness calculation 186
8.4.6 Influence-line oriented identification systems 188
8.5 Other identification methods 193
8.6 Sensitivity factor method 193
8.6.1 General aspects 193
8.6.2 Introduction 193
8.6.3 Linear systems 194
8.6.4 Summary 196
8.7 Gamma prediction method 196
8.7.1 General Remarks 196
8.7.2 Gamma processes for describing the degradation properties 198
8.7.3 Characteristics of stochastic processes 198
8.7.4 Modelling of gamma processes 199

This document is the intellectual property of the fib – International Federation for Structural Concrete. All rights reserved.
This PDF of fib Bulletin 86 is intended for use and/or distribution solely within fib National Member Groups.

8.7.5 Application of gamma processes for deterioration processes 200
8.7.6 Selection of inspection methods 203

9. Probabilistic based models for material degradation processes 205
9.1 Introduction 205
9.2 Degradation and limit states 206
9.2.1 Limit states: General 206
9.2.2 Design for durability 208
9.2.3 Durability limit states 209
9.2.4 Initiation period 210
9.2.5 Propagation period 211
9.3 Deterioration of concrete structures 213
9.3.1 Carbonation 213
9.3.2 Chloride ion ingress 214
9.3.3 Corrosion 215
9.3.4 Frost attack 215
9.3.5 Fire attack 217
9.3.6 Alkali-aggregate reaction 217
9.4 Analytical models for degradation 218
9.4.1 Carbonation 219
9.4.2 Chloride ion ingress 224
9.4.3 Corrosion 227
9.4.4 Frost attack 231
9.4.5 Fire attack 231
9.4.6 Alkali-aggregate reaction 234
9.5 Software 235
9.6 Illustrative examples of Durability Design/Assessment 236
9.6.1 Reinforcement depassivation – assessment of initiation period 237
9.6.2 Loss of reinforcement due to corrosion 238

10. Case studies applications 241
10.1 Reliability based assessment of a segmental bridge – Austria 241
10.2 Reliability based assessment of a prestressed box girder bridge – Italy 243
10.2.1 Deterministic model 243
10.2.2 Probabilistic analysis 246
10.2.3 Ultimate Limit State ULS/Structure 248
10.2.4 Time dependent degradation considerations 249
10.2.5 Strengthening measures 249

This document is the intellectual property of the fib – International Federation for Structural Concrete. All rights reserved.
This PDF of fib Bulletin 86 is intended for use and/or distribution solely within fib National Member Groups.

10.3 Reliability based structural and durability analysis of a prestressed-precast V-beam bridge - Italy 250
10.3.1 Introduction 251
10.3.2 Neumarkt Bridge 252
10.3.3 Inspection 252
10.3.4 Performance assessment activities 254
10.4 Monitoring and analysis for the evaluation of fatigue resistance in existing post-tensioned concrete bridges 271
10.4.1 Background – Behaviour of prestressed concrete bridges subject to fatigue loading 271
10.4.2 Monitoring 272
10.4.3 Measuring set-up 273
10.4.4 Analysis of the concrete strains and the crack width 274
10.4.5 Verification of the service stress range of the tendon coupler assemblies 276
10.4.6 Conclusions 277
10.5 Monitoring and reliability assessment of a jointless bridge structure – Austria 277
10.5.1 Introduction 277
10.5.2 General aspects of the Marktwasser Bridge, S33.24 278
10.5.3 Monitoring systems applied on the Marktwasser Bridge, S33.24 279
10.5.4 Verification of an analytical creep shrinkage model 290
10.5.5 Analysis of the slab detail 292
10.5.6 Conclusion 294
10.5.7 Acknowledgement 294
10.6 Egnatia motorway, Northern Greece: Monitoring based risk assessment of bridges 294
10.6.1 Introduction 295
10.6.2 Risk assessment of bridges 295
10.6.3 Major risks for Egnatia bridges 296
10.6.4 Bridge visual inspection and data base recording 299
10.6.5 Bridge health monitoring activities 302
10.6.6 Conclusions 308
11 References 310

*This document is the intellectual property of the fib – International Federation for Structural Concrete. All rights reserved.*
*This PDF of fib Bulletin 86 is intended for use and/or distribution solely within fib National Member Groups.*

This document is the intellectual property of the fib – International Federation for Structural Concrete. All rights reserved.
This PDF of fib Bulletin 86 is intended for use and/or distribution solely within fib National Member Groups.

# 1. Performance-based design requirements ensuring the life-cycle

## 1.1 Introduction

The design of structures and civil infrastructure systems has to meet certain function-based requirements. Any structure has to remain functional and serviceable over the span of its intended service live. The main aim in the design process is the reduction, and if possible even the thorough prevention, of any risk of possible structural collapse or irretrievable serious damage under extreme condition. The design process also has to safeguard adequate performance under service load conditions. To date, the outlined aims were met by the stipulation of design codes and guidelines which determined explicit and implicit safety factors. These factors were specified according to experience based on previous designs and also contained a great deal of what may casually be dubbed "engineering judgement".

Over the last decades, the theory of structural reliability has been developed to a great degree. It offers a more objective approach for the assessment and quantification of the safety of structural systems (buildings, etc.) and infrastructures (bridges, dams, tunnels, pipelines, etc.). This methodology allows the integration of both aleatory and epistemic uncertainties which are part of any assessment of the safety of structural members, systems and networks.

Aleatory, or parametric uncertainties refer to the natural randomness associated with an uncertain quantity. Since this randomness is inherent in time and in space, it cannot be reduced.

Epistemic, or modelling uncertainties arise from insufficient knowledge about the phenomena that may affect the safety of the system.

Consequently, the theory of structural reliability provides a useful framework for analysing the uncertainties in structural loads and operational demands on a component or a system. It also provides a method for assessing the structural capacities that are required to withstand these demands. The resulting information can be used to determine an instantaneous probability of component or system failure and to conclude the probability of failure during any service period.

While the reliability-based concepts outlined above are sufficiently general to be applicable for most types of structures and infrastructure systems, their tangible employment in engineering practice and codified design has to date been realized to a very different extent for various types of applications and the related engineering communities and industries. Here, we offer a review of both the state of art and the state of practice in the development and application of reliability-based performance criteria for civil structures and for infrastructure systems. For illustration examples concerning existing structures are presented from different countries. The following issues are addressed: component safety, system safety, time-dependent reliability, serviceability, redundancy, and some aspects of robustness.

This document is the intellectual property of the fib – International Federation for Structural Concrete. All rights reserved.
This PDF of fib Bulletin 86 is intended for use and/or distribution solely within fib National Member Groups.

## 1.2 Component safety

Reliability-based structural performance indicators have essentially been applied to assess and consequently safeguard the safety of structural components. The reserve margin of safety ($Z$) is, for the evaluation of component performance, defined as:

$$Z = R - S \tag{1-1}$$

Here, $S$ is the applied load effect or demand and $R$ is the load carrying capacity. Failure probability $P_f$ is expressed as:

$$P_f = P_r\left[R \leq S\right] = 1 - R = F(-\beta) \tag{1-2}$$

Here, $R$ is the reliability defined as the complement of $P_f$. $F$ is the normal probability function and $\beta$ is the reliability index.

To date, the reliability criteria of component levels have been most successful where they were integrated into codes and specifications for design and assessment. On an international scale, these codes and guidelines have been synchronized as to provide consistent levels of component reliability.

## 1.3 Structural system safety

The structural design process is based on examining the safety of each individual member for one particular failure mode. This seemingly straightforward process is made more complicated by the fact that most structures are composed of several members, each of which may be subject to failure in a different mode. The reliability of a structural system is a function of the reliability of its components. More than one interdependency between the reliability levels of its members typically exists.

The performance of structural systems is often evaluated on the basis of probability of failure criteria, and occasionally using system reliability index values. When, however, one starts to investigate the reliability of the individual components, the complexity of what system failure is emerges. In addition to the evaluation of the probability of failure, risk analysis must account for the consequences of failure. This understanding has led to the development of performance-based design criteria. While many of the proposed performance-based design criteria have not been explicitly standardized on the basis of numerical risk assessment, they implicitly include subjective notions of risk as perceived by the code writers based on their experience and their understanding of the public's risk tolerance. Most proposals for performance-based codes distinguish between different building occupancy categories in defining the performance requirements, depending on the consequences of failure[1].

## 1.4 Life-cycle & time dependent reliability

To date, most existing structural reliability studies have concentrated on the analysis of members and systems that are not subject to major changes over time, except for time-dependent models that account for member deterioration, particularly due to corrosion of reinforcing steel bars in concrete and steel members. Even if only few concrete structural failures are attributed to effects of temperature, creep or shrinkage,

*This document is the intellectual property of the fib – International Federation for Structural Concrete. All rights reserved.*
*This PDF of fib Bulletin 86 is intended for use and/or distribution solely within fib National Member Groups.*

these phenomena have been the source of much frustration for long span bridge owners, who frequently need to spend valuable resources on renovation measures in concrete bridges after only a few years of service.

The need to understand the sources of uncertainties in predicting the long term behaviour of concrete and the scale effects is an important issue[2]. To date, the problem was not investigated in sufficient depth particularly for the new generation of advanced concrete.

## 1.5 Serviceability

The primary objective of structural design is to provide structural safety. However, in order to maintain serviceability of structural systems, additional objectives have to be covered, typically including comfort of users, durability and appearance. Serviceability is normally checked by controlling deformations, cracking and stress limits of various components.

Reliability based methods similar to those used in evaluating structural safety can also be used in the treatment of serviceability. In the existing codes this issue is mostly treated by a past practice manner rather than objective scientific evidence or research.

In most cases, the relation between existing criteria and structure's service life, functionality, or users comfort are not well established. For bridges, the guidelines based on the elastic response require that all bridges be designed to avoid "undesirable structural or psychological effects due to their deformations".

The implementation of reliability-based performance indicators for serviceability limit states has been significant issue for many engineers due to a number of reasons. Some argue on the purpose of building codes (protection vs. creativity, innovation, etc.)[3], while others point out the prohibitive computational demands, especially when time-varying load processes and stochastic effects generally have to be considered.

Recent advances in reducing the computational costs associated with characterization of stochastic processes have proved to be efficient for realistic failure probabilities as well. For instance, a novel approach enabling identification of non-stationary stochastic processes as critical input for nonlinear mechanical models in the fully probabilistic framework was proposed in[4].

## 1.6 Durability

Traditionally the durability aspects are included in the structural details by using certain minimum geometrical requirements and material properties. For the future it is quite relevant to verify also the limit states associated with durability. The Model Code 2010 distinguishes between different safety formats:

- probabilistic safety format;
- partial safety factor format;
- deemed-to-satisfy approach;
- avoidance-of-deterioration approach.

This document is the intellectual property of the fib – International Federation for Structural Concrete. All rights reserved.
This PDF of fib Bulletin 86 is intended for use and/or distribution solely within fib National Member Groups.

## 1.7 Fatigue

When designing components that are sensitive to fatigue, it is necessary to obtain the definition of a representative load spectrum to be used with the fatigue properties of the material for assessing the safety of the component over its service life. The problem is complicated by the variability in the underlying load environment, the analysis of the stress response, and shortcomings in the modelling techniques available for the analysis of the fatigue phenomenon. In practice, fatigue analysis techniques frequently make conservative assumptions about the loads and large safety factors on the fatigue properties, which are often represented by S-N curves, for an evaluation of successful performance over a design lifetime.

Despite the tremendous progress that was achieved during recent decades, fatigue damage prognosis of engineering materials and structures still poses a challenging problem. The fatigue process of structural components under service loading is stochastic in nature. The development of probabilistic fatigue damage modelling based on underlying physical mechanisms, rigorous statistical model verification and validation, and systematic uncertainty quantification and management is required for a sound reliability-based performance evaluation of many aerospace structure systems. It is also one of the current focuses of several governmental agencies.

Among the recent and ongoing efforts are the probabilistic damage prognosis, uncertainty quantification and propagation and metrics-based model validation. The latter is considered a critical issue faced by many agencies. The appropriate metrics are lacking, especially for the time-dependent problems. Metrics should be as simple as possible, making them easy to use by field engineers. In addition, the metrics need to take into consideration uncertainties from measurements and modelling to ensure accurate risk assessment.

## 1.8 Structural redundancy, robustness and progressive collapse

Redundancy is defined as the provision of additional capacity. Thus, a redundant structure may be defined as a structure with additional structural capacity and reserve strength, allowing it to carry a greater load than anticipated when considering the capacity of individual members.

Robustness is defined as the capability of performing without failure under unexpected conditions. Structural robustness could therefore be defined as the capability of a structural system to survive extraordinary circumstances, beyond the scope of conventional design criteria[5]. This parallels the definition of robustness by[6], who suggested that structural robustness represents the ability of a structure to survive and continue to carry some load after the removal of a structural component.

The two definitions for redundancy and robustness provided above are both related to system effect and the ability of the system to continue to carry load after the capacity of individual members are exceeded or after the removal of individual members from the system. Consequently, redundancy is the umbrella term for both.

Traditionally, engineers have recognised three types of redundancy: First, there is internal redundancy, where the failure of one element will not result in the failure of

*This document is the intellectual property of the fib – International Federation for Structural Concrete. All rights reserved.*
*This PDF of fib Bulletin 86 is intended for use and/or distribution solely within fib National Member Groups.*

other elements of the same member. Second, we have structural redundancy, which is the result of continuity within a load path. The third type is load path redundancy, which is related to the number of supporting elements. These traditional definitions are however descriptive in nature, a fact that has led many bridge engineers to observe that "the industry lacks a clear, objective, and quantifiable definition of redundancy, and there is no rational minimum benchmark that can be quantified in the design standards" leaving it up to "the bridge owner to select the design criteria of redundancy retrofits such as fracture environment, post fracture capacity, and post fracture performance"[7].

For the design of new structures it is recommended to include redundancy criteria such as proposed by[8]. The formulation of the redundancy criteria should be based on the reliability of the structural system rather than its individual members. System reliability methods will serve to account for the uncertainties associated with estimating a system's capacity, its redundancy, and its robustness.

Several studies have proposed reliability-based approaches to evaluate the probability of system collapse and evaluating system redundancy[9; 10; 8; 11; 12; 13; 14].

For example the NCHRP Report 406[15] developed a process for quantifying redundancy (i.e. robustness according to the European view) in bridge superstructures. Subsequently, this approach was extended to substructures[16]. A bridge is considered safe if:

- it provides reasonable safety against first member failure;
- it provides adequate levels of safety before it reaches its ultimate limit states;
- it does not deform excessively under expected loads;
- it is able to carry some traffic loads even after damage or loss of members.

Consequently, four limit states are defined as:

- *member failure*, which is a check of individual member safety using elastic analysis;
- *ultimate limit state*, which is defined as the ultimate capacity of the bridge system or the formation of a collapse mechanism;
- *functionality limit states*, which is defined as the capacity of the structure to resist a main member live load displacements of specified magnitude;
- *damaged condition limit state*, which is defined as the ultimate capacity after removal of one main load carrying component.

All four limit states are to be checked in order to ensure the adequately safe performance of the bridge system both under extreme and regular conditions. "Adequate" safety margins can be determined using reliability based techniques. A reliability index can be defined for each limit state, thus there will be $\beta_{member}$ for the member failure, $\beta_u$ for the ultimate limit state, $\beta_{funct}$ for the functionality limit state, and the system reliability index $\beta_{damaged}$ for damaged conditions. To study the redundancy of a system, it is valuable to examine the differences between the reliability indices of the system expressed as $\beta_u$, $\beta_{funct}$, and $\beta_{damaged}$ and the reliability index of the most critical member as $\beta_{member}$ . The relative reliability indices are defined as:

This document is the intellectual property of the fib – International Federation for Structural Concrete. All rights reserved.
This PDF of fib Bulletin 86 is intended for use and/or distribution solely within fib National Member Groups.

$$\Delta\beta_u = \beta_u - \beta_{member} \tag{1-3}$$

$$\Delta\beta_f = \beta_{func} - \beta_{member} \tag{1-4}$$

$$\Delta\beta_d = \beta_{damage} - \beta_{member} \tag{1-5}$$

These relative reliability indices give measures of the relative safety provided by the bridge system compared with the nominal safety of first member failure.

The quantitative evaluation of robustness, and consequently the evaluation of the reliability indices related to the robustness, has been treated by several authors. A summary of the main quantitative definitions proposed in the past few years is presented in[17].

Four main approaches exist:

- *Risk-based*: this approach, proposed by[18], is based on the investigations of several risk scenarios, determined on the basis of an event tree. To this end, the assessment of the probability of occurrence of each leaf of the tree is required and an evaluation of the consequence in term of cost is needed in order to calculate the associated risk.

- *Topology-based*: in this method, proposed by[19], a central role is played by the structural hierarchy. Particularly, a parameter called "well-formedness" is identified in the system, which accounts for the level of connection between the structural elements.

- *Energy-based*: this approach, qualitatively described by[20], is based on a comparison between the energy released by an element failure and the energy required for the next element to fail.

- *Damage-based*: this approach considers the degradation of a parameter which represents the structural response due to the presence of a structural damage. Consequently, the response of the nominal integer structural configuration needs to be investigated and compared with the response of a damaged configuration. Different parameters for the response and the damage can be found in literature[13,21]. A damage-based quantitative evaluation of the robustness for a long span suspension bridge can be found for example in[22]. This method considers the ultimate resistance as a parameter for the evaluation of the structural performance and the number of failed elements as parameter for the quantification of the damage level. For each damage degree, all possible structural configurations corresponding to the combinations of removed elements in the structure are investigated by means of an incremental static analysis, and the maximum and minimum of ultimate resistance are stored, giving origin to two curves that provide a lower and upper bound of the structure robustness.

Robustness of structural systems should be related to exposure over their lifetime and should be in balance with the risk acceptance of society as well as the economical constraints[23,24,25].

*This document is the intellectual property of the fib – International Federation for Structural Concrete. All rights reserved.*
*This PDF of fib Bulletin 86 is intended for use and/or distribution solely within fib National Member Groups.*

## 1.9 Resiliency

The "resilience" of structures in terms of time is related to the structural capability to reduce the probability of failure, to minimize the consequences from failures and to optimize time to recover the functionality of the structural system.

## 1.10 Network reliability

Specifically for complex structures and infrastructure systems it is highly recommended to address all safety related aspects not only on the components level but in particular on the network level. For instance, network performance quantification can be based on the clustering of components and their interaction among them.

In the ALA guidelines development[26], maps and collected hazard data are used to identify the potential threats to lifeline systems. Subsequently, fragility curves are used to determine lifeline component damage states, based on which their functionality is established. Clearly, the performance measures defined in the ALA guidelines[26] combine several dimensions, and their evaluation often calls for the experience of multiple operators, rendering the performance assessment process somewhat subjective and complex. Thus, simplified and technically objective measures are still required in practical design and assessment of lifeline network performance today. From a purely topological point of view, every lifeline network may be represented as an abstract graph $G$ ($N$,$K$) with $N$ nodes and $K$ interconnected links. The connections between each pair of nodes are represented by an NxN matrix, whose $\{a_{ij}\}$ entries equal to 1 if there is a connection between node $i$ and node $j$, and equal to 0 otherwise. Under this representation, the performance of a lifeline network is often studied from the perspectives of connectivity and efficiency.

Generic lifeline networks operate under different regimens of flow among supply and demand nodes. It is therefore crucial to establish performance metrics that combine network topology with various flow patterns within the networks, allowing them to reflect different levels of functionality in hazard situations.

Service flow reduction (SFR) and similar metrics are used extensively due to the fact that they take into consideration both flow capacity and supply/demand constraints. They provide information on the amount of flow the network system will be able to handle in relation to its capacity before perturbation[27].

The network performance of a whole highway system subjected to seismic events is addressed by[28], who proposed four performance measures: total number of highway sections open, total length of highway open, total "connected" length of highway open, and total weighted "connected" length of highway open.

A probabilistic model developed by[29] is based on evaluating the effect of repairing bridge damage on the improvement of the network performance in the days following an earthquake. They introduce the "Drivers Delay" metric, which is defined as the increase in total daily travel time for all travellers, including commuters and commercial vehicles, caused by earthquake induced delays.

This document is the intellectual property of the fib – International Federation for Structural Concrete. All rights reserved.
This PDF of fib Bulletin 86 is intended for use and/or distribution solely within fib National Member Groups.

# 2. Risk issues

## 2.1 General overview of risk categories

In general, the risk issues can be categorized in different classes:

- identifiable as well as quantifiable risks
- expectable risks which are non-quantifiable at the relevant time
- non-identifiable and non-quantifiable risks
- unknown and extreme risks

So that a certain danger or a risk does not occur and the condition remains safe, preventive and postventive protective measures can be taken (see below for definition).

Preventive protective measures are taken to forestall a certain risk or danger. But also insurances, rescue services, information activities and confidence-building measures rank among the preventive measures.

Postventive measures are defined here as measures taken to help surmount dangers and risks that have already materialized. Among them are compensation measures as well as restoration and rehabilitation measures.

In the technical sciences, a quantitative measure in the form of a probability of failure value is used to compare the actual risk present with the tolerable risk value as defined by the relevant standards, or a with reasonably acceptable risk.

$$R_{lim} \geq R_{vorh,i} = P_i * I_i$$

$R_{lim}$ = acceptable risk (tolerable risk)

$R_{vorh}$ = actual risk present

$P_i$ = probability for the risk event to occur (usually per year)

$I_i$ = consequences and extent of damage

The problem with the equation above is that it is not possible to use the simple product of the probability of a risk event to occur with its consequences or damage extent (high extent in cases of low occurrence probability) for evaluating the average risk expectation.

In the natural and technical sciences, the theory of extreme values is frequently used for modelling natural phenomena. Essentially, two approaches are used today:

- focus on maximum and minimum values, “block maxima models” with extreme value distribution functions
- analysis of those instances where the actual measures exceeded or fall below relevant limit values, “threshold exceedance models”

An alternative approach would be to focus on the exceedance of limit values. Here, unrelated data are compared with a predefined limit state (for example the Richter or Mercalli scales for earthquakes or the dyke heights or flood levels). In case of exceedance, the values follow a generalized Pareto distribution.

*This document is the intellectual property of the fib – International Federation for Structural Concrete. All rights reserved.*
*This PDF of fib Bulletin 86 is intended for use and/or distribution solely within fib National Member Groups.*

$$P(x) = 1 + \log G(x)$$

For G(x), either an extreme value distribution or, in the event of natural disasters, an exponential distribution may be used.

Table 2-1 identifiable, quantifiable and deterministic risks

| identifiable & quantifiable risks | deterministic risk analysis |
|---|---|
| expectable risks which are non-quantifiable at the relevant time | probabilistic risk analysis |
| non-identifiable & non-quantifiable risks | empirical risk analysis |
| unknown, extreme risks | dynamic phenomenological scenario analysis |

Table 2-2 Terms and definitions given in to ISO 2394[30], ISO/TS 16732[31], ISO/IEC Guide73[32]

| | |
|---|---|
| Qualitative estimation | In qualitative estimation, risk is subjectively estimated and ranked in a verbal expression. Qualitative estimation can be used: 1) as an initial screening activity to identify risks which require more detailed estimation; 2) where the qualitative estimation provides sufficient information for decision making; or 3) where the numerical data or resources are insufficient for a quantitative estimation. |
| Semi-quantitative estimation | In semi-quantitative estimation, a more expanded ranking scale than the one usually achieved in qualitative estimation shall be adopted. It should be noted that the numbers chosen may not properly reflect relativities and this can lead to inconsistent, anomalous or inappropriate outcomes. |
| Quantitative estimation | In quantitative estimation numerical values shall be used rather than the descriptive scales used in qualitative and semi-quantitative estimation for both consequences and likelihood using data from a variety of sources. The quality of the estimation depends on the accuracy and completeness of the numerical values and the validity of the models used. |
| Data for estimation | Data for estimation shall be taken from appropriate source of information. The most pertinent information source and techniques should be used when estimating probability. Information source may include the following:<br>- Past records<br>- Practice and relevant data (field data collection)<br>- Relevant published data (incident data)<br>- Experiments and prototype<br>- Engineering or other models<br>- Specialist and expert judgment (expert opinion) |

The international standard ISO/IEC 31010:2009 incorporates general principles of evaluating the risks involving structural systems. Since structures are endangered by certain hazards, the standard aims at minimizing the risk due such events.

As a part of the whole process of risk management, risk assessment provides owners/authorities with the basis for the risk control consisting of decision making on whether the risk is treated or not and how it would be treated if necessary and risk monitoring on whether the risk is being maintained under the acceptable level. It will give an overview of the standard as a framework of reference and as a methodology for the identification of hazards and for the assessment and handling of risks concerning structures. It will focus on definitions and statements that are necessary for understanding.

This document is the intellectual property of the fib – International Federation for Structural Concrete. All rights reserved.
This PDF of fib Bulletin 86 is intended for use and/or distribution solely within fib National Member Groups.

## 2.2 Normative references

- ISO/IEC 31010:2009[33]: Risk management – Risk assessment techniques is closely associated with the following documents
- ISO 2394:2015-03[30]: General principles on reliability for structures
- ISO 13822:2001[34] : Basis for design of structures – Assessment of existing structures
- ISO/TS 16732[31]: Fire safety engineering - Fire risk assessment – Part 1: General
- ISO/IEC Guide 51[35]: Safety aspects – Guidelines for their inclusion in standards[35]
- ISO/IEC Guide 73[32]: Risk management-Vocabulary – Guidance for use in standards, 2002
- ISO 16204[36]: Durability-service-life-design of concrete structures
- ISO 13823[37] : General principles on the design of structures for durability

## 2.3 Terms and definitions

General principles, terms and definitions associated with risk and reliability issues are addressed in ISO 2394[30], ISO/TS 16732[31], ISO/IEC Guide73 and are listed in the following Tables.

Table 2-3 Basic terminology associated with risk and reliability acc. to ISO 2394[30], ISO/TS 16732[31], ISO/IEC Guide73[32] – part 1

| | |
|---|---|
| Risk level | A level of risk, which an individual or society would accept to secure certain benefits |
| Consequence analysis | A systematic procedure to describe and/or estimate consequences. |
| Cost benefit | An analysis to contribute to decision-making for whether to adopt a project or a plan by quantifying and comparing its costs and benefits |
| Event | An incidence of one or more hazards acting on a system.<br>Note: Extraordinary events are the events that could not be anticipated or expected technologically by experts, or the events whose occurrence probability is estimated extremely low. |
| Hazard | Potential source that could be dangerous for human life and/or cause damage for structures.<br>- Identification process to find, list and characterize hazards.<br>- Curve probability distribution of occurrence of the identified hazard with specified magnitude. |
| Hazard screening | The process of identifying significant hazards which shall be considered among possible hazards. |
| Negative consequence | A quantitative estimate of harm, direct and indirect, stated in terms of personal injury, death, environmental damage, and monetary loss.<br>Note 1: There can be more than one negative consequence from one event.<br>Note 2: Consequences can range from positive to negative. However, consequences are always negative for safety aspects.<br>Note 3: Consequences can be expressed qualitatively or quantitatively. |
| Option | Possible alternatives to mitigate risk<br>Note: nothing-to-do can be a feasible option when other alternatives cannot mitigate the risk against their invested costs. |

*This document is the intellectual property of the fib – International Federation for Structural Concrete. All rights reserved.*
*This PDF of fib Bulletin 86 is intended for use and/or distribution solely within fib National Member Groups.*

Table 2-4 Basic terminology associated with risk and reliability acc. to ISO 2394[30], ISO/TS 16732[31], ISO/IEC Guide73[32] – part 2

| | |
|---|---|
| Reliability | Probability that a unit will perform a required function for given conditions and for a given period of time (from ISO 921: 1997, Nuclear energy - vocabulary). |
| Residual risk | Risk remaining after risk treatment. |
| Risk assessment | Overall process of establishment of structural context, definition of system, identification of hazards and consequences, risk estimation, risk evaluation, and evaluation of treatment alternatives. |
| Risk communication | Exchange or sharing of information about risk among the decision-maker, other stakeholders and engineers.<br>Note: The information can relate to the existence, nature, form, probability, severity, acceptability, treatment or other aspects of risk. |
| Risk control | Actions implementing risk management decisions.<br>Note: Risk control may involve monitoring, re- evaluation, and compliance with decisions. |
| Risk criteria | Terms of reference by which the significance of risk is assessed. Note: Risk criteria can include associated costs and benefits, legal and statutory requirements, socio-economic and environmental aspects, the concerns of stakeholders, priorities and other inputs to the assessment. |
| Risk estimation | Process used to assign values to the probability of events and consequences of a risk.<br>Note: Risk estimation can consider cost, benefits, the concerns of stakeholders, and other variables, as appropriate for risk evaluation. |
| Risk evaluation | Process of comparing the estimated risk against given risk criteria to determine the significance of the risk.<br>Note: Risk evaluation may be used to assist in the decision to accept or to treat a risk. |
| Structural context | Background or reasons why the risk assessment should be implemented from the viewpoint of structures. |
| Stakeholder | Any individual, group, organization or authority that can affect, be affected by, or perceive itself to be affected by, a risk.<br>Note: The decision-maker is also a stakeholder. |
| Structure | A natural or human-made arrangement of materials that must withstand certain forces and/or displacement to perform some intended function. |
| System | A bounded group of interrelated, interdependent or interacting elements forming an entity that achieves a defined objective in its environment through interaction of its parts.<br>Note 1: This definition implies that the system is identifiable, is made up of interacting elements or subsystems, all elements are identifiable, and the boundary of the system can be identified.<br>Note 2: System involving structures includes structural system defined in ISO 2394 as a subsystem.<br>Note 3: In terms of technological hazards, a system is normally formed from a physical subsystem, a human subsystem, their management, and environment. |

This document is the intellectual property of the fib – International Federation for Structural Concrete. All rights reserved.
This PDF of fib Bulletin 86 is intended for use and/or distribution solely within fib National Member Groups.

## 2.4 General framework of risk assessment for structures

Generally speaking, the main objective of risk management is the "optimal" allocation of limited resources to stakeholders such as society, local community, individuals, and various organizations. The process of risk management can be broken down to several discrete steps including establishment of the risk management goals, risk assessment, risk treatment, communication and consultation, and monitoring and review, as outlined below. The process of risk management is not a one way street, but rather an iterative process.

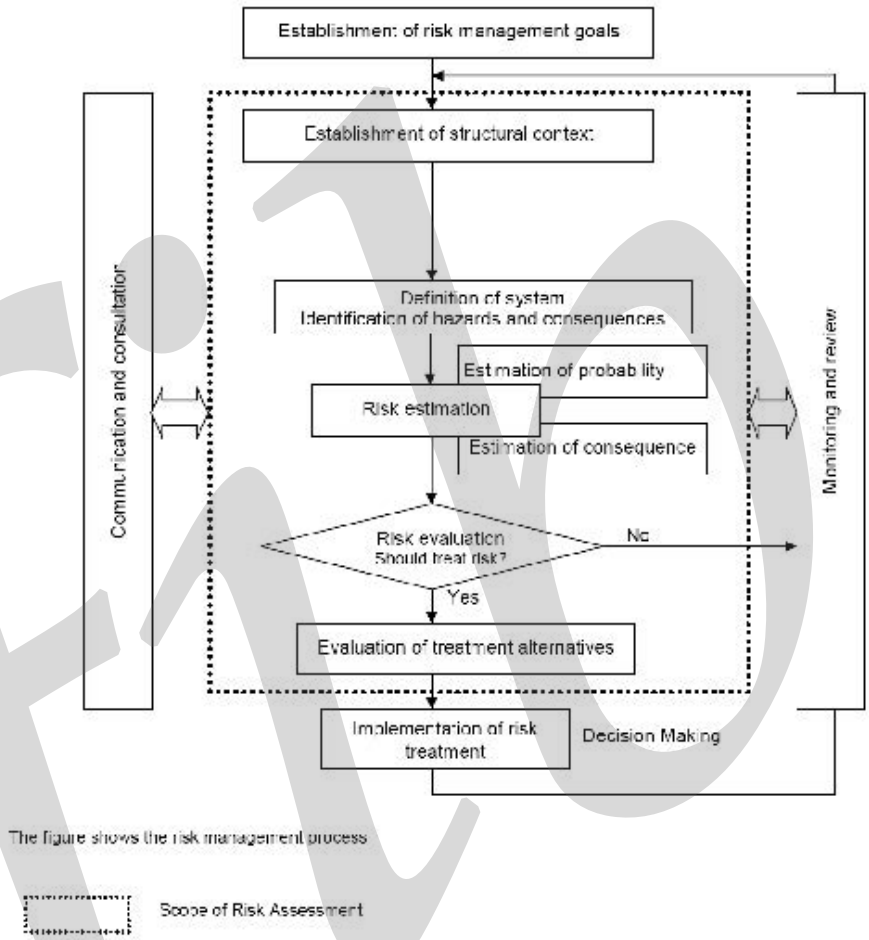


Fig. 2-1 Risk management and scope of risk assessment for structures acc.to (ISO 2394[30])

The following definitions are taken from ISO 2394[30] in order to illustrate the risk assessment process, as shown in Fig. 2-1

- Establishment of risk management goals: To identify the risk management objectives for either new or existing structures, the overall risk is determined on the basis of the planned design specifications and/or the current conditions. A definition of an acceptable risk level is reached by determining risk-induced costs and benefits and by comparing the current case with previous ones.

- Risk assessment: In order to achieve risk assessment in a meaningful way, in the first step, the structural context need to be examined and the structural system has to be determined. Even if these two steps are not generally part of most risk assessment guidelines, they provide essential information. Subsequently, possible hazards and

*This document is the intellectual property of the fib – International Federation for Structural Concrete. All rights reserved.*
*This PDF of fib Bulletin 86 is intended for use and/or distribution solely within fib National Member Groups.*

their consequences are identified, the associated risk is estimated and evaluated and decisions on risk treatment are taken.

- Risk treatment: Once risks have been identified and assessed, decisions are made on how to manage the risk, and any necessary measures are taken. It may be worth mentioning that as part of this decision making process, stakeholders of a structure may decide to accept risks that were found to be unacceptable in the previous assessment on the basis of their values and objectives, thereby implicitly changing the safety objectives.

- Communication and consultation: For any successful risk management, thorough communication and detailed consultation with the stakeholders is essential.

- Monitoring and review: Continuous attention needs to be given to the monitoring of the risk level, regardless of risk treatment. The effectiveness of all risk management elements also needs to be examined on a regular basis. Comprehensive documentation of all elements of the risk management process is crucial for the decision making process and to enable continuous improvement.

Wherever the uncertainty of an input parameter has a significant impact on how a structure may behave in a hazard situation, and accordingly on the consequences of this behaviour, a specific risk evaluation analysis should be performed and mitigation measures assured.

## 2.5 Risk assessment -dire impact on the functioning of a community

The structural context defines the role of risk assessment in the framework of risk management for structures. The typical structural contexts are 1) design basis, 2) assessment of existing structures, and 3) assessment of exceptional structures and/or extraordinary events

Table 2-5 Terms and definitions taken out from ISO 2394[30], ISO/TS 16732[31], ISO/IEC Guide73[32] – part 3

| | |
|---|---|
| Design basis | 1) Any design codes prescribe a series of design criteria for the design of structural members. These criteria are often based on the target reliability levels which must be predetermined by judging the risk due to the exceedance from the limit states of interest. The result from the risk assessment can provide the rational basis for determining the reliability level.<br>2) Risk assessment can be carried out to qualify existing structural design codes. |
| Assessment of existing structures | 1) Risk of any types of existing structures shall be assessed in case that the risk due to possible hazards seems to be large, and then the results from the risk assessment shall be reported qualitatively or quantitatively to the stakeholders. The final results will be translated into the appropriate form in such a way that the stakeholders can make decisions in the framework of risk management.<br>Note: ISO 13822 (Assessment of existing structures) can be used for risk estimation.<br>2) It is necessary to assess the risk due to extraordinary events beyond the design-based events and to verify that the results should be within the acceptable level. The acceptable level should be equivalent to that for newly designed structures; however, the level for existing structures can be determined with cost benefit consideration. |
| Exceptional structures or extraordinary events | Exceptional structures are the ones designed beyond the scope of existing codes. Such structures that have significant consequence due to the structural failure shall be subject to the risk assessment, even if the events of structural failure may not be frequent. Risk assessment shall also be implemented for some extraordinary events such as fires and some critical event scenarios. |

This document is the intellectual property of the fib – International Federation for Structural Concrete. All rights reserved.
This PDF of fib Bulletin 86 is intended for use and/or distribution solely within fib National Member Groups.

## 2.6 Risk assessment - system identification

For the risk assessment the various systems including structures, equipment, environment and their identification have to be considered, as indicated in Table 2-5. Therefore the role of risk assessment considering identification scenarios and the extent of failures have to be taken into account.

Table 2-6 Terms and definitions taken out from ISO 2394[30], ISO/TS 16732[31], ISO/IEC Guide73[32]– part 4

| | |
|---|---|
| Identification of system under consideration | The extent of system that is considered in risk assessment shall be clearly identified. That is, for example, structure(s), equipment, a human subsystem, their management, and environment. The characteristics of each subsystem should also be identified, such as type of structure(s), codes and standards used in the design of the structure(s), use, importance, location and working life. The limit states of the system should also be specified. |
| Identification of scenarios | The extent of scenarios due to failure of the system in time and space shall be specified. The extent should include collapse or damage of the structure(s), loss of functionality, injury or death of human inside and just outside the structure(s), economic and/or social loss caused by the failure of the system concerned to the stakeholders. |

## 2.7 Risk estimation - evaluation

Risk estimation shall be undertaken depending upon the purpose of the estimation, required degrees of details, the information, data and resources available. The types of estimation fall into three broad categories, which are qualitative, semi-quantitative and quantitative, depending on the circumstances. In practice, qualitative estimation is often used, as a preliminary risk estimation, to obtain a general indication of the level of risk and to reveal the risk which should be considered. Later it may be necessary to undertake more specific or quantitative estimation on the revealed risk.

Table 2-7 Terms and definitions taken out from ISO 2394[30], ISO/TS 16732[31], ISO/IEC Guide73[32] – part 5

| | |
|---|---|
| Identification of possible hazards | Structures may be exposed to various possible hazards occurring during their service lives, some of which result from natural sources, some of which are due to human-made sources. Hazards that could cause any unfavourable events shall be identified. Combination of more than one accidental hazard can be ignored due to their extremely low probability of simultaneous occurrence. Some hazard that may follow the occurrence of the other hazard such as earthquake induced fire shall not be ignored. |
| Hazard screening | Although all possible hazards should be taken into consideration, important hazards to a system should be selected on the basis of their significance and will be incorporated in the risk assessment. As each hazard has its inherent property and possible consequence, it is recommended to categorize hazards by original cause, by degree of quantifiability and by degree of significance of consequence, and then to screen out the hazards less important in the risk assessment. The hazard screening can be implemented based on experience and expertise. The result of the risk screening should be documented. |

*This document is the intellectual property of the fib – International Federation for Structural Concrete. All rights reserved.*
*This PDF of fib Bulletin 86 is intended for use and/or distribution solely within fib National Member Groups.*

| | |
|---|---|
| Hazard screening criteria | Preliminary risk estimation should be done to identify the significant risk. The criteria for the hazard screening are, in principle, based on the magnitude of the risk from the preliminary risk estimation. Frequency of the hazard and/or significance of the relevant consequence could also be the useful criteria. Hazards with obviously negligible risk compared with the acceptable risk level can be screened out.<br>The hazard screening criteria should be clearly described in terms of frequency of the event and magnitude of the consequence of interest, both of which are relied on the past experience, people's perception, some given values specified elsewhere. |
| Identification of consequences | Consequences resulting from the hazards and following events should be identified. They should be described in terms of several measures, e.g., monetary loss, human fatalities and environmental damage. Some consequences can be identified by scenario analyses considering the extent of influences due to failure of the system in time and space |

Table 2-8 Terms and definitions given in ISO 2394[30], ISO/TS 16732[31], ISO/IEC Guide73[32] – part 6

| | |
|---|---|
| Risk representation | The results obtained in a risk estimation shall be presented to stakeholders with maximum clarity. A common approach is to group similar hazards and convert them to a common scale, such as lives at risk or lost. This can then be related to the probability of occurrence of various hazards, and might be compared to other hazardous activities or to risk criteria. In qualitative risk representation risk shall be rated as high, moderate, or low importance. In quantitative representation risk shall be presented by a combination of probability and consequence |
| Estimation of probability | Probability can be obtained from any or all of the following three approaches: (1) direct estimation from data, (2) inference from a model that relates the probabilities of interest to other probabilities, and (3) engineering judgment. Where no reliable or relevant past data are available, subjective estimates may be made which reflect an individual's or group's degree of belief that a particular event or outcome will occur.<br>It is preferable to differentiate between uncertainties due to inherent natural variability, model uncertainties and statistical uncertainties. Whereas the first type of uncertainty is often denoted aleatory uncertainty, the two latter are referred to as epistemic uncertainties. In the procedure of quantitative risk estimation, the probability of occurrence of an identified hazard and limit state probability for corresponding identified hazard shall be estimated. |
| Quantitative estimation of probability | An appropriate probabilistic model should represent each hazard. A hazard curve can be obtained as a function of an index that expresses magnitude of hazard.<br>Limit state probability<br>The limit state probability shall be estimated according to the following procedures.<br>(1) Modelling of action<br>(2) Modelling of resistance<br>(3) Structural analysis (response analysis)<br>To represent a conditional limit state probability, a fragility curve can be used as a function of an index of limit state probability corresponding to the magnitude of hazard.<br>* Detail of hazard curves and fragility curves will be described in Annex E. |

*This document is the intellectual property of the fib – International Federation for Structural Concrete. All rights reserved.*
*This PDF of fib Bulletin 86 is intended for use and/or distribution solely within fib National Member Groups.*

Table 2-9 Terms and definitions given in ISO 2394[30], ISO/TS 16732[31], ISO/IEC Guide73[32] – part 7

| | |
|---|---|
| Estimation of consequence | Consequences can be determined by modelling the outcomes of an event or set of events, or by judging from experimental studies or past data.<br>For the quantitative estimation of consequence, it should be expressed numerically to define the extent of human fatality and injuries and/or environmental damage and economic loss. A scenario analysis is performed from the occurrence of an initial event consequence. |
| Sensitivity analysis | Since some of the results made in risk estimation could be imprecise, a sensitivity analysis should be carried out to investigate the effect of uncertainty in assumption and data. Greater sensitivity suggests that more care and/or effort should be required in obtaining data or estimates for the variables concerned. Sensitivity analysis is also a way of examining the appropriateness and effectiveness of potential controls and risk treatment options. |

Table 2-10 Terms and definitions given in ISO 2394[30], ISO/TS 16732[31], ISO/IEC Guide73[32] – part 8

| | |
|---|---|
| Assessment of alternatives for risk treatment | Selecting the most appropriate treatment option involves balancing the costs of implementing each option against the benefits (assume this is the net of gains and losses) derived from it. In general, the cost of managing risks needs to be commensurate with the benefits obtained.<br>When making such cost versus benefit judgments the level of gains and losses as determined by the risk criteria and the level of risk should be taken into account. It is important to consider all direct and indirect costs, gains, and losses whether tangible, intangible, financial or otherwise within the context established.<br>A number of treatment options may be considered and applied either individually or in combination. Sensitivity analysis is one way of testing the effectiveness of different options for treating risk. The organization may benefit through the adoption of a combination of options. An example can be the effective use of contracts and specific risk treatments supported by appropriate insurance and other risk financing.<br>Risk treatment options should consider the values and perceptions of stakeholders and the most appropriate ways to communicate with them. |
| Implementation of risk treatment | After the assessment of alternatives for risk treatment, decisions should consider infrequent but severe risks that may warrant risk treatment actions that are not justifiable on strictly economic grounds. Legal and social responsibility requirements may override simple financial cost benefit analysis in the risk criteria. If the budget for risk treatment is constrained the treatment plan should clearly identify the priority order in which individual risk treatments should be implemented. It is important to compare the cost of not taking action against the budgetary saving.<br>Risk treatment may itself introduce new risks that need to be identified, assessed, treated and monitored.<br>If, after treatment, there is a residual risk, a decision should be taken about whether to retain this risk or repeat the risk treatment process. |

*This document is the intellectual property of the fib – International Federation for Structural Concrete. All rights reserved.*
*This PDF of fib Bulletin 86 is intended for use and/or distribution solely within fib National Member Groups.*

Table 2-11 Terms and definitions given in ISO 2394[30], ISO/TS 16732[31], ISO/IEC Guide73[32] – part 9

| | |
|---|---|
| Examples of exceptional events | (1) Exceptional event is very rare event which causes very severe consequences or frequent event results in large consequences.<br>(2) Exceptional events can be put into two major categories with regard to causes: natural and man-made events.<br>(3) Some examples of natural exceptional events are as follows: huge earthquake, tsunami, hurricane, violent windstorm, extraordinary ocean waves, methane hydrate eruption, volcanic eruption, landslide, shallow debris flow, rock fall, avalanche, flood, heavy snowstorm, ice accretion, atmospheric icing, etc.<br>(4) Man-made exceptional events can be subdivided into two groups: terrorist attacks and unintentional occurrences. Causes of these events are different but consequences are similar. The following examples of man-made exceptional events can be listed as follows: severe fire, gas explosion, bomb blast, impact from projectile, vehicle, ship, helicopter or aircraft, impact from collision of trains or trucks, mining ground deformations, catastrophic erosion, cardinal human error, and others. |
| Examples of exceptional structures | (1) Exceptional structure is a structure with unusual: size, load, environment, application, or/and a structure which has significant influence to a community.<br>(2) Some examples of exceptional structures concerning their unusual features are as follows:<br>- size: high-rise residential and office buildings, long-span roofs and bridges, large train and auto tunnels, dams, storm surge barriers, marine pipelines, offshore structures,<br>- load: nuclear reactor vessels and steam line components, hydraulic structures, offshore platforms, large foundation of turbo-generators, railway bridges, wind mill towers,<br>- environment: nuclear power plants, structures containing highly toxic materials and hazardous waste, storage tanks for liquid natural gas, petroleum and natural gas transmission pipelines, explosives and fire work factories and storages,<br>- application: buildings where loss of the function has extremely negative and very important influences to a community, e.g. hospitals, schools, temples, theatres, museums, bus and train stations, airports, shopping centres, power-generating and rescue stations. |

*This document is the intellectual property of the fib – International Federation for Structural Concrete. All rights reserved.*
*This PDF of fib Bulletin 86 is intended for use and/or distribution solely within fib National Member Groups.*

Table 2-12 Terms and definitions given in ISO 2394[30], ISO/TS 16732[31], ISO/IEC Guide73[32] – part 10

| | |
|---|---|
| Situations recommended for risk assessment | (1) Risk assessment is useful in circumstances where exceptional events can happen or/and exceptional structures are considered.<br>(2) Risk assessment is essential where the socially acceptable level of risk to human life and health as well as to assets, environment and historical heritage can be exceeded.<br>(3) Some examples of situations recommended for risk assessment are as follows:<br>- high-rise residential and office buildings (usually more than 16 stories and/or 500-1000 occupants), considering one or some of the potential hazardous events, first of all: big fires, internal gas explosion, bomb blast, impact from projectile, helicopter or aircraft,<br>- long-span roofs, especially lightweight structures of exhibition and shopping centres, sport and concert hall, stadiums, courtyards, railway and bus stations, having regard to one or some of the potential hazardous events: extreme snow loads, hurricanes or violent windstorm, terrorist attack, internal fire, catastrophic corrosion, cardinal human error,<br>- long-span bridges, in particular suspension and cable-stayed bridges, taking into consideration some possible exceptional events: ship impact from river or canal traffic, or from seagoing vessels, impact from road vehicles, trains, helicopter or aircraft, hurricanes or wind storm, catastrophic corrosion, terrorist attack,<br>- large train and auto tunnels, first of all having regard to internal fire and explosion, but also possible earthquake, mining ground deformations and/ or landslides,<br>- hydraulic structures such as dams storm surge barriers and breakwaters, considering exceptional flood, extraordinary ocean waves or/and catastrophic erosion,<br>- nuclear power plants particularly exposed to huge internal explosion and fire, earthquake, impact from projectile, helicopter or aircraft, and terrorist attacks,<br>- structures containing highly toxic materials and hazardous waste, storage tanks for liquid natural gas, petroleum and natural gas transmission pipelines, taking into consideration some possible exceptional events: earthquake, landslides, mining ground deformations, internal explosion and fire, impact from projectile, terrorist attacks,<br>- major natural and industrial disasters in urban areas, among those most important natural disasters: huge earthquake, tsunami, volcano eruption, flood from river and from sea, cyclones, and large industrial accidents from nuclear power plants, large chemical plants, storage structures for highly toxic or explosive materials. |

A risk assessment requires probabilistic information related to quantifying epistemic or aleatory uncertainties. Such uncertainties are best quantified from analysis of large statistical databases derived from operating experience, and field or experimental studies. However, for many situations the data may be of insufficient extent or quality to provide useful and credible quantitative measures for use in a risk assessment. In such cases it is often necessary to rely on the use of expert opinions where quantitative information obtained from people associated with the parameter to be measured may be solicited. Such information relies, of course, heavily on the experience and knowledge of the people consulted and their ability to make judgements and to convey opinions. Evidently, great care must be taken in the selection of experts, and at least some of their opinions calibrated against known information. In general, however, an expert can be defined as a very skilful person who has much training and has knowledge in some special field.

*This document is the intellectual property of the fib – International Federation for Structural Concrete. All rights reserved.*
*This PDF of fib Bulletin 86 is intended for use and/or distribution solely within fib National Member Groups.*

Table 2-13 Terms and definitions given in ISO 2394[30], ISO/TS 16732[31], ISO/IEC Guide73[32]– part 11

| | |
|---|---|
| Winkler et al.[38] provide the following guidance for selection of experts: | Experts can be identified through literature searches, registries of professional organizations, consulting firms, research laboratories, government agencies, and universities. A formal nomination process is sometimes used, particularly when controversy is possible. The nomination process should be designed to preclude bias in selection. A first step is inviting stakeholders and interested parties to nominate experts. A second step is using an independent external selection panel to evaluate the nominees.<br>The criteria for selection should be specific and documented, including:<br>- Evidence of expertise, such as publications, research findings, degrees and certificates, positions held, awards, etc.;<br>- Reputation in the scientific community, including knowledge of the quality, importance, and relevancy of the nominee's work and the nominee's ability to provide the desired judgements;<br>- Availability and willingness to participate;<br>- Understanding of the general problem area;<br>- Impartiality, including the lack of an economic or personal stake in the potential findings; and<br>- Inclusion of a multiplicity of viewpoints. |

Expert opinions may be obtained from the following approaches[39; 40]:

Table 2-14 Terms and definitions given in ISO 2394[30], ISO/TS 16732[31], ISO/IEC Guide73[32] – part 12

| | |
|---|---|
| Aggregated individual method: | weighted average of expert provided data |
| Iterative methods: | varying levels of interaction among elicited experts before rendering opinions, followed by review of results with opportunity for revision of expert opinions. This process is repeated until complete consensus is achieved. The expert responses are anonymous so that independence of responses is preserved. Typical methods include:<br>- Delphi method<br>- nominal group technique: inter |
| Interactive methods: | meeting of experts to identify and structure the probabilistic data required. |
| Analytical methods: | Bayesian integration of expert opinions based on the confidence of each expert. |

In the risk analyses there are also some non-quantitative parameters to be taken into account. In order to include expert opinions in the risk analyses and in the development of mitigation measures, the skills and experience of the consulted experts have to be evaluated carefully to account for their possible biases. More details are provided in[41].

Methods for obtaining expert opinions or assessments include personal interviews or written questionnaires. The formulation of relevant questions is the key to success. Qualitative questions might target the validity of existing data (gained through experiments or field studies) or prevalent modelling assumptions. Quantitative questions could include probability estimates such as mean, median, variance, upper and lower bounds, confidence limits and probability distribution types. They may take the concrete form of absolute probability judgment, pair comparisons, rankings or indirect numerical estimates.

*This document is the intellectual property of the fib – International Federation for Structural Concrete. All rights reserved.*
*This PDF of fib Bulletin 86 is intended for use and/or distribution solely within fib National Member Groups.*

How a collection of expert reports should be interpreted may be influenced by several factors[42]. Bayesian methods in a possible combination with a fuzzy membership functions could be effectively used to combine expert judgment with a quantitative risk analyses and to account for expert biases.

This document is the intellectual property of the fib – International Federation for Structural Concrete. All rights reserved.
This PDF of fib Bulletin 86 is intended for use and/or distribution solely within fib National Member Groups.

# 3. Methods of structural reliability

## 3.1 Main principles and methods

### 3.1.1 General

A general introduction to the current safety concept of structures is given. This includes a review of basic probability theory and statistics as well as standard methods for the computation of structural reliability. These methods are compared in their application to a simple structural problem involving multiple failure modes. Additional special focus has been put on existing structures. Here often complaint about the possible adaptation to existing structures can be found. Nevertheless the probabilistic safety concept can also be used for such type of structures.

Structural systems are typically designed to stay in service for at least several decades. The structural design and the related structural reliability are formulated with respect to a specified life cycle.

This implies that proper care must be taken to ensure their safety and serviceability in the presence of deterioration as well as changing conditions of utilization. For example, it became clear that unfortunately both deterioration as well as increasing traffic loads put severe constraints on the operating conditions of bridge structures. Without proper inspection and maintenance, the evolution of resistance and load would occur as depicted in Fig. 3-1.

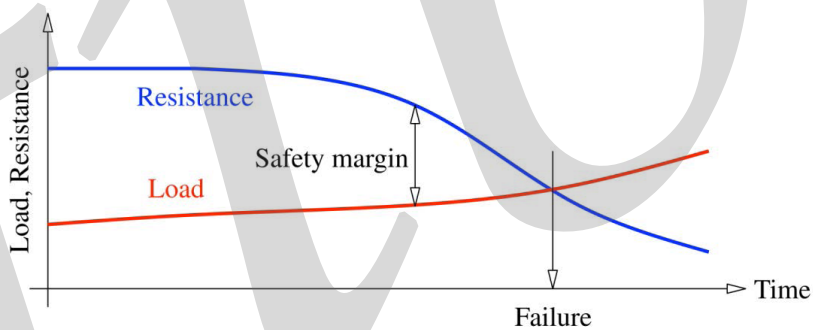


Fig. 3-1 Time dependent load and resistance, no maintenance

Eventually, this leads to a substantial safety problem due to possible structural failure. Even if failure does not occur, the serviceability of the structure will be severely reduced. Hence the need for maintenance should be obvious. Both safety and serviceability may be combined into the notion of structural performance.

This document is the intellectual property of the fib – International Federation for Structural Concrete. All rights reserved.
This PDF of fib Bulletin 86 is intended for use and/or distribution solely within fib National Member Groups.

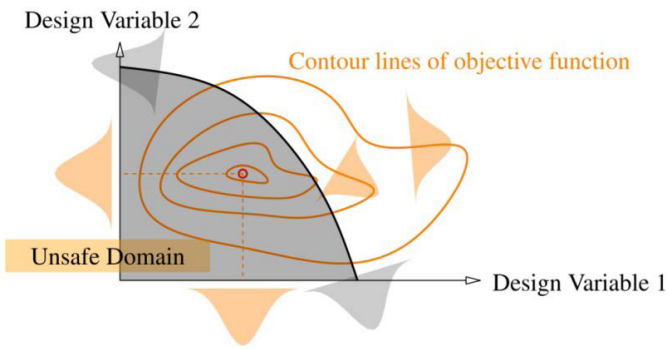


Fig. 3-2 Sources of uncertainty in optimal structural design

Structural design optimization typically aims at high performance levels for a clearly specified set of conditions. Unfortunately, this goal can usually be achieved only by sacrificing robustness of the design. This implies an increased sensitivity of the structure with respect to unforeseen stochastic situations or unavoidable random manufacturing tolerances. In order to prevent structural failure due to loss of robustness it is therefore desirable to incorporate a suitable measure of robustness into the optimization process. This can be achieved by introducing additional constraint conditions or appropriate modifications of the objective function. An example for such a design concept is reliability-based optimization based on the notion of the failure probability. This is most appropriate for high-risk structures. Alternatively, simpler stochastic measures such as variances or standard deviations might be more appropriate for the design of low-risk structural elements. Uncertainties in the structural design optimization process can be attributed to three major sources as shown in Fig. 3-2. These sources of uncertainties or stochastic scatter are:

- Uncertainty of design variables. This means that the manufacturing process is unable to achieve the design precisely. The magnitude of such uncertainty depends to a large extent on the quality control of the manufacturing process.
- Uncertainty in the objective function. This means that some parameters affecting the structural performance are beyond the control of the designer. These uncertainties may be reduced by a stringent specification of operating conditions (e.g. traffic loads). This is typically not feasible for civil structures subjected to environmental loading such as earthquakes or severe storms.
- Uncertainty of the feasible domain. This means that the admissibility of a particular design (such as its safety or serviceability) cannot be determined deterministically. Such problems are at the core of probability-based design of structures and will be discussed in detail subsequently.

A thorough review of optimization in the context of stochastic mechanics is given e.g. by[43]. Dealing with the uncertainties as mentioned above is usually achieved by applying methods based on probability theory and statistics. There are several textbooks explaining these concept in much greater detail [44; 45; 46; 47].

### 3.1.2 Probability theory

In the following some basics are given in a mathematical style in order to create a logical sequence of information to understand the basic principles of probability theory.

*This document is the intellectual property of the fib – International Federation for Structural Concrete. All rights reserved.*
*This PDF of fib Bulletin 86 is intended for use and/or distribution solely within fib National Member Groups.*

The reader might consider additional literature sources for more detailed information and engineering based applications.

#### 3.1.2.1 Random variables

For structural engineering problems the random events $A$ under consideration are defined by the occurrence of a real-valued random value $X$ which is smaller than a prescribed, deterministic value $x$:

$$A = \{X \mid X < x\} \tag{3-1}$$

The probability $P[A]$ associated with this event obviously depends on the magnitude of the prescribed value $x$, i.e. $P[A]=F(x)$. For real valued $X$ and $x$, this function $F_x(x)$[1] is called probability distribution function (or, equivalently cumulative distribution function, cdf):

$$F_X(x) = \mathrm{P}[X < x] \tag{3-2}$$

[1]The index $X$ refers to the random variable $X$, the argument $x$ refers to a deterministic value against which the random variable is compared.

Since real-valued variables must be always be larger than -∞, and can never reach or exceed +∞, we obviously have

$$\lim_{x\to-\infty} F_X(x) = 0; \lim_{x\to+\infty} F_X(x) = 1 \tag{3-3}$$

Differentiation of $F_X(x)$ with respect to $x$ yields the so-called *probability density function* (pdf):

$$f_X(x) = \frac{d}{dx} F_X(x) \tag{3-4}$$

From the above relations it follows that the area under the pdf-curve must be equal to unity:

$$\int_{-\infty}^{\infty} f_X(x)dx = 1 \tag{3-5}$$

A qualitative representation of these relations is given in Fig. 3-3.

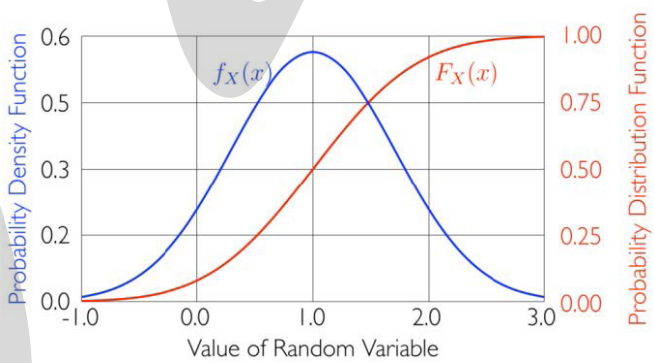


Fig. 3-3 Schematic sketch of probability distribution and probability density functions

This document is the intellectual property of the fib – International Federation for Structural Concrete. All rights reserved.
This PDF of fib Bulletin 86 is intended for use and/or distribution solely within fib National Member Groups.

In many cases it is more convenient to characterize random variables in terms of expected values rather than probability density functions. Special cases of expected values are the mean value $\bar{X}$:

$$\bar{X} = \mathrm{E}[X] = \int_{-\infty}^{\infty} x \cdot f_X(x)\,dx \tag{3-6}$$

and the variance $\sigma_X^2$ of a random variable:

$$\sigma_X^2 = \mathrm{E}[(X-\bar{X})^2] = \int_{-\infty}^{\infty} (x-\bar{X})^2 f_X(x)\,dx \tag{3-7}$$

The positive square root of the variance $\sigma_X$ is called standard deviation.

Frequently, statistical properties such as mean values or standard deviations have to be estimated from samples. The estimators must meet certain requirements. Assume we want to estimate a parameter $\gamma$ from $n$ independent samples $X_1,\ldots,X_n$; using the estimator $\Gamma$: $\Gamma_n = \Gamma(X_1,\ldots,X_n)$. We then require two essential properties of the estimator guaranteeing a truly representative estimate.

Definition: The estimator $\Gamma$ is called *consistent* if:

$$\forall \in > 0 : \lim_{n\to\infty} P[|\Gamma_n - \gamma| < \in] = 1 \tag{3-8}$$

(this means convergence of the estimator to the true value in probability)

Definition: The estimator $\Gamma$ is called *unbiased* if:

$$\mathrm{E}[\Gamma_n] = \gamma \tag{3-9}$$

This means that the random deviations of the estimator from the true value diminish as the sample size increases.

### 3.1.2.2 Types of distributions

Due to its simplicity, the so-called Gaussian or normal distribution is frequently used. A random variable $X$ is normally distributed, if its probability density function is:

$$f_X(x) = \frac{1}{\sqrt{2\pi\sigma_x}} \exp\left[-\frac{(x-\bar{X})^2}{2\sigma_X^2}\right]; -\infty < x < \infty \tag{3-10}$$

Here $\bar{X}$ is the mean value, and $\sigma_X$ is the standard deviation. The distribution function $F_X(x)$ is described by the normal integral $\Phi(.)$:

$$F_X(x) = \Phi\left(\frac{x-\bar{X}}{\sigma_X}\right) \tag{3-11}$$

in which

$$\Phi(z) = \frac{1}{\sqrt{2\pi}} \int_{-\infty}^{z} \exp\left(-\frac{u^2}{2}\right) du \tag{3-12}$$

This integral is not solvable in closed form, however tables and convenient numerical approximations exist. The use of the Gaussian distribution is frequently motivated by the central limit theorem which states that an additive superposition of independent random effects tends asymptotically to the Gaussian distribution.

*This document is the intellectual property of the fib – International Federation for Structural Concrete. All rights reserved.*
*This PDF of fib Bulletin 86 is intended for use and/or distribution solely within fib National Member Groups.*

For cases in which the random variable under consideration must be positive due to physical reasons (such as e.g. the yield strength of structural steel) the log-normal distribution provides a more appropriate stochastic model. A random variable $X$ is *log-normally distributed*, if its pdf is:

$$f_X(x) = \frac{1}{x\sqrt{2\pi s}} \exp\left[ -\frac{\left(\log \frac{x}{\mu}\right)^2}{2s^2} \right]; 0 \le x < \infty \tag{3-13}$$

and its distribution function is given by

$$F_X(x) = \Phi\left( \frac{\log \frac{x}{\mu}}{s} \right) \tag{3-14}$$

In these equations, the parameters $\mu$ and $s$ are related to the mean value and the standard deviation as follows:

$$\mu = \bar{X} \exp\left( -\frac{s^2}{2} \right); s = \sqrt{\ln\left( \frac{\sigma_X^2}{\bar{X}^2} + 1 \right)} \tag{3-15}$$

Two random variables with $\bar{X}$=1.0 and $\sigma_X$ = 0.5 having different distribution types are shown in Fig. 3-4. Normal and log-normal probability density functions. It is clearly seen that the log-normal density function is non-symmetric.

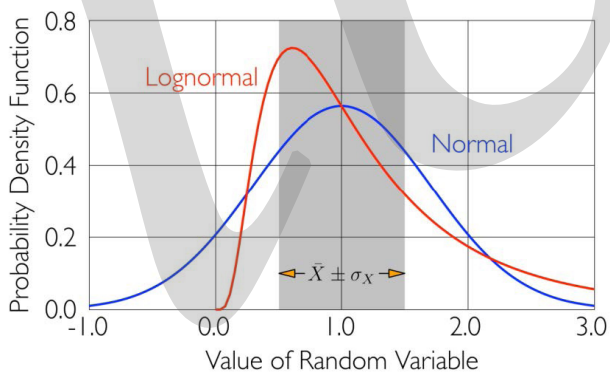


Fig. 3-4 Normal and log-normal probability density functions

Especially in the tail regions the difference becomes significant. The log-normal distribution does not allow any negative values, whereas the Gaussian distribution in this case allows negative values with a probability of 2.2%. In the upper tail, the probabilities of exceeding different values are shown in Table 3-1. The difference is quite dramatic which emphasizes the importance of the appropriate distribution model.

This document is the intellectual property of the fib – International Federation for Structural Concrete. All rights reserved.
This PDF of fib Bulletin 86 is intended for use and/or distribution solely within fib National Member Groups.

Table 3-1 Exceedance probabilities for different distribution models

| Level ξ | 1 | 2 | 3 | 4 | 5 |
|---|---|---|---|---|---|
| Normal | 0.5 | 0.023 | 3.17e-05 | 9.90e-10 | 6.28e-16 |
| Lognormal | 0.5 | 0.071 | 0.010 | 0.0017 | 0.00033 |

### 3.1.2.3 Random vectors

In many applications a large number of random variables occur together. It is conceptually helpful to assemble all these random variables $X_k$; $k = 1...n$ into a random vector $X$ (the symbol $T$ denotes transposition of vectors and matrices):

$$X = [X_1, X_2, ... X_n]^T \tag{3-16}$$

For this vector, expected values can be defined in terms of expected values for all of its components:

### 3.1.2.4 Mean value vector

$$\overline{X} = E[X] = [\overline{X}_1, \overline{X}_2, ... \overline{X}_n]^T \tag{3-17}$$

This is simply a vector containing all the mean values of the individual random variables $X_k$; $k = 1... n$.

### 3.1.2.5 Covariance matrix

This matrix assembles the expectations of all possible pair-wise cross-products of the individual random variables:

$$C_{XX} = \mathrm{E}[(X - \overline{X})(X - \overline{X})^T] \tag{3-18}$$

The dimensionless quantity

$$\rho_{ik} = \frac{\mathrm{E}[(X_i - \overline{X}_i)(X_k - \overline{X}_k)]}{\sigma_{x_i} \cdot \sigma_{x_k}} \tag{3-19}$$

as derived from the elements of the covariance matrix is called coefficient of correlation. Its value is bounded in the interval [-1,1]. Both the covariance matrix $C_{XX}$ and the matrix of correlation coefficients are symmetric and positive definite.

### 3.1.2.6 Joint probability density function models

The pdf of jointly normally (Gaussian) distributed random variables (components of a random vector $X$ is given by

$$f_x(x) = \frac{1}{(2\pi)^{\frac{n}{2}} \sqrt{\det C_{XX}}} \exp\left[ -\frac{1}{2} (x - \overline{X})^T C_{XX}^{-1} (x - \overline{X}) \right]; \quad x \in \mathbb{R}^n \tag{3-20}$$

If all random variables $X_i$ are mutually independent, then the joint probability density function is given by the product of the individual pdfs.

$$f_X(x) = \prod_{i=1}^{n} f_{X_i}(x_i) \tag{3-21}$$

*This document is the intellectual property of the fib – International Federation for Structural Concrete. All rights reserved.*
*This PDF of fib Bulletin 86 is intended for use and/or distribution solely within fib National Member Groups.*

This follows from the multiplication rule for independent events.

The so-called Nataf-model[48, 49] describes the joint probability density function of random variables $X_i$ based on their individual (marginal) distributions and the covariances. The concept is to transform the original variables $X_i$ to Gaussian variables $Y_i$ whose joint density is assumed to be Gaussian. This model can be realized in three steps:

First step: Map all random variables $X_i$ individually to normally distributed random variables $V_i$ with zero mean and unit standard deviation:

$$\left\{X_i; f_{X_i}(x_i)\right\} \leftrightarrow \left\{V_i; \varphi(v_i)\right\} \tag{3-22}$$

which is accomplished by means of the transformation

$$V_i = \Phi^{-1}\left[F_{X_i}(X_i)\right] \tag{3-23}$$

Second step: Assume a jointly normal distribution for all random variables $V_i$

$$\mathrm{E}[V_i] = 0; \;\; \mathrm{E}[V_i^2] = 1; \;\; \mathrm{E}[V_i V_j] = \rho_{V_i V_j} \neq \rho_{X_i X_j} \tag{3-24}$$

Note that at this point, the correlation coefficient $\rho_{V_i V_j}$ is not yet known. The joint pdf for the components of the random vector $V_i$ is then

$$f_V(v) = \frac{1}{(2\pi)^{\frac{n}{2}}\sqrt{\det R_{VV}}} \exp\left(-\frac{1}{2} v^T \cdot R_{VV}^{-1} \cdot v\right) \tag{3-25}$$

From this relation, it follows that

$$f_X(x) = f_V[v(x)] \prod_{i=1}^{n} \left|\frac{dx_i}{dv_i}\right| = f_v[v(x)] \prod_{i=1}^{n} \frac{\varphi[v_i(x_i)]}{f_{X_i}(x_i)} \tag{3-26}$$

Third step: Adjust the correlation coefficients $\rho_{V_i V_j}$ by solving

$$\sigma_{x_i} \cdot \sigma_{x_j} \cdot \rho_{X_i X_j} = \int_{-\infty}^{\infty} (x_i - \overline{X}_i)(x_j - \overline{X}_j) f_{X_i X_j}(x_i, x_j, \rho_{V_i V_j}) dx_i \cdot dx_j \tag{3-27}$$

This is usually achieved by iteration. A known problem of the Nataf-model is that this iteration may lead to a non-positive-definite matrix of correlation coefficients. In this case, this model is not applicable.

### 3.1.3 Structural reliability

#### 3.1.3.1 Definitions

Generally, failure (i.e. an undesired or unsafe state of the structure) is defined in terms of a limit state function $g(.)$, i.e. by the set $F = \{X : g(X) \leq 0\}$ . Frequently, $Z = g(X)$ is called safety margin. As indicated previously, the definition of the limit state function is not unique

This document is the intellectual property of the fib – International Federation for Structural Concrete. All rights reserved.
This PDF of fib Bulletin 86 is intended for use and/or distribution solely within fib National Member Groups.

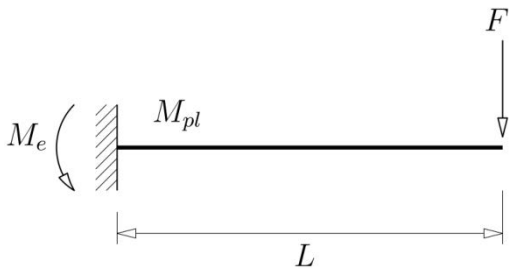


Fig. 3-5 Structural system and failure condition

$$F = \left\{ \left( F, L, M_{pl} \right) : F \cdot L \geq M_{pl} \right\} = \left\{ \left( F, L, M_{pl} \right) : 1 - \frac{F \cdot L}{M_{pl}} \leq 0 \right\}$$

The failure probability is defined as the probability of the occurrence of $F$:

$$\mathrm{P}(F) = \mathrm{P}\left[ \left\{ X : g(X) \leq 0 \right\} \right] \tag{3-28}$$

This quantity is *unique*, i.e. not depending on the particular choice of the limit state function. Assembling load and resistance variables into a random vector, the problem of determining structural reliability can be interpreted as an integration problem. Here the joint pdf of both $R$ and $S$ is integrated over the failure domain. This is shown in Fig. 3-6.

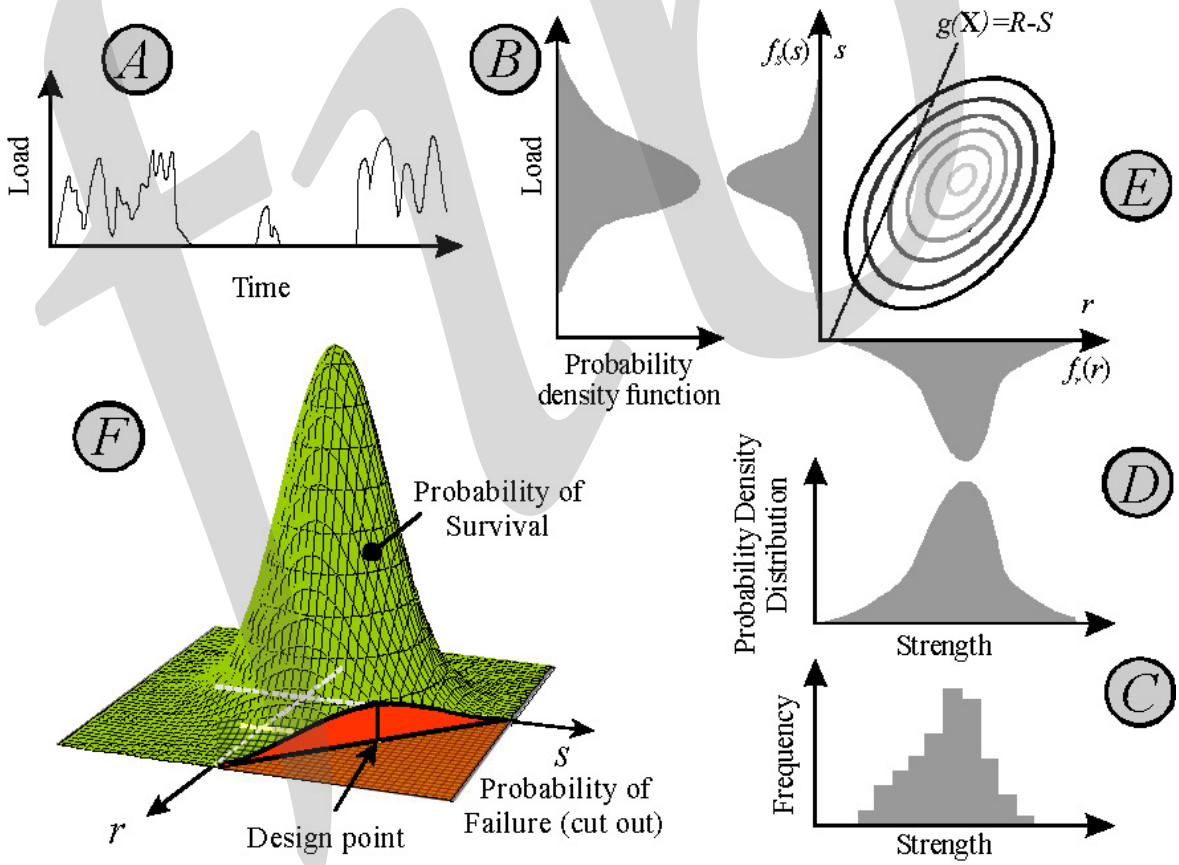


Fig. 3-6 Formulation of Reliability Problem in Structural Engineering

*This document is the intellectual property of the fib – International Federation for Structural Concrete. All rights reserved.*
*This PDF of fib Bulletin 86 is intended for use and/or distribution solely within fib National Member Groups.*

### 3.1.3.2 FOSM First order-second moment concept

The first order-second moment method aims at a representation of the limit state function $g(.)$ by a Taylor series and subsequent calculation of the statistical moments of the safety margin $Z$.

$$g(x) = g(x_0) + \sum_{i=1}^{n} \left.\frac{\partial g}{\partial x_i}\right|_{x=x_0} (x_i - x_{i0}) + \frac{1}{2}\sum_{i=1}^{n}\sum_{k=1}^{n} \left.\frac{\partial^2 g}{\partial x_i \partial x_k}\right|_{x=x_0} \left(x_i - x_{i0}\right)\left(x_k - x_{k0}\right) \tag{3-29}$$

Terminating the series after the quadratic terms yields

$$\mathrm{E}[Z] = \mathrm{E}[g(X)] = g(x)_0 + \sum_{i=1}^{n} \frac{\partial g}{\partial x_i} \mathrm{E}\left[x_i - x_{i0}\right] + \frac{1}{2}\sum_{i=1}^{n}\sum_{k=1}^{n} \frac{\partial^2 g}{\partial x_i \partial x_k} \mathrm{E}\left[\left(x_i - x_{i0}\right)\left(x_k - x_{k0}\right)\right] \tag{3-30}$$

Terminating the Taylor series after the linear terms yields:

$$\mathrm{E}[Z] = \mathrm{E}[g(X)] = g(x_0) + \sum_{i=1}^{n} \frac{\partial g}{\partial x_i} \mathrm{E}\left[x_i - x_{i0}\right] \tag{3-31}$$

If the mean value vector $\bar{X}$ is chosen as expansion point $x_0$ for the Taylor series, then $\mathrm{E}[Z] = g(x_0)$ and the variance becomes

$$\sigma_Z^2 = \mathrm{E}\left[\left(Z - \bar{Z}\right)^2\right] = \mathrm{E}\left[\left(\sum_{i=1}^{n} \frac{\partial g}{\partial X_i}\left(X_i - \bar{X}_i\right)\right)^2\right] = \sum_{i=1}^{n}\sum_{k=1}^{n} \frac{\partial g}{\partial x_i}\frac{\partial g}{\partial x_k} \mathrm{E}\left[\left(X_1 - \bar{X}_i\right)\left(X_k - \bar{X}_k\right)\right] \tag{3-32}$$

Finally the distribution function $F_Z(z)$ is approximated by a normal distribution:

$$F_Z(z) = \Phi\left(\frac{z - \bar{Z}}{\sigma_Z}\right) \tag{3-33}$$

Then we obtain the approximate result:

$$\mathrm{P}(F) = F_Z(0) = \Phi\left(-\frac{\bar{Z}}{\sigma_Z}\right) \tag{3-34}$$

Note that this result does not take into account the types of distributions of the basic variables. It also depends significantly on the choice of the expansion point for the Taylor-series.

### 3.1.3.3 FORM – First order reliability method

The FORM-Concept is based on a description of the reliability problem in standard Gaussian space. Hence transformations from correlated non-Gaussian variables $X$ to uncorrelated Gaussian variables $U$ with zero mean and unit variance are required. This step is called Rosenblatt-transformation. Then a linearization in performed in $u$-space. The expansion point $u^*$ is chosen such as to maximize the pdf within the failure domain. Geometrically, this coincides with the point in the failure domain having the minimum distance $\beta$ from the origin. From a safety engineering point of view, the point $x^*$ corresponding to $u^*$ is called design point. This concept is especially useful in conjunction with the Nataf-model for the joint pdf of $X$. Details can be found in various text books, e.g. in[47].

This document is the intellectual property of the fib – International Federation for Structural Concrete. All rights reserved.
This PDF of fib Bulletin 86 is intended for use and/or distribution solely within fib National Member Groups.

From the geometrical interpretation of the expansion point $u^*$ in standard Gaussian space it becomes quite clear that the calculation of the design point can be reduced to an optimization problem:

$$u^* : u^T \cdot u \rightarrow \text{Min.}; \quad \text{subject to: } g\left[x\left(u\right)\right] = 0 \tag{3-35}$$

Applying standard methods for constrained optimization this leads to the Lagrange-function

$$L = u^T \cdot u + \lambda \cdot g(u) \rightarrow \text{Min} \tag{3-36}$$

In principle, any optimization procedure can be utilized to solve for the location of $u^*$. However, in practical application there may be convergence problems either due to numerical difficulties in computing the partial derivative or due to the existence of multiple local minima. Especially the latter may lead to substantial errors in the computed reliability. In the next step, the exact limit state function $g(u)$ is replaced by a linear approximation $\bar{g}(u)$ as shown in Fig. 3-7.

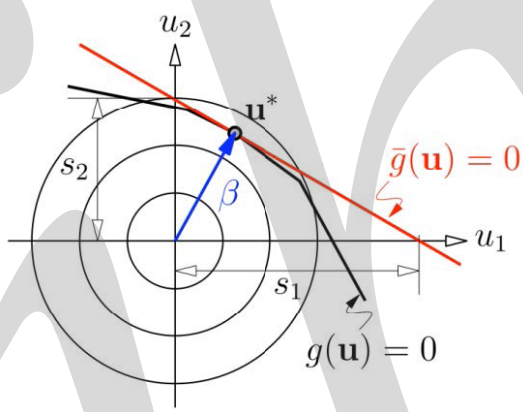


Fig. 3-7 Linearization required for first order reliability method

Geometrically, it is easily seen that $\bar{g}(u)$ is determined from

$$\bar{g} : -\sum_{i=1}^{n} \frac{u_i}{s_i} + 1 = 0; \quad \sum_{i=1}^{n} \frac{1}{s_i^2} = \frac{1}{\beta^2} \tag{3-37}$$

The safety margin $Z = \sum_{i=1}^{n} \frac{U_i}{s_i} + 1$ is normally distributed with the following statistical moments:

$$\mathrm{E}[Z] = 1; \quad \sigma_z^2 = \sum_{i=1}^{n}\sum_{k=1}^{n} \frac{\mathrm{E}\left[U_i \cdot U_k\right]}{s_i \cdot s_k} = \sum_{i=1}^{n} \frac{\mathrm{E}\left[U_i^2\right]}{s_i^2} = \sum_{i=1}^{n} \frac{1}{s_i^2} = \frac{1}{\beta^2} \tag{3-38}$$

$$\rightarrow \sigma_Z = \frac{1}{\beta} \tag{3-39}$$

From this, the probability of failure is easily determined to be

$$\mathrm{P}(F) = \Phi\left(-\frac{1}{\frac{1}{\beta}}\right) = \Phi(-\beta) \tag{3-40}$$

This document is the intellectual property of the fib – International Federation for Structural Concrete. All rights reserved.
This PDF of fib Bulletin 86 is intended for use and/or distribution solely within fib National Member Groups.

This result is exact, if $g(u)$ is actually linear.

Table 3-2 Conversion of Probability of Failure to Safety Index

| Probability of Failure | $10^{-12}$ | $10^{-11}$ | $10^{-10}$ | $10^{-9}$ | $10^{-8}$ | $10^{-7}$ | $10^{-6}$ | $10^{-5}$ | $10^{-4}$ | $10^{-3}$ | $10^{-2}$ | $10^{-1}$ | 0,5 |
|---|---|---|---|---|---|---|---|---|---|---|---|---|---|
| Safety Index | 7.03 | 6.71 | 6.36 | 5.99 | 5.61 | 5.19 | 4.75 | 4.26 | 3.72 | 3.09 | 2.33 | 1.28 | 0.0 |

The explained safety concept can be found in many regulations, such as Eurocode, DIN 1055-100, GruSiBau, JCSS Modelcode, ISO/CD 13822 and so on. Especially the specification of target values of safety indices proves that (Table 3-3). These values are then the basis for the estimation of safety factors, which are introduced for practical reasons.

Table 3-3 Required Values for Safety Index according to the JCSS Modelcode[50].

| Costs of Safety Measure | Consequence of Failure | | |
|---|---|---|---|
| | Low | Medium | High |
| Low Costs | 3.1 | 3.3 | 3.7 |
| Medium Costs | 3.7 | 4.2 | 4.4 |
| High Costs | 4.2 | 4.4 | 4.7 |

### 3.1.3.4 Monte-Carlo-simulation

Generally the failure probability is defined as the probability that the limit state function attains non-positive values:

$$\mathrm{P}(F) = \mathrm{P}\left[g\left(X_1, X_2, \ldots X_n\right) \le 0\right] \tag{3-41}$$

This can be written as an expected value:

$$\mathrm{P}(F) = \int_{-\infty}^{\infty}\int_{-\infty}^{\infty}\ldots\int_{-\infty}^{\infty} I_g(x) f_{X_1\ldots X_n}\, dx_1 \ldots dx_n \tag{3-42}$$

in which $I_g(x_1 \ldots x_n) = 1$ if $g(x_1 \ldots x_n) \le 0$ and $I_g(.) = 0$ else. In order to determine $P(F)$ in principle all available statistical methods for estimation of expected values are applicable. If $m$ independent samples $x^{(k)}$of the random vector $X$ are available then the estimator

$$\overline{\mathrm{P}}(F) = \sum_{k=1}^{m} I_g(x^{(k)}) \tag{3-43}$$

yields a consistent and unbiased estimate for $p_f$.

Problem: For small values of $P(F)$ and small values of $m$ the confidence of the estimate is very low. The variance $\sigma^2_{\overline{P}(F)}$ of the estimate $\overline{P}(F)$ can be determined from

$$\sigma^2_{\overline{\mathrm{P}}(F)} = \frac{\mathrm{P}(F)}{m} - \frac{\mathrm{P}(F)^2}{m} \approx \frac{\mathrm{P}(F)}{m} \tag{3-44}$$

$$\sigma_{\overline{\mathrm{P}}(F)} = \sqrt{\frac{\mathrm{P}(F)}{m}} \tag{3-45}$$

Note: The required number $m$ of simulations is independent of the dimension $n$ of the problem!

*This document is the intellectual property of the fib – International Federation for Structural Concrete. All rights reserved.*
*This PDF of fib Bulletin 86 is intended for use and/or distribution solely within fib National Member Groups.*

### 3.1.3.5 Importance sampling (weighted simulation)

In order to reduce the standard deviation $\sigma_{\overline{P}(F)}$ of the estimator to the order of magnitude of the probability of failure itself $m$ must be in the range of m = $\frac{1}{p_f}$. For values of $p_f$ in the range of $10^{-6}$ this cannot be achieved if each evaluation of the limit state function requires a complex structural analysis. Alternatively, strategies are employed which increase the "hit-rate" by artificially producing more samples in the failure domain than should occur according to the distribution functions. One way to approach this solution is the introduction of a positive weighting function $h_Y(x)$ which can be interpreted as density function of a random vector $Y$. Samples are taken according to $h_Y(x)$.The probability of failure is then estimated from

$$\overline{\mathrm{P}}(F) = \frac{1}{m}\sum_{k=1}^{m}\frac{f_X(x)}{h_Y(x)}I_g(x) = \mathrm{E}\left[\frac{f_X(x)}{h_Y(x)}I_g(x)\right] \tag{3-46}$$

From the estimation procedure as outlined it is seen that the variance of the estimator $\overline{P}(F)$ becomes

$$\sigma^2_{\overline{\mathrm{P}}(F)} = \frac{1}{m}\mathrm{E}\left[\frac{f_X(x)^2}{h_Y(x)^2}I_g(x)\right] \tag{3-47}$$

A useful choice of $h_Y(x)$. can be based on minimizing $\sigma_{\overline{P}(F)}$. An ideal weighting function should reduce the sampling error to zero. However, this cannot be achieved in reality, since such a function should have the property:

$$h_Y \cdot v(x) = \begin{cases} \frac{1}{\mathrm{P}(F)}f_X(x) & g(x) \le 0 \\ 0 & g(x) > 0 \end{cases} \tag{3-48}$$

This property requires the knowledge of $P(F)$ which, of course, is unknown. Special updating procedures such as adaptive sampling 51 can help to alleviate this problem.

### 3.1.3.6 Importance sampling at the design point

Based on the previous FORM analysis it may be attempted to obtain a general importance sampling concept. This can be accomplished in two steps:

1. Determine the design point x* as shown in the context of the FORM-procedure.
2. Choose a weighting function (sampling density) $h_Y(x)$ with the statistical moments $E[X] = x^*$ and $C_{YY} = C_{XX}$ in the following form (multi-dimensional Gaussian distribution)

$$h_Y(x) = \frac{1}{(2\pi)^{\frac{n}{2}}\sqrt{\det C_{XX}}}\exp\left[-\frac{1}{2}(x-x^*)^T C_{XX}^{-1}(x-x^*)\right] \tag{3-49}$$

3. Perform random sampling and statistical estimation according to 3-1.

This document is the intellectual property of the fib – International Federation for Structural Concrete. All rights reserved.
This PDF of fib Bulletin 86 is intended for use and/or distribution solely within fib National Member Groups.

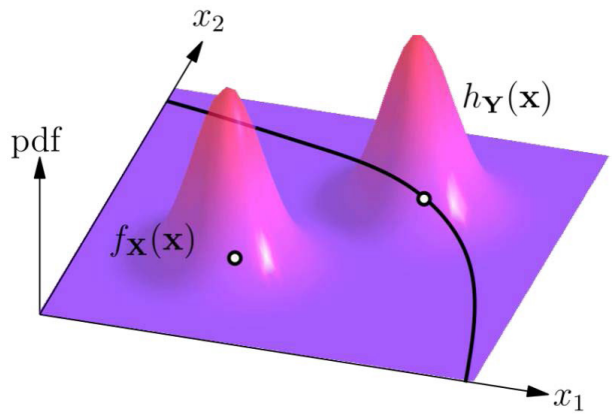


Fig. 3-8 Original and importance sampling probability density functions

The efficiency of this concept depends on the geometrical shape of the limit state function. In particular, limit state functions with high curvatures or almost circular shapes cannot be covered very well. It is also interesting to note that the concept of importance sampling can very well be extended for application in the context of dynamic problems[47].

### 3.1.3.7 Response surface method: General remarks

In many practical situations it is virtually impossible to calculate the value of the safety margin (limit state function) repeatedly so many times as required for Monte-Carlo-Simulation procedures. Here suitable approximations for the limit state function can be very useful, particularly if these approximations are based on relatively simple functions. In the context of structural reliability analysis such approximate limit state functions are called Response Surfaces.

This means that the limit state function $g(X)$ is approximated by a simpler function $\overline{g}(X)$. Note that e.g. this concept of representing complicated mechanical behaviour in terms of simple interpolating functions is the well-established basis of the Finite Element Method. A comprehensive review is given by[52].

### 3.1.3.8 Interpolation scheme for reliability analysis

Such an approximation can be based on interpolating functions taken from a class of polynomials, e.g. of second order:

$$\overline{g}(X) = a + \sum_{k=1}^{n} b_k \cdot X_k + \sum_{k=1}^{n}\sum_{l=1}^{n} c_{kl} \cdot X_K \cdot X_l \tag{3-50}$$

Here $n$ is the dimension of the random vector X. The coefficients $a$, $b_k$, and $c_{kl}$ have to be determined from $N = \frac{n(n+1)}{2} + 1$ points on the actual limit state function $g(X) = 0$. For $n = 2 (N = 5)$ this is shown in the following sketch:

This document is the intellectual property of the fib – International Federation for Structural Concrete. All rights reserved.
This PDF of fib Bulletin 86 is intended for use and/or distribution solely within fib National Member Groups.

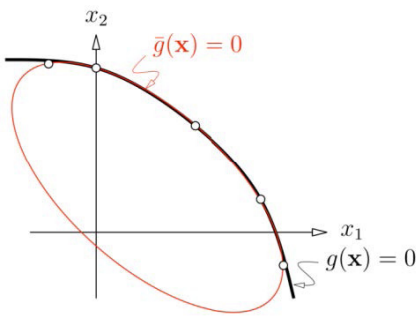


Fig. 3-9 True limit state function and response surface approximation

## 3.1.4 Application example: Collapse of a plane frame

### 3.1.4.1 Description of problem

Consider a plane frame with a uniform cross section whose plastic moment is given by $M_{pl}$. The frame carries a horizontal load $H$ and a vertical load $V$. Both loads are assumed to be Gaussian variables with mean values

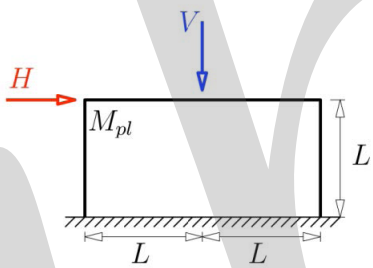


Fig. 3-10 Frame structure and loading conditions

Based on first-order plastic hinge theory there are several possible collapse mechanisms which are defined in terms of a kinematic chain. The relevant modes are shown in Fig. 3-11.

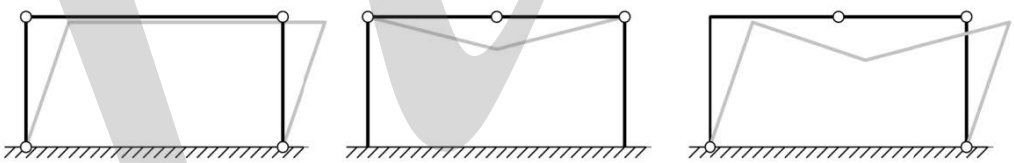

Fig. 3-11 Failure mechanisms of frame structure

These three failure mechanisms are mathematically defined by:

$$g_1(X) = 4\frac{M_{pl}}{L} - H;$$
$$g_2(X) = 4\frac{M_{pl}}{L} - V; \qquad (3\text{-}51)$$
$$g_3(X) = 6\frac{M_{pl}}{L} - H - V;$$
$$\mathrm{X} = \left[H, V\right]^T$$

This document is the intellectual property of the fib – International Federation for Structural Concrete. All rights reserved.
This PDF of fib Bulletin 86 is intended for use and/or distribution solely within fib National Member Groups.

Failure will occur whenever at least one of these functions yields a negative value. The limit state function is shown in Fig. 3-12 below.

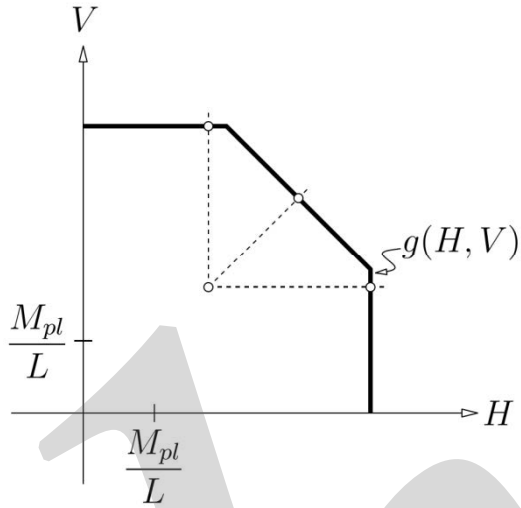


Fig. 3-12 Limit state function for frame structure

For convenience, the limit state functions describing the failure mechanisms are rewritten in terms of standardized variables which are given as

$$u_1 = \frac{H \cdot L - 1.7M_{pl}}{0.5M_{pl}}; \quad u_2 = \frac{V \cdot L - 1.7M_{pl}}{0.5M_{pl}}; \tag{3-52}$$

### 3.1.4.2 FORM Analysis

Applying the FORM-methodology yields three possible design points, which are related to the three relevant failure modes. In standardized space, these points are located at (4.6, 0), (0, 4.6) and (2.6, 2.6) with safety indices of 4.6, 4.6, and 3.677, respectively. The corresponding failure probabilities are $2.1 \cdot 10^{-6}$, $2.1 \cdot 10^{-6}$, and $1.2 \cdot 10^{-4}$. It can be seen that picking the correct design point is absolutely essential for obtaining a reasonable estimate of the failure probability.

### 3.1.4.3 Monte Carlo simulation

Applying Monte Carlo simulation with a sample size of 100.000 yields an estimated probability of failure of about $1.0 \cdot 10^{-4}$. The samples from one such run are shown in Fig. 3-13 below. All samples in blue represent safer states whereas all samples in red represent failure states. It can be seen that only a very small number of samples actually lies in the failure domain thus yielding rather uncertain estimates of the failure probability. Also, note that only one failure mode occurs in these samples (the combined mode).

*This document is the intellectual property of the fib – International Federation for Structural Concrete. All rights reserved.*
*This PDF of fib Bulletin 86 is intended for use and/or distribution solely within fib National Member Groups.*

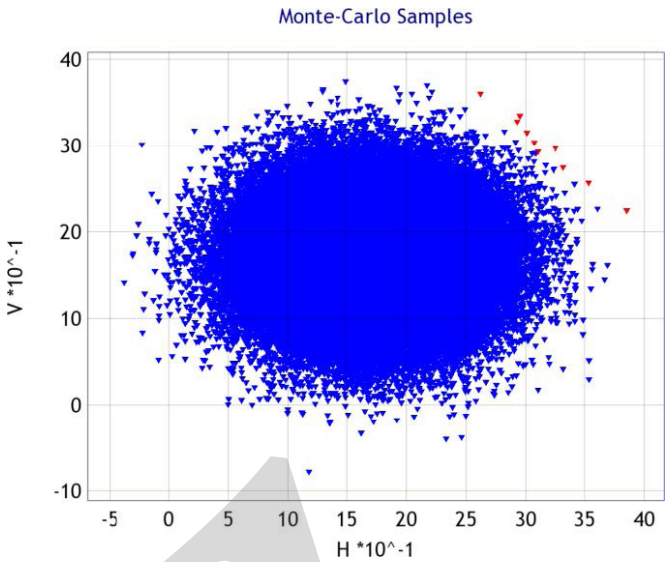


Fig. 3-13 Plain Monte Carlo sampling (100.000 samples)

By shifting the centre of the sampling density to the design point with the smallest reliability index it is possible to obtain good estimates for the failure probability with a significantly smaller sample size. Fig. 3-14 below shows 1000 samples using the design pint of the combined failure mode as centre. The failure probability as estimated from these samples is $1.2 \cdot 10^{-4}$.

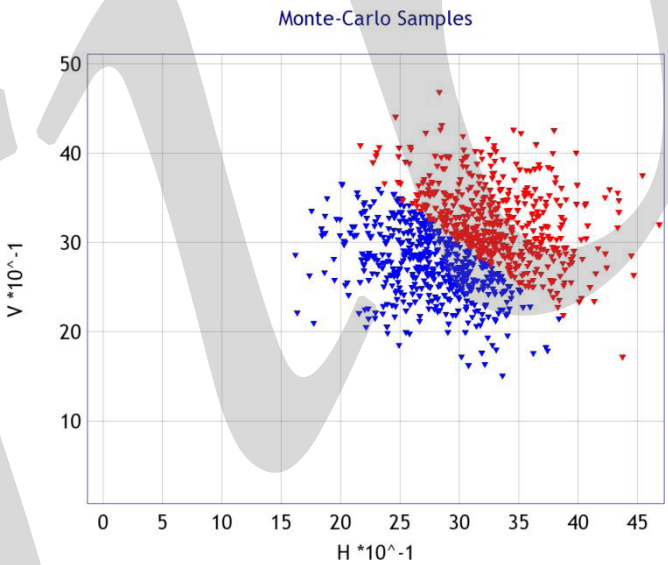


Fig. 3-14 Importance sampling (1000 samples)

### 3.1.4.5 Response surface analysis

Here the search for failure points is starting from mean values which results in the support points as indicated in Fig. 3-15 below.

This document is the intellectual property of the fib – International Federation for Structural Concrete. All rights reserved.
This PDF of fib Bulletin 86 is intended for use and/or distribution solely within fib National Member Groups.

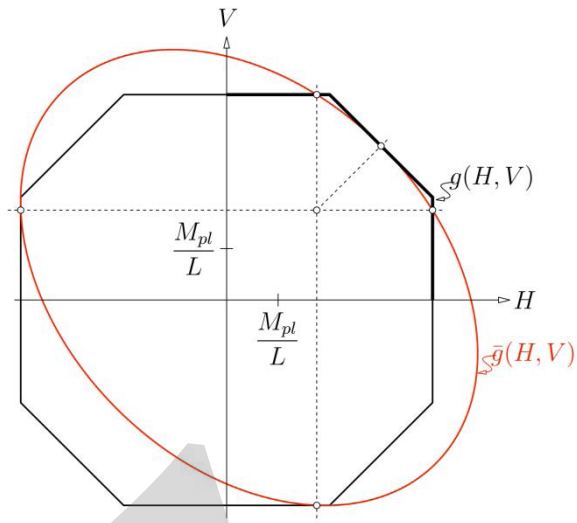


Fig. 3-15 Response surface for frame structure

The response surface in the space of standardized variables $u_1, u_2$ is described by the second order polynomial

$$\bar{g}(H,V) = 1 - 0.1297u_1 - 0.1297u_2 - 0.01907u_1^2; \quad -0.0102u_1 \cdot u_2 - 0.01907u_2^2 \qquad (3\text{-}53)$$

The resulting probability of failure using 100000 Monte Carlo samples is

$$\mathrm{P}(F) = 1.42 \cdot 10^{-4} \qquad (3\text{-}54)$$

which is slightly larger than the exact value.

## 3.2 Reliability methods in engineering practice

### 3.2.1 Stages of the safety concept

In the following, engineering methods, practical aspects, and normative guidelines will be briefly described. The safety and reliability of a structure is subject to the following influence values:

- Distribution of influences and loads
- Distribution of capabilities
- Design errors
- Errors in the implementation
- Errors of use

Human error (can only be estimated by means of a safety concept) . It needs to be taken into consideration that, with regard to all safety models, it is possible to map only those influences which can be identified on the basis of historical data or forecast models. An important part remains inaccessible to us, and is to be accepted with a certain “epistemic humility”[53].

This document is the intellectual property of the fib – International Federation for Structural Concrete. All rights reserved.
This PDF of fib Bulletin 86 is intended for use and/or distribution solely within fib National Member Groups.

### 3.2.2 Failure probability and reliability index

The probabilistic method for assessing reliability is based on the following inequality:

$$E \leq R \tag{3-55}$$

where

$E$ loads and actions / influences

$R$ resistances

In practical applications, this approach is transferred into a reliability method based on partial safety factors, which serve as multipliers for scaling the par values of influences and properties of building materials.

The load $E$ and the resistance $R$ can be set down with stochastically independent normal distributions, as characterized by ($\mu_E$; $\sigma_E$) or ($\mu_R$; $\sigma_R$) respectively, as shown in Fig. 3-16:

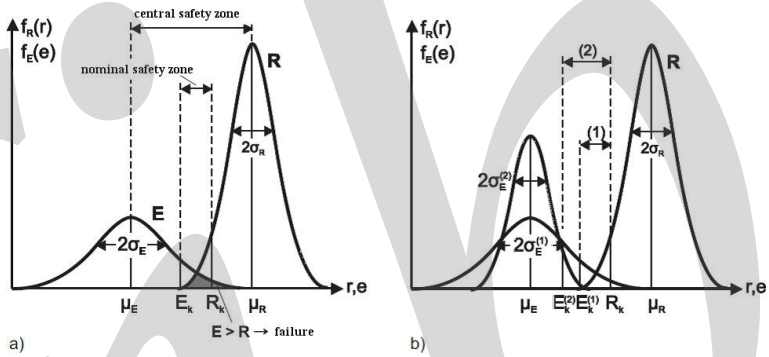


Fig. 3-16 Density distribution function of load $E$ and resistance $R$. a) Definition of the safety zones. b) Impacts of changes within the scattering on the probability of failure

The two density functions have areas of overlap with $r < e$ (the loads/actions are greater than the resistances), where the load bearing capacity no longer exists. As it is practically impossible to avoid such overlaps, absolute safety cannot be ensured.

The distribution $f_R(r)$ in Fig. 3-16 can be moved to the right by increasing the resistance. Therefore, the area of overlap $r < e$ and consequently, the probability of failure $p_f$ decreases. The central question in the course of reliability based concepts of analysis is to choose a suitable or at least acceptable distance between the density distribution functions. The scattering of the density distribution functions can be characterized by the following definitions of the safety zones:

- Central safety zone = distance between the median values $\mu_R$ and $\mu_E$,
- Nominal and/or decentralized safety zone = distance between the characteristic values $E_k$ and $R_k$.

Fig. 3-16 also illustrates that for significantly smaller uncertainties on the action side, i.e. $\sigma_{E\,(2)} < \sigma_{E\,(1)}$, and for the same resistance $R$, the probability of failure decreases as well (see Fig. 3-16b). The limit state function

$$G = R - E = 0 \tag{3-56}$$

*This document is the intellectual property of the fib – International Federation for Structural Concrete. All rights reserved.*
*This PDF of fib Bulletin 86 is intended for use and/or distribution solely within fib National Member Groups.*

makes it possible to distinguish between the failure area $G < 0$ and the survival area $G \geq 0$. For independent normal distribution of E and R, a normally distributed density distribution function G with the following median value arises:

$$\mu_G = \mu_R - \mu_E \tag{3-57}$$

with the following standard deviation

$$\sigma_G = \sqrt{\sigma_R^2 + \sigma_E^2} \tag{3-58}$$

The inverse variation coefficient of the density distribution function $G$ results into the reliability index

$$\beta = \frac{\mu_G}{\sigma_G} = \frac{\mu_R - \mu_E}{\sqrt{\sigma_R^2 + \sigma_E^2}} \tag{3-59}$$

Accordingly, the multiplication of the standard deviation $\sigma_G$ with the reliability index $\beta$ results in the distance of the median value $\mu_G$ of the density distribution function from the point of failure $g = 0$. The operative probability of failure $p_f$ (f for failure) corresponds with the area underneath the density function for $G \leq 0$ and is mathematically defined as follows:

$$p_f = p_{(G<0)} = F_G(g=0) = \int_{-\infty}^{0} f_G(g)dg = \Phi\left(\frac{\mu_G}{\sigma_G}\right) = \Phi(-\beta) \tag{3-60}$$

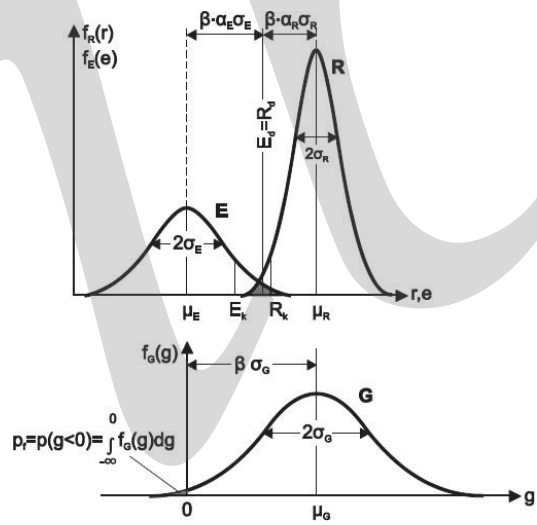


Fig. 3-17 Correlation between the probability of failure $p_f$ and the safety index $\beta$ of the normally distributed state function $G = R - E$

As illustrated by Fig. 3-17 the probability of failure pf and the safety index $\beta$ are directly correlated for standard normal distributions. Table 3-4 represents for selected failure probabilities pf their corresponding reliability indices, applied to a one year period and a fifty year period respectively. The failure probabilities $P_f$ for the 50 year period can be calculated as follows:

$$P_f = \sum_{i=1}^{n} p_{fi} \text{ with } n = 50 \tag{3-61}$$

This document is the intellectual property of the fib – International Federation for Structural Concrete. All rights reserved.
This PDF of fib Bulletin 86 is intended for use and/or distribution solely within fib National Member Groups.

Reliability in a mathematical sense represents the complement to the probability of failure: the probability of survival $p_r = 1 - p_f$. Assuming a normal distribution the respective ß index can be calculated as shown in Table 3-4.

Table 3-4 The operative probability of failure $p_f$ and the corresponding reliability indices $\beta$ $p_f$ *bzw.* $P_f = p_f / P_f$ respectively

| $P_f / p_f$ | $10^{-1}$ | $10^{-2}$ | $10^{-3}$ | $10^{-4}$ | $10^{-5}$ | $10^{-6}$ | $10^{-7}$ |
|---|---|---|---|---|---|---|---|
| $\beta$(1 year) | 1.28 | 2.32 | 3.09 | 3.72 | 4.27 | 4.75 | 5.20 |
| $\beta$(50 years) | - | 0.21 | 1.67 | 2.55 | 3.21 | 3.83 | 4.41 |

### 3.2.3 Partial safety factors for engineering practice

The measuring procedures in engineering are performed on the basis of the quantile values of loads and resistances, where the quantile values from the statistical moments can be determined using quantile factors $K_{p,E}$ and $K_{p,R}$ (<0!) as follows:

$$E_k = \mu_E + K_{p,E} \cdot \sigma_E \tag{3-62}$$

$$R_k = \mu_R + K_{p,R} \cdot \sigma_R \tag{3-63}$$

Note that this is a nonlinear relationship of $\sigma_G$ with the standard deviations $\sigma_E$ and $\sigma_R$. The definition of the weighting factors $\alpha_E$ and $\alpha_R$ facilitates the following indirect linearization:

$$\sigma_G = \sqrt{\sigma_R^2 + \sigma_E^2} = \alpha_R \cdot \sigma_R + \alpha_E \cdot \sigma_E \tag{3-64}$$

where

$$\alpha_E = \frac{\sigma_E}{\sqrt{\sigma_R^2 + \sigma_E^2}} \tag{3-65}$$

and

$$\alpha_R = \frac{\sigma_R}{\sqrt{\sigma_R^2 + \sigma_E^2}} \tag{3-66}$$

From Eq. (6-58), it follows that

$$\alpha_E^2 + \alpha_R^2 = 1 \tag{3-67}$$

Using the weighting factors on Equations (6-59) and (6-60), we can calculate as follows:

$$\mu_R - \mu_E = \beta\sqrt{\sigma_R^2 + \sigma_E^2} = \beta \cdot \alpha_R \cdot \sigma_R + \beta \cdot \alpha_E \cdot \sigma_E \tag{3-68}$$

Assigning parts of this equation to the load or the resistance side results in the general equation for verification of the limit state as follows:

$$\mu_R - \beta \cdot \alpha_R \cdot \sigma_R = R_d \tag{3-69}$$

$$\mu_E - \beta \cdot \alpha_E \cdot \sigma_E = E_d \tag{3-70}$$

The design values $R_d$ and $E_d$ are referred to as the coordinates of the rating point. The quotient of the design values and the characteristic values results in the following partial safety factors $\gamma_R$ and $\gamma_E$ respectively. Using these values, the level of reliability defined by $\beta$ is achieved on the basis of normally distributed values:

This document is the intellectual property of the fib – International Federation for Structural Concrete. All rights reserved.
This PDF of fib Bulletin 86 is intended for use and/or distribution solely within fib National Member Groups.

$$\gamma_E = \frac{E_d}{E_k} = \frac{\mu_E + \beta \cdot \alpha_E \cdot \sigma_E}{\mu_E + K_{p,E\sigma_E}} = \frac{1 + \beta \cdot \alpha_E \cdot V_E}{1 + K_{p,E\sigma_E}} \tag{3-71}$$

and, respectively,

$$\gamma_R = \frac{R_k}{R_d} = \frac{\mu_R + K_{p,R\sigma_R}}{\mu_R - \beta \cdot \alpha_R \cdot \sigma_R} = \frac{1 + K_{p,R} \cdot V_R}{1 - \beta \cdot \alpha_R \cdot V_R} \tag{3-72}$$

For lognormally distributed resistance values, the desired partial safety value $\gamma_R$ can be determined on the basis of Eq. (3-69)

$$\gamma_R = \frac{R_k}{R_d} = \exp\left(\alpha_R \cdot \beta \cdot V_R - k_R\right) \tag{3-73}$$

In practice, the design values $R_d$ and $E_d$ are determined by multiplying and/or dividing the characteristic values with their corresponding partial safety values.

$$E_d = E_k \cdot \gamma_E \tag{3-74}$$

and, respectively,

$$R_d = \frac{R_k}{\gamma_R} \tag{3-75}$$

Generally, $\gamma_R \geq 1$ and $\gamma_E \geq 1$ applies. A substantial advantage of this approach is the transparent attainability of sensitivity factors on the partial safety factors $\gamma_R$ and $\gamma_E$.

## 3.3 Reliability assessment of existing structures

### 3.3.1 General aspects

In the following section some reflections about the reliability assessment and the probabilistic modelling of existing structures are given. Faber[54] addressed the efforts in the last century, that went into the development of an efficient framework for design procedures and modern design codes[55,56, 57, 58] for buildings. The objectives were to include economic design, construction and operation in compliance with assumed required operating conditions, safety of people and safety of environment. For instance modern design codes such as[59] have been based on the principles of economical decision analysis and modern reliability methods.

In the past, design and construction of new buildings had been at the heart of historical civil engineering. The past centuries have seen an accelerated deterioration of an increasing number of key structures, many of them vital for society. Therefore society now justifies a significantly increased interest in the assessment of existing structures[54].

The Bayesian probabilistic framework turned out to be useful as the theoretical basis for such an assessment of existing structures[54]. Investigations along these lines were to a large degree driven by the requirements for the assessment of existing structures in offshore and bridge engineering.

Any comprehensive condition assessment of structures generally includes inspection, testing, monitoring and calculation. In addition, plans for strengthening measures,

This document is the intellectual property of the fib – International Federation for Structural Concrete. All rights reserved.
This PDF of fib Bulletin 86 is intended for use and/or distribution solely within fib National Member Groups.

maintenance and repair guidelines or even changes in the use of structures are an integral part of such an assessment.

What makes the assessment of existing structures so different from the design of new ones is the amount of accessible information. Probabilistic frameworks for the assessment of existing structures can therefore be seen as extensions of the probabilistic concept for the design of structures[54]. They make it possible to take into account new information; knowledge that was not available at the point in time when the structure was designed.

The JCSS[60] and ISO 9126 (1:1999) are two of the few policies that address these issues. In particular, the JCSS and ISO provide the philosophical basis and the theoretical framework for the assessment of structures and offer a suitable background for the development of codes.

In the following, a framework is outlined for the assessment of existing structures by means of Bayesian probability theory. First a general overview of the theory is given and then identification of key probabilistic models and applications required for different types of assessment problems will be provided. In addition the textbooks by[61] and[62] for further reading are recommended.

Uncertainties regarding geometry, material properties, loading and environmental conditions affect the knowledge about the actual condition ("as built") during the design and construction phase. Natural variations, for example in material properties or load characteristics, may lead to such uncertainties. Overall, however, they mainly result from insufficient information.

To illustrate this point, the uncertainties within for example the material properties from the design phase to the final structural performance, are significant since the manufacturer and the material batch characteristics may be unknown. The probabilistic models that are applied to the planning and assessment of a structure merely reflect the existing gap in the available information about the structure. This knowledge gap may (partially) be closed by updating the probabilistic model with information about the structure at the outset of and during operation[54].

Reassessment can be considered as a decision process. The objective is to find suitable measures for an economical and efficient fulfilment of the defined requirements[54]. A set of adequate measures may include inspection of the structure and collection of relevant information about the geometry, the material properties, the degree of deterioration, the static and dynamic behaviour and the loading conditions on the structure[54], followed by strengthening measures or change of allocation or "intended use".

Finally, any proposed measures need to be evaluated and compared to their alternatives, taking into account their consequences both on the safety and on the financial situation over the span of the planned service life[54].

### 3.3.2 Assessment decision process

The number of possible alternative measures that turn up in the course of structural assessment, as for example inspections, strengthening and maintenance activities, among others, can be overwhelming. Efficient tools for a systematic analysis of these alternatives and their consequences are therefore of fundamental importance. A suitable framework is

*This document is the intellectual property of the fib – International Federation for Structural Concrete. All rights reserved.*
*This PDF of fib Bulletin 86 is intended for use and/or distribution solely within fib National Member Groups.*

provided by the Bayesian decision analysis (see e.g.[63, 64, 65]), as it is allows the integration of even subjective and frequentest information into the analysis.

### 3.3.3 Decision tree

A helpful tool in any decision finding process is its visualization via decision/ event trees. Fig. 3-18 presents Faber's[54] version of a decision / event tree that is suitable to address the aforementioned requirements. Here, *d* refers to a decision rule, Θ refers to an uncertain state of nature and u is the utility associated with the decision and the uncertain state of nature.

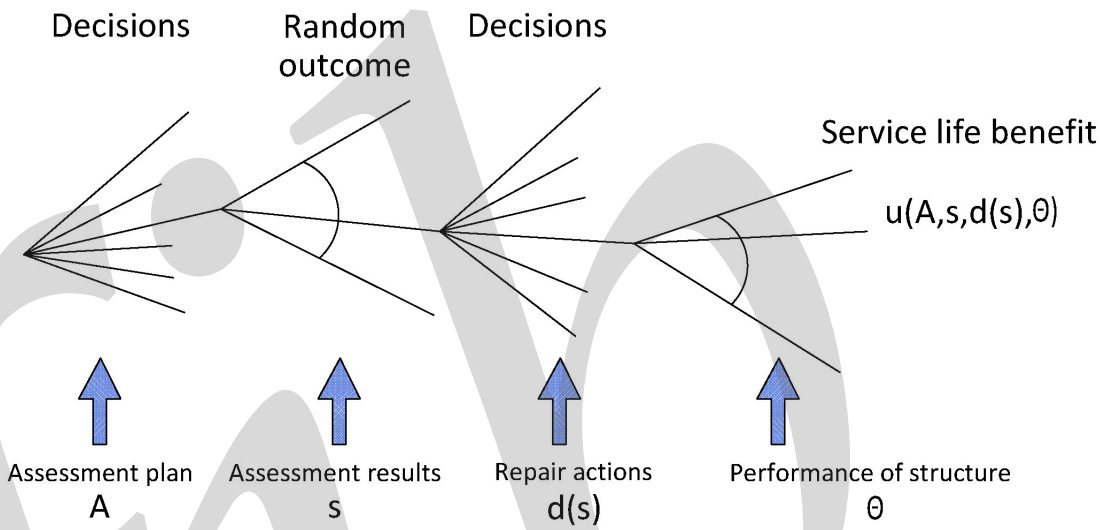


Fig. 3-18 Decision / event tree (adapted from[54])

The theoretical framework for decision analysis and associated applications in structural engineering are outlined in more detail in the literature[66,67,68,69,70].

Following[71], the assessment of existing structures is a sequential process. The model is designed, the consequences are evaluated, the resulting information and new findings are introduced into the re-design of the model, the structure is modified or the use of the structure is changed (see Fig. 3-19). Based on this aspects[54] has defined the most important issues as follows:

- Formulation of probabilistic models
- Formulation of limit state functions
- Evaluation of benefits/consequences
- Updating of probabilistic models
- Evaluation of probabilities
- Setting acceptable levels for the probability of failure

This document is the intellectual property of the fib – International Federation for Structural Concrete. All rights reserved.
This PDF of fib Bulletin 86 is intended for use and/or distribution solely within fib National Member Groups.

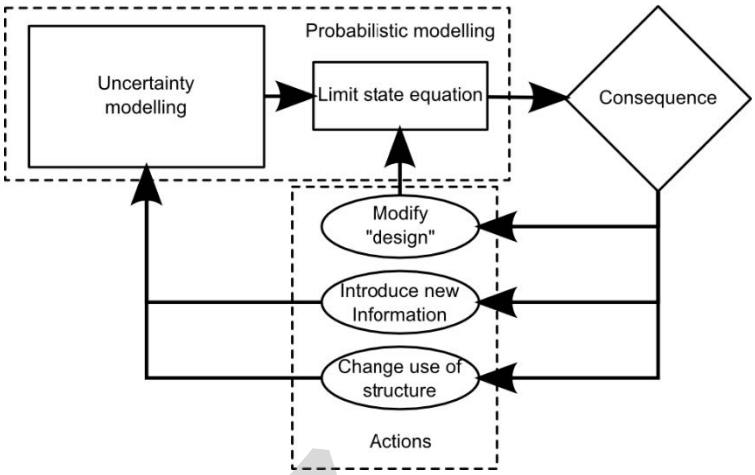


Fig. 3-19 Bayesian probabilistic assessment of structures (adapted from[72])

## 3.3.4 Probabilistic modelling

To capture different kinds of uncertainties, such as physical, statistical or, measurement uncertainties, model uncertainties or uncertainties related to the precision of new information, basic variables are used. Statistical analysis methods, as for example the methods of moments and the maximum likelihood method, enable estimating the distribution parameters for available test results or observations of an uncertain quantity, as soon as the family of probability distribution is known[73,74].

Physical arguments may also be used for some uncertainties in order to identify the suitable family of distribution functions, the choice of which is, to some degree, flexible.

In the framework of the Bayesian analysis, one or more of the parameters $q$ of the distribution function $F_X(x,q)$ may be considered as uncertain variables for any probabilistic modelling of the basic variable $X$. Then, any most frequently occurring or subjective information available about $X$ may be integrated via so-called prior probabilistic modelling of $q$, e.g. $f'_Q(q)$. The problem determines whether an uncertain parameter is modelled by a random variable, a random process or a random field[54].

Numerous random processes and/or fields can be represented as an assessment problem in terms of their extreme characteristics, enabling their capture as random variables. Both the probabilistic modelling and the verification of the applicability must be performed very carefully and with attention to detail in this approach.

Numerous examples for uncertainties in probabilistic modelling can be found in the literature[75, 76, 61, 77, 78]. The two JCSS documents[79, 80] provide numerous recommendations for the probabilistic modelling of resistance and load variables, respectively.

## 3.3.5 Limit state functions for assessment

Limit state functions are generally well suited to describe events relevant for decision finding processes, whether adverse or favourable. Examples for adverse events include structural failure, excessive degradation or similar conditions. Favourable events include positive proof load test results, inspection results that rule out degradation or similar findings[54]. Even the fact that an existing structure has not failed previously can be seen as a favourable event. The formulation of appropriate limit state functions for such events is outlined below.

*This document is the intellectual property of the fib – International Federation for Structural Concrete. All rights reserved.*
*This PDF of fib Bulletin 86 is intended for use and/or distribution solely within fib National Member Groups.*

The limit state functions applied to the structural assessment are commonly based on a physical understanding of the problem. Due to various simplifications and approximations, empirical elements are to some extent also included. These empirical elements are taken into account by the so-called model uncertainty. This model uncertainty needs to be taken into account in what is commonly called uncertainty modelling (see e. g.[81]).For clarity, we distinguish between events representing adverse states of the structure on the one hand and new information about the performance of the structure or the loading situation on the other hand.

Adverse events F may be defined as according to[54]:

$$F = \left\{ x \mid g(x) \leq 0 \right\} \tag{3-76}$$

Events defining new information about the structure, such as inspection and test results, are expressed as

$$I = \left\{ x \mid h(x) * 0 \right\} \tag{3-77}$$

where * stands for either ≤, >or =, depending on the type of information

### 3.3.6 Evaluation of benefits and consequences

According to[82], those decisions can be considered as optimal which maximize the expected value of the utility function, a function that describes the decision-maker's preferences in terms of the consequences. The consequences are generally expressed in monetary terms.There are, for example, numerous situations where the marginal utilities are associated with the events of failure, repair and inspection. The expected utility, in monetary terms $E$[CT(tinst)] for one particular decision can be expressed as

$$E[CT(tinst)] = PICI + PfCf + PRCR = E[CI] + E[Cf] + E[CR] \tag{3-78}$$

E[CI] being the expected cost of inspection, E[Cf] the expected cost of failure and E[CR] the expected cost of repair, all of them represented by their mean values according to decision theory.

### 3.3.7 Updating of probabilities

Information that may be exploited for a successful assessment of existing structures includes according to[54]:

- Survival of the structure.
- Material characteristics from different sources.
- Geometry.
- Observations of damage and deterioration.
- Proof load test results.
- Static and dynamic response to controlled loading.

Reliability updating technique can help to integrate such new information into the prior probabilistic models, resulting in so-called posterior probabilistic models which may be used as an enhanced basis for the reassessment engineering decision

This document is the intellectual property of the fib – International Federation for Structural Concrete. All rights reserved.
This PDF of fib Bulletin 86 is intended for use and/or distribution solely within fib National Member Groups.

analysis. Two types of quantitative information are relevant for use in reliability updating techniques:

- information of the equality type,
- information of the inequality type

Examples for information of the equality type are measuring results for a basic strength, load or response variable. In a probabilistic evaluation procedure, measurement errors should be modelled as random variables, with their mean values (which is zero for unbiased estimates), their standard deviations and, wherever necessary, their correlation patterns[54]. The standard deviation is a property of the measurement technique, but it may also depend on the circumstances. The degree of correlation between observations at different places and different points in time is a crucial and very complex modelling element.

When dealing with information of the inequality type, knowledge about the observed variable is limited to a certain threshold value. For example, a crack in the structure may be present, but less than the observation threshold, or a limit state of collapse either may be reached or not. Uncertainty in the threshold value should be taken into account. The distribution function for the minimum threshold level is often referred to as the probability of detection curve (POD curve). Also here, correlations for the probability of detection in various observations should be known. The POD plays an essential role in the quantification of information gained by testing existing structures. In many cases, the POD curve is modelled as follows[54]:

$$F(a) = \Delta\left[1 - \exp\left(-\frac{a - a_0}{\lambda}\right)\right] \tag{3-79}$$

where a is the threshold and * is a number smaller than 1, which represents the probability that detection does not take place, regardless of what the threshold value may be. The constants $a_0$ and j are characteristic for the applied inspection method. Examples for the modelling of POD curves for different types of inspection methods were described in detail in the literature[83,84,85].

### 3.3.8 Updating of random variables

Results of structural inspections or testing that bear a direct relation to random variables can enter the updating process. Initially, and prior to any update, the distribution parameters are modelled. Now, by applying the Bayes theorem (see e.g.[73,86,87]), the prior distribution functions, which are assessed by any combination of frequentist and subjective information, are updated and thereby transformed into posterior distribution functions.

If we assume that a random variable $X$ has the probability distribution function $F_X(x)$ and density function $f_X(x)$ and that one or more of the distribution parameters, (e.g. the mean value and standard deviation of $X$ are uncertain when the probability density function is $f_Q(q)$, then the probability distribution function for $Q$ may be updated on the basis of observations of $X$, i.e. $x_L$. The general updating scheme is

$$f_Q''(q \mid \hat{x}) = \frac{f_Q'(q) \cdot L(q \mid \hat{x})}{\int_{-\infty}^{\infty} f_Q'(q) \cdot L(q \mid \hat{x})\, dq} \tag{3-80}$$

This document is the intellectual property of the fib – International Federation for Structural Concrete. All rights reserved.
This PDF of fib Bulletin 86 is intended for use and/or distribution solely within fib National Member Groups.

where $f_Q(q)$ is the distribution function for the uncertain parameters $Q$ and $L(q \mid x_L)$ is the probability of the observations in $x_L$. '' denotes the posterior and ' the prior probability density functions of $Q$. $x_L$ may be used not only for updating the distribution of the uncertain parameters $Q$, but also the probability distribution of $X$. The updated probability distribution function for $X$ is often referred to as the predictive distribution or the Bayes distribution. The predicted distribution may be assessed according to[54] through

$$f_X^U(x) = \int_{-\infty}^{\infty} f_X(x \mid q) \cdot f_Q''(q \mid \hat{x}) dq \tag{3-81}$$

For further examples of closed-form solutions to the posterior and the predictive distributions for special types of probability distribution functions, the so-called natural conjugate distributions, please refer to the literature[63,74,88]. Several examples are also collected in JCSS[60]. These solutions are useful for updating random variables, and they cover a number of distribution types relevant to reliability based structural reassessment. Yet evidently, practical situations may always arise where no analytical solution is available. In such cases FORM/SORM techniques[45] can be used to integrate over the possible outcomes of the uncertain distribution parameters and thereby assess the predictive distribution.

### 3.3.9 Engineering aspects

For new structures only the beginning and the end of the expected lifetime of the structure are considered, and the changes of the safety conditions over time is neglected. For existing structures in most cases neither the inner nor the outer conditions of the structure are well known. In an example of a 100 year old concrete arch bridge, usually the original design load of the bridge is unknown, and if the standard loads for new bridges are used in calculations, in most cases this results in calculated overload. Nevertheless the bridge still exists. The inner structure of the bridge might also be unknown, if original plans are not available or the bridge has experienced major alterations over its life time, without the keeping of records of the work. In addition, historical loads at some time might have reached the ultimate load bearing capacity of the structure. In simple terms, whereas a new structure is a well-known mechanism, an existing structure is very often a “black box”. The differences between new and existing structures are summarized in Fig. 3-20 in terms of a flow of actions and conditions.

In contrast to the mentioned disadvantages existing structures feature one property: existing structures can be intensively investigated. In the flowchart of several authors about the investigation of existing structures, this plays a major part Fig. 3-21.

Nevertheless for both cases, new and existing structures, not all conditions will be determined completely. This indetermination is described in codes in terms of probability and randomness. The incorporation of randomness into the design and assessment process can be done using random variables. Such random variables can extend the traditional choice of one number as input value into an isomorphism instead of using a function diversity of numbers for the input value. These functions are based on statistical historical knowledge. All as random variables chosen input variables are building then a multidimensional random function. According to a criterion of choice this multidimensional random function can then be disintegrated into two multidimensional spaces. The criteria of choice are mainly limit state function formulae of load bearing behaviour of a structure or a structural element, limit state functions of serviceability or limit state functions of durability. The uncertainty of

This document is the intellectual property of the fib – International Federation for Structural Concrete. All rights reserved.
This PDF of fib Bulletin 86 is intended for use and/or distribution solely within fib National Member Groups.

the formulation of the limit state function is sometimes considered as a model uncertainty factor, sometimes not. Fig. 3-21 summarizes this explanation.

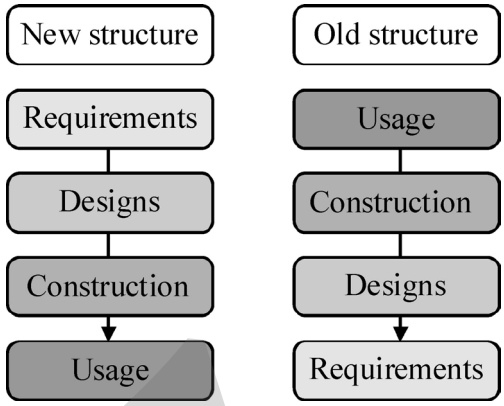


Fig. 3-19 Bayesian probabilistic assessment of structures (adapted from[72])

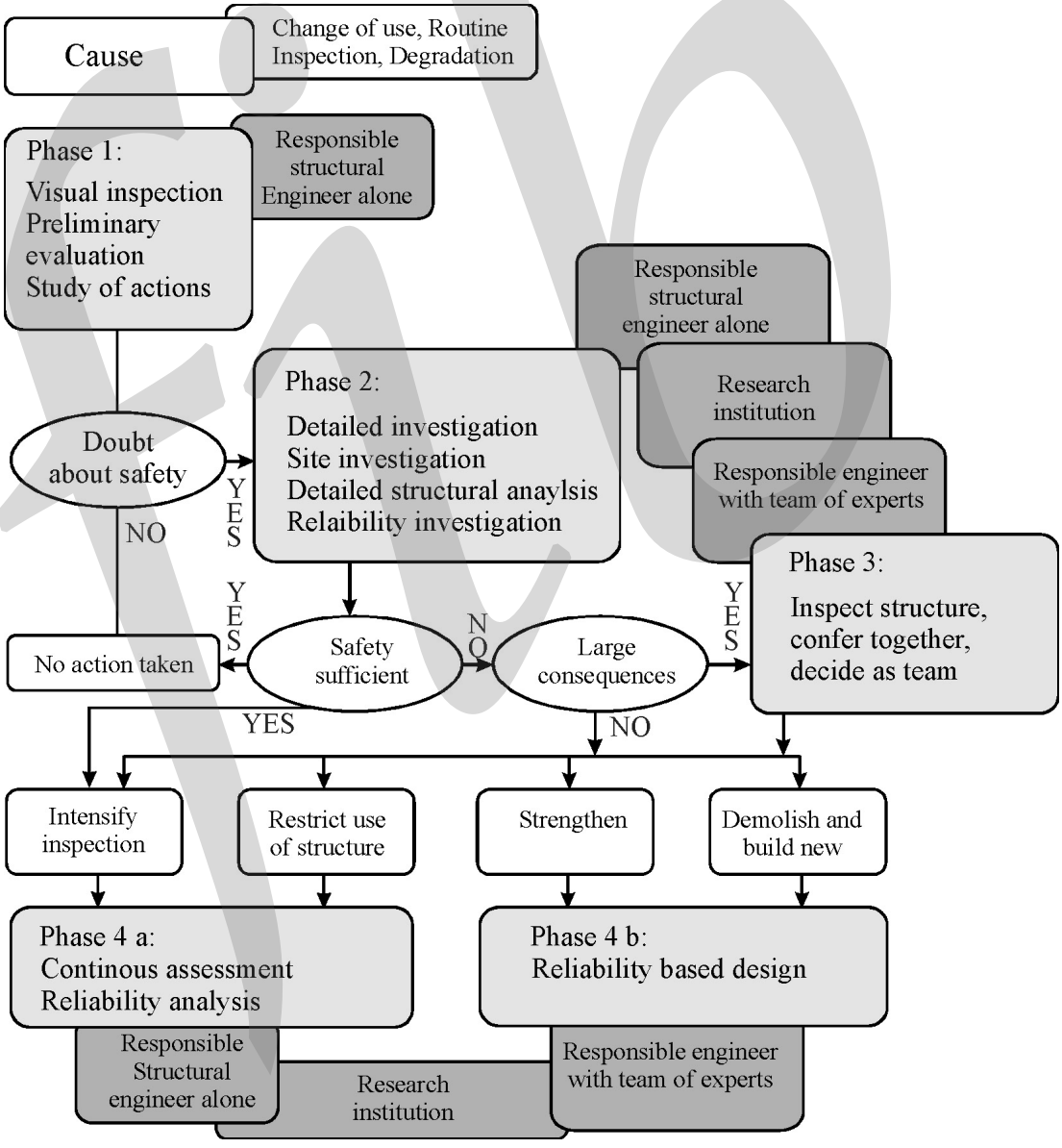


Fig. 3-21 Global framework for the assessment of existing structures acc. to[89] and[90]

This document is the intellectual property of the fib – International Federation for Structural Concrete. All rights reserved.
This PDF of fib Bulletin 86 is intended for use and/or distribution solely within fib National Member Groups.

As mentioned before, existing structures show different properties of safety compared to structures under planning. This is explained in detail in Fig. 3-22

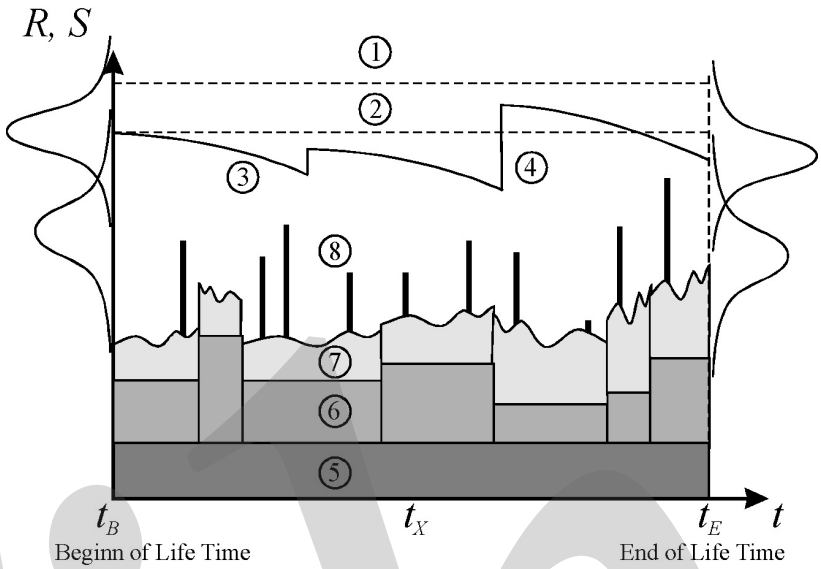


Fig. 3-22 Development of Resistance and Stress on a structure over time

Line ① corresponds with the designed load bearing behaviour. Especially for historical structures this line might show major differences due to the simple models for estimating the load bearing behaviour of the structure. Line ② corresponds to the real load bearing behaviour of the structure. Not only structural changes, but also human errors in construction are included here. Line ③ shows the time and damage dependent development of the load bearing behaviour of the structure. In general it is assumed, that the ultimate load of a structure will decrease over time. Theoretical considerations, which permit a rise of the ultimate load are considered as part of the nonlinear behaviour and therefore included in the original line ②. Line ④ represents the load bearing after restoration. Such a restoration can be a partial reconstruction, or a complete reconstruction and result in an increase in the load bearing over the original value of the structure. In addition, it is possible, that reconstructions do more harm than help and result in a reduction of the ultimate load capacity or to an increase of the degradation process. Line ⑤ represents the load from self-weight. Line ⑥ represents loads from modifications such as replacement of structural elements with a lifetime less than that of the entire structure. Line ⑦ describes continuously changing loads, such as wind. For many historical concrete structures such loads are of minor importance. For bridges traffic loads can be included in this class of loads and then this load will be of major importance. Line ⑧ deals with a special type of load, which occurs for an extremely short time of action, such as impacts or explosions.

For new structures only $t_B$ and $t_E$ are of interest. In contrast for existing structures, $t_X$ and $t_E$. For the evaluation of the safety of an existing concrete structure the estimation of the resistance of the structure as well as of the loading conditions is of major importance. The resistance capacity of the structure depends on the life time as well as on the history of the structure. Historical damage might influence the load bearing in a stepped way, whereas over time continuous degradation processes might decrease the load bearing capacity. Such degradation functions have been proposed by several authors. The following damage function for the load bearing behaviour is used by [91] and [92].

This document is the intellectual property of the fib – International Federation for Structural Concrete. All rights reserved.
This PDF of fib Bulletin 86 is intended for use and/or distribution solely within fib National Member Groups.

$$g = 1 - a \cdot t^b \tag{3-82}$$

Examples for exponents are shown in Table 35.

Table 3-5 Examples of exponents for the damage function according to different degradation process for concrete structures[91, 92]

| Function type | Exponent | Example |
|---|---|---|
| Root law | $b = 0.5$ | Diffusion (Chloride migration) |
| Linear | $b = 1.0$ | Corrosion |
| Parabolic | $b = 2.0$ | Sulphate attack |

In addition to such models, special circumstances of the structure can be considered using target values of the safety index. Table 3-6 shows the possibility of adaptation of this parameter according to

$$\beta = \beta_T - (\Delta_S + \Delta_R + \Delta_P + \Delta_I \geq 2.0 \tag{3-83}$$

Table 3-6 Variable Safety Index subject to different Conditions according to the Canadian Standard CAN/CSA-S6-88: Canadian Limit States Design Standard in modified form taken from[93]

| | |
|---|---|
| Adjustment for System behaviour: | $\Delta_S$ |
| failure leads to collapse, likely to impact occupants | 0.00 |
| failure is unlikely to lead to collapse, or unlikely to impact occupants | 0.25 |
| failure is local only, very unlikely to impact on occupants | 0.50 |
| Adjustment for Risk Category: | $\Delta_R$ |
| high number of occupants ($n$) exposed to failure ($n$ = 100-1000) | 0.00 |
| normal occupancy exposed to failure ($n$ = 10-99) | 0.25 |
| low occupancy exposed to failure ($n$ = 0-9) | 0.50 |
| Adjustment for Past Performance: | $\Delta_P$ |
| no record of satisfactory past performance | 0.00 |
| satisfactory past performance or dead load measured | 0.25 |
| Adjustment for Inspection: | $\Delta_I$ |
| component not inspectable | -0.25 |
| component regularly inspected | 0.00 |
| critical component inspected by expert | 0.25 |

If the safety index is the basis for the calculation of partial safety factors, then such adaptations of existing structures must need special partial safety factors for existing structures. Indeed[93] have investigated special safety factors for loadings on a historical arch bridge (Table 3-6). Sadovský[94] and Žnidarič & Moses[95] introduce a variable safety factor for the dead load of existing structures. See also[96].

*This document is the intellectual property of the fib – International Federation for Structural Concrete. All rights reserved.*
*This PDF of fib Bulletin 86 is intended for use and/or distribution solely within fib National Member Groups.*

Table 3-7 Partial safety factor for actions using an adapted safety index according to[93]

| $\Delta_S + \Delta_R + \Delta_P + \Delta_I \leq 1.5$ | Partial Safety Factor for Dead Load | Partial Safety Factor for Live Load | Factor of Combination |
|---|---|---|---|
| -0.25 | 1.42 | 1.56 | 0.69 |
| 0.00 | 1.35 | 1.50 | 0.70 |
| 0.25 | 1.28 | 1.45 | 0.71 |
| 0.50 | 1.22 | 1.39 | 0.72 |
| 0.75 | 1.16 | 1.34 | 0.73 |
| 1.00 | 1.10 | 1.29 | 0.74 |
| 1.25 | 1.05 | 1.25 | 0.75 |
| 1.50 | 1.00 | 1.20 | 0.76 |

Other authors, such as Melchers and Faber[97] have adapted the partial safety factor of resistance of the structure. They consider the damage process, but also the protection measures and the inspection when considering the safety factors:

$$\gamma_M = \gamma_{M0} \cdot \varphi_P \cdot \varphi_D \cdot \varphi_M \tag{3-84}$$

In general, it can be stated, that the probabilistic safety concept allows the adaptation to existing structures. The development of safety elements from the safety concept in terms of safety factor and characteristic values will be dealt with in the section about safety factors.

This document is the intellectual property of the fib – International Federation for Structural Concrete. All rights reserved.
This PDF of fib Bulletin 86 is intended for use and/or distribution solely within fib National Member Groups.

# 4. Safety concepts for design

## 4.1 Lifetime orientated design and remaining lifetime

### 4.1.1 Introduction

The design task can be defined as visionary, a concrete implementation plan as well as a detailed instruction to reach an aim and as far as the building industry is concerned a practical building. From today's perspective this includes the consideration of economic and sustainability aspects in addition to the technical task. An optimum long term solution under variable constraints is sought. A successful long term concept requires the designer to look ahead.

It builds on the general recognised state of the art and as a consequence on standards and directives current at the time. It is constrained by the boundaries known at the point of planning and compilation. During the design phase the basic characteristics which will mainly affect the lifetime of the building should be defined. Later on it is usually not possible to influence the lifetime to the same degree. The correctly removal of material such as the pressure gouging of arch bridges, or the redundancy of support systems prevail for a long life time and a provide robust load bearing behaviour. Historically, structures were built without considering their expected life. Their planning and execution often took place without a guaranteed time of use. The primary technical challenge was the creation of the structure itself. During the planning process stress comparisons and criteria of the usability dominated. Aspects of durability were introduced in technical regulations just a few years ago. It is a process which lasts until today. In retrospect we know that it was because of the non-consideration of the variability and degeneration of materials over their life time. Often newly developed materials were introduced in a short time without the possibility of testing their long time behaviour. It is well known that the majority of existing bridges around the world were constructed in the 60's and 70's of the 20$^{th}$ century. In European countries this is attributed to the efforts of the reconstruction after the end of the Second World War. At this time prestressed concrete was developed just in time, in order to allow the bridging of huge spans in an economical way. Meanwhile it was also possible to use high-strength steels which were available in necessary sizes at this time. Since this historical boom the number of new bridges has decreased continuously in many countries. Preservation, repair, and reinforcement measures are becoming more and more in the focus of civil engineering.

Nowadays caused by ageing and increased impairment, caused by heavy load traffic, more and more bridges reach their operating life within 50 to 80 years and sometimes even earlier. Against this background the responsible authorities develop guidelines in order to evaluate the bearing capacity[98].

A new challenge concerning this evaluation is rising, such as the need related to disposal medium, to document the plan dossier, notes about special load events, local inspections as well as inspection intervals and, if it is needed, experimental investigations of the existing structure, to obtain information about the history of the structure. The primary goal of these investigations is the exact evaluation of the relevant values for different models, for example a numerical discrete finite model of support structures or the specific model of material including any existing damage, in order to determine the remaining life time. Today it is largely accepted that these values mentioned above have huge imponderabilities and significantly influence

*This document is the intellectual property of the fib – International Federation for Structural Concrete. All rights reserved.*
*This PDF of fib Bulletin 86 is intended for use and/or distribution solely within fib National Member Groups.*

the results of recalculations. A good example is given by the traffic load history on bridges. In order to meet forecasts and to keep this idealisation as realistic as possible it is necessary to minimize the spread which is linked with the traffic load. In order to prove the quality of a model, measurements and investigations on the existing structure can be carried out.

Firstly there is a need for holistic design concepts of new structures, which ensure that the concepts are optimal in the long term, not just at the point of construction. Secondly dealing with existing structures needs sound concepts to prove safety and handling in an economic and sustainable way.

### 4.1.2 Design concepts

The resistance *R* of a concrete structure should be higher than the impact *S* on this structure until the end of its usability $t_d$. *R* and S are variable in the long term as well as disperse and vague values and the dispersal range of each becomes wider over time. Due to degradation in the case of *R* and an enhancement of *S*-events the individual *R* and *S* distributions come closer to each other over time such that the safety with respect to reliability will reduce[99, 100, 101]. Integrated monitoring can be helpful for a better correlation of the model parameters and can lead to a reduction of uncertainty in the context of probabilistic structure investigations. Fig. 4-1 relates to a design concept in which the structure resistances have a sufficient amount of reserves in order to secure its use throughout life $t_d$ without the need for repairs.

As an alternative concept it is possible to start with provision of just a few reserves and continue with upgrading measures and if necessary to make an overhaul at certain time intervals, in order to ensure the safety until the end of life. Upgrading measures which can be done once or several times are still scheduled in this alternative concept. Often a coordinated cost benefit ratio is useful for a strategic design of maintenance measures. Subsequent negative surprises concerning the useful life should not appear. In order to ensure the usability $t_d$ a broad quality management (QM) is needed which not only is concerned with the design, the calculations and the construction and implementation on the construction site but also includes checks and maintenance during its lifetime.

Also the individual tasks of the QM should be coordinated. In the case of remaining life estimation of existing buildings it comes down to the actual quality condition, which should be broadly determined. Based on this a forecast concerning the actual state of the remaining lifetime can be given and a control for the intended life estimation can be set. Dependent on the buildings class it exist different expectations concerning the lifetime. This lifetime is about a few years on 'temporary buildings' (exhibition pavilions) and three to four decades on industrial buildings. In the case of chemical facilities ease of adaptation is more important than overdesigning because the product lines can change in a few years.

Bridges are expected to have a lifetime of about 100 years and in the case of tunnels it is even more. Dams have an expected life time of 150 years and landfills considerably more. There are two extremes concerning the target use of life: a maintenance free design with enough reserves in order to avoid further maintenance measures or a reduced design at the beginning but anticipating the need for repairs later on. If the target is to reach an economic optimum it would be worth carrying out a cost assessment comparison for the different options (none, a few or a lot of maintenance effort). These cost assessments need to include secondary costs as well, such as prospective interest on capital and costs as a result of the loss of use during maintenance works. Depending on the class and manner of use of the building the cost comparisons can be different e.g.[13].

This document is the intellectual property of the fib – International Federation for Structural Concrete. All rights reserved.
This PDF of fib Bulletin 86 is intended for use and/or distribution solely within fib National Member Groups.

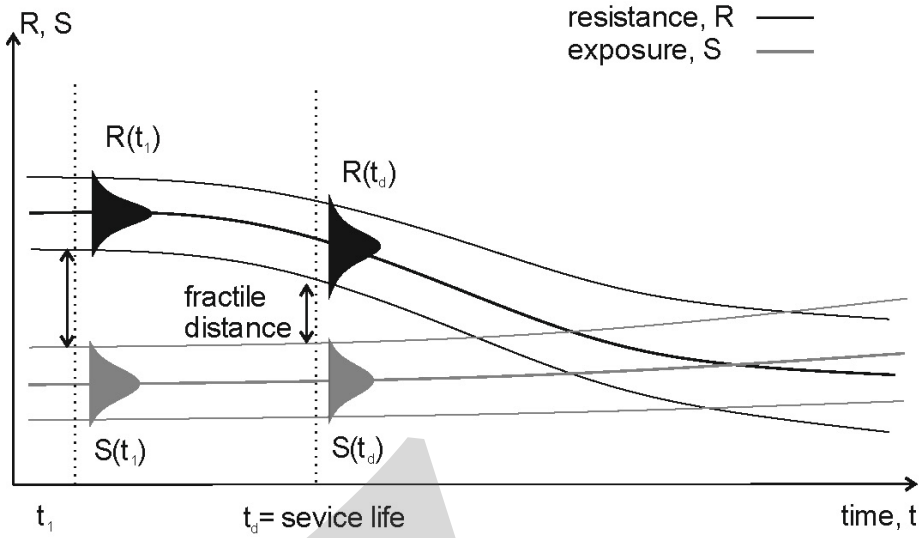


Fig. 4-1 Design concept

## 4.1.3 Remaining lifetime

### 4.1.3.1 Assessment of life history

Reinforced concrete structures which were built in the 1950's for example were erected with different guidelines, standards, quality management systems and methods than at present. Even the material classifications are not comparable to those used today[102, 103]. It is necessary to understand the circumstances at that time in order to reach a realistic base of operation. The inverse simulation can be useful to examine the records of a bridge in which special events (such as information of heavy load transports) are recorded. These extreme loads can have a significant impact on the deterioration of the bridge. It is also necessary to investigate the present condition at the start of a possible remaining life time. This condition should be informed by the results of the simulations of the ageing process. In the case of widely scattered results it should be close to the mean value rather than being on the edge areas. Otherwise the simulation might include assumptions which do not match the actual deterioration history. Under certain assumptions it might be possible to improve them by variation. Thereby a basis is given in order to evaluate the safety conditions of a structure at the start for a possible remaining use of life. In the case of too small reserves of reliability it may be concluded that the end of usability is close or even reached. Huge reserves allow a possible remaining lifetime which can be further extended by maintenance measures.

### 4.1.3.2 Prediction and control of remaining life time

The inverse simulation which is the link between the original state in the past and the present condition includes the deterioration history of the whole lifetime. Forecasts can be updated by the simulation including future improvement measures. Maintenance measures in conjunction with quality management are not only tools for through-life coverage but furthermore, depending on the range, they can enhance the remaining lifetime.

*This document is the intellectual property of the fib – International Federation for Structural Concrete. All rights reserved.*
*This PDF of fib Bulletin 86 is intended for use and/or distribution solely within fib National Member Groups.*

## 4.2 Safety factor formats

### 4.2.1 Introduction

The stochastic based safety concept has been introduced in structural engineering. Nevertheless the direct proof of safety of structures using probabilistic procedures in daily use remains impracticable. Therefore substitutes have to be provided, which are on one hand based on the stochastic description and on the other hand easy to use. Such elements are the safety factors and the characteristic values. This section focuses on the history, development and diversity of safety factors in the field of structural engineering.

The stochastic based safety concept of structural safety has introduced the measure of probability of failure as measure of reliability and safety. Nevertheless under everyday conditions this measure is not practicable and instead simpler types of proof of safety have to be used for structures. Therefore the probabilistic safety concept has to be transformed into a semi-probabilistic safety concept, which means simply developing substitutes for the probability of failure proof, which are easier to use. Such substitutes are the safety factors, characteristic values and the design values. They are developed on some basic simplification. The major advantage for these elements is the long tradition of the application of safety factors.

### 4.2.2 Global safety factors

It has been estimated that the first application of a global safety factor goes back up to 300 years before[104]. He introduced the global safety factor in terms of:

$$\gamma = \frac{\text{Resistance}}{\text{Load}} \tag{4-1}$$

Even empirical geometrical rules remained valid almost over the next two millennia. Only in the last few centuries have the application of safety factors become widespread. Over time several different values were developed for different materials. In most cases the values reduced significantly during the last century. For example whereas for brick masonry in 1880 almost a factor 10 was required, only ten years later the factor was chosen between 7 and 8. In the 20$^{th}$ century the values ranged from factor 5, 4 and now for the recalculation of historical structures with that material the factor 3 is chosen[105, 106, 107, 108, 109]. This decline of safety factors could also be observed for other materials, such as steel. The development of new materials led to particular concerns about the safe application of that material. The different developments for safety factors for materials in the beginning of the 20$^{th}$ century lead to first efforts to develop material-independent factors, like shown in Table 4-1 and Table 4-2.

This document is the intellectual property of the fib – International Federation for Structural Concrete. All rights reserved.
This PDF of fib Bulletin 86 is intended for use and/or distribution solely within fib National Member Groups.

Table 4-1 Global safety factor according to Visodic[110]

| Safety factor | Knowledge of load | Knowledge of material | Knowledge of environment |
|---|---|---|---|
| 1,2-1,5 | Excellent | Excellent | Controlled |
| 1,5-2,0 | Good | Good | Constant |
| 2,0-2,5 | Good | Good | Normal |
| 2,5-3,0 | Average | Average | Normal |
| 3,0-4,0 | Average | Average | Normal |
| 3,0-4,0 | Low | Low | Unknown |

Table 4-2 Global safety factor acc. to Norton[111]

| Safety factor | Knowledge of load | Knowledge of material | Knowledge of environment |
|---|---|---|---|
| 1,3 | Extremely well known | Extremely well known | Likewise tests |
| 2 | Good approximation | Good approximation | Controllable environment |
| 3 | Normal approximation | Normal approximation | Moderate |
| 5 | Guessing | Guessing | Extreme |

As the tables show, a further decline of global safety factors seems to be limited; otherwise the major requirement for safety of structures might not be fulfilled anymore. Therefore more advanced changes might be considered to meet the demanding requirements for economic and safe structures. Such development would be special safety factors for the different columns in the table, for example a safety factor for the load and a safety factor the material. This indeed is the idea of the partial safety factor concept. It does not necessarily result in lower safety factors, but it leads to a more homogenous level of safety.

The development of partial safety factors is strongly connected to the development of the probabilistic safety concept in structural engineering. First proposals about probabilistic based safety concepts can be found by Mayer in Germany[112], Chocialov (1929) and Prot (1936) in France[113]. Already in 1944 in the Soviet Union the introduction of the probabilistic safety concept for structures was forced by politicians[114]. The development of probabilistic safety concepts in general experienced a strong impulse during and after World War II, not only in the field of structures, but also in the fields of aeronautics. In 1947 Freudenthal[115] published his famous work about the safety of structures. Until now a model code for the probabilistic safety concept of structures has been published by the JCSS. Further investigation into the development of safety concept in structural engineering is given by[116] and[117].

The practical application of partial safety factors based on probabilistic safety concepts took further decades.

### 4.2.3 Partial safety factors

There exist several methods to develop partial safety factors for a certain material or a certain type of structure. But in general, all procedures rely on a statistical description of the inherent uncertainty about the material. Additionally historical partial safety factors remain valid, if they have proven to provide safe and reasonably economic structures.

This document is the intellectual property of the fib – International Federation for Structural Concrete. All rights reserved.
This PDF of fib Bulletin 86 is intended for use and/or distribution solely within fib National Member Groups.

#### 4.2.3.1 CEB-Method

First a historical procedure is introduced which permits the development of partial safety factors for concrete only on the coefficient of variation, an assumption about the type of probability distribution function and the class of the structure[113] (Table 4-3 and Table 4-4).

Table 4-3 Partial safety factor for a lognormal distributed strength

| Class of structure | Coefficient of variation | | | |
|---|---|---|---|---|
| | 0.05 | 0.10 | 0.15 | 0.20 |
| Dam | 1.26 | 1.58 | 1.95 | 2.43 |
| Bridge. Theatre. Cultural buildings | 1.23 | 1.49 | 1.82 | 2.16 |
| Residential buildings. Office buildings | 1.20 | 1.40 | 1.65 | 1.91 |
| Lager . Bunker. Frames | 1.15 | 1.31 | 1.46 | 1.62 |
| Secondary buildings | 1.10 | 1.17 | 1.22 | 1.25 |

Table 4-4 Partial safety factor for a normal distributed strength

| Class of structure | Coefficient of variation | | | |
|---|---|---|---|---|
| | 0.05 | 0.10 | 0.15 | 0.20 |
| Dam | 1.24-1.30 | 1.46-1.85 | | |
| Bridge. Theatre. Cultural buildings | 1.21-1.26 | 1.41-1.67 | 1.60-2.47 | |
| Residential buildings. Office buildings | 1.18-1.22 | 1.35-1.53 | 1.50-2.00 | 1.65-2.86 |
| Lager . Bunker. Frames | 1.15-1.16 | 1.27-1.37 | 1.38-1.61 | 1.49-1.92 |
| Secondary buildings | 1.10-1.11 | 1.17-1.19 | 1.21-1.25 | 1.23-1.28 |

Usually the coefficient of variations for concrete depending on the production conditions lies around 10%[118; 119].

#### 4.2.3.2 JCSS method

The Eurocode is heavily based on works and suggestions by the Joint Committee of Structural Safety. The Eurocode model will be explained later in this bulletin in detail. But in the background document of the Eurocode provided by the JCSS an example for the development of a partial safety factor is presented. The general description for such a factor is:

$$R = \Theta \cdot a \cdot x \tag{4-2}$$

with $\Theta$ as uncertainty factor for the calculation model, $a$ as geometrical factor and $x$ as material strength. The resistance design value is then:

$$R_d = \frac{\Theta_k \cdot a_k \cdot x_k}{\gamma_M} \tag{4-3}$$

The three parameters might then be considered as independent random variables with a lognormal distribution. However it should be noted that this is not true for many materials. The material partial safety factor can then be evaluated according to:

$$\gamma_M = \exp(a_R \cdot \beta(V_x + 0.4V_a + 0.4V_\Theta) - 1.64V_x \tag{4-4}$$

The results are shown in Table 4-5.

This document is the intellectual property of the fib – International Federation for Structural Concrete. All rights reserved.
This PDF of fib Bulletin 86 is intended for use and/or distribution solely within fib National Member Groups.

Table 4-5 Material partial safety factor according to some coefficient of variation

| $V_\Theta$ | $V_a$ | $V_x$ | $\delta_M$ |
|---|---|---|---|
| 0.05 | 0.05 | 0.05 | 1.21 |
| 0.05 | 0.05 | 0.15 | 1.30 |
| 0.05 | 0.05 | 0.25 | 1.49 |
| 0.10 | 0.05 | 0.05 | 1.29 |
| 0.10 | 0.05 | 0.15 | 1.38 |
| 0.10 | 0.05 | 0.25 | 1.59 |
| 0.20 | 0.05 | 0.05 | 1.45 |
| 0.20 | 0.05 | 0.15 | 1.67 |
| 0.20 | 0.05 | 0.25 | 1.92 |

Formulation according to Melchers & Faber

Melchers & Faber[97] introduce a damage function, which is included in the material safety factor.

$$\gamma_M = \gamma_{M0} \cdot \varphi_P \cdot \varphi_D \cdot \varphi_M \tag{4-5}$$

The factors consider deterioration processes, protection against deterioration and intensity of inspection.

#### 4.2.3.4 Factors for new structures

An overview of partial safety factors regarding building materials is shown in Table 4-6.

Table 4-6 Material safety factors

| Production type | Code | $\gamma_c$ | $m_b$ | res.$\gamma_c$ |
|---|---|---|---|---|
| Precast concrete | DIN 1045-1 [120] | 1.35 | – | 1.35 |
| | ETV concrete | 1.30 | 1.00 | 1.30 |
| In-situ concrete | DIN 1045-1 [120] | 1.50 | – | 1.50 |
| | ETV concrete with TGL 33403, with adaptation for the pouring type | 1.30 | 0.80 | 1.63 |
| | | | 0.85 | 1.53 |
| | | | 0.90 | 1.44 |
| | | | 0.95 | 1.37 |
| Reinforcement steel | DIN 1045-1 [120] | 1.15 | | 1.15 |
| | ETV concrete | 1.16 | 1.00 | 1.15 |

Table 4-7 Material safety factors-Part I

| Material | Norm | Limit state of ultimate load | Accidental load conditions | Limit state of serviceability |
|---|---|---|---|---|
| Concrete (up to C 50/60) | DIN1045-1 [120] | 1.50 | 1.30 | 1.50 |
| Concrete higher then C 50/60 | DIN1045-1[120] | $\frac{1.50}{1.1-\frac{f_{ck}}{500}}$ | $\frac{1.30}{1.1-\frac{f_{ck}}{500}}$ | - |
| Non reinforced concrete | DIN1045-1[120] | 1.80 | 1.55 | - |
| Non reinforced concrete | FU-B[121] | 1.25 | | |
| Precast concrete | DIN1045-1[120] | 1.35 | | - |
| Collateral evasion | DIN1045-1[120] | 2.00 | - | - |

*This document is the intellectual property of the fib – International Federation for Structural Concrete. All rights reserved.*
*This PDF of fib Bulletin 86 is intended for use and/or distribution solely within fib National Member Groups.*

| | | | | |
|---|---|---|---|---|
| Reinforcement steel | DIN1045-1[120] | 1.15 | 1.00 | 1.15 |
| Prestressing steel | DIN1045-1[120] | 1.15 | 1.00 | 1.15 |
| Steel yield strength | EC 4 [122] | 1.10 | 1.00 | |
| Steel tensile strength | EC 4 [122] | 1.25 | 1.00 | |
| Steel tensile strength | EC 4 [122] | 1.00 | 1.00 | |
| Wood | EC 5 [123] | 1.30 | 1.00 | 1.00 |
| Masonry (Category A) | EC 6[124] | 1.7 (I)/2.0 (II) | 1.20 | |
| Masonry (Category B) | EC 6[124] | 2.2 (I)/2.5 (II) | 1.50 | |
| Masonry (Category C) | EC 6[124] | 2.7 (I)/3.0 (II) | 1.80 | |
| Masonry - Steel | EC 6[124] | 1.50/2.20 | | |
| Masonry | DIN 1053-100 | 1.50-1.875 | 1.30-1.625 | |

*1 Consider construction conditions[125]

*2 Recent researches indicates lower values

*3 A Partial safety factor for a system.

Table 4-8 Material safety factors-Part II

| Material | Norm | Limit state of ultimate load | Accidental load conditions | Limit state of serviceability |
|---|---|---|---|---|
| Masonry (Category K. A-C) | EC 6 [126] , [124] | 2.50 | 1.20 | |
| Float glass | [127] | 1.80 | 1.40 | 1.40 |
| Prestressed glass | [127] | 1.50 | 1.30 | 1.30 |
| Silicon glass | [127] | 5.00 | 2.50 | 2.50 |
| Glass fibre | | 1,3 | | |
| Carbon fibre | [128; 125] | 1.20 | | |
| Carbon fibre | [125] | 1.30 *[1] | | |
| Carbon fibre cable | [125] | 1.20 *[1] | | |
| Carbon fibre glue | [125] | 1.50 *[1] | | |
| Cladding | DIN 18 516 [129] | 2.00 | | |
| Aluminium yield strength | EC 9 [130] | 1.10 | | |
| Aluminium tensile strength | EC 9 [130] | 1.25 | | |
| Bamboo as building material | [131] | 1.50 | | |
| Textile reinforced concrete | [132] | 1.80 *[2] | | |

*[1] Consider construction conditions[125]

*[2] Recent researches indicates lower values

*[3] A Partial safety factor for a system.

Table 4-9 Material safety factors -Part III

| Material | Norm | Limit state of ultimate load | Accidental load conditions | Limit state of serviceability |
|---|---|---|---|---|
| Concrete under multiaxial loading | [133] | 1.35-1.70 | | |
| Granodiorite tensile strength | [132] | 1.50-1.70 | | |
| Historical masonry arch bridges | UIC-Codex[134] | 2.00 *[3] | | |
| Historical non reinforced arch bridges | [135] | 1.80 *[3] | | |

*[1] Consider construction conditions[125]

*[2] Recent researches indicates lower values

*[3] A Partial safety factor for a system.

This document is the intellectual property of the fib – International Federation for Structural Concrete. All rights reserved.
This PDF of fib Bulletin 86 is intended for use and/or distribution solely within fib National Member Groups.

#### 4.2.3.5 Factors for existing structures

An extensive inspection is necessary any time the assessment of an existing structure will be carried out, independently of whether partial safety factors for a static recalculation will be modified or not. It should be noted that every existing structure represents an individual case and that the assessment has to be done individually. In general, the inspection methods are separated into a qualitative inspection and a quantitative inspection. The following noticeable problems have to be checked in a qualitative inspection, for example for a concrete structure:

- Cracks
- Corrosion
- Damaged concrete surfaces with spalling
- Appearance of chloride or carbonation
- Geometry
- Dead loads, live loads
- Change in use, including increased load requirements
- Check of the documentation of the existing structure

This qualitative inspection is the first step of the assessment. In the next step, a quantitative inspection has to be carried out. With such an inspection a set of values of measured parameters characterize the condition of the structure. For a concrete structure the necessary information for a static recalculation is:

- Measurement of concrete compression strength on samples of drilling cores or by non-destructive testing methods
- Measurement of steel yield strength on samples or by non-destructive testing methods
- Corrosion area and depth
- Crack depth and length
- Geometry and displacements
- Determination of chloride and carbonation on the samples of drilling cores
- Static system of the structure

In general, if more information on the structure is available, the assessment can be done more accurately. Additionally, the quality of modified partial safety factors depends on the depth and intensity of the inspection and the results from the measurement of the material properties. This is shown clearly in chapter 4.3 which demonstrates the dependence of the value of the partial safety factors on the coefficient of variation of the parameters from the materials. New developments of non-destructive testing methods for existing structures allow an increasing amount of information on the existing structure. A good overview of the testing methods is shown on the homepage of the German Federal Institute for Materials Research and Testing[136]. With these new technologies, most parameters of the materials of a structure can be identified very well. Additionally, the use of monitoring systems for loads and for the structural response of existing structures gives information about the behaviour of structures, especially about the variation of the

*This document is the intellectual property of the fib – International Federation for Structural Concrete. All rights reserved.*
*This PDF of fib Bulletin 86 is intended for use and/or distribution solely within fib National Member Groups.*

monitored parameters. The monitoring data lead to a decrease of uncertainty and give an input for the calibration of the safety level.

For existing structures the structural analysis does not provide a forecast in the way that the planning of new buildings does, because essential information about the structure, for example the material strength and the geometry, can be determined by measurements.

In German code (DIN 1055-100[137]), in the Eurocode[40] and in specific codes for various materials which are based on the semi-probabilistic safety concept, there are no regulations for modifying the partial safety factors in the case of existing structures. In Germany there are additional documents which allow such a modification of the partial safety factors for use in practice for concrete structures. In Table 4-10 there is a summary of the current developments. The values from DIN 1045-1[120] (column 2) show the reference values without modification.

Table 4-10 Modified partial safety factors for existing structures (columns 3 to 5)

| 1 | 2 | 3 | 4 | 5 |
|---|---|---|---|---|
| | DIN 1045-1 [120] | DAfStb Heft 467[138] | Richtlinie Belastungsversuche an Massivbauwerken[139] | Fingerloos / Schnell [102] |
| Dead load – general $\gamma_G$ | 1.35 | 1.35 | 1.35 | 1.35 |
| Dead load – existing structure $\gamma_G$ | 1.35 | 1.15 | 1.15 | 1.35 |
| Live Loads $\gamma_Q$ | 1.50 | 1.50 | 1.50 | 1.5 |
| Concrete $\gamma_C$ | 1.50 | 1.40 | 1.40 | 1.20 – 1.50 |
| Reinforcing steel $\gamma_S$ | 1.15 | 1.10 | 1.10 | 1.05 – 1.15 |

The modified partial safety factors suggested by Dafstb[138, 139] can be used if the characteristic values of the material strength of concrete and steel and of the dead load of the structure are known. If the characteristic values have to be determined from tests, the Annex D of the Eurocode – Basis of structural design[40] shows the calculation according to the number of samples and the general test criteria. The modified values of $\gamma_c$ and $\gamma_S$ are based in principle on the regulation of the Model Code 90[140], which allows the reduction if specific limitations of the tolerances in the geometry of the concrete elements, of the cover or of the position of steel are observed. The modified partial safety factors[138; 139] are not quantified based on a probabilistic analysis, but rather from the experience.

In the assessment of an existing structure it has to be decided which code will be chosen for the static recalculation. There are generally two questions: The original code at the time of building or the current new code format with for example the semi-probabilistic safety concept and the newest developments of the limit states. The calibration of the partial safety factors depends on the statistical parameters of the materials and loads and on the target reliability. In the case of an existing structure, the additional information can be used for the calibration of the partial safety factors for a static recalculation. The most influential document in practical and illustrative terms for a code calibration procedure is the work of Ellingwood[141].

For a probabilistic analysis of existing structures with the First Order Reliability Method (FORM) or the Second Order Reliability Method (SORM), the Joint Committee on Structural Safety (JCSS) has published the JCSS document "Assessment of existing structures"[50]. This document contains instructions for inspection techniques, for reliability updating such as the Bayes theory and for tentative target reliability indices $\beta$. The tentative target reliability

*This document is the intellectual property of the fib – International Federation for Structural Concrete. All rights reserved.*
*This PDF of fib Bulletin 86 is intended for use and/or distribution solely within fib National Member Groups.*

$\beta$ according to JCSS[50] is differentiated to the relative cost of safety measures and to the consequences of failure. For the semi-probabilistic safety concept there is no advice for modified partial safety factors.

The investigations of[41] the reliability of reinforced structural elements in existing structures subjected to shear force shows that the model uncertainties for the shear force capacity have considerable influence on reliability[103]. The investigations are based on the German Code DIN 1045-1[120] with the limit state functions for shear force bearing capacity of structures without shear force reinforcement $V_{Rc,t}$, the bearing capacity of the shear force reinforcement $V_{Rs,y}$ and the bearing capacity of the compressive strut $V_{Rd,max}$. The investigations consider the special case of an existing structure with different statistical parameters than for new structures. The investigations show that the coefficient of variation of the concrete compression strength of existing structures can increase by up to 40% for a fifty-year-old building. Experience shows that the concrete quality of bridges is in most cases better than that of buildings. This probably depends on the stronger control mechanism in the construction phases of bridges. For a new structure the coefficient of variation of concrete is normally 10% to 20%. The effect of the value of the coefficient of variation to the reliability index $\beta$ for the compressive strut due to shear load ($V_{Rd,max}$) is shown in Fig. 4-2.

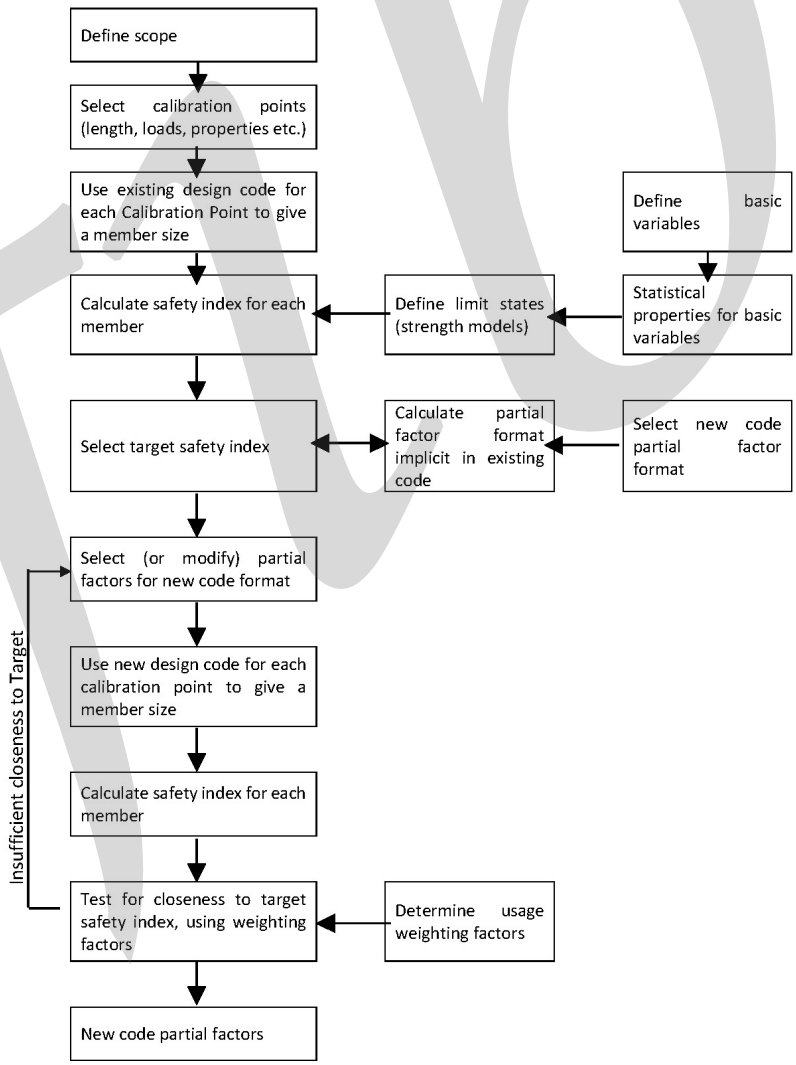


Fig. 4-2 Flow chart for calibration of code safety-checking format Ellingwood[141]

This document is the intellectual property of the fib – International Federation for Structural Concrete. All rights reserved.
This PDF of fib Bulletin 86 is intended for use and/or distribution solely within fib National Member Groups.

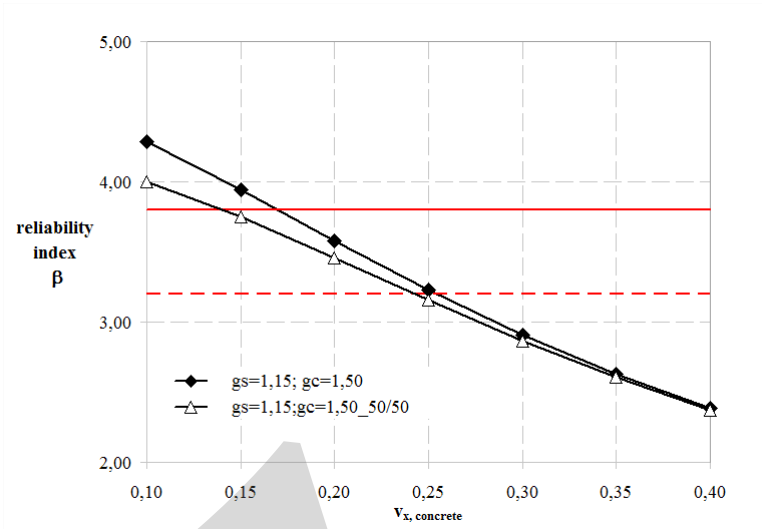


Fig. 4-3 Reliability of the compressive strut due to shear load ($V_{Rd,max}$) for different coefficients of variation of concrete compressive strength for a reference period of 50 years with $\gamma_c$ = 1.50 (concrete); $\gamma_S$ = 1.15 (steel) and $\gamma_G$ = 1.35 (dead load), $\gamma_Q$ = 1.50 (live load)[103]

In the case of building components with a very high thickness, as in the case of the ground slab of a high-rise building or a nuclear power plant with a usual cross-sectional thickness of 3.0 metres up to 5.0 metres or in the case of bridges with a very high dead load, the influence of the coefficient of variation of the geometry is very high. The distribution function type for dead load is usually a normal distribution.

For example, a coefficient of variation of $v_x$ = 5% – 10% for the dead load of a concrete structure means a deviation of 0.25 m – 0.50 m in the case of 5.0 m thick ground slab. In practice this is very unrealistic.

Especially in the case of existing structures the geometry and thickness can be measured and the coefficient of variation can be calculated exactly. The influence on the partial safety factor for dead loads can be easily illustrated. The calculation according to Eurocode[40] is:

$$\gamma_G = 1 + 0.7\beta \cdot V_G \tag{4-6}$$

$V_G$ is the coefficient of variation for load factor and for model uncertainty:

$$V_G = \sqrt{\left(V_g^2 + V_{Ed}^2\right)} \tag{4-7}$$

with:

$V_g$ = Coefficient of variation of the dead load

$V_{Ed}$ = Coefficient of variation of model uncertainty (according to EC0[40] $V_{Ed}$ = 10%)

With a coefficient of variation $V_g$ = 10% and $V_{Ed}$ = 10% and a target reliability of $\beta$ = 3.8 the partial safety factor can be calculated to:

$$\gamma_G = 1 + 0.7 \cdot 3.8\sqrt{\left(0.10^2 + 0.10^2\right)} = 1.37 \approx 1.35 \tag{4-8}$$

This is the chosen partial safety factor for dead loads in the Code[40]. In the case of an existing structure with a measured coefficient of variation $V_g$ = 3%, equivalent to a deviation of 15 cm in a 5 m thick ground slab, and $V_{Ed}$ = 5% in accordance to JCSS[142], the partial safety factor is:

This document is the intellectual property of the fib – International Federation for Structural Concrete. All rights reserved.
This PDF of fib Bulletin 86 is intended for use and/or distribution solely within fib National Member Groups.

$$\gamma_G = 1 + 0.7 \cdot 3.8 \cdot \sqrt{\left(0.01^2 + 0.05^2\right)} = 1.15 \approx 1.15 \tag{4-9}$$

This simple example shows the high influence of the coefficient of variation on partial safety factors.

This calculation shows the importance of insitu geometrical measurements specifically for the determination of the dead load. In general a smaller coefficient of variation can be obtained and in consequence a smaller safety factor for dead load can be assumed.

Another approach is given in the Canadian National building code. There is a specific distinction in terms of partial safety factors for dead load depending on the inspection availability and results. The investigations of Allen[143] for the Canadian National Building Code show the influence of the type of inspection on the partial safety factors of actions:

Table 4-11 Changes of partial factor for dead load for evaluation of existing buildings Allen[143]

| Inspection performance | Adjustment of $\beta$ with $\Delta\beta$ | Load factor for dead load $\gamma_G$ |
|---|---|---|
| No inspection or drawings | - 0.4 | 1.35 |
| Inspected for identification/location | 0.0 | 1.25 |
| Satisfactory performance or dead load measured | 0.25 | 1.20 |

These aspects should be included in the calibration procedure of partial safety factors for existing structures. The use of modified partial safety factors needs a quantitative inspection of the existing structure. With new developments in the field of destructive and non-destructive testing methods, the grade of information is very high. The procedure in[144] can be recommended for the calibration of modified partial safety of existing structures in individual cases with a new code format. For practical use, the modified partial safety factors in Table 4-10 can be used if the regulations for the inspection and the determination of the characteristic values have been carried out. However, it should be noted that the values are based on experience and not on a probabilistic calibration.

#### 4.2.3.6 Factors for load and material combinations

The same approach can be used also for the resistance side, e.g. the partial safety factors for materials. If the failure mode is controlled by one material (e.g. partial safety factor for a concrete compression strut in a reinforced concrete section) the partial safety factors of the other materials (e.g. steel reinforcement) must be equal to 1.0.

### 4.2.4 Proof loading

Additionally there exist simplified rules for the development of design values including material partial safety factors based on testing of materials. Such procedures have been intensively discussed by Reid[145]. The procedures include some main assumptions, for example the probability distribution function of the load and the resistance. Examples are the Australian Standard Procedure for Statistical Proof Loading, Australian Standard Procedure for Probabilistic Load Testing or the Standard for Probabilistic Load tests. Most of the procedures consider the variance of the material strength, the variance of the load, some condition factors, the number of tests or a correction factor and the required safety index.

*This document is the intellectual property of the fib – International Federation for Structural Concrete. All rights reserved.*
*This PDF of fib Bulletin 86 is intended for use and/or distribution solely within fib National Member Groups.*

Val & Stewart[146] describe a procedure for the evaluation of partial safety factor for the resistance mainly for existing structures. The safety factor is split into two parts, the partial safety factor $\gamma_m$ for the material strength and $\gamma_\eta$ as factor for the consideration of additional uncertainties, $f_{k,est}$ is the estimated characteristic material strength. The design value for the strength is therefore:

$$f_d = \frac{f_{k,est}}{\gamma_m \cdot \gamma_\eta} \tag{4-10}$$

Table 4-12 and Table 4-13 show some examples taken from the publication by Val & Stewart[146]. Here no a-priori information was available whereas in Table 4-13 a-priori information could be used. It becomes clear, that additional information is of major importance, especially for existing structures, for keeping safe and efficient structures. As already seen in the JCSS example, the consideration of modelling uncertainty, however in which way, builds a major part of many expansions of the traditional way for the development of partial safety factors. Here it becomes visible, that the clear rule for the application of statistics might sometimes be a drawback for a realistic estimation of the safety of a structure.

Table 4-12 Example of material partial safety factors without a-priori and with six tested samples 146

| Coefficient of variation of the samples | $\gamma_m$ | $\gamma_\eta$ Coefficient of variation of the calibration factor | | |
|---|---|---|---|---|
| | | 0.05 | 0.10 | 0.15 |
| 0.04 | 1.1 | 1.07 | 1.19 | 1.27 |
| 0.08 | 1.4 | 1.05 | 1.17 | 1.24 |
| 0.12 | 1.6 | 1.04 | 1.15 | 1.21 |
| 0.16 | 1.9 | 1.03 | 1.10 | 1.19 |
| 0.20 | 2.2 | 1.02 | 1.07 | 1.15 |

Table 4-13 Example of material partial safety factors with a-priori and with six tested samples[146]

| A priori-coefficient of variation | $\gamma_m$ |
|---|---|
| 0.05 | 1.36 |
| 0.10 | 1.25 |
| 0.15 | 1.21 |

## 4.3 Safety formats for non-linear analysis

### 4.3.1 Introduction

Engineering design practice is experiencing growing use of numerical methods, which are based on advances in material science offered by the research community[147,148,149, 150, 151, 152].

Nonlinear finite element programs can simulate the resistance of elements, or whole structures and offer a virtual testing, which very much resembles a real structural performance, and a real failure. In this approach a typical representative value is a global resistance, described for example by a force, which can be used for a verification of safety.

This document is the intellectual property of the fib – International Federation for Structural Concrete. All rights reserved.
This PDF of fib Bulletin 86 is intended for use and/or distribution solely within fib National Member Groups.

However, the present safety formats based on partial factor method is here not directly applicable. It has been developed for a different approach, in which safety assessment is made in local points or cross sections and safety check on a global level is not made. It will be shown that the safety on a global level can be evaluated based on generally accepted safety principles agreed by Joint Committee of Structural Safety. In general the limit state function includes contributions of actions as well as resistance. In some cases, we restrict our formulations only to the resistance part, assuming that the safety due to actions and resistance can be decoupled, which is a simplification usually accepted in the present codes.

### 4.3.2 Safety formats

In general a verification of limit states is required by the current design codes. An admissible limit state can be described by the condition

$$g(s,r) > 0 \tag{4-11}$$

whereas the remaining range of limit states

$$g(s,r) \leq 0 \tag{4-12}$$

represents the failure. In this $g(s,r)$ is the limit state function, $s$ describes actions and $r$ resistance. However, due to random nature of these functions the limit state condition is fulfilled only with certain probability $P_f = Prob\{g(s,r) \leq 0\}$. The limit state function can be separated to the action function $s(s)$ and resistance function $r(r)$ and consequently the design condition can be rewritten as

$$s(s) \leq r(r) \tag{4-13}$$

In general the resistance $r(r)$ describes the response of a structure to given load actions. It is a result of interaction of many random effects, which are in the end reflected in the value of limit resistance. In case of ultimate limit states this can be, for example, an ultimate load of a structure. The resistance can be described by a scalar, vector or a function, depending on type of the limit state formulation.

The safety assessment of design condition can be performed in various ways, often referred as safety formats, which can be according to its probabilistic approach classified into three classes: (1) Full probabilistic analysis, (2) Global safety factor method, (3) Partial safety factor method. From a probabilistic viewpoint, the full probabilistic method is theoretically most rational, global safety method is rational but simplified and partial safety factor method has the lowest value since it lacks a global concept. We shall describe the character of these approaches briefly.

Full probabilistic analysis is the most general method based on a rational theoretical concept. However, it requires detail information about probabilistic parameters of the limit state function and a realistic computational model of resistance. It usually requires a large computational effort, especially, when numerical methods are employed for both, probabilistic and structural models. The details of this approach is outside of the scope of this chapter. Full probabilistic analysis can be performed by numerical methods and available software tools as described by Novak et al.[153].

In the global safety factor approach condition can be rewritten as

$$S_d \leq R_d \tag{4-14}$$

This document is the intellectual property of the fib – International Federation for Structural Concrete. All rights reserved.
This PDF of fib Bulletin 86 is intended for use and/or distribution solely within fib National Member Groups.

where $S_d$ is the design value of actions, which can be determined for a certain probability required for design. Alternatively, the method used for partial factors can be applied in which the design action can be schematically written as $S_d = s(S,\gamma_s)$, where actions $S$ (permanent and variable loads, etc.) are scaled by the partial factors $\gamma_s$. Design value of resistance $R_d$ can be obtained as

$$R_d = R_m / \gamma_R^* \tag{4-15}$$

where $R_m$ is the mean resistance and $\gamma_R^*$ is the global safety factor of resistance. Note, that unlike in partial factors for materials $\gamma_M$, which are applied to characteristic values, the global safety factor of resistance, hence marked by asterisk *, is applied to the mean value of resistance.

In general, action and resistance, which appear in design equation (4-14), can include many components (for example vertical and horizontal forces, body forces, temperature, etc.,) and can be described by a point in a multi-dimensional space. It is useful for safety evaluation to define a resistance scaling factor $k_R$, which describes the ratio between design actions and mean resistance:

$$k_R = \frac{R}{S_d} \tag{4-16}$$

Then, the design condition can be rewritten as:

$$\gamma_R < k_R \tag{4-17}$$

Where $\gamma_R$ is the global safety factor for resistance. Factor $k_R$ can be used to calculate the relative safety margin $m_R$ of resistance

$$m_R = k_R - 1 \tag{4-18}$$

It was argued by some investigators, that the value of global factor is strongly related to the type of limit state function. Consequently, for required probability of attainment of the limit state condition (4-1), the value of global factor cannot be unique for all limit state situations and should be related to the variability of the resistance. This idea is reflected in the method ECOV described later.

Model uncertainty, if relevant, can be included in eq. (4-20), or into the left hand side of condition (4-13) in actions. However, in case of numerical models with high level of accuracy this uncertainty should be considered in broad sense and reflect unforeseen effects, rather than coarse mechanical models.

Partial safety factor method is the safety format used in present codes. In this method the design condition (4-19) is not applied to a global response, but to local response of cross sections.

$$S_d \le r(f_d,\ldots) \tag{4-19}$$

where $r(f_d,\ldots)$ is the resistance function of the cross section, $f_d$ is the design value of material parameters

$$f_d = f_k / \gamma_M, \quad \gamma_M = \gamma_m \cdot \gamma_{Rd} \tag{4-20}$$

in which $\gamma_M$ is partial safety factor of material property accounting for model uncertainty and dimension variation, $\gamma_M$ is partial safety factor of material property and $\gamma_{Rd}$ is partial safety factor for model uncertainty and dimension variation.

This document is the intellectual property of the fib – International Federation for Structural Concrete. All rights reserved.
This PDF of fib Bulletin 86 is intended for use and/or distribution solely within fib National Member Groups.

The partial safety factor method represents the lowest level of probabilistic approach. It does not allow an assessment of the safety of the structure under consideration as whole, but rather then that it performs checks of local points, usually cross sections.

### 4.3.3 Methods of global safety verification

#### 4.3.3.1 Introduction

A need for global safety assessment emerged with the spread of nonlinear analysis, which is becoming a frequent tool for design of new and assessment of existing structures. This development is supported by the rapid increase of computational power as well as by new capabilities of the available software tools for numerical simulation of structural performance. The non-linear analysis is by its nature always a global type of assessment, in which all-structural parts, or sections interact. It resembles more a virtual testing of designed structures rather than simplified mechanical models.

On the other hand the code provisions provide very little guidance how to use the results of non-linear analysis for structural assessment or design. The safety formats and rules that are usually employed in the codes are tailored for classical assessment procedures based on beam models, hand calculation, linear analysis and local section checks. Until recently the codes did not allow applying the method of partial safety factors for non-linear analysis, and therefore, a new safety format was expected to be formulated. Certain national or international codes have already introduced new safety formats based on overall/global safety factors to address this issue. Such codes are, for instance, German standard DIN 1045-1[120] or Eurocode 2 EN 1992-2[154].

Global safety approach was also studied by other investigators with the aim to provide more information about structural safety obtained by design according to partial safety factor method. Holicky[155] used probabilistic analysis to demonstrate safety in typical structural elements and found a large variation of global safety. He indicated that in some cases such design could be unsafe. [156] argued that unsafe situations are prevented by empirical code provisions. They demonstrated a suitability of the global safety factor method proposed in Eurocode 2 for nonlinear analysis.

#### 4.3.3.2 Design variable of resistance

Global resistance is represented by variable $R$ in Eq. (4-21). In a simple case this can be a single variable, such as loading force, or intensity of a distributed load, in general it can include a set of actions with their loading history. The resistance is used to evaluate the safety of limit state and is effected by random variation of basic variables such as material parameters, dimensions and possibly others.

Random variation of resistance can be described by statistical distribution with parameters: $R_m$- mean value of resistance, $R_k$ - characteristic value of resistance, (corresponding to the probability 5%), $R_d$ - design value of resistance. Theoretically, other parameters of higher order can be introduced, but we will simplify our approach to those mentioned above. For further derivations it is important to realize that the characteristic and design values reflect the random scatter of the resistance, which in probabilistic terms means that they reflect distribution function of resistance and its parameters, namely the standard deviation, and which we consider as most important for description of global safety.

*This document is the intellectual property of the fib – International Federation for Structural Concrete. All rights reserved.*
*This PDF of fib Bulletin 86 is intended for use and/or distribution solely within fib National Member Groups.*

The resistance is determined for a certain loading pattern, which is here introduced by the symbol of actions $S$. It is understood that unlike material parameters and dimensions, which enter the limit state function $r$ as basic variables, the loading is scalable, and includes load type, location, load combination and history. It is important to note that the global safety in this approach is defined for a unique load combination and load history. The reasons for this are different theoretical assumptions in linear and nonlinear models. In partial safety factor method a superposition of load case results is assumed due to linear models, while this is not possible in nonlinear models.

In general, action and resistance, which appear in design equations, can include many components (for example vertical and horizontal forces, body forces, temperature, etc.,) and can be described by a point in a multi-dimensional space. It is useful for safety evaluation to define a resistance scaling factor $k_R$, which describes the ratio between design actions and mean resistance:

$$k_R = \frac{R}{S_d} \tag{4-21}$$

Then, the design condition can be rewritten as:

$$\gamma_R < k_R \tag{4-22}$$

where $\gamma_R$ is required global safety factor for resistance. Factor $k_R$ can be used to calculate the relative safety margin $m_R$ for resistance

$$m_R = k_R - 1 \tag{4-23}$$

Two methods for determining global resistance for the purpose of design condition are described in the following Section. Method proposed Eurocode EN1992-2[154] is based on a unique global safety factor. Method ECOV is based on a random variation of resistance.

#### 4.3.3.3 Global safety format according to EN 1992-2[154]

Design resistance is calculated from

$$R_d = r\left(\tilde{f}_{ym}, \tilde{f}_{cm} \ldots\right) / \gamma_R = R_{mc} / \gamma_R \tag{4-24}$$

Material properties used for resistance function are considered by modified mean values. The mean steel yield strength $\tilde{f}_{ym} = 1.1 f_{yk}$. Mean strengths of concrete is reduced to account for greater random variation of concrete properties $\tilde{f}_{cm} = 1.1 = \frac{\gamma_s}{\gamma_c} f_{yk}$ , where $\gamma_s$ and $\gamma_c$ are partial safety factors for steel and concrete, respectively. Typically this means that the concrete compressive strength should be calculated as $\tilde{f}_{cm} = 0.843 f_{ck}$. This method allows treating of both failure modes, due to steel and due to concrete, in a unified way.

The global factor of resistance shall be $\gamma_R = 1.27$. It should be noted that a part of safety is covered by the resistance $r(\tilde{f}_{ym} \tilde{f}_{cm})$.

Note should be made to the "mean" resistance $R_{mc}$ formulated in this method. This resistance does not correspond to the real mean resistance, since it is based on reduced concrete strength. Thus a part of the global safety is included in the reduced mean resistance $R_{mc}$ and the rest is in the global factor $\gamma_R$.

This document is the intellectual property of the fib – International Federation for Structural Concrete. All rights reserved.
This PDF of fib Bulletin 86 is intended for use and/or distribution solely within fib National Member Groups.

#### 4.3.3.4 ECOV method – estimate of coefficient of variation

This method is based on the idea, that the random variation of resistance described by the coefficient of variation $V_R$, can be estimated from mean $R_m$ and characteristic values $R_k$ values of resistance[157]. The underlying assumption is that random distribution of resistance is according to lognormal distribution, which is typical for structural resistance[155]. Consequently, it is possible to express the coefficient of variation as:

$$V_R = \frac{1}{1.5}\ln\left(\frac{R_m}{R_k}\right) \tag{4-25}$$

Global safety factor $\gamma_R$ of resistance is then estimated as:

$$\gamma_R = \exp\left(\alpha_R \cdot \beta \cdot V_R\right) \tag{4-26}$$

where $\alpha_R$ is the sensitivity (weight) factor for resistance reliability and $\beta$ is the reliability index. The above procedure enables to estimate the safety of resistance in a rational way, based on the principles of reliability accepted by the codes. Appropriate code provisions can be used to identify these parameters. According to Eurocode 2 EN 1991-1, typical values are $\beta = 4.7$ (one year) and $\alpha_R = 0.8$. In this case, the global resistance factor is:

$$\gamma_R \cong \exp(-3.76 V_R) \tag{4-27}$$

and the design resistance is calculated as:

$$R_d = R_m / \gamma_R \tag{4-28}$$

The key steps in the proposed method include the determination of mean and characteristic values of resistance $R_m$, $R_k$. It is proposed to estimate them using two separate nonlinear analyses using mean and characteristic values of input material parameters:

$$R_m = r(f_m, \ldots), \quad R_k = r(f_k, \ldots) \tag{4-29}$$

In a similar manner the random effect other parameters important for resistance, for example dimensions or load positions, can be included.

The method is general and reliability level $\beta$ and distribution type can be changed if required. It reflects all types of failure. Its sensitivity to random variation of all material parameters is automatically included. Thus, there is no need of special modifications of concrete properties in order to compensate for greater random variation of certain properties. However, the method requires two separate non-linear analyses.

### 4.3.4 Partial factor method

It can be argued, why one should not calculate $R_d$ directly from Eq. (4-24). One of the reasons is the fact that design material values $f_d$ are extremely low and do not represent a real material. A simulation of real behaviour should be based on mean material properties and safety provision should be related to it. Analysis based on extremely low material properties may result in unrealistic redistribution of forces, which may not be on the conservative side. It may also change the failure mode. Therefore, the characteristic value $f_k$, which is not so far from the mean, but well reflects the scatter, is preferred for this purpose. However the recent studies including the present one do not confirm these arguments and indicate that a calculation of design resistance based on design input values is possible, as will be shown in the examples.

This document is the intellectual property of the fib – International Federation for Structural Concrete. All rights reserved.
This PDF of fib Bulletin 86 is intended for use and/or distribution solely within fib National Member Groups.

### 4.3.5 Nonlinear analysis

Examples in this chapter are analysed with program ATENA for non-linear analysis of concrete structures. ATENA is capable of a realistic simulation of concrete behaviour in the entire loading range with ductile as well as brittle failure modes as shown in papers by Cervenka[158; 159]. The numerical analysis is based on the finite element method and non-linear material models for concrete, reinforcement and their interaction. Tensile behaviour of concrete is described by smeared cracks, crack band and fracture energy, compressive behaviour of concrete is described by a damage model with hardening and softening. In the examples presented the reinforcement is modelled by truss elements embedded in two-dimensional isoparametric concrete elements. The nonlinear solution is performed incrementally with equilibrium iterations in each load step.

### 4.3.6 Examples of application

The performance of safety formats presented will be tested on several examples ranging from simple statically determinate structures with bending failure mode up to statically indeterminate structures with shear failure modes.

#### 4.3.6.1 Example 1: Simply supported beam in bending

A simply supported beam is uniformly loaded as shown in Fig. 4-4. The beam has a span of 6 m, rectangular cross/-section of $h$ = 0.3 m, $b$ = 1 m. It is reinforced with 5Φ14 along the bottom surface. The concrete type is C30/37 and reinforcement has a yield strength of 500 MPa. The failure occurs due to bending with reinforcement yielding.

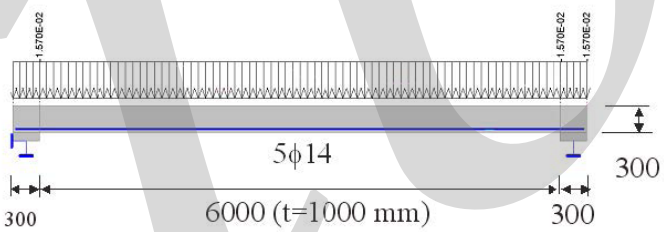


Fig. 4-4 Beam geometry with distributed design load for example 1

#### 4.3.6.2 Example 2: Deep beam

A continuous deep beam with two spans is shown in Fig. 4-5 and Fig. 4-6. It corresponds to one of the beams tested at Delft University of Technology by Asin[160]. It is a statically indeterminate structure with a brittle shear failure.

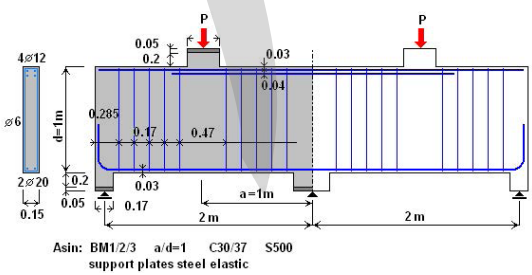


Fig. 4-5 Deep beam in Example 2

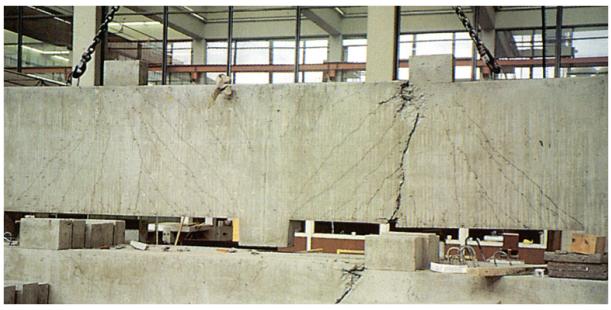

Fig. 4-6 Laboratory test of deep beam

This document is the intellectual property of the fib – International Federation for Structural Concrete. All rights reserved.
This PDF of fib Bulletin 86 is intended for use and/or distribution solely within fib National Member Groups.

#### 4.3.6.3 Example 3: Bridge pier

This example is chosen in order to verify the behaviour of the various safety formats in the case of a problem with second order effect (i.e. geometric nonlinearity). It is adopted from a practical bridge design in Italy that was published by[156]. It is a bridge pier loaded by normal force and moment in the top, Fig. 4-7.

Fig. 4-7 Bridge pier in Example 3

Fig. 4-8 Railway bridge in Example 4. Top – model, bottom real structure

#### 4.3.6.4 Example 4 : Railway frame bridge

The bridge frame structure in Sweden shown in Fig. 4-8 fails by a combined action of bending and shear. It is an existing bridge that was subjected to a field test up to failure by a single load in the middle of the left span.

#### 4.3.6.5 Example 5: Large shear beam

The large beam tested by Yoshida at the University of Toronto[161], Fig. 4-9, was experimentally investigated in a project about "Shear Reinforcement for Large Lightly Reinforced Concrete Members". In this beam no vertical reinforcement was provided. It failed in a brittle way due to formation of a diagonal crack. The large size is remarkable, with depth/length/thickness = 2/12/0.3 m, which exceeds the size range usually investigated. Probabilistic analysis was done by Dolezel and Novak at the Technical University in Brno[162].

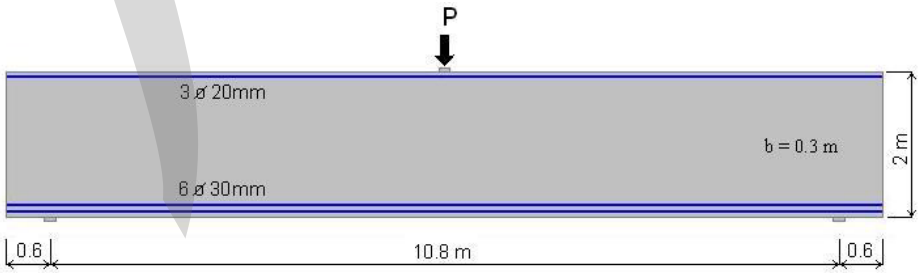


Fig. 4-9 Large beam tested by Yoshida[161]

This document is the intellectual property of the fib – International Federation for Structural Concrete. All rights reserved.
This PDF of fib Bulletin 86 is intended for use and/or distribution solely within fib National Member Groups.

#### 4.3.6.6 Case study

All examples were calculated by non-linear analysis, where the load was gradually increased up to failure. Typical results are illustrated on the case of the simple supported beam of Example 1. Fig. 4-10 shows the beam response for increasing load using various safety formats described in Section 3. The straight dashed line denoted as EN 1992-1 represents the load-carrying capacity given by standard design formulas based on beam model (plane section, hand calculation) and critical section check by partial factor method. The curve denoted as PSF corresponds to the nonlinear analysis with material parameters according to partial factor method. These two methods are based on the same safety format, PSF, and the differences are only due to different analysis models used: cross section analysis with zero tensile strength of concrete (hand calculation) and FE analysis utilizing design tensile strength. The other curves correspond to the analyses with different material properties as specified by the safety format approaches that are presented in Section 2.

The response curve EN 1992-2[154] is obtained from an analysis, where the material parameters are given by Section 3.3. For the ECOV method (Section 3.4), two separate analyses are needed: one using mean values of material properties and other with characteristic values. The results from these two analyses are denoted by the labels "Mean" and "Char." respectively.

For each example, a full probabilistic analysis was performed. Each probabilistic analysis consisted of several (from 32 to 64) non-linear analyses with randomly chosen material properties based on LHS sampling. The design resistance is then obtained by a probabilistic analysis of randomly generated resistances.

Calculated design resistances for all examples and various methods are compared in Fig. 4-10. The design resistances are normalized with respect to the values obtained by full probabilistic analysis. The probabilistic analysis served as a reference for the most exact result.

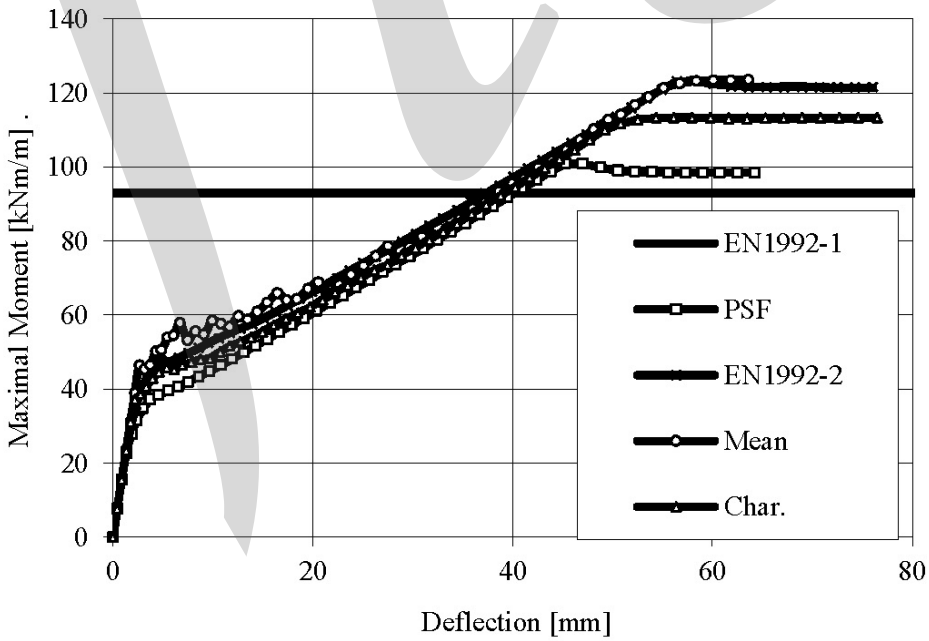


Fig. 4-10 Load-displacement diagrams for beam in Example 1

This document is the intellectual property of the fib – International Federation for Structural Concrete. All rights reserved.
This PDF of fib Bulletin 86 is intended for use and/or distribution solely within fib National Member Groups.

Table 4-14 Comparison of various safety formats.

| | $R_d / R_d^{prob}$ | | | |
|---|---|---|---|---|
| | PSF | ECOV | EN 1992-2 | Probabilistic |
| Example 1 Bending | 1.04 | 1.04 | 0.99 | 1.0 |
| Example 2 deep beam | 1.02 | 1.04 | 1.0 | 1.0 |
| Example 3 bridge pier | 0.98 | 1.04 | 0.96 | 1.0 |
| Example 4 bridge frame | 0.99 | 0.96 | 0.92 | 1.0 |
| Example 5 shear beam | 1.03 | 0.98 | 1.02 | 1.0 |
| average | 1.01 | 1.01 | 0.98 | 1.0 |

### 4.3.7 Concluding remarks

Two methods of global safety format applied to the safety assessment by nonlinear analysis were presented and verified in a case study. The method ECOV (Estimate of Coefficient Of Variation) can capture the random variation of resistance. It requires two non-linear analyses with mean and characteristic values of input parameters, respectively. Other safety formats suitable for non-linear analysis that are based on global resistance are also presented. They are: the global approach proposed by EN 1992-2, fully probabilistic analysis and a simple approach based on design values of input parameters, i.e. characteristic parameters reduced by partial safety factors (PSF). The last approach is usually not recommended by design codes, but practicing engineers often overlook this fact, and use this approach. The case study shows that PSF method gives results comparable with other more sophisticated methods. The safety formats discussed are tested on five examples. They include ductile as well as brittle modes of failure and second order effect (of large deformation). For the range of problems investigated, all the methods provide consistent results.

Based on the limited set of examples the following conclusions are drawn:

- The differences between all methods are not significant. None of the methods, PSF, EN 1992-2 and ECOV is superior to others.
- EN 1992-2 method using a fixed global factor $\gamma_R$ = 1.27 gives slightly more conservative results comparing to other methods.
- The proposed ECOV method gives results consistent with PSF and Probabilistic method.
- The PSF method, gives results consistent with Probabilistic analysis. It is a natural extension of the conventional PSF approach to the design based on non-linear analysis.

Fully probabilistic analysis is sensitive to the type of random distribution assumed for input variables. It offers a rational safety assessment in which real random properties of materials and other parameters can be utilized. The presented study was too limited to draw generally valid conclusions. However, it supports the authors experience that nonlinear analysis can be applied using any of the presented safety formats. The choice of an appropriate safety format depends on the specific situation (design of new structure, assessment of existing structure, knowledge of specific material data). The methods are currently subjected to further validation for other types of structures and failure modes.

This document is the intellectual property of the fib – International Federation for Structural Concrete. All rights reserved.
This PDF of fib Bulletin 86 is intended for use and/or distribution solely within fib National Member Groups.

# 5. Testing for assessment and design

## 5.1 Testing for design

In numerous fields of structural and civil engineering, experimental investigations aim at the development of resistance models based on the experimental data and at raising the design quality to sufficient safety levels. Load capacity, serviceability and also durability of structures depend significantly on the mechanical characteristics of the materials used. These characteristics are frequently measured using simplified, occasionally even idealized, test methods. At the same time, different load and ambient conditions are simulated in the laboratory in order to reproduce reality. Such tests may be performed by directly determining the load resistance or serviceability of structures or their elements for specific load conditions (e.g. fire, snow or concentrated loads). Alternatively, the reduction of uncertainties regarding specific parameters of the resistance model may be tested. This category of experiments also covers tests of components or groups of components, as for example sheet or plate constructions.

### 5.1.1 Design and planning

In the design and planning of the test series, several points need to be taken into consideration (see Fig. 5-1). The objectives and the range of applications should be clearly specified in advance. This includes the definition of the required characteristics, the identification of the influence of specific parameters, the potential limits of the test and possibly the necessary transfer function of the model regularities.

All essential characteristics and factors, such as geometrical imperfections, construction production methods and size and sequence effects, have to be taken into consideration for a successful prediction of the experimental results. The expected types of failure and the computational models need to be described in relation to these parameters of influence. Pre-tests for further test planning are advisable in cases where the relevant type of failure is not known (e.g. for prototypes).

The construction conditions should be carefully reproduced as realistically as possible when defining test elements and specimens. This is relevant for the dimensions and the tolerances as well as for the production and the sampling methods. The quantity of test elements and specimens depends on existing experience or prior information. It is essential to choose statistically representative sampling specimens.

The load conditions and the ambient conditions need to include load initiation and variation in time, temperature, relative humidity and influences by fluid or gaseous media. The loading sequence should be defined such that the specified conditions for the structure include not only merely typical, but even especially demanding conditions. Adequate test facilities and measuring methods are necessary for obtaining results of sufficient quality, and the accuracy of the sensors and the signal solution play a decisive role in the digital processing. Further attention needs to be paid to sufficient resistance and stiffness of the construction of both load initiation and bearings and to an unrestricted deformation path. A detailed measuring schedule needs to be developed in preparation for each test.

This document is the intellectual property of the fib – International Federation for Structural Concrete. All rights reserved.
This PDF of fib Bulletin 86 is intended for use and/or distribution solely within fib National Member Groups.

### 5.1.2 Derivation of design values

Two methods are commonly used to derive design values for characteristics of construction materials or element resistances:

- Determination of the characteristic value, division by a partial safety factor and (in some cases) multiplication with a transfer factor.
- Direct determination of the design value under implicit or explicit consideration of the transfer function and the required reliability.

Prior information gained from previous tests or theoretical reflections may be used in those cases where influences like scale effects, time or duration dependencies or ambient, load and constraint conditions do not provide sufficient information. The evaluation of the test results should be based on statistical methods. The application of distribution functions and their parameters is essential as well. In those cases where significant inconsistencies between the experimental results and the prediction emerge, additional tests are necessary, as for example tests under different conditions or modifications of the theoretical models. The methods presented in this chapter are suitable only in those cases where the statistical data are valid for specific basic populations which are distributed with sufficient homogeneity, and where a sufficient number of measurement results are available. Where a single property $X_i$ determines the resistance $R$ of a product (e.g. the compressive strength of concrete), the design or characteristic value may be specified directly with the corresponding partial safety factor. Where several properties $X_i$ influence the resistance R, the derivation of the design value has to take into consideration effects by other properties $X_j$, model uncertainties, and other effects such as scale or volume.

### 5.1.3 Outlier test

In those cases where single values exhibit significant deviations within a test run that cannot be explained by systematic failures, as for example measurement, calculation, write or data logging errors, an outlier test may facilitate meaningful evaluation. Such a test provides critical information on whether a differing single value is to be assigned to the population accumulated by the other single values or not.

No random deviation of a single value is possible, and so an excluded single value may be defined as an outlier and therefore omitted from the analysis. It needs to be indicated in the analysis records that this single value was eliminated as an outlier. Repeated application of the outlier test to the remaining single values is not acceptable!

#### 5.1.3.1 David-Hartley-Pearson-Test

In those cases where n readings of a sample are realizations of a Gaussian distribution, the David-Hartley-Pearson-Test hypothesis may be useful. $H_0$: The largest (or smallest) reading belongs to the sample. The hypothesis $H_0$ will be abolished on level $\alpha$, if the following can be applied:

$$Q = \frac{R}{S} = \frac{x_{\max} - x_{\min}}{\sqrt{\frac{1}{n-1}\sum_{i=1}^{n}\left(x_i - m_x\right)^2}} > Q_{n;1-\alpha} \tag{5-1}$$

*This document is the intellectual property of the fib – International Federation for Structural Concrete. All rights reserved.*
*This PDF of fib Bulletin 86 is intended for use and/or distribution solely within fib National Member Groups.*

Several quantiles $Q_{n;y}$ for an evaluation of the David-Hartley-Pearson-Test are given in Table 5-1.

Table 5-1 Quantiles $Q_{n;y}$ of the David-Hartley-Pearson-Test

| n | 3 | 4 | 5 | 6 | 7 | 8 | 9 | 10 | 12 | 15 | 20 | 30 | 40 | 50 | 100 |
|---|---|---|---|---|---|---|---|---|---|---|---|---|---|---|---|
| $Q_{n;0,95}$ | 2.00 | 2.43 | 2.75 | 3.01 | 3.22 | 3.40 | 3.55 | 3.69 | 3.91 | 4.17 | 4.49 | 4.89 | 5.15 | 5.35 | 5.90 |
| $Q_{n;0,99}$ | 2.00 | 2.45 | 2.80 | 3.10 | 3.34 | 3.54 | 3.72 | 3.88 | 4.13 | 4.43 | 4.79 | 5.25 | 5.54 | 5.77 | 6.36 |

In those cases where the hypothesis $H_0$ will be abolished, the smallest $x_{min}$ or the largest $x_{max}$ value of the test series will be assessed as an outlier, depending on which of the two has the larger distance to the mean value $m_x$. In those cases where both are at an equal distance, both values will be eliminated.

#### 5.1.3.2 Grubbs-Test

The Grubbs outlier test is another test based on the assumed Gaussian distribution for the population from which a present test series $x_1,...x_n$ and in respect $x_{min},...x_{max}$ was taken. The hypothesis $H_{01}$:$x_{min}$ is not an outlier will be abolished on the level $\alpha$, if

$$T_1 = \frac{m_x - x_{\min}}{s} > T_{n;1-\alpha} \tag{5-2}$$

and the hypothesis $H_{01}$: $x_{max}$ is not an outlier will be abolished on the level $\alpha$, if

$$T_n = \frac{x_{\max} - m_x}{s} > T_{n;1-\alpha} \tag{5-3}$$

Table 5-2 Critical values for $T_{n;y}$ in the Grubbs-Test

| n | 3 | 4 | 5 | 6 | 7 | 8 | 9 | 10 | 12 | 15 | 20 | 30 | 40 | 50 | 100 |
|---|---|---|---|---|---|---|---|---|---|---|---|---|---|---|---|
| $T_{n;0,95}$ | 1.15 | 1.46 | 1.67 | 1.82 | 1.94 | 2.03 | 2.11 | 2.18 | 2.29 | 2.41 | 2.56 | 2.75 | 2.87 | 2.96 | 3.21 |
| $T_{n;0,99}$ | 1.16 | 1.49 | 1.75 | 1.94 | 2.10 | 2.22 | 2.32 | 2.41 | 2.55 | 2.71 | 2.88 | 3.10 | 3.24 | 3.34 | 3.60 |

### 5.1.4 Design values

#### 5.1.4.1 General remarks

For the determination of design values $X_d$, various aspects such as experimental design, sampling assessment and evaluation of the quantile factors $k_n$ need to be investigated in detail.

This document is the intellectual property of the fib – International Federation for Structural Concrete. All rights reserved.
This PDF of fib Bulletin 86 is intended for use and/or distribution solely within fib National Member Groups.

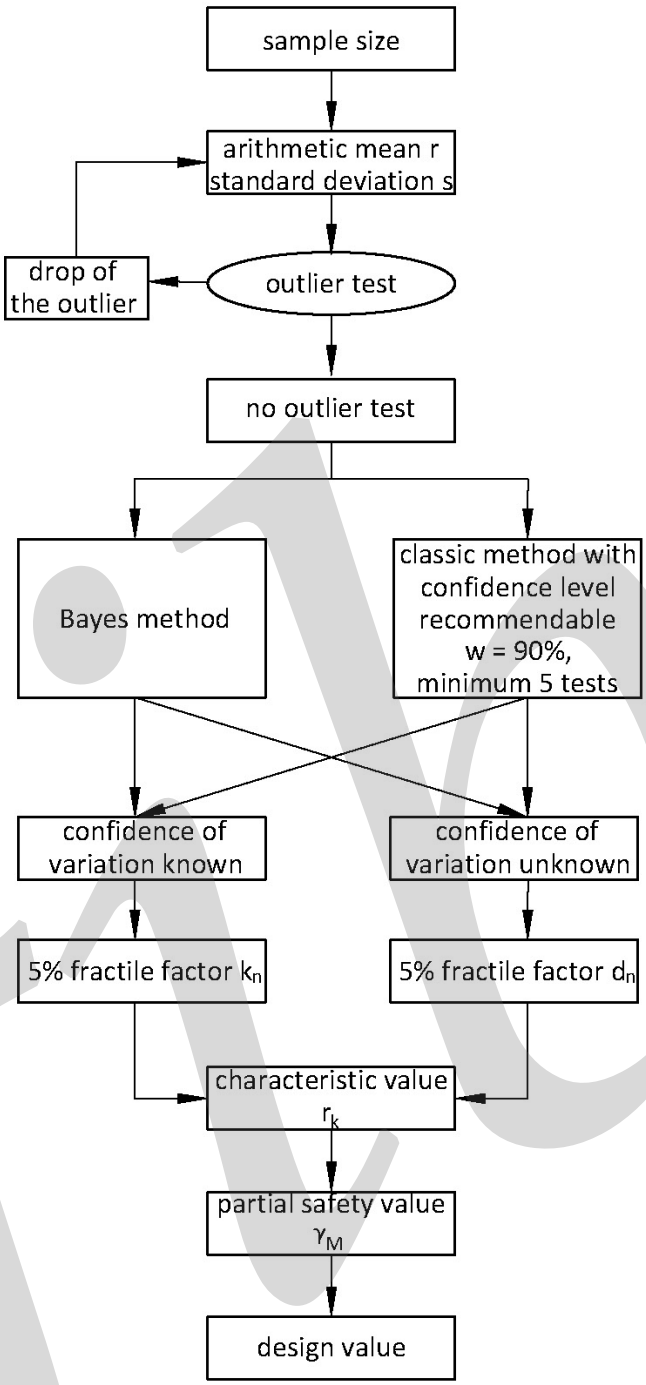


Fig. 5-1 illustrates a schematic sequence for the determination of design values based on experiment

### 5.1.4.2 Determination of the design values based on characteristic values

In the following chapter, text passages quoted from design codes (cursive) and in particular from EN 1990 shall lead to a better understanding. The method of determining the design values on the basis of the characteristic values is generally preferable, given that the partial safety is predetermined by the design method (e.g. Eurocode). Depending on the prior information, the following assumptions can be made:

- $V_x$ known: full prior information about the coefficient of variation exists
- $V_x$ unknown: no prior information about the coefficient of variation exists

*This document is the intellectual property of the fib – International Federation for Structural Concrete. All rights reserved.*
*This PDF of fib Bulletin 86 is intended for use and/or distribution solely within fib National Member Groups.*

The design value of a parameter is determined by

$$X_d = \eta_d \frac{X_k}{\gamma_m} = \frac{\eta_d}{\gamma_m}\left(m_X - k_n \cdot s_X\right) \tag{5-4}$$

The conversion factor $\eta_d$ depends both on the type of tests being performed and on the materials used. The values for $k_n$ (which is determined by the number of samples) are listed in Table 5-3 with a confidence level of 95%.

The line "$V_x$ known" is to be used where the coefficient of variation or an upper estimated value is known from prior information (e.g. earlier comparable tests). One example of use is the quality control of a continuous production. The line "$V_x$ unknown" is to be used where the coefficient of variation is not known from prior information and has to be estimated on the basis of the tests by

$$s_X^2 = \frac{1}{n-1}\sum_{i=1}^{n}\left(x_i - m_X\right)^2 \tag{5-5}$$

$$V_X = \frac{s_X}{m_X} \tag{5-6}$$

One example is the extension of a known product:

Table 5-3 Values $k_n$ for the characteristic values (5-%-fractile)

| n | 1 | 2 | 3 | 4 | 5 | 6 | 8 | 10 | 20 | 30 | ∞ |
|---|---|---|---|---|---|---|---|---|---|---|---|
| $V_x$ known | 2.31 | 2.01 | 1.89 | 1.83 | 1.80 | 1.77 | 1.74 | 1.72 | 1.68 | 1.67 | 1.64 |
| $V_x$ unknown | - | - | 3.37 | 2.63 | 2.33 | 2.18 | 2.00 | 1.92 | 1.76 | 1.73 | 1.64 |

COMMENT 1: This table is based on a Gaussian distribution

COMMENT 2: Applying a log-normal distribution becomes equation

$$X_d = \frac{\eta_d}{\gamma_m}\exp\left[m_Y - k_n \cdot s_Y\right]$$

whereas:

$$m_Y = \frac{1}{n}\sum \ln\left(x_i\right)$$

In the case $V_x$ is known from prior information,

$$s_Y = \sqrt{\ln\left(V_X^2 + 1\right)} \approx V_X$$

In the case $V_x$ is not known from prior information,

$$s_Y = \sqrt{\frac{1}{n-1}\sum\left(\ln x_i - m_Y\right)^2}$$

$k_n$-factors according to Table 5-4 are to be used in correspondence with the confidence level together with prior information about the coefficient of variation, and in such cases where the tests are executed on prototypes.

This document is the intellectual property of the fib – International Federation for Structural Concrete. All rights reserved.
This PDF of fib Bulletin 86 is intended for use and/or distribution solely within fib National Member Groups.

Table 5-4 5%-fractile for different confidence levels

| n | w = 75% | | w = 90% | | w = 95% | |
|---|---|---|---|---|---|---|
| | *s* known | *s* unknown | *s* known | *s* unknown | *s* known | *s* unknown |
| 2 | 2.12 | 5.12 | 2.55 | 13.09 | 2.81 | 26.26 |
| 3 | 2.03 | 3.15 | 2.38 | 5.31 | 2.59 | 7.66 |
| 4 | 1.98 | 2.68 | 2.28 | 3.96 | 2.47 | 5.14 |
| 5 | 1.94 | 2.46 | 2.22 | 3.4 | 2.38 | 4.21 |
| 6 | 1.92 | 2.33 | 2.17 | 3.09 | 2.32 | 3.71 |
| 7 | 1.9 | 2.25 | 2.13 | 2.89 | 2.27 | 3.4 |
| 8 | 1.88 | 2.19 | 2.1 | 2.75 | 2.23 | 3.19 |
| 9 | 1.87 | 2.14 | 2.07 | 2.65 | 2.19 | 3.03 |
| 10 | 1.85 | 2.1 | 2.05 | 2.57 | 2.16 | 2.91 |
| 15 | 1.82 | 1.99 | 1.98 | 2.33 | 2.07 | 2.57 |
| 20 | 1.8 | 1.93 | 1.93 | 2.21 | 2.01 | 2.4 |
| 30 | 1.77 | 1.87 | 1.88 | 2.08 | 1.94 | 2.22 |
| 40 | 1.75 | 1.83 | 1.85 | 2.01 | 1.9 | 2.13 |
| 50 | 1.74 | 1.81 | 1.83 | 1.96 | 1.88 | 2.06 |
| 100 | 1.71 | 1.76 | 1.77 | 1.86 | 1.81 | 1.93 |

### 5.1.5 Direct determination of design values

In order to directly determine the design value, both the relevant limit states and the required safety levels need to be taken into consideration. The relevant assumptions need to be compatible with the assumptions for the load and the expected service life has to be considered wherever necessary. The design value $X_d$ of a parameter $X$ will be determined as follows:

$$X_d = \eta_d \left( m_X - k_{d,n} \cdot s_X \right) \tag{5-7}$$

The value $\eta_d$ covers all uncertainties not covered by the test. Values for the specific quantile values $k_{d,n}$ are given in Table 5-5.

Table 5-5 Value $k_{d,n}$ for the design value for the proof of the load capacity

| n | 1 | 2 | 3 | 4 | 5 | 6 | 8 | 10 | 20 | 30 | ∞ |
|---|---|---|---|---|---|---|---|---|---|---|---|
| $V_X$ known | 4.36 | 3.77 | 3.56 | 3.44 | 3.37 | 3.33 | 3.27 | 3.23 | 3.16 | 3.13 | 3.04 |
| $V_X$ unknown | - | - | - | 11.4 | 7.85 | 6.36 | 5.07 | 4.51 | 3.64 | 3.44 | 3.04 |

COMMENT 1: The table is based on the assumption that the design value corresponds with the product $\alpha_R \cdot \beta = 0.8 \cdot 3.8 = 3.04$ and $X$ is Gaussian distributed. The probability to under-run is app. 0.1%. This assumptions are based on EN 1990.

COMMENT 2: Using a log-normal distribution the argument will be determined accordingly $X_d = \eta_d \exp[m_X - k_n \cdot s_X]$

This document is the intellectual property of the fib – International Federation for Structural Concrete. All rights reserved.
This PDF of fib Bulletin 86 is intended for use and/or distribution solely within fib National Member Groups.

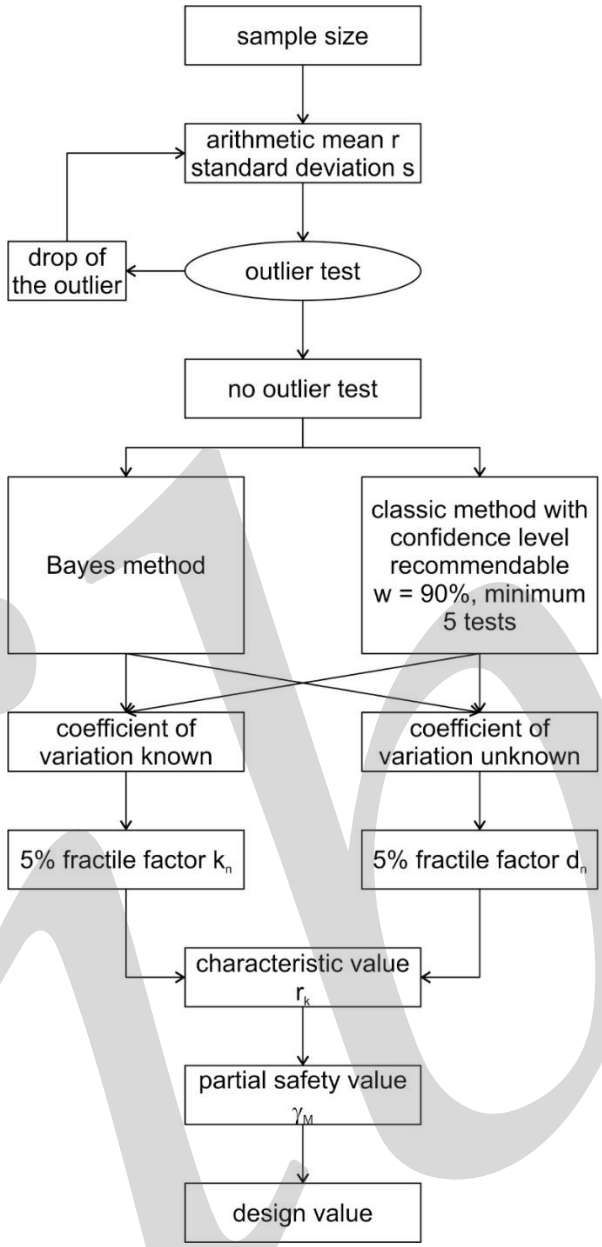


Fig. 5-2 Schematic sequence for the determination of design values based on experiment

### 5.1.5.1 Statistical determination of a resistance models

The following section deals closely with the EN 1990[40] norm. Parts of the design code text will be quoted and then illustrated by an example. This clause is mainly intended to define procedures (methods) for the calibration of resistance models and for the derivation of design values from tests and series of tests. Available prior information (knowledge or assumptions) will be used.

Based on the observation of actual behaviour in tests and on theoretical considerations, a "design model" should be developed, leading to the derivation of a resistance function. The validity of this model should be then checked by means of a statistical interpretation of all available test data. If necessary, the design model is then adjusted until sufficient correlation is achieved between the theoretical values and the test data. Deviation in the predictions obtained by using the design model (i.e. the variation of the "range of dispersion *d*") should also be determined from the tests. This deviation will need to be

This document is the intellectual property of the fib – International Federation for Structural Concrete. All rights reserved.
This PDF of fib Bulletin 86 is intended for use and/or distribution solely within fib National Member Groups.

combined with the deviations of the other variables in the resistance function in order to obtain an overall indication of deviation.

These other variables include:

- Deviation in material strength and stiffness
- Deviation in geometrical properties.

The characteristic resistance should be determined by taking account of the deviations of all the variables. These methods are presented as a number of discrete steps and some assumptions regarding the test population are made and explained; these assumptions are to be considered to be no more than recommendations covering some of the more common cases.

### 5.1.5.2 Standard evaluation procedure

- For the standard evaluation procedure, the following assumptions are made:
- The resistance function is a function of a number of independent variables $X_i$;
- A sufficient number of test results is available;
- All relevant geometrical and material properties are measured;
- There is no correlation (statistical dependence) between the variables in the resistance function;

All variables follow either a normal or a log-normal distribution.

NOTE: Adopting a log-normal distribution for a variable has the advantage that no negative values can occur. The standard procedure consists of seven steps, which will in the following be illustrated by means of an example. In our example, a single span girder is mounted on two supports and stressed at its centre with a single load.

Step 1: Development of a design model

(1) Development of a design model for the theoretical resistance $r_t$ of the member or structural detail considered, represented by the resistance function

$$r_t = g_{rt}(\underline{X}) = g(x_1,...,x_n) \tag{5-8}$$

In our example, the applicable load causing an approved deflection $w$ shall be determined for a single span girder.

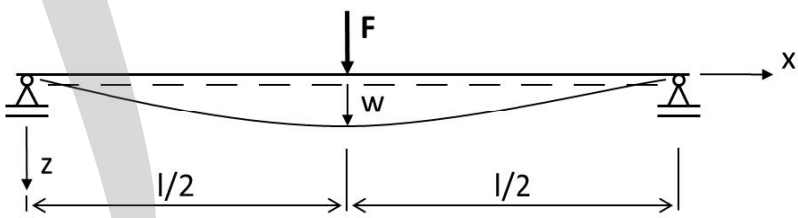


Fig. 5-3 Problem statement for the statistical determination of a resistance model

The deflection $w(z)$ may be calculated from theoretical considerations according to Eq. (5-9). In the modelling, ideal bearing conditions and elastic material behaviour are assumed.

This document is the intellectual property of the fib – International Federation for Structural Concrete. All rights reserved.
This PDF of fib Bulletin 86 is intended for use and/or distribution solely within fib National Member Groups.

$$w = l^3 \cdot F \Big/ 48E \cdot I_y \tag{5-9}$$

The design model for the determination of the resistance $r_t$ for a prescribed deformation may be obtained after a simple transformation according to Eq. (5-10).

$$g_n(X) = r_t = (48E \cdot I_y \cdot w) \Big/ l^3 \tag{5-10}$$

(2) The resistance function should cover all relevant basic variables ($X_1,\ldots,X_n$) that affect the resistance at the relevant limit state. The basic parameters $X$ (according to Table 5-6) can be defined for the design model mentioned. Every basic parameter can be described by the mean value and coefficient of variation $V_x$ The coefficient of variation $V_x$ is calculated by dividing the standard derivation by the mean value.

Table 5-6 Stochastic parameters for the considered problem

| Description | Symbol | Unit | $m_X$ | $V_X$ |
|---|---|---|---|---|
| Young's modulus | $E$ | [kN/m²] | 23000 | 0.05 |
| Moment of inertia | $I_y$ | [m4] | 0.0036 | 0.08 |
| Span | $l$ | [m] | 5.00 | 0.01 |
| Deflection | $w(z)$ | [m] | 0.01 | 0.50 |

(3) All basic parameters should be measured for each test specimen and should be available for use in the evaluation. According to this demand, all parameters included in Eq. (5-9) need to be measured previous to the tests. For parameter $I$, all required determinants ($I = b \cdot h^3/12$) need to be measured respectively. The survey of these parameters for each specimen provides a dataset that enables derivation of both the mean value and the scattering value – standard derivation, $V_x$.

Step 2: Comparison of experimental and theoretical values

(1) Substitute the actual measured properties into the resistance function so as to obtain theoretical values $r_{ti}$ to form the basis of a comparison with the experimental values $r_{ei}$ from the tests.

Table 5-7 Comparison of the values $r_{ti}$ and $r_{ei}$

| Test | $E$ [kN/m²] | $I_y$ [m⁴] | $L$ [m] | $w(z)$ [m] | $r_{ti}$ [kN] | $r_{ei}$ [kN] |
|---|---|---|---|---|---|---|
| 1 | 22607000 | 0.0036 | 8.94 | 0.0082 | 44.83 | 46.96 |
| 2 | 22019000 | 0.0037 | 6.60 | 0.0086 | 116.98 | 103.92 |
| 3 | 22922000 | 0.0037 | 6.34 | 0.0081 | 129.39 | 142.85 |
| 4 | 22176000 | 0.0035 | 9.19 | 0.0124 | 59.52 | 47.91 |
| 5 | 22894000 | 0.0036 | 8.15 | 0.0111 | 81.12 | 86.88 |
| 6 | 22139000 | 0.0036 | 9.67 | 0.0121 | 51.19 | 50.72 |
| 7 | 22935000 | 0.0037 | 5.68 | 0.0128 | 284.52 | 335.29 |
| 8 | 22353000 | 0.0036 | 8.04 | 0.0112 | 82.24 | 69.02 |
| 9 | 22199000 | 0.0037 | 5.22 | 0.0129 | 357.56 | 397.50 |

The first five columns of Table 5-7 show the measured values of the specimens for 9 test readings. The 6th column shows the calculated value for the specific specimen and the 7th column shows the experimental value $r_{ei}$. Plotting the calculated value of the 6th column versus the experimental value of the 7th column in a diagram complies with the following demand:

This document is the intellectual property of the fib – International Federation for Structural Concrete. All rights reserved.
This PDF of fib Bulletin 86 is intended for use and/or distribution solely within fib National Member Groups.

(2) The points representing pairs of corresponding values ($r_{ti}$,$r_{ei}$) should be plotted on a diagram, as indicated in Fig. 5-4.

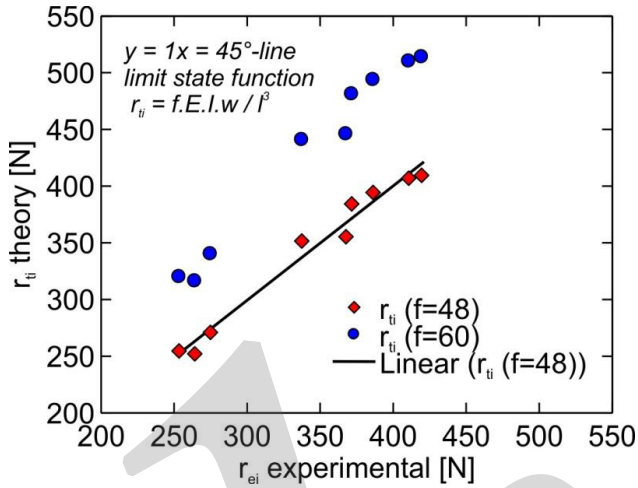


Fig. 5-4 Pairing of values ($r_{ti}$, $r_{ei}$) to demonstrate the model uncertainty

(3) If the resistance function is exact and complete, then all of the points will lie on the bisector line. In practice the points will show some scatter, but the causes of any systematic deviation from that line should be investigated to check whether this indicates errors in the test procedures or in the resistance function.

The diagram provides information about the quality of the model equation. In the current case, the obtained values exhibit good applicability of the chosen design model, as can be seen from the relatively small scattering around the bisecting line.

The values $r_{t,60}/r_{ei}$ show a systematic error. It is obvious that these values range above the bisecting line. This systematic error results from the change of the constant factor 48 to the factor 60 for the design equation.

$$g_n(X) = r_{t,60} = \left(60E \cdot I_y \cdot w\right) / l^3 \tag{5-11}$$

Step 3: Estimate of the mean value correction factor *b*

(1) Represent the probabilistic model of the resistance *r* in the format:

$$r = b \cdot r_t \cdot \delta \tag{5-12}$$

Here, the uncertainties which are hidden in the deterministic calculated value $r_t$ are included with the spread and the correction of the mean value. A similar formulation for the calculation of the resistance can be found in Schneider et al.[163], compare Eq. (5-13).

$$R = M \cdot F \cdot A \tag{5-13}$$

This formulation, according Schneider, considers the model fuzziness *M*, the material characteristics (strength, Young's modulus …) and the dimensions, as the resulting parameters such as moment of inertia of 1st and 2nd order, or the area (*A*), emerge as scattered parameters in terms of scattered values.

Model fuzziness[163]: Due to the fact that certain influences will usually be neglected, knowingly or unknowingly, in the set-up of a design model, deviations between calculation and test results are to be expected. The model variable M can be determined from tests by dividing the test results $r_{EXP}$ by the corresponding calculated value from the model $r_{Mod}$:

This document is the intellectual property of the fib – International Federation for Structural Concrete. All rights reserved.
This PDF of fib Bulletin 86 is intended for use and/or distribution solely within fib National Member Groups.

$$M = \frac{r_{Exp}}{r_{Mod}} \cdot \frac{r_{ei}}{r_{ti}} \tag{5-14}$$

From a large number of tests, a histogram $M$ can be obtained to extract the mean value $m_M$ and the standard deviation $s_M$. A distribution describing the histogram in a good approximation shall be chosen and $m_M = \mu_M$ and $s_M = \sigma_M$ shall be related.

For good models, the result is $\mu_M \approx 1$. Due to the fact that usually, conservative models are used, the result is $\mu_M > 1$. Accordingly, the value of $\sigma_M$ turns out to be rather diverse. For good models (e.g. for the bending resistance of steel or concrete cross-sections), coefficients of variation of a few percent can be expected, while for models of lesser quality (shear resistance or punching of reinforced concrete), 10 to 20% can be expected. The mean value $\mu_R$ and the coefficient of variation $V_R$ of $R$ will be calculated by the common rule for products.

$$\mu_R = \mu_M \cdot \mu_F \cdot \mu_A \tag{5-15}$$

$$v_R = \sqrt{v_M^2 + v_F^2 + v_A^2} \tag{5-16}$$

As mentioned previously, the resistance tends to be log-normal distributed, as it appears as product or variables. Ceteris paribus negative resistances are inconceivable. Examples for distributions of resistance parameters can be taken from Vrouwenvelder & Siemes[164].

The main difference of the formulation (4-12) is a result of considering all variables as scattered values. In equation (4-11) of the preliminary version of EN 1990, only parameter $\delta$ is considered a scattered value. The mean value correction b is considered a deterministic parameter. In the following, the determination of these 2 parameters is shown.

$b$ is the "Least Squares" best-fit to the slope, given by:

$$b = \frac{\sum r_{ei} \cdot r_{ti}}{\sum r_{ti}^2} \tag{5-17}$$

Table 5-8 was prepared for the example "single span girder" discussed previously.

Table 5-8 Calculation of the mean value deviation $b$

| Test | $r_{ti}$ | $r_{ei}$ | $r_{ei}\, r_{ti}$ | $r_t^2$ |
|---|---|---|---|---|
| 1 | 44.83 | 46.96 | 2105.22 | 2009.73 |
| 2 | 116.98 | 103.92 | 12155.52 | 13681.98 |
| 3 | 129.39 | 142.85 | 18483.36 | 16741.77 |
| 4 | 59.52 | 47.91 | 2851.60 | 3542.63 |
| 5 | 81.12 | 86.88 | 7047.71 | 6580.45 |
| 6 | 51.19 | 50.72 | 2596.36 | 2620.42 |
| 7 | 284.52 | 335.29 | 95396.71 | 80951.63 |
| 8 | 82.24 | 69.02 | 5745.22 | 6928.90 |
| 9 | 357.56 | 397.50 | 142130.10 | 127849.15 |
| | | | 288511.80 | 260906.66 |

For the discussed example, a mean value correction $b$ = 288511.8/260906.66 = 1.106 (ca. 10%) is obtained. With this mean value correction, the mean value of the theoretical

This document is the intellectual property of the fib – International Federation for Structural Concrete. All rights reserved.
This PDF of fib Bulletin 86 is intended for use and/or distribution solely within fib National Member Groups.

resistance function $r_m$ may be determined, according to the next point mentioned in EN 1990, where the design function $g_{rt}$ is calculated with the mean values of the basic variable $X_m$.

(2) The mean value of the theoretical resistance function, calculated using the mean values $X_m$ of the basic variables, can be obtained from:

$$r_m = b \cdot r_t(X_m) = b \cdot g_{rt}(X_m)\delta \tag{5-18}$$

For the discussed problem, the result is the dataset listed in Table 5-9 $g_{rt}(X_m)$ of 31.80 kN. The still unknown scattering value $\delta$ will be discussed in the following step.

Table 5-9 Stochastic parameters for the calculation of the unknown scattering value $\delta$

| Description | Symbol | Unit | $m_X$ | $V_X$ |
|---|---|---|---|---|
| Young's modulus | $E$ | [kN/m²] | 23000000 | 0.05 |
| Moment of inertia | $I_y$ | [m⁴] | 0.0036 | 0.08 |
| Span | $l$ | [m] | 5.00 | 0.01 |
| Deflection | $w(z)$ | [m] | 0.01 | 0.50 |

$$g_n(X) = r_t = (48E \cdot I_y \cdot w)\big/ l^3 \tag{5-19}$$

$$g_n(X) = r_t = \left(48 \cdot 2300000 \cdot 0.0036 \cdot 0.01\right)\big/ 5^3 \tag{5-20}$$

$$g_n(X) = r_t = 31.80 \tag{5-21}$$

Step 4: Estimate the coefficient of variation of the errors $\delta$

(1) The error term $\delta$ for each experimental value should be determined from following expression:

$$\delta_i = \frac{r_{ei}}{b \cdot r_{ti}} \tag{5-22}$$

This formulation is presented in the form of a table for the current problem. The last column shows the scattering values $\delta_I$ for each experimental value. These scattering values are logarithmized according to the demands of point (2) and result in the values $\Delta_i$ of the last column.

Table 5-10 Calculation of the scattering value $\delta_i$.

| Test | $r_{ti}$ | $r_{ci}$ | $\delta_i$ | $\Delta_i$ |
|---|---|---|---|---|
| 1 | 44.83 | 46.96 | 0.947 | -0.054 |
| 2 | 116.98 | 103.92 | 0.803 | -0.219 |
| 3 | 129.39 | 142.85 | 0.998 | -0.002 |
| 4 | 59.52 | 47.91 | 0.728 | -0.318 |
| 5 | 81.12 | 86.88 | 0.969 | -0.032 |
| 6 | 51.19 | 50.72 | 0.896 | -0.110 |
| 7 | 284.52 | 335.29 | 1.066 | 0.064 |
| 8 | 82.24 | 69.02 | 0.750 | -0.288 |
| 9 | 357.56 | 397.50 | 1.005 | 0.005 |

(2) From the values of $\delta_i$, an estimated value for $V_\delta$ is to be determined by defining:

$$\Delta_i = \ln(\delta_i) \tag{5-23}$$

*This document is the intellectual property of the fib – International Federation for Structural Concrete. All rights reserved.*
*This PDF of fib Bulletin 86 is intended for use and/or distribution solely within fib National Member Groups.*

After determining the logarithmized values $\Delta_i$, the mean value $\Delta$ or the expected value $E(\Delta)$ according to point (3) of EN1990 may be determined.

(3) The estimated value $\Delta$ for $E(\Delta)$ should be obtained from:

$$\bar{\Delta} = \frac{1}{n} \cdot \sum_{i=1}^{n} \Delta_i \tag{5-24}$$

Applied to the current problem, an expected value is obtained as follows:

$$\bar{\Delta} = \frac{1}{9} \cdot (-0.953) = -0.1059 \tag{5-25}$$

The standard derivation as well as the coefficient of variation of this scattering parameter $D$ can be determined according to point (4) of EN1990:

(4) The estimated value $s_\Delta^2$ for $\sigma_\Delta^2$ should be obtained from:

$$s_\Delta^2 = \frac{1}{n-1} \sum_{i=1}^{n} \left(\Delta_i - \bar{\Delta}\right)^2 \tag{5-26}$$

(5) The expression:

$$V_\delta = \sqrt{\exp\left(s_\Delta^2\right) - 1} \tag{5-27}$$

may be used as the coefficient of variation $V_\delta$ of the $\delta$ error terms.

For the discussed problem, a coefficient of variation of app. 14% is the result:

$$s_\Delta^2 = \frac{1}{9-1} \cdot 0.1508 = 0.01885 \tag{5-28}$$

$$V_\delta = \sqrt{\exp(0.01885) - 1} = 0.138 \tag{5-29}$$

Step 5 : Analysis of the compatibility

(1) The compatibility of the test population with the assumptions made in the resistance function should be analysed.

(2) If the scatter of the $(r_{ei} \cdot r_{ti})$ values is too high to give economical design resistance functions, this scatter may be reduced in one of the following ways:

- Correction of the design model to take into account parameters which had previously been ignored;
- Modification of $b$ and $V_\delta$ by dividing the total test population into appropriate sub-sets for which the influence of such additional parameters may be considered to be constant.

(3) To determine which parameters have most influence on the scatter, the test results may be split into subsets with respect to these parameters.

NOTE: The purpose is to improve the resistance function per sub-set by analysing each subset using the standard procedure. The disadvantage of splitting the test results into sub-sets is that the number of test results in each sub-set can become very small.

(4) When determining the fractile factors $k_n$ (see step 7), the $k_n$ value for the sub-sets may be determined on the basis of the total number of the tests in the original series.

This document is the intellectual property of the fib – International Federation for Structural Concrete. All rights reserved.
This PDF of fib Bulletin 86 is intended for use and/or distribution solely within fib National Member Groups.

NOTE: Attention is drawn to the fact that the frequency distribution for resistance can be better described by a bi-modal or a multi-modal function. Special approximation techniques may be used to transform these functions into a uni-modal distribution.

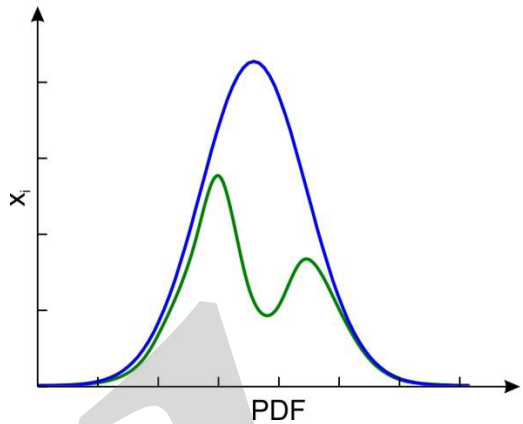


Fig. 5-5 Approximation of a multimodal distribution by a unimodal distribution

Step 6: Determination of the coefficients of variation $V_{Xi}$ of the basic variables

If it can be shown that is fully representative of the variation in reality the coefficients of variation $V_{Xi}$ of the basic variables in the resistance function may be determined on the basis of the test data. However, since this is not generally the case, the coefficients of variation VXi will usually need to be determined on the basis of some prior knowledge.

NOTE: Prior information can be taken from investigations of product data, test data on structures or from the literature. Among the substantial references for construction material characteristics and load conditions are JCSS[165, 166, 119].

Step 7: Determination of the characteristic value $r_k$ of the resistance

(1) If the resistance function for *j* basic variables is a product function of the form

$$r = b \cdot r_t = b\left\{X_1 \cdot X_2 \ldots X_j\right\}\delta \tag{5-30}$$

the mean value $E(r)$ may be obtained from:

$$\mathrm{E}(r) = b\left\{\mathrm{E}\left(X_1\right)\cdot \mathrm{E}\left(X_2\right)\ldots \mathrm{E}\left(X_j\right)\right\} = b \cdot g_{rt}\left(\underline{X}_m\right) \tag{5-31}$$

and the coefficient of variation may be obtained from the product function:

$$V_r^2 = \left(V_\delta^2 + 1\right)\left[\prod_{i=1}^{j}\left(V_{X_i}^2 + 1\right)\right] - 1 \tag{5-32}$$

(2) Alternatively, for small values (V ≤ 10%) of $V_\delta^2$ and $V_{X_i}^2$ the following approximation may be used:

$$V_r^2 = V_\delta^2 + V_{rt}^2 \tag{5-33}$$

with

$$V_{rt}^2 = \sum_{i=1}^{j} V_{X_i}^2 \tag{5-34}$$

*This document is the intellectual property of the fib – International Federation for Structural Concrete. All rights reserved.*
*This PDF of fib Bulletin 86 is intended for use and/or distribution solely within fib National Member Groups.*

Since the formulation of the discussed design model shows a product form and the coefficients of variation are comparatively small, the following statement can be applied:

$$V_{rt}^2 = V_E^2 + V_I^2 + V_l^2 + V_w^2 \tag{5-35}$$

*E* Young's modulus

*I* Moment of inertia

*l* Span

*w* Deflection

$$V_{rt}^2 = 0.05^2 + 0.08^2 + 0.01^2 + 0.5^2 = 0.259 \tag{5-36}$$

$$V_r^2 = V_\delta^2 + V_{rt}^2 \tag{5-37}$$

$$V_r^2 = 0.138^2 + 0.259^2 = 0.086 \tag{5-38}$$

(3) If the resistance function is a more complex function of the form:

$$r = b \cdot r_t \cdot \delta = b \cdot g_{rt}\left(X_1, X_2 ..., X_j\right)\delta \tag{5-39}$$

the mean value $E(r)$ may be obtained from:

$$\mathrm{E}(r) = b \cdot g_{rt}\left(\mathrm{E}\left(X_1\right), ..., \mathrm{E}\left(X_j\right)\right) = b \cdot g_{rt}\left(\underline{X}_m\right) \tag{5-40}$$

and the coefficient of variation $V_{rt}$ may be obtained from:

$$V_{rt}^2 = \frac{VAR\left[g_{rt}\left(\underline{X}\right)\right]}{g_{rt}^2\left(\underline{X}_m\right)} = \frac{1}{g_{rt}^2\left(\underline{X}_m\right)} \sum_{i=1}^{j} \left( \frac{\partial g_{rt}}{\partial X_i} \sigma_i \right)^2 \tag{5-41}$$

An example "metal anchors in concrete" is quoted in the appendix. This example illustrates how the partial derivatives of equation (5-41) have to be handled in order to obtain the required coefficient of variation $V_{rt}$. An alternative to the calculation of mean values and coefficients of variation is given by the probabilistic software packages "VAP"[167], "FREET"[168] and "CALREL[169].

(4) If the number of tests is limited (say $n < 100$), allowance should be made in the distribution of $\Delta$ for statistical uncertainties. The distribution should be considered as a central t-distribution with the parameters $\overline{\Delta}$, $V_{\Delta(r)}$ and $n$.

(5) In this case the characteristic resistance $r_k$ should be obtained from:

$$r_k = b \cdot g_R\left(\underline{X}_m\right) \exp\left(-k_\infty \cdot \alpha_{rt} \cdot Q_{rt} - k_n \cdot \alpha_\delta \cdot Q_\delta - 0.5 \cdot Q^2\right) \tag{5-42}$$

According to this formulation the 5% fractile is determined with a confidence level of approximately 75%. Within this formulation, the $Q$ factor describes the standard derivation in logarithmic notation. The a factors are factors of weighting, that measure the particular influence on the characteristic value, and the $k$ factors serve the calculation of the fractile values. These $k$ factors are a function of test number and confidence level as well as of prior information (see Table 5-3). The standard derivation in logarithmic notation is calculated by:

$$Q_{rt} = \sigma_{\ln(rt)} = \sqrt{\ln\left(V_{rt}^2 + 1\right)} \tag{5-43}$$

This document is the intellectual property of the fib – International Federation for Structural Concrete. All rights reserved.
This PDF of fib Bulletin 86 is intended for use and/or distribution solely within fib National Member Groups.

$$Q_\delta = \sigma_{\ln(\delta)} = \sqrt{\ln\left(V_\delta^2 + 1\right)} \tag{5-44}$$

$$Q = \sigma_{\ln(r)} = \sqrt{\ln\left(V_r^2 + 1\right)} \tag{5-45}$$

The related weighting factors can be calculated by:

$$\alpha_{rt} = \frac{Q_{rt}}{Q} \tag{5-46}$$

$$\alpha_\delta = \frac{Q_\delta}{Q} \tag{5-47}$$

where

$k_n$ is the characteristic fractile factor from Table 5-4 ($W$ = 75%) for the case "$V_x$ unknown";

$k_\infty$ is the value of $k_n$ for $n \to \infty$ [$k_\infty$ = 1.64];

$\alpha_{rt}$ is the weighting factor for $Q_{rt}$;

$\alpha_\delta$ is the weighting factor for $Q\delta$.

NOTE: The value of $V_\delta$ is to be estimated from the test sample under consideration.

Calculating the 5% fractiles for the discussed problem, the following values will be obtained:

$$Q_{rt} = \sigma_{\ln(rt)} = \sqrt{\ln\left(0.259^2 + 1\right)} = 0.255 \tag{5-48}$$

$$Q_\delta = \sigma_{\ln(\delta)} = \sqrt{\ln\left(0.138^2 + 1\right)} = 0.137 \tag{5-49}$$

$$Q = \sigma_{\ln(r)} = \sqrt{\ln\left(0.293^2 + 1\right)} = 0.286 \tag{5-50}$$

$$\alpha_{rt} = \frac{0.255}{0.286} = 0.892 \tag{5-51}$$

$$\alpha_\delta = \frac{0.137}{0.286} = 0.479 \tag{5-52}$$

$$\begin{aligned} r_k &= 1.106 \cdot 31.80 \\ &\quad \cdot \exp\left(-1.645 \cdot 0.892 \cdot 0.255 - 1.87 \cdot 0.479 \cdot 0.137 - 0.5 \cdot 0.286^2\right) \\ &= 20.54 \end{aligned} \tag{5-53}$$

(6) If a large number of tests ($n \geq 100$) is available, the characteristic resistance $r_k$ may be obtained from:

$$r_k = b \cdot g_{rt}\left(\underline{X}_m\right) \exp\left(-k_\infty \cdot Q - 0.5Q^2\right) \tag{5-54}$$

Standard evaluation procedure (method (b))

(1) In this case, the procedure is the same as before, with the exception that step 7 is adapted by replacing the characteristic fractile factor $k_n$ by the design fractile factor $k_{d,n}$

This document is the intellectual property of the fib – International Federation for Structural Concrete. All rights reserved.
This PDF of fib Bulletin 86 is intended for use and/or distribution solely within fib National Member Groups.

equal to the product $\alpha_R \cdot \beta$ assessed at 0.8 ·3.8 = 3.04 (as commonly accepted) to obtain the design value $r_d$ of the resistance.

(2) For the case of a limited number of tests (e.g. $n < 100$) the design value $r_d$ should be obtained from

$$r_d = b \cdot g_{rt}\left(\underline{X}_m\right)\exp\left(-k_{d,\infty} \cdot \alpha_{rt} \cdot Q_{rt} - k_{d,n} \cdot \alpha_\delta \cdot Q_\delta - 0.5Q^2\right) \tag{5-55}$$

where:

$k_{d,n}$ is the design fractile factor from table 5 for the case "$V_x$ unknown";

$k_{d,\infty}$ is the value of $k_{d,n}$ for n → ∞ [$k_{d,\infty}$ = 3.04];

NOTE: The value of $V_\delta$ is to be estimated from the test sample under consideration.

(3) For the case of a large number of tests the design value $r_d$ may be obtained from:

$$r_d = b \cdot g_{rt}\left(\underline{X}_m\right)\exp\left(-k_{d,\infty} \cdot Q - 0.5Q^2\right) \tag{5-56}$$

Use of additional prior knowledge

(1) If the validity of the resistance function $r_t$ and an upper bound (conservative estimate) for the coefficient of variation $V_t$ are already known from a significant number of previous tests, the following simplified procedure may be adopted when further tests are carried out.

(2) If only one further test is carried out, the characteristic value $r_k$ may be determined from the result $r_e$ of this test by applying:

$r_k = \eta_k \cdot r_e$

where:

$\eta_k$ is a reduction factor applicable in the case of prior knowledge that may be obtained from

$$\eta_k = 0.9\exp\left(-2.31V_r - 0.5V_r^2\right) \tag{5-57}$$

where:

$V_r$ is the maximum coefficient of variation observed in previous tests.

(3) If two or three further tests are carried out, the characteristic value $r_{em}$ may be determined from the mean value $r_k$ of the test results by applying:

$$r_k = \eta_k \cdot r_{em} \tag{5-58}$$

where: $\eta_k$ is a reduction factor applicable in the case of prior knowledge that may be obtained from:

$$\eta_k = \exp\left(-2.00V_r - 0.5V_r^2\right) \tag{5-59}$$

where: $V_r$ is the maximum coefficient of variation observed in previous tests provided that each extreme (maximum or minimum) value $r_{ee}$ satisfies the condition:

$$\left|r_{ee} - r_{em}\right| \le 0.10r_{em} \tag{5-60}$$

This document is the intellectual property of the fib – International Federation for Structural Concrete. All rights reserved.
This PDF of fib Bulletin 86 is intended for use and/or distribution solely within fib National Member Groups.

(4) The values of the coefficient of variation $V_r$ may be assumed for the types of failure to be specified (e.g. in the relevant design Eurocode), leading to the listed values $\eta_k$ given in Table 5-11 according to expressions (6-51) and (6-53).

Table 5-11 Reduction factors $\eta_k$

| Coefficient of variation $V_r$ | Reduction factor $\eta_k$ | |
|---|---|---|
| | For one test | For 2 or 3 tests |
| 0.05 | 0.80 | 0.90 |
| 0.11 | 0.70 | 0.80 |
| 0.17 | 0.60 | 0.70 |

### 5.1.5.3 Example for the determination of a design value

In the following an example is given for the calculation of the design resistance by means of a resistance model for anchors in concrete. The peak load $r_t$ of an undercut anchor in cracked concrete for a concrete disruption failure type can be calculated according the following:

$r_t = 9.5 \cdot \sqrt{f_c} \cdot h_{ef}^{1.5}$

$r_t$ Peak load [kN]

$f_c$ Concrete compressive strength [MPa]

$h_{ef}$ Anchoring depth [mm]

Fig. 5-6 compares the theoretical values with the experimental values of 90 tests according, where the anchoring depth as well as the concrete compressive strength was varied.

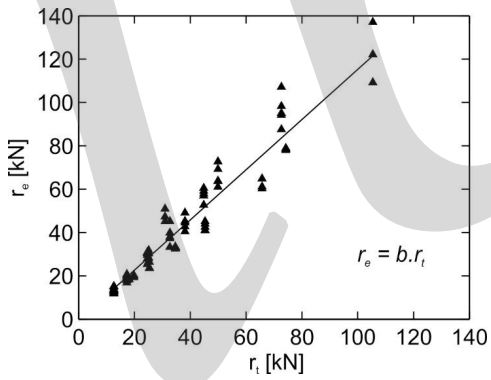


Fig. 5-6 Comparison of the experimental and the theoretical failure load of undercut anchors

Using the relationships outlined in the previous chapters, the mean value correction and the coefficient of variation for the scattering value $\delta$ can be obtained as follows:

$b = 1.029$

$V_\delta = 0.146$

Now, the characteristic resistance of an undercut anchor M10 is calculated with the parameters listed in Table 5-12. The partial derivatives of the coefficient of variation $V_{rt}$ need to be calculated due to the fact that the resistance function is a complex function of the basic variables $f_c$ and $h_{ef}$:

$$\frac{\partial g_{rt}}{\partial h_{ef}} = 1.5 \cdot 9.5 \sqrt{h_{ef} \cdot f_c} \tag{5-61}$$

This document is the intellectual property of the fib – International Federation for Structural Concrete. All rights reserved.
This PDF of fib Bulletin 86 is intended for use and/or distribution solely within fib National Member Groups.

$$\frac{\partial g_{rt}}{\partial h_{ef}} = 0.5 \cdot 9.5 h_{ef}^{1.5} \cdot f_c^{-0.5} \tag{5-62}$$

Table 5-12 Parameter for the calculation of the characteristic resistance

| $h_{ef}$ [mm] | $f_c$ [MPa] | $\sigma_{hef}$ [mm] | $\sigma_{fc}$ [MPa] | $k_n$ | $k_\infty$ | $r_m$ [kN] | $\gamma_M$ |
|---|---|---|---|---|---|---|---|
| 50 | 29.58 | 1 | 5.86 | 1.7[1)] | 1.64 | 18.27 | 1.8 |

$$V_{rt}^2 = \frac{1}{r_m^2}\left[\left(1.5 \cdot 9.5\sqrt{h_{ef} \cdot f_c}\,\sigma_{hef}\right)^2 + \left(0.5 \cdot 9.5 h_{ef}^{1.5} \cdot f_c^{-0.5} \cdot \sigma_{fc}\right)^2\right] = 0.01 \tag{5-63}$$

$$V_r^2 = V_\delta^2 + V_{rt}^2 = 0.032 \tag{5-64}$$

$$Q_{rt} = \sqrt{\ln\left(V_{rt}^2 + 1\right)} = 0.103 \tag{5-65}$$

$$Q_\delta = \sqrt{\ln\left(V_\delta^2 + 1\right)} = 0.146 \tag{5-66}$$

$$\alpha_{rt} = \frac{Q_{rt}}{Q} = 0.58 \tag{5-67}$$

$$\alpha_\delta = \frac{Q_\delta}{Q} = 0.819 \tag{5-68}$$

As $n < 100$ the characteristic value $r_k$ of the failure load is determined by

$$r_k = b \cdot r_m \exp\left(-k_\infty \cdot \alpha_{rt} \cdot Q_{rt} - k_n \cdot \alpha_\delta \cdot Q_\delta - 0.5Q^2\right) = 12.4kN \tag{5-69}$$

$$r_d = \frac{r_k}{\gamma_M} = 6.8kN \tag{5-70}$$

A standard derivation of 5 mm is assumed for the anchoring depth (possible e.g. for expansion anchors without clear mark for the anchoring depth). Consequently, the design value is reduced by approximately 7%. The design value is less sensitive with regard to the variation of the standard derivation of the concrete compressive strength.

a) Calculation of the design resistance from a test series

The mean value and standard derivation will be determined from a test series of 5 tests taking as a basis a Gaussian distribution:

$r_{em}$ = 17.04kN

$s$ = 1.66kN

The fractile for a confidence level of 90% and for unknown standard derivation needs to be calculated. The corresponding fractile factor is to be taken from Table 5-5 and yields 3.4. As a result

$$r_k = r_{em} - k_n \cdot s = 11.4kN \tag{5-71}$$

$$r_d = r_k / \gamma_M = 6.3kN \tag{5-72}$$

This document is the intellectual property of the fib – International Federation for Structural Concrete. All rights reserved.
This PDF of fib Bulletin 86 is intended for use and/or distribution solely within fib National Member Groups.

The compliance with the design value calculated for point a) is quite good. Due to the fact that there is no failure model for other failure types of metal anchors, as for example anchor slips (frequent in expansion anchors) or disruption of the concrete at present, the design values need to be determined by testing.

### 5.1.6 Probabilistic-based assessment of sampling

A frequent problem in engineering practice lies in the evaluation of samples $X$ from the resistance side (for example the load carrying capacity of small and large structural components) with regard to the specific design situation $R_d \geq S_d$ as defined in the relevant design standards.

An objective assessment of sample $X = (x_1,..x_n)$ with its more or less scattering properties requires a transformation of the individual realizations of the sample $x_i$ into a probability density function PDF (e.g. Normal distribution, Lognormal distribution, Weibull distribution etc.) using goodness-of-fit tests, examples of which are the $X^2$ test or the Kolmogoroff Smirnov test. Both these tests are possible with a total sample number $n$ that is in general smaller than the basic population $N$.

Alternatively, the PDF received after the goodness of fit test can be corrected for its standard deviation in order to then perform a $K$-factor correction of the fractile value. The $K$-factor correction depends on the total number of samples (see chapter 4.3).

Acceptance H0 or rejection H1 of sample $X$ with regard to its compliance with the design situation Rd ≥ Sd can be tested in the following ways (see also Fig. 5-7):

a) The exceedance probability $P_u$ of $X$ is determined with regard to the lower bound design value $R_d$ and compared with an acceptable probability $P_{rd}$.

$$P_u = P\left\{\left(X,n\right) \leq R_D\right\} \leq R_{Rd} \tag{5-73}$$

The sample X is accepted H0 or rejected H1 on the reliability level of the design value $R_d$ with an acceptable exceedance probability $P_{rd}$. The reliability level is contained implicitly in the relevant norm specifications (e.g., by the reliability index $\beta$ or the probability of failure pf respectively).

b) The exceedance probability $P_u$ of $X$ is determined with regard to the lower tail of the distribution $R$ and compared with an acceptable probability $P_R$.

$$P_u = P\left\{\left(X,n\right) \leq R\right\} \leq P_R \tag{5-74}$$

The sample X is accepted H0 or rejected H1 on the reliability level of the distribution $R$ with an acceptable exceedance probability $P_{Rd}$ of the lower tail of $R$. This formulation requires a reconstruction of distribution $R$ on the basis of the standards specific fractile values $r_k$. The acceptance probability of this formulation is usually higher than that of the formulation outlined in (a), as the tail of $R$ is taken into consideration and the safety zone defined by the partial safety factor $g_R$ is neglected.

c) The exceedance probability $P_u$ of $X$ is determined with regard to the design value $S_d$ and compared with an acceptable exceedance probability $P_{Sd}$.

$$P_u = P\left\{\left(X,n\right) \leq S_D\right\} \leq P_{Sd} \tag{5-75}$$

*This document is the intellectual property of the fib – International Federation for Structural Concrete. All rights reserved.*
*This PDF of fib Bulletin 86 is intended for use and/or distribution solely within fib National Member Groups.*

The sample $X$ is accepted H0 or rejected H1 on the reliability level of the load design value $S_d$ with an acceptable exceedance probability $P_{Sd}$. The reliability level is contained implicitly in the relevant norm specifications, as mentioned previously. This formulation neglects the safety margin on the resistance side. This fact needs to be taken in consideration when determining the acceptable exceedance probability $P_{Sd}$.

The exceedance probability $P_u$ of $X$ is determined with regard to the higher tail of the load distribution $S$ and compared with an acceptable probability $P_S$.

$$P_u = P\{(X,n) \leq S\} \leq P_S \tag{5-76}$$

The sample $X$ is accepted H0 or rejected H1 on the reliability level of the distribution $S$ with an acceptable exceedance probability $P_S$. This formulation requires as for concept (b) a reconstruction of distribution $S$ on the basis of the standards specific fractile values $s_k$. The acceptance probability of this formulation is generally higher than that of the formulations (a) to (c), as the tail of $S$ is taken into consideration and the safety zone defined by the partial safety factors $g_S$ and $g_R$ is neglected. This fact needs to be taken into consideration, similar as in (b) when determining the acceptable exceedance probability $P_{Sd}$.

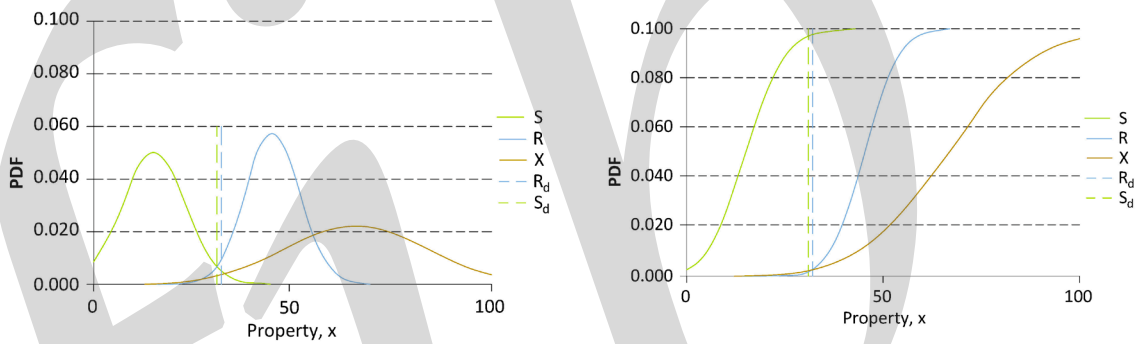


Fig. 5-7 Assessment of sample $X$ with regard to the design situation $R_d \geq S_d$. (a) PDF representation, (b) CDF representation

Fig. 5-8 and Fig. 5-9 present the practical procedure with respect to case (a)

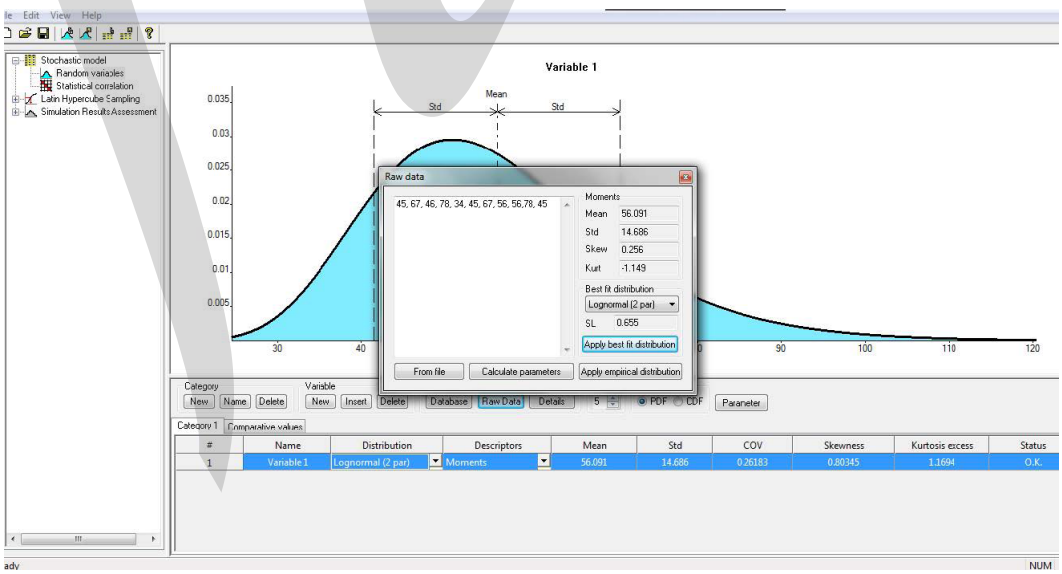

*This document is the intellectual property of the fib – International Federation for Structural Concrete. All rights reserved.*
*This PDF of fib Bulletin 86 is intended for use and/or distribution solely within fib National Member Groups.*

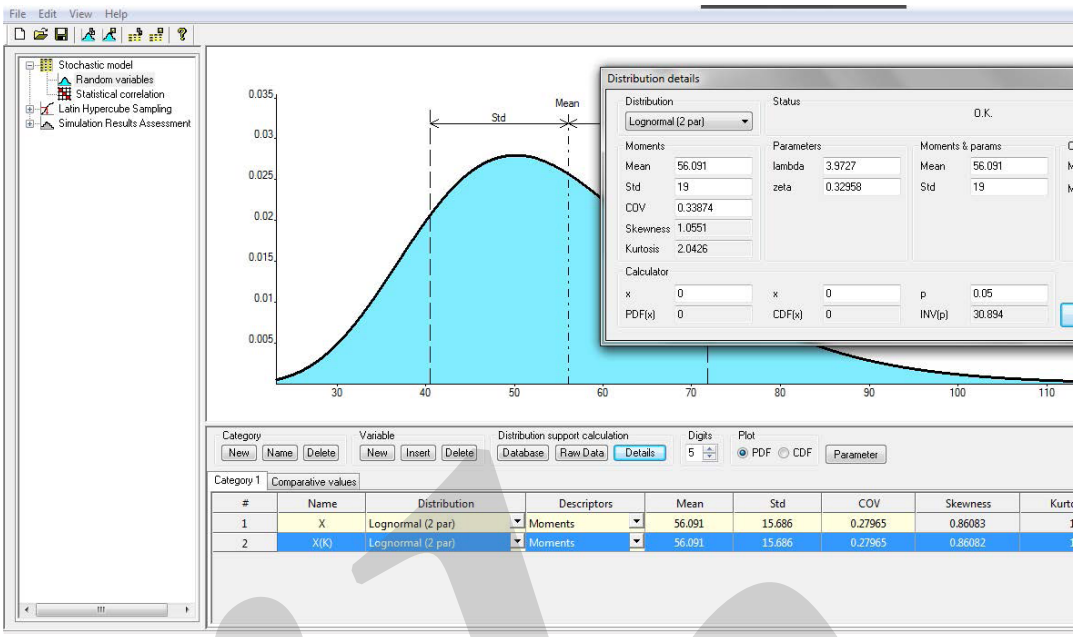


Fig. 5-8 Determination of exceedance probability $P_u$ with respect to $R_d$ (a) Data acquisition of 11 sample data in FREeT, (b) $X^2$ Curve Fitting on sample data and correction of the standard deviation in order to fit the *K*-factor corrected fractile value

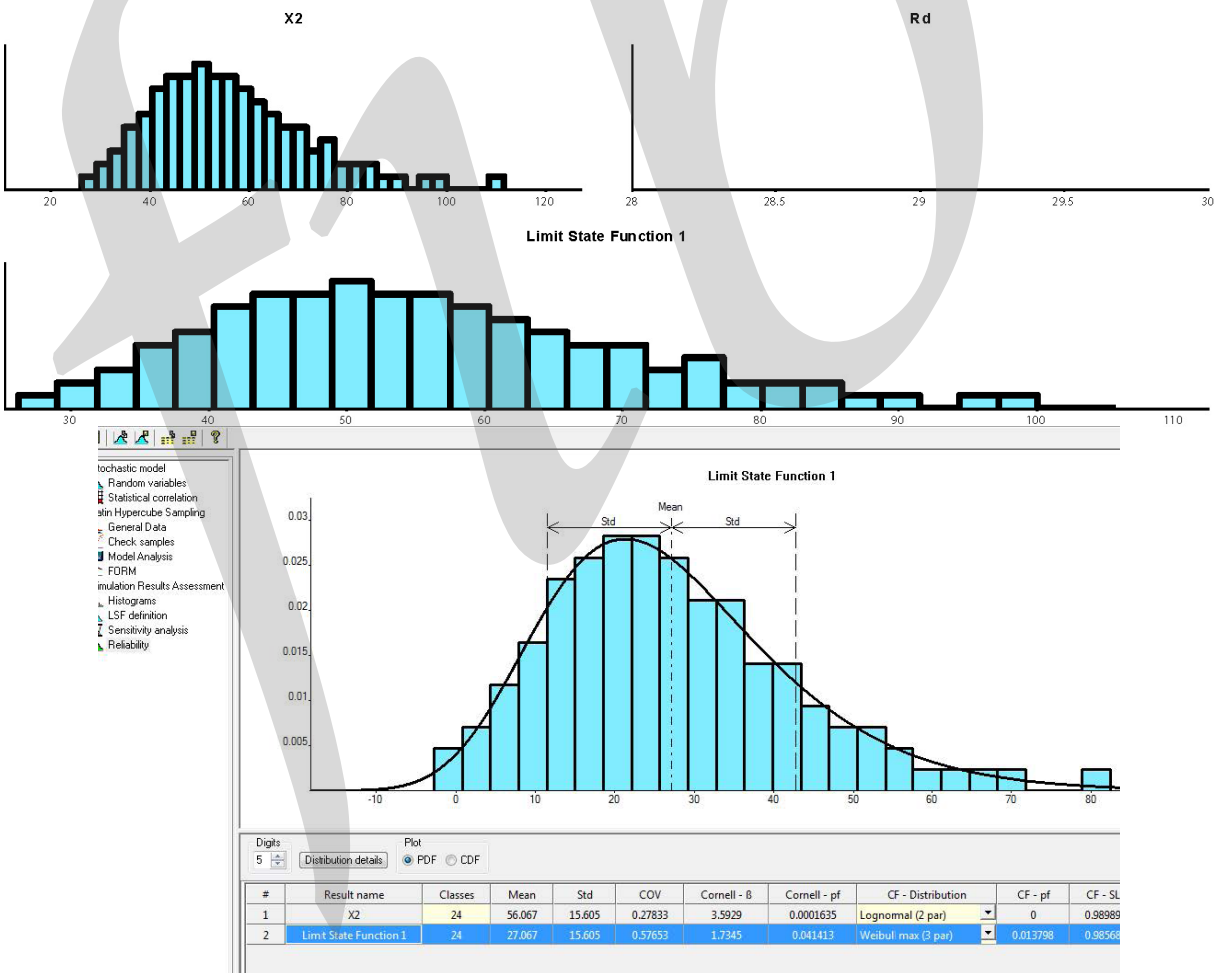


Fig. 5-9 Determination of exceedance probability $P_u$ with respect to $R_d$ (c) Sampled *R* with respect to deterministic design value $R_d - G = R - R_d = 0$; (d)simulated exceedance probability $p_f = 4\%$ based on $G = R - R_d$

*This document is the intellectual property of the fib – International Federation for Structural Concrete. All rights reserved.*
*This PDF of fib Bulletin 86 is intended for use and/or distribution solely within fib National Member Groups.*

### 5.1.6.1 Testing recommendations for the determination of design values

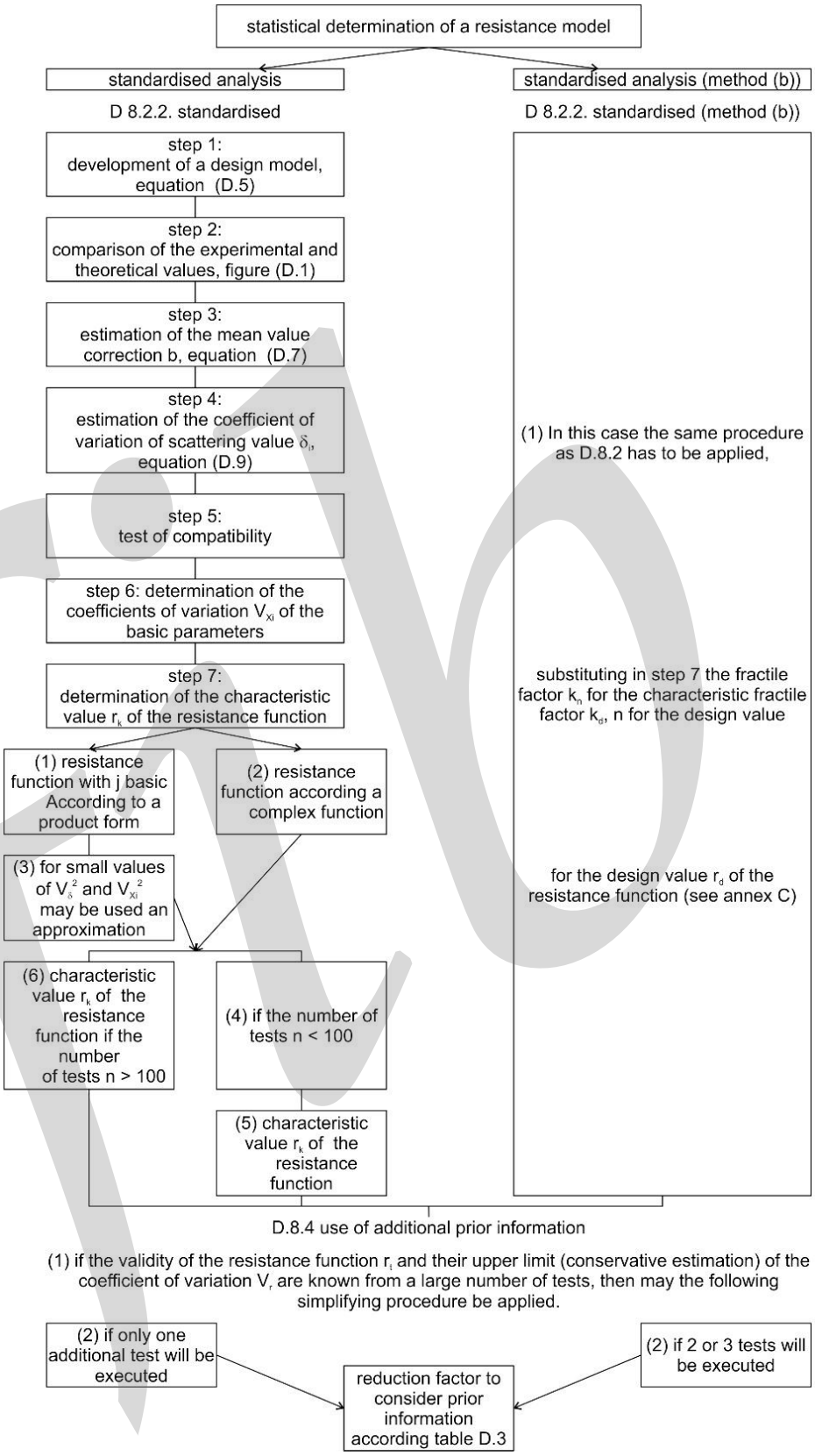


Fig. 5-10 Basic procedure

*This document is the intellectual property of the fib – International Federation for Structural Concrete. All rights reserved.*
*This PDF of fib Bulletin 86 is intended for use and/or distribution solely within fib National Member Groups.*

## 5.2 Stochastic models for design

### 5.2.1 Stochastic models for the resistance of structural engineering

In this chapter, several stochastic models relevant for structural engineering are presented. The derived statistical properties are extracted from state of the art literature sources, such as ANG TANG, JCSS, etc. and various research projects.

In general the correlation Matrix presented in the Table 5-13 to Table 5-34 are based on expert knowledge and there experience.

#### 5.2.1.1 Stochastic parameters of TT Roof Elements – Austria

Basic variables used and Correlation matrix used for the simulation of the TT Roof elements[170]

Table 5-13 Concrete mix I (C50/60 B4 - 28 Days)[170]

| Param. | Mean | Cov [%] | PDF | Unit | Material model Comment: |
|---|---|---|---|---|---|
| $f_c$ | 77 | 6.4 | GMB min EV I | MPa | 3D Nonlinear Cementitious 2 |
| $f_t$ | 3.9 | 10.6 | GMB max EV I | MPa | |
| $E$ | 34.8 | 10.6 | WBL min (3 par) | GPa | |
| $G_f$ | 219.8 | 12.8 | GMB max EV I | J.m$^{-2}$ | |
| $\rho$ | 2.3 | 4 | Normal | t/m$^3$ | |

Correlation Matrix:

| | $f_c$ | $f_t$ | $E$ | $G_f$ |
|---|---|---|---|---|
| $f_c$ | 1 | -0.7 | -0.8 | -0.6 |
| $f_t$ | -0.7 | 1 | 0.5 | 0.8 |
| $E$ | -0.8 | 0.5 | 1 | 0.5 |
| $G_f$ | -0.6 | 0.8 | 0.5 | 1 |

Table 5-14 Steel reinforcement (Bst 550B)[170]

| Param. | Mean | Cov [%] | PDF | Unit | Material model Comment: |
|---|---|---|---|---|---|
| $E$ | 200 | 2 | Normal | GPa | Multilinear diagram |
| $f_y$ | 610 | 4 | Normal | MPa | |

Correlation Matrix:

| | $E$ | $f_y$ |
|---|---|---|
| $E$ | 1 | 0.6 |
| $f_y$ | 0.6 | 1 |

Table 5-15 Tendons (Cables - St 1570/1770) 170

| Param. | Mean | Cov [%] | PDF | Unit | Material model Comment: |
|---|---|---|---|---|---|
| $E$ | 195 | 2.5 | Normal | GPa | Bilinear diagram with hardening |
| $f_y$ | 1387.88 | 2 | Normal | MPa | |

Correlation Matrix:

| | $E$ | $f_y$ |
|---|---|---|
| $E$ | 1 | 0.6 |
| $f_y$ | 0.6 | 1 |

Table 5-16 Prestressing force 170

| Param. | Mean | Cov [%] | PDF | Unit | Numerical model Comment: |
|---|---|---|---|---|---|
| $P$ | 0.0835 | 6 | Normal | MN | Initial strain for reinforcement line |

*This document is the intellectual property of the fib – International Federation for Structural Concrete. All rights reserved.*
*This PDF of fib Bulletin 86 is intended for use and/or distribution solely within fib National Member Groups.*

Table 5-17 Loss of prestressing (Uncertainties) 142

| Param. | Mean | Cov [%] | PDF | Unit | Numerical model Comment: | Correlation Matrix: | Im. | Lo. |
|---|---|---|---|---|---|---|---|---|
| Immediate loss uncertainty | 1 | 30 | Lognormal | MN | Initial strain for reinforcement line | Im. | 1 | 0.5 |
| Long-term loss uncertainty | 1 | 30 | Lognormal | MN | Temperature load | Lo. | 0.5 | 1 |

### 5.2.1.2 Stochastic parameters of Gossensass Bridge – Italy

Basic variables and Correlation matrix used for the simulation of the Gossensass Bridge

Table 5-18 Concrete C30/35[170]

| Param. | Mean | Cov [%] | PDF | Unit | Material model Comment: | Correlation Matrix: | $f_c$ | $f_t$ | $E$ | $G_f$ |
|---|---|---|---|---|---|---|---|---|---|---|
| $f_c$ | 42.5 | 10 | Lognormal | MPa | | $f_c$ | 1 | -0.8 | -0.9 | -0.6 |
| $f_t$ | 3.2 | 18 | Weibull | MPa | | $f_t$ | -0.8 | 1 | 0.7 | 0.9 |
| $E$ | 37 | 15 | Lognormal | GPa | | $E$ | -0.9 | 0.7 | 1 | 0.5 |
| $G_f$ | 135 | 20 | Weibull | J.m$^{-2}$ | | $G_f$ | -0.6 | 0.9 | 0.5 | 1 |
| $\rho$ | 23 | 10 | Normal | t/m$^3$ | | | | | | |

Table 5-19 Steel reinforcement[142]

| Param. | Mean | Cov [%] | PDF | Unit | Material model Comment: | Correlation Matrix: | $E$ | $f_y$ |
|---|---|---|---|---|---|---|---|---|
| $E$ | 210 | 3 | Lognormal | GPa | Multilinear diagram | $E$ | 1 | 0 |
| $f_y$ | 500 | 5 | Lognormal | MPa | | $f_y$ | 0 | 1 |

Table 5-20 Tendons[142]

| Param. | Mean | Cov [%] | PDF | Unit | Material model Comment: | Correlation Matrix: | $E$ | $f_y$ |
|---|---|---|---|---|---|---|---|---|
| $E$ | 210 | 3 | Normal | GPa | Bilinear diagram with hardening | $E$ | 1 | 0 |
| $f_y$ | 850 | 3 | Lognormal | MPa | | $f_y$ | 0 | 1 |

Table 5-21 Ratio 142

| Param. | Mean | Cov [%] | PDF | Unit | Source | Material model Comment: | Correlation Matrix: | $E$ | $f_y$ |
|---|---|---|---|---|---|---|---|---|---|
| $r_{y=}A_s/A_c$ | 0.003 | 10 | Normal | - | | | $E$ | 1 | 0 |
| $r_M=A_s/A_c$ | 0.003 | 10 | Normal | - | | | $f_y$ | 0 | 1 |

This document is the intellectual property of the fib – International Federation for Structural Concrete. All rights reserved.
This PDF of fib Bulletin 86 is intended for use and/or distribution solely within fib National Member Groups.

### 5.2.1.3 Stochastic parameters of Neumarkt bridge – Italy

Basic variables and Correlation matrix used for the simulation of the Neumarkt Bridge, B300 (C30/37).

Table 5-22 Statistical data for the compressive strength of classical concrete acc. to[119]

| Quality of manufacture and control | Coefficient of variation of concrete with an average compressive strength $f_{cm} < 20 N/mm^2$ | Standard deviation of variation of concrete with an average compressive strength $f_{cm} < 20 N/mm^2$ | Correlation Matrix: | $E$ | $f_y$ |
|---|---|---|---|---|---|
| Concrete plants with good raw materials. trained personnel and flawless production control | $V_x$ = 0.125...0.20<br>0.15 | $\sigma_x$ = 2.5...4.0<br>3.0 | $E$ | 1 | 0 |
| Larger sites and ready-mixed concrete with normal manufacturing and test conditions | $V_x$ = 0.20...0.275<br>0.225 | $\sigma_x$ = 4.0...5.5<br>4.5 | $f_y$ | 0 | 1 |
| Smaller sites with production of concrete on the construction site | $V_x$ = 0.275...0.35<br>0.30 | $\sigma_x$ = 5.5...0.7<br>6.0 | | | |

Table 5-23 Coefficient of variation of concrete strength according to[171, 144]

| Construction type | one component | multiple components | Correlation Matrix: | $E$ | $f_y$ |
|---|---|---|---|---|---|
| from one concrete mixture | $V_x = \sqrt{\left(V_M^2 + V_T^2\right)}$<br>0.067 | $V_x = \sqrt{\left(V_M^2 + V_T^2 + V_{TT}^2\right)}$<br>0.084 | $E$ | 1 | 0 |
| from multiple concrete mixtures | $V_x = \sqrt{\left(V_M^2 + V_T^2 + V_{MM}^2\right)}$ | $V_x = \sqrt{\left(V_M^2 + V_T^2 + V_{MM}^2 + V_{TT}^2\right)}$ | $f_y$ | 0 | 1 |
| situ concrete: | 0.120 | 0.130 | | | |
| precast concrete: | 0.90 | 0.103 | | | |

Table 5-24 Comparison of statistical data on the compressive strength of normal strength concrete[144]

| Compressive strength acc. to DIN 1045[120] | DIN 1045-1 2008 [120] | | | | Tue. N. V. 2007[172] | | DAfStb Heft 206 1969 [173] | |
|---|---|---|---|---|---|---|---|---|
| | | $f_{ck}$ calib. | $F_{cm}*v_x$ | $V_x$ for $s$ = 5 [N/mm²] (const.) | From Fig. 4.4 | From $f_{ck}$ extracted | From Fig. 4.3 | Computed |
| | $f_{cm}$ [N/mm²] | $V_x$ [] | $s$ [N/mm²] | $V_x = s/f_{cm}$ | $V_x$ [] | $f_{cm}$ [N/mm²] | $S$ [N/mm²] | $V_x$ [] |
| C8/10 | 16 | 0.392 | 6.272 | 0.313 | 0.312 | 13.9 | 3.8 | 0.238 |
| C12/15 | 20 | 0.291 | 5.820 | 0.250 | 0.210 | 17.3 | 4.6 | 0.230 |
| C16/20 | 24 | 0.233 | 5.592 | 0.208 | 0.163 | 21.2 | 5.0 | 0.200 |
| C20/25 | 28 | 0.195 | 5.460 | 0.179 | 0.135 | 25.2 | 5.2 | 0.186 |
| C25/30 | 33 | 0.162 | 5.346 | 0.152 | 0.120 | 30.7 | 5.2 | 0.158 |
| C30/37 | 38 | 0.138 | 5.244 | 0.132 | 0.090 | 34.9 | 5.2 | 0.137 |
| C35/45 | 43 | 0.121 | 5.203 | 0.116 | 0.080 | 40.0 | 5.2 | 0.121 |
| C40/50 | 48 | 0.108 | 5.184 | 0.104 | 0.075 | 45.4 | 5.2 | 0.108 |

This document is the intellectual property of the fib – International Federation for Structural Concrete. All rights reserved.
This PDF of fib Bulletin 86 is intended for use and/or distribution solely within fib National Member Groups.

| | | | | | | | | |
|---|---|---|---|---|---|---|---|---|
| C45/55 | 53 | 0.097 | 5.141 | 0.094 | 0.070 | 50.6 | 5.2 | 0.098 |
| C50/60 | 58 | 0.088 | 5.104 | 0.086 | 0.065 | 55.7 | 5.2 | 0.090 |

Table 5-25 Coefficient of variation of concrete tensile strength (strength values in [N/mm²])

| $f_{ck}$ | 8 | 12 | 16 | 20 | 25 | 30 | 35 | 40 | 45 | 50 |
|---|---|---|---|---|---|---|---|---|---|---|
| $f_{cm}$ | 16 | 20 | 24 | 28 | 33 | 38 | 43 | 48 | 53 | 58 |
| $f_{ctm}$ | 1.2 | 1.6 | 1.9 | 2.2 | 2.6 | 2.9 | 3.2 | 3.5 | 3.8 | 4.1 |
| $f_{ctk\,0.05}$ | 0.84 | 1.1 | 1.3 | 1.5 | 1.8 | 2.0 | 2.2 | 2.5 | 2.7 | 2.9 |
| $V_{X,fctm}$ | 0.21 | 0.22 | 0.22 | 0.22 | 0.21 | 0.22 | 0.22 | 0.20 | 0.20 | 0.20 |
| $V_{X,fck}$ | 0.39 | 0.29 | 0.23 | 0.20 | 0.16 | 0.14 | 0.12 | 0.11 | 0.10 | 0.09 |
| $\Delta V_X$ | -0.18 | -0.07 | -0.01 | +0.02 | +0.05 | +0.08 | +0.10 | +0.09 | +0.10 | +0.11 |

Table 5-26 Stochastic modelling of model uncertainties of resistance $\theta_R$ according to[174]

| Failure due to | PDF | mean | coefficient of variation |
|---|---|---|---|
| Normal force | LN / N | 1.00 | 0.05 (0.01 to 0.15) |
| Bending | LN / N | 1.025 | 0.07 (0.01 to 0.15) |
| Shear | LN / N | 1.10 | 0.10 (0.01 to 0.15) |
| Punching | LN / N | 1.10 | 0.015 (0.05 to 0.25) |

Table 5-27 Stochastic modelling of model uncertainties of resistance $\theta_R$ according to JCSS 2000[142]

| Failure due to | PDF | mean | coefficient of variation |
|---|---|---|---|
| Normal force | LN | 1.00 | 0.05 |
| Bending | LN | 1.20 | 0.15[1)] |
| Shear | LN | 1.40 | 0.25 |
| Punching | LN | 1.00 | 0.10 |

[1)] takes into account the simultaneous effects of axial and shear forces and Theory II. order

Table 5-28 Statistical parameters of the model uncertainties on the resistance[144]

| Failure due to | PDF | mean | coefficient of variation |
|---|---|---|---|
| Normal force | LN | 1.00 | 0.05 |
| Bending | LN | 1.10 | 0.07 |
| Shear due to continuous loads | LN | 1.10 | 0.15 |
| Shear due to single load | LN | 1.40 | 0.20 – 0.25 |

Table 5-29 Statistical parameters of the model uncertainties on the resistance $\theta_R$ for shear[144]

| Source | PDF | mean | coefficient of variation |
|---|---|---|---|
| JCSS 2000 [142] | LN | 1.40 | 0.25 |
| Faber. M. H. 2005[144] | LN | 1.00 | 0.10 – 0.20 |
| Brehm. E. et al. 2008 [175] | LN | 1.00 | 0.20 |
| Hansen. M. 2004 [174] | LN / N | 1.10 | 0.10 |
| Kautsch. R. 2010 (ETB) [176] | LN / N | 1.17 | 0.16 |
| Kautsch. R. 2010 (TB) [176] | LN / N | 1.49 | 0.27 |

This document is the intellectual property of the fib – International Federation for Structural Concrete. All rights reserved.
This PDF of fib Bulletin 86 is intended for use and/or distribution solely within fib National Member Groups.

Table 5-30 Statistical parameters of the model uncertainties on the resistance $\theta_R$ for shear[144]

| Type of failure | PDF | mean | coefficient of variation |
|---|---|---|---|
| $V_{Rd,ct}$ | LN | 1.00 | 0.15 |
| $V_{Rd,sy}$ | LN | 1.10 | 0.10 |
| $V_{Rd,max}$ | LN | 1.10 | 0.15 |

Table 5-31 Stochastic parameter of concrete are to Fischer 144

| Basic variable resistance | | | PDF | stat. characteristics | | comment |
|---|---|---|---|---|---|---|
| | | | | $m_{X,i}/X_{k,i}$ | $V_{X,i}$ | |
| Concrete compressive | $f_{cm}$ | N/mm² | LN | 20/12 | 0.292 | C12/15 |
| Concrete compressive | $f_{cm}$ | N/mm² | LN | 28/20 | 0.195 | C20/25 |
| Concrete compressive | $f_{cm}$ | N/mm² | LN | 38/30 | 0.138 | C30/37 |
| Concrete compressive | $f_{cm}$ | N/mm² | LN | 58/50 | 0.088 | C50/60 |
| Concrete compressive | $f_{ctm}$ | N/mm² | LN | 1.6/1.1 | 0.216 | C12/15 |
| Concrete compressive | $f_{ctm}$ | N/mm² | LN | 2.9/2.0 | 0.215 | C30/37 |
| Concrete tension | $f_{ctm}$ | N/mm² | LN | 4.1/2.9 | 0.200 | C50/60 |
| Steel tensile strength | $f_{ym}$ | N/mm² | LN | 240/220 | 0.054 | Bst I |
| Steel tensile strength | $f_{ym}$ | N/mm² | LN | 460/420 | 0.054 | Bst III |
| Steel tensile strength | $f_{ym}$ | N/mm² | LN | 550/500 | 0.054 | Bst IV |
| Geometry | $b \cdot h$ | m | N | 1.00/1.00 | 0.02 | - |
| Effective depth | $d$ | m | N | 1.00/1.00 | 0.02 | - |
| Margin reinforcement | $d_1$ | m | N | 1.00/0.80 | 0.125 | - |

Table 5-32 Model uncertainties for a general mechanical loading[144]

| Basic variable model uncertainty | | | PDF | stat. characteristics | | comment |
|---|---|---|---|---|---|---|
| | | | | $m_{X,i}/X_{k,i}$ | $V_{X,i}$ | |
| Normal force resistance | $\theta_{R1}$ | - | LN | 1.00/1.00 | 0.05 | - |
| Shear force resistance | $\theta_{vRd,ct}$ | - | LN | 1.10/1.10 | 0.15 | Equal distributed load |
| Shear force resistance | $\theta_{vRd,sy}$ | - | LN | 1.10/1.10 | 0.10 | Equal distributed load |
| Shear force resistance | $\theta_{R2}$ | - | LN | 1.10/1.10 | 0.20 – 0.25 | Single load |
| Shear force resistance | $\theta_{vRd.m}$ | - | LN | 1.10/1.10 | 0.15 | Equal distributed load |
| Bending resistance | $\theta_{MRd}$ | - | LN | 1.10/1.10 | 0.07 | |

Table 5-33 Stochastic Characteristics of Concrete Used for the Finite Element Reliability Assessment of the Girder T2 in the Middle Field of the Neumarkt Bridge based on[177]

| Characteristics | | Units | Probability density function | Mean | Standard deviation | Coefficient of variation |
|---|---|---|---|---|---|---|
| Cube strength. | $f_{cu}$ | MPa | | 60 | | |
| Elastic modulus. | $E$ | MPa | Log-normal | 39270 | 1964 | 0.05 |
| Poisson's ratio. | $\mu$ | - | | 0.20 | | |

This document is the intellectual property of the fib – International Federation for Structural Concrete. All rights reserved.
This PDF of fib Bulletin 86 is intended for use and/or distribution solely within fib National Member Groups.

| | | | | | | |
|---|---|---|---|---|---|---|
| Tensile strength. | $f_t$ | MPa | Log-normal | 3.68 | 0.29 | 0.08 |
| Compressive strength. | $f_c$ | MPa | Normal | 51.00 | 3.06 | 0.06 |
| Specific fracture energy. | $G_f$ | MN/m | Weibull | 9.2 x 10^-5 | 1.6 x 10^-5 | 0.18 |
| Critical compressive displacement. | $W_d$ | M | | -5 x 10^-4 | | |
| Compressive strain at compressive strength. | | - | | 2.597 x 10^-3 | | |
| Reduction of compressive strength due to cracks | $\varepsilon$ | | | 0.80 | | |
| Specific material weight. | $\rho$ | MN/m | | 0.023 | | |
| Coefficient of thermal expansion. | $\infty$ | 1/K | | 1.2 x 10^-5 | | |

Table 5-34 Stochastic Characteristics of Prestressing and Mild Steel Used for the Finite Element Reliability Assessment of the Girder T2 in the Middle Field of the Neumarkt Bridge based on[177]

| Characteristics | Units | Probability density function | Mean | Standard deviation | Coefficient of variation |
|---|---|---|---|---|---|
| | | Prestressing steel | | | |
| Elastic modulus. $E$ | MPa | Log-normal | 210000 | | 0.03 - 0.05 |
| Yield strength. $f_y$ | MPa | Log-normal | 1540 | 46 | 0.03 |
| Specific material weight. $\rho$ | MN/m | | 0.0785 | | |
| Coefficient of thermal expansion. $\infty$ | 1/K | | 1.2 x10$^{-5}$ | | |
| | | Mild steel | | | |
| Elastic modulus. $E$ | MPa | Log-normal | 210000 | 6300 | 0.03 |
| Yield strength. $f_y$ | MPa | Log-normal | 440 | 22 | 0.05 |
| Specific material weight. $\rho$ | MN/m | | 0.0785 | | |
| Coefficient of thermal expansion. $\infty$ | 1/K | | 1.2 x 10$^{-5}$ | | |

This document is the intellectual property of the fib – International Federation for Structural Concrete. All rights reserved.
This PDF of fib Bulletin 86 is intended for use and/or distribution solely within fib National Member Groups.

# 6. Inspection and monitoring

## 6.1 Introduction

Inspection and monitoring strategies for existing load-bearing structures, and in particular for bridges, aim at the evaluation and assessment of structural safety and reliability (load carrying capacity, serviceability) with the ultimate objective of determining the traffic safety on such structures[178]. Evaluation and assessment actions are typically performed in the course of conversion and development work on supporting structures, as any significant alterations introduced by such reconstruction work may result in significantly changes both to the static concepts and to the loading conditions.

In the new code specifications, monitoring and evaluation measures are recommended with the aim of improving the understanding and the general assessment of the condition of the structure or also as a special inspection which enables the identification and localization of damage in time. The ultimate objective is to safeguard the performance over the whole life-span.

The basis of any kind of monitoring is always a detailed inspection.

Such inspections may be subdivide in four time-related categories:

- Visual inspections, e.g. yearly basis.
- Simple checks, for instance 3 years after every main inspection.
- Main inspections, for instance every 6 years.
- Special inspections, following exceptional occurrences or incidents.

The first examination of a structure has to take place prior to expiry of the warranty. Every inspection is to be performed by an experienced engineer or by specially trained staff. Such training may take place either by internal training actions of the building maintainer or through external training seminars. Intervals for inspections should not be no longer than 2 years. Shorter intervals are to be applied whenever the condition of the structure or any of its components indicates it. In addition, special inspections may be required whenever damage by unusual occurrences (e.g. accidents, fire, floods or rock falls etc.) cannot be ruled out.

In case of defects or deficiencies, special inspections and further tests or examinations have to be conducted with the aim of assessing whether or not these defects have any impact on the serviceability of the structure. On this basis, it shall be decided whether the deficiencies and/or damage are to be repaired in the course of the next maintenance action. In general, in-depth examinations should be performed at intervals of no longer than 6 years.

The aim of monitoring is to ensure both the functionality and the serviceability of the single structural element as well as for the whole system. The results of the individual monitoring tasks can be transferred into a general and objective evaluation system via an evaluation matrix. The key elements of the evaluation system are the assessment of any reductions of functionality and the decisions regarding necessary measures. The necessary measures are prioritised, either to be performed immediately or in the course of the next scheduled maintenance action.

This document is the intellectual property of the fib – International Federation for Structural Concrete. All rights reserved.
This PDF of fib Bulletin 86 is intended for use and/or distribution solely within fib National Member Groups.

## 6.2 Inspection framework for maintenance of structures

### 6.2.1 General remarks

The maintenance of structures should be supported by database frameworks.

Through database systems a comprehensive overview of general and technical parameters for decision making are available.

An infrastructure database should be able to support daily work of those responsible in road administration. The need of information at project level as well as for management is typical for such systems. The project engineer needs data sheets, a drawing or a picture for a particular part of his work. A manager is interested in accumulated information, or in specific performance indicators. For the development of a yearly maintenance program a database can provide essential information.

Concerning for instance bridges the heterogeneous scenery of bridge systems and the different approach of administration and users concerning the topic "bridge" must be mapped. The key for this is a dynamic and modular structure and employment of modern software tools ( e.g. Austrian guideline RVS 13.10.61[179]). For example, for highway infrastructures there are the seasons of examination in spring and autumn, the preparation of the repair works plan during summer and the repair works season from April till October which necessitates the amount and type of information gathered during the year[180].

### 6.2.2 Hierarchical structure of databases

Databases should give a relational view of the realistic problem, for example of a bridge. Bridges can be built very simply and be similar to many others or they can be a very complex construction, and be unique. Some databases (e.g. BAUT) uses a hierarchical approach, where the descriptive components, how the structure is set up, are selected dynamically.

Basic features like high value is attached to analyses, as the history of each object, for instance a bridge, is included in the database and can be seen by each user of the database.

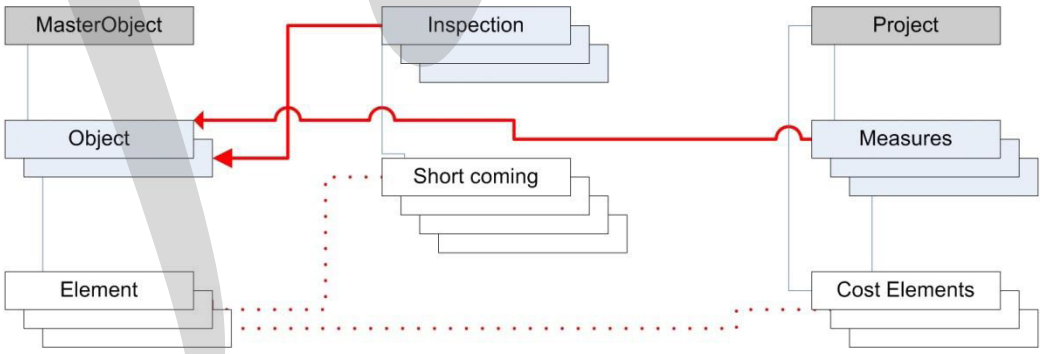


Fig. 6-1 Hierarchical Structure

The database should be structured hierarchically. In the diagram the master object should be a complex attribute, which consists of one or more objects. On this level general and administration relevant attributes should be stored. The objects hold all their technical attributes. Every object can be specified by none, one or more elements

This document is the intellectual property of the fib – International Federation for Structural Concrete. All rights reserved.
This PDF of fib Bulletin 86 is intended for use and/or distribution solely within fib National Member Groups.

representing deteriorating parts of the structure. Elements can be allocated dynamically to each object. This allows a customized description of the structure, which will be important concerning condition rating or statistical queries. In addition to this general attributes like regulations or links can be stated[181].

Regarding the structure of inspection events, the database distinguishes between inspection events and shortcomings found. Inspections are related to each single object, because in a serial system the failure of an object can cause the failure of the whole system. Shortcomings are related to elements as a rough localization. Pictures taken from them are also stored into the database. Inspections and shortcomings give a rating to objects and elements.

Projects and measures taken can influence the condition of an object. A project consists of one or more measures and the cost elements for the measures as well as the cost elements for the project.

Within the database several modules of maintenance management might be recorded.

## 6.3 Structural monitoring

### 6.3.1 General remarks

Some important documents already in Industry. Some of these associated with monitoring are listed which cover general principles, terms and definitions and detailed information regarding the monitoring of structures.

- Innovative Monitoringstrategien für Bestandsbauwerke[182]
- Global monitoring concepts for bridges[183]
- Instrumentation and Data Acquisition techniques in Structural Health Monitoring[184]
- Monitoring und Strukturidentifikation von Betonbrücken[185]
- Bauwerksüberwachung der Autobahnbrücke Gossensaß[186]
- Monitoring and safety evaluation of existing concrete structures. State-of-art report)[187]

In general, the assessment of degrading processes of ageing engineering structures is performed by visual inspection methods. However, most of these visual strategies do not have the capability for detecting the initiation of corrosion, fatigue, and cracks. The observation of changes in a physical property of a structure e.g. by non-destructive evaluation (NDE) methods can complement visual inspection strategies and can allow detection of the initial degradation processes.

NDE methods are not able to provide information about the lifetime performance of a whole structure, since they are limited to discrete locations in space at discrete time points. Sensor-based monitoring systems can overcome this constraint to time and space discrete performance information. They have the ability to provide data associated with structural physical properties on a continuous basis. A smart combination of monitoring devices (sensors) combined with probabilistic assessment methods applied to prediction models will provide a comprehensive maintenance planning tool for engineering structures. The aim of this chapter is: (a) to briefly review sensor systems traditionally used for monitoring of engineering structures, and (b) to investigate factors associated with

This document is the intellectual property of the fib – International Federation for Structural Concrete. All rights reserved.
This PDF of fib Bulletin 86 is intended for use and/or distribution solely within fib National Member Groups.

condition assessment under uncertainty by using sensors (e.g. displacements, corrosion indicators, strain fields, crack widths, accelerations.

### 6.3.2 Introduction

Physical and chemical properties, like stiffness and material conditions, of a structure can vary considerably due to loading and environmental conditions or others in space and time. Corrosion is one of the chemical deterioration processes that even affect the physical properties of engineering structures. For instance, corrosion of steel in concrete can be detected by traditional non-destructive evaluation (NDE) methods or by sensors. The half-cell potential survey, linear polarization measurements, radar survey, infrared thermography, and ultrasonic tests are possible devices for detecting corrosion activities[188,189, 190, 191, 192, 193, 194, 195, 196]. In addition to corrosion, other environmental and/or mechanical stressors can affect the safety and/or serviceability of structures. Performance indicators for these stressors are, for example, strains, displacements and accelerations. These indicators can be detected by sensors such as electrical strain gauges[197, 198, 199, 200, 201], linear variable differential transformers, accelerometers, and fibre bragg grating sensors[202].

The decision basis on whether structural components should be repaired, replaced, or left in their current state, for example can be provided by sensor based monitoring systems associated with advanced probabilistic assessment methods. Nevertheless, it must be noted that devices or sensors are applied at discrete locations of a structure (e.g. on a discrete point of a cross section) and only the combination of them with mechanical properties of the structure allows a comprehensive structural assessment. This fact underlines the necessity for accuracy of instrument-based evaluation methods as well as sensor-based monitoring methods.

Accuracy describes the closeness of measured to real physical quantities or properties. The accuracy of device or sensor-based monitoring methods is determined by comparison of assessments made by the methods to the actual condition of the structural components.

The term “correctly” entails both damage intensity and damage location[190]. The assessment and the effective planning of monitoring systems and methods require knowledge about (a) the physical and mechanical properties and processes of a structure, (b) sensors and their operation properties, (c) sensors errors defined as the difference between the measured and true value, (d) statistical assessment methods, and (e) costs of monitoring systems including direct and operating costs[203].

These issues are fundamental for the evaluation of inspection devices, sensors, and monitoring systems.

### 6.3.3 Principles of monitoring structures

Monitoring of structures is a non-destructive method for evaluating a structure’s condition which is based on measurement data. It may be applied either manually or mathematically at defined intervals. The collected measurement data may describe either the load side or the resistance side. Depending on the measurement task, various physical values can be collected at different intervals. The advantage of structural monitoring lies essentially in the fact that distinct information about a physical value is collected over a longer period of time at defined intervals. This may under certain

This document is the intellectual property of the fib – International Federation for Structural Concrete. All rights reserved.
This PDF of fib Bulletin 86 is intended for use and/or distribution solely within fib National Member Groups.

circumstances enable predictions on the future behaviour of any of the physical values of the structure. As an added bonus, any change in a physical value (structural property) can be observed over time.

Under no circumstances can monitoring actions replace detailed structural inspection. Monitoring should be always complementary to inspections and add additional information on individual physical parameters regarding the prescription of maintenance works.

#### 6.3.3.1 Terms and definitions

*Global vs. local monitoring*: Global monitoring can be described as a set of methods for determining physical values which describe the overall behaviour of a load-bearing structure. Local monitoring can be described a procedure where discrete parts of the system are measured and evaluated.

*Temporary vs. permanent monitoring*: Temporary monitoring is used for a limited period of time during the structure's life time. The collection of physical data can thereby be adapted, as circumstances require, to the condition of the supporting structure or parts thereof. Permanent monitoring collects information on physical values in predefined intervals throughout the time span the structure is used. The intervals are determined according to the respective physical values to be measured.

Any monitoring system may in general be described by a set of components as follows:

*Measurement sensor*: Electromechanical or electronic device which converts the measured physical value into an electrical signal.

*Data logger*: Unit that converts the analogue electrical signal into a digital signal.

*Computer / evaluation device*: In this part of the monitoring system, the measured data are converted into such measurement indicators as are necessary for further evaluation. Here, basic calculations (such as averaging functions or determination of extreme values), statistical analyses and further calculations are performed.

*Alarm device*: If present, this unit is part of the monitoring system serves to alert the responsible person/s in case certain predefined alarm and limit values are exceeded. Such an alert may take the form of an SMS text message, an e-mail or a visual-acoustical signal.

*Transmission unit*: Transmits the collected and/or pre-processed data to a central office. It is used to facilitate data backup, which may then be performed centrally, or serves the public communication of the measured data via the internet.

#### 6.3.3.2 Classification of monitoring systems

There is a distinction between direct and indirect measuring data. Direct measuring values on the one hand are data where the sensor output corresponds directly with the required information (e.g. linear displacement as measured by a linear variable differential transformer (LVDT)). Indirect measuring values on the other hand need to be processed after measurement by the sensor in order to achieve the required physical value. To assess for instance the deflection of a structure via inclinometers, a numerical integration process is required. Such subsequent calculations are generally imprecise to varying degrees. Direct measurement is preferable wherever possible.

A general overview over the applicability of different sensors for different measuring tasks is provided in Table 6-7. The evaluation matrix provides information about the

*This document is the intellectual property of the fib – International Federation for Structural Concrete. All rights reserved.*
*This PDF of fib Bulletin 86 is intended for use and/or distribution solely within fib National Member Groups.*

suitability of a certain sensor type for the determination of a structural physical value. The measurement precision of a sensor is the property which is most essential for the choice of the optimum sensor for a certain measuring task. Table 6-11 provides (according to[204]) an overview of the achievable accuracy when determining the linear displacement via different sensors and measuring devices and of the expected costs of these devices. The costs presented here are based on experience and only provide an indication of the cost scale to be expected.

As can be seen from the list according to[205], the cost of a system is not always correlated with its accuracy in terms of the physical value it is designed to collect. Consequently, several parameters need to be taken into account when choosing a monitoring system for a distinct measuring task. Simply put, the most expensive system is not always the most suitable for a certain purpose.

#### 6.3.3.3 Evaluation of monitoring data

Any evaluation of monitoring data is performed by converting the raw data compiled by the individual sensors into interpretable data. In the field of measurement technology, this process is referred to as signal analysis. Depending on the issue at hand, the measuring system and the sensors used, various procedures are necessary to achieve this end. The following list of evaluation methods is therefore only a very basic, by no means exhaustive, listing of possibilities:

- Digital filters
- Integration and/or differentiation
- Frequency analysis (FFT)

Subsequent to the basic signal processing, further procedures usually are necessary to convert the processed measuring data (e.g. acceleration, linear displacement) into the structurally relevant values which required for further interpretation. The following methods may be used:

- Random decrement method for determining both the system immanent frequency and the system attenuation,
- SSI – stochastic subspace identification
- FDD – frequency domain decomposition
- and other methods

By applying these or numerous other methods, values are gained that are relevant for the structure, as for example for the adaptation of numerical models or for explicit system identification.

#### 6.3.3.4 Interpretation of monitoring data

The core task of monitoring is the interpretation of the gathered data in terms of the structural condition itself or of a representative model. In recent years, new methods have been designed as existing technologies were further developed, some of which will be described in detail below.

This document is the intellectual property of the fib – International Federation for Structural Concrete. All rights reserved.
This PDF of fib Bulletin 86 is intended for use and/or distribution solely within fib National Member Groups.

## 6.3.4 Monitoring associated model updating

### 6.3.4.1 General remarks

The basic idea behind the model updating (model calibration) approach lies in the adaptation of a calculation model in terms of measured values with the aim of minimizing any inconsistency between the measured values (e.g. deflection) and the calculated values. In practice, this is done by modifying individual model parameters, as for example the modulus of elasticity in concrete, within the calculation model. Due to its relatively simple application and due to the fact that no additional software is required, this is one of the most widely used methods. An efficient minimization of the inconsistencies between measured and model-based calculated values is only possible in those cases where the variables are both independent from each other and normally distributed. Only in rare cases has this been achieved on existing structures.

### 6.3.4.2 Bayesian inference

The first step in the Bayesian-inference method is to formulate a model that is sufficient to describe a given problem. For the relevant parameters of the model, a distribution is formulated which appears to be suitable in advance (informative prior distribution) to describe them. With the gathered data, the initial distribution of the variables is adapted as follows[206]:

$$P\left(\theta \middle| y\right) = \frac{P\left(y \middle| \theta\right) P\left(\theta\right)}{P\left(y\right)} \tag{6-1}$$

where

$P(\theta)$ Informative prior distribution of the variables

$y$ Measured data

$P(y|\theta)$ Likelihood function for informative prior distribution of the variables

Based on the new distributions of the variables in combination with the model, statements can be made about the future behaviour of the variables (see also Goulet (2012)).

### 6.3.4.3 Model falsification

The approach of model falsification is a popular one. It was developed by Karl Popper and later adapted for engineering structures by[207]. The basic idea is that any model can never be fully verified, for example through measured data. It can only be disproved and thereby falsified / rejected. This principle is applied in the method of model falsification: For a set of model instances (e.g. models that vary with regard to their geometrical and mechanical dimensions), the modelling errors are compared with the measured sensor errors to aid the decision of either acceptance or rejection of the respective model as suitable for reflecting the real behaviour of a structure. The acceptance and rejection limits are defined via a criterion for error probability[207]. The definition of this criterion is essentially deduced subjectively, on the basis of prior experience with model uncertainties[207]. distinguishes several methods according to their degree of required individual evaluation and their degree of simplified hypotheses.

This document is the intellectual property of the fib – International Federation for Structural Concrete. All rights reserved.
This PDF of fib Bulletin 86 is intended for use and/or distribution solely within fib National Member Groups.

### 6.3.5 Sensors for monitoring systems: A brief review

In the following, electrical strain gauges, linear variable differential transformer (LVDT), fibre bragg grating sensors, accelerometers, corrosion sensors, and half-cell potential, are briefly presented to allow an insight in their performance and the costs to be expected by using them in a monitoring system.

#### 6.3.5.1 Electrical strain gauges (ESG)

A strain gauge is a device used to measure deformation (strain) of an object. The principal idea of the strain gauge was developed by Simmons in 1938[197, 199, 208]. The most common type of a strain gauge consists of an insulating flexible backing which supports a metallic foil pattern[208]. The gauge has to be attached to the object by a suitable adhesive. As the object is deformed, the foil is deformed, causing its electrical resistance to change. This resistance change, usually measured using a Wheatstone bridge, is related to the strain by a quantity known as the gauge factor[199]. For metallic foil gauges, the gauge factor is about 2. Foil gauges typically have active areas 2-10 mm in size. With careful installation, the correct gauge, and the correct adhesive, strains up to at least 10 % can be measured. Electrical strain gauges are frequently used as monitoring systems. These are quite reliable. Nevertheless the right interpretation of the results requires the knowledge about possible sources of errors. Table 6-1 shows types of errors which have to be included in the interpretation of measurements. These errors are obtained from the technical data sheets accessible on http://www.vishay.com[209] and the data sheets of Hottinger Baldwin Messtechnik[201]. The measurement accuracy of electrical strain gauge systems are time independent[210], if a mechanical damage, a corrosion influence or moisture influence on the ESG is prevented. In practice sensors are used redundantly, e.g. two sensors measuring the same physical quantity or arranging the sensors in groups. The errors to be expected for an electrical strain gauge monitoring system as shown in Table 6-1 have to be taken into account in the interpretation of the results.

Table 6-1 Electrical Strain Gauge (ESG) System: Errors* in Measurements

| Cause of errors | Minimum | Maximum | Reference |
|---|---|---|---|
| Sensor | 1.00 % | 3.00 % | Bäumel[211] |
| Misalignment | 0.00 % | 3.00 % | vishay.com[209] |
| Linear deviation | 0.03 % | 0.10 % | Hesse (2006) |
| Creep | avoidable | Avoidable | DMS-Katalog[201] |
| Fatigue (cycle) | avoidable | Avoidable | DMS-Katalog[201] |
| Wires of sensors (noise) | 0.14 % | 0.30 % | Bäumel[211] |
| Data acquisition system | 0.03 % | 0.05 % | Bäumel[211] |
| Application | 0.00 % | user dependent | Klarer[210] |

* Error = ratio between the difference of measured and the true value

#### 6.3.5.2 Linear variable differential transformer (LVDT)

The linear variable differential transformer (LVDT) is a sensor used to measure displacements. The sensor is a transformer with three solenoidal coils placed end-to-end around a tube. The outer coils are the secondaries while the middle one is the primary coil. A cylindrical ferromagnetic core is placed along the axis of the tube[197, 208, 212]. The

This document is the intellectual property of the fib – International Federation for Structural Concrete. All rights reserved.
This PDF of fib Bulletin 86 is intended for use and/or distribution solely within fib National Member Groups.

ferromagnetic core is on one side in contact with the object whose position is to be measured and slides on the other side friction less along the axis of the tube. An alternating current is driven through the primary, which induces a voltage in the secondary proportional to its mutual inductance with the primary. The movement of the core causes in consequence a change in the mutual inductances and the voltage in the secondaries. The alternating current is in general in the range of 1 to 10 kHz. The coils are connected in reverse series, so that the output voltage is the difference between the two secondary voltages; when the core is in its central position, equidistant between the two secondaries, equal but opposite voltages are induced in these two coils, so the output voltage is zero. The movement of the core in one direction is combined with increase of voltage in one coil and the decrease in the other. The voltage of the coil is in phase with the primary voltage. The phase of the voltage indicates the direction of the movement. The magnitude of the output voltage is proportional to the distance moved by the core; therefore the device is called a linear variable differential transformer. Since the sliding core does not touch the inside of the tube the LVDT is a highly reliable device. As mentioned for the ESG system (e.g., based on the measured physical quantity, on the interpreted physical quantity and sensor errors) the LVDT systems can provide an extremely reliable monitoring system. Nevertheless it requires the knowledge about the sources of errors for the right interpretation of the measurements. Table 6-2 shows types of errors which have to be included in the interpretation of LVDT measurements. These data are mainly obtained from the technical data sheets accessible on www.macrosensors.com[212]. There are two types of LVDT. The first is based on inductivity and the second is based on the measurement of the resistance. Table 6-2 is valid for both of them. It could be of interest, since the LVDT are more resistant against time dependent actions, how the monitoring costs changes using the LVDT system instead of an ESG monitoring system. Since the LVDT system is much more reliable than the ESG system, it is sometimes preferable to choose a more expensive solution.

Table 6-2 LVDT System: Errors in Measurements

| Cause of errors | Minimum | Maximum | Reference |
|---|---|---|---|
| Sensor / Nonlinearity | | 0.25 % | Macro Sensors[212] |
| Sensor / Hysteresis | | 0.01 % | Macro Sensors[212] |
| Sensor / Repeated Errors | | 0.01 % | Macro Sensors[212] |
| Wires of sensors (noise) | 0.14 % | 0.30 % | Bäumel[211] |
| Data acquisition system | 0.03 % | 0.05 % | Bäumel[211] |
| Application | 0.00 % | user dependent | Klarer[210] |

### 6.3.5.3 Fibre optical sensors

In the following different fibre optical sensors are described through different ways of categorization[213]:

- By the sensor's material: Silica optical fibers and polymer optical fibers. The optical, mechanical and chemical properties of these different materials determine the physical quantities that can be measured and the application fields.
- By arrangement: Many techniques of transferring the measurands into an optical signal are performed within a discrete device, allowing point-wise measurements of the quantity. Some point-wise sensors can be arranged in chains or arrays,

*This document is the intellectual property of the fib – International Federation for Structural Concrete. All rights reserved.*
*This PDF of fib Bulletin 86 is intended for use and/or distribution solely within fib National Member Groups.*

allowing a quasi-distributed measurement of the structure. In contrast, distributed sensors provide a (practically) continuous signal in at least one spatial dimension.

- By optical parameter: Depending on the nature of the interaction between the measurand and the optical signal, different properties of the light will be affected and will contain the information about the measurand. In interferometric sensors, the phase of the optical signal is altered, leading to characteristic interference patterns after superposition with a reference signal; in systems using pulse reflectometry, the time of flight is used; in spectrometric sensors as well as sensors using non-linear optical effects, the characteristic wavelength spectrum of the optical signal is recorded and analysed.

Some of the most relevant fibre optic sensing techniques for applications in structural health monitoring are listed according to[213] as follows:

- Fibre optic extrinsic Fabry Perot interferometers (EFPI) for point-wise dynamic deformation monitoring. In this technique, two silica optical fibres are placed into a capillary in such a way that their end faces form a cavity of a few micrometres. Injected light is partially reflected at the two surfaces and superposed inside the fibres. The characteristic interference pattern depends on the phase difference of the two superposed optical signals and thereby contains information about the deformation of the capillary.
- Fibre Bragg gratings (FBG) are interference filters that are inscribed into silica and polymer optical fibres. An optical signal is injected into the fibre and fed through the grating. According to the Bragg relation, characteristic parts of the optical spectrum will be reflected at the grating. Since this spectral response depends on the grating period, it will change with temperature and strain applied to the optical fibre in longitudinal direction at the position of the grating. By aligning several gratings along one optical fibre, a quasi-distributed deformation or temperature sensor over a length of several hundred meters can be realized.
- Fibre bragg grating sensors are based on the principle of low-coherence interferometer. The infrared emission of a light emitting diode (LED) is launched into a standard single mode fibre and directed, through a coupler, towards two fibres mounted on or embedded in the structure to be monitored[214]. The fibre a which is used for the measurement of e.g. the physical quantity of elongation or shortening has to be in mechanical contact with the structure and will therefore follow its deformations, the fibre *b* is called the reference fibre, and is installed free in the same pipe. Mirrors at the end of both fibres are used to reflect the light back to the coupler[214]. Table 6-3 shows types of errors which have to be included in the interpretation of the measurements.

Table 6-3 Fibre Bragg Grating System: Errors in Measurements

| Cause of errors | Minimum | Maximum | Reference |
|---|---|---|---|
| Sensor / Nonlinearity | | 0.50 % | Inaudi et al. [214] |
| Misalignment | | 3.00 % | Vishay[209] |
| Wires of sensors (noise) | 0.14 % | 0.30 % | Bäumel[211] |
| Data acquisition system | 0.03 % | 0.05 % | Bäumel[211] |
| Application | 0.00 % | user dependent | Klarer[210] |

This document is the intellectual property of the fib – International Federation for Structural Concrete. All rights reserved.
This PDF of fib Bulletin 86 is intended for use and/or distribution solely within fib National Member Groups.

Distributed Raman sensing in silica optical fibres uses a non-linear optical effect known as stimulated Raman backscattering for distributed measurement of temperature. While being entirely insensitive to mechanical stress, distributed Raman sensors allow temperature monitoring over lengths of several kilometres.

Polymer optical fibres (POF) are more robust to resist mechanical stresses and are easier to handle during the installation process in difference to silica fibres. Since in polymer fibres applied strain leads to a roughly linear increase of the intensity of Rayleigh backscattering, pulse reflectometry can be used to perform a distributed measurement of the strain profile of the fibres. The feasibility of this method for monitoring of geotechnical and masonry structures has been shown. Due to the high optical losses of polymer fibres, the measurement range of such a distributed sensor is limited to a few hundred meters.

Distributed POF sensing overcomes the problem of discrete measurement points; in this technique, an absolute relation of the measurement trace to the monitored structure is even facilitated by the insertion of defined fault locations in the sensing fibre.

Distributed Brillouin sensing allows to measure a continuous profile of the longitudinal strain as well as the temperature along a silica optical fibre over a length of several ten kilometres. This forms a truly distributed sensor (each infinitesimal spatial point along the fibre provides information on the local quantity of strain and temperature) over a long distance.

#### 6.3.5.4 Accelerometers

The accelerometers, used by ATLSS Center, are triaxial accelerometers that measure shock and vibration in three mutually perpendicular axes. They are designed in a unique flat package and built in a welded, environmentally sealed, stainless steel case, providing years of reliable operation. These sensors feature a higher operating temperature up to 330°F (165°C) and range from 0.3 to 1000 Hz. They are protected against thermal transients and transverse acceleration. Details about this type of sensors can be found at www.intertechnology.com/Kistler[215]. The used quartz sensing elements in these sensors ensure a long-term stability superior to other sensing materials. Table 6-4 gives the possible errors in acceleration measurements.

Table 6-4 Accelerometer System: Errors in Measurements

| Cause of errors | Minimum | Maximum | Reference |
|---|---|---|---|
| Sensor / Nonlinearity | | 1.00 % | Kistler[215] |
| Wires of sensors (noise) | 0.14 % | 0.30 % | Bäumel[211] |
| Data acquisition system | 0.03 % | 0.05 % | Bäumel[211] |
| Application | 0.00 % | user dependent | Klarer[210] |

#### 6.3.5.5 Corrosion sensors

Most permanently embedded sensors for civil infrastructure systems can be categorized according to the type of data they collect, including displacement/strain gauges, load cells, crack monitors, and corrosion/ temperature probes (Parker and Ansari, 2003). Strain gauges and load cells, such as weight in motion sensors are useful for quantifying the actual load conditions experienced by a structure. In combination, a refined estimate of the safety margin (resistance minus load effect) and the probability of failure can be obtained by corrosion sensors[188].

This document is the intellectual property of the fib – International Federation for Structural Concrete. All rights reserved.
This PDF of fib Bulletin 86 is intended for use and/or distribution solely within fib National Member Groups.

The sensors can be electrochemical probes designed to measure the corrosion rate of steel directly. This type of sensors relies on direct electrical potential measurements between the reinforcing steel and a reference electrode to determine the instantaneous rate of corrosion of the steel. The most extensively used method for determining rebar corrosion rates in reinforced concrete is the linear polarization resistance (LPR) measurement[216]. LPR sensors quantitatively measure the corrosion current density (CCD) at the rebar level in units of μA/cm². The corrosion current density, $I_{corr}$, is directly related to the instantaneous corrosion rate, $J_r$ and the penetration rate, $P_r$ through Faraday's Law as follows[217],

$$J_r = \left(\frac{W}{F_c}\right) I_{corr} \tag{6-2}$$

$$P_r = \left(\frac{W}{F_c \cdot \rho_{st}}\right) I_{corr} \tag{6-3}$$

where $W$ = equivalent weight of steel = 27.925 g, $F_c$ = Faraday's constant = 96,487 A-seconds, $\rho_{st}$ density of steel (7.85 g/cm³), $I_{corr}$ = corrosion current density (A/cm²), $J_r$ = instantaneous corrosion rate (g/cm²/s), and $P_r$ = penetration rate (cm/s). As previously mentioned, corrosion rate sensors that use the LPR method directly measure the CCD in units of μA/cm², but as the above relations show, the CCD is directly proportional to both the instantaneous corrosion rate and the penetration rate. For this reason, these three terms may be used interchangeably[188].

### 6.3.5.6 Half Cell potential surveys

The deterioration of highway and bridge infrastructure is mainly influenced by corrosion of steel reinforcement. The assessment of the severity of corrosion in reinforced concrete structures can be based on the half-cell potential measurement. This is an electrochemical technique which measures the corrosion potential. The corrosion potential is qualitatively associated with the steel corrosion rate. The half-cell potential measurement offers a survey of the condition of a reinforced concrete structure and is therefore the first step towards its rehabilitation and the validation of the remaining service life[193, 194]. The potential difference can be measured between a standard portable half-cell, normally a copper/ copper sulphate (Cu/CuSO4) standard reference electrode placed on the surface of the concrete with the steel reinforcement underneath[218]. The reference electrode is connected to the positive end of the voltmeter and the steel reinforcement to the negative. An indication of the relative probability of corrosion activity was empirically obtained through measurements during the 1970s[218]. This work formed the basis of the ASTM standard C876, which provides general guidelines for evaluating corrosion in concrete structures as outlined in Table 6-5.

Table 6-5 ASTM Standard C876 Guidelines for Corrosion in Concrete Structures

| Half-cell potential reading | Corrosion activity |
|---|---|
| less negative than - 0.200 V | 90% probability of no corrosion |
| between -0.200 V and - 0.350 V | an increasing probability of corrosion |
| more negative than - 0.350 V | 90% probability of corrosion |

Nevertheless the half-cell potential measurements are significantly influenced by 218: (a) oxygen concentration at the interface of the steel reinforcement and concrete,

This document is the intellectual property of the fib – International Federation for Structural Concrete. All rights reserved.
This PDF of fib Bulletin 86 is intended for use and/or distribution solely within fib National Member Groups.

(b) concrete carbonation, (a reaction between the carbon dioxide in the atmosphere and calcium hydroxide in the concrete), (c) chloride-induced corrosion, (d) corrosion inhibitors, (e) epoxy coated and galvanized steel reinforcement, (f) concrete resistance, and (g) organic coated and sealed structures.

The interpretation of half-cell potentials is the determination of whether the measured half-cell potential corresponds to damage or no damage at the test location. This is performed by an interpretation function which can be built from the probability density functions (PDFs) of half-cell potentials in good and delaminated areas. There are two types of interpretations: threshold interpretations and continuous, probability based interpretations[190].

Other NDE Inspections are: (a) Radar survey[191, 193, 194, 219, 220] (b) Ultrasonic flow[197, 192, 193, 194, 195, 221], and (c) Infrared Thermography[197, 189, 196]. As mentioned previously, the measured data are not identical with the mechanical quantities that an engineer is looking for Table 6-6 shows the relation between the measured and interpreted quantities for various monitoring systems.

Table 6-6 Measured and Interpreted Quantity of Monitoring Systems

| Monitoring system | Measured quantity | Interpreted quantity |
|---|---|---|
| Electrical strain gauges (ESG) | Volt (mV) | strain (μm/m) |
| Linear variable differential transformer (LVDT) | Volt (mV) | displacement (mm) |
| Fibre bragg grate sensors (FBG) | infrared emission of a light emitting diode (LED) | strain (μm/m) |
| Accelerometer | Volt (mV) | acceleration (m/sec$^2$) |
| Corrosion sensor | linear polarization resistance (LPR) | corrosion current density (μA/cm$^2$) |
| Half-cell potential | Volt (mV) | corrosion potential |

Yen (2007), however, pointed out that, in general, the idealization of mechanical models used for the verification of the measurements contains high errors. The decision for the application of a monitoring system is mainly based on the cost of the system and the cost saving possibilities in the maintenance planning. The costs are highly dependent on the kind of operation of the monitoring system. Monitoring can be at discrete time intervals, or continuously over specified time periods, or even over the entire life of a structure.

For example, the Lehigh River Bridge SR-33 in Pennsylvania was monitored during the construction period (July 2, 2001 to October 23, 2001) and during a controlled and uncontrolled live load period (January 4, 2002 to March 11, 2005), (Connor and Santosuosso 2002). The monitoring was necessary due to a new method of combining the concrete bridge deck with the truss system. Since the truss system does not have high redundancy against fatigue it was of special interest to proof the influence of the concrete aging on the truss system, in the first years. An electrical strain gauge (ESG) system and vibrating wire sensor (VW) system were used for monitoring the strain in the structure. It was of special interest to analyse the cost of the four year operating monitoring system for the above mentioned Lehigh River Bridge SR-33, since these cost data provide the basis for the extrapolation of monitoring cost functions valid for the whole lifetime. The analyses show that the monitoring costs can be divided into four parts[222].

This document is the intellectual property of the fib – International Federation for Structural Concrete. All rights reserved.
This PDF of fib Bulletin 86 is intended for use and/or distribution solely within fib National Member Groups.

### 6.3.6 Cost models for monitoring systems

The expenses for monitoring campaigns are usually related to the following processes:

- General preparation / project coordination
- Maintenance of sensors, wiring and harnessing, data acquisition system
- Analysis and reporting
- Permanent observation and evaluation of the data

Each category mentioned above covers both personnel and material costs. For comparatively brief monitoring periods (less than 3 years), there are in general no automation effects in categories (c) and (d). Long-term monitoring programs have a high potential for automation and continuous evaluation of the data, and consequently for an improved cost efficiency. However, monitoring systems are also based on software and data exchange systems, which in turn are subject to rapid changes due to technological progress. Consequently it often becomes necessary to adapt and update the monitoring architecture. One possible cost model for a monitoring system can be described as follows:

$$C(t) = C_D\left(1 + m \cdot t\right) + C_S \cdot t \cdot n \tag{6-4}$$

where

$C(t)$ Total costs of the monitoring system up to the point in time $t$

$C_D$ Direct material costs

$C_S$ Personnel costs per year

$n$ Automation factor

$m$ Upgrading rate for the adaptation and updating of the monitoring equipment and software

### 6.3.7 Strategies for inspection and monitoring

The major objective for inspection and monitoring is to establish a balance between the effort for inspection, monitoring, maintenance and the available financial budget. In the following Fig. 6-2 some aspects are shown for bridge maintenance.

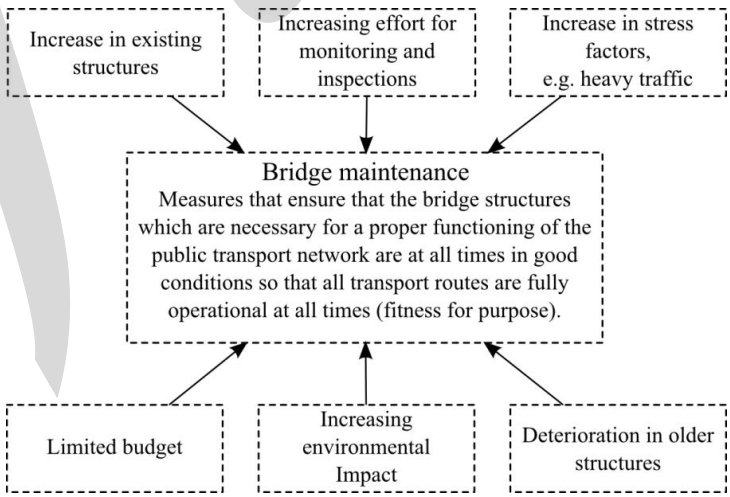


Fig. 6-2 Perspectives of bridge maintenance and structural monitoring

*This document is the intellectual property of the fib – International Federation for Structural Concrete. All rights reserved.*
*This PDF of fib Bulletin 86 is intended for use and/or distribution solely within fib National Member Groups.*

In order to set up an efficient structural monitoring program some key elements have to be taken into account. In the following tables key elements and constraints are presented mainly taken from the Austrian guideline RVS 13.03.11[223, 224].

Table 6-7 Key elements of continuous monitoring

| | |
|---|---|
| General | Assessment of the functional capability of the structure and traffic safety of the road surface and the bridge equipment<br>Identification of any externally visible damage that can be observed by means of skilled visual inspection |
| Execution | Extraordinary changes in the structure<br>Damage to the road surface<br>Damage to the drainage systems |
| Result | Defects, damage or changes are to be reported in writing to the responsible body<br>Wherever traffic safety is compromised, suitable measures are to be put into effect immediately<br>Written documentation is not required |

Table 6-8 Key elements of detailed inspections

| | |
|---|---|
| General | Identification, documentation and evaluation of any changes in the structural condition by means of visual inspection, without instruments or equipment<br>Execution by a skilled engineer or by specially trained technical personnel |
| Execution | Inspection of:<br>- Substructure<br>- Superstructure<br>- Bridge equipment (bearings, joints, expansion joints etc.) |
| Result | Documentation of discovered defects or damage<br>Instigation of measures that may require immediate attention due to the defects or damage<br>Repair of the respective defects / damage<br>If assessment of defects or damage is not possible -> in-depth examination |

Table 6-9 Key elements of in-depth examinations

| | |
|---|---|
| General | Identification, documentation and evaluation of the structural condition<br>Execution by an expert engineer with experience in bridge assessment or bridge construction |
| Execution | Result<br>Position and height verification<br>Examination of the substructure<br>Examination of the superstructure<br>Examination of the bridge equipment |
| Report: | Functional capacity and loading capacity of the object in its current scope<br>Identification of necessary measures to safeguard structural safety, robustness and stability (scheduling)<br>Recommended measures<br>Specific instructions for the detailed inspections<br>Scheduling of any special inspections, if necessary<br>Scheduling of the next in-depth examination (year) |

*This document is the intellectual property of the fib – International Federation for Structural Concrete. All rights reserved.*
*This PDF of fib Bulletin 86 is intended for use and/or distribution solely within fib National Member Groups.*

Table 6-10 Evaluation system based on RVS 13.03.11[223]

| Evaluation degree | Description |
|---|---|
| 1 | No or very slight damage, normal age-related wear and tear, aesthetic damage.<br>*No decrease* in load carrying capacity, serviceability and predicted life time.<br>*No measures* required. |
| 2 | Slight damage, production defects with no signs of further deterioration.<br>*No decrease* in load carrying capacity and serviceability.<br>If no suitable measures are taken, the predicted life time will decrease. Repair measures are required in the course of the next maintenance action. |
| 3 | Moderate to severe damage with *no decrease* in load carrying capacity and serviceability.<br>*Signs of deterioration* regarding load carrying capacity and serviceability.<br>*Medium-term maintenance* and repair actions are necessary in order to preserve the serviceability and expected life time of the structure. |
| 4 | Severe damage, with *no decrease* in load carrying capacity.<br>*Deterioration* in terms of serviceability and expected life time can already be observed.<br>*Maintenance measures* are to be instigated as soon as possible in order to safeguard the serviceability and the expected life time. Such measures may be substituted by additional special inspections within a defined time frame. |
| 5 | Extreme damage with impact on the load carrying capacity of the structure.<br>Repair and maintenance measures must be performed immediately. |

Table 6-11 Evaluation matrix for physical measuring values with regard to possible sensor types

| | Measuring value | Displacement sensor | Inclinometer | Water level | Optical path measurement | Strain gauge | Tachymeter | Fibre optics | Weighing cell | Pressure sensor | Acceleration sensor | Velocity sensor |
|---|---|---|---|---|---|---|---|---|---|---|---|---|
| Static / quasi-static | Vertical drift [m] | OOO | O | OOO | OOO | OOO | OOO | OOO | O | O | O | O |
| | Horizontal drift [m] | OOO | O | O | OOO | OOO | OOO | OOO | O | O | O | O |
| | Torsion [degree] | OO | OOO | OO | OO | O | OOO | O | O | O | Contingent on sensor | |
| | Settlement [m] | OO | OO | OOO | OO | O | OOO | OO | OO | OO | O | O |
| | Linear Expansion [‰] | OO | O | O | O | OOO | O | OOO | O | O | O | O |
| | Force [N] | O | O | O | O | OOO | O | OOO | OOO | OO | Rope forces | |
| Dynamic | Pressure [N/m²] | O | O | O | O | OO | O | O | O | OOO | O | O |
| | Acceleration [m/s²] | O | O | O | O | O | O | O | O | O | OOO | OO |
| | Vibration velocity [m/s] | O | O | O | O | O | O | O | O | O | O | OOO |
| | Natural frequency [Hz] | OO | O | O | OO | OO | O | OO | O | O | OOO | OOO |
| | Attenuation [%] | OO | O | O | OO | O | O | O | O | O | OOO | OOO |

OOO = Highly suitable, OO = Suitable, O = Unsuitable

This document is the intellectual property of the fib – International Federation for Structural Concrete. All rights reserved.
This PDF of fib Bulletin 86 is intended for use and/or distribution solely within fib National Member Groups.

Table 6-12 Selection of various measurement methods and their accuracy

| | Measuring accuracy | | | Comments |
|---|---|---|---|---|
| | Up to 10 m | Up to 30 m | Up to 100 m | |
| Levelling measurements | 0.1 mm | 0.2 mm | 0.3 mm | |
| Angle measurements | 0.1 mm | 0.2 mm | 0.8 mm | Error in cross-section |
| Tachymetry | 1 mm | 1 mm | 2 mm | More than one station required for larger objects |
| Laser | 1 mm | 1 mm | 2 mm | |
| Optical height measurements | 0.1 mm | 0.3 mm | 0.5 mm | 4 positions required for determination of height |
| Spirit level | 0.5 mm | 1 mm | 10 mm | Differential measurement; invariable precision due to a 0.5 m grid |
| GPS-survey | Static measurement – 3 mm (measurement over 8 hrs) Dynamical measurement – 10 mm | | | Postprocessing required |
| Photogrammetry | 2 mm | 2 mm | 6 mm | |
| Videogrammetry | 20 mm | 20 mm | 60 mm | |
| Laser distomat | 3 mm | 5 mm | 15 mm | |
| Inclinometer | < 1 mm | | | Precision depends on the number of devices |
| Fibre optics | ~1 mm | | | Depends on the number of measuring cells |
| Strain gauge | Length: 10 µm | | | |

## 6.3.8 Model uncertainties resulting from the structural inspection

Specifically for inspection the skills and the experience of inspection experts is quit important. For the determination of inspection based reliability performance indicators can be taken into account[227]. The statistical evaluations by[225] and[226] demonstrate that in bridges without or with only slight defects and damage, the assessment by the building inspectors is subject to less scattering than where severely damaged bridges are concerned. Accordingly the uncertainty of building inspectors in introduced in[227]. The following model uncertainties are given particular attention:

$U_{BW,d}$ Model uncertainty building inspector for the assessment of spalling

$U_{BW,f}$ Model uncertainty building inspector for the assessment of the compressive strength of the concrete

$U_{BW,A}$ Model uncertainty building inspector for the assessment of the corrosion of the steel reinforcement

With the aid of such information about the model uncertainties of building inspectors, it is possible to adapt the basic variables of individual limit states with the following multiplicative approach according to[227]:

$$d_{BW} = U_{BW,d \cdot d} \tag{6-5}$$

$$f_{c,BW} = U_{BW,f \cdot fc} \tag{6-6}$$

$$A_{s,BW} = U_{BW,A \cdot As} \tag{6-7}$$

This document is the intellectual property of the fib – International Federation for Structural Concrete. All rights reserved.
This PDF of fib Bulletin 86 is intended for use and/or distribution solely within fib National Member Groups.

where

$d_{BW}$ Model uncertainty building inspector – adjusted basic variable of the statistical effective depth in the event of damage by spalling

$f_{c,BW}$ Model uncertainty building inspector – adjusted basic variable of the compressive strength of the concrete in the event of damage by concrete corrosion

$A_{s,BW}$ Model uncertainty building inspector – adjusted basic variable of the cross section of the steel reinforcement in the event of damage by corrosion of the steel reinforcement

Based on the assumption of stochastic independence of the model uncertainty building inspector for the assessment of the various types of damage and the assumption of normally distributed independent random variables, the model uncertainty building inspector in its entirety is calculated as follows:

$$U_{BW,ges} = U_{BW,d} \cdot U_{BW,f} \cdot U_{BW,} \tag{6-8}$$

The variation coefficient $V_{UBW,ges}$ assessment is calculated, based on the law of the propagation of variance, as follows:

$$V^2_{U_{BW,ges}} = V^2_{U_{BW,d}} + V^2_{U_{BW,f}} + V^2_{U_{BW,A}} \tag{6-9}$$

and

$$V_{U_{BW,ges}} = \sqrt{V^2_{U_{BW,d}} + V^2_{U_{BW,f}} + V^2_{U_{BW,A}}} \tag{6-10}$$

From the investigations and research of[227] it follows that:

In those cases where no or only slight or occasional defects or damage are present, the variation coefficient for the model uncertainty building inspector can be set as VBW = 5% for $U_{BW,d}$, $U_{BW,f}$ and $U_{BW,a}$ respectively. For cases of stochastically independent damage, the variation coefficient $V_{BW,ges}$ can be calculated as follows:

$$V_{U_{BW,ges}} = \sqrt{0.05^2 + 0.05^2 + 0.05^2} = 0.0866 = 8.7\% \tag{6-11}$$

In those cases where distinct or severe defects and damage is present, the variation coefficient for the model uncertainty building inspector can be set as $V_{BW}$ = 10% for $U_{BW,d}$, $U_{BW,f}$ and $U_{BW,a}$ respectively. The variation coefficient $V_{BW,ges}$ can consequently be calculated as follows:

$$V_{U_{BW,ges}} = \sqrt{0.10^2 + 0.10^2 + 0.10^2} = 0.173 = 17.3\% \tag{6-12}$$

### 6.3.8.1 Standardized limit state functions

A primary aim of the limit state functions suggested by[227] is the development of a generally applicable evaluation system for the load carrying capacity of damaged reinforced concrete structures. In particular, standardized limit state functions and their inherent dimensionless parameters enable the development of diagrams for condition assessment for the evaluation of, for example, bridges with varying spans, static systems and construction materials on the basis of the reliability analysis. In the course of the standardized limit state functions, the dimensional basic variables $X$ are calculated as follows:

This document is the intellectual property of the fib – International Federation for Structural Concrete. All rights reserved.
This PDF of fib Bulletin 86 is intended for use and/or distribution solely within fib National Member Groups.

$$X = X_{Wert} \cdot X_0 \tag{6-13}$$

where

$X_{Wert}$ Main variable representing the expected value / average value of the basic variables

$X_0$ Transfer variable in the form of a distribution function for the description of the stochastic properties of the basic variables

### 6.3.8.2 Dimensionless parameters

The following definition of the ratio value $\rho_g$ (see Equation (6-14)) which indicates the proportion of internal forces as a consequence of permanent loads to all influences enables e.g. an approach to reinforced concrete bridges that is independent of their span:

$$\rho_g = \frac{S_G}{S_{Ges}} \tag{6-14}$$

where

$S_G$ Internal forces as a result of permanent loads (intrinsic weight of both construction load and additional load)

$S_{Ges}$ Internal forces as a result of both permanent loads and variable loads

### 6.3.8.3 Standardized limit state function for the bending load

The standardized limit state function of the resistance model for the bending load without the normal force and without compression reinforcement for a square cross-section of reinforcing concrete may be expressed as follows:

$$g_0\left(M_R\right) = U_{RM}\left[\frac{A_{s,0}}{b_0 \cdot d_0}\frac{f_{y,0}}{f_{c,0}}D_M - \frac{k_\alpha}{\alpha_R \cdot \alpha}\left(\frac{A_{s,0}}{b_0 \cdot d_0} \cdot \frac{f_{y,0}}{f_{c,0}}D_M\right)^2\right] - U_E \frac{\left(M_{G,0} \cdot \rho_{gM} + M_{Q,0}\left(1 - \rho_{gM}\right)\right)b_0}{f_{c,0} \cdot b_0 \cdot d_0^2}\mu_M \tag{6-15}$$

Where the dimensionless values are

$$D_M = \frac{A_{s,Wert}}{b_{Wert} \cdot d_{Wert}}\frac{f_{y,Wert}}{f_{c,Wert}} \tag{6-16}$$

and/or

$$\mu_M = \frac{M_{Ges,Wert}}{f_{c,Wert} \cdot b_{Wert} \cdot d_{Wert}^2} \tag{6-17}$$

and

$$\rho_{gM} = \frac{M_G}{M_{Ges}} \tag{6-18}$$

This document is the intellectual property of the fib – International Federation for Structural Concrete. All rights reserved.
This PDF of fib Bulletin 86 is intended for use and/or distribution solely within fib National Member Groups.

where

| | |
|---|---|
| $M_G$ | Bending moment as a result of variable loads |
| $M_{Ges}$ | Bending moment as a result of both permanent loads and variable loads |
| $m_M$ | Dimensionless applied bending moment |
| $D_M$ | Dimensionless material and geometry parameter |

### 6.3.8.4 Relevance for construction practice

Standardized limit state functions facilitate the calculation of the reliability indicator $\beta$ for e.g. the cross-sectional failure of a reinforced concrete component that is independent of the material properties and of the geometry. Evaluation diagrams based on categories of damage[227] and their underlying stochastic models as well as diagrams based on single basic variables may developed in this way. Fig. 6-3 shows such a developed evaluation diagram for the flexural strength of a square cross section of reinforced concrete without the normal force and without compression reinforcement.

Consequently, the reliability indicator $\beta$ for the limit state of the flexural strength of a cross section of reinforced concrete is correlated with the input parameter $D_M$, $\mu_M$ and the load ratio $\rho_{GM}$ (see Fig. 6-3). Through the dimensionless diagrams it becomes possible to determine the reliability of reinforced steel cross sections with varying properties. The information about the properties of the respective cross section contains the dimensionless parameters.

An approximation method for construction practice was developed in[227] where they investigate, for relevant limit states, diagrams of the reliability level for such damage profiles as shown in[227] and for varying load conditions $\rho_G$ for a time frame of 50 years. Because of the vast number of diagrams and the resulting problems for user convenience, a software tool[226] which facilitates was developed, in addition to the reliability assessment, also recommendations for restrictions of use:

"The evaluation of the extent of the damage of the respective damage profile is performed via a five-point rating system, with grades ranging from 0 to 4, following[227] in methodology. The building inspector enters the data gathered in the damage evaluation into the developed software tool and receives for severely damaged structures a recommendation for restricted use without decrease in the level of security", quoted from[227].

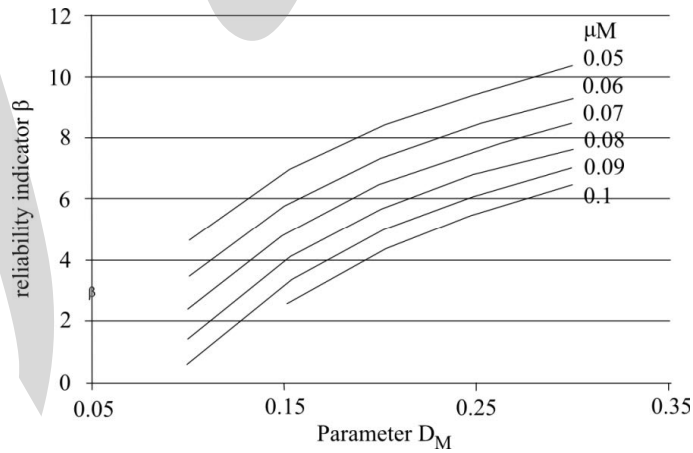


Fig. 6-3 Evaluation diagram for determining the reliability indicator $\beta$ in dependence of the parameters $D_M$ and of the influence ratio $\rho_{GM}$ = 0.6 for the limit state of the flexural strength without the normal force and without compression reinforcement

This document is the intellectual property of the fib – International Federation for Structural Concrete. All rights reserved.
This PDF of fib Bulletin 86 is intended for use and/or distribution solely within fib National Member Groups.

## 6.4 Monitoring based reliability assessment

### 6.4.1 General remarks

Current advanced reliability assessment methods rely on measured data obtained via monitoring systems. A comprehensive approach is necessary, as the task at hand is very complex. Multiple basic principles need to be taken into consideration, such as the design of a monitoring system, the optimum number of sensors, the required quality of sensors, the monitoring frequency, the duration or possible interruption, the transformation of monitored physical quantities to reliability based quantities, the development of prediction functions among others. In the following, we will outline methods for determining the optimum number of sensors, the effective incorporation of monitoring data into the present reliability assessment, and reliability profile prediction.

### 6.4.2 Introduction

Strauss et al.[228] were able to experimentally demonstrate that the optimum number of sensors placed on engineering structures for monitoring purposes can be based on acceptance sampling concepts as they are used for production and material testing. Acceptance sampling is also useful for adjusting monitoring systems. It enables the determination of the number of sensors necessary for recording concrete physical quantities. They[228] have outlined several distinct steps for the integration of monitoring data into a reliability assessment concept: (a) definition of monitoring periods, (b) determination of the associated extreme values, (c) computation of the extreme values distributions according to the accessible sample size and (d) computation of the reliability index with respect to the extreme value distributions and the defined thresholds. The application of extreme value distributions in combination with reliability assessment methods enables (a) the capability for time dependent reliability assessment based on sample size related extreme value predictions and (b) an efficient detection tool for degrading processes by comparison of present and future extreme value behaviour.

### 6.4.3 Design of monitoring systems

The definition of acceptance criteria and acceptance sampling concepts is crucial for any realistic structural assessment in combination with the implementation of monitoring systems. With the help of these concepts on criteria, the number of sensors $n$ that is required for any meaningful determination of the monitored physical quantities may be decided. Engineering structures obviously contain numerous structural components where measurable physical quantities can indicate a violation of a performance threshold. Two types of acceptance criteria are established: (a) acceptance by attributes, and (b) acceptance by variables[228].

### 6.4.4 Acceptance by attributes

Structural monitoring systems are based on the pooling of structural components in batches (or lots) according to their similarities in mechanical or environmental loading, geometrical dimensions and/or the significance of physical quantities. It is, in general, not feasible or practical, not only for economic reasons, to install sensors on all structural elements $N$ of one lot[228]. In general, it is sufficient to place sensors on a limited number

This document is the intellectual property of the fib – International Federation for Structural Concrete. All rights reserved.
This PDF of fib Bulletin 86 is intended for use and/or distribution solely within fib National Member Groups.

$n$ of selected elements of a lot for an efficient assessment the entire lot of $N$ structural components (i.e., where $n < N$) as follows.

If threshold violations are detected by more than $r$ out of $n$ sensors, the performance of the observed lot $N$ is predicted to be inadequate; otherwise the performance will be sufficient. Each monitored element is to be equipped with one sensor, and way in which the sensors are mounted onto the elements should not be parallel or correlated. If a sample (e.g., $n$ sensors) is randomly taken from the lot $N$, the probability of defective items in the sample is given by the hypergeometric distribution. The principle of acceptance monitoring[46] is based on the hypergeometric distribution. The probability of accepting a lot $N$ with an actual fraction $f$ of threshold violations can be obtained from

$$P(f) = \sum_{x=0}^{r} \frac{\binom{N \cdot f}{x}\binom{N \cdot h}{n-x}}{\binom{N}{n}} \tag{6-19}$$

where $h = 1 - f$. For small $n$ relative to $N$, It was demonstrated[229] that Eq. (6-19) can be approximated by

$$P(f) \approx \sum_{x=0}^{r} \binom{n}{x} f^x \cdot h^{n-x} \tag{6-20}$$

As shown by[46] the lot will be accepted in those cases where there are $r$ or less sensors indicating threshold violation. Following[228], equations (6-19) and (6-20) are suitable for:

- Finding the probability $P(f)$ of accepting a lot of size $N$ with an actual fraction of threshold violations $f$ monitored by $n$ sensors, out of which $r$ sensors have indicated threshold violations.
- Finding the necessary number of sensors $n$ by limiting the probability of accepting a defined actual fraction $f$ of threshold violations.

Interpretations of the monitoring results similar to quality assurance sampling methods allows statements about the necessary number of sensors $n$, which should with a reliability $h$ and a confidence level $C$ be sufficient to assess the condition of the investigated structure or structural component. The claim for no threshold violation $r = 0$ out of $n$ sensor measurements leads to the probability of accepting a lot $N$ with an actual fraction $f$ of threshold violations as follows[46]

$$P(f) \approx \sum_{x=0}^{r=0} \frac{n!}{x!(n-x)!} f^x \cdot h^{n-x} \tag{6-21}$$

and therefore, when $h = 1 - f$

$$P(1-h) = h^n \tag{6-22}$$

This probability of acceptance, given a confidence level $C$, should be limited to

$$h^n = 1 - C \tag{6-23}$$

Consequently, the required number of sensors $n$ for a specified reliability $h$, a specified confidence level $C$, for no threshold violation $r = 0$, can be determined from[46]

This document is the intellectual property of the fib – International Federation for Structural Concrete. All rights reserved.
This PDF of fib Bulletin 86 is intended for use and/or distribution solely within fib National Member Groups.

$$n = \frac{\ln(1-C)}{\ln h} \tag{6-24}$$

or

$$n = \frac{\ln(1-C)}{\ln(1-f)} \tag{6-25}$$

In the following an example, assuming a certain number of sensors in order to determine some physical quantities is presented.

If we assume that a monitoring system that consists e.g. of $n$ = 5 sensors measures the same physical quantity (e.g. the strain range for the fatigue assessment (AASHTO)) of nominal identical mechanical components of an engineering structure out of $N$ = 288 components, then the reliability $h$ associated with no critical elements on a confidence level $C$ = 0.95 can be determined from

$$\ln(h) = \frac{1}{n}\ln(1-C) \tag{6-26}$$

or

$$h = (1-C)^{\frac{1}{n}} = (1-0.95)^{\frac{1}{5}} = 0.549 \tag{6-27}$$

Finally, it is reasonable to predict that 0.549 · 288 = 158 components out of $N$ = 288 are in good condition (with no symptoms of fatigue) on a confidence level $C$ = 0.95. For the concept outlined here, the size of the lot $N$ has no bearing on the required number of sensors $n$ (see Eq. (6-25)). Another advantage lies in the fact that it enables the system designer to specify the necessary number of sensors $n = \ln(1 - C)/\ln(1 - f)$ with given confidence $C$ and reliability $h$ levels[228]. The necessary number of sensors $n$ increases with both the prescribed confidence and reliability levels.

### 6.4.5 Acceptance by variables

What is missing in the approach outlined above, namely the method of monitoring attributes, is the complete utilization of all the information that may be gained from the sensor measurements. Since it only distinguishes between "good" or "bad" measurement results – with respect to predefined thresholds – the gleaned measuring data are only put to use to a rather inadequate degree[228].

A more efficient alternative which allows the statistical integration of the measurement results is the method of monitoring by variable. Another advantage of this method is the fact that the quality of the monitored components can be evaluated via various statistical methods, by making use of the mean and standard values of the monitoring results. The method also shows certain advantages when in comparison to the acceptance by attributes concept: the necessary number of sensors can be significantly reduced without overall quality loss. Most methods that use monitoring or sampling by variables are based on Gaussian distribution[46]. In the following, the mean value $\mu_G$ of a monitored lot represents a good physical quantity, whereas the mean value $\mu_B$ represents a poor physical quantity. Acceptance planes are based on the concept of minimizing both the probability $\kappa$ that a good physical quantity $N(\mu_G \cdot \sigma_G)$ will be rejected and the probability $\lambda$ that a poor physical quantity $N(\mu_G \cdot \sigma_B)$ will be accepted[228]. These probabilities provide the basis for determining the threshold $\gamma$ and the required number of sensors $n$. Assuming

This document is the intellectual property of the fib – International Federation for Structural Concrete. All rights reserved.
This PDF of fib Bulletin 86 is intended for use and/or distribution solely within fib National Member Groups.

that the standard deviation of the variable $\sigma_B = \sigma_G = \sigma$ is known in advance, the sample mean $\overline{X}$ can be considered as Gaussian with a standard deviation $\sigma/\sqrt{n}$[46].

Furthermore, if the monitored conditions are acceptable, the sample mean $\overline{X}$ will be $N(\mu_G, \sigma/\sqrt{n})$. Nevertheless, the sensor measurements will indicate a bad condition or violation of the threshold if the sample mean $\overline{X}$ is less than a threshold $\gamma$. This probability $\kappa$ can be determined as:

$$P\left(\overline{X} < T \middle| \mu_G\right) = \Phi\left(\frac{\gamma - \mu_G}{\sigma/\sqrt{n}}\right) = \kappa \tag{6-28}$$

In those cases where the monitored conditions turn out to be poor, there the sample mean $X$ will result in $N(\mu_B, \sigma/\sqrt{n})$. The measurement results will indicate that the monitored conditions are good if the sample mean $\overline{X}$ is larger than $\gamma$. This probability $\lambda$ can be computed as:

$$P\left(\overline{X} > T \middle| \mu_B\right) = 1 - \Phi\left(\frac{\gamma - \mu_B}{\sigma/\sqrt{n}}\right) = \lambda \tag{6-29}$$

In previous equations we determine the necessary number of sensors $n$ and the threshold $\gamma$ with respect to the defined characteristics (e.g., $\kappa$, $\lambda$, $N(\mu_B, \sigma_B)$) and the given characteristics $N(\mu_G, \sigma_G)$, assuming that the standard measurement deviation $\sigma$ is known in advance (e.g. from experience) and the measurement distribution is Gaussian.

In the following an example is presented.

Our objective here is to determine the mean value $\mu_G$ of the acceptable effective stress range (acceptable sample) with respect to a defined poor sample $\mu_B$. The mean value $\mu_G$ is a function of the number of sensors n. Consequently, the allowable mean value $\mu_G = \mu_{\beta f}$ of the acceptable monitored condition needs to be determined for a given number of sensors $n$ while keeping the risk of fatigue at a minimum. This allowable mean value $\mu_G$ and, in consequence, a critical lifetime $t_c$ can be obtained via equation (6-29). For example, assuming $n = 6$ sensors for the assessment of the fatigue behaviour $\sigma_G = \sigma_{\beta f} = 0.3$ and $\kappa = 0.05$ k results in $\mu_G = 2.24$ and the threshold $\gamma = 2.04$. If we install $n = 36$ sensors instead, the result is $\mu_G = 2.10$, $\gamma = 2.02$. These values clearly illustrate the influence of the number of selected sensors on the assessment characteristics.

### 6.4.6 Extreme value distributions for monitoring based predictions

Recorded extremes (i.e. maximum and minimum values) of physical quantities are of special interest and importance for monitoring programs the predictions they generate. We will address this topic in detail below. A detailed discussion can be found in[230].

Examples for extreme values, the largest and smallest values from a pool of recorded data (which can be a monitored sample of size $n$ of a known or unknown population) can be represented with a probability distribution[230]. These probability distributions may be classified as exact or as asymptotic distributions.

This document is the intellectual property of the fib – International Federation for Structural Concrete. All rights reserved.
This PDF of fib Bulletin 86 is intended for use and/or distribution solely within fib National Member Groups.

#### 6.4.6.1 Exact distributions

A physical quantity that is measured at a defined point on a structure can be considered as a random variable $X$ (or population). The monitored sample of size $n$ from this population will have a largest and a smallest value which is related to the probability distribution $f_X(x)$ or $F_X(x)$. These extreme values will also have their respective distributions which in turn are correlated with the distribution of the initial variable X[230].

The monitored sample of size n may be considered as a set of observations ($x_1$, $x_2$, ... $x_n$) representing the first, second,…., n[th] observed values. Yet, the monitored values are unpredictable, with an underlying set of random variables ($X_1$, $X_2$, ..., $X_n$). Consequently, we focus on the maximum and minimum values of ($X_1$, $X_2$, ..., $X_n$), which can be expressed as follows:

$$Y_n = \max(X_1, X_2, ..., X_n) \tag{6-30}$$

and

$$Y_1 = \min(X_1, X_2, ..., X_n) \tag{6-31}$$

It is possible to develop the exact probability distributions of $Y_1$ and $Y_n$ if we take into account certain assumptions. Consider a specified value y. If $Y_n$ is less than $y$, then all the sample associated random variables $X_1$, $X_2$, ..., $X_n$ must also be less than $y$. Assuming that $X_1$, $X_2$, ..., $X_n$ are statistically independent and identically distributed, this leads us to

$$F_{X_1}(x) = F_{X_2}(x) = ...F_{X_n}(x) = F_X(x) \tag{6-32}$$

The corresponding CDF of $Y_n$ may be obtained as follows:

$$F_{Yn}(y) = P\left(X_1 \le y, X_2 \le y, ..., X_n \le y\right) = \left[F_X(y)\right]^n \tag{6-33}$$

The PDF can be represented as

$$f_{Yn}(y) = \frac{dF_{Yn}(y)}{dy} = n\left[F_X(y)\right]^{n-1} f_X(y) \tag{6-34}$$

where $F_X(y)$ and $f_X(y)$ are, respectively, the CDF and PDF of the initial variable $X$. An analogue equation, survival function which is the complement of the CDF, can be used for the minimum $Y_1$ as follows:

$$1 - F_{Y_1}(y) = P\left(X_1 > y, X_2 > y, ..., X_n > y\right) = \left[1 - F_X(y)\right]^n \tag{6-35}$$

thus the CDF of $Y_1$ is

$$F_{Y_1}(y) = 1 - \left[1 - F_X(y)\right]^n \tag{6-36}$$

and the corresponding PDF is

$$f_{Y_1}(y) = n\left[1 - F_X(y)\right]^{n-1} f_X(y) \tag{6-37}$$

This derivation illustrates that the exact distribution of the extreme values from samples of size $n$ is a function of the distribution of the initial variate.

This document is the intellectual property of the fib – International Federation for Structural Concrete. All rights reserved.
This PDF of fib Bulletin 86 is intended for use and/or distribution solely within fib National Member Groups.

### 6.4.6.2 Extreme data concerning exponential function

The initial variate $X$ of a monitored physical quantity can for example be captured by an exponential PDF as follows:

$$f_X(x) = \lambda \cdot e^{-\lambda \cdot x} \quad x \geq 0 \tag{6-38}$$

or by the corresponding CDF of $X$ as

$$F_X(x) = 1 - e^{-\lambda \cdot x} \tag{6-39}$$

Also, the CDF of the maximum value $Y_n$ for $X$, can be determined following to Eq. (6-35) as follows:

$$F_{Yn}(y) = \left(1 - e^{-\lambda \cdot y}\right)^n \tag{6-40}$$

and the corresponding PDF can be determined as

$$f_{Yn}(y) = \lambda \cdot n\left(1 - e^{-\lambda \cdot y}\right)^{n-1} e^{-\lambda y} \tag{6-41}$$

These Eqs. illustrate that any increase of sample size with time will affect both PDFs and CDFs. Fig. 6-4 and Fig. 6-5 show the PDF and CDF of $Y_n$ for a range of different sample sizes $n$, from 1 to 100 and a $\lambda = 1.0$. It can be demonstrated that the PDF and its mode, and in consequence also the, CDF shift to the right with the increase in $n$. For large $n$, the CDF of the largest value from an exponential population approaches the double exponential function as follows[46]:

$$F_{Yn}(y) = \exp\left(-n \cdot e^{-\lambda \cdot y}\right) \tag{6-42}$$

Structural monitoring is a continuous process, and the sample sizes $n$ will increase with time. Equations (6-41) and (6-42) can be used to draw conclusions for the allowed future behaviour of physical quantities that are measured on engineering structures. By applying both of those equations to the points in time available from the present monitored data and computing the distributions for a future time horizon, the elements of a prediction model are developed. Significant deviations of the distributions in the future time that are calculated for a new monitored sample size $n$ can be used to indicate processes in the structure[228].

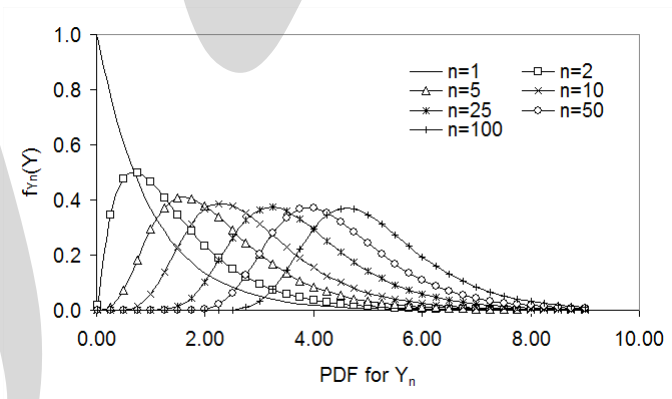


Fig. 6-4 Sample size $n$ dependent exponential PDF of the extreme value $Y_n$

This document is the intellectual property of the fib – International Federation for Structural Concrete. All rights reserved.
This PDF of fib Bulletin 86 is intended for use and/or distribution solely within fib National Member Groups.

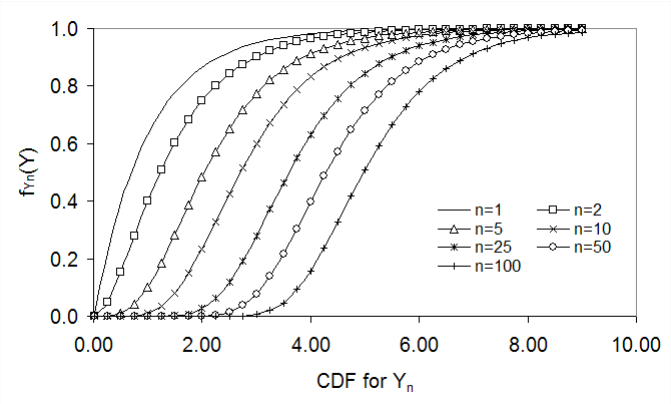


Fig. 6-5 Sample size $n$ dependent exponential CDF of the extreme value $Y_n$

### 6.4.6.3 Asymptotic distributions

As illustrated by the findings above, it is possible to develop exact solutions via asymptotic distributions. The CDF of the maximum value from samples of size $n$ of the initial exponential distribution for example approaches the double exponential distribution with the increase of $n$. Also referred to as the asymptotic distribution of the largest value, the exact distribution of $Y_n$ converges with the asymptotic (e.g. double exponential) distribution as $n \rightarrow \infty$. Three types of such asymptotic distributions subject to the tail behaviour of the initial PDFs were proposed[231]:

**Type I**: The double exponential

**Type II**: The single exponential

**Type III**: The exponential with an upper (or lower) bound

The following lines of reasoning were developed[46]: First, the extreme value from an initial distribution with an exponential decaying tail (in the direction of the extreme) will converge asymptotically to the Type I, Eq.(6-42). Second, the distribution of an extreme value of an initial variate with a PDF that decays with the polynomial tail will converge to the Type II, Eq.(6-43). And third, if the extreme value is limited, the corresponding extremal distribution will converge asymptotically to the Type III, Eq. (6-44).

$$F_{Yn}(y) = (1 - e^{-\lambda \cdot y})^n \text{ Type II} \tag{6-43}$$

$$F_{Yn}(y) = (1 - e^{-\lambda \cdot y})^n \text{ Type III} \tag{6-44}$$

In the following an example, by assuming the Type II single exponential function using the data of Wisconsin. The approaches outlined above can directly be applied to monitoring programs of existing structures.

This approach was applied[232] for the evaluation of monitored data gained from sensor measurements at the I-39 Northbound Bridge over the Wisconsin River. The bridge was constructed in 1961 in Wausau, Wisconsin, USA. The total length of the five span continuous steel plate girder bridge is 196.04 m (643.2 ft). The monitoring of this bridge included measurements of the strain/stress behaviour of specified structural elements.

In Fig. 6-6 a, the following data are presented: the maximum daily stress based on the monitoring during 97 days, its lognormal PDFs, and the Type II extreme PDFs based on each lognormal PDF after 20, 40, 60, 80 days. Fig. 6-6 b indicates the lognormal PDF

This document is the intellectual property of the fib – International Federation for Structural Concrete. All rights reserved.
This PDF of fib Bulletin 86 is intended for use and/or distribution solely within fib National Member Groups.

of the maximum daily stress based on 97 monitoring days, Type II extreme PDFs for 200 days and 1000 days, respectively, which are calculated from the lognormal PDF at 97 days as the initial distribution.

The monitoring of any safe structure requires that its resistance $R$ is greater than the monitored load effect $X$. This requirement (i.e. $R > X$) may be expressed as

$$g(Y) = R - X > 0 \tag{6-45}$$

The reliability index of assumed normal distributions is given as

$$\beta = \left(\mu_R - \mu_X\right) / \left(\sigma_R^2 + \sigma_X^2\right)^{1/2} \tag{6-46}$$

where $\mu_R$ and $\mu_X$ = mean resistance and mean monitored load effect, respectively; and $\sigma_R$ and $\sigma_X$ = standard deviation of the resistance and the standard deviation of the monitored load effect, respectively. Sensors are generally mounted at different locations within a structure. The recorded data can give a positive or a negative result (for example compression or tension). It is not always possible to anticipate if a sensor should produce a positive or a negative reading. Consequently, the grouping of sensor data for calculating the mean $\mu_X$ entails a certain risk of misinterpretation. It is therefore more practical to calculate an associated reliability index for each sensor $i$.

$$\beta_i = \left(\mu_R - \mu_{Xi}\right) / \left(\sigma_R^2 + \sigma_{Xi}^2\right)^{1/2} \tag{6-47}$$

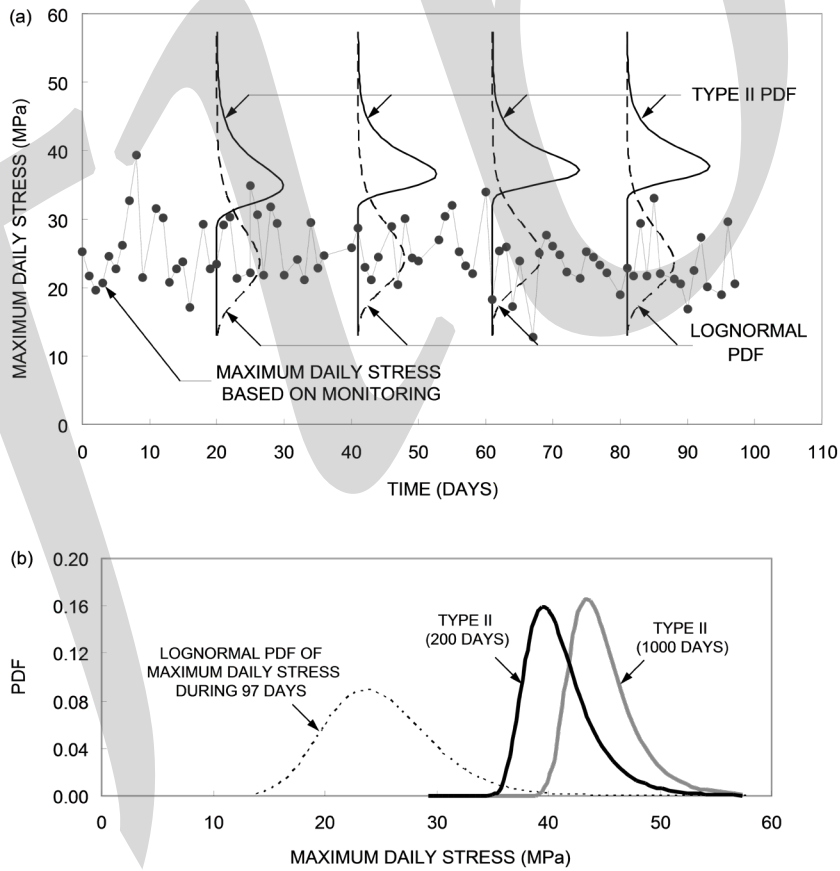


Fig. 6-6 Monitored data associated with sensor CH15: (a) maximum daily stress, lognormal PDFs of the maximum daily stress, and the Type II PDFs calculated from the lognormal PDFs after 20, 40, 60, 80 days, and (b) lognormal PDF based on 97 monitoring days, the Type II PDF for 200 days, and the Type II PDF for 1000 days

This document is the intellectual property of the fib – International Federation for Structural Concrete. All rights reserved.
This PDF of fib Bulletin 86 is intended for use and/or distribution solely within fib National Member Groups.

As outlined above, Fig. 6-6 (a) illustrates the maximum daily stress $X_m^0$ recorded by sensor CH15. A scenario simulating an increase of $X_m^0$ with time can be expressed as:

$$X_m = X_m^0 \left(1 + a \cdot t + b \cdot t^2\right) \tag{6-48}$$

where $X_m$ = modified monitored data, $X_m^0$ = existing monitoring data, $a$ and $b$ are constants for the assumed scenario, and t = time (in days). In order to evaluate the loss of reliability index with per unit time and the remaining time until a defined reliability threshold is violated, the reliability degradation ratio $\eta$ can be defined as:

$$\eta = \frac{\beta_{EXI}}{\beta_{INI}} \tag{6-49}$$

where $\beta_{INI}$ = initial reliability index on the first monitoring day and $\beta_{EXI}$ = reliability index at time $t$. Fig. 6-7 illustrates the reliability degradation ratio for three assumed scenarios as described by $a$ = 1/500, $a$ = 1/100, $a$ = 1/50 and $b$ = 20,000.

The last scenario will cause a loss in the initial reliability index by about 28 % after 97 days. In all scenarios outlined above, the reliability index was determined on the basis of the yield strength of steel.

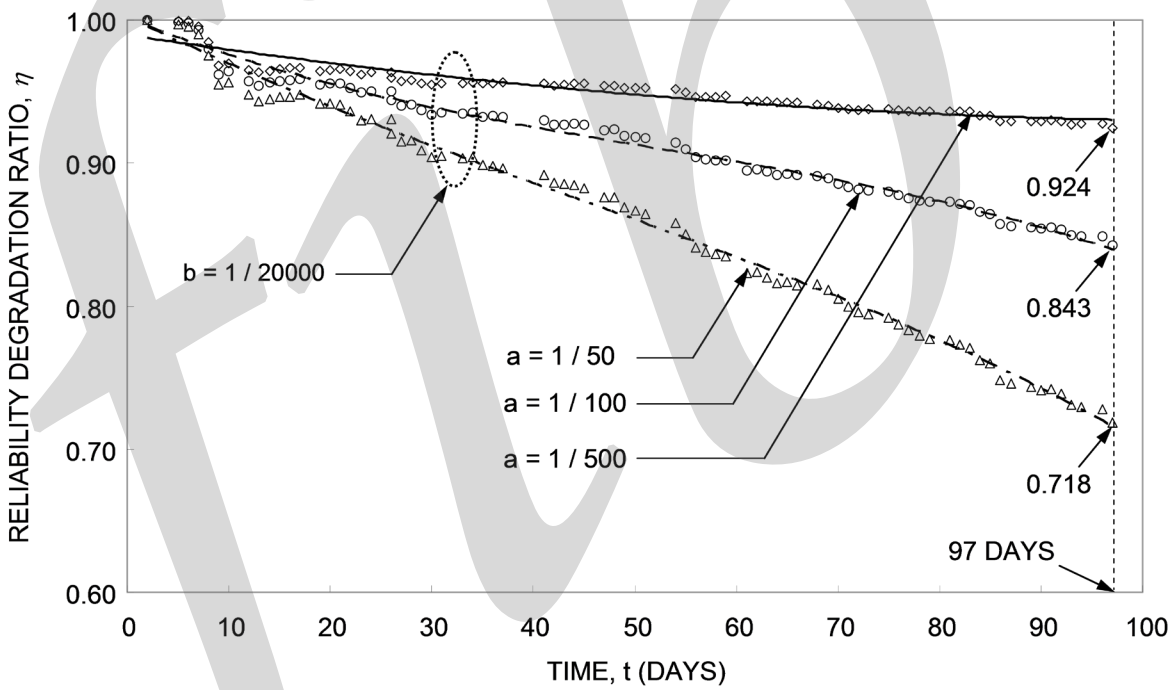


Fig. 6-7 Reliability degradation ratio versus time

This example showed the applicability of the approximate extreme value distribution to predict the structural performance using monitoring information.

### 6.4.7 Reliability assessment based on monitoring information

Reliability analyses via FORM provide in many cases already very close approximations for both linear and nonlinear conditions. Optimization procedures for the calculation of the reliability indicator and the corresponding probabilities of failure for non-deterministic systems under random influences are supported by software packages such as RELSYS[233], FREET[168] or VAP[167].

This document is the intellectual property of the fib – International Federation for Structural Concrete. All rights reserved.
This PDF of fib Bulletin 86 is intended for use and/or distribution solely within fib National Member Groups.

The monitoring of reference values of structures is linked with the stipulation that the observed limit value (resistance value) $R$ is larger than the observed influence value $M$. This stipulation ($R > M$) can be mathematically represented as follows:

$$g(X) = R - M > 0 \tag{6-50}$$

The related reliability indicator follows:

$$\beta = \left(\mu_R - \mu_M\right) \Big/ \left(\sigma_R^2 + \sigma_M^2\right)^{1/2} \tag{6-51}$$

where

$\mu_R$, $\mu_M$ average resistance effect, average influence effect

$\sigma_R$, $\sigma_Q$ standard deviation of the observed effects of resistance and influence

Sensors of monitoring systems are usually fixed in or to a structure at different locations. The observed data may be positive (tension) values or negative (compression) values. Not in all cases can it be anticipated whether a sensor will record positive or negative values. Consequently, the categorization of sensor data and the calculation of the mean value $\mu_M$ may be subject to misinterpretations. Consequently, the calculation of the corresponding reliability indicator for each sensor $i$ is best described in the following way:

$$\beta_i = \left(\mu_R - \mu_{Mi}\right) \Big/ \left(\sigma_R^2 + \sigma_{Mi}^2\right)^{1/2} \tag{6-52}$$

where

$\mu_{Mi}$ average of the observed influence effects of sensor $i$

$\sigma_{Mi}$ standard deviation of the observed influence effects of sensor $i$

The average of the observed influence effects $\mu_{Mi}$ can be determined as the average of the observed maximum and minimum values throughout the duration of a monitoring process. Consequently, the maximum influence during the whole duration of an influence process can be viewed as a random variable which is characterized by the average value $\mu_{oMi}$ and the following standard deviation:

$$\sigma_{oMi} = \mu_{oMi} \cdot \sigma_R / \mu_R \tag{6-53}$$

These descriptive statistical values lead to the following reliability index:

$$\beta_{oi} = \left(\mu_R - \mu_{oMi}\right) \Big/ \left\{\sigma_R \left[1 + \left(\mu_{oMi} / \mu_R\right)^2\right]^{1/2}\right\} \tag{6-54}$$

In addition to the uncertainties regarding the material properties and the influence effects, the uncertainties of sensor $e_s$ (%) can be included in the reliability assessment by introducing the following factor:

$$f_s = 1 + e_s \tag{6-55}$$

It follows that:

$$\beta_{oi,e} = \left(\mu_R - \mu_{oMi} \cdot f_s\right) \Big/ \left\{\sigma_R \left[1 + \left(\mu_{oMi} / \mu_R\right)^2\right]^{1/2}\right\} \tag{6-56}$$

In the following example, the probabilistic assessment of the structural condition of the Lehigh River Bridge SR-33[234] is reduced to the use of the quasi-static and the fatigue stress of the steel frames based on the observed sensor data and on the construction

This document is the intellectual property of the fib – International Federation for Structural Concrete. All rights reserved.
This PDF of fib Bulletin 86 is intended for use and/or distribution solely within fib National Member Groups.

information. The steel grade is a significant factor for both the quasi-static stress and the fatigue stress. In the case of the Lehigh River Bridge SR-33, the used steel is of the grade M270 variety. The nominal yield strength of this steel grade is 345 MPa. The statistical values of the yield strength $f_y$ of the steel truss girders of the bridge were determined from examinations with an average value of 380 MPa and a standard deviation of 28 MPa.

These statistical values serve as the average value $\mu_R$ and the standard deviation $\sigma_R$ of the resistance. The sensors at Lehigh River Bridge SR-33 delivered the strains in the form of loads ($\mu$m/m). The calculation of the reliability indicator $\beta^0_{i,e}$ per sensor requires a transformation of the measured strains into tensions. To achieve this transformation, the linear Hooke's law was used in combination with a modulus of elasticity of 200.000 MPa. In this way, the measured strains were transformed into the average value $\mu^0_{Mi}$ and the standard deviation $\sigma^0_{Mi}$.

In the following, the loading condition 1 (LC1) concerns the inherent weight of the supporting structure, the loading condition 2 (LC2) concerns the inherent weight of the permanent additional loads and the loading condition 3 (LC3) concerns traffic loads from moving traffic and also from load tests.

The standard deviations which cannot be measured on the resistance side can be determined in a first approximation upon presuming that the variation coefficient from the measured loads equals that of the resistance.

The maximum variable strains (extreme values) resulting from the inherent weight of the supporting structure (LC1) are determined with the help of the following probabilistic indicators: $\mu^0_{Mi}$, LC1, $\sigma^0_{Mii}$, LC1. The maximum variable strains (extreme values) resulting from the additional loads (LC2) are determined using $\mu^0_{Mi}$, LC2, $\sigma^0_{Mi}$, LC2. The average values of the maximum variable strains resulting from a combination of LC1 and LC2 are calculated as follows:

$$\mu^\circ_{Mi(1)} = \mu^\circ_{Mi,LC1} + \mu^\circ_{Mi,LC2} \tag{6-57}$$

The standard deviations in the sensors $i$ are presented as:

$$\sigma^0_{Mi(1)} = \left[\left(\sigma^0_{Mi,LC1}\right)^2 + \left(\sigma^0_{Mi,LC2}\right)^2\right]^{1/2} \tag{6-58}$$

Under the conservative assumption that the variation coefficient on the resistance side ($v = \sigma_R/\mu_R$) are the same and the variation coefficient equals observed maximum variable strains are determined as:

$$\sigma^0_{Mi(1)} = v\left[\left(\mu^0_{Mi,LC1}\right)^2 + \left(\mu^0_{Mi,LC2}\right)^2\right]^{1/2} \tag{6-59}$$

And consequently:

$$\sigma^0_{Mi(1)} = \sigma^0_{Mi,LC1}\left[1 + \left(\mu^0_{Mi,LC2}/\mu^0_{Mi,LC1}\right)^2\right]^{1/2} \tag{6-60}$$

The reliability indicator $\beta_{i,e,y}$ (where y stands for the yield point) can be determined on the basis of equations (6-56) and (6-55) as follows:

$$\sigma^0_{Mi(1)} = \sigma^0_{Mi,LC1}\left[1 + \left(\mu^0_{Mi,LC2}/\mu^0_{Mi,LC1}\right)^2\right]^{1/2} \tag{6-61}$$

This document is the intellectual property of the fib – International Federation for Structural Concrete. All rights reserved.
This PDF of fib Bulletin 86 is intended for use and/or distribution solely within fib National Member Groups.

To also take into consideration the observed strains that result from the traffic loads (LC3) with the probabilistic indicators μoMi, LC3 and $\sigma^0_{Mi}$, LC3, it is necessary to combine them with the average values of load conditions LC1 and LC2:

$$\mu^0_{Mi(2)} = \mu^0_{Mi,LC1} + \mu^0_{Mi,LC2} + \mu^0_{Mi,LC3} \tag{6-62}$$

$$\sigma^0_{Mi} = \sigma^0_{Mi,LC1}\left[1+\left(\mu^0_{Mi,LC2}/\mu^0_{Mi,LC1}\right)^2+\left(\mu^0_{Mi,LC3}/\mu^0_{Mi,LC1}\right)^2\right]^{1/2} \tag{6-63}$$

Consequently, the reliability index for the assessment of the observed load with regard to the yield point of steel $\beta^0_{i,e,y}$ can be calculated at the location of every sensor *i* for the loading conditions LC1, LC2 and LC3 according to Eq. (6-56).

The determination of the reliability with regard to the long term influences from temperature, creep and shrinkage can be performed in a similar form on the basis of Eq. (6-57) to (6-63). The extreme values from the long term influences and the long term temperature effects may be combined, e.g. in $\mu_{Mi}$, LC3.

The reliability against fatigue stress of steel, concrete and reinforced concrete structures as a result of cyclical traffic loads is another key factor for the performance capacity of a structure. For the assessment of the existing reliability and the prediction of the remaining life time, information gathered by monitoring systems with regard to regulations such as[235] or Model Code 2010[236] are suitable tools.

It is general practice to compare the observed stress ranges with material characteristics (Woehler curves) which were acquired experimentally according to the above mentioned regulations and which decrease in correlation with the number of stress cycles. The probabilistic assessment of the fatigue behaviour of steel, concrete and reinforced concrete structures via the reliability index $\beta^0_{i,e,f}$ and taking into consideration the acquired sensor data can be performed as follows:

$$\beta^0_{i,e,f} = \left(\mu_f - \mu^0_{Mi}\cdot f_s\right)\Big/\left[\sigma^2_f + \left(\sigma^0_{Mi}\right)^2\right]^{1/2} \tag{6-64}$$

where

| | |
|---|---|
| $\mu_f$ | effective stress range in accordance with the guidelines |
| $\sigma_f = \mathrm{v}\cdot\mu_f$ | standard deviation of the effective permissible strange range, where the variation coefficient of the influence (monitoring information) is adopted as a first approximation of the resistance |
| $\mu^0_{Mi}$ | average value of the stress range resulting from the sensor information *i* |
| $\sigma^0_{Mi}$ | standard deviation of the stress range resulting from the sensor information *i* |
| $f_s$ | factor for sensor errors |

## 6.5 Monitoring based performance indicators

A comprehensive life-cycle performance assessment of bridges requires the definition of performance indicators. These indicators, which provide an easier and time efficient assessment procedure, are recognised as significant quantities. In general, the quantities of the performance indicators are derived from (a) deterministic numerical or analytical

This document is the intellectual property of the fib – International Federation for Structural Concrete. All rights reserved.
This PDF of fib Bulletin 86 is intended for use and/or distribution solely within fib National Member Groups.

investigations of the structural system, (b) probabilistic numerical or analytical investigations, (c) from pure statistical considerations, and (d) from monitoring information with respect to natural or code specific given limit states. The incorporation of monitoring processes and associated code specifications in the performance indicator concept is not yet performed, since this needs the specific preparation and adaptation of existing to fully probabilistic code specifications and the specific treatment of monitoring systems.

Therefore, in order to meet this task, the targets are the analysis and definition of (1) Code specific given limit states and associated monitored quantities (2)Properties of monitoring systems and associated sensors, (3) Optimizing of monitoring systems and sensor properties with respect to performance indicators, (4) of monitoring based performance indicators, (5) Monitoring networks vs. performance indicators:

### 6.5.1 Code specific given limit states and associated monitored quantities

The modern European standards in structural engineering are based primarily on the semi probabilistic reliability assessment procedure and thus has a directly reference to the limit state formulations in terms of the probabilistic analysis.

These standards contain a variety of semi probabilistic assessment procedures in the service ability and the ultimate limit state, among others. Therefore, an objective must be the definition of the code specific semi probabilistic formulations by probabilistic limit state functions and its associated random variables, as already performed in the JCSS model code for some considerations. It should be noted, that this definition needs specific probabilistic considerations for a limited number of variables, since many random variables in the semi-probabilistic code specifications.(e.g., Load models and Load combinations) are not used by their 5 % or 95 % fractile.

The collection of monitoring information based on extreme value statistics, as proposed by[237] enables the setup of prediction models associated with the e.g., mechanical or environmental properties of interest. Bayesian updating approaches allow the efficient weighted incorporation of short term monitored information into historical information based prediction models. These extreme value based predictions are essential stress ($S$) quantities for the characterization of the prediction of time-varying failure probabilities with respect to code specific limits (resistance $R$), e.g., such as the maximum concrete or steel stress.

### 6.5.2 Properties of monitoring systems and associated sensors

Monitoring itself must be a carefully planned activity which generally has to cover the following steps: (a) definition of the objective of the monitoring work, (b) selecting the monitoring method and the locations to be monitored, (c) execution of the monitoring activity, (d) evaluation and interpretation of data, (e) adjustment of processes based on the monitoring data (model-updating, numerical simulation), and (f) decision about a possible intervention such as maintenance or repair among others. Hence, a monitoring based performance assessment and the definition of performance indicators require a detailed knowledge about the current possible facilities in monitoring. The stability and reliability of monitoring systems and the associated software and related algorithms should be evaluated. In the next step the recorded data and parameter provided by the monitoring system, which will be the inputs for performance indicators and the code

This document is the intellectual property of the fib – International Federation for Structural Concrete. All rights reserved.
This PDF of fib Bulletin 86 is intended for use and/or distribution solely within fib National Member Groups.

based limit states, should be tested against random and systematic errors and the stability in time. The results and findings are a necessary fundamental knowledge.

### 6.5.3 Optimizing monitoring systems and sensor properties with respect to performance indicators

For a monitoring based performance assessment of structures the appropriate selection and location of the sensors are significant for the achievable quality of the statement. For instance, an in proper selected sensor will cause a misinterpretation of recorded values due to an insufficient measurement range. Therefore, the aim must be the development of a decision matrix for the proper sensor selection in dependence to the monitoring task. This matrix can be developed on the results and experiences from various field tests and on results from numerical simulations. In contrast to the proper selection of the sensor, the optimum localization of the sensors is a much more challenge.

### 6.5.4 Definition of monitoring based performance indicators

The key ingredients of a maintenance optimization process are the performance indicators upon which maintenance decisions are made; the list of maintenance options to be optimized. One of the roles that a performance indicator plays in the maintenance planning process is an alarm which is triggered when that performance indicator reaches a specified threshold. It is a tool by which the safety and integrity of the structural system is ensured by preventing the performance indicators from crossing their thresholds. Needless to say, a performance indicator used for the maintenance optimization process is required to be able to accurately represent a specific type of performance and predict its future variations. Frangopol and[238] have identified numerous commonly encountered and used life-cycle performance measures. Examples of these measures and their applications in the literature are: the point-in-time reliability index[239], the point-in-time probability of system failure and redundancy[240].

### 6.5.5 Advanced monitoring system

Recent progress in the area of information and communication technology (e.g., wireless sensor networks) allows monitoring system users to increase spatial resolution and lower data acquisition costs. Upon closer examination the new paradigm of “physical computing” may imply further advantages and possibilities. So called intelligent sensors have the potential to process signals and data in a distributed manner in order to observe only relevant events or even predict structural conditions. But on the other hand there are several issues e.g. reliability and security of such systems left unaddressed. These monitoring systems shall be investigated in terms of system reliability and cost effectiveness. A key criterion of monitoring systems, which directly influences the accuracy of the total system, is the system reliability. This is defined in ISO 9126 (1991) as the probability of error-free operation over a determined period of time and in a particular environment. In consequence, the monitoring sub-systems (such as sensor, signal processing, communications and data transmission, data processing, data storage, data access control and distribution, information systems – in particular algorithms and models, visualization, alarm system, expert decision support system, among others)have to be analysed on their error rate and/or their influence on the overall accuracy. Subsequently relevant standards, guidelines for preventing against errors have to be considered. These include process standards for development of safety-critical

This document is the intellectual property of the fib – International Federation for Structural Concrete. All rights reserved.
This PDF of fib Bulletin 86 is intended for use and/or distribution solely within fib National Member Groups.

embedded systems such as IEC 61508, EN 50126, 50128, 50129 and standards for radio transmission, protocols, etc. (ISO / EN, CENELEC, IEEE, ETSI, FCC). In addition, technical and safety aspects such as confidentiality, data integrity, authentication and availability of data and higher safety goals as accountability, data authenticity, non-repudiation, accessibility control (data management) must be investigated.

## 6.6 Risk based inspections

### 6.6.1 General remarks

Risk Based Inspection planning (RBI) aims at identifying the inspection strategy that minimizes the total expected life cycle cost while ensuring compliance with risk acceptance criteria. RBI for structures is based on a probabilistic modelling of the deterioration processes and the inspection quality. The effect of inspections on the reliability of the structure is accounted for by means of Bayesian up-dating and the expected cost are computed by application of Bayesian decision theory. The chapter out-lines the current state-of-the-art and presents an example of RBI for welded joints in steel structures.

### 6.6.2 Introduction

Operators and owners of technical facilities are facing deterioration of their structures and require effective strategies for ensuring structural integrity. Because most deterioration phenomena on structures are of a highly uncertain nature, inspections represent an efficient tool for the reduction of the related risk. If quantitative inspection performance models as well as physically based models of the deterioration phenomena are available, the effect of inspections on the reliability and the risk can be quantified. Such approaches were first published by[241] as well as[242] and allow for a quantitative optimization of the inspection efforts[243]. This optimization is termed Risk Based Inspection planning (RBI). When combined with Structural Reliability Analysis (SRA), these methods provide a powerful tool for consistent asset integrity management, see[244, 245] or[246]. However, the fact that such optimization procedures are computationally highly demanding has for a long time been prohibitive for a widespread application of RBI on structures, and only few applications have been reported[247, 248, 249, 250]. To over-come the practical problems associated with the computations, applying RBI procedures on a set of generic representations of the actual components was proposed[251]. Inspection plans for individual components are then derived from the generic plans by simple interpolation algorithms. This approach, which was later refined[252], is now successfully applied in practice[253, 254].

The basic principle of the optimization is shown in Fig. 6-8. To reduce the cost of deterioration or, in other words, to optimize the life-cycle cost of structures, a balance must be achieved between the benefit of risk reduction (through improved design and maintenance, including inspections) and the cost associated with these measures. For structures in service, the design is often fixed and maintenance and inspections are the only feasible risk reduction measures. Therefore, the problem is to determine the inspection strategy that leads to the economically optimal reliability of the structure, but complies with given societal acceptance criteria. The RBI methods, as summarized in this article, facilitate the computation of the expected cost of failure as a function of the inspection efforts (the risk) and the identification of the minimal inspection efforts

This document is the intellectual property of the fib – International Federation for Structural Concrete. All rights reserved.
This PDF of fib Bulletin 86 is intended for use and/or distribution solely within fib National Member Groups.

required to achieve a certain level of reliability of the structural components. Due to their quantitative format, they allow documenting compliance of a given inspection strategy with prescribed risk acceptance criteria.

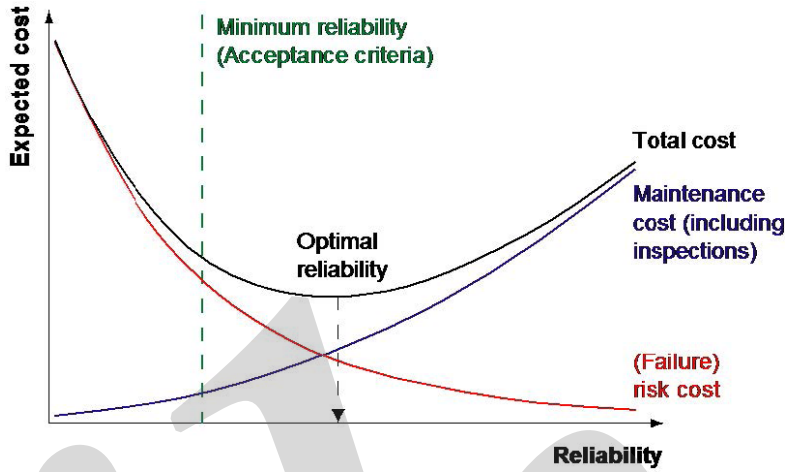


Fig. 6-8 The optimization problem for structures in service

An introduction in the RBI methodology based on Bayesian decision analysis will be given. The following section provides a brief overview on the principles of the analysis and the computation of the expected costs. Thereafter, the probabilistic modelling of deterioration and inspections is introduced through an example considering fatigue in welded joints. An outline of the generic approach to RBI and a discussion of system effects conclude the article.

### 6.6.3 Risk based inspection planning for structures

Traditionally, RBI is performed for individual structural elements separately. This section is thus limited to RBI for single structural elements; the inclusion of system effects is discussed later.

RBI is based on the pre-posterior analysis from the Bayesian decision theory as presented, e.g., in[63] or[64]. Based on probabilistic models of both the deterioration and the inspection performance, it aims at minimising the total expected cost of an inspection and maintenance plan, $E[C_T]$, which is the sum of the expected costs of failure, inspection and repair, Eq. (6-65).

$$\mathrm{E}\left[C_T\right]=\mathrm{E}\left[C_F\right]+\mathrm{E}\left[C_I\right]+\mathrm{E}\left[C_R\right] \tag{6-65}$$

The different expected costs are evaluated considering the different branches in the decision tree, illustrated in Fig. 6-9. All branches in the decision tree are characterized by their branching probability of occurrence and the associated costs.

Each branch in the decision tree represents an intersection of different decisions and random out-comes. When several inspections are planned, the total number of these branches becomes prohibitive for the full evaluation of the decision tree, because the calculations of the branching probabilities are computationally demanding. Therefore all published approaches use a simplified decision tree to limit the number of branches that must be computed. As an example consider the simplified decision tree from[255] shown in

This document is the intellectual property of the fib – International Federation for Structural Concrete. All rights reserved.
This PDF of fib Bulletin 86 is intended for use and/or distribution solely within fib National Member Groups.

Fig. 6-10: The decision tree is simplified by differentiating only between repair and no-repair events after the inspection and by representing the repaired structural element by a model identical to a new element (where the element after repair is stochastically independent of the element before repair). The branching probabilities in this decision tree are then given by the probability of failure given no repair, $p_F$, and the probability of repair after the inspections, $p_R$. The probability of repair is evaluated by calculating the probabilities of the different possible inspection outcomes (as a function of the considered inspection technique) and by relating the repair decision to the outcome by means of a decision rule *d*. Typical decision rules are, e.g., that every defect indicated by an inspection is repaired or that every defect with a measured size *s* larger than some limit $s_R$ is repaired. A limit state function (LSF) for the repair event *R* is then defined by combining the decision rule *d* with the inspection performance model. These calculations are described in detail in the literature, see, e.g.,[245] or[255].

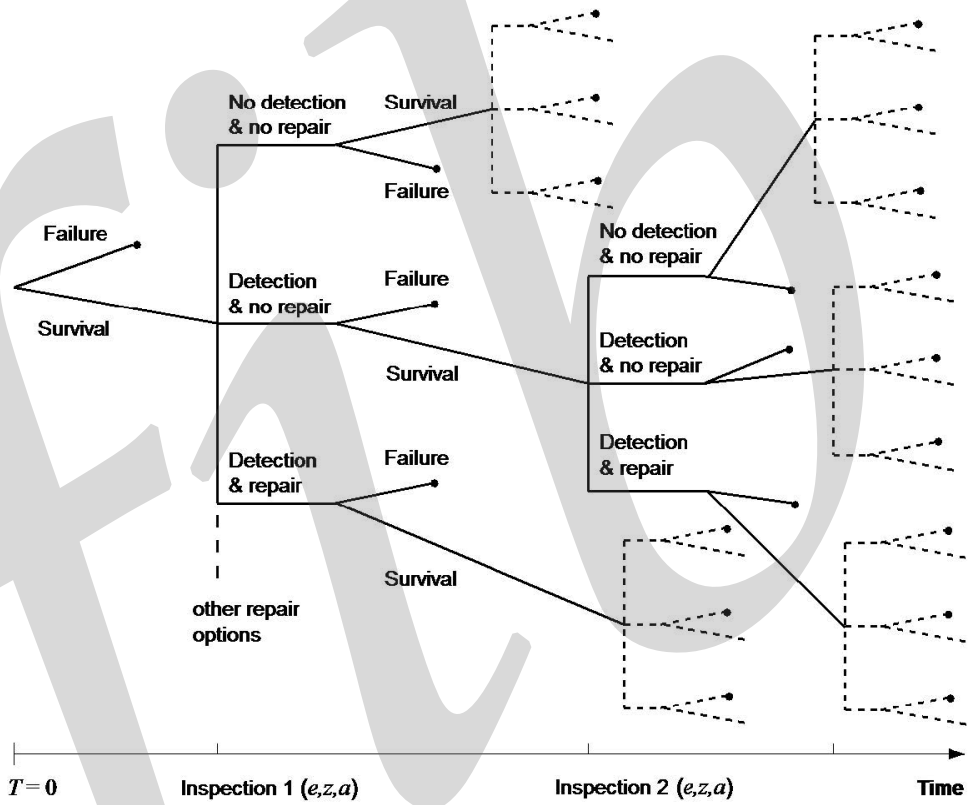


Fig. 6-9 The general event tree for risk based inspection planning (for a given inspection/repair strategy)

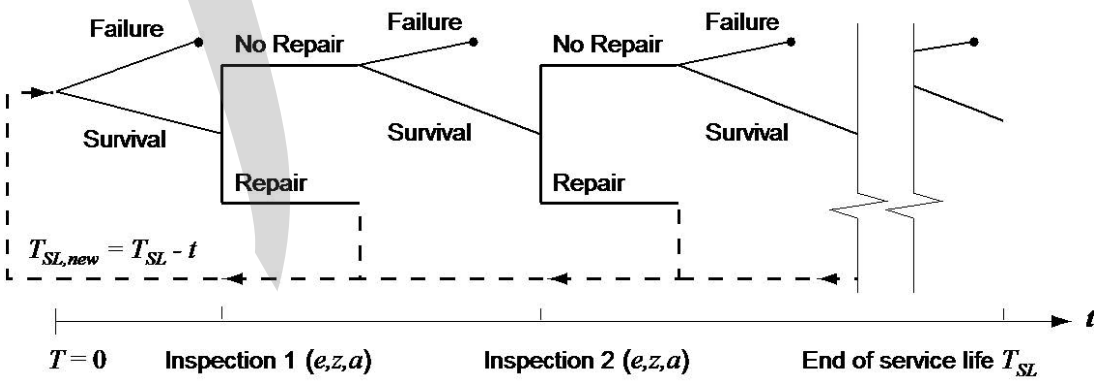


Fig. 6-10 The simplified event tree for risk based inspection planning

This document is the intellectual property of the fib – International Federation for Structural Concrete. All rights reserved.
This PDF of fib Bulletin 86 is intended for use and/or distribution solely within fib National Member Groups.

Based on the probabilities and the (monetary) consequences related to the individual events, the expected costs are calculated as net present values following the decision tree in Fig. 6-10. As an example, the expected cost of failure is given for a particular inspection strategy *e* as:

$$\mathrm{E}\left[C_F\left(e,d,T_{SL}\right)\right]=\sum_{t=1}^{T_{SL}}\left[\left(1-p_R\left(e,d,t-1yr\right)\right)\frac{c_1}{\left(1+r\right)^t}\right] \tag{6-66}$$

$$c_1=\left(p_F\left(e,d,t\right)-p_F\left(e,d,t-1yr\right)\right)c_F+\left(p_R\left(e,d,t\right)-p_R\left(e,d,t-1yr\right)\right)\mathrm{E}\left[C_F\left(e,d,T_{SL}-t\right)\right]$$

where *e* is a vector describing the inspection times and qualities, *d* is the decision rule on the repair actions, $T_{SL}$ is the anticipated service life of the structure given in years, $c_F$ is the cost of failure and *r* is the real rate of interest. The notation $p_F(e,d,t)$ and $p_R(e,d,t)$ is introduced to express that both the cumulative probability of failure and the cumulative probability of repair at time are conditional on no-repair at all inspections; they are thus a function of *e* and *d*. The calculation of $p_F(e,d,t)$ and $p_R(e,d,t)$ is described in the following section. The first additive term in $c_1$ in Equation (6-66) represents the cost of failure at time without a repair, the second corresponds to the expected cost of failure over the years following a repair at time *t* (in the anticipated remaining service life period $T_{SL}^{new} = (T_{SL} - t)$. Because of this latter term, Equation (6-66) is recursive. Alternatively, the classical renewal models may be applied, e.g.[256]. The calculation of the expected cost of inspections and repairs is in analogy to Eq. (6-66), the interested reader is referred to[255] for details.

## 6.6.4 Optimization of inspection strategies

An inspection strategy is defined by *e* and *d*; the aim of RBI is thus the identification of the set of *e* and *d* that yields the minimum expected total cost, i.e.,

$$\min_{e,d}\ \mathrm{E}\left[C_T\left(e,d,T_{SL}\right)\right] \tag{6-67}$$

subject to $\Delta p_F(e,d,t) \leq \Delta p_F^{\max}$, $t = 0,\ldots,T_{SL}$

where $\Delta p_F^{\max}$ is the acceptable probability of failure per year (the acceptance criterion) and must be determined in accordance with the relevant code and the preferences of the owner or operator of the structure[257]. $\Delta p_F(e,d,t)$ is the annual probability of failure (also known as the failure rate), defined as

$$\Delta p_f\left(e,d,t\right)=\frac{P_F\left(e,d,t\right)-p_F\left(e,d,t-\Delta t\right)}{\Delta t\left(1-p_F\left(e,d,t-\Delta t\right)\right)} \tag{6-68}$$

The decision rule *d* to apply is often prescribed by the operator of the structure, otherwise the number of feasible decision rules is in general limited and the identification of the optimal d is straightforward. The number of possible *e* (the possible combinations of inspection times and methods over the service life time of the structure) on the other hand is very large and thus prohibitive for the direct evaluation of Equation (6-68). For this reason, the threshold approach and the equidistant approach to inspection planning were introduced, as described in[251]. In the equidistant approach the number of possible *e* is limited by prescribing that the time between subsequent inspections is a constant; the inspection times are then fully described by the length of the inspection $\Delta T_{Insp}$ interval

This document is the intellectual property of the fib – International Federation for Structural Concrete. All rights reserved.
This PDF of fib Bulletin 86 is intended for use and/or distribution solely within fib National Member Groups.

respectively the total number of inspections $n_{Insp}$ (for given service life). When $e$ denotes the type of inspection to perform, the general optimization problem can be rewritten as

$$\min_{e,n_{Insp},d} \; \mathrm{E}\left[C_T\left(e,\Delta T_{Insp},d,T_{SL}\right)\right] \tag{6-69}$$

subject to $\Delta p_F(e,\Delta T_{insp},d,t) \leq \Delta p_F^{\max}$, $t = 0,\ldots,T_{SL}$

Applying the threshold approach, inspections are planned in the year before the annual probability of failure exceeds a threshold $\Delta p_f^T$ as illustrated in Fig. 6-11. The obtained inspection intervals increase with time. This is commonly observed for many deterioration phenomena and is explained by the decrease in uncertainty after each inspection, which is accounted for by the Bayesian updating of the probabilities following an inspection.

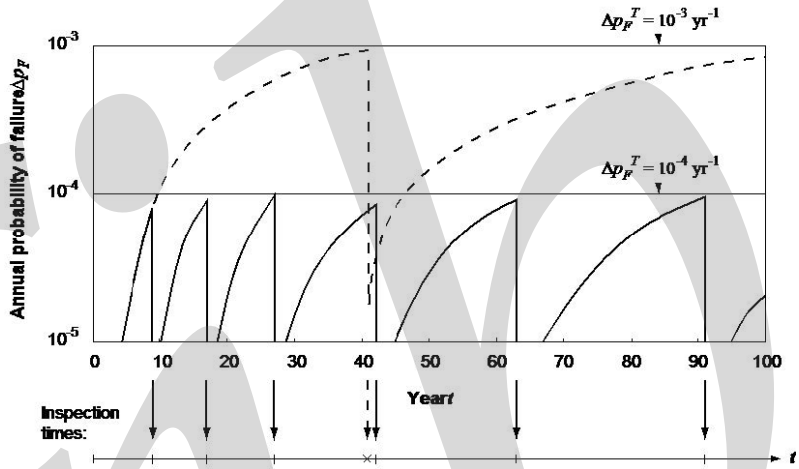


Fig. 6-11 Determination of the inspection times as a function of the threshold on the annual probability of failure for the welded joint as described by the probabilistic model in[18]

For the threshold approach, the optimization problem is written as

$$\begin{aligned} &\min_{e,\Delta p_F^T,d} \left[C_T\left(e,\Delta p_F^T,d,T_{SL}\right)\right] \\ &s.t. \quad \Delta p_F^T \leq \Delta p_F^{\max} \end{aligned} \tag{6-70}$$

The threshold approach has the advantage that the constraint is formulated directly on the optimization parameter. This facilitates the interpretation of the optimization results because it is immediately recognisable if an inspection plan complies with the requirements in terms of the acceptable annual probability of failure $\Delta p_F^{max}$.

The optimization with both the threshold approach and the equidistant approach is carried out by evaluating the total expected costs for different values of the optimization parameters. For the threshold approach, the obtained solution is only an approximation because the threshold is a continuous variable, yet the accuracy is in general sufficient for any practical purpose. Fig. 6-12 shows the optimization using both approaches; it is observed that the calculated minimal expected costs are approximately the same for both approaches.

This document is the intellectual property of the fib – International Federation for Structural Concrete. All rights reserved.
This PDF of fib Bulletin 86 is intended for use and/or distribution solely within fib National Member Groups.

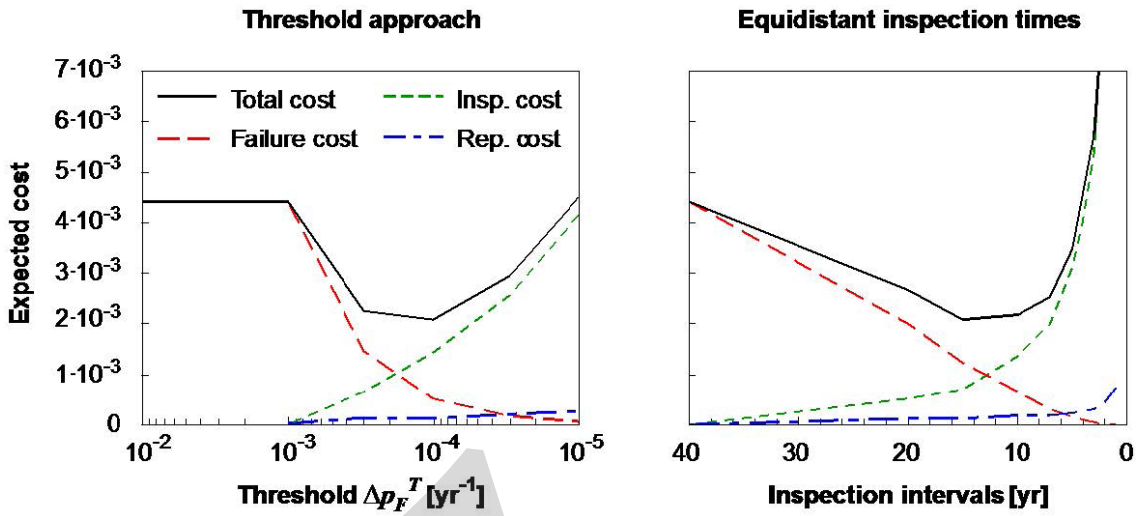


Fig. 6-12 Optimization of inspection efforts: Comparing the threshold and the equidistant approach[252]

### 6.6.5 Example on deterioration using Risk Based Inspection (RBI) modelling

Most deterioration phenomena on structures are of a highly stochastic nature; the models describing these processes consequently involve large variations and uncertainties. Therefore, deterioration mechanisms are represented by stochastic models of the defect size as a function of time. A review of various probabilistic models for fatigue, corrosion and combinations thereof is provided in[255]. Inspections can reduce the uncertainty associated with deterioration; in doing so, they facilitate the purposeful application of mitigation actions. However, the performance of inspections is subject to uncertainty itself, which is typically represented by Probability of Detection (PoD) models and estimations of the Probability of False Indication (PFI). In this section, the probabilistic modelling of deterioration and inspections is presented through an example of fatigue deterioration and associated inspections. It is then demonstrated how these models are applied to compute the conditional probabilities of failure and repair as a function of time, $p_F(e,d,t)$ and $p_R(e,d,t)$. All numerical results presented here are computed with the parameter values given in[252].

The specific example considered is a typical welded joint in a tubular offshore structure subject to fatigue. Failure of such an element can be described by the SN limit state function, Eq. (6-71).

$$g_{SN}(t) = \Delta - D_{tot}(t) \tag{6-71}$$

where $\Delta$ is the failure criteria and $D_{tot}(t)$ is the accumulated damage at time t according to the Palmgren-Miner rule, which is a function of the stress ranges and the SN curve representing the type of detail and environment. In many instances analytical solutions for $D_{tot}(t)$ exist, e.g., for the fairly typical situation when the stress ranges can be modelled by a Weibull distribution, see[255] for details. Because the Bayesian updating of fatigue reliability after an inspection requires that the limit state function describing fatigue performance contains the same (geometric) parameters as the inspection performance model, a fracture mechanics based crack growth model (FM model) must be used that explicitly contains the crack dimensions as a model parameter. Therefore a FM model is calibrated to the SN model, in such a way that the evaluated reliability is the same for the two models, as shown in (6-15).

This document is the intellectual property of the fib – International Federation for Structural Concrete. All rights reserved.
This PDF of fib Bulletin 86 is intended for use and/or distribution solely within fib National Member Groups.

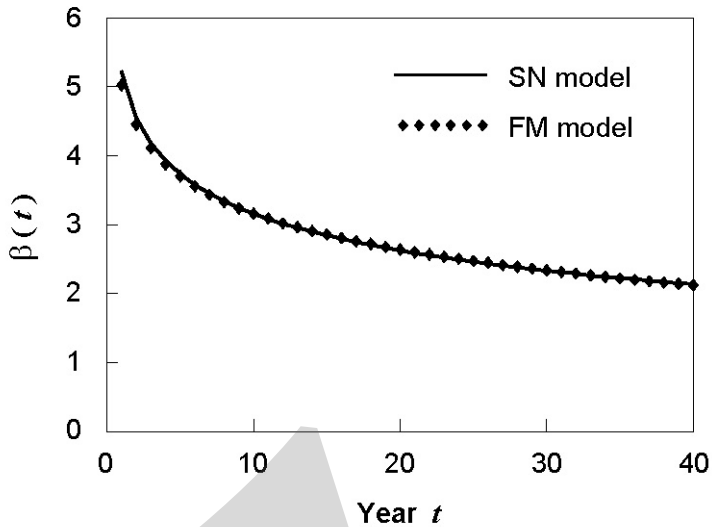


Fig. 6-13 The reliability of the considered fatigue example as evaluated using the SN and the FM approach

The limit state function describing ductile fatigue failure using the FM approach is

$$g_{FM}(t) = N_I + N_P - \upsilon t \tag{6-72}$$

where $N_I$ is the number of cycles to crack initiation and $N_P$ is the number of cycles it takes for the crack to grow from the initial crack size to the failure size. $N_I$ can be determined according to[258] as:

$$N_I = N_{I_0} \frac{\left(150 Nmm^{-2}\right)^{m_1}}{\Delta S_e^{m_1}} \tag{6-73}$$

where $\Delta S_e$ is the equivalent stress range, $m_1$ is the slope parameter of the *SN* curve and $N_{I_0}$ is the number of cycles to initiation at the normalizing mean stress range equal to 150 Nmm-2. $N_{I_0}$ is cor-related to the crack propagation parameter $C_P$. $N_P$ is calculated by solving a coupled differential equitation based on Paris' law, Eq. (6-74). This model is based on the assumption of a semi-elliptical crack shape with crack depth *a* and length 2*c*.

$$\begin{aligned} \frac{da}{dN} &= C_{P,a}\left(\Delta K_a\left(\Delta S_e, a, c, DoB\right)Y\right)^{m_{FM}} \\ \frac{dc}{dN} &= C_{P,c}\left(\Delta K_c\left(\Delta S_e, a, c, DoB\right)Y\right)^{m_{FM}} \end{aligned} \tag{6-74}$$

*N* is the number of cycles, $C_{P,a}$, $C_{P,c}$ and $m_{FM}$ are (empirical) parameters describing the crack growth. $\Delta K_a(\Delta S_e,a,c)$ and $\Delta K_a(\Delta S_e,a,c)$ are the stress intensity factor ranges in the *a* and *c* direction and are calculaced using the empirical solutions from[259] as a function of the equivalent stress range $\Delta S_e$ and the degree of bending *DoB*. *DoB* is the fraction of the stresses at the hot spot which are due to bending (in the undamaged condition). *Y* is the model uncertainty related to the stress intensity factors. The boundary conditions for the solution of Equation (6-74) is given by the initial crack size as $a(N = N_I) = a_0$, $c(N = N_I) = c_0$. The value of $\Delta S_e$ is calculated from the design fatigue life $T_{FL}$ by setting all parameter values in the *SN* model equal to their design values and by determining the stress range for which the fatigue life becomes equal to $T_{FL}$.

This document is the intellectual property of the fib – International Federation for Structural Concrete. All rights reserved.
This PDF of fib Bulletin 86 is intended for use and/or distribution solely within fib National Member Groups.

The inspection performance is modelled by means of Probability of Indication (PoI) models. The PoI corresponds to the Probability of Detection (PoD) where additionally the probability of a false error is included, i.e., the probability that a defect is indicated where none is present, see also[260]. The applied PoI model is dependent on the crack depth *a* and given as:

$$PoI(a) = PoD(a) + \left(1 - PoD(a)\right)PFI$$
$$PoD(a) = \frac{\exp\left(\alpha_D + \beta_D \ln(a)\right)}{1 + \exp\left(\alpha_D + \beta_D \ln(a)\right)} \tag{6-75}$$

The parameters of the PoI are given as $\alpha_D$ = 0.63, $\beta_D$ = 1.16 and PFI = 0.138. The event of indication of a crack with depth *a* at the inspection is described by a limit state function, Eq. (6-76), in accordance with Hong[261].

$$g_I(t) = z - \Phi^{-1}\left(PoI\left(a(t)\right)\right) \tag{6-76}$$

Z is a standard normal distributed random variable and $\Phi^{-1}(.)$ is the inverse of the standard normal distribution function.

A repair is performed when a defect is indicated and measured as being deeper than 1 mm. This is the applied decision rule d, see[255] for other possible rules. The event of repair therefore requires the definition of an additional measurement limit state, defined as:

$$g_M(t) = a_R - a(t) - \varepsilon_m \tag{6-77}$$

with $a_R$ being the repair criterion (here $a_R$ = 1 mm) and $\varepsilon_m$ the measurement uncertainty, modelled as Normal distributed random variable with zero mean and standard deviation $\sigma_{\varepsilon_m}$ = 0.5. mm.

The probabilities $p_F(e,d,t)$ and $p_R(e,d,t)$ to be applied in Equations (6-78) and (6-79) are now computed from the limits state functions using crude Monte Carlo simulation (and structural reliability analysis for validation purposes). The probability of repair at the first inspection is given as

$$P_R\left(\underline{e}, d, t = t_{Insp_1}\right) = P\left(g_I\left(t_{Insp_1}\right) \le 0 \cap g_m\left(t_{Insp_1}\right) \le 0\right) \tag{6-78}$$

The probability of failure in the first *t* years given no repair at previous inspections is calculated from

$$p_F(\underline{e}, d, t) = \frac{P\left(g_{FM}(t) \le 0 \cap \left(\cap_{i=1}^{n_{Insp}(t-1yr)}\left(g_I(t_i) > 0 \cup g_M(t_i) > 0\right)\right)\right)}{P\left(\cap_{i=1}^{n_{Insp}(t-1yr)}\left(g_I(t_i) > 0 \cup g_M(t_i) > 0\right)\right)} \tag{6-79}$$

$n_{Insp}(t - 1\text{yr})$ is the number of inspections that are planned in the interval $[0, t - 1\text{yr}]$ and $t_i$ are the times of inspections, as prescribed by the inspection vector *e*. The conditional probability of repair after an inspection in year is evaluated accordingly as

$$p_R(\underline{e}, d, t) = \frac{P\left(\left(g_I(t) \le 0 \cap g_m(t) \le 0\right) \cap \left(\cap_{i=1}^{n_{Insp}(t-1yr)}\left(g_I(t_i) > 0 \cup g_M(t_i) > 0\right)\right)\right)}{P\left(\cap_{i=1}^{n_{Insp}(t-1yr)}\left(g_I(t_i) > 0 \cup g_M(t_i) > 0\right)\right)} \tag{6-80}$$

This document is the intellectual property of the fib – International Federation for Structural Concrete. All rights reserved.
This PDF of fib Bulletin 86 is intended for use and/or distribution solely within fib National Member Groups.

### 6.6.6 Generic approaches to risk based inspection (RBI)

The probability calculations, Equations (6-79) and (6-80) are computationally demanding, especially for fatigue problems. This has hindered the application of the RBI methodology in practice and has been prohibitive for the consideration of the system effects. The generic approach to RBI was developed to overcome these limitations, see[255] and[252]. The core of the generic approach to RBI is the pre-fabrication of inspection plans for generic hot spots which are representative for the particular hot spots in the considered structures. These pre-fabricated plans are termed Generic Inspection Plans. The inspection plans for the individual hot spots in a structure are then obtained from the generic inspection plans through an interpolation procedure. All hot spots that are represented by the model are fully described by the so-called generic parameters. These are the input parameters to the model that vary from hot spot to hot spot and which are indicators of the relevant deterioration mechanism. For structures subjected to fatigue, typical examples of such generic parameters are, e.g., the calculated design fatigue life $T_{FL}$ (respectively the dimensionless Fatigue Design Factor FDF; The FDF is a deterministic safety factor, defined as the ratio of the calculated design fatigue life to the design service life), other loading characteristics, the applied SN curve (which is representative for the detail type and the environment) and geometrical parameters such as the wall thickness at the hot spot. Because these parameters are obtained from standard fatigue evaluation procedures, the RBI can, in principle, be performed without specialist knowledge once the generic inspection plans are available.

The computational efficiency of the generic approach rests on the replacement of the demanding probability evaluations by an interpolation of the probabilities, which are calculated previously and stored in the generic database. Although the calculations of the generic inspection plans are still demanding, these are performed at a previous stage; the extraction of inspection plans for particular structures from the generic database on the other hand is very efficient and can be integrated in the daily asset integrity management procedures of the owner or operator of the structure. When simulation is applied, the generic approach reduces the CPU time required for the calculation of the inspection plans by a factor which is in the order of[104] (from hours and days to few seconds). Details on the computational aspects are provided in[252].

As an example of the generic approach consider Fig. 6-14. The required inspections to comply with given acceptance criteria can be evaluated as a function of the FDF. For fixed values of all other parameters, the inspection times are obtained as a function of the FDF. Similarly the expected costs can be expressed as a function of the FDF, Fig. 6-15.

This document is the intellectual property of the fib – International Federation for Structural Concrete. All rights reserved.
This PDF of fib Bulletin 86 is intended for use and/or distribution solely within fib National Member Groups.

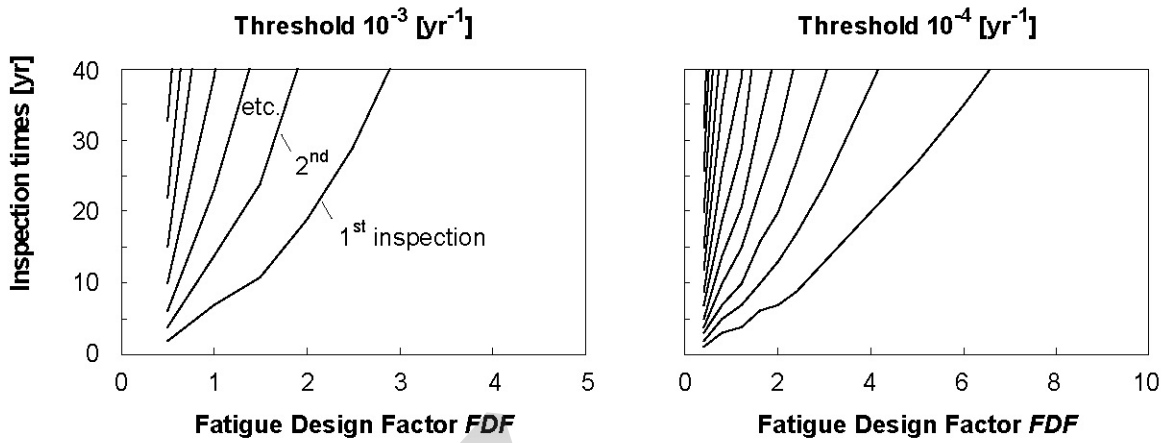


Fig. 6-14 Inspection times as a function of the FDF for two different thresholds on the annual prob-ability of failure[252]

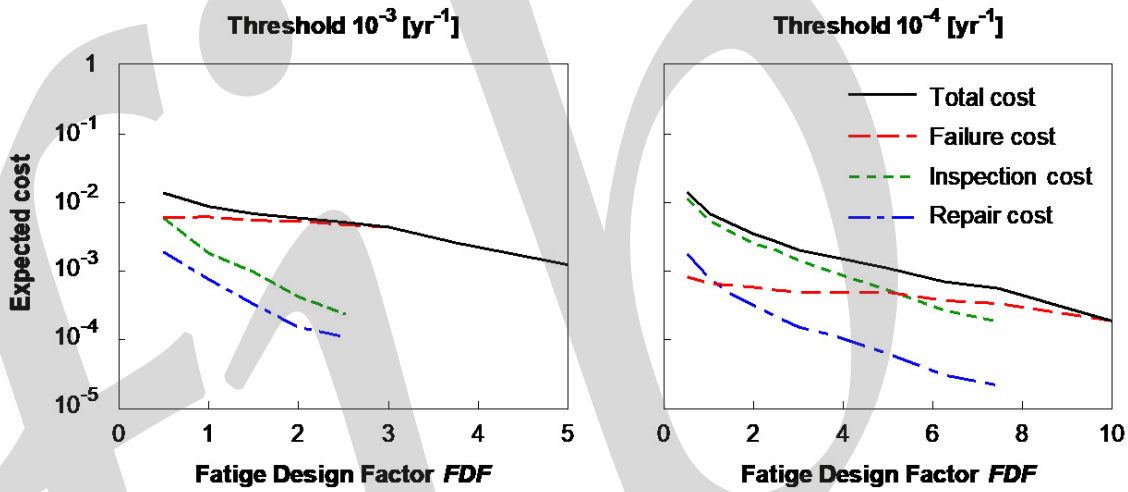


Fig. 6-15 Expected costs as a function of the FDF for two different thresholds on the annual prob-ability of failure[252]

## 6.6.7 System effects in risk based inspection

It has been realized that for large structural systems, considerations of system effects in risk based inspection (RBI) is required to ensure an optimal inspection planning[262, 263]. As an example, consider ship hulls that contain thousands of structural details, for which detailed inspection of all elements would be sub-optimal and often is not feasible. Therefore, it is required that in addition to optimizing the inspection plans for the individual elements, the inter-dependences among the elements are considered in the analysis. In the following, these dependences are shortly outlined.

### 6.6.7.1 Dependences in deterioration phenomena

Interdependences between the deterioration at the individual components arise from a) common influencing factors, such as the composition and temperature of a gas along the pipeline, as well as from b) common statistical and model uncertainties. Although this dependence among the deterioration states from one location to another is often inherently assumed (If only part of the system is inspected, any extrapolation of the outcomes to the

This document is the intellectual property of the fib – International Federation for Structural Concrete. All rights reserved.
This PDF of fib Bulletin 86 is intended for use and/or distribution solely within fib National Member Groups.

non-inspected components is based on this dependency.), it is rarely modelled explicitly in inspection planning. It not only influences the system failure probabilities, but also the amount of information gained by a partial inspection of the system.

#### 6.6.7.2 Dependences in inspection performance

Inter-dependences between the inspection performances at different components are modelled and investigated by[260]. It is found that for well-controlled inspections, the influence of the dependencies on the system reliability after the inspections is relatively small. The cost of inspections is in general not increasing linearly with the number of inspected components $N_I$, instead the marginal cost is often decreasing with increasing $N_I$. If, e.g., scaffolding is the main contributor to the inspection cost, the cost per inspected component decreases with increasing $N_I$.

#### 6.6.7.3 Dependences in failure consequences

In many systems, failures of the individual components only have limited consequences, whereas failure of the entire system can be safety critical and may induce substantial cost. In such systems, the cost of a component failure is a function of the influence that the component has on the overall system reliability, which can be expressed by the redundancy of the system with respect to failure of the component. Simple indicators for the redundancy, as presented by[257], are available. However, a full model must take into account the combined effect of several component failures, commonly modelled by a cut-set of the component failure events. Such a model is proposed in[264].

An approach for fully including system effects in RBI has been presented in[265]. It is based on an optimization of the individual structural elements, using the generic approach previously outlined, combined with an explicit consideration of the inter-dependence in the system as discussed above. As an example, the effect of an inspection of one element on the reliability of the other elements is computed and included in the analysis by modifying the models of the non-inspected elements accordingly. Due to the considerable computational efforts required for such an approach, to date, a full implementation of a systems approach to RBI is not realistic, but simplified models derived from the approach have been used in practice, e.g.[252].

### 6.6.8 Conclusions

In the past, RBI methods have sometimes been confronted with the somewhat imprecise reproach of being “too theoretical”. Underlying this statement are two arguments, which are often well-justified, namely that the methods are computationally too demanding and thus not economical and that the methods are too difficult to understand and may therefore cause gross errors. The first argument has become obsolete through recent developments, such as the generic approach to RBI outlined in this article. For large structural systems, RBI has a huge potential benefit for optimizing the inspection and maintenance efforts, which quickly exceeds the cost of establishing a database containing the generic inspection plans and a software for the application of the RBI procedure on a daily basis. The second argument is more severe, but it is reminded that the procedures presented in this article must be embedded in a general asset integrity management strategy, which considers all possible failure modes. As discussed in[266], such strategies must be robust in regard to the underlying model assumptions. In industrial applications that followed these principles,

*This document is the intellectual property of the fib – International Federation for Structural Concrete. All rights reserved.*
*This PDF of fib Bulletin 86 is intended for use and/or distribution solely within fib National Member Groups.*

RBI methods have proven to be a practical and consistent approach to the planning of inspections in structures. The financial benefits in terms of the expected total life-cycle cost can be huge as compared to traditional prescribed inspection intervals. Furthermore, RBI plans ensure compliance of the structures with risk acceptance criteria during the entire service life of the structure, which is not generally guaranteed by application of prescribed inspection intervals.

This document is the intellectual property of the fib – International Federation for Structural Concrete. All rights reserved.
This PDF of fib Bulletin 86 is intended for use and/or distribution solely within fib National Member Groups.

# 7. Life cycle performance

## 7.1 General

Environmental and mechanical stressors create a degradation process for most structures that are at the beginning of the service life. This degradation process progressively deteriorates the resistance of these structures. In order to keep a structure in a safe state, it needs to be maintained. In maintenance, either the degradation process is repressed or its effects are reversed. The actions taken to maintain a structure are more effectively selected if they are determined as part of an optimum life-cycle maintenance strategy. Such strategy can be best obtained by life-cycle planning and maintenance optimization. In this chapter, some of the fundamentals of the maintenance optimization process are presented and some optimization techniques are provided.

## 7.2 Prediction of life-cycle performance

Maintenance is essentially performed to structures in order to keep their performance above prescribed levels. The structural performance generally degrades over time. Traditionally, a performance threshold is set such that the degrading performance should never cross it. If crossed, the structure is deemed not fit or safe for use. Maintenance actions are selected based on their effects on the structural performance and the cost of their application. In most cases, the selection of a maintenance action at some point in time is dependent upon the sequence of selected maintenance actions over the structural life-cycle and their overall effects on the life-cycle performance. Therefore, a profile for the maintained performance has to be predicted in order to be used for the selection of the optimum maintenance actions.

Life-cycle performance is quantified by indicators. The safety and serviceability of the structures are ensured by preventing the performance indicators from crossing their thresholds. Needless to say, a performance indicator used for the maintenance optimization process is required to be able to accurately represent a specific type of structural performance. [267] have identified several commonly encountered and used life-cycle performance indicators. Examples of these indicators and their applications are: the point-in-time reliability index[268, 269, 270, 271, 239, 272], the point-in-time probability of system failure and redundancy index[240], the cumulative probability of failure[273, 274, 275, 276, 277], the lifetime probability of failure or the unavailability[278, 279, 280, 281, 281, 238], condition and safety indices[282, 283, 284, 285, 286, 287, 288, 289].

Choosing the performance indicators to be used in maintenance planning can be challenging. Different factors influence the choice. These factors include: the type of structural performance (e.g., serviceability, ultimate), the level of modelling detail required (i.e., component, system, network; or network of networks), the degree of accounting for uncertainty, the accuracy, and computational speed[290,286,291, 292, 293, 294, 295]. Additional information on maintenance of structures using probabilistic and/or optimization concepts can be found in [296] and [297].

This document is the intellectual property of the fib – International Federation for Structural Concrete. All rights reserved.
This PDF of fib Bulletin 86 is intended for use and/or distribution solely within fib National Member Groups.

### 7.2.1 Point-in-time reliability

Structural reliability has been recognised as a powerful tool for design and assessment under uncertainty. The topic has also found its way into the maintenance planning field. Structural reliability defines safety as the condition in which failure will not occur. In its most basic forms, the structural reliability problem is formulated as the problem of calculating the probability that failure will occur due to loading (i.e., demand) exceeding the resistance. However, its calculation is generally tedious. Computer programs are available for computing the structural and the system reliability such as RELSYS[233] and CALREL[298].

In the following an example on determining the point-in-time reliability index profile for a simply supported beam of span L = 5 m, loaded at midspan by a concentrated load *P* is presented. The applied load is a time-invariant normal random variable with mean 10 kN and standard deviation 2 kN. The flexural resistance of the beam M is a lognormal random variable with mean 40 kN.m and standard deviation 6 kN.m. The resistance degrades with time, where the mean decreases in a rate of 0.01/year and the standard deviation increases with a rate of 0.01/year. The lifespan of the beam is assumed as 40 years. The point-in-time performance function associated with flexural failure of the mid-span section is

$$g(t) = M(t) - \frac{P \cdot L}{4} \tag{7-1}$$

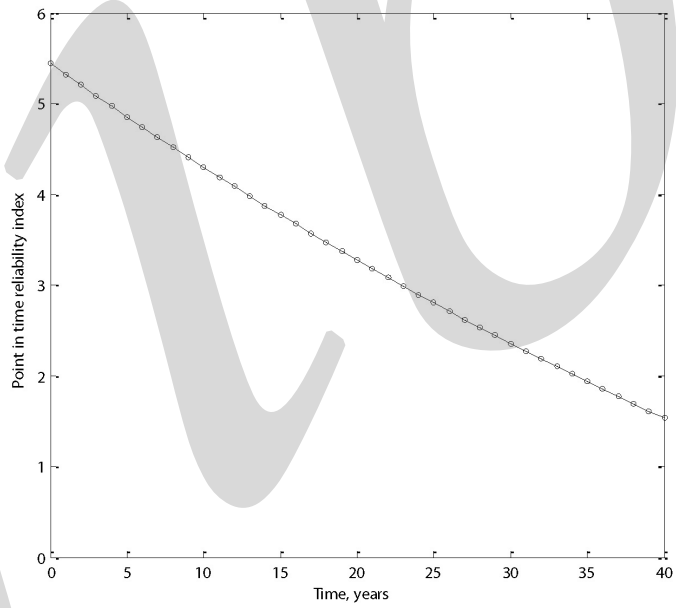


Fig. 7-1 Point-in-time reliability index profile for a simply supported beam

In order to solve this problem, the general purpose time-invariant reliability software used for determining the point-in-time reliability index is RELSYS. The input file is updated at each time increment, RELSYS is run, and the results are extracted from the output file. The resulting point-in-time reliability index profile is shown in Fig. 7-1. The deterioration in the performance of this simply supported beam is evident in this figure. If a threshold was set to $b = 3$, an essential maintenance action should clearly be needed by the year 23, or preventive maintenance actions could be applied before the year 23. If an essential maintenance action that restores the structural performance to its initial condition is applied at the year 23, the point-in-time reliability index profile becomes as shown in Fig. 7-2.

This document is the intellectual property of the fib – International Federation for Structural Concrete. All rights reserved.
This PDF of fib Bulletin 86 is intended for use and/or distribution solely within fib National Member Groups.

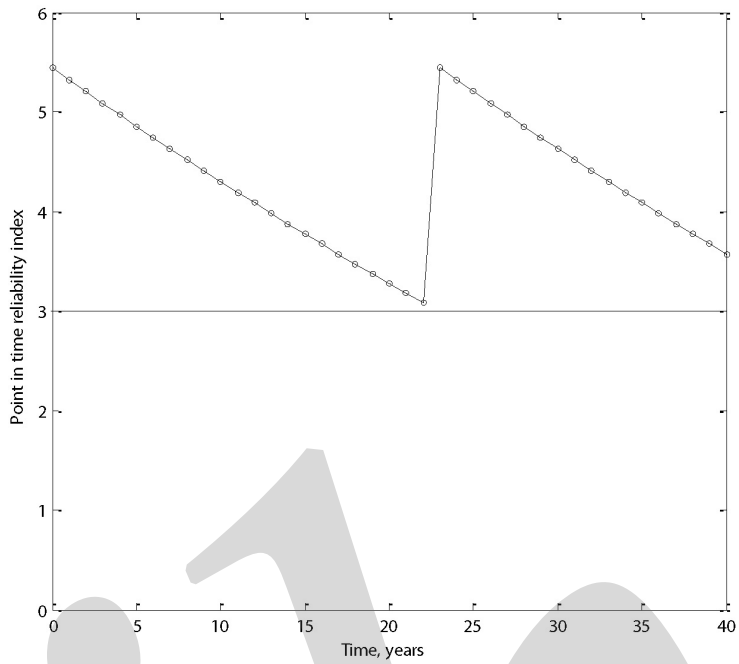


Fig. 7-2 Point-in-time reliability index profile for a simply supported beam considering an essential maintenance action at year 23

## 7.2.2 Unavailability

The fact that the unavailability is one of the most computationally effective performance indicator for automated maintenance optimization was demonstrated by[299]. Unavailability is one of the representations of lifetime functions. Lifetime functions are probabilistic distributions that represent the lifetime performance of components and structures. Statistical records of the ages of components and structures are used to determine an appropriate distribution for their time to failure probability density function (PDF). Typically, the time to failure PDF is the source used to generate the different representations of lifetime functions. The time to failure is a random variable and is defined as the time elapsing from the time the component is put into operation until it fails for the first time. Having the time to failure PDF, the unavailability profile can be determined.

A component is unavailable at time t if it is not functioning at time t. The unavailability *An*(*t*) can be calculated by integration of the PDF of the time to failure[300]. The unavailability of a component without maintenance can be calculated by

$$An(t) = P\left(T < t\right) = \int_0^t f(u)\,du \tag{7-2}$$

where *T* is the time to failure and *f*(*t*) is its PDF. Structural components typically have lifetime functions modelled by the Weibull distribution. Hence, the unavailability can be given as:

$$An(t) = \begin{cases} 1 - e^{-(\lambda t)^{\kappa}} & \text{for } t \geq 0 \\ 0 & \text{otherwise} \end{cases} \tag{7-3}$$

where *l* is a scale parameter and *k* is a shape parameter.

The system unavailability may also be used as the performance indicator in maintenance planning. The system unavailability can be established by the minimal cut set method[300].

This document is the intellectual property of the fib – International Federation for Structural Concrete. All rights reserved.
This PDF of fib Bulletin 86 is intended for use and/or distribution solely within fib National Member Groups.

A minimal cut set is a set of components in the system which by failing causes the system to fail, but if one doesn't fail the system doesn't fail. Once the minimal cut sets are determined, the system unavailability can be established as:

$$An_s(t) = 1 - \prod_{j=1}^{n_K} \left[ 1 - \prod_{i \in K_j} An_i(t) \right] \tag{7-4}$$

where $K_j$ is the $j^{th}$ cut set, and $n_K$ = the number of cut sets and $An_i(t)$ is the unavailability of component i from the cut set $K_j$.

In the following an example on determining the unavailability profile for a simply supported beam with lifetime function modelled by the Weibull distribution having its scale parameter $l$ = 1/150 and shape parameter $\kappa$ = 2.5 is presented. The life-span of the beam is assumed as 40 years.

Equation 7-4 is solved at 1 year increments and the results are shown in Fig. 7-3. Note that the unavailability at time $t$ = 0 is $An(0)$ = 0. However, realistic components have an initial unavailability. In this example, it is assumed that $An(0)$ = 10-6. Again, the deterioration in the performance of this simply supported beam is evident in the figure. If a threshold was set to $An$ = 10-2, an essential maintenance action should clearly be needed by the year 24, or preventive maintenance actions could be applied before the year 24. If an essential maintenance action that restores the structural performance to its initial condition is applied at the year 24, the unavailability profile becomes as shown in Fig. 7-4.

## 7.3 Optimization of maintenance

### 7.3.1 Introduction

The primary goal in the maintenance planning process is the minimization of cost. The objective is typically to find the maintenance solution with minimum life cycle cost. Additional objectives may include improving performance. Hence, the problem may require fulfilling multiple conflicting objectives. Generally, the maintenance planning process involves multiple variables and parameters that make finding the solution practically impossible to obtain without using an efficient solution tool. Optimization is used as such tool.

In optimization, one can find the solution to a mathematical problem that maximizes or minimizes one or more objectives without violating preset constraints. The solution is represented by variables, called the design variables, that make up the objectives and constraints. The objectives and constraints are formulated as explicit or implicit mathematical functions of the design variables. Therefore, to solve the maintenance planning problem using optimization, the first step is to interpret the problem into a proper mathematical formulation that satisfies its needs and is capable of being solved using a proper optimization technique. In some advanced cases, the problem formulation and solution technique are set up and adjusted to accommodate each of their capabilities and restraints. For instance, using certain types of variables in the problem formulation may require adjusting the operations inside the solution technique to accommodate this variable; or the problem formulation has to be modified because the solution technique is unable to handle it properly or efficiently.

This document is the intellectual property of the fib – International Federation for Structural Concrete. All rights reserved.
This PDF of fib Bulletin 86 is intended for use and/or distribution solely within fib National Member Groups.

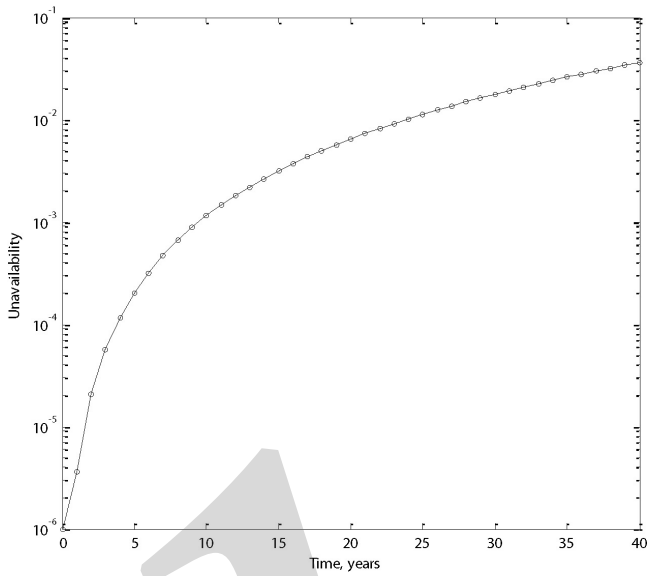


Fig. 7-3 Unavailability profile for a simply supported beam

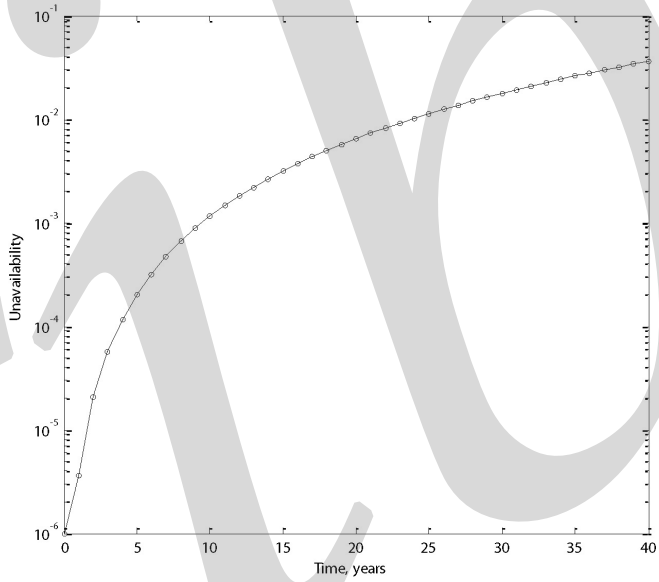


Fig. 7-4 Unavailability profile for a simply supported beam considering an essential maintenance action at year 24

Developing mathematical formulations for the maintenance optimization problem is a process in continuous growth. In this chapter, some of these formulations are presented. Developing optimization solution techniques have also exhibited significant progress. Currently, Genetic Algorithms (GA) are the most commonly used tools in maintenance optimization. In this section, some of the fundamentals of mathematical optimization and GA are reviewed.

#### 7.3.1.1 The basic problem

Ingredients of an optimization problem are: (a) the design variables, which the problem aims to find best values for, (b) objective functions, which the problem aims to improve by minimizing or maximizing, and (c) constraints, which the problem must not violate for the optimum solution. As shown in Fig. 7-5, global solutions to single objective optimization problems, if exist, are unique.

This document is the intellectual property of the fib – International Federation for Structural Concrete. All rights reserved.
This PDF of fib Bulletin 86 is intended for use and/or distribution solely within fib National Member Groups.

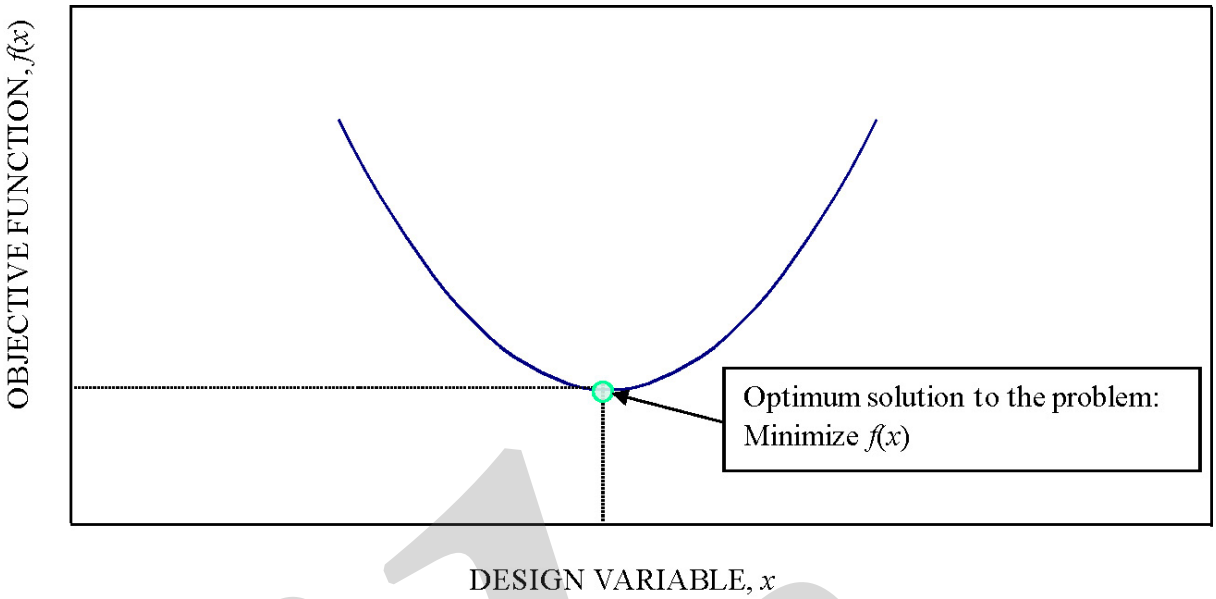


Fig. 7-5 Sketch of a qualitative solution of a one dimensional single objective optimization problem: Minimize $f(x)$

It is shown in the following example, how the optimum values of the design variables: $X_1$ and $X_2$ can be defined. To maximize the objective function:

$$Z = 2X_1 + 3X_2 \tag{7-5}$$

Subject to the constraints:

$$g_1 = X_1 + 2X_2 \leq 10 \tag{7-6}$$

$$g_2 = X_1 + X_2 \leq 8 \tag{7-7}$$

$$g_3 = X_2 \leq 4 \tag{7-8}$$

$$X_1; X_2 \geq 0 \tag{7-9}$$

This problem can be solved using several methods. Since there are only two design variables, a graphical solution can be found in the ($X_1$, $X_2$) space. Fig. 7-6 shows the objective and constraints (Equations (7-6) through (7-9)) drawn in the ($X_1$, $X_2$) space. These constraints divide the ($X_1$, $X_2$) space into a region that contains the combinations of $X_1$ and $X_2$ that satisfy the constraints (i.e. the feasible region) and a region in which these combinations violate the constraints (i.e. the infeasible region). Contour lines of the objective function $Z$ (Equation (7-5)) can be drawn on the figure, where each line represents all the combinations of values of $X_1$ and $X_2$ that give the same value of $Z$. The point of intersection of the constraints with the contour line that gives the maximum $Z$ inside the feasible space is the optimum solution ($X_1$ = 6, $X_2$ = 2, $Z$ = 18).

This document is the intellectual property of the fib – International Federation for Structural Concrete. All rights reserved.
This PDF of fib Bulletin 86 is intended for use and/or distribution solely within fib National Member Groups.

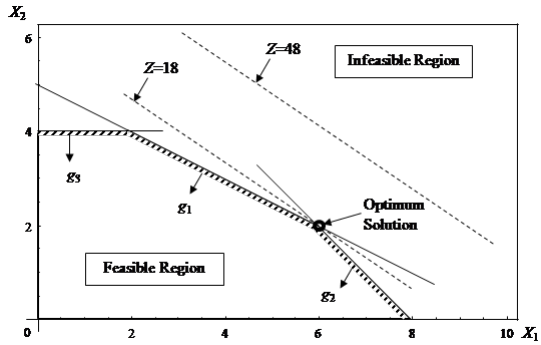


Fig. 7-6 Graphical solution for the single optimization example

### 7.3.1.2 Multi objective optimization

Some applications of optimization, such as in the field of civil infrastructure management, involve multiple competing objectives that need to be simultaneously minimized or maximized. However, in the case of multi-objective optimization problems, one cannot improve an objective without compromising another competing one .Therefore, there exists a set of solutions, known as the set of Pareto-optimal (or non-dominated) solutions, that are optimum trade-offs among all objectives. A solution is Pareto-optimal if there doesn't exist another solution that improves at least one objective without worsening another one[301].

In the qualitative bi-objective optimization problem shown in Fig. 7-7. Solution A presents a solution that best improves (minimizes) the first objective while most compromising (increasing) the second objective. The opposite can be said about Solution B. Moving in the set from Solution A to Solution B improves (minimizes) the second objective and compromises (increases) the first objective. Solutions that don't belong to the Pareto-optimal set are called non-Pareto or dominated and they are not optimum solutions.

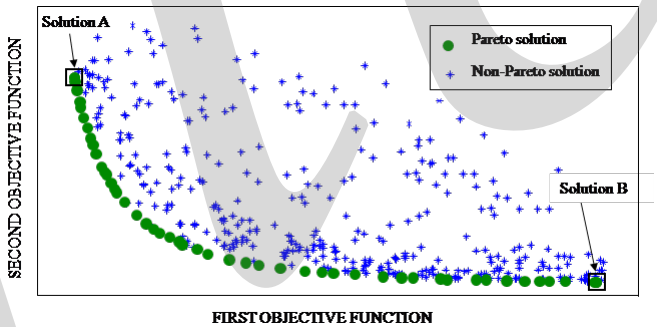


Fig. 7-7 Sketch of a qualitative solution of a bi-objective optimization problem: (Minimize Objectives 1 and 2 simultaneously)

### 7.3.1.3 Genetic algorithms

GAs are optimization techniques inspired by evolutionary biology such as inheritance, mutation, selection, and crossover. GAs have become the method of choice for optimization problems that are too complex to be solved using deterministic techniques such as linear programming or gradient (Jacobian) methods. The large number of applications and continuously growing interest in this field are due to several advantages of GAs compared to gradient based methods for complex problems. For instance, GAs use objective function information not derivatives or other auxiliary knowledge, GAs search from a population of points, not a single point, and GAs can handle discrete variables.

*This document is the intellectual property of the fib – International Federation for Structural Concrete. All rights reserved.*
*This PDF of fib Bulletin 86 is intended for use and/or distribution solely within fib National Member Groups.*

The terminology used in GA subjects stems from both natural genetics and computer science. A generation in the GA process is a parallel term to an iteration in optimization terminology. During a generation, a population goes through mathematical (genetic) operations to obtain its offspring. A population is a set of design points at the current generation coded in a particular manner (e.g. binary, real). Coded and decoded design points are known as chromosomes and individuals, respectively. Each individual contains values for all design variables. The offspring population is the set of new design points obtained by performing genetic operations to a parent population.

#### 7.3.1.4 Multi objective genetic algorithm: NSGA-II

An advanced GA called non-dominated sorting genetic algorithm with controlled elitisms, NSGA-II, has gain much popularity since its appearance[302]. The algorithm is shown in the flowchart in Fig. 7-8 and can be shortly described by the following five steps[302]:

1. Randomly create an initial population $P_o$ of size $N$;
2. Generate the offspring population $Q_i$ of size $N$ using selection, crossover and mutation.
3. Combine the two populations $P_i$ and $Q_i$ to form the population $R_i$ of size $2N$;
4. Evaluate the objective and use non-dominated sorting and crowding distance assignment to select the $N$ fittest values of $R_i$composing $P_i$+1; and
5. Repeat the process from Step 2 (i.e., computing the offspring population $Q_i$) using the population selected above.

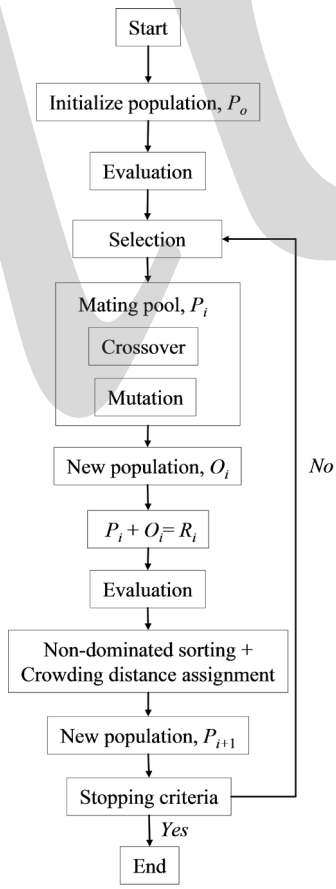


Fig. 7-8 Flowchart for NSGA-II

This document is the intellectual property of the fib – International Federation for Structural Concrete. All rights reserved.
This PDF of fib Bulletin 86 is intended for use and/or distribution solely within fib National Member Groups.

## 7.3.2 Types of maintenance actions

### 7.3.2.1 Essential vs. preventive maintenance

Maintenance actions are scheduled to either delay the occurrence of reaching a performance indicator to its threshold or improve the state of the performance indicator if its threshold is reached. Thus, maintenance types may be categorized into two general groups: preventive (PM) and essential (EM)[303, 304, 305]. PMs are usually time-based, that is, they are applied at pre-specified time instants over the life-cycle of the structure. In contrast, EMs are performance-based in that they are applied when some performance indicators reach pre-defined target values[285]. Fig. 7-9 shows the difference in the impact of EM and PM on the performance of a deteriorating structural component.

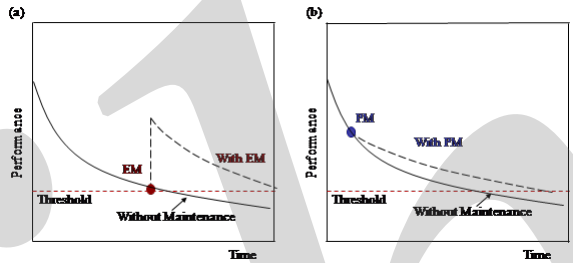


Fig. 7-9 The effects of (a) EM and (b) PM on the performance of a deteriorating structural component

### 7.3.2.2 Effects of maintenance on performance

In order to prioritize the maintenance actions in an optimum schedule, their effects on the performance need to be established[306]. The application of a maintenance action requires proper modification of the formulas used for determining the life-cycle performance. This modification should mathematically reflect the actual effects of the maintenance action on the life-cycle performance. For instance, [240] provided formulas that reflect the effects of applying EM and PM, separately and combined, on the unavailability. For example, the effect of EM on the unavailability of a structural component is[240].

$$An(t) = An(t - T_i) \qquad T_i < t < T_{i+1} \tag{7-10}$$

where $An^*(t)$ = the unavailability after EM, and $T_i$ = the time of application of EM $i$ ($T_0 = 0$ and $T_{n+1} = \infty$). Equation (7-10) was used in obtaining the unavailability profile in Example before. Also, the unavailability of a structural component considering the application of PM can be calculated by[238]

$$An^*(t) = \begin{cases} An(t) & \text{if } t < Tpm_1 \\ 1 - \left(1 - An(t - Tpm_i)\right) \cdot \prod_{j=1}^{i} \left(1 - An(Tpm_j - Tpm_{j-1})\right) & \text{if } Tpm_i \le t < Tpm_{i+1},\ i \ge 1 \end{cases} \tag{7-11}$$

where $Tpm_1$, $Tpm_2$, …, Tpmq are the times at which $q$ preventive maintenance actions are applied to a deteriorating structural component and $Tpm_0 = 0$ and $Tpm_{n+1} = \infty$. It is assumed in Equation (7-11) that the application of PM restores the rate of change in the availability to its original value.

### 7.3.2.3 Maintenance types, problem formulations and solution techniques

The type of maintenance actions considered is the driving factor in the formulation of the maintenance optimization problem and accordingly the solution technique. Given

*This document is the intellectual property of the fib – International Federation for Structural Concrete. All rights reserved.*
*This PDF of fib Bulletin 86 is intended for use and/or distribution solely within fib National Member Groups.*

that EMs are performance-based, the timing of applying EM is determined analytically by determining the times that the performance reaches a pre-specified threshold. The optimization is then performed in order to find the best EM type among the available list of EM types. Accordingly, EM optimization is a combinatorial problem. This type of problem formulation is implicit and solved with exclusive algorithms. In other words, design variables may be absent, making it unnecessary to use an optimization search method to solve. On the other hand, PMs are time-based. PMs can be applied at any time prior to reaching the performance to a threshold. Hence, the task of the optimization is geared towards determining the optimum timings of each PM type. Clearly, the timings of PM applications lend themselves to be modelled with design variables. With a proper problem formulation and solution technique, the optimum values for the timings of application of the PM types can be determined.

The details of the problem formulation and solution technique also depend on the desired frequency of PM application. In other words, a problem formulation and its solution technique for optimization of uniform time-interval PM may be different from optimization of non-uniform time-interval PM. [307] used two design variables for PM: one for the time of first application of PM and the other for the time interval between subsequent applications. Thus the obtained PM solutions had a uniform time-interval frequency.

To obtain non-uniform time-interval PM strategies, coded design variables in a form of numerical strings were used. [285] used a real value string with a bit length equal to the designated life-cycle in years. Each bit may take an integer value representing one of the identifiers (ids) given for the considered maintenance options. In fact, the difference between PM and EM is removed; only the effects of each maintenance type on the performance are retained[285]. In other words, the time and choice of application of both PM and EM was determined by the optimum coded string found by the optimization problem, and with no regard to any performance threshold. Alternatively, [308] used binary strings for describing the ids of the maintenance options. The result was a binary matrix in which each row represented the maintenance action at a given year and the binary code in that row represented one of the considered maintenance options.

Other similar representations were used[281, 283, 287, 309]. However, treating EM as a time-based maintenance[281, 283, 284, 285, 308] may result in obtaining uneconomical solutions, where EM is applied sooner than the time of reaching the threshold of a performance indicator. [307] combined EM with PM in the optimization and EM was treated indeed as performance-based. However, only one EM type was used. Thus, the need to optimize the EM was absent. The considered EM type is applied at the time the performance indicator reaches its threshold.

In[240, 238], a new algorithm was proposed for optimizing EM. In addition, this algorithm was embedded in a GA to combine PM and EM. PM was considered at regular or irregular time intervals and EM was considered as performance-based with multiple applications. In order to do so, a number of continuous design variables are considered where each represents the time of a PM application, in addition to an integer design variable for each PM type. This ensures that the program has the ability to decide the optimum number of applications for each type of PM.

This document is the intellectual property of the fib – International Federation for Structural Concrete. All rights reserved.
This PDF of fib Bulletin 86 is intended for use and/or distribution solely within fib National Member Groups.

### 7.3.3 Optimization of essential maintenance

EM optimization generally aims to select an action each time a performance threshold is reached. The selection of the EM action is typically driven by its cost effectiveness. There are two available approaches for determining the cost effectiveness of applying an EM action. The first selects the EM type that has the lowest cost per year increase of service life. In this approach, the selection is made irrespective of the previous or next EM applications. An algorithm is available for EM optimization based on this approach and is referred to as EMO1. The second approach selects the EM action if it is one of the set of EM actions required to maintain the performance of the structure above the threshold(s) throughout the life-cycle and have the lowest total cost of maintenance. Therefore, the selection of an EM action at one performance threshold reaching depends on previous and next applications. Accordingly, all maintenance scenarios have to be investigated to select the optimum among them. This can be done with an event tree type of analysis. However, [240] have developed an algorithm referred to as EMO2 which is enhanced with checkpoints that avoid investigating scenarios that can be predicted not to be optimum. The algorithm is an efficient systematic technique for finding the optimum EM solution. It was also demonstrated in[240] that algorithms EMO1 and EMO2 can both find the optimum EM solution in most cases. However, EMO2 was shown to provide the optimum solution all the time whereas EMO1 did not.

For the Colorado Bridge E-17-AH, described in[270], the time of the first reaching of performance to its threshold and select the optimum EM option to be applied at that time based on the lowest cost per year increase of service life criterion will be determined. The reinforced concrete slab of the bridge is supported by nine steel girders[310]. The system unavailability is used as the performance indicator with threshold of $10^{-2}$. Weibull distributions are adopted to model the unavailability of the components of this bridge. The parameters of these distributions are based on the best fit of the data summarized in[311]. The shape and scale parameters, $\kappa$ and $\lambda$, respectively, are $\kappa = 2.37$ and $\lambda = 0.0077$ for the deck, and $\kappa = 2.86$ and $\lambda = 0.0106$ for the girders. The system failure is assumed to occur by the failure of any three adjacent girders or the deck. Four essential maintenance options are considered to maintain the system unavailability under its thresholds. These essential maintenance actions and their associated costs are[270]; Replace deck ($225,600); Replace exterior girders ($229,200); Replace exterior girders and deck ($341,800); and Replace superstructure ($487,100).

The first step in solving this problem is setting up the equations for predicting the unavailability. The unavailability of the deck $An_d(t)$, interior girders $An_i(t)$, and exterior girders $An_e(t)$ can be predicted using Equation 6. Even though the interior and exterior girders have the same parameters of the Weibull function, they are modelled with different distributions here because there is an option of replacing the exterior girders separately. The minimal cut sets can be determined from the system failure criterion (i.e., failure of any three adjacent girders or the deck). These cut sets are: (a) deck, (b) three interior girders, and (c) two interior girders and an exterior girder. There are five combinations of the cut set (a) since there are seven interior girders and there are two combinations of the cut set (c) for the girders on both sides of the bridge. Hence, the system unavailability can be established using Equation (7-11) as:

$$An_s(t) = 1 - \left(1 - An_d(t)\right)\left(1 - An_i(t)^3\right)^5 \left(1 - An_e(t) An_i(t)^2\right)^2 \tag{7-12}$$

This document is the intellectual property of the fib – International Federation for Structural Concrete. All rights reserved.
This PDF of fib Bulletin 86 is intended for use and/or distribution solely within fib National Member Groups.

Equation (7-12) is used to first generate the system unavailability profile without maintenance. This is shown in Fig. 7-10. It can be found from the figure and values of $An_d(t)$ that the threshold is reached for the first time at the time $t$ = 18.6 years.

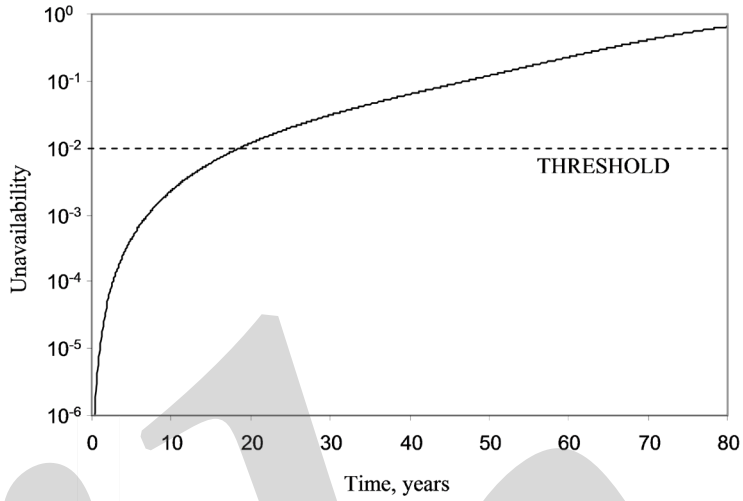


Fig. 7-10 Unavailability of the Colorado Bridge E-17-AH without maintenance

Now, at time $t$ = 18.6 years, an EM maintenance needs to be selected for application. The service life extension of each maintenance action needs to be determined. In order to do so, the time of the first unavailability threshold reaching following the application of each EM is found. For instance, replacing the deck improves the unavailability as shown in Fig. 7-11. Accordingly, the next unavailability threshold reaching is at time $t$ = 36 years. Hence, the service life extension is 36 – 18.6 = 17.4 years. The cost per year increase of service life for this EM action is $225,600/ 17.4 years = 12966 $/year. Similarly, the cost per year increase of service life for the other three EM actions can be found as: Replace exterior girders = 0 $/year (this EM action offers no improvement to the unavailability); Replace exterior girders and deck = 19310 $/year; and Replace superstructure = 25910 $/year. Therefore, replacing the deck is selected for replacement as an EM action at time $t$ = 18.6 years since it gives the lowest cost per year increase of service life. This procedure can be repeated every time the unavailability reaches the threshold until a pre-specified service life is reached.

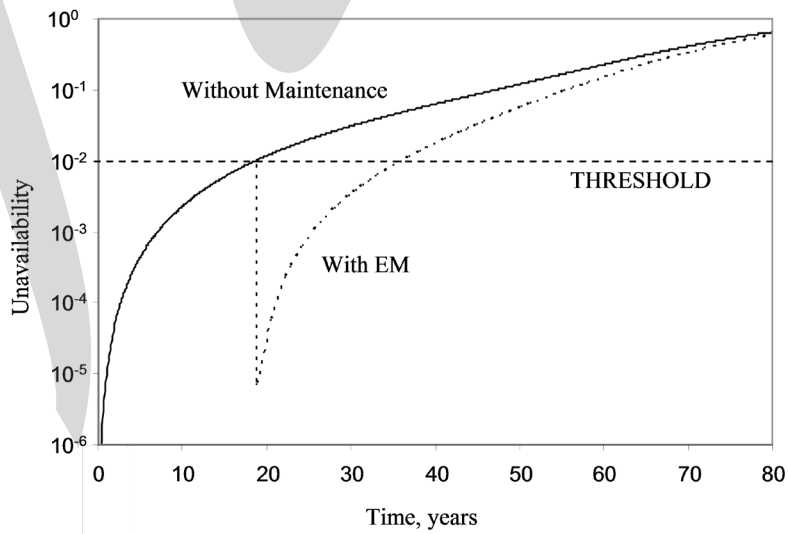


Fig. 7-11 Unavailability of the Colorado Bridge E-17-AH with EM

This document is the intellectual property of the fib – International Federation for Structural Concrete. All rights reserved.
This PDF of fib Bulletin 86 is intended for use and/or distribution solely within fib National Member Groups.

### 7.3.4 Optimization of preventive maintenance

Since the time of application of PM is not restricted by the reaching of the performance to its threshold, optimization of PM involves determining the optimum time of application of each PM action. This can be done by treating the PM time of application as a continuous design variable in a maintenance optimization problem. Generally, the goals of performing the optimization of maintenance are to find the maintenance solution providing the maximum performance with minimum cost. Hence, a multi-objective optimization formulation is a suitable tool for this problem. In the most basic case, one may decide to apply one type of PM once during the service life of the structure and he seeks to find the optimum time of application of this PM action. The problem can thus be formulated as:

*Find*: Time of application of PM, tp

To *maximize*: Performance

and to *minimize*: Cost

Clearly, the cost of one PM action is the same, which may pose a question regarding the need to minimize the cost in this example. The answer to this question lies in the effect of the discount rate. In order to compare the costs of different solutions where the PM is applied at different times, all costs are calculated at their present value:

$$C_{PV} = \frac{C}{\left(1+\upsilon\right)^{t}} \tag{7-13}$$

where $C_{PV}$ = present value of PM cost, $C$ = cost of PM action at time of application, $\upsilon$ = discount rate of money, and $t$ = time of application of repair.

For the Colorado Bridge E-17-AH described previously, it is decided to apply Silane treatment to the deck one time over the service life of 50 years. This PM action is assumed to restore the rate of change in the unavailability of the structure to its original value. The cost of the Silane treatment is $50,000. It is desired to treat the maximum unavailability reached over the service life as an indicator for the performance. Considering a discount rate of money of 2%, plot the cost of Silane treatment vs. the time of its application. Also, plot the variation of the maximum unavailability reached over the service vs. the time of Silane treatment. Additionally, plot the maximum unavailability vs. cost and comment.

In order to capture the effect of Silane treatment, Equation (7-12) is used to compute the unavailability of the deck. The rest of the computations for generating a single unavailability profile follow that of the previous example. The time of application of the PM action is incremented at one year increments. For each year, the maximum unavailability is obtained. For example, Fig. 7-12 shows the unavailability profile with applying PM at the year 25. The maximum (worst) unavailability in this case is the value that the unavailability reaches at the year 50.

Fig. 7-13 shows the variation of the maintenance cost vs. the time of applying the Silane treatment. Clearly, owing to the discount rate, the present cost decreases over time. From a pure financial point of view, it is more economical to delay the PM application. However, Fig. 7-14, which represents the variation of the maximum unavailability with the time of Silane treatment, shows otherwise. Delaying the PM improves the unavailability until the year 25 is reached. Then it starts to deteriorate again until the year 50. Clearly, the lowest (best) unavailability is reached by applying the PM at the middle of the service

*This document is the intellectual property of the fib – International Federation for Structural Concrete. All rights reserved.*
*This PDF of fib Bulletin 86 is intended for use and/or distribution solely within fib National Member Groups.*

life, year 25. This should be intuitive since the PM restores the rate of change in the unavailability to its original value.

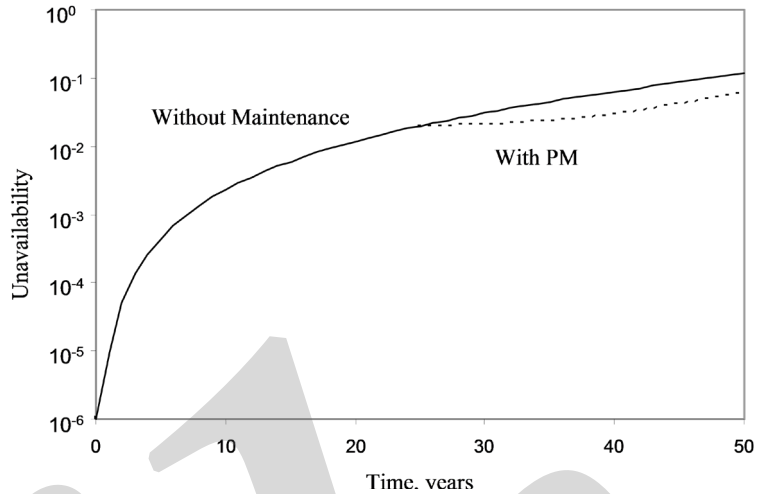


Fig. 7-12 Unavailability of the Colorado Bridge E-17-AH with and without PM

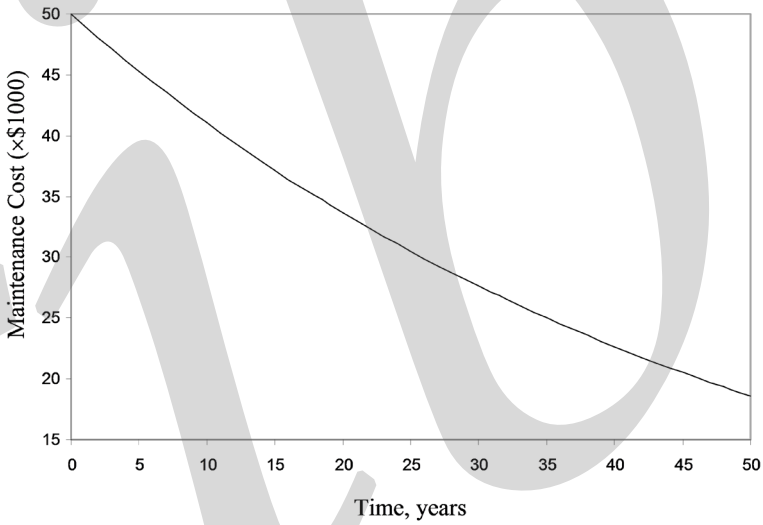


Fig. 7-13 Maintenance cost vs. the time of applying the Silane treatment

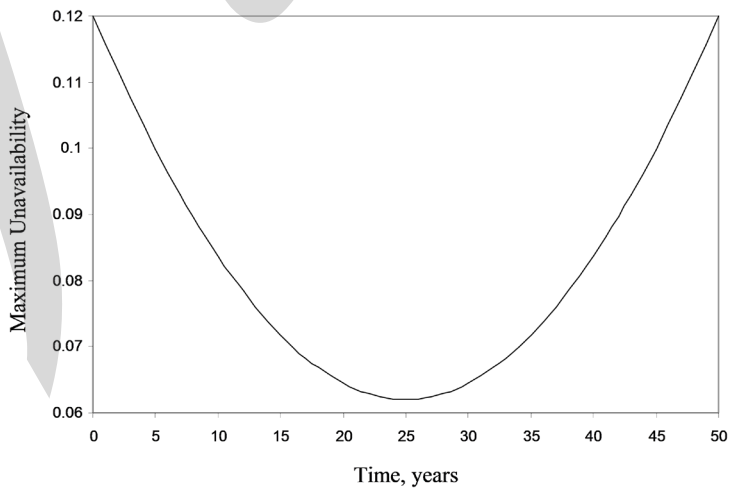


Fig. 7-14 Maximum unavailability vs. the time of applying the Silane treatment

This document is the intellectual property of the fib – International Federation for Structural Concrete. All rights reserved.
This PDF of fib Bulletin 86 is intended for use and/or distribution solely within fib National Member Groups.

Fig. 7-15 plots the maximum unavailability vs. the maintenance cost. Shown on the figure are the PM solutions with applications at the times t = 0, 25, and 50 years. The conflict in the two objectives is clear in this figure. Applying PM at year 50 gives the best maintenance cost but worst unavailability, as the time of application is reduced towards the year 25, the unavailability improves but the maintenance cost worsens. Hence, the points between the application at times t = 25 and 50 years constitute the Pareto-optimal solution set that shows all the compromised solutions between the two considered criteria. Interestingly, reducing further the time of application towards the time zero worsens both criteria, thus these solutions are not Pareto-optimal.

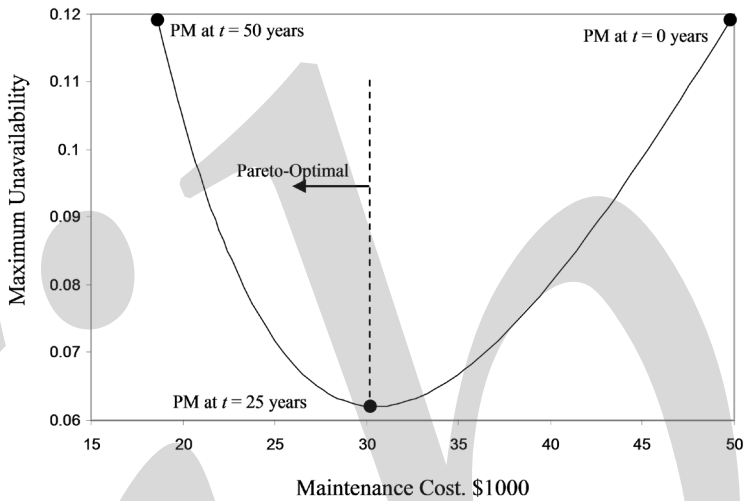


Fig. 7-15 Maximum unavailability vs. maintenance cost of applying the Silane treatment

For the same example of the Colerado Bridge a Pareto-optimal set of maintenance solutions that minimize the maximum unavailability and minimize the maintenance cost have been considered. These solutions must have the optimum numbers and optimum times of Silane treatment and girder repaintings. Irregular time-interval PM maintenance must be allowed. Up to 10 applications of each PM type are allowed. It is desired not to apply maintenance anytime in the first or last two years of the service life of the structure. In addition, a minimum time span of two years between any two consecutive maintenance applications of the same type is required.

In order to solve this problem, the approach in[240] is followed. This approach has been previously presented. Twenty two design variables are considered in this problem. These design variables are: ten continuous design variables for the time of application variables for the Silane treatment of the deck $Td_i$ ($i$ = 1,2,..10), an integer design variable for the number of applications of the preventive maintenance for the deck $N_d$ (where $N_d$ = 0,1,2,…,10), ten continuous design variables for the time of application variables for the girder repaintings $Tg_j$ ($j$ = 1,2,..10); and an integer design variable for the number of applications of the preventive maintenance for the girders $N_g$ (where $N_g$ = 0,1,2,…,10). The problem is formulated as follows:

Find: $Td_i$, $N_d$, $Tg_j$, $N_g$

to achieve the following two objectives:

Minimize Anmax

Minimize LCC

This document is the intellectual property of the fib – International Federation for Structural Concrete. All rights reserved.
This PDF of fib Bulletin 86 is intended for use and/or distribution solely within fib National Member Groups.

Subject to the constraints:

$$2 \text{ years} \leq Td_i \leq 73 \text{ years}$$

$$2 \text{ years} \leq Tg_j \leq 73 \text{ years}$$

$$Td_i - Td_{i-1} \geq 2 \text{ years}$$

$$Tg_j - Tg_{j-1} \geq 2 \text{years}$$

$$N_d, N_g = \{0, 1, 2, \ldots, 10\}$$

where $i, j = 1,2,..5$. The resulting Pareto-optimal set of the optimization problem is shown in Fig. 7-16. Any point on the figure is an optimum solution that has values for the design variables above and can be selected. Clearly, the reduction in the unavailability is associated with a higher life-cycle cost (LCC).

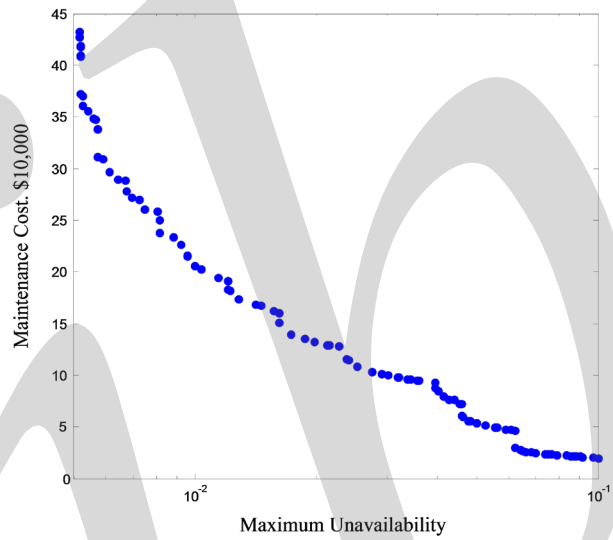


Fig. 7-16 Pareto-optimal set for considering only PM

## 7.3.5 Optimization of combined maintenance

Thus far in this chapter, it has been shown that optimization of only EM computationally has a different nature from that of optimization of only PM. In addition, each of these two optimization problem categories has different methods to be used with. In combining both types of EM and PM, the same type of optimization approach for one may not work with the other. A proper mathematical platform for combining the two types of maintenance needs to be used. Even in the case of combined maintenance optimization, different methods have been used. However, each method suites a certain set of conditions. As shown in a previous Section, some methods where limited to considering only one EM type and considered only uniform time-interval PM maintenance. Others treated EM as time-based. The only approach where EM was treated as performance based, multiple EM types where used, and PM was treated in non-uniform time intervals (or uniform if optimum) was proposed in[240]. The key in combining the two maintenance types was embedding (nesting) the considered algorithm of EM optimization into the genetic algorithm where design variables for the PM optimization where solved for. These design variables included a number of continuous design variables where each represents the time of application of a PM application, in addition to an integer design variable for each PM type that determines the number of applications that are actually considered out of the ones provided.

*This document is the intellectual property of the fib – International Federation for Structural Concrete. All rights reserved.*
*This PDF of fib Bulletin 86 is intended for use and/or distribution solely within fib National Member Groups.*

Considering a discount rate of 2 %, find and plot Pareto-optimal set of maintenance solutions that minimize the maximum unavailability and minimize the maintenance cost. These solutions must have the optimum numbers and optimum times of Silane treatment and girder repaintings. Irregular time-interval PM maintenance must be allowed. Up to 5 applications of each PM type is allowed. It is desired not to apply maintenance anytime in the first or last two years of the service life of the structure. In addition, a minimum time span of two years between any two consecutive maintenance applications of the same type is required.

The example discussed in the previous chapters using the combined maintenance approach (EM and PM) treats as a design variable the unavailability threshold $An_{th}$.

The EMO1 algorithm is embedded in the genetic algorithm. The problem is formulated as follows:

Find: $An_{th}, Td_i, N_d, Tg_j, N_g$

To achieve the following two objectives:

Minimize Anmax (18a)

Minimize LCC (18b)

Subject to the constraints:

$2\text{years} \leq Td_i \leq 73 \text{ years}$

$2\text{years} \leq Tg_j \leq 73 \text{ years}$

$Td_i - Td_{i-1} \geq 2 \text{ years}$

$Tg_j - Tg_{j-1} \geq 2 \text{ years}$

$N_d, N_g = \{0, 1, 2, \ldots, 5\}$

where $i, j = 1,2,..5$. The resulting Pareto-optimal set of the optimization problem is shown in Fig. 7-17. Any point on the figure is an optimum maintenance solution that has values for the design variables above and an optimum EM schedule that can be selected.

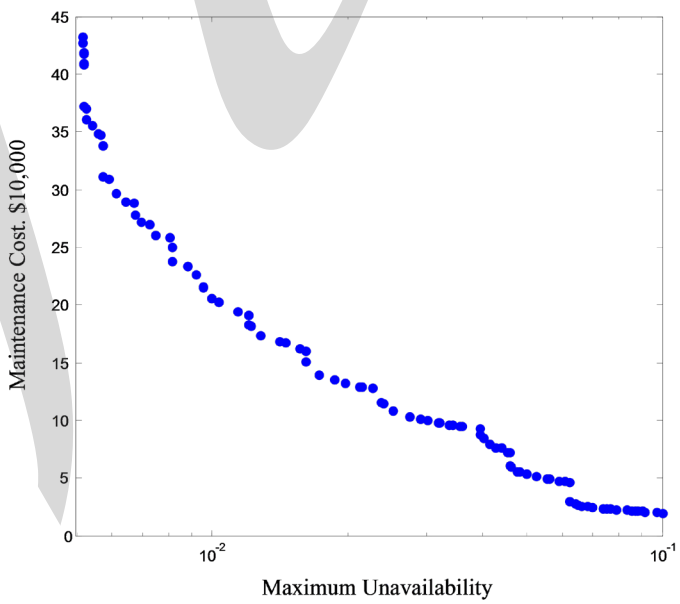


Fig. 7-17 Pareto-optimal set for considering combined PM and EM

This document is the intellectual property of the fib – International Federation for Structural Concrete. All rights reserved.
This PDF of fib Bulletin 86 is intended for use and/or distribution solely within fib National Member Groups.

# 8. Structural identification and prediction methods

## 8.1 Introduction

Early detection of the level and/or the localization of the damage using non-destructive methods are getting more and more important nowadays also due to the increasing maintenance costing. A dynamic experiment is a well-known technique. Using vibration measurements, the natural frequencies and mode shapes are obtained. The real dynamic behaviour is then compared with a FEM computational model.

Damage identification methods may be categorized as global or local techniques. A typical example in the literature is the linear-elastic behaviour of the system in the damaged states. In most cases, linear behaviour of the material properties is foreseen in the literature. The material properties thus are unrelated to the amplitude of oscillation. While changes in modal characteristics are a result of changes in geometry, boundary conditions or material properties of the structure, the structural response may still be modelled via a linear equation of motion.

Novel damage assessment techniques are frequently assessed by comparison with numerical simulations *n* a first step. In a second step, the methods are applied in laboratory tests and real-life cases. Noise in the experimental data cannot be avoided, as acquisition systems can only provide a limited degree of accuracy. For details, refer to the statistical study of signal versus noise in damage detection by[312]. A widely used classification system divides damage identification methods into four levels[313].

Level 1: Damage detection: spotting of damage present in the structure

Level 2: Damage localization: pinpointing of the geometric location of the damage

Level 3: Quantification of damage degree

Level 4: Prediction of the remaining service life of the structure

Continuous health-monitoring of structures (bridges) is essential part of its maintenance[314]. Damage localization and its level is the subject of research of both academic and industrial research groups during last decade. Non-destructive testing – vibration measurements to get modal data (frequencies, modal shapes) is the most promising technique as it can be performed using a structure in usage. The task is based on the fact that damaged structure has smaller stiffness in some parts – and this difference will affect vibration (modal data). The comparison of vibration of virgin (undamaged) structure and damaged structure can be used for the detection of damaged parts (localization of damage). An effectiveness of identification procedure is based on positioning of sensors used in health-monitoring, sensors placed very close to damage are usually the most sensitive[315]. An inverse analysis should consider also other aspects – operational conditions (e.g. temperature changes, etc.), see[316].

"The model updating method" is the term frequently used in identification[317, 318]. "Updating" means that individual parameters of FEM model are iteratively changed in order to minimize the difference between experimentally measured and calculated response.

The aim of this chapter is to show efficiency and possibilities of selected techniques: Damage identification using artificial neural network based approach[319] and sensitivity based

This document is the intellectual property of the fib – International Federation for Structural Concrete. All rights reserved.
This PDF of fib Bulletin 86 is intended for use and/or distribution solely within fib National Member Groups.

approach[320]. Integral part of research is the study of modal properties and analysis of its applicability for damage identification. Both techniques are briefly described. The efficiency of techniques for damage identification is illustrated using selected numerical examples.

Reinforced concrete structures are not made to last forever. Over time, they are damaged by service loads and environmental and accidental action. In order to detect any defects at an early stage and to determine the safety and reliability of the structure, inspection and condition assessment is necessary on a regular basis. Early damage detection and pinpointing the damage location enables an exact scheduling of maintenance and repair works, thereby minimizing costs.

The state of the art in damage detection methods includes visual or localized experimental methods such as acoustic or ultrasonic methods, magnet field methods, radiographs, eddy-current methods and thermal field methods. A prerequisite of any of these experimental techniques is that the location of the damage is known beforehand and that the portion of the structure being inspected is accessible. In those cases where the structural damage is small or where it is in the interior of the system, visual detection is impossible.

A useful, though more elaborate, non-destructive evaluation (NDE) tool is vibration monitoring. Damage or fault detection as determined by changes in the dynamic properties or response of structures is a subject that has received considerable attention in literature. The basic idea is that the occurrence of damage or loss of integrity in a structural system leads to a changed response to dynamic forces caused by changes in the dynamic properties of the structure (eigenfrequencies, modal damping rates, mode shapes and/or transfer functions). Extensive research is carried out on the development of non-destructive damage assessments methods and the translation of changes of modal characteristics in occurred damage in a structure.

The health of civil engineering structures by vibration monitoring may be evaluated in two steps.

Firstly, monitoring measurements are taken with a limited number of sensors on the structure (as for example a reference accelerometer, a strain gauge at a critical section or a temperature sensor). With state of the art software and hardware, it is possible to take such measurements continuously.

Secondly, a full-scale dynamic survey is to be performed, often focusing on indications gathered in the first step where the structures 'health condition' needs further attention. For a full modal analysis, usually many sensors are required, as for example accelerometers to extract modal displacements at many locations, and in some instances complemented by sensors for strain and temperature.

For the cornerstones of a robust damage detection scheme, please refer to[321, 322]. Crucial steps are the identifying damage that may have occurred very early in the life-time of the structure, pinpointing the damage location within the applied sensor resolution, estimating the degree of the damage and predicting the remaining life-span of the structure. As far as possible, the method is to be independent of the engineering judgment of the user or of any analytical model of the structure. Nonetheless, several damage assessment methods require in-depth knowledge of the initial, baseline measurement of the undamaged structure. Many of the damage identification methods in the literature commonly assume that damage does not change the mass of a structure to any significant degree.

This document is the intellectual property of the fib – International Federation for Structural Concrete. All rights reserved.
This PDF of fib Bulletin 86 is intended for use and/or distribution solely within fib National Member Groups.

Novel developments in vibration based damage detection technology are due to innovations in Fast Fourier Transform analysers and digital computing hardware, as for example non-contact and remote sensors.

Where the initially linear-elastic structure behaves in a non-linear manner after the damage has occurred, the literature speaks of non-linear damage, as for example the formation of a fatigue crack that subsequently opens and closes within the usual vibrations of its operation. Additional stiffness has to be taken into consideration whenever the crack closes. Other examples of non-linear damage include loose connections that may rattle, and non-linear material behaviour.

A further classification system of linear methods relates to model-based and non-model based methods. The basis of model based methods is the assumption that any structure will respond in a certain calculable manner, thus making it possible to model its response via finite element analysis. The location of the damage may also be pinpointed without a (detailed) model of the structure by making use of the change in eigenfrequencies, mode shapes or changes in its derivatives, or also changes in flexibility matrices compiled from the measured modes and eigenfrequencies.

The theoretical basis of the current work is established within the framework of linear damage assessment methods. Those applications of vibration based damage detection which have emerged within the technology of rotating machinery have been the most successful ones to date. Many of these date back to the 1970s and 1980s, when the oil industry pushed the development of vibration based damage detection for offshore platforms. Damage detection in such structures is an enormous challenge, as the damage location is not known and much of the structure cannot be accessed easily. At about the same time, in the late 1970s and early 1980s, aerospace industry started to examine possibilities for vibration based damage assessment. Subsequently, in the early 1980s, the trend was taken up by civil engineering: damage assessment techniques were finally applied to bridges.

In that particular field, the challenges lie within the environmental and condition variability to bridge monitoring application. An additional challenge is posed by the physical size and diversity of the test structures[323]. An advantage of vibration based damage identification methods as compared to local NDE methods is the fact that it is not necessary to know the location of the damage in advance. It is also not necessary that the sensors are located in the vicinity of the damage, and only a limited number of sensors is needed for detecting and pinpointing the location of the damage, and to eventually quantify it. Suitable as NDE tools are measurements of the dynamic characteristics, eigenfrequencies and damping, since they can be performed independent of sensor location.

## 8.2 State of the art

The development of vibration monitoring of civil engineering structures (e.g. bridges, buildings, dams) has attracted considerable interest in the course of the past years. As yet, it remains unresolved whether the measured deviations suffice as an indicator for damage or deterioration. Sensitivity studies using finite element (FE) models and in-situ-test of artificially damaged bridges have shown that the decrease of eigenfrequencies may remain below a certain threshold. Even if the local stiffness drop at a crack may be high, the global stiffness may only give rise to minor frequency changes which are detectable

This document is the intellectual property of the fib – International Federation for Structural Concrete. All rights reserved.
This PDF of fib Bulletin 86 is intended for use and/or distribution solely within fib National Member Groups.

only with very precise measurement and identification procedures. It has been suggested, even if not sufficiently proven, that higher modes might be more sensitive to certain types of damage. Natural changes caused by the environment (e.g. temperature changes) may also obstruct the process of comparing the dynamic properties of a structure in the initial and the damage states. Another unresolved issue remains the pinpointing of the damage starting from any observed shift in dynamic properties. Proving the feasibility of vibration monitoring techniques is a necessary next step in order to convince the engineering community of its value as a tool for structural assessment. This may be performed via short term loading failure tests on existing structures (not only on laboratory beams), thereby proving that changes in dynamic properties are not only large enough to be statistically relevant, but can also be linked to damage in a particular part of the structure. An extensive review of the literature on vibration damage detection methods and their application to mechanical, civil and aerospace structures has been performed by[322]. The techniques for damage assessment that are defined in more detail below are categorized on the basis of the damage indicator.

## 8.2.1 Methods based on changes of basic modal parameters

### 8.2.1.1 Eigenfrequencies

Damage assessment techniques using eigenfrequency changes have been dealt with extensively in the literature. Due to the somewhat low sensitivity of frequency shifts to damage, either very precise measurements or significant damage are necessary for successful damage determination. [321] state that the statistical variation on eigenfrequencies nevertheless is less than on other modal parameters. Due to the fact that eigenfrequencies are a global property of a structure, it is harder to identify damage at levels 2 and 3. Frequently the number of experimental eigenfrequencies is not sufficient to locate the damage location in the structure. In the abovementioned literature review[324], a distinction is made between the forward problem, which usually falls into the category of level 1 damage identification, and the inverse problem, which is typically level 2 or level 3 damage identification.

The pioneering paper by [325] describes the use of vibration monitoring by eigenfrequency shifts in a composite material as a good example for the forward problem. The paper provides a formulation to detect damage in composite materials from frequency shifts. Starting point is the ratio between frequency shifts for a pair of eigenmodes. The authors consider a grid of possible damage points. An error term is defined to relate the experimental frequency shifts to those predicted by a model based on a local stiffness reduction. The pair giving the lowest error indicates the location of the damage. The authors suggest using a number of mode pairs for each potential damage location. The formulation does not account for possible multiple-damage locations. The inverse problem consists of calculating the damage parameters (e.g. crack lengths and/or location) from the frequency shifts.

A further damage identification technique using the sensitivity of eigenfrequency changes was developed by[326]. Their method is based on the experimental eigenfrequencies in combination with a numerically generated sensitivity matrix. The method enables exact pinpointing of the location in the structure and provides assessment of the degree of damage. The method was tested experimentally in the laboratory using cantilever beams [327, 328].

Another approach was established by[329]. They developed a system where the shifts in eigenfrequencies within a structure are rank-ordered, and then relations to the damage

*This document is the intellectual property of the fib – International Federation for Structural Concrete. All rights reserved.*
*This PDF of fib Bulletin 86 is intended for use and/or distribution solely within fib National Member Groups.*

are established using a finite element model. However, the rank-ordering is insensitive to the degree of damage. The authors claim that sensitivity to minor inaccurate in boundary conditions is negligible, and that their method is relatively robust to uncertainty on the eigenfrequency measurements. A method of assessing damage in beams where the intersection of various bending stiffness versus faulted beam element location curves indicates the location of the damage is provided by[330]. The intersections represent the possible fault location and magnitudes (Young's modulus), resulting in the appropriate changes in eigenfrequencies. A drawback of this method is that it remains impossible to uniquely detect damage within a symmetrical structure. The possibility of damage detection by comparing the vector of measured changes due to damage and the vector of predicted changes in natural frequency due to damage at a known location was explored by[331].

Consequently, the Multiple Damage Location Assurance Criterion (MDLAC) was defined by using a correlation approach similar to that of the Modal Assurance Criterion (MAC), which is used for comparing mode shapes. The method was successfully applied to a damage pin-jointed truss model. [332] has used the equations of motion of a simple beam for calculating both position and size of a crack in a rod via a pair of eigenfrequencies. [333] provides a thorough literature review on structural damage detection through changes in eigenfrequencies. The major advantage of using only eigenfrequencies in the damage assessment of structures is its efficiency: the cost of acquisition is low, and the approach therefore provides a low-cost assessment technology. However, special attention needs to be given to filtering out the influence of environmental conditions, as for example the influence of temperature on the stiffness of a structure, and the boundary conditions[334]. A disadvantage of techniques based solely on eigenfrequencies is that in some cases, unrealistic damage patterns may emerge. Using such methods, it remains impossible to distinguish damage at symmetrical locations in a symmetrical structure, and the number of measured eigenfrequencies is usually lower than the number of unknown model parameters, thereby resulting in a non-unique solution. Consequently, eigenfrequencies-based methods are often combined with mode shapes for an extensive damage assessment.

#### 8.2.1.2 Mode shapes

Mode shape based methods combine the change of experimental eigenfrequencies with the change of experimental mode shapes for damage assessment. A method was developed by[335] where they measure the amplitude of a steel beam at two points during forced vibration at an eigenfrequency, and then use a model of the beam to predict crack length and position by fitting the amplitudes to the equations of motion at the eigenfrequency. They assume that the transverse surface crack extends uniformly along the width of the structure. It is possible to use single-number measures of the mode shape changes. The Modal Assurance Criterion, one of the more common single number measures, turned out to be rather insensitive to a limited degree of damage in the structure. The MAC value of two modes $\varphi$ A and $\varphi$ B (e.g. a mode shape in the undamaged and damaged state) is defined using *n* modal degrees of freedom. The MAC value indicates the degree of correlation between two modes and varies from 0 to 1, with 0 for no correlation and 1 for full correlation. The deviation from 1 may be interpreted as an indicator for damage in structures. The Co-ordinate Modal Assurance Criterion differs from the MAC definition, as it gives local information and combines information of different modes. The COMAC value at modal co-ordinate i and for m modes is defined as a modal displacements in a co-ordinate *i* from two sets of measurements are identical, the COMAC value equals 1 for

This document is the intellectual property of the fib – International Federation for Structural Concrete. All rights reserved.
This PDF of fib Bulletin 86 is intended for use and/or distribution solely within fib National Member Groups.

this co-ordinate. An overview on the use of MAC values and related assurance criterions is given by 336. 337 present various methods of comparing mode shape information and validate them on a numerical cantilever FE beam model.

#### 8.2.1.3 Damping

The use of damping factors for damage assessment is still in an its early, experimental, stage, partly due to the lack of accuracy in determining damping ratios from system identification techniques[338].

[339] explored the damping mechanism and possibilities for using damping as an indicator in structural health monitoring (SHM) in order to assess damage in partially cracked reinforced concrete (RC) beams. An energy based method was applied. Two phenomena were in the focus of attention: the strain energy redistribution caused by stress transfer between steel and concrete when cracks occur, and the energy dissipated by friction forces in the interface at the crack edges. It appears that both effects act in the opposite way on the RC loss factor (related to dissipated energy). In the mentioned tests, the RC loss factor is governed by the friction dissipated energy. As a result, the measured damping increases with increasing damage. Attempts have been made to use damping rations as a measure of damage, but with limited success.

Two damping-based localization techniques are presented by[340]. The first method is based on the variation of an energetically equivalent modal damping ration, the first on distinguishing the contribution of a viscous and friction component in damping and identification of the damage via friction detection and characterization. Both methods are applied on a cracked hollow panel. The method based on modal friction damping delivers promising results.

[341] have performed tests on partially cracked concrete beams. The results give no clear indication of a relation between crack growth and an increase of damping. Tests on a steel girder bridge with concrete decking were performed by[342]. Even if damping rations are affected by deterioration, they proved to be unsuitable as indicators for damage as they increase initially and subsequently decrease with increasing damage. This result is substantiated by[343], who proved that the damping of a steel plate girder bridge does not consistently increase or decrease with damage.

Structural repairs played a role in the tests by[344], whose measurements before and after repair did not indicate a clear trend in damping values.

Several methods of interpreting the mode shape data were suggested to date, some of them making use of derived quantities rather than the experimental modes themselves.

#### 8.2.1.4 Modal strain energy

The change of modal strain energy (MSE) is another common indicator for structural damage. [345] base their so-called damage index method on the decrease in modal strain energy between two structural degrees of freedom, as defined by the curvature of the measured mode shapes. When the authors applied their method to a damaged steel bridge, damage was localized using three eigenmodes[346]. The feasibility of the method was also tested with a limited set of modal parameters).

[347] present a further structural damage detection method based on the change in modal strain energy. With this technique, it is possible not only to pinpoint the location, but

*This document is the intellectual property of the fib – International Federation for Structural Concrete. All rights reserved.*
*This PDF of fib Bulletin 86 is intended for use and/or distribution solely within fib National Member Groups.*

also to define the extent of the damage. In addition, single as well as multiple damage can be detected. However, the extent of the damage can only be predicted successfully for low noise levels. Data that are measured incompletely are expanded in the process. Further methods include[348] and[349], who use changes in strain energy to localize damage respectively in a space truss structure and a beam-like structure.

#### 8.2.1.5 Mode shape curvatures

When compared to modal displacements, which usually hardly change for realistic damage with respect to the initial mode shapes of the undamaged structure, modal curvatures prove to be more sensitive. For beams, curvature and bending strain are in direct relation: where $\varepsilon$ is the strain, R is the radius of curvature, $\kappa$ is the curvature and $y$ the distance to the neutral axis. The curvatures can be obtained either by calculation from the modal displacements or by measuring the curvatures/strains directly. As a result of a bending crack, bending stiffness decreases (EI), resulting in a local increase in curvature, equal to the bending moment divided by bending stiffness.

[350] were the first to introduce the concept of curvature mode shapes. The curvature values are computed from the displacement mode shape using the central difference approximation. A finite element model of a simply-supported beam is applied, where the reduction in $E$ is 50% at one third of the span. Consequently, the modal curvature is a much more sensitive damage indicator than the MAC or COMAC values.

[351] expands this damage detection method. The curvature of the damage beam can be studied without previous knowledge of the undamaged structure. Ratcliffe's method makes use of the Laplace operator Li for a discrete mode shape.

It is proportional to the difference quotient. Severe damage is indicated by a noticeable jump in the Laplacian. Minor damage necessitates a comparison between the Laplacian at each point and a cubic fit to the Laplacian, using the two points at either side of the point in question. The method is reasonably successful in predicting the damage location in a steel beam. The remaining challenge is the exact determination of modal curvatures from experimental data.

#### 8.2.1.6 Flexibility

The dynamically measured flexibility matrix is another parameter that may be used to estimate changes in the static behaviour of an engineering structure. The flexibility matrix, as the inverse of the static stiffness matrix, relates the applied static force to the resulting structural displacement. Therefore, each column of the flexibility matrix represents a set of nodal displacements of the structure due to a unit force applied at one of the degrees of freedom (DOF). The measured flexibility matrix F is estimated from the mass normalized measured mode shapes and frequencies and may be calculated by means of the analytical mass matrix. For output-only measurements, mode shapes are not scaled but techniques are available to mass-normalise the experimental modes. [352] describe a controlled mass addition experiment, and[353] have developed an acoustic excitation method. Only the first few modes of the structure are measured, and consequently, the formulation of the flexibility matrix is approximate. The synthesis of the complete static flexibility matrix would require measuring all of the mode shapes and frequencies. Typically, flexibility matrices are used to detect damage by comparing the flexibility matrix synthesized using the modes of the damaged structure to the flexibility matrix synthesized using the modes

This document is the intellectual property of the fib – International Federation for Structural Concrete. All rights reserved.
This PDF of fib Bulletin 86 is intended for use and/or distribution solely within fib National Member Groups.

of the undamaged structure or the flexibility matrix from a FE model. The measured flexibility matrix is most sensitive to changes of the modes in the lower frequency range because of the inverse relationship to the square of the modal frequencies. The flexibility matrix converges rapidly with increasing values of frequency, an advantage of using flexibility instead of stiffness.

The damage detection and location method presented by[354] is based on changed in the structure's measured flexibility. The authors test their method first with numerical examples, and subsequently with experimental data collected on a wide flange steel beam. It was shown that measuring the first two modes is sufficient for estimating the damage condition and pinpointing the damage location[355].

[356] also calculate flexibility using the mode shapes and conclude that it is a superior indicator to examine the raw mode shape data. They note that higher modes would reveal local damage but that these higher modes are more difficult to identify experimentally on a bridge.

Another flexibility based damage localization method is proposed by[357]. The damaged elements of the structure are classified as belonging to the set of elements whose internal forces under the action of a certain set of load vectors are zero. These so-called Damage Locating Vectors (DLV) define a basis for the null space of the change in flexibility. The mass matrix is assumed to be diagonal. Single and multiple damage locations are pinpointed by numerical tests, without the need for a reference model of the structure. A final robustness test is yet to be validated in experiment.

### 8.2.2 Methods based on updating of structural parameters

A further class of damage identification techniques is based on the modification of structural modal parameters to reproduce as closely as possible the measured static and/or dynamic response. These parameters include stiffness, mass and damping. Alternative updating techniques may be formulated based on the choice of the objective function to be minimized, on the constraint conditions of the problem and on the numerical scheme used to solve the minimization problem. Model based techniques for damage assessment imply the development of a numerical model (in most cases a FE model) of the structure. In FEM updating, an optimization problem is established where differences between experimental and numerical modal data are minimized by adjusting uncertain model parameters[358, 359]. The congruence between numerical model and real structure must be maximized in order to detect, localize and quantify the damage by examining the tuned model.

At the heart of the solution lies the minimization of the residual between the experimental modal model and the analytical modal model that describe the dynamics of the structure. The choice of updating parameters is another crucial factor. Such updating parameters include (spring) stiffnesses of supports, bending and torsional stiffnesses of individual beam elements, parameters of mathematical expressions that describe the damage over several elements (damage functions) and others.

The composition of the residual is another aspect of the process of minimization. It may, apart from the resonance frequencies, contain modal displacements, modal curvatures and many other dynamic features of the system, such as elements of the MAC matrix, frequency response functions, or elements of the orthogonality matrices. Various terms

This document is the intellectual property of the fib – International Federation for Structural Concrete. All rights reserved.
This PDF of fib Bulletin 86 is intended for use and/or distribution solely within fib National Member Groups.

in the residue are frequently weighted to express the reliability of the measured dynamic parameters of the system, and constraints of the updating parameters often imposed.

[360] state that the first-order perturbation of the eigenvalue problem may yield the relationship between the variation of global stiffness and eigenvalues. The variation in the stiffness matrix is then expressed as the sum of the changes proportional to the element matrices. The result is a set of simultaneous equations that set the local stiffness decrease in relation to the eigenfrequency decreases. In the optimization process, one of three criteria is minimized: the changes in the element stiffnesses, the norm of the damaged stiffness matrix, or the residuals of the eigenvalue problem. A parameter study was performed on a two-bay steel frame structure with 10 floors. The findings were that five frequencies are sufficient for determining moderate damage in any of the beams. A method for pinpointing the cracked portion of concrete beams by using a non-linear least-squares method to identify the equivalent moments of inertia for beam elements in a FE model was developed by[361]. The method is based on minimizing the error between measured eigenfrequencies and modal amplitudes and those calculated by FEM. The actual boundary conditions for the beam are also evaluated using the same method. Sensitivity based updating methods are commonly used for solving the optimization problem. Basis is the first Taylor series expansion of the error function. An alternative to sensitivity based methods to solve the optimization may be methods that search for the global minimum of a cost function. Such methods are currently in the development stages.

[362] have developed a method to correlated their mathematical model with the measurements by minimizing an objective function consisting of functions that incorporate parameters related to the damaged structure, such as eigenfrequency differences, modal curvature differences and normalized mode shape differences. The method initially uses data obtained via FEM, where calibration of the coefficient for the cost function and the parameters appearing in the optimization procedure through genetic algorithms are possible. The so-called Coupled Local Minimizers (CLM) method is another global minimization method. Here, a cooperative search mechanism is established using a population of local optimizers, each starting from a different point in the search space. Via interaction and information exchange, the local optimization processes are then coupled online. The fast convergence resulting from the derivative information used in the local algorithms combined with the capability of finding the global minimum resulting from the parallel strategy, promises an efficient global optimization algorithm[363, 317, 364] solved the inverse problem of damage assessment with special attention to the parameter selection. The inverse problem is often ill-posed and necessitates regularization. The problem of high dimensionality of the update parameter space, which requires reduction as far as possible, has been dealt with. The reduced subset of dominant parameters has to be able to describe the damage scenario. It should finally concentrate on those parameters corresponding to the damaged sub-regions of the structure. A parameter reduction method is necessary. Only such parameters persist whose contribution exceeds a threshold value to reconstruct the residual vector that has to be minimized in the updating process[365]. [366] explore the optimization of Frequency Response Functions (FRF) for damage determination. Their assumption is that finite element model of the structure has been correlated to match the frequency response of the actual undamaged structure. A damage vector using the mass, stiffness and damping matrices of the undamaged model and the damaged mode shapes is calculated, resulting in degrees of freedom at which damage has occurred. The method is tested by generating a damaged frequency response function for a simply-supported truss bridge using the model of the bridge.

This document is the intellectual property of the fib – International Federation for Structural Concrete. All rights reserved.
This PDF of fib Bulletin 86 is intended for use and/or distribution solely within fib National Member Groups.

This method provides the means to distinguish between noise and small damage levels to a reasonable degree. The authors fail to address the robustness of the technique when applied to a real structure. The influence of the number of frequency points and eigenfrequencies on damage assessment techniques based on FRF based model updating procedures is explored by[367]. Several FRF based detection methods are applied to a damaged free-free steel beam in the laboratory by[368]. For an overview of model updating in structural mechanics, please refer to 369,370. In the following, we will discuss several user-friendly identification methods.

## 8.3 Identification method based on artificial neural network

### 8.3.1 Introduction

Inverse problems appear in civil engineering disciplines under similar forms. In principle, the solutions are often identical, but occur under different names (e.g. inverse analysis, identification, model updating). The goal is to identify parameters (e.g. structural and material parameters) of the system (e.g. a structure) based on the observation of its response. The complexity of the system identification approaches is obvious[371].

Constraining our focus to problems of engineering computational mechanics mainly solved by the finite element method (FEM), there are several basic inverse analysis tasks. For a better orientation and simple reference, the symbols IP (identification parameters) and MD (measured data) will be used.

Gaining information on the loads acting on a structure, based on the observation of the response (e.g. deformation, stresses), represents a typical identification problem. Maincon[372, 373] suggests a procedure of the inverse finite element method (iFEM), formulated and applied successfully mainly for linear problems of computational mechanics. Problem classification: IP = load, MD = response in selected points.

Early detection of the level and/or the localization of the damage using non-destructive methods are getting more and more important nowadays also due to the increasing maintenance costing. A dynamic experiment is a well-known technique. Using vibration measurements, the natural frequencies and mode shapes are obtained. The real dynamic behaviour is then compared with a FEM computational model. For the application in bridge engineering, approaches called “model updating” are developed, e.g.[318, 374, 375, 317, 376]. Problem classification: IP = material model parameters, MD = frequencies and mode shapes based on the dynamic experiment.

A strong interest has been developed for formulating inverse analysis methods to determine the quasi-brittle fracture behaviour of concrete. There are basically two groups of inverse analysis techniques[377]: (1) those that use the complete load-displacement curve of one specimen size and shape; (2) those that use the peak loads of specimens of different sizes and shapes capturing the size effect phenomenon. Out of many recent works belonging to this category let us mention e.g.[378, 379, 380, 381, 382, 383, 384]. Problem classification: IP = material model parameters, MD = load-deflection curve or part of it.

However, there is a higher statistical level of identification: Instead of deterministic MD used for inverse analysis to consider the measured statistical data in form of histograms and to identify IP as unknown random variables. Such a higher level of identification can be called the statistical or probabilistic inverse analysis[385, 386, 387, 380]. Problem classification:

This document is the intellectual property of the fib – International Federation for Structural Concrete. All rights reserved.
This PDF of fib Bulletin 86 is intended for use and/or distribution solely within fib National Member Groups.

IP = statistical parameters of computational model (mean, standard deviation), MD = statistical characteristics of structural response based on measurements.

A new approach of inverse analysis is based on the coupling of a stochastic simulation and an artificial neural network (ANN). The identification parameters play the role of basic random variables with a scatter reflecting the physical range of potential values. A novelty of the approach is the utilization of the efficient small-sample simulation method Latin Hypercube Sampling (LHS) used for the stochastic preparation of the training set utilized in training the neural network. Once the network has been trained, it represents an approximation consequently utilized in an opposite way: To provide the best possible set of model parameters for the given experimental data.

Damage identification based on model data can be performed using the proposed inverse analysis approach. The efficiency of this application was tested and verified by numerical examples, laboratory scale beam tests and applications to bridges for which monitoring information was available..

### 8.3.2 Latin Hypercube Sampling statistical simulation

The basic step of the neural networks-based identification procedure is statistical simulation using a computational model of Monte Carlo type which can be time consuming (e.g. in the nonlinear FEM analysis). The utilization of LHS appeared to be very useful as the whole multi-dimensional space of IP is covered perfectly by relatively small number of simulations[388, 389, 390].

The basic feature of LHS is that the probability distribution functions $F_i(x)$ for all random variables $X_i$ are divided into $N_{Sim}$ equivalent intervals ($N_{Sim}$ is a number of simulations); then the values from the intervals are used in the simulation process (random selection, middle of interval or mean value). This means that the range of the probability distribution function of each random variable is divided into intervals of equal probabilities. The samples are then chosen directly from the distribution function based on the inverse transformation of the distribution function. The representative parameters of variables are selected randomly, being based on the random permutations of integers 1, 2,..., j, $N_{Sim}$. Every interval of each variable must be used only once during the simulation in order to achieve the best simulation.

It has been proved that the best LHS strategy which simulates the means and variances as close as possible is the method suggested by[391]. The random mean of each interval should be chosen as (8-1):

$$x_{i,k} = \frac{\int_{y_{i,k-1}}^{y_{i,k}} x \cdot f_i(x)\,dx}{\int_{y_{i,k-1}}^{y_{i,k}} f_i(x)\,dx} = N_{sim} \cdot \int_{y_{i,k-1}}^{y_{i,k}} x \cdot f_i(x)\,dx, \quad y_{i,k} = F_i^{-1}\left(\frac{k}{N_{sim}}\right) \tag{8-1}$$

where $f_i$ is the probability density function of random variable $X_i$, and $y_{i,k}$ are integration limits.

This document is the intellectual property of the fib – International Federation for Structural Concrete. All rights reserved.
This PDF of fib Bulletin 86 is intended for use and/or distribution solely within fib National Member Groups.

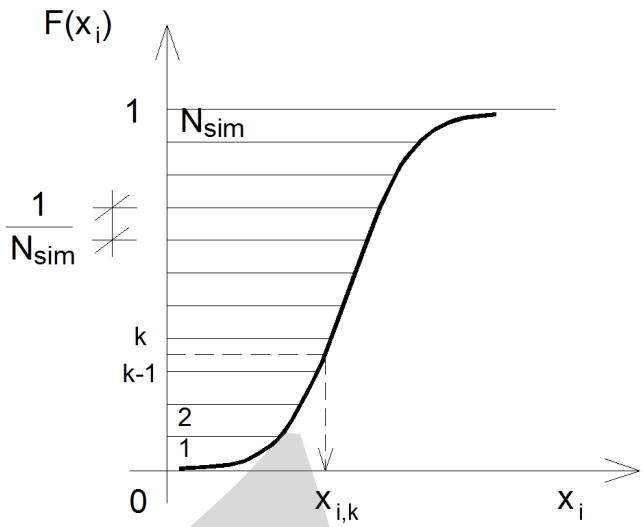


Fig. 8-1 Illustration of LHS technique

### 8.3.3 Statistical correlation

LHS realizations cover multi-dimensional space of random variables – parameters for identification (IP) very well. If the statistical correlation among IP is known (or at least assumed), it is recommended to consider it in the random samples preparation. It can be done by using different techniques published in the literature on LHS (e.g.[392]); 4, however, we found some serious limitations while using them.

A robust technique to impose the statistical correlation based on the stochastic method of optimization called simulated annealing has been recently proposed by[393]. The imposition of the prescribed correlation matrix into the sampling scheme can be understood as an optimization problem: The difference between the prescribed *K* and the generated *S* correlation matrices should be as small as possible. A suitable measure can be introduced, e.g. a norm using the deviations of all correlation coefficients:

$$E_{overall} = \sqrt{\sum_{i=1}^{N_V-1} \sum_{j=i+1}^{N_V} \left( S_{i,j} - K_{i,j} \right)^2} \tag{8-2}$$

Norm *E* has to be minimized from the point of view of the definition of the optimization problem using simulated annealing optimization approach, Nv random variables realizations are related to the ordering in the sampling scheme.

Note that using small numbers of simulations (tens, hundreds) can result in random spurious statistical correlation. Such undesired spurious correlation can influence the consequent training, therefore it is recommended to use simulated annealing to diminish such a correlation as much as possible. The concept is the same - the correlation matrix of statistically independent random variables is the unit matrix we need to impose in the same way as explained above.

### 8.3.4 Sensitivity analysis

An important task in the inverse analysis is to determine the significance of parameters which are subject to identification. The selection of the set of IP should be done with respect to the dominancy of parameters. Dominating variables have to be incorporated

This document is the intellectual property of the fib – International Federation for Structural Concrete. All rights reserved.
This PDF of fib Bulletin 86 is intended for use and/or distribution solely within fib National Member Groups.

in the model but all irrelevant variables should be discarded to avoid "noise" which can bring troubles to train the network. This problem is generally known and solved by different techniques, e.g.[394].

With respect to the small-sample simulation techniques described above, the straightforward and simple approach can be used based on the non-parametric rank-order statistical correlation between the basic random variables and the structural response variable[395, 389]. The sensitivity analysis is obtained as an additional result of LHS, and no additional computational effort is necessary.

The relative effect of each basic variable on the structural response can be measured using the partial correlation coefficient between each basic input variable (IP) and the response variable (MD). The method is based on the assumption that the random variable which influences the response variable most considerably (either in a positive or negative sense) will have a higher correlation coefficient than other variables. Since the model for the structural response is generally nonlinear, a non-parametric rank-order correlation is used by means of the Spearman correlation coefficient or Kendall $\tau$.

### 8.3.5 Artificial neural networks

The basic idea of artificial neural network was to model numerically processes in brain. Nowadays this approach is used in various fields of technical practice. In our identification technique a classical feed-forward neural network, multi-layer-perceptron (MLP), is used (e.g.[396]). A keystone of this network is McCulloch-Pitts's perceptron. All neurons in one layer are connected with all neurons in the following layer. The connecting paths among neurons are weighted, which models their conductivity. At the level of neuron the bias is added to the sum of the weighted impulses from each neuron of the preceding layer. Then, an activation function is applied. Three types of transfer functions can be used: hard-limit, linear and nonlinear (e.g. sigmoid) transfer functions. Synaptic weights, biases and transfer functions determine behaviour of neurons and the whole neural network.

For the network training, a set of training parameters is needed. This set consists of ordered pairs $[\boldsymbol{p}_i, \boldsymbol{y}_i]$, where $\boldsymbol{y}_i$ are the expected output vectors (in our case the random realizations of parameters selected for the identification) which yields from the simulation of the network with the input vectors $\boldsymbol{p}_i$ (MD). A novelty of our approach rests in using the stratified simulation LHS to get these pairs for training of the neural network. Here LHS is used for the efficient preparation of training set. The well-known backpropagation algorithm (gradient descent method with the momentum or Levenberg – Marquardt method) is finally used to train the network. Output from single neuron can be calculated as:

$$y = f(x) = f\left(\sum_k \left(w_k \cdot p_k\right) + b\right) \tag{8-3}$$

where: $k$ – number of input impuls (1,...,$K$), $w_k$ – synaptic weight of connecting path from $k$ -th neuron of previous layer, $p_k$ – impuls from $k$-th neuron of previous layer, $b$ – bias of neuron and $f$ – transfer function of neuron. If the output vector of whole neural network is required, output vectors have to be calculated layer by layer from the input layer to the output layer of network. Output of $u$-th layer of network is:

$$y_k^u = f^u\left(\sum_{j=1}^{J} \left(w_{kj}^u \cdot y_j^{u-1}\right) + b_k^u\right) \tag{8-4}$$

This document is the intellectual property of the fib – International Federation for Structural Concrete. All rights reserved.
This PDF of fib Bulletin 86 is intended for use and/or distribution solely within fib National Member Groups.

where: $k$ – number of component in output vector in $u$-th layer (1,...,$K$ = number of neurons in $u$-th layer), $j$ – number of component in output vector in ($u$ – 1)-th layer (1,...,$J$ = number of neurons in ($u$ – 1)-th layer), $y_k^u$ – one component of output vector, $w_{kj}^u$– synaptic weight – it is connecting $k$-th neuron of $u$-th layer with $j$-th in ($u$ – 1)-th layer, $y_j^{u-1}$– one component of output vector in previous layer, $b_k^u$ – bias of $k$-th neuron in $u$-th layer and $f^u$ – transfer function in $u$-th layer. If $u$ is the number of the last layer then $y^u$ is the output vector.Artificial neural network works in two phases – active and adaptive. In active phase signal passes through the connecting paths from the input layer to the output layer of the network. To obtain correct results of that process, weights and biases must have appropriate values. To assign those values, adaptive phase must be used. This process is called training of neural network. For network training a set of training parameters is needed. This set consists of ordered pairs [$\boldsymbol{p}_i$,$\boldsymbol{y}_i$], where $\boldsymbol{y}_i$ are expected output vectors, which yields from simulation of network with input vectors $\boldsymbol{p}_i$ (in our case points on load-deflection curves). The main aim during training is to minimize following criterion:

$$E = \frac{1}{2}\sum_{i=1}^{N}\sum_{k=1}^{K}\left(y_{ik}^{\upsilon} - y_{ik}^{*}\right)^2 \tag{8-5}$$

where: $N$ – number of ordered pairs input – output in training set, $y_{ik}^*$– required output value of $k$-th output neuronat $i$-th inputand $y_{ik}^{\upsilon}$– real output value (at same input). For minimization of criterion $E$ some optimization technique is used.

## 8.3.6 Basic concept of the identification method

Proposed method for damage detection is based on artificial neural networks (ANN) in combination with stochastic analysis. The damage is defined as a stiffness reduction (bending or torsion) in certain part of a structure. ANN then serves as an approximation for following inverse task: what damage has caused the given change of structural response?

The whole procedure of inverse analysis can be itemized as follows:

1. The computational model of a particular problem has to be first developed using the dynamic finite element method (FEM) software. In case of dynamic damage identification identified parameters (IP) are usually values of stiffness varied along the structure, often Young modulus of elasticity. Measured data (MD) are modal parameters (eigenfrequencies, mode shapes). Note, that an initial guess of IP has to be done based on testing, engineering judgement and virtual computational simulation. Parameters are estimated only roughly and therefore next identification can and should follow. Without any idea about the values of IP proposed methodology cannot guarantee good results. Fortunately, this is not case happening in engineering computational mechanics as there is usually a rough idea on values of parameters.

2. IP of the computational model are considered as random variables described by a probability distribution; the rectangular distribution is a “natural choice” as the lower and upper limits represent the bounded range of the physical existence of IP. However, also other distributions can be used, e.g. the Gaussian one. IP are simulated randomly based on the Monte Carlo type simulation, the small-sample simulation LHS is recommended. The results are random realizations of IP (vector y, see Fig. 8-2). A statistical correlation between some parameters may be taken into account too. If correlation is known, then it can help to the inverse analysis in

This document is the intellectual property of the fib – International Federation for Structural Concrete. All rights reserved.
This PDF of fib Bulletin 86 is intended for use and/or distribution solely within fib National Member Groups.

consequent stochastic training – keeping the consistency of computational parameters in a computational model.

3. A multiple calculation (simulation) of FEM model using random realizations y of IP is performed, a statistical set of the virtual response p (see Fig. 8-2) is obtained. The selection of number of simulations is driven by many factors, mainly by complexity of the problem (computational demand), structure of ANN and variability of IP.
4. Random realizations y (outputs of ANN) and the random responses from the computational model p (inputs of ANN) serve as the basis for the training of an appropriate ANN. This key point of the whole procedure is sketched in Fig. 8-2 (here for the FEM model response in the form of eigenfrequencies).
5. The trained neural network is ready to give an answer to the key task: To select the best parameters IP so that the calculation may result in the best agreement with MD, which is performed by means of the network simulation using MD as an input. This results in an optimal set of parameters yopt.
6. The last step is the results verification – the calculation of the computational model using optimal parameters yopt. A comparison with MD will show to what extent the inverse analysis was successful.

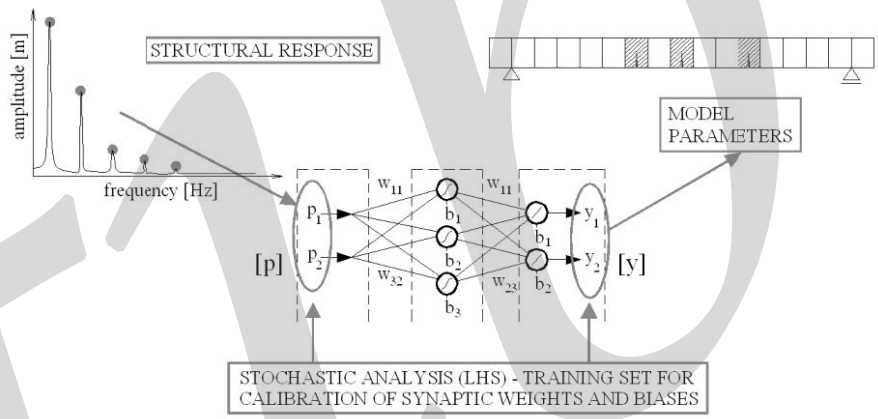


Fig. 8-2 A scheme of ANN-based damage detection

## 8.3.7 Software tools

Damage detection procedure described above consists of structural dynamic analysis, statistical and sensitivity analyses and artificial neural network simulation. For automation of such relatively time-consuming task, several software tools must be combined. Since efficient stochastic and soft-computing techniques and methods are required the following tools are suggested:

- FReET[397, 398] – the multipurpose probabilistic software for statistical, sensitivity and reliability analysis of engineering problems. First, it is used for preparation of the training set for artificial neural network. Second, when damage is identified, it can be consequently used for reliability assessment of given problem using the results from inverse analysis.
- DLNNET[399] – artificial neural network software which enables preparation, training and simulation of appropriate network. It is a corner stone of inverse analysis

This document is the intellectual property of the fib – International Federation for Structural Concrete. All rights reserved.
This PDF of fib Bulletin 86 is intended for use and/or distribution solely within fib National Member Groups.

which communicates with FReET and FEM software. At the end of inverse analysis procedure, it provides the values of stiffness of analysed structure which indicate positions and size of damage.

- FEM computational software – FEM software for performing structural dynamic analysis of a particular problem, e.g. SOFiSTiK. Since FEM analyses are performed repetitively for different sets of input data a special dynamic-link library was created to directly connect SOFiSTiK to FReET and fully automate simulation process.

## 8.4 Direct stiffness identification method

### 8.4.1 Introduction

Another method to identify the structural performance can be based on the direct stiffness approach. The effects of bending cracks on the bending stiffness of beams with a few spans by means of nonlinear numeric models have been studied[400]. In the same way, the reaction of columns of reinforced concrete due to large enforced displacements was described[401]. However, appliance of nonlinear FE-models for the identification of systems is limited as a result of the unknown history of loading. Hence relations between crack characteristics, decay of stiffness and the condition of the structure can be made and they may be used as initial information for planning the maintenance of the structure. This offers the possibility to distinguish between unimportant or intended losses of stiffness and critical damage.

Describing the bending stiffness from existing cracks (potential damage) can be done by using a discrete or a smearing approach, in the same way as FE-models for modelling cracks are created. Even though the discrete approach is more realistic and it enables the localisation of the decay of stiffness inside the cracks, are there no serious advantages in using this approach. In addition, there is no significant difference in the response of the structure[402]. Most of the existing identification approaches use the smeared approach; there are lots of various appliances. In[403], they divide structures in segments with constant stiffness along their longitudinal axis. In contrast to this, a structure can be considered as undamaged and single damage can be simulated as local decays of the stiffness, which in case of bending cracks can be analytically described by a parabolic profile along the longitudinal axis[404]. A further possibility is to describe the stiffness linearly between a structure's interpolation points[405]. Fig. 8-3 shows the linearised description of the bending stiffness along a damaged, haunched bridge with three spans. It is important for the appliance to minimise the essential identification values (in this case $n$ interpolation points $EI_i$ of the stiffness distribution) and to maximise the reliability of the results.

As depicted in Fig. 8-3 on a bridge with three spans, there can be changes in the geometry along the axis of the structure, like haunches. The distribution of their stiffness is a mathematical function of a higher grade (in this case cubic), and has to be rebuilt for acceptable identification results. Furthermore, an adequate number of interpolation points is required to represent the decay of stiffness due to cracks in damaged structures, which have a parabolic profile for bending cracks[406, 404].

This document is the intellectual property of the fib – International Federation for Structural Concrete. All rights reserved.
This PDF of fib Bulletin 86 is intended for use and/or distribution solely within fib National Member Groups.

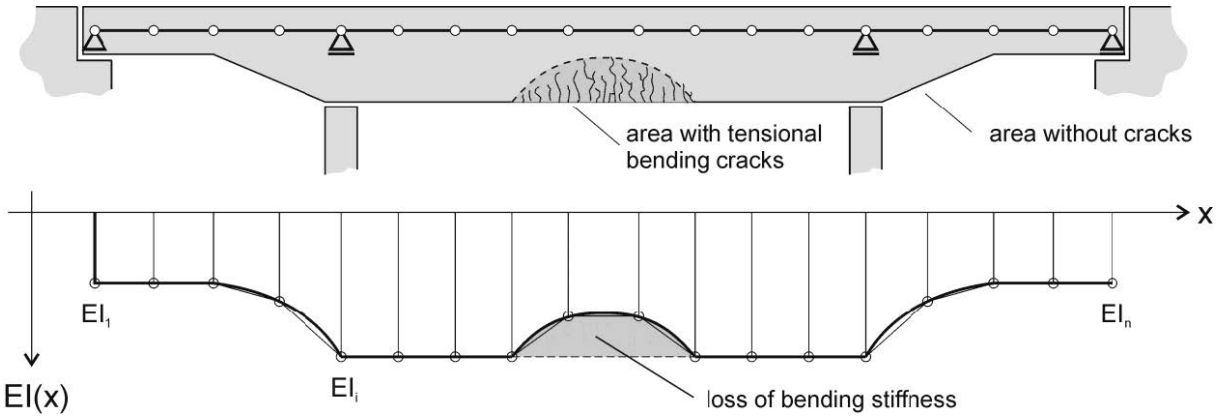


Fig. 8-3 Bending stiffness distribution due to geometry and damage[402]

Although a reinforced concrete structure shows a nonlinear performance, a linear performance of the stiffness can be used to describe the current condition of a structure. This assumes a stress independent and constant performance of the stiffness, as long as the monitoring is executed. The bending stiffness, which is simulated to be linearly distributed along the longitudinal axis in the FE-model, is a value in between the idealised state I $EI^{I}$ and the cracked state II $EI^{II}$, as shown in Fig. 8-4, which describes the relationship between moment and coving of a partially cracked reinforced concrete profile[407]. Depending on the history of loading, the stiffness of the observed section is still in the elastic region, and has not reached the point of formation of the first cracks (1) or is on a point (2) between state I and II. In case of loadings, which do exceed the load maximum, the performance can be described as linear-elastic.

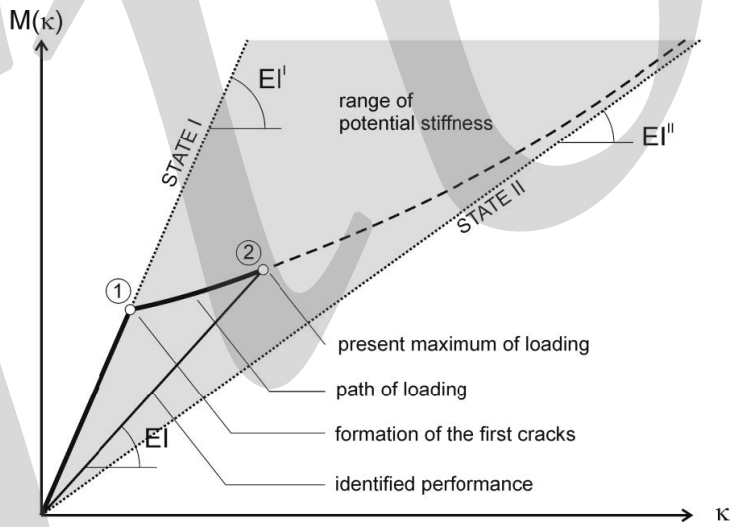


Fig. 8-4 Nonlinear performance of RC structures[402]

## 8.4.2 Elements of a monitoring and system-identification system (MIS)

The quantitative recording of a structure's condition by means of a monitoring system is the groundwork for any health-monitoring-system (SHM) or life-cycle-management (LCM). In addition to the initial interpretation of measured data, they can be used for methods of system identification, as described in[408]. There are lots of greatly varying approaches[409, 410, 411], which essentially differ in the way the structure is actuated: ambient influences (ambient excitation[412]) or defined loadings (enforced excitation, test loading).

This document is the intellectual property of the fib – International Federation for Structural Concrete. All rights reserved.
This PDF of fib Bulletin 86 is intended for use and/or distribution solely within fib National Member Groups.

The ambient approach allows an undisturbed usage of the structure while testing, and in case of a permanent installed monitoring system the system is highly over determined because of the high amount of available data. If defined loading is applied, the measured data is usually better due to the higher and tuned actuation, but the structure can only partially or not at all be used during the whole testing procedure. Choosing the correct concept is influenced by different criteria, e.g. the importance of the structure for transport, the chosen measuring quantity and above all, the differentiation between a new construction and existing structures. In case of new constructions a permanently installed ambient system should be preferred, in case of existing structures, defined loading and mobile measuring systems are more effective.

An application oriented identification approach should not allow for manual data correction or unadvised filtering in order to avoid a biased possibly wrong identification result which might in the worst case lead to disaster and fatalities. Filtering and smoothing techniques require a high degree of knowledge and should therefore be only very carefully applied or not at all[403, 402].

### 8.4.3 Structural model

System identification in most cases means the determination of structural parameters using available observed data. However, it is necessary to draw up a relation between measured data and observed data. Theoretically, this connection can be solved in a closed analytic form, mostly it is a complex iterative optimising problem.

The description of the structural behaviour, depending on a few structural parameters which must be optimised like segmental stiffness, can be carried out in an analytic way for practical problems, as Hoffmann describes for the relation between the influence line of bearing reaction and the distribution of the bending stiffness[403]. In most of the other cases, adapted FE-models are used, by reason of requirements of a practically usable identification method, e.g. the level of automation, robustness, efficiency of the mathematical description and low efforts for modelling. Moreover, FE-models can be adapted to specific requirements of the identification easily[402].

With an adequate high number of finite elements, each structural problem can be described, however this causes a significant increase in computational demand. By adapting the properties of the finite elements, their number can be reduced without reduction of accuracy.

An efficient illustration of the stiffness along a real structure needs the capability to determine a linear stiffness distribution inside of a finite element for representing both geometrically and damage-caused changes in stiffness.

Beams are the most important structural elements in civil engineering. Their principal duty is to transfer loads which act perpendicular to the beam axis. In the case of real beams this happens mainly by bending or by a combination of bending and shear force deformation. In most cases, beams and frame members, which are solely loaded by axial forces, are adequate for modelling real bridge structures.

Conventional theory on beams uses the Bernoulli-Euler-Hypothesis. This means that the cross sections are plane and normal to the longitudinal axis and also that they remain in this condition in the displaced state. Load transfer takes place exclusively by bending; shear deformation due to shear force is not considered. In many cases, also in questions

This document is the intellectual property of the fib – International Federation for Structural Concrete. All rights reserved.
This PDF of fib Bulletin 86 is intended for use and/or distribution solely within fib National Member Groups.

of vibration analyses, if shear deformation is neglected, it causes unreliable results[402]. By means of the Timoshenko-Theory even shearing effects can be considered. The basic assumption that the cross sections remain plane is upheld, but there is no thesis that it remains in a normal position to the longitudinal axis in the deformed state[413].

### 8.4.4 System identification

Many available methods for system identification are types of a model-update, which has to be seen as an optimising problem. These methods can vary in the type of data they use, e.g. the analytic model ILIAS[403] is based on influence lines, and the way the simulated structural response is obtained, e.g. the modal method MOBEL uses finite elements[402]. Literature shows several approaches for identification and classification of system identification methods[408].

The core of system identification is to optimise the unknown system parameters (basic variables for optimisation, e.g. interpolation points of stiffness distribution, springs stiffness, etc.) based on observing the structural response at a defined load level. Therefore it is necessary to define a numerical criterion for describing the quality of congruence. This criterion constitutes the objective function. Hence optimising the basic variables according to this criterion means minimising the objective function.

$$f^*(x^*) = \min f(\vec{x}) \left| \begin{array}{l} h_i(\vec{x}) = 0, i = 1,\ldots,n \\ g_j(\vec{x}) \leq 0, j = 1,\ldots,m \end{array} \right. \tag{8-6}$$

in which:

$f(\vec{x})$ = objective function

$f^*(x^*)$ = ideal value of the objective function at the position of the optimum $x^*$

$(\vec{x})$ = vector of the basic variables, which obeys to the theorem of $i$ equations $h_i(\vec{x})$ and the theorem of $j$ inequations $g_j(\vec{x})$ as boundary condition

In many cases the system identification is an adaption of a curve, e.g. of the measured and calculated bending line. The objective function can be considered as deviation between observed and calculated monitoring values, whose minimum represents the optimum of identification.

$$f_i(\vec{x}) = \left(\vec{x}_{c,i} - \vec{x}_{m,i}\right)^T \left(\vec{x}_{c,i} - \vec{x}_{m,i}\right) \tag{8-7}$$

in which

$\vec{x}_{c,i}$ = vector of the calculated monitoring values for loading/date $i$

$\vec{x}_{m,i}$ = vector of the measured monitoring values

Generally there are linear and nonlinear optimising problems and challenges with and without boundary conditions (constrained and unconstrained). In case of linear optimisations, the objective function depends linearly on the basic variables and linear boundary conditions. Many practical problems can be described easily by means of linear relations and particularly linear boundary conditions, or these issues can be simplified to a linear problem with sufficient accuracy. Luenberger[414] gives a description of various optimisation problems in some detail. Optimising of common types of objective functions can be performed by commercial available software programs, like “lsqcurvefit”, which is an MATLAB-application[415].

This document is the intellectual property of the fib – International Federation for Structural Concrete. All rights reserved.
This PDF of fib Bulletin 86 is intended for use and/or distribution solely within fib National Member Groups.

Lots of problems of structural identification are highly nonlinear problems, due of the complex relations between structural parameters and monitoring value (e.g. stiffness and bending line) and the large reciprocal relation between the basic variables. In contrast to linear optimising (linear programming) these nonlinear problems can only be solved by iterative methods, which cause large additional efforts. Moreover, nonlinear objective functions may have a few minima, which make it quite difficult to detect the global one. The "genetic algorithm", which was developed by Holland[416] and the "simulated-annealing" method, proposed by[417] are standard approaches for solving problems caused by local minima. Both approaches can be used for system identification, as[362] have shown. Furthermore, there is the method of "coupled local minimisers" for identification of bending stiffness[418, 404] and the "response surface method"[419].

### 8.4.5 Direct stiffness calculation

There are many identification methods based on dynamic properties of structures. Some consider mainly eigenfrequencies others include also Eigen form and damping.

Unlike other approaches which are based on some kind of model update, 'Direct Stiffness Calculation' (DSC) allow direct calculation of a structure's stiffness distribution.

In course of project 'AIFIT' conducted at BOKU university different identification tools – both static and dynamic – have been applied to measurement data of several simple two-span reinforced concrete beams and their operability verified against each other. Based on those studies it can be concluded that direct stiffness methods are able to identify stiffness distributions correctly. The results are comparable to those obtained by other dynamic methods like sensitivity based model update.

The original Direct Stiffness Calculation was developed by[420] in 2003. This technique makes use of experimentally determined eigenfrequencies and mode shapes of a structure and is able to estimate bending and torsional stiffness along the structure respectively. It is assumed that a (local) loss of stiffness is caused by some kind of (localized) damage. Basically no accurate model of the structure is needed. However the comparison of the theoretical undamaged stiffness distribution with the identified one allows interpretation of the results more usefully.

The most important input information is modal curvatures which can be derived from measured mode shapes. They are highly sensitive to damage and thus contain much valuable information. On the other hand small errors in measurement have a huge impact on 2$^{nd}$ derivatives of measured displacements. Thus the input data has to be prepared in advance by certain filtering and smoothing techniques. For DSC a technique called 'mixed approach' was developed by[420] based on differences between approximations for rotations and curvatures and respectively the first and second derivatives of modal displacements using penalty factors $\alpha$ and $\beta$. A short comparison between 'mixed approach' and more classical techniques like global smoothing, moving polynomial or b-splines is given by Maeck[420].

The calculation of the bending stiffness $EI$ in each section by direct stiffness calculation (DSC) is based on the relation between modal bending moment $M$ in that section divided by the corresponding modal curvature as second derivative of the bending mode $\varphi^b$, Eq.(8-8). In the same manner the torsion stiffness $GJ$ can be calculated using modal torsional moment $T$ and modal torsion rate as first derivative of the torsion mode $\varphi^t$, Eq.(8-9). This has to be done separately for every mode shape available.

This document is the intellectual property of the fib – International Federation for Structural Concrete. All rights reserved.
This PDF of fib Bulletin 86 is intended for use and/or distribution solely within fib National Member Groups.

$$E \cdot I = \frac{M}{d^2 \cdot \varphi^b / dx^2} \tag{8-8}$$

$$G \cdot J = \frac{M_T}{d \cdot \varphi^t / dx} \tag{8-9}$$

Consequently the modal internal forces $M$ and $T$ respectively have to be calculated accurately and the modal curvatures or modal torsion rates have to be determined.

Based on the free vibration dynamic equilibrium equation Eq. (8-10) the generalized eigenvalue problem can be formulated by Eq. (8-11)according to[421].

$$M_a \cdot \ddot{U} + K \cdot U = 0 \tag{8-10}$$

where $M_a$ is the analytical mass matrix and $K$ the stiffness matrix.

$$K \cdot \varphi_m = \omega_m^2 \cdot M_a \cdot \varphi_m \tag{8-11}$$

where $\varphi_m$,is the vector of measured modal displacement and $\omega_m$ are measured circular eigenfrequencies.

Considering equation Eq. (8-11) as pseudo static, the right-hand side $\omega_m{}^2 \cdot M_a \cdot \varphi_m$ are forces acting on a structure with stiffness matrix $K$ resulting in deformation $\varphi_m$. Thus for a known mass distribution and measured modal displacements a set of inertia forces can be calculated[420]. In practice the experimental mass matrix is for simplicity substituted by the analytical one.

Considering several measured mode shapes and corresponding eigenfrequencies one obtains exactly as many sets of inertia forces. The length of each vector is determined by the number of measured modal displacements, thus only a discrete pattern of inertia load is determined. By linear interpolation of the measured displacements finally an approximately distributed load can be calculated.

Consequently shear forces $V_i$, bending moments $M_i$ and torsional moments $T_i$ can be computed according to[420], assuming that only inertia load is acting on the beam – equations Eq. (8-12) to Eq. (8-14).

$$M_{i+1} = M_i + T_i\left(x_{i+1} - x_i\right) - \int_{x_i}^{x_{i+1}} \omega_m^2 \cdot \rho \cdot A \cdot \varphi_m^b(x)\left(x_{i+1} - x\right)dx \tag{8-12}$$

$$V_{i+1} = V_i - \int_{x_i}^{x_{i+1}} \omega_m^2 \cdot \rho \cdot A \cdot \varphi_m^b(x)dx \tag{8-13}$$

$$T_{i+1} = T_i - \int_{x_i}^{x_{i+1}} \omega_m^2 \cdot i_\alpha \cdot \varphi_m^t(x)dx \tag{8-14}$$

Where $\rho$, $A$, $i_\alpha$ are respectively density, cross area and polar moment of inertia of the structure.

Alternatively internal forces can be calculated using simple finite element software. This is especially useful for hyperstatic structures, as was necessary for the two-span beam considering in project AIFIT. Theoretically the calculation of internal forces has to be done iteratively because stiffness distribution and internal forces are coupled.

This document is the intellectual property of the fib – International Federation for Structural Concrete. All rights reserved.
This PDF of fib Bulletin 86 is intended for use and/or distribution solely within fib National Member Groups.

However it could be shown by Maeck[420] that for realistic damage changes in internal forces are relatively small.

### 8.4.6 Influence-line oriented identification systems

In the following, simple criteria and approaches for influence line orientated system identification focusing on the modal based approach are discussed (MOBEL)[402]. Fig. 8-5 shows the principal elements and the constitution of the approach.

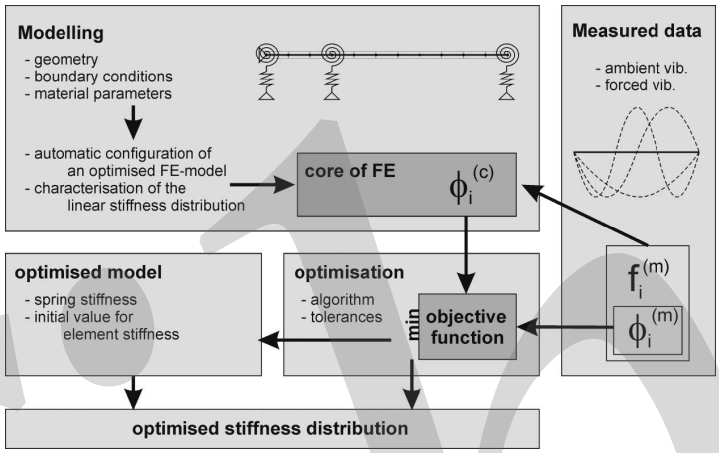


Fig. 8-5 Scheme of the influence line based system identification MOBEL[402]

The general concept of the identification method MOBEL is based on a pseudo-static view on measured mode shapes. As a result it is possible to use modal information for system identification without solving the eigenvalue problem as it is extremely sensitive to the hardly ascertainable geometrical boundary conditions. Transforming the homogenous moving equation yields to the generalised eigenvalue problem, as formulated by[421]:

$$M \cdot \ddot{\vec{x}} + K \cdot \vec{x} = 0 \tag{8-15}$$

$$K \cdot \vec{\Phi} = \omega^2 \cdot M \cdot \vec{\phi} \tag{8-16}$$

in which

$\omega$ = considered angular frequency

$\vec{\Phi}$ = associated mode shape

This dynamic equation can also be transformed to a static situation. The right part describes the inertia forces, which operate on the system. They are equal to the forces which are required to induce the deformation $\vec{\Phi}$ considering the stiffness matrix $K$[420]. As a result the measured mode shape can be expressed as a bending line. On a general oscillating bar-construction in space, there are six degrees of freedom on each node, three deformations and three rotations. To calculate the inertia forces and moments, which are connected to a certain mode shape, it is necessary to take the mass inertia for translational components and the rotary inertia for the rotatory components into consideration. If the geometry of a structure is thus far known that it can be described with the theoretical values of the cross sections, the inertia forces are determined by means of the displacements of the nodes.

This document is the intellectual property of the fib – International Federation for Structural Concrete. All rights reserved.
This PDF of fib Bulletin 86 is intended for use and/or distribution solely within fib National Member Groups.

$$\vec{F}(x) = \omega^2 \cdot m(x)\vec{\Phi}^t(x) \tag{8-17}$$

in which

$\vec{\Phi}^t(x)$ = modal displacement of the node towards the three axes at $x$

$m(x) = \int \rho(x)\, dA\, dx$

The rotary inertia is calculated analogously.

$$\vec{F}^r(x) = \omega^2 \cdot J(x)\vec{\Phi}^r(x) \tag{8-18}$$

in which

$\vec{\Phi}^t(x)$ = rotation of the node around the three axes in position $x$ $J(x)$ = tensor of inertia at position $x$

For applying a method of system identification it is necessary to have an adequate amount of measured data in a sufficient quality. The quasi-static consideration on eigenmodes and general mode shapes according to the equations above enables the usage of any measured mode conditions for system identification – not only eigenmodes with associated eigenfrequencies. The reason is that the relation between inertia forces at maximal dynamic deflection, stiffness and static deflection is generally admitted at equivalent static load[402]. Both ambient measured mode shapes and measurements with forced vibration can be taken for identification. By means of a selective excitation of the eigenfrequency of a structure, the modal response has one dominant mode shape and hence a robust and clear signal. Additionally considerable amplitudes can be reached by usage of the dynamic enlargement by excitation in resonance for structures with little damping. In this case, the measurement range of the sensor is better utilised, enhancing the quality of the measured mode shapes.

Although the elegance of modal model-updating – system identification with just a few measured variables – gets lost, the reliability of results is increased, as hardly any a priori knowledge is necessary. For the application of system identification the boundary conditions and structural properties like stiffness or material properties are usually not known in advance. Temperature effects can also cause significant shifts in the eigenfrequencies[422] and make updating of the eigenfrequencies more difficult. These effects however can be neglected in a first step by the proposed approach. In case of MOBEL there are is no need for comparative measurements or calibrations of the model in an undamaged state. Hence, the temperature effects are only considered during interpretation of the identified stiffness distributions and the boundary conditions, which show the general condition at the time when the measurements were taken. The demand for high stability in the identification (optimisation) process calls for a high grade of over-determination. To reach this over-determination, it is necessary, to have lots of measured mode shapes $\vec{\Phi}_i^{(m)}$ and to have them with a high density of measurement points. An adequate formulation of the objective function with the principle of least-square curve fits is used to handle a large number of measuring points.

Editing and preparation of data is an important point concerning the application of structural analysis and system identification. Especially in working with time series and signals in a time range, filter (e.g. high-pass and low-pass filter), smoothing and transformation processes (e.g. Fast-Fourier-Transformation) between time domain and frequency domain are used. To avoid negative influences as a result of a wrong appliance, methods should either work with the raw data or should give the operator the alternative to choose between various data preconfigured processing techniques[402]. MOBEL does not

This document is the intellectual property of the fib – International Federation for Structural Concrete. All rights reserved.
This PDF of fib Bulletin 86 is intended for use and/or distribution solely within fib National Member Groups.

need any methods of editing data, in contrast to other methods like the "direct stiffness calculation" DSC[420]. In MOBEL, the high grade of over determination and the used Curve-Fitting-Method enable the compensation for random measurement errors.

The build-up of an adequate FE-model for a specific topic is generally not easy. Hence it is necessary to automate this challenge and to reduce the user's interventions to a minimum. Taking into account the variability of the structures and types, a full automation is obviously not possible. In the following, the application is limited to continuous beams with a variable number of spans, which makes it quite easy to automate the modelling. With the creation of templates for the most common types of structures it is possible to enable a simple input and an automated modelling even for more sophisticated structures.

The chosen restriction to two-dimensional continuous beams causes a reduction of the input parameters: mode shapes, including the position along the axis, amplitudes and frequencies, the dimensions of the spans and the cross section values. These parameters can be used to estimate the oscillating mass and offers a favourable selection of the initial values of the stiffness. In case of a fine FE-mesh, it may be required not to consider each sectional value as a basic variable for optimisation to ensure a sufficient over determination. MOBEL uses an approach for interpolating the residual section values. Each element describes a linear distribution of the stiffness, where the values at the elements ends can be found by linear interpolation. In order to be able to accurately enough describe the stiffness distribution and to localise and quantify damage, it is necessary to have approximately ten nodes at each span[402].

Boundary conditions are quite important for the reliability of calculations, especially in cases of dynamic problems – both the eigenvalue problem and the quasi-static approach. MOBEL allots translational and rotational springs to each support point. The properties of these are updated along with the stiffness distribution. As a result the boundary conditions have not to be constituted a priori.

In addition to an accurate description of the system stiffness of a structure, the correct characterisation of the mass distribution is important, too. For an efficient FE-modelling, a realistic mass matrix $M$ has to be identified, including rotational and translational contributions, which have a direct influence on the eigenvalue problem and the calculation of the inertia forces. Theoretically, it is necessary to determine the whole tensor of inertia, but for low eigenmodes the rotary fractions can be neglected[420], it follows:

$$\vec{f}_i^{(m)} = M \cdot \omega^2 \cdot \vec{\Phi}_i^{(m)} \tag{8-19}$$

in which:

$M$ = diagonal matrix of node-concentrated masses

$\vec{f}_i^{(m)}$ = vector of known nodes of the distributed inertial load

After the generation of the FE-mesh (nodes, bars, supports), the structural response is calculated for each mode shape separately. The steps of the calculation are firstly to calculate the distributed inertia load, then solving the stiffness equations and finally the extraction of node displacements associating to measured amplitudes. As a result we get for each measured (m) mode shape $\vec{\Phi}_i^{(m)}$ a corresponding calculated ($c$) $\vec{\Phi}_i^{(c)}$, which have to be the same, if the modelled structure accords to the real structure.

Obviously, the FE-model for the quasi-static approach does not only calculate the bending lines in association with the mode shapes, but also can be used for each further

*This document is the intellectual property of the fib – International Federation for Structural Concrete. All rights reserved.*
*This PDF of fib Bulletin 86 is intended for use and/or distribution solely within fib National Member Groups.*

static or quasi-static loading. The identification uses all system values of the model, in addition to the dynamic information, a static test loading can be applied for further optimisation. Moreover, influence lines for reactions can be included by means of generating a unity moving load to compare this values to the measured ones, similarly as[403] describes it in his analytical approach.

The real core of MOBEL is the optimisation of the unknown system parameters (basic variables for optimisation). As discussed above, MOBEL yields to i measured mode shapes $\vec{\Phi}_i^{(m)}$ with their corresponding bending lines $\vec{\Phi}_i^{(c)}$. The optimal choice of the basic variables means therefore the highest achievable congruence. The objective function is determined by deviance, as usual in fitting curves. The objective function $f_i(\vec{x})$ can be defined for each available mode shape *i*, as pointed out in the following equations. The weighting factors $\alpha_0$, $\alpha_1$ and $\alpha_2$ enable the variation of the influence of displacement, slope and coving inside of the objective function. The measured respectively calculated deflections are used for calculating the objective function.

$$f_i(\vec{x}) = \alpha_0 \cdot \Delta\vec{\Phi}_i^T \cdot \Delta\vec{\Phi}_i + \alpha_1 \cdot \Delta\vec{\Phi}_i'^T \cdot \Delta\vec{\Phi}_i' + \alpha_2 \cdot \Delta\vec{\Phi}_i''^T \cdot \Delta\vec{\Phi}'' \tag{8-20}$$

in which:

$$\vec{\Phi}_i' = \frac{d\vec{\Phi}_i}{dx};\ \vec{\Phi}'' = \frac{d^2\vec{\Phi}_i}{dx^2}$$

$\Delta\vec{\Phi}_i, \Delta\vec{\Phi}_i', \Delta\vec{\Phi}''$= vector of deviance in the i-n$^{th}$ mode shape or their derivative according to location

$\alpha_0$, $\alpha_1$, $\alpha_2$ = weighting factors to express the form

Connecting all available *i* mode shapes, the whole optimising problem can be seen as a minimisation of the multi-objective function, the additional factor $\beta$ assesses the measurements in their relative quality.

$$\min_{\vec{x}} \sum_i \beta_i \cdot f_i(\vec{x}) = \min_{\vec{x}} \sum_i \beta_i \left( \alpha_0 \cdot \Delta\vec{\Phi}_i^T \cdot \Delta\vec{\Phi}_i + \alpha_1 \cdot \Delta\vec{\Phi}_i'^T \cdot \Delta\vec{\Phi}_i' + \alpha_2 \cdot \Delta\vec{\Phi}_i''^T \cdot \Delta\vec{\Phi}'' \right) \tag{8-21}$$

in which:

$\beta_i$ = weighting factors for input of *i* mode shapes

Due to the fact that weighting factors intervene in a very manipulating way into optimising, they should be used quite carefully and set to 1,0. If necessary, the multi-objective function can be extended to build in additional measurement categories. Then the $\beta$-factor has to selected in an adequate way to ensure a solid optimisation process[402].

The identification of the stiffness distribution of a structure is a complex issue as the basic variables are not independent. This is especially true, if variables with dominant impact on the objective function (e.g. boundary elements like springs at supports) are to be identified simultaneously. Hence a two-step iterative strategy was developed as sketched in Fig. 8-6.

This document is the intellectual property of the fib – International Federation for Structural Concrete. All rights reserved.
This PDF of fib Bulletin 86 is intended for use and/or distribution solely within fib National Member Groups.

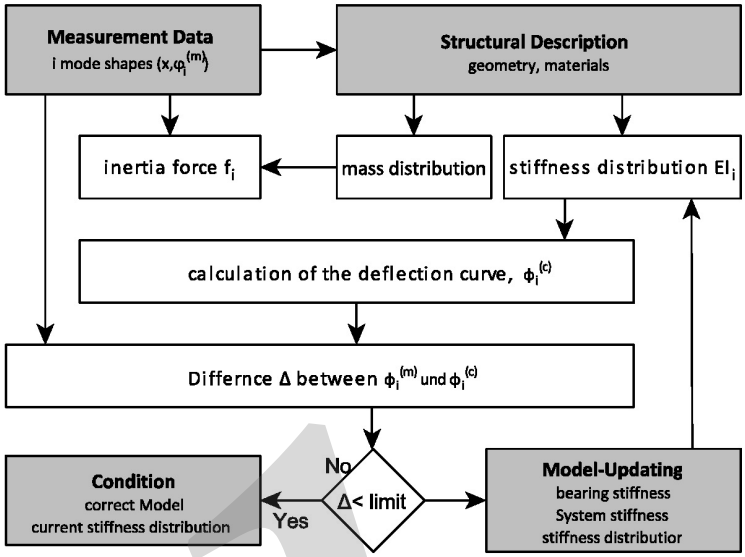


Fig. 8-6 Optimisation strategy for MOBEL

In the first step a single basic value for the stiffness of the superstructure and the spring stiffness values of the supports are considered as optimising values (basic variables), because they hold a large influence on the objective function. The stiffness of the supports is modelled by springs, the initial values are assumed to be well above real values, out of the reason that this means a simple choice. The stiffness of the superstructure is described with a single variable. To offer the possibility of stiffness changes along the structure, the section values can be used to estimate the relative stiffness distribution along the structure. The results of the first optimisation can be taken as good estimations of the initial values for the real optimising process in which only the relative changes of stiffness have to be optimised both of the elements and of the supports. The initial assumption of a constant stiffness which only depends on the section geometry along the structure yields to a wrong identification of support stiffness in case of damaged structures. Those wrong stiffness influences the determination of the stiffness distribution. The distribution, which is received from a second optimising step, can be used to get a better distribution, because it is already a good approximation. Due to the separated optimisation of the boundary conditions and the stiffness distribution by means of an iterative approach, the solution of the complex optimisation problem can be received automatically.

The application of the optimisation problem inside of the algorithm MOBEL is based on the procedure "lsqcurvefit"[415], which is provided by MATLAB and has the capability to solve nonlinear problems with boundary conditions. The same algorithm was applied by Hoffmann[403] to identify the stiffness based on measured influence lines for reaction forces. The procedure "lsqcurvefit" uses a large-scale algorithm for the present optimisation problem, operating with the "subspace trust region method", which is based on the "interior-reflective Newton method" by[423]. This method has a rather complicated algorithm, each iteration step means the approximate solution of a large linear system of equations with the "preconditioned conjugate gradients method" (PCG)[424]. If the Jacobian matrix is available, it can be provided, otherwise it has to be approximated by means of "lsqcurvefit" by the finite differences model. Further information about the applied algorithm can be found in[415]. The most important advantages of "lsqcurvefit" are the simple configuration, the possibility to define initial values for optimisation, to fix upper and lower boundaries and to vary the

*This document is the intellectual property of the fib – International Federation for Structural Concrete. All rights reserved.*
*This PDF of fib Bulletin 86 is intended for use and/or distribution solely within fib National Member Groups.*

convergence criteria[403]. However the algorithm cannot overcome local minima, as they frequently occur in structural engineering. The objective function is decreasing monotonously coming from an overestimation of the stiffness values, therefore a robust optimisation with a value nearby the global minimum can be achieved, if the initial values are chosen correctly.

## 8.5 Other identification methods

Other identification methods are described in[343] in detail.

## 8.6 Sensitivity factor method

### 8.6.1 General aspects

Design sensitivity analysis plays a critical role in inverse and identification studies, as well as numerical optimization, and reliability analyses. However, the concepts presented in this may be readily extended to compute sensitivities for complex systems via numerical techniques such as the finite element, boundary element, and finite difference methods.

### 8.6.2 Introduction

For inverse and identification analyses, error functions quantify the discrepancy between experimentally measured and analytically predicted response data. Sensitivity analyses are then preformed to evaluate the gradients of the error functions with respect to the model parameters used in the analysis. The sensitivities are then used to modify the unknown model parameters to correlate the predicted and experimental response data. For example, the stiffness parameters in a structural model are modified through sensitivity analysis to correlate the frequency data. Sensitivity information is also valuable in its own right. Indeed, we may determine how the value of a given response function, say F, changes with respect to a given change in the model parameters, say $\Delta x$. For small perturbations $|\Delta x|$, this information is e.g. obtained through a first-order Taylor series expansion,

$$F(x+\Delta x) = F(x) + \nabla F(x)\Delta x + o\left(\left|\Delta x\right|\right) \tag{8-22}$$

where $x$ is the vector of the model parameters. If the response function $F$, e.g. the stress at a point of a structural system, is evaluated through a numerical analysis such as a finite element method, then we may predict how the response function value varies for small perturbations in the model parameters without performing a re-analysis (see[425] for structural mechanic and[426] for nuclear reactor design applications). Thus, the sensitivities offer an efficient means to predict the performance of modified models. Much work has been performed in the field of design sensitivity analysis. Most notably, perhaps, is the work in structural mechanics with applications to structural optimization. For example see the books[427, 428, 429, 430, 431, 432, 433] the journal Structural and Multidisciplinary Optimization[434] and the NATO ASI proceedings[435, 436, 437] for a wide range of sensitivity derivations with applications to numerous structural systems. Some of the pioneering work in this field traces back to the analytical optimization of simple structures via adjoint approaches and variational principles[438, 439, 440, 441, 442].

*This document is the intellectual property of the fib – International Federation for Structural Concrete. All rights reserved.*
*This PDF of fib Bulletin 86 is intended for use and/or distribution solely within fib National Member Groups.*

Numerical evaluation of the sensitivities appeared sporadically prior to the eighties after which it became commonplace. Sensitivities are derived for numerous structural systems. For example, in linear elastostatics, we cite derivations for continuum systems[425, 443, 444, 445, 446, 447, 448, 449, 450, 451, 452, 453, 454, 455, 456, 457, 458, 459] and structural systems (i.e. beams, plates, and shells)[460, 461, 462 463, 464, 465, 466, 467, 468, 469, 470, 471, 472, 473]. Sensitivities are derived with respect to material parameters which may be used, for example in the design of composite materials[448, 462, 466, 470, 471, 472], sectional parameters which describe beams, plates, and shells[461, 463, 464, 468] and shape parameters which describe the body's geometry[425, 445, 446, 447, 474, 450, 475, 452, 453, 454, 455, 476, 456, 457, 458, 459, 465, 467, 469, 473]. Sensitivities have also been derived for nonlinear structural systems.

Nonlinear elastic formulations may be found in[477, 478, 479, 480, 481, 482, 483, 484] viscoelastic formulations appear in[485, 486, 487] and history dependent material response (e.g. plasticity) formulations appear in[488, 489, 490, 491, 492, 493, 494, 495]. Eigenvalue and frequency response sensitivity formulations are investigated in[496, 497, 498, 499, 500]. Finally, sensitivities for elastodynamic systems appear in[501, 502, 503, 504] and for contact problems see[505, 506] Sensitivities have also been derived for other classes of problems. For example, sensitivities for thermal systems are derived in[507, 508, 509, 510, 511, 512, 513, 514]. These results are combined with structural sensitivity analyses to formulate sensitivities for thermoelastic systems in[515, 516, 517, 518, 519]. In the area of rigid body mechanics, see[520, 521, 522, 523] for sensitivity results.

Sensitivity applications are numerous. In addition to their application in structural optimization, we cite optimization applications for various other systems, for example see the proceedings Multi-Disciplinary Optimization Conferences[524]. Sensitivities are also embedded in inverse conduction[525, 526, 527, 528, 529] and inverse elasticity [530, 531] analyses. Likewise, sensitivities appear in non-destructive evaluation[532, 533], modal identification[534, 535] chaos prediction [536], nonlinear programming[537, 538, 539] and reliability, probability and stochastic analyses[540, 541, 542, 543, 544, 545].

### 8.6.3 Linear systems

Presently, we focus our attention on linear elliptic systems. For such systems, we may evaluate the response $u$ at any point in the body through the following equation

$$K(x) \cdot u(x) = P(x) \tag{8-23}$$

subject to the appropriate boundary conditions. Here $K$ is a linear differential operator in space and is an explicit function of the n-dimensional design vector $x$. The elements of $x$ comprise the set of design parameters and are used to describe the material response, sectional properties, load data, and geometry of the domain. The load data $F$, is also an explicit function of the design $x$. Finally, the response $u$, is an implicit function of the design $x$ as seen through the above equation. The above system governs many problems, for example linear elastostatics and linear steady-state conduction.

Without loss of generality, we discretize the above system for the numerical evaluation of u, e.g. by the finite element, boundary element, or finite difference methods. Then $K$, $F$ and $u$ are the m×m stiffness matrix, the $m$-dimensional load vector, and the m-dimensional displacement vector, respectively, where $m$ is the number of degrees of freedom. One performs a finite element (or similar) analysis to evaluate the system response u and then uses this system response to evaluate the response function $F$ which we define through

This document is the intellectual property of the fib – International Federation for Structural Concrete. All rights reserved.
This PDF of fib Bulletin 86 is intended for use and/or distribution solely within fib National Member Groups.

$$F(x) = G(u(x), x) \tag{8-24}$$

The objective of the sensitivity problem, then, is to compute the derivative, or sensitivity, of the above, i.e. where we invoked the chain rule.

$$\frac{DF}{Dx}(x) = \frac{\partial G}{\partial u}(u(x), x)\frac{Du}{Dx}(x) + \frac{\partial G}{\partial x}(u(x), x) \tag{8-25}$$

The difficulty of evaluating the above is due to the presence of the derivative $\frac{Du}{Dx}$ which is implicitly defined through equation (8-1), and therefore it is generally unknown.

Example 1 Consider a spring system. We may compute the deflection $u$ by solving the system

$$K \cdot u = P \tag{8-26}$$

where

$$K = \begin{bmatrix} k_1 + k_2 & -k_2 \\ -k_2 & k_2 \end{bmatrix}, \text{ and } P = \begin{bmatrix} P_1 \\ P_2 \end{bmatrix} \tag{8-27}$$

The result is seen to be $u$ = [3,4] for the case in which $k_1 = 1$, $k_2 = 2$, $P_1 = 1$, and $P_2 = 2$. We can also evaluate this result symbolically as

$$u_1 = \frac{(P_1 + P_2)}{k_1} \tag{8-28}$$

$$u_2 = \frac{\left(k_2 \cdot P_1 + (k_1 + k_2)P_2\right)}{k_1 \cdot k_2} \tag{8-29}$$

In regard to the sensitivity analysis, we consider u as the system response and $x = [k1, k2, P1, P2]$

$\in \Re^4$ as the design parameter vector.

Now suppose we treat the load as fixed, i.e. $P1$ and $P2$ are not allowed to vary. This seems reasonable for design problems, for we could otherwise reduce to zero the structural weight by merely eliminating the load. At any rate, the design then reduces to the spring constants, x = $[k1, k2] \in \Re^2$, which is specified by the engineer who designs the system. Suppose we wish to determine how the compliance of the design is affected by a change in the spring constants. The compliance is computed from

$$F(x) = G(u(x), u) = P_1 \cdot u_1(x) + P_2 \cdot u_2(x) = \frac{P_1(P_1 + P_2)}{k_1} + \frac{P_2(k_2 \cdot P_1 + (k_1 + k_2)P_2}{k_1 \cdot k_2} \tag{8-30}$$

from which we obtain

$$\nabla F(x) = \begin{bmatrix} -\frac{-(P_1 + P_2)^2}{k_1^2} \\ -\frac{P_2^2}{k_2^2} \end{bmatrix} = \begin{bmatrix} -9 \\ -1 \end{bmatrix} \tag{8-31}$$

Thus, an increase in the stiffness of spring 1 would decrease the compliance nine times greater than an equal increase of spring 2. From the above, we also find that

This document is the intellectual property of the fib – International Federation for Structural Concrete. All rights reserved.
This PDF of fib Bulletin 86 is intended for use and/or distribution solely within fib National Member Groups.

$$Du(x) = \begin{bmatrix} \frac{Du_1}{Dk_1} & \frac{Du_1}{Dk_2} \\ \frac{Du_2}{Dk_1} & \frac{Du_2}{Dk_2} \end{bmatrix} = \begin{bmatrix} -\frac{P_1+P_2}{k_1^2} & 0 \\ -\frac{P_1+P_2}{k_1^2} & --\frac{P_2}{k_2^2} \end{bmatrix} = \begin{bmatrix} -3 & 0 \\ -3 & -0.5 \end{bmatrix} \tag{8-32}$$

In the previous example, we evaluated the response symbolically so that the response $u$ and response function $F$ are explicit in the design $x$. In general this is not possible, so we devise means to evaluate the sensitivities when $u$ and hence $F$ are not explicit functions of $x$. Nevertheless, the afore mentioned procedure can be applied in a similar way to methods like the finite difference method, the direct differentiation method, and the adjoint method and the Finite element methods.

### 8.6.4 Summary

Sensitivity analyses play an integral role in many engineering design problems. Here, we attempted to present the sensitivity formulations in a straightforward manner. A simplistic example was used to demonstrate the efficiency of the analyses. These same concepts are used to formulate sensitivities for numerous other problems; please see the citations for specific details.

## 8.7 Gamma prediction method

Stochastic process modelling methods such as gamma processes are becoming increasingly popular in the maintenance management of infrastructure buildings. Gamma process based methods are very well suited to process classical structural information from visual inspections as for example crack formations or deflections, but also on near-surface stress or strain evolution. Gamma process based forecast models are able to provide aid for the process of determining suitable inspection intervals and maintenance measures.

### 8.7.1 General Remarks

Numerous industrially advanced countries use various different management systems to ensure the safety level of their infrastructure buildings (such as motorway bridges) as required by their national economies. Since each of these engineering structures is unique and because of the diversity of processes that take place within each structure, very extensive and complex sets of data may emerge in the course of the structural management, much of which is irrelevant for the proprietors' decision-making processes.

Furthermore, a wide variety of modern monitoring technologies and numerical methods has been developed in the last few decades, ranging from innovative sensors in monitoring systems to new video-imaging routines.

These new developments provide the means to examine and bring into accordance established technical and physical methods for assessing quality, diversity and location specific data. They also serve to improve and adapt inspection routines and, in a next step, to optimize temporally and methodically the relevant maintenance and management systems.

In general, concrete structures are subject to aging processes that result from mechanical, environmental and chemical stresses which go hand in hand with a continuous deterioration

*This document is the intellectual property of the fib – International Federation for Structural Concrete. All rights reserved.*
*This PDF of fib Bulletin 86 is intended for use and/or distribution solely within fib National Member Groups.*

of the safety level. In order to control the progression of these processes and to adapt the scheduling of maintenance measures accordingly, standards and regulations (DIN 1076: 1999[546], DIN EN 1076: 2004[547], FSV RVS 13.71[548]) where inspection intervals are set down with clear and unambiguous descriptions of the scope of the examination have been introduced in most countries world-wide.

Currently, most monitoring efforts are based on visual inspections and the resulting assessment of both structural components and building equipment by trained specialists. This procedure is subjective by its very nature[549] and consequently delivers an in some cases quite limited picture of both load carrying capacity and serviceability of a structure.

In particular for prestressed reinforced concrete structures which are subject to aggressive environmental conditions (e.g. excessive application of road salt), this can lead to considerable assessment errors.

The deterioration of the structural condition over time and the attainable service life are strongly affected by conservation strategies, maintenance measures and reinforcements – ultimately, by the management methods applied by the proprietors, which in turn are subject to varying budgetary and societal constraints.

The inspection routines established in the countries of Germany and Austria are divided into monitoring actions, continuous control measures and regular inspections. These individual steps are performed either in regular intervals or prompted by specific conditions or events. For a comprehensive assessment of the structures, in general, an inspection is performed. There are numerous advantages to these historically developed inspection routines, yet a few failings also need to be mentioned:

- Inspection data may (in part) be of questionable quality and therefore not suitable for systematic documentation.
- Only in rare cases are inspection data useful for a quantitative analysis.
- The integration of alternative inspection techniques into life cycle assessment efforts is problematical.
- Quantitative information on the effectiveness of various inspection techniques is not available.
- The translation of the inspection results into the optimization of maintenance and repair work is, in the best case, performed via modelling with random variables.
- Only a very limited amount of structure specific inspection data suitable for any comprehensive evaluation is available.

Nevertheless, each inspection generates an extensive amount of documentation, most of which is, due to both format and nature of the generated data, unsuitable for aiding the decision making process regarding suitable measures. The main inspection of a newly constructed engineering structure will usually lead to unambiguous and useful results that are subject to time-dependent processes only to a very limited degree.

Nevertheless, the main inspection of an older structure delivers no more than a snapshot of the current structural condition, providing only limited insight about the temporal degradation processes, due to the fact that traditional visual inspection methods are not suited for this task.

This document is the intellectual property of the fib – International Federation for Structural Concrete. All rights reserved.
This PDF of fib Bulletin 86 is intended for use and/or distribution solely within fib National Member Groups.

The ultimate goal in developing optimized structure specific inspection programs is to provide the proprietors of infrastructures with effectual access to control data and to serviceable inspection data. It should be noted that the components of infrastructure buildings have prototypical characteristics regarding structural type, type of use, boundary conditions (composition of the ground), environmental influences (chloride contamination) and so on. It is the designer's responsibility to devise the complete structure with allowance for the varied demands placed on the structure throughout its planned life cycle.

The fact that current inspection methods used in main inspections exhibit a limited grasp of deterioration processes in their beginning stages further justifies the need for stochastic process modelling.

Efficient life cycle assessment methods are divided into the following stages:

1. Characterization of the initial deterioration profile on the basis of expert experience.
2. Specification of both inspection methods and inspection intervals for the identified deterioration profile.
3. Implementation of the chosen inspection method.
4. Adaptation of the deterioration profile according to the inspection results.
5. Specification of the succeeding inspection method and the next inspection interval.
6. Repetition of the sequence 1 to 5 over the complete life cycle of the structure.

This adaptive process makes it possible to optimize all conservation measures with regard to both time and method and consequently provides an essential basis for the decision making process. Preventive conservation methods are an integral part of the decision making cycle outlined above. All further conservation efforts are structure specific and will be initiated on the basis of the inspection results.

### 8.7.2 Gamma processes for describing the degradation properties

Degradations or deterioration processes within a structure can be described through non-negative and continuous functions. Stochastic deterioration processes of mechanical components are frequently calculated using gamma processes. The use of gamma processes for deterioration processes in engineering structures as well has been suggested by[550] and by[551].

### 8.7.3 Characteristics of stochastic processes

The reliability assessment of engineering structures such as bridges is based on the assumption of incomplete information about, for example, material properties, quality of implementation, stresses and other factors. As a result of this incompleteness of information, lifetime distributions – which are frequently derived from very small error rates – are often inconsistent and cannot be expressed unambiguously. Consequently, time dependent and highly uncertain properties and processes, as for example an average deterioration rate per time unit, are often captured through random values. Especially well-suited for this method is the class of Markov processes (see Chapter 6.6.3), i.e. stochastic processes with independent development increments. Markov processes can be divided into discrete and continuous processes, as for example Brownian motion with drift, or Poisson, Levy and Gamma processes. In general, discrete stochastic models are not suited for capturing

This document is the intellectual property of the fib – International Federation for Structural Concrete. All rights reserved.
This PDF of fib Bulletin 86 is intended for use and/or distribution solely within fib National Member Groups.

deterioration processes in engineering. Continuous gamma processes are generally much better suited for this task. [551] demonstrated the suitability of gamma processes for mapping continuous stochastic processes, capturing the gradual accumulation of deterioration in small increments over time. The positive development increments can be determined using gamma distribution with identical standard parameters and temporal side actions. Using this type of process, it is possible to particularly determine: wear and tear, material fatigue, creep, crack formation, corrosion and similar phenomena. Furthermore, gamma processes provide the advantage of a relatively straightforward mathematical description.

In the first step of the gamma process model, the random variable $X$ of the gamma distribution, which is characterized by the shape parameter $\alpha > 0$ and the scale parameter $\beta > 0$, is defined as follows:

$$Ga\left(x\middle|\alpha,\beta\right) = \frac{\beta^{\alpha}}{\Gamma(\alpha)} x^{\alpha-1} \cdot \exp\left(-\beta \cdot x\right) \tag{8-33}$$

where

$$\Gamma(\alpha) = \int_{z=0}^{\infty} z^{\alpha-1} \cdot e^{-z} \cdot dz \tag{8-34}$$

is the gamma function for $\alpha > 0$.

## 8.7.4 Modelling of gamma processes

The gamma process distributions Ga are independent from each other for different, temporally variable $\alpha(t)$. Consequently, it is possible to design, purely on the basis of the current observation, the conditional distribution of the variable $X$. This property is very well suited for mapping deterioration processes in common engineering structures. However, when using this type of forecast model, it is necessary to consider not only current observations, but also past events that have caused the current status. In other words, historical deterioration profiles need to be integrated into such forecast models.

The shape parameter $\alpha(t)$ mentioned above is a constantly increasing, right-sided, real-valued function for $t \geq 0$ where $\alpha(0) = 0$. The gamma process with the shape function $\alpha(t) > 0$ and the scale parameter $\beta > 0$ is a continuous stochastic process {X(t), t ≥ 0} with the following properties:

$$P\left(X(0) = 0\right) = 1 \tag{8-35}$$

and

$$X(\eta) - X(t) = Ga\left(\alpha(\eta) - \alpha(t), \beta\right) \tag{8-36}$$

for

$\eta > t \geq 0$

where $X(t)$ is characterized by independent increments. Consequently, the probability density function of $X(t)$ with the time variable t follows the gamma process below:

$$f_{X(t)}(x) = Ga\left(x, \alpha(t), \beta\right) \tag{8-37}$$

This document is the intellectual property of the fib – International Federation for Structural Concrete. All rights reserved.
This PDF of fib Bulletin 86 is intended for use and/or distribution solely within fib National Member Groups.

The attendant expected value therefore becomes:

$$E\left(X(t)\right) = \frac{\alpha(t)}{\beta} \tag{8-38}$$

while the variance is:

$$Var\left(X(t)\right) = \frac{\alpha(t)}{\beta^2} \tag{8-39}$$

The temporally mutable variation coefficient is derived from the relation between the standard deviation and the median value as follows:

$$COV\left(X(t)\right) = \frac{\sqrt{Var\left(X(t)\right)}}{E\left(X(t)\right)} = \frac{1}{\sqrt{\alpha(t)}} \tag{8-40}$$

### 8.7.5 Application of gamma processes for deterioration processes

For gamma deterioration processes, the following power law approach is particularly well suited to derive the shape function $\alpha(t)$:

$$\alpha(t) = c \cdot t^b \tag{8-41}$$

This is a standard formulation which, according to[552], takes for example linear form ($b$ = 1) for the corrosion of the steel supports within reinforced concrete structural components, a parabolic form ($b$ = 2) for sulphate corrosives and a square root form ($b$ = 0.5) for ageing processes caused by diffusion. The deterioration rate for $X(t)$ at time $t$, where $t \geq 0$, can therefore be expressed in a simplified form with the shape function $\alpha(t) = c \cdot t^b$ and the scale parameter $\beta$. In engineering, the form of the expected deterioration is known in most cases, and b is considered to be constant[306]. However, c and $\beta$ remain unknown and need to be determined by either expert judgment or statistical information. The three most common methods to determine those parameters are the maximum likelihood method, the statistical moment method and Bayes statistics[551]. Determining the parameters of the basic population via the statistical moments of the samples is the easiest way and usually provides very good results in a first approximation. Provided that the main parameters of the expected value and of the variance of the cumulative deterioration at time $t$ are known, the non-stationary gamma process can easily be transformed into a stationary gamma process. This is achieved by a monotonic transformation of the real time into a standardized time period[551] as follows:

$$z(t) = t^b \cdot t(z) = z^{\frac{1}{b}} \tag{8-42}$$

The expected value therefore becomes:

$$E\left(X\left(t(z)\right)\right) = \frac{c \cdot z}{\beta} \tag{8-43}$$

and the equation for variance is written as follows:

$$Var\left(X(t)\right) = \frac{c \cdot z}{\beta^2} \tag{8-44}$$

The transformation of the inspection intervals can be performed in a similar way: $z_i = t_i^b$ for $I = 1, \ldots, n$. For the inspection interval between two inspection dates, this will be:

This document is the intellectual property of the fib – International Federation for Structural Concrete. All rights reserved.
This PDF of fib Bulletin 86 is intended for use and/or distribution solely within fib National Member Groups.

$$w_i = t_i^b - t_{i-1}^b \tag{8-45}$$

and

$$\gamma_i = X_i - X_{i-1} \tag{8-46}$$

as proposed by[553]. The deterioration increments $\gamma_i$ are approximately gamma distributed with a shape factor $c \cdot w_i$ and a scale factor $\beta$ for all $I = 1,2, \ldots, n$. Van Noortwijk suggests the method of moments for estimating parameters $\hat{c}$ and $\hat{\beta}$ using the following formulation:

$$\frac{\hat{c}}{\hat{\beta}} = \frac{\sum_{i=1}^{n} \gamma_i}{\sum_{i=1}^{n} w_i} = \frac{x_n}{t_n^b} \tag{8-47}$$

or with

$$\frac{\hat{c}}{\hat{\beta}} = \bar{\gamma} \cdot \frac{x_n}{\hat{\beta}} \left( 1 - \frac{\sum_{i=1}^{n} w_i^2}{\left[ \sum_{i=1}^{n} w_i \right]^2} \right) = \sum_{i=1}^{n} \left( \gamma_i - \bar{\gamma} \cdot w_i \right)^2 \tag{8-48}$$

The method of moments leads to simplified formulations for parameter assessment and can provide first approximations for the probability equations. The intervals $w_i$ are intervals between the main inspections and may relate to shorter or longer periods of time. This is of special interest for choosing the most suitable inspection methods and inspection intervals. As outlined above, gamma processes are very well suited for characterizing and collecting information e.g. from inspections and monitoring, but also for analysing mechanical changes within the structure.

One example: Over a longer period of time, a gradual reduction in cross-section caused by corrosion was observed in the reinforcing bars of the road surface of a reinforced concrete bridge. The progression of the corrosion and the corrosion model (as shown in Table 8-1) are based on empirical studies[550]. The represented inspection dates were chosen at random.

Table 8-1 Simplified empirical corrosion model (according to 554).

| Inspection date [year] | Corrosion rate [mm/a] | $A_{before}$ [mm²] | $A_{after}$ [mm²] | $A_{corr}$ [mm²] |
|---|---|---|---|---|
| 0 | 0 | 201 | 201 | 0 |
| 9 | 3 | 201 | 174 | 27 |
| 13 | 2.3 | 174 | 165 | 36.2 |
| 17 | 2 | 165 | 157 | 44.2 |
| 21 | 1 | 157 | 153 | 48.2 |

$A_{before}$ area of the cross section at the beginning of the respective inspection interval

$A_{after}$ area of the cross section that has been reduced due to corrosion, at the time of inspection

$A_{corr}$ accumulated area that has been lost to corrosion

The gamma process parameters which were determined using the statistical moment method outlined above are shown in Table 8-2.

This document is the intellectual property of the fib – International Federation for Structural Concrete. All rights reserved.
This PDF of fib Bulletin 86 is intended for use and/or distribution solely within fib National Member Groups.

Table 8-2 Parameters for the gamma process characterization

| Age [years] | $w_i$ [year] | $x_i$ [%] | $\gamma_i$ [%] |
|---|---|---|---|
| 0 | - | 0 | - |
| 9 | 9 | 13.4 | 13.4 |
| 13 | 4 | 18 | 5.2 |
| 17 | 4 | 22 | 4.8 |
| 21 | 4 | 24 | 2.6 |

Table 8-1 shows the gamma process parameters at different inspection dates, as determined on the basis of Table 8-2.

Table 8-3 Gamma process parameters for defined inspection dates

| Time | $\beta$ | $C$ | $\alpha(t)$ |
|---|---|---|---|
| 0 | - | - | - |
| 9 | $\beta_{expj}$ | $c_{expj}$ | $\alpha(t)_{expj}$ |
| 13 | 14.3 | 20.5 | 2.665 |
| 17 | 8.45 | 11.57 | 1.966 |
| 21 | 1.72 | 2.13 | 0.447 |

It should be noted that the parameters of the first years were not determined on the basis of the first inspection but by expert judgment (Index expj for expert judgment), since there are limitations to the applicability of the method of moments. The reduction in cross section on the basis of the gamma process based inspection performed in year 13 is shown in.

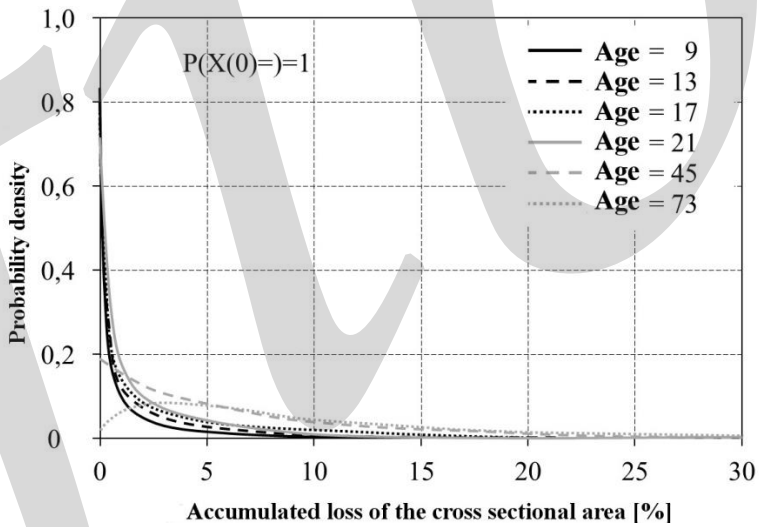


Fig. 8-7 Reduction of the rebar cross section over time, in form of a gamma process representation based on the inspection in year 13

Due to the reduction in cross section, the curves are positive and asymmetrical. The specification of "age" refers to the time period of the current inspection year (13). The forecasts for the reduction in cross section between the time intervals are non-negative. Fig. 8-8 shows the forecast based on the inspection in year 21.

This document is the intellectual property of the fib – International Federation for Structural Concrete. All rights reserved.
This PDF of fib Bulletin 86 is intended for use and/or distribution solely within fib National Member Groups.

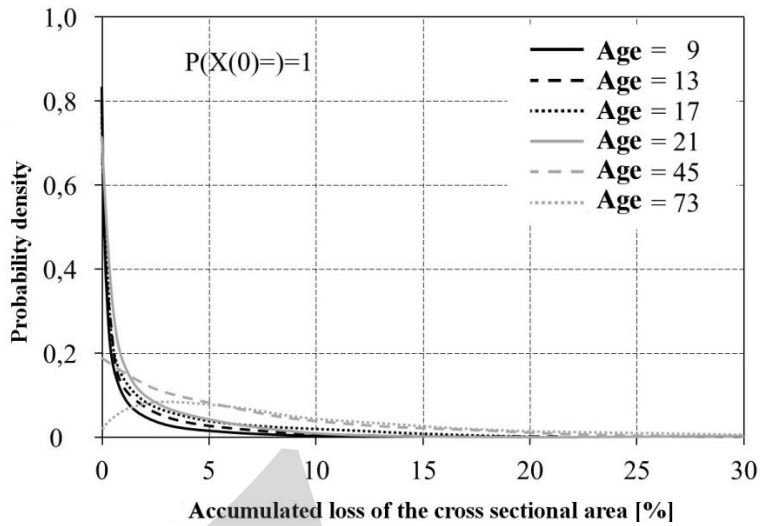


Fig. 8-8 Reduction of the rebar cross section over time, in form of a gamma process representation based on the inspection in year 21

Since the prognoses are independent, it is also possible to adequately take into consideration any repair works performed.

## 8.7.6 Selection of inspection methods

A suitable method for a sensible sequence of inspections is the selection of suitable inspection methods and their local application on the structure as appropriate. The inspection methods are characterized by their specific costs and assessment criteria.

The determination of suitable inspection methods enable the proprietors of the structure to make informed decisions about sensible inspection sequences and also about the use of more expensive inspection methods (that may provide e.g. information about damage detection probability) and also over longer periods of time. The optimization of costs incurred by inspections, conservation measures and damage repair can be seen as the rational basis for the decision-making process.

The density distribution functions shown in Fig. 8-9 for the time periods T1 and T2 enable the characterization of a quantitative value for the deterioration over a certain period of time which is essential for the owner.

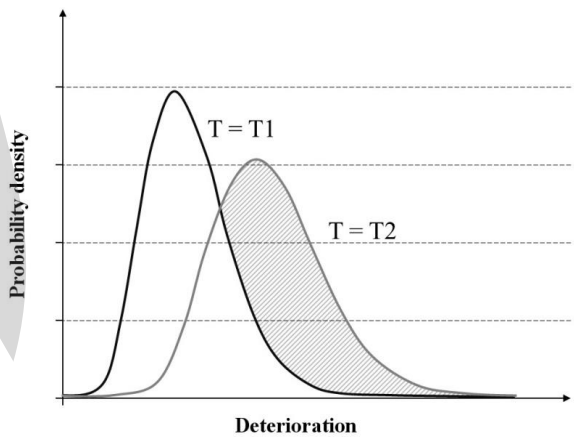


Fig. 8-9 Accumulated reduction of the cross section of the rebar, in form of a gamma modelling

*This document is the intellectual property of the fib – International Federation for Structural Concrete. All rights reserved.*
*This PDF of fib Bulletin 86 is intended for use and/or distribution solely within fib National Member Groups.*

The accumulated degree of deterioration as shown in Fig. 8-9[553] (shaded in grey) can be estimated via the standardized formulations[553]. These estimates (which relate to certain intervals) provide the means for determining suitable inspection methods and inspection intervals.

- Other prediction methods
- Continuous State Degradation Models
- Elementary Damage Models
- Shock Models with Damage Accumulation
- Models for Progressive Deterioration
- Approximations to Continuous Degradation Via Jump Processes
- Increasing Degradation Models
- Damage Accumulation with Annealing
- Models with Correlated Shock Sizes and Shock Times

Discrete State Degradation Models

- Discrete Time Markov Chains
- Continuous Time Markov Chains
- Markov Renewal Processes and Semi-Markov Processes
- Phase-Type Distributions
- Numerical Considerations for PH Distributions
- Phase-Type Distributions for Modelling Degradation

Generalized Approach to Degradation

- Lévy Process
- Modelling Degradation via Subordinators

Above shown methods are topics treated in Task Group 3.3 and Task Group 8.4 of the *fib*.

*This document is the intellectual property of the fib – International Federation for Structural Concrete. All rights reserved.*
*This PDF of fib Bulletin 86 is intended for use and/or distribution solely within fib National Member Groups.*

# 9. Probabilistic based models for material degradation processes

## 9.1 Introduction

Safety and economy have to be ensured for a structure during its service life. From this emerges the necessity for:

- A reliability assessment technique for newly designed as well as existing structures (i.e. an assessment of a design or residual reliability level);
- The design of structures for durability;
- Instruments for balancing service life vs. initial costs, maintenance and repair costs.

Time is the decisive variable and the durability issues are pronounced. This is clearly reflected also in recent standardization activities where design for durability is dealt with:

- ISO 13823 (2008) "General Principles on the Design of Structures for Durability"[555] – the objectives of this standard are (i) to improve the evaluation and design of structures for durability by the incorporation of building science principles into structural engineering practice, and (ii) to provide a framework for the development and employment of mathematical models to predict the service life of components of a structure from any type of material (these models are material dependent and therefore are not encompassed in this standard); the limit state method for durability assessment is introduced.
- ISO 16204 (2012) 36: Durability – Service life design of concrete structure. This represents the implementation of fib MC 2010 recommendations.
- the *fib* Model Code 2010 236: In chapter 5 about maintenance and condition control following levels are distinguished:
    1. The full probabilistic approach;
    2. The partial safety factor approach;
    3. The deemed–to-satisfy approach; and
    4. avoidance-of-deterioration.
- *fib* Bulletin 34[556]: Model code for service life design. The document is based on probabilistic approaches and introduce the design of structures for durability – i.e. a time-dependent limit state approach with service life consideration.

In chapter 9 the following deterioration mechanisms are treated:

- Carbonation–induced corrosion,
- Chloride–induced corrosion, and,
- Freeze-thaw attack with or without de-icing agents.

Predictive models are needed to estimate how resistance (and/or loads) will change over time. The text of this chapter is based on the above-mentioned codes and is focused on the enhancement of information by dealing with the broader variety of deterioration

This document is the intellectual property of the fib – International Federation for Structural Concrete. All rights reserved.
This PDF of fib Bulletin 86 is intended for use and/or distribution solely within fib National Member Groups.

effects and appropriate models to enhance effective design practice. The choice of models is useful in many design situations, e.g. due to problems with the availability of statistical data or the testing method for the input variables of each model, and/or the authenticity of the model when using the available data in relation to the required design accuracy level.

The utilization of design for durability may bring positive economical and sustainability impacts. It should be noted that the level of reliability in the context of durability should be left to the client's decision as well as the choice of appropriate serviceability criteria; unfortunately there is a lack of recognition from investors in this respect, in spite of the fact that the mutual impact of these values on the cost of the project may be crucial. Thus, the durability and reliability issues should be addressed during the design process and discussed with the client; the application of a performance-based approach is advocated. Broad utilization of such an approach is, unfortunately, still prevented by the insufficient dissemination of basic ideas, relevant knowledge or by the lack of relevant experimental test methods and suitable models and of efficient and user-friendly design instruments (software and other). The present chapter may be viewed as an attempt to overcome this barrier.

## 9.2 Degradation and limit states

### 9.2.1 Limit states: General

Reinforced concrete is a durable and widely used construction material. Despite the fact that the majority of reinforced concrete structures show good long-term performance and high durability, there are still a large number of failures of these structures. When considering the Limit States (LS) caused by the degradation of reinforced concrete structures, four kinds of attack may be distinguished:

(i) mechanical (mechanical load – static or dynamic),

(ii) chemical (carbonation, chloride and acid attack, alkali-aggregate reaction),

(iii) electrochemical (corrosion of reinforcement) and

(iv) physical (freeze-thaw, abrasion, fire and others).

The present chapter focuses on cases (ii) - (iv); case (i) is treated in Chapts. 1 to 4 of this bulletin. Owing to either carbonation of the concrete or the ingress of chlorides into the concrete, depassivation of reinforcing steel occurs leading to steel corrosion. For the purposes of durability assessment usually the initiation period (depassivation of the reinforcement's surface) and the propagation period of the corrosion process are distinguished. These periods (see Fig. 9-1 and in more details Fig. 9-3), i.e. the description of relevant LS and degradation models are dealt with in the present as well as in the following sections.

This document is the intellectual property of the fib – International Federation for Structural Concrete. All rights reserved.
This PDF of fib Bulletin 86 is intended for use and/or distribution solely within fib National Member Groups.

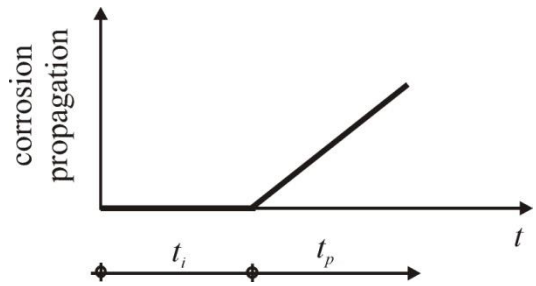


Fig. 9-1 Exposition time periods

Modelling of degradation processes may be based on different levels of sophistication:

(i) macro-level;

(ii) meso-level (simplified models, probabilistic approach);

(iii) micro-level.

The (i)-level is the most simple, often called the "deemed-to-satisfy" set of rules and is not suitable for the direct design/assessment of a specified service life with a specified reliability level. In some countries (e.g. Norway) these deemed-to-satisfy provisions are probability based. In the present revision of the European concrete standards (EN 1992/ EN 13670/EN 206) the procedure to derive the deemed-to-satisfy provisions are also according to ISO 16204[36], *fib* MC 2010[236], *fib* Service life design[556].

The (ii)-level comprises simple models (often semi-empirical), verified by comparison with the results of testing under experimental and real conditions. The variables may be treated as random quantities, and therefore the outputs are also capable of expressing statistical and probabilistic quality with respect to time evolution (service life assessment). In the present work this level is dealt with.

The (iii)-level is the most refined; the models are complex and are developed making use of fundamental physical laws and often constitutive laws of mechanics, thus leading to the problem of needing to solve partial differential equations. This level of sophistication is not suitable for everyday design practice.

LS have been incorporated in the basic approach utilized for structural design all over the world during the last few decades – see also the current codes of practice, e.g. ISO 2394[30], EN 1990[40]. The Ultimate Limit State (ULS) and the Serviceability Limit State (SLS) are assessed while designing/assessing a concrete structure. The general condition for the probability of failure $P_f$ reads:

$$P_f = P(A \geq B) \leq P_d \tag{9-1}$$

where $A$ is the action effect, $B$ is the barrier and $P_a$ is the design (acceptable, target) probability value. The index of reliability $\beta$ is alternatively utilized instead of the probability of failure in practice; both these quantities are interconnected by the transformation rule:

$$\beta = -\Phi^{-1}\left(P_f\right) \tag{9-2}$$

where $\Phi$ is the cumulative distribution function of the standardized Normal distribution.

Generally, both $A$ and $B$ (and hence the $P_f$) are time dependent; this has not been considered for common cases of ULS or SLS in design practice very frequently up to now. Two exceptions have to be mentioned: (i) fatigue limit states – in this case (presumably

This document is the intellectual property of the fib – International Federation for Structural Concrete. All rights reserved.
This PDF of fib Bulletin 86 is intended for use and/or distribution solely within fib National Member Groups.

ULS) the time domain is usually transformed into a number of load cycles and (ii) creep and shrinkage effects – time-dependent special issues that mostly concern concrete structures, do not usually affect ULS and are not related to durability. It should be noted that the reliability approach (and hence the design process) has to cover safety (ULS), serviceability (SLS) and durability – see EN 1990[40]. Durability is related to the design working life (or service life). The most generally used design method – the partial safety factor method – does not assess the reliability level directly, i.e. it does not arrive at a specified value of relevant reliability level and is not suitable for service life assessment. This situation can be amended by utilization of the full probabilistic approach (which is legally applicable according to both documents EN 1990[40] and ISO 2394[30], but is not yet commonly accepted in practice). This approach is described in the present work.

### 9.2.2 Design for durability

Two safety formats for service life design (or durability design) may be considered: Service life format and Limit state format.

The service life format consists of considering a design service life $t_D$ of the component or structure and assessing the predicted service life $t_{PS}$ which shall meet or exceed the design life, i.e.:

$$t_{PS} \geq t_D \tag{9-3}$$

Within the probability framework: the probability of failure $P_f$ is determined and compared to a specified design (target, acceptable) probability $P_d$:

$$P_f(t_D) = P\left\{t_{PS}\left(X_i, t\right) \leq t_D\right\} \leq P_d \tag{9-4}$$

$t_{PS}$ is the predicted value modeled as a function of the basic variables $X_i$ ($i = 1,2,...,n$) and time $t$;$n$ is the number of input parameters involved in the model in question. However, in both *fib*[556] and ISO 13823[555] the partial safety factor approach is described, too.

In the case where a structural component is protected against degrading agents (e.g. concrete covering reinforcement, a coating of steel or others), $t_{PS}$ can be determined as the sum of two service-life predictors:

$$t_{PS} = t_i + t_P \tag{9-5}$$

where $t_i$ is the time to the initiation of degradation (initiation period) and is modelled as a function of the basic variables for degradation agent transfer, $X_i$ and time $t$. Time $t_p$ is the service life after the initiation of degradation (often called the propagation period) and is a function of those basic variables which describe the damage or resistance. Basically, the variables $X_i$ are random variables (or random fields; some of them might be treated as deterministic values in certain situations).

It should be recognised that the service life $t_{PS}$ can be considered as a random variable having its own PDF.

The basic requirement of the limit state format for the ULS during the design life $t_D$ is:

$$R\left(t_D\right) \geq S\left(t_D\right) \tag{9-6}$$

where $R(t_D)$ is the resistance capacity of the structural component at the design life $t_D$ and represents the barrier $B$. $S(t_D)$ represents a cumulative degradation of the component at the

*This document is the intellectual property of the fib – International Federation for Structural Concrete. All rights reserved.*
*This PDF of fib Bulletin 86 is intended for use and/or distribution solely within fib National Member Groups.*

design life ($t_D$ or in other words the action $A$ of "environmental load". Both, $R(t)$ and $S(t)$ may be modelled as a function of basic variables $X_i$ and $t$. The LS condition in Eq. (9-6) is verified by checking that:

$$P_f\left(t_D\right) = P\left\{R\left(t_D\right) - S\left(t_D\right) \leq 0\right\} \leq P_d \tag{9-7}$$

Either the resistance $R$ or the load action $S$ or both can be time-dependent quantities. Thus, the failure probability is also a time-dependent quantity. The above formulation applies to material deterioration and deformation which is cumulative and applies in cases where the functions $R$ and $S$ are considered to be monotonous, which is a prevailing situation in concrete structures. The basic requirement for the LS during the design life of the component $t_D$ is:

$$S\left(t_D\right) \leq S_{\lim} \tag{9-8}$$

where $S_{\lim}$ represents the limit value. The Eq. (9-8) is again verified by checking the condition Eq. (9-7) and interchanging $R(t_D) \rightarrow S_{\lim}$. In some design strategies it might be advisable to use a conservatively defined limit state by simplifying the Eq. (9-5) into the form:

$$t_{PS} = t_i \tag{9-9}$$

This kind of limit state precedes the occurrence of other SLS or ULS and represents a simplified limit state aimed at the prevention of the onset of deterioration. Such a LS belongs to a more general category - Durability limit states (DLS), which are dealt with in Section 9.2.3 in more detail and which may serve in the optimization of the service life (or assessment of the residual service life). Such LS are also dealt with in both documents ISO 13823[555] and *fib*[236,556]. Note: the determination of $t_{PS}$, $R(t_D)$, $S(t_D)$ and $P_f(t_D)$ requires the utilization of suitable and well verified models of degradation processes. Some appropriate models for concrete structures are described in 9.4.

To accomplish the time-dependent limit state evaluation successfully, the utilization of a suitable stochastic approach is necessary: a combination of analytical models and simulation techniques providing statistical and sensitivity analyses as well as reliability level assessment. Evidently, some efficient and specialized software tools are needed – some are briefly described in 9.5.

### 9.2.3 Durability limit states

The service life of a building or structure is determined by its design, construction, ageing and maintenance during use. While assessing the service life, the combined effect of both structural performance and ageing should be considered.

As mentioned above, structural design based on current building codes deals with ULS and SLS. A new category of LS – the DLS has been introduced. DLS may be formally regarded as belonging in the SLS category (or rarely in the ULS category).

As stated in the basic design code EN 1990[557], the recommended value of the reliability index for SLS (irreversible state) is 1.5, which is relevant to a 50-year design service life. It should be noted that the values of $0.8 < \beta_d < 1.5$ for the DLS are currently under discussion (e.g. the recommendation of the *fib* Model Code[236] reads $\beta_d = 1.5$). The level of reliability in the context of durability should be left to the client's decision together with the target service life. When considering the degradation of reinforced concrete structures, the corrosion of reinforcement is the dominating effect.

This document is the intellectual property of the fib – International Federation for Structural Concrete. All rights reserved.
This PDF of fib Bulletin 86 is intended for use and/or distribution solely within fib National Member Groups.

Different aggressive agents affect the structural material during the service life. In 9.3 the degradation effects are briefly described; some analytical models are shown in 9.4. In the following the probability limit conditions relevant to concrete structures are introduced. In the context of the initiation period only one DLS can be recognised/defined: depassivation of reinforcement due to carbonation or chloride penetration creating the possible starting point for reinforcement corrosion.

## 9.2.4 Initiation period

### 9.2.4.1 Carbonation

The durability-oriented limit state condition Eq. (9-7) specialized for the case of carbonation may be written as:

$$P_f\left(t_D\right) = P\left\{a - x_c\left(t_D\right) \le 0\right\} \le P_d \tag{9-10}$$

where a is the concrete cover and $x_c$ is the depth of carbonation at time $t_D$ - design service life. Note that the carbonation process is driven by the diffusivity of $CO_2$ in concrete and the reactivity of $CO_2$ with concrete. The main factors affecting concrete carbonation are the type and content of binder, the water-binder ratio, the degree of hydration, the concentration of $CO_2$ and the relative humidity.

The measurements of $CO_2$ concentration are seldom reported and rarely based on continuous monitoring. They are more likely to be recorded in non-urban (remote) environments so as to monitor the background level of $CO_2$ concentrations needed to help assess the magnitude of "global warming". Therefore, it might be useful to report on actual $CO_2$ measurements recorded by the metrological station of BUT Brno, Civil Engineering Faculty, in an urban environment, i.e. the industrial city of Brno in the Czech Republic, representing thus a typical urban location in Central Europe. From the measured data collected from 1999 to 2005 the minimum hourly $CO_2$ concentration is 682 mg/m$^3$ and the maximum recorded value 1650 mg/m$^3$. A steady increase has been encountered as shown in Fig. 9-2 (approximately 19 mg/m$^3$ yearly). A daily average $CO_2$ concentration at about 840 mg/m$^3$ was found at this location in the year 2006.

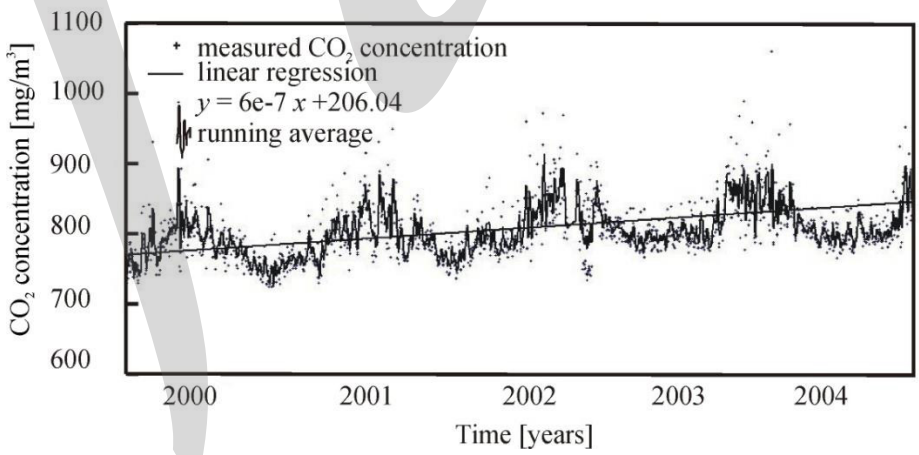


Fig. 9-2 Measurement of carbon dioxide in Brno, Czech Republic (1999-2005), daily at 3p.m.GMT

*This document is the intellectual property of the fib – International Federation for Structural Concrete. All rights reserved.*
*This PDF of fib Bulletin 86 is intended for use and/or distribution solely within fib National Member Groups.*

Considering chloride ingress (e.g. due to de-icing salts) we arrive at the formula:

$$P_f\left(t_D\right) = P\left\{C_{cr} - C_a\left(t_D\right) \le 0\right\} \le P_d \tag{9-11}$$

where $C_{cr}$ is a critical concentration of dissolved Cl- leading to steel depassivation and $C_a$ is a concentration of Cl- at the reinforcement at time $t_D$. The limit conditions, Eq. (9-10) and Eq. (9-11), represent the initiation period limits and are - in the sense of degradation - conservative limits; they describe a situation where corrosion has not propagated yet. Typically, these conditions fall into the DLS category.

The relevant values of variables $x_c$, $C_a$ (which are random quantities) are to be assessed by utilization of a suitable degradation model.

Note: In the region of cracks, carbonation and chlorides can penetrate faster; conversely, in the case of crack widths of up to 0.4 mm a certain degree of 'self-healing' due to dirt and rust deposits tends to diminish the reinforcement corrosion. Due to this, longitudinal cracks and/or the concrete cracking on horizontal surfaces directly affected by chloride-contaminated water (de-icing salts) may be more harmful.

## 9.2.5 Propagation period

Concentrating on reinforcing bar corrosion several LS may be specified:

### 9.2.5.1 Concrete cracking due to reinforcement corrosion

Once the corrosion of reinforcement starts (after depassivation), its degradation effects take place. The rate of steel corrosion is governed by (among other factors) the availability of water and oxygen. Also, the presence of chlorides in the concrete surrounding the steel bars, humidity and temperature may influence the corrosion. The volume expansion of rust products develops tensile stresses in the surrounding concrete leading to the delaminating of concrete cover. The relevant limit condition (DLS) may be constructed either with the tensile stress limit or the crack width limit:

$$P_f\left(t_D\right) = P\left\{\sigma_{cr} - \sigma\left(t_D\right) \le 0\right\} \le P_d \tag{9-12}$$

$$P_f\left(t_D\right) = P\left\{w_{cr} - w_a\left(t_D\right) \le 0\right\} \le P_d \tag{9-13}$$

where $\sigma_{cr}$ is a critical tensile stress that initiates a crack in concrete (on an interface with a reinforcing bar), $\sigma$ is a tensile stress in concrete at the end of the design service life $t_D$, $w_{cr}$ is a critical crack width on the concrete surface and $w_a$ is a crack width on the concrete surface generated by reinforcement corrosion at time $t_D$. Eq. (9-12) is typically a DLS, while Eq. (9-13) is either a DLS or an SLS depending on the $w_{cr}$ value. Note that the exceeding of $w_{cr}$ or $\sigma_{cr}$ depends not only on structural degradation caused by the corrosion of reinforcement but also may co-act with a stress field developed due to other acting loads depending on the type of structure and its configuration.

### 9.2.5.2 Spalling of concrete

When the corrosion progress and consequently the crack opening continue, the spalling of concrete cover may occur. Such a state is either an SLS or an ULS – depending on the location, the severity of this effect, and on the structure's configuration.

This document is the intellectual property of the fib – International Federation for Structural Concrete. All rights reserved.
This PDF of fib Bulletin 86 is intended for use and/or distribution solely within fib National Member Groups.

### 9.2.5.3 Loss of reinforcement

A decrease in the effective reinforcement cross-section due to the corrosion, leading to excessive deformation, loss of bearing capacity and finally to collapse, may fall into the SLS (deformation capacity) or ULS (load bearing capacity) categories. The limit condition reads:

$$P_f\left(t_D\right) = P\left\{A\left(t_D\right) - A_{\min} \le 0\right\} \le P_d \tag{9-14}$$

where $A$ is the reinforcement cross-sectional area at time $t_D$ and $A_{\min}$ is the minimum acceptable reinforcement cross-sectional area with regard to either SLS or ULS. Both pitting and/or a uniform type of corrosion may be considered while evaluating the Eq. (9-14).

A sketch depicting the sequence along the time axis of the above-mentioned LS together with the indicative values of reliability index is shown on Fig. 9-2 (which is a more detailed version of Fig. 9-1).

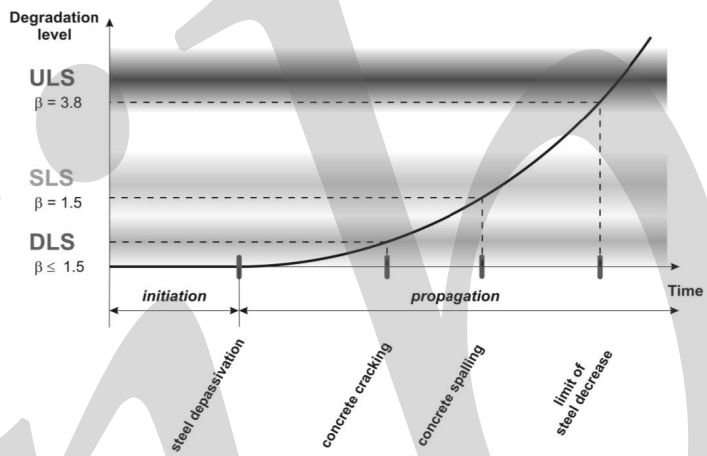


Fig. 9-3 Limit states along the time axis

### 9.2.5.4 Stress corrosion cracking

Special corrosion problems may arise in older bridge structures with quenched and tempered prestressing wires that are sensitive to hydrogen-induced stress corrosion cracking (SCC). The underlying mechanisms of SCC are yet to be fully understood as it depends upon complex chemical and mechanical interactions. Furthermore, in such cases there are large uncertainties related to the deterioration of the materials and the parameters describing the materials' behaviour and consequently the structural member's behaviour. In cases when the linear fracture mechanics approach by[558] is adopted, the limit state condition reads:

$$P_f\left(t_D\right) = P\left\{K_{SCC} - K_I\left(t_D\right) \le 0\right\} \le P_d \tag{9-15}$$

where $K_{SCC}$ is the steel fracture toughness – a material parameter, considered here as a limit value for stress corrosion development. It is supposed that when the equality $K_I = K_{SCC}$ is reached, the crack growth becomes unstable. Such a state can be either an SLS or an ULS. Due to the fact that pit geometry cannot be viewed as a crack, the approach presented in[558] is not realistic enough; as pointed in[559] the consideration of the loss of effective reinforcement area due to pitting and consequently the yielding of the wire may be a more realistic LS.

This document is the intellectual property of the fib – International Federation for Structural Concrete. All rights reserved.
This PDF of fib Bulletin 86 is intended for use and/or distribution solely within fib National Member Groups.

#### 9.2.5.5 Loss of bond

Due to reinforcement corrosion, bond capabilities are changed: during the beginning stage the bond capacity increases slightly, later it decreases. It would not be practical to construct a limit condition Eq. (9-7) considering bond capacity. Instead, the gradual decrease of bond due to the actual degree of rebar corrosion (time dependent) may be reflected in changes of bond stress-slip function and incorporated directly e.g. as in the NLFEM code while assessing the SLS or ULS of a structure in question. In this respect the "bond of corroded reinforcement" is not considered a DLS and it is mentioned here only for the sake of completeness. The bond stress-slip function influenced by corrosion has been shown e.g. by[560].

#### 9.2.5.6 Comments on modelling

Note1: When working with the above-listed limit states the relevant values of variables such as $\sigma$, $w_a$, $A$ and others (which are random quantities) are to be assessed by utilization of a suitable degradation model (9.4).

Note 2: Usually, single models can be used to construct different LS. In some cases LS have to be described by more than one model: a series of two or more models must be used considering the fact that some degradation processes may be subjected to the existence of a state described by another model. Thereby the consecutive model (in time) is conditional on the accomplishment of the previous one. For example, a limit state based on reinforcement corrosion described by a model (say model B) is dependent on the existence of depassivation, i.e. a limit state treated by model A. Such a sequence of models will be called "chained" models in the following text and may be assessed in one of the following ways:

- if the models A, B, etc. chained together are stochastically independent, the conditional probability (a total probability – product of individual probabilities) can be computed for different time steps. Then, the time (service life) relevant to acceptable reliability may be assessed too – for an application see[561];
- individual models' outputs are times (random variables) at which the particular limit is reached. Such a variable serves subsequently as an input for the consecutive model. This approach is applied in FReET-D software, see 9.5 of the present chapter; it has also been utilized in[562].

Note 3: When publishing Model Code 2010[236] , no models with broad international consensus were available for predicting the length of the corrosion period until cracking, spalling or collapse of the structure occurs. For this reason service life designs are normally done with the limit state of depassivation. The direct consequence of passing this limit state is only that possible future protective measures for repair become more expensive. This rather conservative limit state is therefore normally linked to a corresponding relaxed target reliability level for failing, often in the order of 10-1 to 10-2.

## 9.3 Deterioration of concrete structures

### 9.3.1 Carbonation

Carbonation of concrete is a chemical process in concrete driven by ambient $CO_2$ penetrating from the surface and decreasing pH to a value below 9. When the carbonation

*This document is the intellectual property of the fib – International Federation for Structural Concrete. All rights reserved.*
*This PDF of fib Bulletin 86 is intended for use and/or distribution solely within fib National Member Groups.*

depth equals the concrete cover, the steel is depassivated and corrosion may start (when oxygen and moisture is present). The rate of carbonation progress from the concrete surface to the reinforcement depends on many parameters, e.g. concrete cover thickness and permeability, the ambient temperature, relative humidity and carbon dioxide content, whereas the concrete cover permeability itself depends on the concrete mix type and composition, the aggregates' grading and the processing and curing of the concrete.

### 9.3.2 Chloride ion ingress

The source of chlorides in concrete may be internal (admixtures containing chloride) or more commonly external (de-icing salts or a marine environment) when the chlorides enter concrete from the outside. There are two main sources of chlorides: NaCl and $CaCl_2$. Chlorides supplied by the external environment dissolve in water in the pore system of the concrete and penetrate inwards mainly by diffusion in stationary pore water. In a structural element which is intermittently loaded with a chloride-contaminated solution, interrupted by dry periods of air storage during which the water in the concrete close to the surface evaporates, any subsequent re-wetting provokes a process of capillary suction of chloride-bearing water in the surface zone – see[556, 563]. This zone is usually referred to as the "convection zone". Compared to diffusion processes, capillary action leads to the rapid transport of chlorides into the concrete down to the depth of convection zone $\Delta x$, where the chlorides can accumulate over time until they create a saturation concentration, $C_{sat}$.

Not all of the chlorides in concrete are mobile and thus available for initiating or enhancing corrosion. Part of the chlorides dissolved in pore water chemically reacts with calcium aluminates and their hydration products (chemically bounded chlorides). Others are physically adsorbed on the constituents of hardened cement paste or on the surface of aggregate particles (physically bounded chlorides) – this binding is not permanent and the chlorides may be released again. Only free chlorides (dissolved in pore water) destroy the passive film of the steel rebar. and make corrosion attack possible as they reduce the pH of the pore water, decrease the solubility of $Ca(OH)_2$ and increase the electrical conductivity and the moisture content due the hygroscopic properties of chloride salts[563, 564].

The chloride threshold concentration may be presented by means of the total amount of chloride by weight of cement, the amount of free chloride, the concentration ratio of free chloride ions to hydroxyl ions or the ratio of acid-soluble chloride content and the acid neutralization capacity (the content of acid needed to reduce the pH of concrete and cement paste suspended in water to a particular value)[565]. In terms of currently used representations, the total chloride content related to the cement weight is considered the best alternative. This representation results in a reduction in the range of determined values of the critical chloride concentration and represents the total potential chloride aggressive ion content expressed relatively to the hydroxide ion content rising from hydrolysis of cement concentration ratio Cl-/OH-[419, 566, 421, 422].

The mean value of 0.6 [wt.- %/cem] of total chloride concentration (beta distribution, $s$ = 0.15, $a$ = 0.2 and $b$ = 2.0) are currently suggested as the chloride threshold concentration[566, 567] in the case of ordinary mild steel. The mean threshold value of free chlorides is lower, usually < 0.20.

Note: safe limit values of chloride content in concrete mixture are also presented in EN 206[568].

This document is the intellectual property of the fib – International Federation for Structural Concrete. All rights reserved.
This PDF of fib Bulletin 86 is intended for use and/or distribution solely within fib National Member Groups.

### 9.3.3 Corrosion

The most frequent type of degradation of reinforced concrete structures is probably the corrosion of steel reinforcement. Reinforcing bars are protected from corrosion by a thin oxide layer that forms on their surface due to the high alkalinity of the surrounding concrete (steel passivation). Corrosion may start when this layer is destroyed (steel depassivation).

The detrimental effect of corrosion is due to the fact that a rust product has a volume 2 - 6 times larger than the original steel. Consequently, it causes volume expansion, developing tensile stress in the surrounding concrete. Reinforcement corrosion takes place during the propagation period, and its rate is governed mainly by the availability of water and oxygen on the steel surface (e.g. in concrete permanently submerged in water no significant corrosion is likely due to the limited availability of oxygen). Due to corrosion, the effective area of the steel decreases and rust products grow, causing at a certain stage longitudinal cracking, and later, the spalling of concrete cover (delamination). Generally, two types of corrosion are distinguished: the uniform (or general) type and the pitting (localized) type of corrosion.

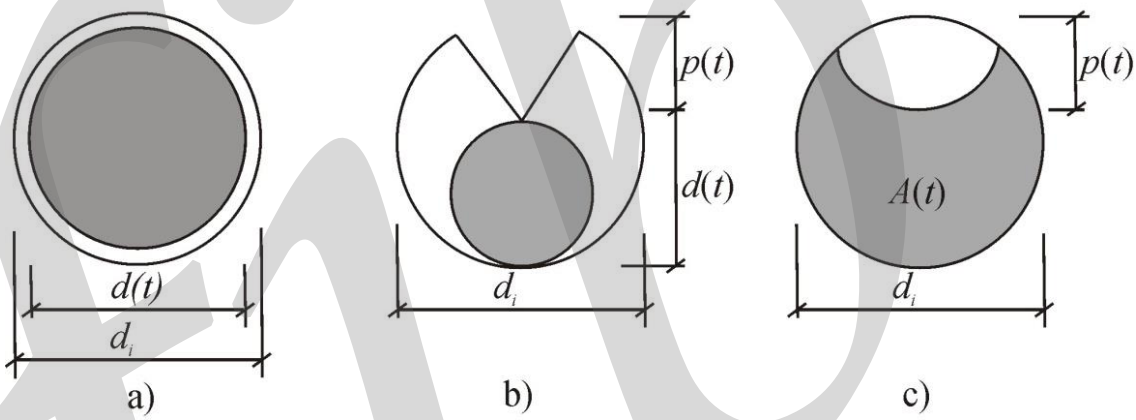


Fig. 9-4 Simplified geometries of corroded steel rebars: a) uniform corrosion[569]; b) pitting corrosion[569] and alternatively c) pitting corrosion[570]

Fig. 9-4 presents highly simplified geometries of corroded steel rebars. The uniform corrosion is however only on the part of the steel surface where the oxide layer is destroyed. The figure 9-4a is thus misleading as it represents the "final stage" - it is assumed that the corrosion is uniform around the perimeter of the rebar; this simplification is utilized in thick-wall cylinder model (Section 9.4.3). In reality, the oxide layer on the rebar surface closest to the concrete surface will start corroding certain time before the oxide layer at rear part of the rebar is destroyed.

### 9.3.4 Frost attack

The frost resistance of concrete is regarded as being a material property. Repeated freezing and thawing of concrete (freeze-thaw cycles) leads to the gradual weakening or disintegration of concrete structure (surface and/or internal parts). Water freezing in capillary pores increases in volume by about 9 %, micro-cracks may develop, and the strength of concrete and its E-modulus as well as other mechanical quantities may decrease/change.

This document is the intellectual property of the fib – International Federation for Structural Concrete. All rights reserved.
This PDF of fib Bulletin 86 is intended for use and/or distribution solely within fib National Member Groups.

The frost resistance of concrete depends on:

- pore structure (governed by w/c ratio, entrained air, curing, concrete composition, strength and other conditions);
- environmental conditions (de-icing salts and their concentrations, the frequency and duration of freeze-thaw cycles, temperature variations and extreme values).

Usually, two degradation mechanisms are distinguished:

- scaling of thin concrete surface layers (mainly in the presence of de-icing salts); depends on (among other variables) the number of freeze-thaw cycles. This deterioration is often measured by weighting (loss of mass);
- internal damage to concrete (loss of mechanical properties). The degree of such damage is usually expressed/measured by the relative dynamic modulus (as a % of the modulus of undamaged concrete) and depends mostly (apart from on the concrete's characteristics) on the extreme (minimum) temperature. The effect of freeze-thaw cycles is less pronounced.

Several freezing and thawing theories have been proposed, e.g. the theory of hydraulic pressure, the theory of osmotic pressure, micro-ice lens theory, the concept of a critical degree of saturation in freezing concrete and a theory based on thermodynamics[571, 572, 573].

The frost resistance problem is of a stochastic nature and differs from the majority of other deterioration effects due to the poorly-defined time functionality. E.g. considering the corrosion of reinforcement, increased exposure time causes increased damage up to a certain limit and to service life ending (a cumulative and monotonous effect). In contrast, with the frost damage problem, increased exposure time does not necessarily imply an increased risk of damage – a single occurrence of freezing with above-critical moisture content may cause severe damage; the occurrence of this dangerous situation is not necessarily a function of exposure time. It is perhaps possible to make a statement about service life with regard to the frost resistance of a given structure in a given environment when environmental characteristics are transformed into an internal moisture-time field in the structure. Such an approach is partially applied in *fib*[556]. The rational way to ensure a required service life is to design the pore structure of concrete in such a way that the probability of reaching the critical moisture level will be low. It may be achieved by air entrainment.

With regard to load-carrying capacity and deformations, the traditional design should include localized or global changes in mechanical properties due to frost damage, whenever applicable. As mentioned above, damage is usually described by the relative dynamic modulus; the functionality of the decrease of dynamic modulus regarding other mechanical properties involved in the structural design process (strength, fracture characteristics, Yang modulus) has not been investigated yet. Some experimental findings according to[574] are as follows (specimens with different w/c ratio; pre-saturated with moisture content above the critical, severe freeze-thaw, i.e. such conditions can be only rarely encountered in a real structure):

Cube compressive strength: Maximal strength reduction observed is 35 %. A regression analysis gives the following mean relation $f_{c,damaged} = 0.96 \cdot f_{c,0} - 9$, where $f_{c,damaged}$ is the compressive strength of frost damaged concrete [MPa] and $f_{c,0}$ is the compressive strength of undamaged concrete [MPa]. Thus, the mean loss in compressive strength is about 10 MPa.

*This document is the intellectual property of the fib – International Federation for Structural Concrete. All rights reserved.*
*This PDF of fib Bulletin 86 is intended for use and/or distribution solely within fib National Member Groups.*

Split tensile strength: Frost attack causes a more severe reduction in tensile strength than in compression (up to 70 %); the mean value determined by regression analysis is $1.2f_{t,0} - 3$, where $f_{t,0}$ is the split tensile strength for an undamaged specimen [MPa].

The mean relation between compressive and tensile strength is $\Delta f_t/f_{t,0} = 1.1 \cdot (\Delta f_c/f_{c,0}) + 29$ where $\Delta f_t/f_{t,0}$ is the relative change in split tensile strength [%] and $\Delta f_c/f_{c,0}$ is the relative change in compressive strength [%].

*Dynamic E-modulus*: No well-defined relation between the E-moduli for damaged and undamaged concrete is found; the decrease is rather severe – the lowest E-modulus measured is 5 GPa.

*Bond*: On average, 50 % of the bond strength is lost in the case of ribbed bars; for plain bars it is up to 90 %.

It appears the reduction of the mechanical characteristics of concrete due to frost under high humidity might be considerable.

### 9.3.5 Fire attack

Extensive research is being currently conducted into the fire safety of engineering structures including tunnels[575, 576, 577], infrastructure, bridges and viaducts, high-rise buildings, containment shells (in nuclear power plants and chemical plants), as well as airport runways ($t$ >150 ºC)[578], as they are at the risk of exposure to elevated temperatures.

In the case of concrete structures under extreme temperature conditions, attention must be paid to generally two types of concrete disintegration due to elevated temperature: (1) gradual degradation of material due to chemical and physical processes and (2) abrupt failure called explosive spalling caused by physical processes resulting in high pore pressures. The following text is focused on the gradual type of disintegration.

Heating temperatures influence the behaviour of concrete at different structural levels. At the micro and meso levels concrete exhibits physical and chemical changes which affect the behaviour on the macro level quantified e.g. by mechanical parameters such as compressive strength, tensile strength, modulus of elasticity, fracture energy, etc.

Various authors have described processes in cement paste and concrete subjected to high temperatures:

- 30-105 °C release of free and physically bound water[579]
- 110-170 °C decomposition of gypsum 579; 580, decomposition of ettringite[581] and dehydration of part of hydrated calcium aluminate [582]
- 180-300 °C dehydration and decomposition of CSH gel and hydrated calcium aluminate[583, 579, 584]
- 450-550 °C decomposition of portlandite[579, 580]
- 700-900 °C calcite decomposition[579, 585].

### 9.3.6 Alkali-aggregate reaction

The majority of aggregates used for concrete manufacturing are more or less chemically inert. However, some of them undergo reaction with the alkali hydroxides present in

This document is the intellectual property of the fib – International Federation for Structural Concrete. All rights reserved.
This PDF of fib Bulletin 86 is intended for use and/or distribution solely within fib National Member Groups.

concrete matrix. It leads to expansion and cracking. Two forms of alkali-aggregate reaction (AAR) exist – alkali-silica reaction (ASR) and alkali-carbonate reaction (ACR).

ASR occurs more often. In this case aggregates that contain certain amorphous forms of silica react with alkali cations and hydroxide ions from concrete pore solutions. This chemical reaction will produce alkali-silica gel. As the second step the expansion of the gel occurs due to moisture adsorption from the surrounding concrete matrix or the environment. The swelling of gels leads to major internal stress redistribution and thus the formation of cracks in the surrounding concrete and/or concrete spalling across critical joints.

To reduce ASR certain supplementary cementitious materials can be utilized – silica fume, fly ash or ground granulated blast-furnace slag.

ACR occurs with certain dolomitic rocks and is relatively rare. Dedolomitization and subsequent crystallization of brucite may lead to significant expansion.

It follows that especially structures with a very high moisture supply such as dams are jeopardized by this type of degradation.

## 9.4 Analytical models for degradation

In this section a brief review of some relevant and available analytical models for reinforced concrete degradation assessment and their partial evaluation are presented, focusing on simplification of modelling process.

Degradation models are time-dependent mathematical functions that show the average increase of degradation with time. These models are parameterized with several material, structural and environmental parameters. The main criteria in selecting the degradation model for each specific use are e. g.:

- type of relevant limit state and exposure conditions;
- availability of statistical data or the testing method for the variables of each model;
- accuracy of the model when using the available data in relation to the required design accuracy level.

Note 1: Recalling equations Eq. (9-2) to Eq. (9-14) it follows that in the model used the variables involved have to be treated in a statistical manner, i.e. the input as well as output quantities are to be random variables (or random fields).

Note 2: Performance-related methods for concrete specification may be based on the use of proven predictive models – see[586, 587].

Note 3: The models introduced in this Section are 1D type temporal models as they describe a time-dependent process merely in one location/point/direction - the only exception being the Cellular Automaton shown in 9.4.2 which represents a 2D description. For RC structures it is highly probable that the deterioration is distributed spatially (e.g. the characteristics of the processes causing the initiation and progress of reinforcement corrosion). The modelling of such effects has received the attention of researchers in recent years[588]. The spatial variability is modelled by identifying zones with common properties further subdivided into elements and their dependency structure (e.g. the correlation length of parameters governing the degradation process which are modelled

*This document is the intellectual property of the fib – International Federation for Structural Concrete. All rights reserved.*
*This PDF of fib Bulletin 86 is intended for use and/or distribution solely within fib National Member Groups.*

as random variables in temporal models; random fields are utilized for these purposes). Such an approach is highly involved and is not yet feasible in the design process. For a complex description and further references see[589].

Note 4: When modelling the deterioration effects or assessing the durability and safety issues in reliability-based methods the physical, statistical and model uncertainties have to be considered. The latter may be treated either by (i) introducing a factor of model uncertainty $\psi$ – a general multiplier provided as an input random variable (a recommendation of JCSS may be used: a two-parametric Lognormal PDF with a mean value of 1.0 and a standard deviation e.g. equal to 0.15), or, (ii) splitting the uncertainty representation into separate factors for capacity and loading description[590].

Note 5: Service life assessments which do not include the synergy between mechanical and environmental loading are neglecting a factor that can have a significant impact on structural safety[591,592]. In order to make service life design realistic it is necessary to consider both of these factors acting simultaneously. This chapter does not deal with such advanced modelling, albeit it is currently under the development[593].

Note 6: In the following some models taken from literature are represented. They are meant to be used for predictions of initiation period when designing new structures. Such use of modelling gives a much higher influence of model and data uncertainties than when using models for assessing service life of existing structures.

### 9.4.1 Carbonation

The mathematical models of concrete carbonation introduced in Table 9-1 are based on the diffusion of CO2 in the pore system of concrete, which can be derived from Fick's 2nd law:

$$\frac{\partial C}{\partial t} = D_{eff} \frac{\partial^2 C}{\partial x^2} \tag{9-16}$$

where $C$ is the concentration of the diffusing agent, $x$ is the distance from the concrete surface, $t$ is time and $D_{eff}$ is the diffusion coefficient, which depends on the properties of the concrete and the environment. The relationship between the carbonation depth $x_c$ and time $t$ can be generally expressed as:

$$x_c = A \cdot t^n \tag{9-17}$$

where parameter $A$ has the meaning of a diffusion coefficient and has to be determined either experimentally or by using the appropriate model; $n$ is a coefficient that may theoretically vary from 0 to 1. For the following models listed in Table 9-1 $n = 0.5$ applies; the models differ in their parameter A. Other models were published also by[594] or are included in the Program Documentation of FReET-D[595].

This document is the intellectual property of the fib – International Federation for Structural Concrete. All rights reserved.
This PDF of fib Bulletin 86 is intended for use and/or distribution solely within fib National Member Groups.

Table 9-1 A list of analytical degradation models proposed by various authors for the modelling of carbonation

| Model's primary reference | No. of inputs | Output | Note |
|---|---|---|---|
| Papadakis et al.[596] | 12 | Carbonation depth at time *t*; time to depassivation | Concretes from Portland cement; variants *a* and *b* differ by RH function |
| Papadakis et al.[597] | 5 | | Ditto; simplified model |
| Morinaga[598] | 7 | | Concretes from Portland cement; influence of temperature |
| Papadakis[599] | 8 | | Concretes from blended cements; model variants *a* and *b* differ by RH function |
| *fib*[556] | 11 | | Concretes from blended cements |

### 9.4.1.1 Papadakis et al. (1992)[596]

The model developed by[596] and denoted as model a was derived from the law of conservation of mass of $CO_2$, $Ca(OH)_2$ and CSH gels (calcium silicate hydrates). Parameter A is defined here in a more general way; the composition of concrete mix is described by 9 parameters; altogether 12 input variables are utilized. The model can be applied for the determination of carbonation depth depending on environmental, technological and material conditions. According to the authors´ experience the model does not provide satisfactory results for higher values of RH. This inaccuracy has been overcome by the authors by implementing an alternative function *f*(RH) based on the combination of experimental works[600, 601, 602] – see Fig. 9-5; the solid line thus creates model *b*.

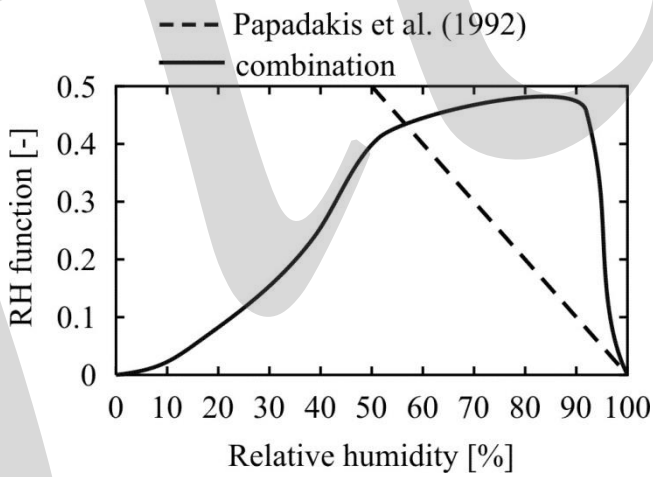


Fig. 9-5 RH functions proposed by Papadakis et al. (1992) and the alternative function

Table 9-2 provides a comparison of analytical results (obtained by both models a and b) with the findings of tests carried out on an existing structure - an RC cooling tower. The tower was investigated at the age of 19.1 years and the depth of carbonation was measured at 75 locations, on both the indoor and outdoor surfaces[603]. A full description of all input values can be found in Table 9-3. The results obtained with model *b* fit the experimental results better compared to model *a*. Some other comparisons have been published in[604].

This document is the intellectual property of the fib – International Federation for Structural Concrete. All rights reserved.
This PDF of fib Bulletin 86 is intended for use and/or distribution solely within fib National Member Groups.

Table 9-2 Carbonation depths in a cooling tower: comparison of analytical models with an experiment

| Surface | Mean value [mm] | | |
|---|---|---|---|
| | In-situ measurements[603] | Model *a* | Model *b* |
| Outdoor (RH = 70 %) | 14.9 | 12.4 | 13.2 |
| Indoor (RH = 97 %) | 8 | 11.5 | 8.2 |

Table 9-3 Input parameters for the calculation of carbonation depths in a cooling tower

| Input parameter | Unit | Mean value | COV | PDF |
|---|---|---|---|---|
| Time of exposure | years | 19.1 | - | Deterministic |
| $CO_2$ content in the atmosphere | mg/m$^3$ | 800 | 0.20 | Normal |
| Relative humidity - outdoor- indoor | % | 70<br>93 | 0.20<br>0.03 | Beta (bounds 0 and 100) |
| Unit content of cement in concrete | kg/m$^3$ | 342 | 0.03 | Normal |
| Unit content of water in concrete | kg/m$^3$ | 188 | 0.03 | Normal |
| Unit content of aggregate (0-4 mm) | kg/m$^3$ | 834 | 0.05 | Normal |
| Unit content of aggregate (4-8 mm) | kg/m$^3$ | 373 | 0.05 | Normal |
| Unit content of aggregate (8-16 mm) | kg/m$^3$ | 614 | 0.05 | Normal |
| Specific gravity of cement in concrete | kg/m$^3$ | 3100 | 0.02 | Normal |
| Specific gravity of aggregate (0-4 mm) | kg/m$^3$ | 2590 | 0.02 | Normal |
| Specific gravity of aggregate (4-8 mm) | kg/m$^3$ | 2540 | 0.05 | Normal |
| Specific gravity of aggregate (8-16 mm) | kg/m$^3$ | 2660 | 0.05 | Normal |
| Uncertainty factor of model | - | 1 | 0.15 | Lognormal (2 par) |

#### 9.4.1.2 Papadakis et al. (1992) – simplified model[597]

The simplest of the introduced models is also proposed by[597]. It has only 5 input variables. The composition of the concrete mix is described here by the *w/c* ratio and the model can serve merely for a rough estimate of the carbonation depth in situations when only limited input data is available. Similarly to the previous model both *f*(RH) functions may be used (model *a* and *b*).

#### 9.4.1.3 Morinaga (1998)[598]

Since temperature affects the kinetics of chemical reactions, this variable is considered to be one of the parameters affecting the carbonation process. Namely, the transport of $CO_2$ in concrete and its reaction rate with concrete's components $Ca(OH)_2$ and CSH gel are temperature-dependent. Increasing temperature leads to higher mobility of $CO_2$ molecules and to a higher reaction rate. The empirical model published by[598] takes into account the ambient temperature and parameter A varies here according to the *w/c* ratio.

#### 9.4.1.4 Papadakis (2000) – concrete from blended cement[605]

According to recent estimates, the cement industry is responsible for producing about 7 % of total global anthropogenic $CO_2$ emissions, which is especially connected with the production of ordinary Portland cement (OPC). Efforts to reduce these emissions are appearing. One approach is in the utilization of solid industrial by-products (fly ash, silica fume and metallurgical slag) as supplementary cementitious materials (SCM) for the production of blended cement leading to the reduction of used OPC.

*This document is the intellectual property of the fib – International Federation for Structural Concrete. All rights reserved.*
*This PDF of fib Bulletin 86 is intended for use and/or distribution solely within fib National Member Groups.*

When designing concretes with SCM the effects of such supplements on mechanical properties and durability should be taken into account. In this model the effect of SCM on carbonation progress is expressed by means of the k-value concept. The k-value takes into account the efficiency of the SCM used, and it differs according to the amounts and types of SCM in concrete. The determination of k-value depends further on the concrete's properties described such as compressive strength, carbonation and chloride ingress resistance. This concept is incorporated in EN 206[606]. Unfortunately, the values of the k-factor recommended in EN 206[606] were most probably developed for compressive strength representation and are different from those established experimentally by[605]. The comparison of both types of k-values has been discussed and the dominancy of the latter values shown[602, 607].

This model[605] is theoretically suitable for assessing the carbonation rate for all types of concrete compositions with SCM. As mentioned above the value of the *k*-factor is different for different amounts and types of SCM in concrete, and creates in this way a decisive input parameter – unfortunately not available for all variants.

The alternative *f*(RH) function (see Fig. 9-5) may be also used for the improvement of this model (model *b*).

#### 9.4.1.5 *fib* (2006)[556]

This model is the most complex one (from those quoted in the present text) and is quite involved in terms of input data quantification. It requires a special carbonation test under accelerated carbonation conditions (ACC-test) to be performed, and the gaining of statistical data for humidity conditions from the closest weather station (meso-climatic conditions due to wetting events on the concrete's surfaces including the probability of driving rain for vertical members, which depends on their geographical orientation). Due to such facts this model with 11 input parameters is less user-friendly; on the other hand it is the only model which is incorporated in the international document *fib* Model Code 2010[236].

Table 9-4 Input parameters for comparison of carbonation models; deterministic calculations (see results in Table 9-5)

| Input parameter | Unit | Value | References to models |
|---|---|---|---|
| Time of exposure | years | 50 | Papadakis (1992); Papadakis (1992) s.m.; Morinaga (1998); Papadakis (2000); Fib (2006)[556] |
| $CO_2$ content in the atmosphere | mg/m³ | 820 | Papadakis (1992); Papadakis (1992) s.m.; Morinaga (1998); Papadakis (2000) [608]; Fib (2006)[556] |
| Relative humidity | % | 70 | Papadakis (1992); Papadakis (1992) s.m.; Morinaga (1998); Papadakis (2000) [608]; Fib (2006)[556] |
| Temperature of structural element or ambient air | °C | 20 | Morinaga (1998) |
| Unit content of cement in concrete | kg/m³ | 313 | Papadakis (1992); Papadakis (1992) s.m.; Morinaga (1998); Papadakis (2000) [608] |
| Unit content of water in concrete | kg/m³ | 185 | Papadakis (1992); Papadakis (1992) s.m.; Morinaga (1998); Papadakis (2000) [608] |
| Unit content of supplementary cementitious materials (SCM) in concrete | kg/m³ | 0 | Papadakis (2000) [608] |
| Unit content of aggregate (0-4 mm) | kg/m³ | 847 | Papadakis (1992) |
| Unit content of aggregate (4-8 mm) | kg/m³ | 386 | Papadakis (1992) |

This document is the intellectual property of the fib – International Federation for Structural Concrete. All rights reserved.
This PDF of fib Bulletin 86 is intended for use and/or distribution solely within fib National Member Groups.

| | | | |
|---|---|---|---|
| Unit content of aggregate (8-16 mm) | kg/m³ | 625 | Papadakis (1992) |
| Specific gravity of cement in concrete | kg/m³ | 3100 | Papadakis (1992); Papadakis (2000)[608] |
| Specific gravity of aggregate (0-4 mm) | kg/m³ | 2590 | Papadakis (1992) |
| Specific gravity of aggregate (4-8 mm) | kg/m³ | 2540 | Papadakis (1992) |
| Specific gravity of aggregate (8-16 mm) | kg/m³ | 2660 | Papadakis (1992) |
| Efficiency factor of SCM | - | 1 | Papadakis (2000) [608] |
| Exponent of regression of execution transfer parameter function $k_c$ | - | -0.567 | *fib* (2006)[556] |
| Curing period | days | 7 | *fib* (2006)[556] |
| Inverse effective carbonation resistance of dry concrete from ACC-test | $\frac{m^2/s}{kg/m^3}$ | $1.34 \cdot 10^{-10}$ | *fib* (2006)[556] |
| Regression parameter of function $R^{-1}_{NAC;0}$ | - | 1.25 | *fib* (2006)[556] |
| Error term of function $R^{-1}_{NAC;0}$ | $\frac{m^2/s}{kg/m^3}$ | $1 \cdot 10^{-11}$ | *fib* (2006)[556] |
| Days with rainfall $h_{ND}$ > 2.5 mm per year | days | 40 | *fib* (2006)[556] |
| Probability of driving rain | - | 0.01 | *fib* (2006)[556] |
| Exponent of regression of weather function $w$ | - | 0.446 | *fib* (2006)[556] |
| Ratio of carbonation velocity of finishing material | - | 1 | Morinaga (1998) |

s.m. = simplified model

Table 9-5 Comparison of carbonation models

| Model's primary reference | | | | | | | |
|---|---|---|---|---|---|---|---|
| Papadakis (1992) {Papadakis, 1992 #297 model *a* | Papadakis (1992) {Papadakis, 1992 #297 model *b* | Papadakis (1992) {Papadakis, 1992 #297 s.m. model *a* | Papadakis (1992) [596]s.m. model *b* | Morinaga (1998) | Papadakis [599] model *a* | Papadakis [599] model *b* | *fib* (2006)[556] |
| Depth of carbonation [mm] | | | | | | | |
| 15.7 | 24.1 | 15.6 | 24.0 | 18.2 | 20.0 | 32.0 | 17.0 |

The referred model given in *fib* Bulletin 34[556] has to be considered as an example as referred in the MC 2010, clause 5.1.13.2 as a way to predict the carbonation ingress when a design has to be based on no a priori information.

Under clause 7.8.2 MC 2010[236] it is however recommended to use a more robust design approach where information of existing structures exposed to similar climate and having similar mix design is also taken into account, Eq. (9-17) or *fib* MC 2010[236], equation 7.8-3.

### 9.4.1.6 Comparison of carbonation models

A comparison of the above-presented carbonation models is discussed in this section. The models are conceptually different and operate on different sets of input parameters, so to compare them is not a simple and straightforward task. For illustrative purposes this problem is restricted to the comparison of carbonation depth at the age of 50 years for OPC concrete of modest quality in a medium indoor environment. A description of input values can be found in Table 9-4). The results of the deterministic analysis for all models are shown in Table 9-5.

This document is the intellectual property of the fib – International Federation for Structural Concrete. All rights reserved.
This PDF of fib Bulletin 86 is intended for use and/or distribution solely within fib National Member Groups.

### 9.4.2 Chloride ion ingress

Several different approaches exist for the description of the time-dependent process of chloride ingress in concrete. Many authors have based their calculations on Fick's 2nd law of diffusion, taking into account the fact that observations indicate that mainly diffusion controlled transport of chlorides in concrete occurs, and that the convection zone is relatively small[564] – see also chapter 9.3.2. The Fick's 2nd law apply the difference between the surface concentration and the initial chloride content as the driving potential.

It was[609] who were probably the first to apply the Crank solution[610] to Fick's 2nd law for the diffusion of chlorides through concrete resulting in a prediction model based on an error function complement solution. This solution is widely used – see e.g.[611].

The simplest model takes the apparent diffusion coefficient and the surface chloride concentration as a constant in time and space. The chloride binding and the refinement of the pore structure over time results in a retarding effect on the diffusion process or for instance in a beneficial effect of the interaction of sea water (*fib* MC 2010[236], clause 7.8.3.1.2).

In some advanced models the time dependency of the apparent chloride diffusion coefficient was taken into account. The proper mathematical analysis for the time-dependent diffusion coefficient[612] and a comparison of possible errors caused by some oversimplified mathematical expressions commonly used in some models are given by[613].

As the transport mechanisms inside the convection zone are mainly capillary suction controlled, the approach of Fick's 2nd law of diffusion yields no satisfactory approximation for chloride penetration inside the convection zone. In order to still describe the penetration of chlorides for an intermittent load using Fick's 2nd law of diffusion, the effect of the convection zone, which may deviate considerably from ideal diffusion behaviour, is neglected and Fick's 2nd law of diffusion is applied starting at depth $\Delta x$ with a substitute surface concentration $C_{s,\Delta x}$.

With this simplification, Fick's 2nd law of diffusion yields a very good approximation of the chloride distribution at depth $x \geq \Delta x$. This simplification has been employed in the *fib*-Model Code[236] models[556].

The physical ClincConc model proposed by[614] has recently been converted into a more engineer-friendly version. The model predicts free chloride penetration through the pore solution in concrete using a flux equation based on the principle of Fick's 2nd law, and then converts the free chloride concentration to total chloride content. It can be used for marine submerged and splash conditions and also with certain modifications for marine atmospheric conditions or in a road environment.

For an estimation of the depth of chlorination at time $t$ (i.e. $x_{Cl}$), time to depassivation (i.e. $t_i$) and the concentration of chlorides at an arbitrary depth and time (i.e. $C$), the models listed in Table 9-6 may be utilized, although several other models exist. A brief description of the models from Table 9-6 follows.

This document is the intellectual property of the fib – International Federation for Structural Concrete. All rights reserved.
This PDF of fib Bulletin 86 is intended for use and/or distribution solely within fib National Member Groups.

Table 9-6 A list of analytical degradation models proposed by various authors for the modelling of chloride ingress

| Model's primary reference | No. of inputs | Output | Note |
|---|---|---|---|
| Papadakis et al. (1996)[563] | 14<br>15 | Depth of chlorination at time *t*; time to depassivation | Alternatives *a* and *b*. Model *b* provides calculation of saturation concentration of $Cl^-$ by analytical formula |
| Tikalsky (2005)[611] | 4<br>5 | Concentration of chlorides at depth *x* and time *t* | Alternatives *a* and *b*. Model *b* provides calculation of diffusion coefficient by experimentally derived formula |
| *fib* (2006)[556] | 9<br>10 | | *fib*-Model Code ; model *b* provides calculation of surface $Cl^-$ concentration for specific conditions by analytical formula |

### 9.4.2.1 Papadakis et al. (1996)[563]

These models[563] of the physicochemical processes of diffusion-adsorption of chlorides in concrete allow for computation of the depth of chlorination from the surface $x_{Cl}$ at a given time *t*, and also of the critical time to depassivation $t_i$. They are based on the assumption of the formation of a moving "chlorination front", where all the adsorption and binding of chlorides takes place at any point in time without the chloride ingress effect.

Unfortunately, the effective diffusivity in these models is given by a semi-empirical expression applicable only for fully saturated, fully hydrated OPC concrete. In model *b*, the input value of saturation concentration of $Cl^-$ in concrete, $C_{sat}$, may be calculated on the basis of an experimentally derived formula proposed also in[563] (in model a it is a direct input parameter). This formula requires knowledge of the saturation concentrations of $Cl^-$ in cement and aggregate which in[563] were determined only for NaCl as the source of chlorides. For different design situations the user may choose one of the following models.

### 9.4.2.2 Tikalsky (2005)[611]

Model a, which is based on an error function complement solution, involves 5 input parameters, one being the variable $D_c$, the diffusion coefficient of chloride through concrete which depends on concrete mix, curing conditions and other parameters. This creates a considerable drawback for this model as it is not an easy task to gain suitable data (including statistical parameters). Moreover, the use of the diffusion coefficient as a constant in time and space is according to[613] too conservative due the lack of consideration of the decrease in the coefficient over time that results from chloride binding. As mentioned above, for the probabilistic prediction of chloride diffusion[611] utilized a set of data from the in-situ measurement of chloride penetration from 230 bridge decks, which were constructed under identical construction and design specifications over a 13-year period and exposed to de-icing salts as well as normal environmental cycles.

There have been some attempts to express the diffusion coefficient in an analytical manner, with a dependence on various parameters. In model b the value of $D_c$ is calculated on the basis of the formula proposed by[615]. They have derived a formula for the diffusion coefficient as a function of time for (i) a control mix made of OPC only, and (ii) concretes with

*This document is the intellectual property of the fib – International Federation for Structural Concrete. All rights reserved.*
*This PDF of fib Bulletin 86 is intended for use and/or distribution solely within fib National Member Groups.*

30 % of fly ash and (iii) with 70 % of slag as a partial replacement for OPC. Unfortunately, this mathematical oversimplification may not be quite correct[613].

#### 9.4.2.3 *fib* (2006)[556]

This model is also based on an error function complement solution, is rather complex and may be utilized for all kinds of concretes. It should be noted that the time dependent apparent chloride diffusion coefficient is represented in this model as an averaged constant (over the entire considered time period).

Two variants are presented: $C_{s,\Delta x}$ is either a direct input parameter (model a), or an experimentally derived formula may be utilized for $C_{s,\Delta x}$, where the horizontal distance from the roadside and height above the road surface are needed as input values (model b). However, it may take a considerable effort to gain all the input data; e.g. the data from a weather station nearby (for the determination of ambient temperature) or the results of the Rapid Chloride Migration method (RCM) for the given concrete mixture. Therefore, these models are less user-friendly. Note that only these models are to be incorporated in the international document *fib*-Model Code 2010.

Table 9-7 Comparison of chloride ingress models

| Model's primary reference | | | |
|---|---|---|---|
| Tikalsky (2005) model *a* [611] | Tikalsky (2005) model *b*[611] | *fib* (2006) model *a*[556] | *fib* (2006) model *b*[556] |
| Chloride concentration [wt.-%/cement] | | | |
| 0.01274 | 0.01588 | 0.01275 | 0.01269 |

#### 9.4.2.4 Comparison of chloride ingress models

Due to the inconsistency of outputs, only some models[611, 556] may be compared with each other. Here, the compared output is chloride concentration at the depth of 30 mm and at a time of 50 years. A full description of all input values can be found in Table 9-8. The results of the deterministic analysis are shown in Table 9-7.

Table 9-8 Input parameters for the comparison of chloride ingress models; deterministic calculations (see results in Table 9-7)

| Input parameter | Unit | Value | Model's primary reference |
|---|---|---|---|
| Depth, usually concrete cover | mm | 30 | Tikalsky (2005) [611]<br>*fib* (2006) [556] |
| Time of exposure, *t* | years | 50 | Tikalsky (2005) [611]<br>*fib* (2006) [556] |
| Concentration of chlorides on nearest surface | wt.-%/cement | 0.02 | Tikalsky (2005) [611] |
| Diffusion coefficient of concrete | $m^2/s$ | $1.28 \cdot 10^{-12}$ | Tikalsky (2005) [611] * |
| Diffusion coefficient of concrete in 28 days | $m^2/s$ | $8 \cdot 10^{-12}$ | Tikalsky (2005) [611] ** |
| Exponent of function $D_t(t)$ | - | 0.1 | Tikalsky (2005) [611] ** |
| Depth of the convection zone | mm | 0 | *fib* (2006) [556] |
| Initial chloride content in concrete | wt.-%/cement | 0 | *fib* (2006) [556] |

This document is the intellectual property of the fib – International Federation for Structural Concrete. All rights reserved.
This PDF of fib Bulletin 86 is intended for use and/or distribution solely within fib National Member Groups.

| | | | |
|---|---|---|---|
| Chloride content in concrete at $\Delta x$ and $t$ | wt.-‰/cement | 0.02 | *fib* (2006)* [556] |
| Chloride migration coefficient | $m^2/s$ | $8.9 \cdot 10^{-12}$ | *fib* (2006) [556] |
| Ageing exponent | - | 0.3 | *fib* (2006) [556] |
| Regression variable | °C | 4526.9 | *fib* (2006) [556] |
| Temperature of structural element or ambient air | °C | 20 | *fib* (2006) [556] |
| Horizontal distance from the roadside | m | 5 | *fib* (2006)** [556] |
| Height above road surface | m | 6.3 | *fib* (2006)** [556] |

* input only for model *a*

** input only for model *b*

#### 9.4.2.5 Nilsson and Carcasses[616]

This model is also based on the widely used Crank's solution to Fick's 2nd law of diffusion with the erf function, however it employs the proper mathematical analysis[613] for time-dependent diffusion coefficient. It can be applied only under the implicit assumption that chloride binding is time-dependent and linearly proportional to the free chloride concentration.

#### 9.4.2.6 Cellular automaton

A cellular automaton (CA) is an effective modelling approach to simulate the diffusion process in concrete. Specifically, this technique may be utilized for chloride penetration predictions[617] based on Fick's 2nd law. The CA technique is a very effective 2D solution while assessing the variation of surface applied chlorides at a time and position with the consequence of the response from the concrete material which may also vary significantly in space and time[618]. In such a way the regions where a critical chloride concentration is reached are recognised and the effect of seasonal de-icing salt application[619] may be studied more effectively compared to the 1-D models mentioned above.

### 9.4.3 Corrosion

Roughly the following phases of reinforcement corrosion propagation in concrete may be specified (Fig. 9-6). Firstly, stage I, when no corrosion is yet present as illustrated in Fig. 9-6a. Next is stage II, where the porous zone at the reinforcement-concrete interface is filled by corrosion products and the surrounding concrete starts to be stressed due to corrosion, see Fig. 9-6b. When the tangential stress in concrete exceeds its tensile strength, cracks start to develop (Fig. 9-6c, stage III). After a certain time a crack propagates through the concrete cover (see Fig. 9-6d) and we are able to observe the crack on the concrete surface, stage IV. At this stage, spalling of the concrete cover may occur. This process does not take place in reality as a rotationally symmetrical one, as depicted. A situation that the whole perimeter of the rebar is depassivated at the same time will never happen. In this respect models based on such representation (thick-wall cylinder models) are (over) simplified and their application is therefore limited.

The described process of degradation might not be valid in the case of prestressed concrete structures.

This document is the intellectual property of the fib – International Federation for Structural Concrete. All rights reserved.
This PDF of fib Bulletin 86 is intended for use and/or distribution solely within fib National Member Groups.

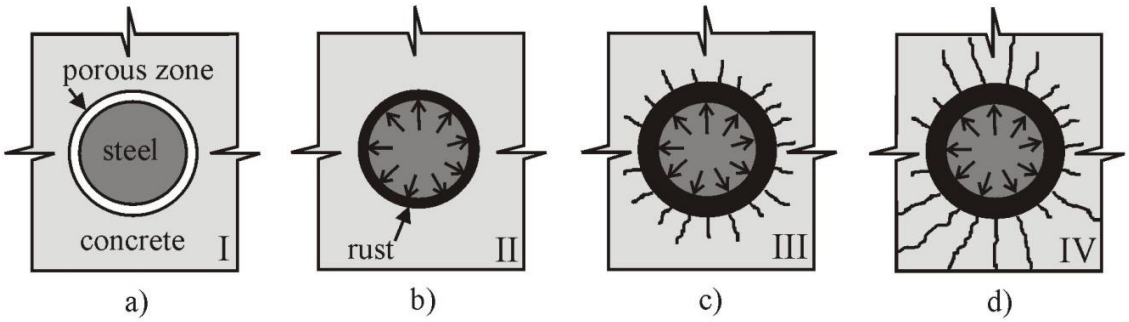


Fig. 9-6 Scheme of the cracking process in reinforced concrete due to corrosion

The key factor for the modelling of steel corrosion as a time-dependent process is the corrosion rate, which is usually expressed through current density, icorr. This variable is strongly affected by ambient conditions such as humidity[620] and temperature, moisture and oxygen availability at the steel level, the degree of concrete carbonation and amount of chlorides[598, 621, 622] thus, it depends on the diffusion characteristics of concrete[623] that are affected e.g. by the water to cement ratio[624] or cracks in the concrete cover[625]. According to[626], the rate of corrosion is inversely proportional to concrete resistivity. This approach may be applied for carbonated concrete structures, but especially for chloride contaminated concrete it should be modified by several factors[627] considering the influence of chloride content, galvanic effects, the formation of rust products and the availability of oxygen. However, sufficient data for factor evaluation is lacking. The effect of the oxygen concentration, chloride concentration and pH of the anodic areas on corrosion propagation have been investigated[621]. According to their studies oxygen controls the rate of corrosion and the chloride concentration affects the amount of areas where corrosion initiates. Decreasing the pH of anodic areas helps to re-initiate the corrosion in the moisture cycle following the drying cycle.

In[628] were specified four ranges of resistivity for the orientation classification of corrosion rate (corresponding current densities were identified[629]): $i_{corr} < 0.1\,\mu A/cm^2$ is low, $0.1 < i_{corr} < 0.5\,\mu A/cm^2$ is low to moderate, $0.5 < i_{corr} < 1\,\mu A/cm^2$ is moderate to high and $i_{corr} > 1\,\mu A/cm^2$ is a high rate of corrosion.

The following text provides a brief description of the models available for the modelling of corrosion in RC structures listed in Table 9-9.

### 9.4.3.1 Andrade et al. (1996)

As already mentioned, the uniform and the pitting type of corrosion are generally distinguished from each other. The formula for the time related net rebar diameter $d(t)$ at exposure time $t$ [years] for the prediction of uniform corrosion reads[630], see also Fig. 9-4a:

$$d(t) = d_i - 0.0116 i_{corr} \cdot R_{corr}(t - t_i) \text{ for } t_i < t \le t_i + d_i \Big/ \left(0.0116 i_{corr} \cdot R_{corr}\right) \tag{9-18}$$

where $d_i$ is the initial bar diameter [mm], $t$ is the time of exposure and parameter $R_{corr}$ [-] expresses the type of corrosion. Apart from parameter $R_{corr}$ , other coefficients may be present in the formula, relating to the influence of chlorides, humidity, pH, etc. Such coefficients may be applied only when appropriate data is available. The constant 0.0116 is a conversion factor from $\mu A/cm^2$ to mm/years under the assumptions that steel (Fe) has $n = 2$ (number of electrons freed by the corrosion reaction), $M = 55.85$ g/mol (atomic mass) and $\rho = 7.88$ g/cm$^3$ (specific gravity).

This document is the intellectual property of the fib – International Federation for Structural Concrete. All rights reserved.
This PDF of fib Bulletin 86 is intended for use and/or distribution solely within fib National Member Groups.

Table 9-9 A list of analytical degradation models proposed by various authors for the modelling of corrosion

| Model's primary reference | No. of inputs | Output | Note |
|---|---|---|---|
| Andrade et al. (1996) | 5 | Net rebar diameter at time *t* | Uniform corrosion |
| Gonzales et al. (1995) | 4 | Pit depth at time *t* | Pitting corrosion |
| Val and Melchers (1998) | 2 | Net cross-sectional area of rebar at time *t* | Pitting corrosion |
| Morinaga (1988) | 3 | | Regression on experimental data |
| Bažant (1979) | ~17 | Time to cracking due to corrosion | Uniform corrosion |
| Liu and Weyers (1998) | 11 | | Uniform corrosion |
| Maaddawy and Soudki (2007) | 8 | | Uniform corrosion |
| Bhargava et al. (2005) | ~15 | Cracking process due to corrosion over time | Five modifications of the model; uniform corrosion |
| Li et al. (2006) | 13 | Crack width due to corrosion at time *t* | Uniform corrosion |
| Izquierdo et al. (2001) and Tada et al. (2000) | 4 | Stress intensity factor at the pit tip at time *t* | Prestressed reinforcement, pitting corrosion |

### 9.4.3.2 Gonzales et al. (1995)[631]

The same approach may be applied to the pitting type of corrosion. Then, the depth of pit $p(t)$ reads[631]:

$$p(t) = 0.0116 i_{corr} \cdot R_{corr} \left(t - t_i\right) \tag{9-19}$$

The studies by[631] on concrete with chloride added to the cement show that the maximum rate of corrosion penetration in the case of pitting corrosion is 4-8 times that of uniform corrosion. Thus, they recommend $R_{corr}$ = 4-8 for the pitting type of corrosion. According to[632], $R_{corr}$ = 4-10 for pitting corrosion, while others[559] suggest $R_{corr}$ = 8-11. So, this factor is highly uncertain and additional investigations are needed. Note: the studies by[631] were performed on reinforcing steel embedded in concrete with a constant amount of chlorides added to the cement for both natural and accelerated conditions. Accelerated tests on prestressed wires embedded in concrete with a constant amount of chlorides added to the cement was performed[559]. The effect of chlorides and used an external voltage source as a corrosion accelerator was not considered by[632].

Note: The effect of chloride concentration on reinforcement corrosion has been incorporated into the model via the $i_{corr}$ value[619].

### 9.4.3.3 Rodrigues et al. (1996)[569]

A very simplified approach for the calculation of the net cross sectional area was suggested by[569]. Accordingly, the net rebar area consists of a circular area with the diameter $d(t)$ as illustrated in Fig. 9-4b.

This document is the intellectual property of the fib – International Federation for Structural Concrete. All rights reserved.
This PDF of fib Bulletin 86 is intended for use and/or distribution solely within fib National Member Groups.

#### 9.4.3.4 Val and Melchers (1998)[570]

The residual reinforcement cross section $A(t)$ (see Eq. (9-14) and Fig. 9-4c)) in the case of pits can be predicted by their simplification into a hemispherical form as proposed by[570]. This leads to a more realistic geometry for the residual reinforcement cross section then the simplification used by[569].

#### 9.4.3.5 Morinaga (1988)[598]

The model for calculation of the time to crack initiation in concrete cover proposed by[598] is an empirical equation based on experimental data. This model takes into account only the initial bar diameter, concrete cover thickness and rate of corrosion. It does not include any of the mechanical parameters of concrete.

#### 9.4.3.6 Bažant (1979) [633]

In[633 is] proposed a physical-mathematical model for the calculation of initiation time to corrosion cracking taking into account concrete cover depth, reinforcing bar diameter and spacing, the mechanical properties of concrete, etc. This model also solves the time of steel depassivation due to critical chloride concentration.

#### 9.4.3.7 Liu and Weyers (1998)[634]

Bažant's model was extended by[634], who proposed a model for the time of crack initiation based on a comparison of the minimum stress required to cause cracking (which equals the tensile strength of the concrete cover) with the expansive pressure in concrete developed over time due to the growth of corrosion products. Concrete is considered to be a homogeneous elastic material shaped like a thick-wall cylinder. It differs from Bažant´s model mainly by taking into account the type of corrosion products and porous zone at the steel-concrete interface and the growth of rust, which is proportional to the amount (thickness) of rust products.

#### 9.4.3.8 Maaddawy and Soudki[635]

A simple mathematical model for the prediction of the time to cracking due to corrosion by[635] aims for the further improvement of models proposed by[633] and[634]. The authors have developed a relationship between steel mass loss and the internal radial pressure caused by rust growth. The time to corrosion cracking is estimated on the basis of Faraday´s law.

#### 9.4.3.9 Bhargava et al. (2005)[636]

In[636] was developed a model describing the entire cracking process after crack initiation. The problem is modelled as a boundary value problem with governing equations expressed in terms of radial displacement. Concrete is treated as a 2-zone material: cracked and uncracked, with consideration of tensile softening. Five modifications of the model are proposed to reproduce various experimental trends. Besides the common mechanical parameters of concrete, the following special inputs are required: modulus of elasticity and Poisson's ratio for cracked concrete and also for a combination of steel and expansive corrosion products.

This document is the intellectual property of the fib – International Federation for Structural Concrete. All rights reserved.
This PDF of fib Bulletin 86 is intended for use and/or distribution solely within fib National Member Groups.

#### 9.4.3.10 Li et al. (2006)[637]

In[637] was proposed a model describing the whole cracking process in concrete due to corrosion with the possibility of calculating the width of a crack on a concrete surface. The concrete is divided into cracked and uncracked parts. It is assumed that the cracks in the inner cracked concrete cylinder are smeared and uniformly circumferentially distributed and that concrete is a quasi-brittle material. The residual tangential stiffness is represented by $a_{stiff}E_{ef}$, where $a_{stiff}$ (<1) is the tangential stiffness reduction factor[638] and $E_{ef}$ is the effective modulus of elasticity of concrete.

#### 9.4.3.11 Izquierdo et al. (2001)[558]

Mathematical model fundamentals describing SCC in prestressed wire have been proposed by[558]. The model is based on the fracture mechanics approach. It is assumed in this model that the corrosion develops in the form of pits that are considered to be stress concentrators; the position and range of the pitting corrosion is random, the worst pit is taken into account here and the geometry of the crack/pit is considered to be semi-elliptical and loaded via the mode I opening. A key parameter of this model, which is a geometry function, may be calculated e.g. according to[639]. The output of this model is the stress intensity factor.

#### 9.4.3.12 Andrade et al.[640]

A simplest model for propagation period, i.e. the advance of the accumulated corrosion (or corrosion penetration) is introduced as the result of multiplying the average (representative) corrosion rate by the propagation time. For pitting corrosion the "pit factor" is utilized (suggesting its average value as 10.0). Note, this factor is also mentioned in 9.4.3.1 and 2 as $R_{corr}$.

#### 9.4.3.13 Osterminski and Schiessl 641

This damage model of German Research Unit 537 is physically well-defined macrocell corrosion model which allows a detailed analysis of all mechanisms occuring in reinforcement corrosion.

### 9.4.4 Frost attack

According to the authors' best knowledge no well-established numerical model for the prediction of concrete damage due to frost attack exists. Note: the probability limit conditions of type (9-1) introduced in *fib*[556] for both the scaling of and internal damage to concrete is not based on mathematical models – the failure probabilities are assessed utilizing experimental results based on considerable laboratory efforts.

### 9.4.5 Fire attack

A widely-used tool for the design and assessment of concrete and reinforced concrete structures is numerical modelling using the finite element method. In the case of the assessment of structures subjected to high temperatures, it is necessary to take into account the effect of temperature on the material properties of analysed materials/structures. These parameters change due to physical and chemical processes in materials during temperature loading. In the case of concrete structures, the important data are properties in compression

*This document is the intellectual property of the fib – International Federation for Structural Concrete. All rights reserved.*
*This PDF of fib Bulletin 86 is intended for use and/or distribution solely within fib National Member Groups.*

and tension; mainly the fracture energy that affects the development of tensile cracks and material toughness, thereby the ductility/brittleness of the structure. The main restriction (among others) for efficient numerical modelling of high temperature-loaded structures is the lack of input parameters, mainly their temperature history dependence.

A temperature history, i.e. the dependence of temperature on time may be characterized by four fundamental thermal parameters. Namely, they are heating rate, exposure time, cooling rate and maximum heating temperature. At present, some dependencies exist - e.g. that of 'common' material parameters (compressive strength, modulus of elasticity) on the maximum temperature. Some of the dependencies are proposed by current guides and recommendations for the design of structures for high temperatures, and some were proposed by[642] on the basis of a large literature survey. The codes and design guides which specify design rules for computing concrete parameters at elevated temperatures include EN 1992-1-2 (2003) and EN 1994-1-2 (2001), CEB (1991) and RakMK B4 (1991). ACI 216R-89 (1989) Guide for Determining the Fire Endurance of Concrete Elements does not suggest any general dependencies/relationships for the mechanical properties of concrete on/with temperature; it only refers to various publications. It provides plots of experimental data on compressive strength obtained by[643] and[644], modulus of elasticity by[645] and[646] and stress-strain curves by[647]. The CEB[140] model code recommends practical design curves for the modulus of elasticity (lightweight concrete and other types), the tensile strength of siliceous aggregate concrete and the compressive strength of normal dense concrete (siliceous) and lightweight concrete. The EN 1992-1-2[648] and EN 1994-1-2[122] make a distinction between normal strength concrete (NSC) with siliceous aggregate and that with calcareous aggregate, and also proposes two rules for high strength concrete (HSC) according to compressive strength - C>55/67 to C≤80/95 and C>80/95 to C≤90/105. It also proposes a prescription for the tensile strength and stress-strain relationship for concrete in compression at elevated temperatures. The Concrete Association of Finland's RakMK B4[649] prescribes different design rules for HSC and NSC. HSC is concrete with designated strength grades of K70 to K100 (concretes with a compressive strength of 70 MPa to 100 MPa if 150 mm cubes are used or 62 to 90 MPa if 150 × 300 mm cylinders are used). NSC is concrete with designated strength grades of K10 to K70 (concretes with a compressive strength of 10 MPa to 70 MPa if 150 mm cubes are used or 7 MPa to 62 MPa if 150 x 300 mm cylinders are used). The RakMK B4 also prescribes different design rules for concrete in service (stressed, 30% preload) and for concrete which is not (unstressed). Phan and Carino have proposed a rule for HSC. They suggest, after comparison of residual, hot stressed (in service) and hot unstressed (not in service) data, that there should be only one rule for all these cases as the data did not show considerable differences. The plots of the rules for the mechanical parameters of concrete at high temperatures proposed in the above-mentioned publications are given in Fig. 9-7 to Fig. 9-11.

This document is the intellectual property of the fib – International Federation for Structural Concrete. All rights reserved.
This PDF of fib Bulletin 86 is intended for use and/or distribution solely within fib National Member Groups.

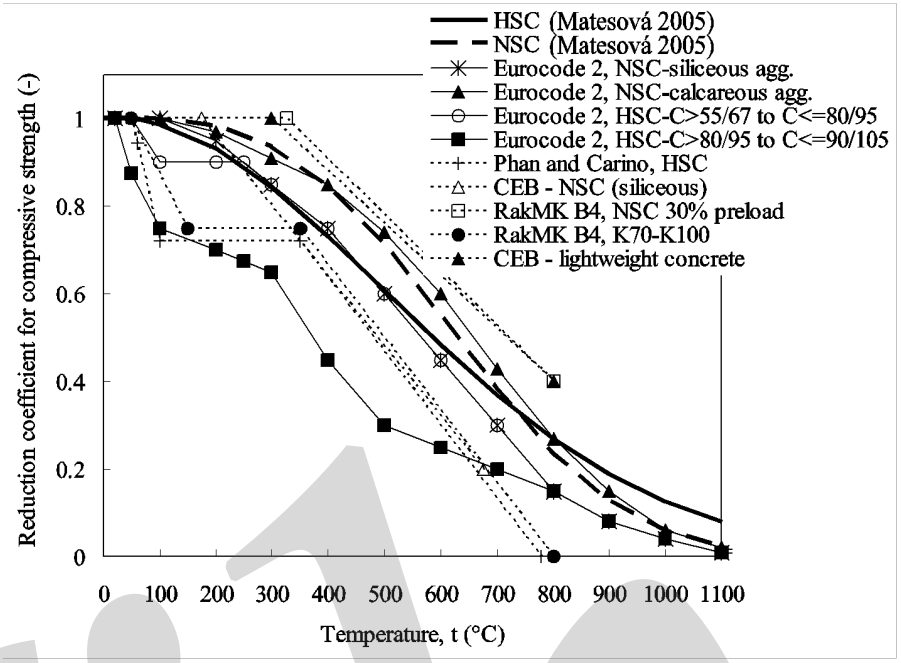


Fig. 9-7 Reduction coefficients for compressive strength vs. temperature from various sources

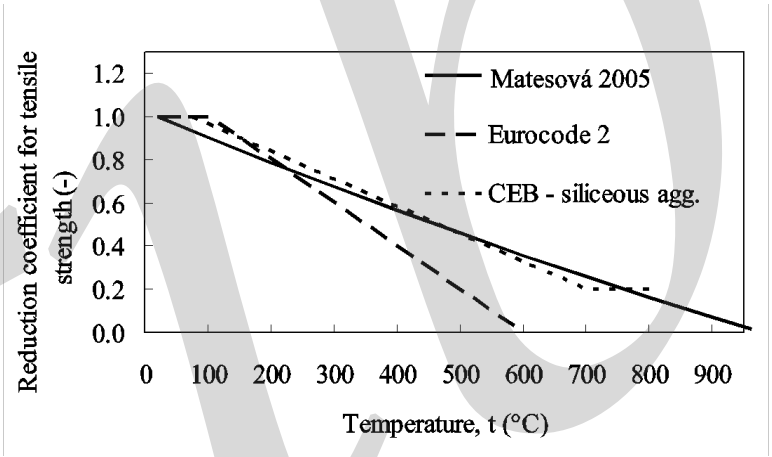


Fig. 9-8 Reduction coefficients for tensile strength vs. temperature from various sources

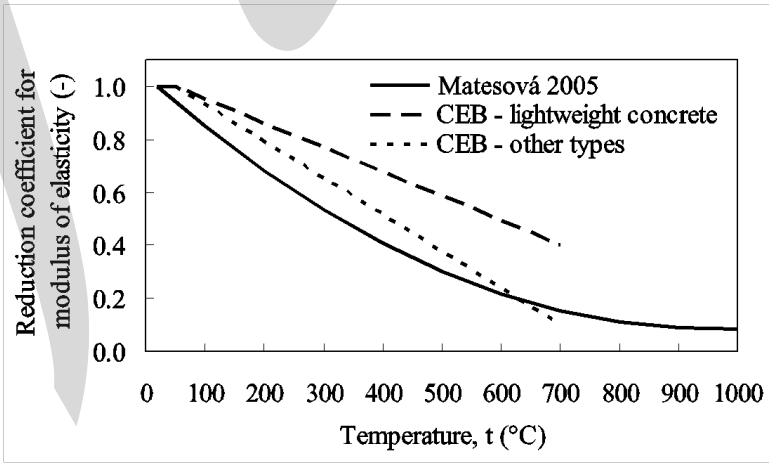


Fig. 9-9 Reduction coefficients for modulus of elasticity vs. temperature from various sources

This document is the intellectual property of the fib – International Federation for Structural Concrete. All rights reserved.
This PDF of fib Bulletin 86 is intended for use and/or distribution solely within fib National Member Groups.

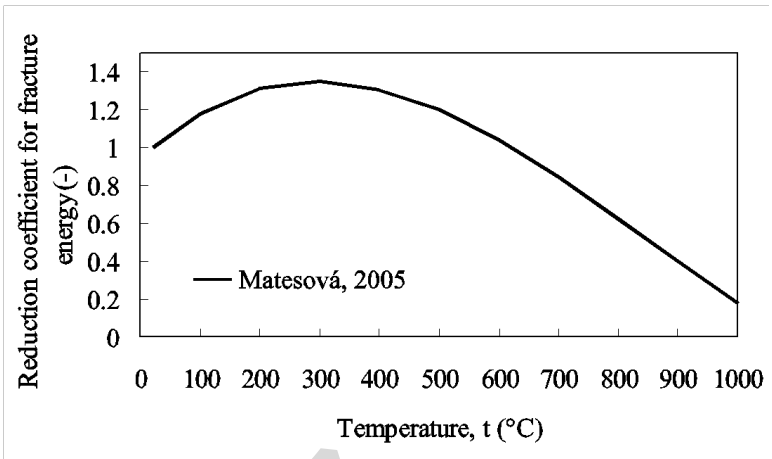


Fig. 9-10 Reduction coefficients for fracture energy vs. temperature

It follows from Fig. 9-7 to Fig. 9-11 that the most observed material parameter is compressive strength. For this parameter several dependencies on temperature exist (Fig. 9-7), distinguished by the type of aggregate and strength level. This is not true for other parameters and beyond this, the dependencies for the fracture energy and Poisson ratio are based on a very limited number of experimental observations. The effect of other thermal parameters (exposure time, heating rate and cooling) is missing in the above-mentioned temperature investigations. There are already a limited number of experimental works on the effect of heating rate[650, 651, 652, 653], exposure time[654, 652] and cooling rate[652] on the material parameters of concrete. The most important factors affecting the high temperature resistance of concrete are strength (HSC vs. NSC) and the type and amount of aggregate[655, 653, 656].

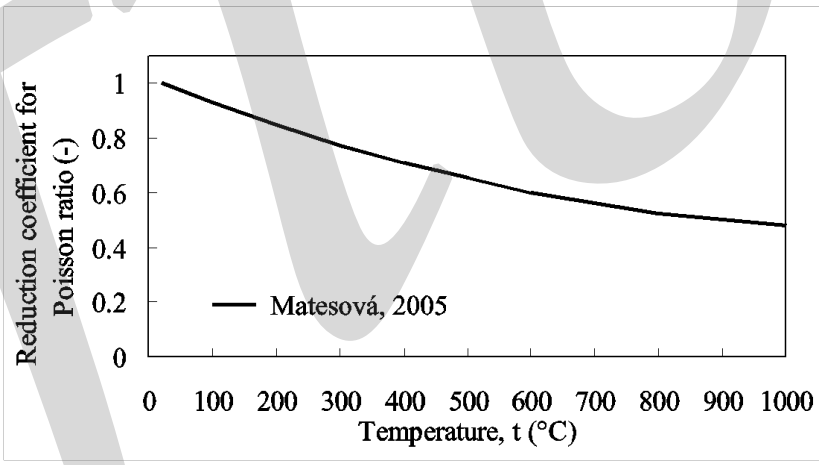


Fig. 9-11 Reduction coefficients for Poisson ratio vs. temperature

## 9.4.6 Alkali-aggregate reaction

In the case of AAR it is quite hard to find a model useable for engineering practice. Let us omit micro and meso-level models and mention some of the macro-level models with the emphasis on a global numerical model for the analysis of a structure. Probably the earliest models are by[657] and[658], who specified critical issues related to AAR – the stress dependency – according to them there is no AAR expansion under a compressive stress of approximately 8 MPa, and the expansion is similar to that of the thermal type.

This document is the intellectual property of the fib – International Federation for Structural Concrete. All rights reserved.
This PDF of fib Bulletin 86 is intended for use and/or distribution solely within fib National Member Groups.

Models that involve the kinetics or even the mechanical model of AAR have been proposed by[659, 660, 661, 662, 663, 664, 665]. The model by[666] seems to be the one applicable to real engineering structures. It is a finite element based model and its utilization for the formulation of the limit state condition, e.g. in the form of Eq. (9-12), would be desirable.

## 9.5 Software

In this section the software products which are suitable for efficiently handling the issues of the durability design or assessment of concrete structures are briefly described and referenced. Note: this list of products is certainly far from complete; only those known to the authors or developed at the Faculty of Civil Engineering, BUT Brno, are dealt with. Most probably, other software of this type does exist.

Life-365 – This computer program for predicting the Service Life and Life-Cycle Costs of reinforced concrete exposed to chlorides (by M.D.A. Thomas and E.C. Bentz) on a deterministic basis is freely accessible on http://www.silicafume.org/specifiers-lifecycle.html; the download package contains an extensive manual that explains the basis of the model and also includes instructions for its use.

Currently, Version 1.1 (2000) of the model is in use in the industry in the USA and represents only the first phase of a longer-term goal to develop a comprehensive service life and life-cycle cost model for reinforced concrete. As explained in the manual, the current version has many limitations in that a number of assumptions or simplifications have been made to deal with some of the more complex phenomena or areas where there is insufficient knowledge to permit a more rigorous analysis.

The analyses carried out within Life-365 can be split into four separate steps as follows:

(i) Predicting the time to the onset of corrosion, commonly called the initiation period, $t_i$,

(ii) Predicting the time for corrosion to reach an unacceptable level, commonly called the propagation period, $t_p$,

(iii) Determining the repair schedule after the first repair,

(iv) Estimating life-cycle costs based on the initial concrete (and other protection) costs and future repair costs.

The model predicts the initiation period assuming diffusion to be the dominant mechanism. The governing differential equation is Fick's second law. The chloride diffusion coefficient is a function of both time and temperature. The propagation period, $t_p$, is fixed at 6 years. In other words, the time to repair, $t_r$, is simply given by $t_r = t_i + 6$ years. The only protection strategy that influences the duration of the propagation period is the use of epoxy-coated steel, which increases the period to $t_p = 20$ years. The total life cycle costs are calculated as the sum of the initial construction costs and the discounted future repair costs over the life of the structure.

Details of the various corrosion protection schemes under consideration are input by selecting a scenario (the options "Automatic Definition" or "User Defined" are offered).

This document is the intellectual property of the fib – International Federation for Structural Concrete. All rights reserved.
This PDF of fib Bulletin 86 is intended for use and/or distribution solely within fib National Member Groups.

RC LifeTime is a web page focused on initiation period[604]. It uses the model for the carbonation process, considers the input data as random variables and performs statistical and reliability analyses utilizing a stochastic simulation technique. It is freely accessible on www.freet.cz. The RC LifeTime offers the following options:

"Service Life Assessment", which provides an evaluation of service life tPS and its statistical characteristics based on the equality condition of carbonation depth and concrete cover - cf. Eq.(9-10). Optionally, the service life corresponding to the target value of reliability index $\beta$ is provided.

"Concrete Cover Assessment", which provides a statistical evaluation of concrete cover a. The reliability index $\beta$ relevant to the required concrete cover may be gained.

A simple check of the $CO_2$ emissions and costs for the concrete mix in question.

RC LifeTime encompasses the modelling of both concrete made from Portland cements as well as from blended cements, based on deterministic models[597, 605].

EUCON[667] computer software, used for the estimation of concrete service life, has been recently introduced. The features of this software are in a certain way similar to those of RC LifeTime, described above: they both are based on models for carbonation[597, 605]. In contrast with RC LifeTime, however, EUCON is not a probabilistic software package and does not offer reliability assessment; on the other hand it provides options for chloride ingress modelling and detailed economical as well as environmental effect optimization.

FReET-D, a complex software tool for the degradation assessment of concrete structures, has been developed recently for assessing the potential degradation of newly designed as well as existing concrete structures. The tool is based on the probabilistic multipurpose software package FReET[668, 397]. In FReET -D, 30 different models for concrete or reinforcement degradation are incorporated: carbonation of concrete, corrosion of reinforcement (mild or prestressing steel), chloride attack. Also, it enables the incorporation of any closed-form numerical model in the form of a limit state/response function. The statistical and probabilistic evaluation of conditions such as Eq. (9-1) or Eq. (9-7) is possible according to the user's requirements. The consideration of input parameters as random variables (statistically independent or dependent), together with the provision of statistical sensitivity options may be essential for probabilistic based assessment and decision making. FReET -D is supposed to be part of a complex software system for the structural analysis and reliability assessment of concrete structures, or it can be used as a stand-alone software package. More details can be found on www.freet.cz or in[669, 397].

## 9.6 Illustrative examples of Durability Design/Assessment

Utilizing the FReET-D software introduced in 9.5, for the statistical analysis of the following examples the Latin Hypercube Sampling method was applied – for more details about this simulation technique[389, 670]. For the output quantities the best fit for the probabilistic distribution function (PDF) was found using the Kolmogorov Smirnov goodness-of-fit test. The parametric approach is utilized in order to support the designer while making decisions (design alternatives, concrete mix and others).

This document is the intellectual property of the fib – International Federation for Structural Concrete. All rights reserved.
This PDF of fib Bulletin 86 is intended for use and/or distribution solely within fib National Member Groups.

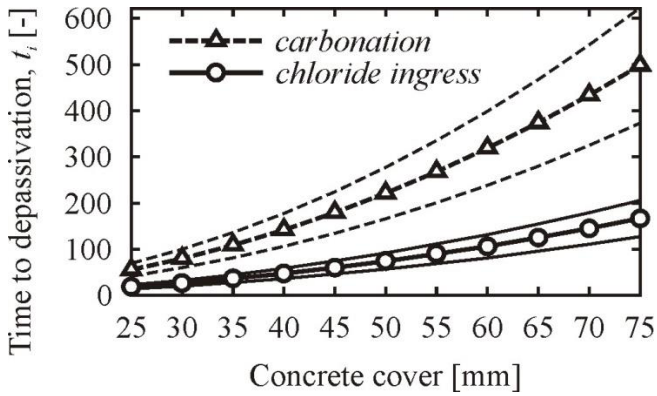


Fig. 9-12 Time to depassivation (average ± standard deviation) due to carbonation and chloride ingress vs. concrete cover

### 9.6.1 Reinforcement depassivation – assessment of initiation period

For this example models by[597] denoted as model *b* (see section 9.4.1) and[563] (see section 9.4.2) were applied for depassivation due to carbonation and chloride ingress, respectively. The calculation of time to reinforcement depassivation, $t_i$, due to carbonation and/or chloride ingress dependent on the concrete cover thickness (this quantity being assumed here in the range from 25 to 75 mm) is presented here. The full description of all input values is given in Table 9-11; firstly let us list here the most important ones. For carbonation they are the $CO_2$ content in the atmosphere: N (820, 98.4) mg/m$^3$, and relative humidity: Beta (70,$a$ = 0, $b$ = 100) %. For chloride ingress they are the concentration of chlorides (de-icing salts) on the concrete surface assumed by the deterministic value of 50 mol/m$^3$ and the critical concentration of $Cl^-$ in pore solution represented by the deterministic value of 13.4 mol/m$^3$.

The results of the statistical analysis are shown in Fig. 9-12, where mean values together with standard deviations are plotted. Considering a specific concrete cover and applying the conditions, Eq. (9-10) and (9-11). Then e.g. for a cover of 45 mm and the target design life $f_{ct}$ = 50 years we obtain $\beta$ = 2.85 ($P_f$ = 2 ·10–3) and $\beta$ = 0.7 ($P_f$ = 2´10–1, not an acceptable value) for depassivation due to carbonation and chloride ingress, respectively. The well-known fact that the rate of chloride ingress is higher compared to the carbonation rate with respect to time to depassivation is also evident from this example.

This document is the intellectual property of the fib – International Federation for Structural Concrete. All rights reserved.
This PDF of fib Bulletin 86 is intended for use and/or distribution solely within fib National Member Groups.

Table 9-10 Input parameters for the calculation of time to reinforcement depassivation

| Reflection of | Variable | Unit | Mean value | COV | PDF |
|---|---|---|---|---|---|
| Models | Uncertainty factor of model | - | 1 | 0.15 | Lognormal (2par) |
| Environment | $CO_2$ content in the atmosphere | mg/m³ | 820 | 0.12 | Normal |
| | Relative humidity | % | 70 | 0.07 | Beta (a = 0, b = 100) |
| Concrete Mix | Unit content of OPC cement | kg/m³ | 313 | 0.03 | Normal |
| | Unit content of water | kg/m³ | 185 | 0.03 | Normal |
| | Unit content of aggregate (0-4 mm) | kg/m³ | 847 | 0.03 | Normal |
| | Unit content of aggregate (4-8 mm) | kg/m³ | 386 | 0.03 | Normal |
| | Unit content of aggregate (8-16 mm) | kg/m³ | 625 | 0.03 | Normal |
| | Specific gravity of cement | kg/m³ | 3100 | 0.02 | Normal |
| | Specific gravity of aggregate (0-4 mm) | kg/m³ | 2590 | 0.02 | Normal |
| | Specific gravity of aggregate (4-8 mm) | kg/m³ | 2540 | 0.02 | Normal |
| | Specific gravity of aggregate (8-16 mm) | kg/m³ | 2660 | 0.02 | Normal |
| Other | Concrete cover | mm | 25 - 75 | - | Deterministic |
| | Concentration of $Cl^-$ on nearest concrete surface | mol/m³ | 50 | - | Deterministic |
| | Saturation concentration of $Cl^-$ in solid phase | mol/m³ | 140 | - | Deterministic |
| | Threshold concentration of $Cl^-$ in liquid phase | mol/m³ | 13.4 | - | Deterministic |
| | Diffusion coefficient of $Cl^-$ in infinite solution | m²/s | $1.6 \cdot 10^{-9}$ | - | Deterministic |

Note: In practice, the different levels of site control should result in different characteristics of expected cover scatter, i.e. the cover would be input as a random variable described by a suitable PDF which will also affect the resulting value of reliability index $\beta$.

## 9.6.2 Loss of reinforcement due to corrosion

A model by Andrade et al. 630 (section 9.4.3) was applied in this example. Assuming an initial reinforcement diameter to be log-normally distributed (2 par): $d_i$ = LN(30; 0.75) mm, and that the critical loss of the reinforcement area is assessed to be 10% (such a loss may e.g. lead to the exceeding of the reliability level for the ULS or SLS which depends on the structure and loading configuration and is not treated in this example). This limit corresponds to the critical net rebar diameter of 28.46 mm. The main input parameters are current density: $i_{corr}$ = N(1; 0.2) mA/cm² and time to corrosion initiation: $t_i$ = LN (47.4; 11.5) years. The full description of the input parameters is given in Table 9-11. The resulting decrease in rebar diameter over time is plotted in Fig. 9-13. The mean values of ti and td,crit (the time of a critical drop in rebar diameter) are marked in this figure.

*This document is the intellectual property of the fib – International Federation for Structural Concrete. All rights reserved.*
*This PDF of fib Bulletin 86 is intended for use and/or distribution solely within fib National Member Groups.*

The best-fitted PDFs for output net rebar diameters are LN (2 par) for 0, 10 and 20 years, Student t for 30 years, Laplace for 40 and 50 years, LN (2 par) for 60, 70, 80, 90 and 100 years, LN (3 par) for 110 and 120 years and LN (2 par) for 130, 140 and 150 years. Chosen histograms of output parameters together with fitted PDFs are depicted in Fig. 11-62 showing the complexity of the statistical description of the problem solved. Note that lognormal PDFs appear for time intervals of 0-20 and 60-150 years. In the first interval the steel is not yet depassivated, while in the second time interval the steel is already depassivated in the majority of stochastic realisations. Therefore, the standard deviation (std) of the output net rebar diameter in the time interval of 0 to 20 years is influenced by the standard deviation of the input initial bar diameter while the standard deviation in the time interval of 60-150 years is affected by the scatter of all input variables. In the time interval between these (i.e. 30-70 years) the standard deviation gradually increases (see Fig. 9-13).

Applying the limit state condition given by Eq. (9-14), replace the cross sections by diameters and assume a design service life of 50 years, a reliability index is obtained of $\beta = 0.38$ (a non-acceptable level of reliability – according to *fib* MC236 $\beta = 1.5$ aplies for an irreversible state).

Table 9-11 Input parameters for calculation of loss of reinforcement due to corrosion

| Input parameter | Unit | Mean value | COV | PDF |
|---|---|---|---|---|
| Initial bar diameter | mm | 30 | 0.025 | Lognormal (2 par) |
| Time to corrosion initiation | years | 47.4 | 0.244 | Lognormal (2 par) |
| Current density | $\mu$A/cm$^2$ | 1 | 0.2 | Normal |
| Coefficient of corrosion type | - | 2 | - | Deterministic |
| Uncertainty factor of model | - | 1 | 0.15 | Lognormal (2 par) |

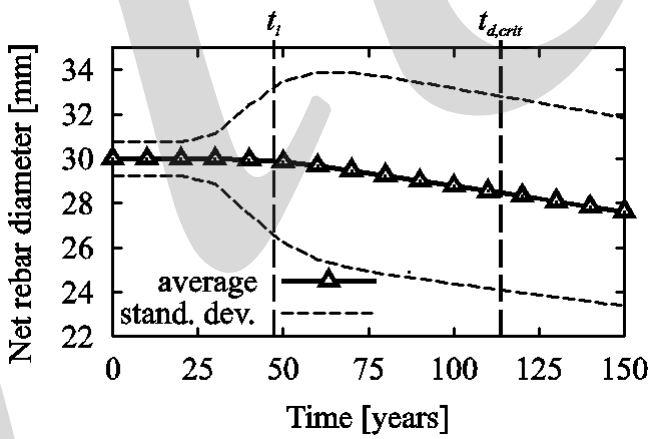


Fig. 9-13 Net rebar diameter (± standard deviation) vs. time

This document is the intellectual property of the fib – International Federation for Structural Concrete. All rights reserved.
This PDF of fib Bulletin 86 is intended for use and/or distribution solely within fib National Member Groups.

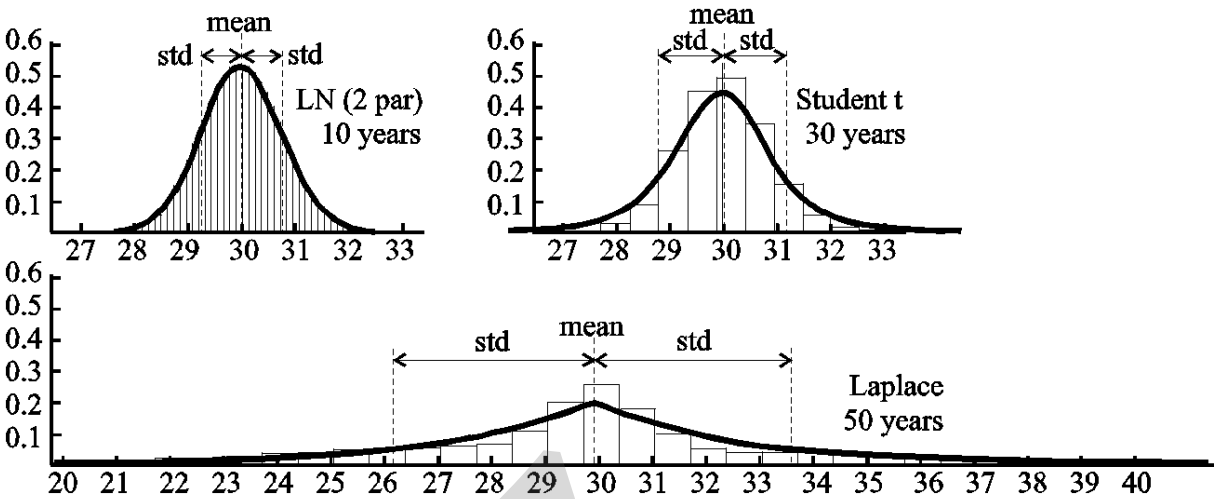


Fig. 9-14 Histograms of output net rebar diameter plotted in Fig. 9-13 (decreased due to corrosion) together with the best-fitted PDFs in chosen time steps

This document is the intellectual property of the fib – International Federation for Structural Concrete. All rights reserved.
This PDF of fib Bulletin 86 is intended for use and/or distribution solely within fib National Member Groups.

# 10. Case studies applications

## 10.1 Reliability based assessment of a segmental bridge – Austria

The 25 years old single span bridge in Vienna over the Highway A23 was, due to an ongoing construction project, demolished in 2002. During the demolition several non-destructive tests as well as a partial and a full destructive load test were performed by the Technical University of Vienna. The planning and optimization of the test setup and finally the reliability assessment are based on SARA[314, 736].

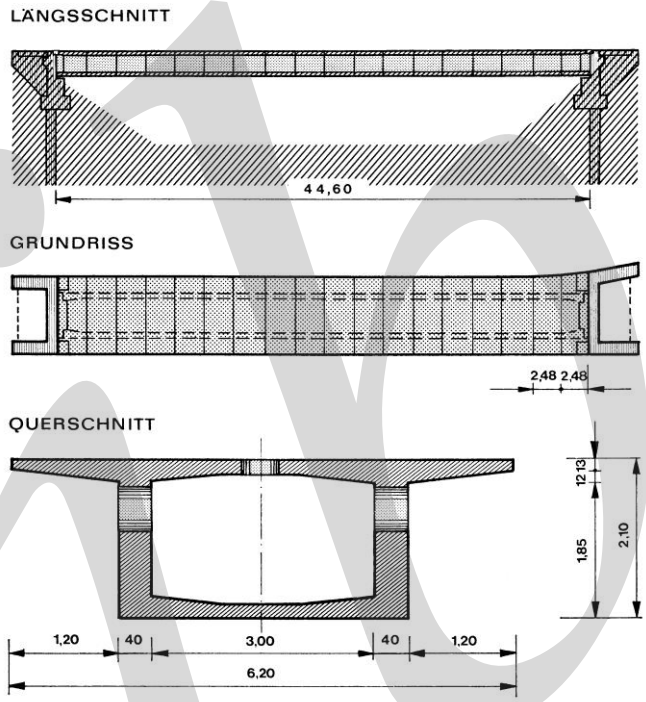


Fig. 10-1 Side elevation of the bridge from the west

The length of the bridge is 44.60 m, the width 6.40 m and the height 2.10 m (Fig. 10-1). The fully post-tensioned box-girder bridge was made of 18 segments with lengths of 2.485 m each. The segmental joints were filled with epoxy resin. The segments were cast from concrete B500 and are rein-forced with mild steel St 50. The post-tensioning tendons consist of 20 strands St 160/180. The bridge was pre-stressed and then loaded with prescribed displacement in the middle of the span. The ultimate failure load and the descending branch of the stress-strain relationship were obtained. The bridge girder failed typically in the middle of the span. First the prestressing tendons yielded, tensile cracks developed, and consequently the concrete in the compression flange of the box girder crushed and split. Mean values of the material properties for concrete B500 were generated using ATENA defaults (based on recommendations by CEB, *fib*, RILEM etc.). Tensile cracking model in ATENA is based on the smeared crack approach, which replaces the discrete cracks, occurring in real concrete structures, by strain localization in a continuous displacement field.

This document is the intellectual property of the fib – International Federation for Structural Concrete. All rights reserved.
This PDF of fib Bulletin 86 is intended for use and/or distribution solely within fib National Member Groups.

Concrete fracture is covered by nonlinear fracture mechanics based on fracture energy with an exponential softening law derived experimentally by[737] demonstrated in Fig. 10-2 and Eq. (10-1). The objectivity of the finite element solution is assured by crack band approach - the descending branch of the stress-strain relationship is adjusted according to the finite element size and mesh orientation.

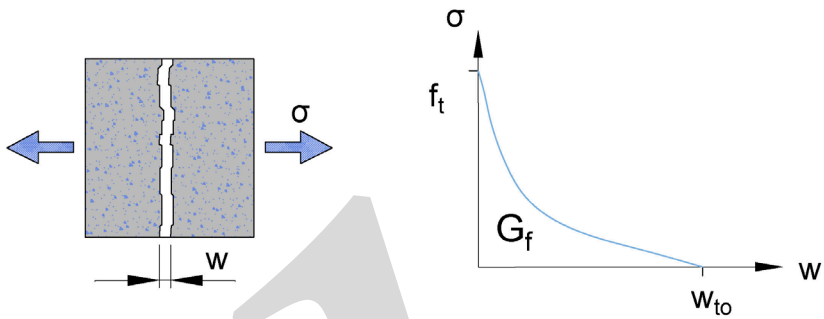


Fig. 10-2 Stress - crack-opening law according to[737]

$$\frac{\sigma}{f_t} = \left(1 + c_1 \frac{w}{w_{t0}}\right)^3 \exp\left(-c_2 \frac{w}{w_{t0}}\right) - \frac{w}{w_{t0}}\left(1 + c_1^3\right)\exp(-c_2) \tag{10-1}$$

$$\text{with } c_1 = 3,\ c_2 = 6.93 \text{ and } w_{t0} = 5.14\frac{G_f}{f_t} \tag{10-2}$$

The used mean values, coefficients of variation and suitable pdfs of the concrete and steel properties are presented in Table 10-1. Statistical correlation among random variables was considered according to the prescribed correlation matrix as shown in the upper triangle of Table 10-2.

The computation of the ultimate load was based on different sample sizes, which are gained from the estimated statistical parameters of the material properties. The sample sizes = 8 and 32 samples already provided comparable results. Furthermore the results have been used to estimate a reliability index for the structure considering different levels of the load, described by the mean and two alternatives of variability (coefficient of variation COV = 0.1 and 0.2). The analysis verified the feasibility of the used complex stochastic nonlinear program system integrating nonlinear fracture finite element analysis with probabilistic tools.

Table 10-1 Basic variables used for the simulation.

| Variable | Material | Properties | Units | Distribution | Mean | CoV |
|---|---|---|---|---|---|---|
| $E_c$ | Concrete | Modulus of elasticity | Gpa | Lognormal | 36.95 | 0.15 |
| $\nu$ | | Poisson' ratio | - | Lognormal | 0.2 | 0.05 |
| $f_t$ | | Tensile strength | MPa | Weibull | 3.275 | 0.18 |
| $f_c$ | | Compressive strength | MPa | Lognormal | 42.5 | 0.10 |
| $G_f$ | | Fracture energy | N/m | Weibull | 81.43 | 0.20 |

This document is the intellectual property of the fib – International Federation for Structural Concrete. All rights reserved.
This PDF of fib Bulletin 86 is intended for use and/or distribution solely within fib National Member Groups.

| | | | | | | |
|---|---|---|---|---|---|---|
| $\varepsilon_\chi$ | | uniaxial compressive strain at compressive strength | - | Lognormal | 0.0023 | 0.15 |
| | | reduction of compressive strength due to damage | | | | |
| $c_{Red}$ | | critical compressive displacement | - | Rectangular | 0.8 | 0.06 |
| | | specific material weight | | | | |
| $w_d$ | | Modulus of elasticity | m | Lognormal | 0.0005 | 0.10 |
| | | Yield strength | | | | |
| $r$ | | Prestressing force | MN/m³ | Normal | 0.023 | 0.1 |
| $E_s$ | Pre-stressed steel | Area of strands | GPa | Lognormal | 200 | 0.03 |
| $f_{yp}$ | | | MPa | Lognormal | 630 | 0.03 |
| $F_p$ | | | MN | Normal | 21.85 | 0.04 |
| $A_s$ | | | m² | Normal | 0.0237 | 0.001 |

Table 10-2 Correlation matrix for concrete properties.

| Parameter | $E_c$ | $f_t$ | $f_c$ | $G_f$ | $\varepsilon_c$ |
|---|---|---|---|---|---|
| $E_c$ | 1 | 0.7 | 0.9 | 0.5 | 0.9 |
| $f_t$ | 0.7 | 1 | 0.8 | 0.9 | 0.6 |
| $f_c$ | 0.9 | 0.8 | 1 | 0.6 | 0.6 |
| $G_f$ | 0.5 | 0.9 | 0.6 | 1 | 0.5 |
| $\varepsilon_c$ | 0.9 | 0.6 | 0.6 | 0.5 | 1 |

## 10.2 Reliability based assessment of a prestressed box girder bridge – Italy

### 10.2.1 Deterministic model

The main objectives of the probabilistic analysis performed were a comprehensive reliability and condition assessment of the thirteen years old Colle Isarco Viaduct and the validation of the developed SARA procedure. The Colle Isarco Viaduct is a cantilever construction beam bridge in Italy with a total length of 1,000 m. It was built in 1969 and is a fully post-tensioned box-girder bridge and is part of the Brenner Highway in Italy. Several structures of this type are found in the two separated lanes which form this bottleneck crossing the Alps.

#### 10.2.1.1 Geometry

The northern cast-in-place balanced cantilever beams are the most sensitive elements of the bridge. Therefore, these elements, with varying box girder depths, have been chosen for the analyses. The total length of the beams is 167.5 m. They are subdivided by the mid-span with a length of 91 m and the cantilever beams with a length of 59 m and 17.5 m, see Fig. 10-3.

This document is the intellectual property of the fib – International Federation for Structural Concrete. All rights reserved.
This PDF of fib Bulletin 86 is intended for use and/or distribution solely within fib National Member Groups.

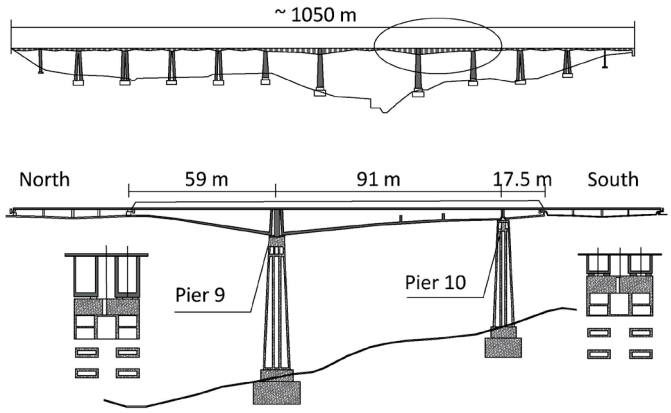


Fig. 10-3 Side elevation of the Colle Isarco Viaduct from the west

The top slab has a width of 10.60 m and the lower girder slab a width of 6.00 m. Both of them have a thickness of about 0.20 m. The height of the box girder varies from 10.80 m over the middle support to 2.85 m at the end of the cantilever beams. A summary of the geometric data used for the analysis is given in Table 10-3.

Table 10-3 Deterministic Geometric Data used for the Analysis.

| Component | Location | Magnitude (m) |
|---|---|---|
| Cantilever north | North of pier 9 | 59.0 |
| Middle-span | Pier 9 to pier 10 | 91.0 |
| Cantilever south | South of pier 10 | 17.5 |
| Width of top slab | Entire slab | 10.6 |
| Box section width | Entire box | 6.0 |
| Box section height | Pier 10 | 4.5 |
| Box section height | Pier 9 | 10.8 |
| Box section height | Both ends | 2.85 |
| Total length | - | 167.5 |

### 10.2.1.2 Finite element model

The finite element model was built in ATENA by using the previously mentioned geometric data. The basic assumption regarding the Constitutive Model SBETA was the application of a plane stress state. In addition, the smeared reinforcement and crack approach was used for the description of the existing material properties.

The material model SBETA includes the following properties:

(a) non-linear behaviour in compression,

(b) hardening and softening effects,

(c) fracture properties of concrete in tension based on the nonlinear fracture mechanics,

(d) biaxial strength failure criterion,

(e) reduction of compressive strength after cracking,

(f) tension stiffening effect,

(g) reduction of the shear stiffness after cracking (variable shear retention),

This document is the intellectual property of the fib – International Federation for Structural Concrete. All rights reserved.
This PDF of fib Bulletin 86 is intended for use and/or distribution solely within fib National Member Groups.

(h) two crack models, and

(i) fixed crack direction and rotated crack direction.

The discretisation of the structure was performed by 2D-Quadrilaterals CCIsoQQuad Elements[671], where the maximum element size of 0.1 m of the two-dimensional mesh resulted in a total number of 5,682 elements with 24,478 nodes. The elements could be grouped in 38 macro elements by considering elements with similar material and geometrical qualities. This grouping permits an efficient calculation process. Detailed descriptions regarding the discretisation and grouping can be found in[672].

#### 10.2.1.3 Load cases

A structure is exposed to numerous stressors. The probabilistic consideration of the Gossensass bridge takes into account (a) the dead weight of the structure, (b) the pre-stressing, (c) selected traffic loads, and (d) the boundary conditions according the initial static of the bridge. The adjacent hinge beams of the considered main girder are considered proportional according to their dead weight and traffic loading. A non-linear ATENA pre-investigation of the model showed that the constant linear distributed line load over the whole length of the girder with a magnitude $p$ = 10 kN/m (according to the original static) is the authority traffic load case for the ultimate strength of the structure.

*Load Case a* – applied once: The dead weight of the structure could be automatically assigned to FE Model by routines included in ATENA.

*Load Case b* – applied once: The pre-stressing of the structure is characterized by 211 bar elements of diameter $d$ = 32 mm, a yield strength $f_y$ = 850 MPa and an ultimate strength $f_u$ = 970 MPa, ST(850/970). In order to take into account the pre-stressing associated affects of wedge slip, shrinkage and creep only 80% of $f_y$ is applied to the model. The pre-stressing had no direct effect on the supports or bearings due to the statically determinate nature of the system.

*Load Case c* – applied incremental: As mentioned previously, a constant distributed line load over the whole length of the girder was incrementally applied. The non-linear computation of the ultimate strength required incremental increases of $p$ ($\Delta p$ = 2 kN/m) until the occurrence of fracture.

Load Case d – applied once: The boundary conditions of the modelled structure are: fixed horizontal and vertical displacements $w$ and $u$ between pier 9 and the girder, all rotations $\varphi_i$ are free, and a fixed vertical displacement $w$ between the pier 10 and the girder, the horizontal displacement $u$ and all the rotations $\varphi_i$ are free.

#### 10.2.1.4 Monitoring of the structural response:

Monitoring points were located along the structure (Fig. 10-4) in agreement with sensors already mounted on the structure. The points allowed the evaluation of the serviceability and the ultimate limit strength of the structure by specified physical quantities, such as displacements, stresses and reaction forces. A monitoring program has already been in operation for more than three years[178]. During the simulation process, for each incremental increase of the line load $p$, the monitoring points recorded the structural response – mainly the vertical deflection. Furthermore, monitoring point M6 serves as the sensing element for the applied force, which was used for the validation of the ultimate limit strength of the structure. Table 10-4 gives detailed information about the locations of the essential monitoring points.

This document is the intellectual property of the fib – International Federation for Structural Concrete. All rights reserved.
This PDF of fib Bulletin 86 is intended for use and/or distribution solely within fib National Member Groups.

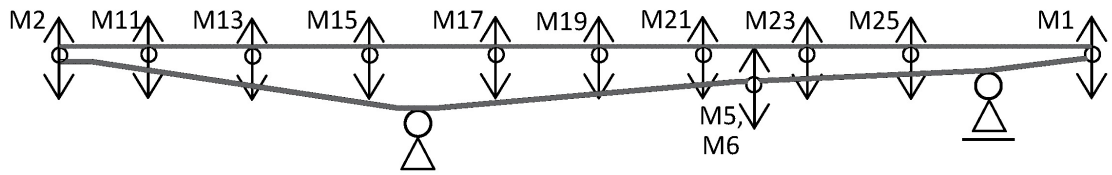


Fig. 10-4 Monitoring points + FEM - discretized structure

Table 10-4 Location of the essential monitoring points

| N° | Monitoring Point | Location x (m) | y (m) |
|---|---|---|---|
| 1 | M1 | 107.84 | -1.95 |
| 2 | M2 | -59.39 | -1.97 |
| 5 | M5 | 45.00 | -6.30 |
| 11 | M11 | -50.77 | -0.44 |
| 13 | M13 | -33.69 | -0.55 |
| 15 | M15 | -11.51 | -0.58 |
| 17 | M17 | 9.98 | -0.43 |
| 19 | M19 | 25.07 | -0.36 |
| 21 | M21 | 40.13 | -0.30 |
| 23 | M23 | 59.15 | -0.29 |
| 25 | M25 | 78.19 | -0.23 |

## 10.2.2 Probabilistic analysis

### 10.2.2.1 Stochastic models

Material and geometrical properties are subject to uncertainties. These uncertainties can be caused by natural influences such as different aggregate densities of concrete or varying production conditions. The SARA based method allows taking into account both geometrical and material scattering by PDFs The PDFs of the essential parameters of this structure are described by the first two statistical moments and a distribution type, see Table 10-5. The disperse material and geometrical characteristics used for this structure were derived from the original production control of the "Colle Isarco Viaduct", from independent structural material inquiries[385] and recommendations by the *fib*.

Table 10-5 Basic variables used for the simulation.

| Variable* | Material | Properties | Units | Distribution | Mean | CoV |
|---|---|---|---|---|---|---|
| $E_c$ | Concrete | Modulus of elasticity | GPa | Lognormal | 37 | 0.15 |
| $f_t$ | | Tensile strength | MPa | Weibull | 3.26 | 0.18 |
| $f_c$ | | Compressive strength | MPa | Lognormal | 42.5 | 0.10 |
| $G_f$ | | Fracture energy | N/m | Weibull | 135 | 0.20 |
| $\rho$ | | Specific material weight | MN/m³ | Normal | 0.023 | 0.10 |
| $E_s = E_p$ | Steel | Modulus of elasticity | GPa | Lognormal | 210 | 0.03 |
| $f_{ys}$ | Reinforcement | Yield strength | MPa | Lognormal | 500 | 0.05 |
| $f_{yp}$ | Pre-stressed Steel | Yield strength | MPa | Lognormal | 850 | 0.03 |
| $r_V$ | Reinforcement | Ratio vertical $A_s/A_c$ | - | Normal | 0.003 | 0.10 |
| $r_M$ | Reinforcement | Ratio horizontal $A_s/A_c$ | - | Normal | 0.003 | 0.10 |

This document is the intellectual property of the fib – International Federation for Structural Concrete. All rights reserved.
This PDF of fib Bulletin 86 is intended for use and/or distribution solely within fib National Member Groups.

#### 10.2.2.2 Correlation

In nature, there is an interaction between physical characteristics; therefore, it is essential to include them in simulation processes as well. In general, SARA encourages the formulation of correlations between material parameters and geometrical parameters. Table 10-5 shows the correlation matrix used. Values of this matrix are obtained partly by experiments[385].

Table 10-6 Correlation matrix of concrete properties.

| Parameter | $E_c$ | $f_t$ | $f_c$ | $G_f$ |
|---|---|---|---|---|
| $E_c$ | 1 | 0.7 | 0.9 | 0.5 |
| $f_t$ | 0.7 | 1 | 0.8 | 0.9 |
| $f_c$ | 0.9 | 0.8 | 1 | 0.6 |
| $G_f$ | 0.5 | 0.9 | 0.6 | 1 |

#### 10.2.2.3 Serviceability

The probability simulation of the structure is based on 30 samples created by the Latin hypercube sampling method (LHS). Loading was applied incrementally by using the Newton-Rapson method for the first steps and the arc-length method for the latter. A calculation time of about 30 hours shows the feasibility of nonlinear FEM computations in the field of probabilistic modelling.

The serviceability considerations of the Gossensass Bridge mainly focus on the vertical displacements. Four different load cases are taken into account:

N° 1 dead load and pre-stressing

N° 2 dead load, pre-stressing and single traffic load $p$ =10 kN/m

N° 3 dead load, pre-stressing and double traffic load $p$ =20 kN/m

N° 4 dead load, pre-stressing and quadruple traffic load $p$ =40 kN/m

Pre-stressing caused a vertical displacement of about 160 mm with a standard deviation of about 30 mm at the end of the longer cantilever. This simulated high deflection never actually occurred because the pre-stressing effects had been continuously compensated during the free-cantilevered construction process. Nevertheless, this analysis is of interest, since the sensitivity analysis performed provides the order of the dominant basic variables responsible for the vertical deflection at the end of pre-stressing.

The sensitivity analysis showed that the concrete qualities in the region of the cantilever and the reinforcement qualities in the region of the middle play a dominant role with respect to the vertical structural displacements. Details regarding the correlation between the scattering basic variables (e.g., $f_c$, $G_F$) and the computed statistical responses in the monitoring points are given in Strauss et al. (2006).

The limit states functions ($g = R - S$) regarding the vertical deflection, especially the restriction $R$, are not well-defined by codes.

Since there are not well defined thresholds regarding the restriction of the vertical displacements in bridge engineering, the computed vertical displacements $S$ are compared to three selected restrictions: $R_1 = L_{Cantilever}/1000$, $R_2 = L_{Cantilever}/500$, $R_3 = L_{Cantilever}/250$ and a coefficient of variation COV = 0.10. The evaluations of the limit state functions $g = R_i - S$ were performed for the dominate monitoring points with the First Order Reliability Method

This document is the intellectual property of the fib – International Federation for Structural Concrete. All rights reserved.
This PDF of fib Bulletin 86 is intended for use and/or distribution solely within fib National Member Groups.

FORM, which is an element of the software FREeT. Fig. 10-5 displays the condition indexes with respect to the defined constraints.

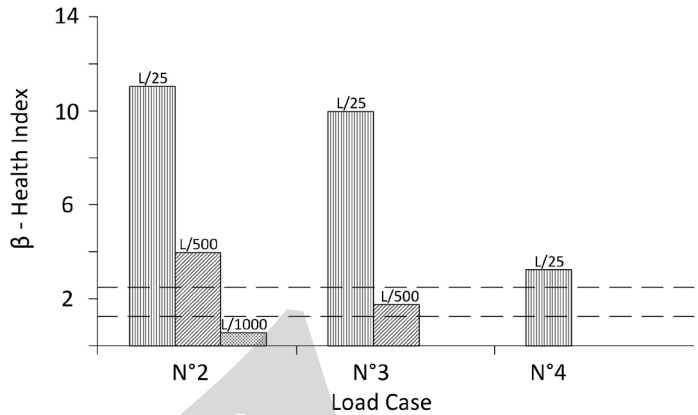


Fig. 10-5 Condition index vs. vertical constraints at the end of the cantilever

Only load case N° 2 satisfies the vertical displacement restriction of *L*/500 with respect to an allowable condition index of 2.8. The restriction of *L*/250 is covered by all load cases.

### 10.2.3 Ultimate Limit State ULS/Structure

The ultimate limit state (ULS) assessment was based according the degree of degradation on three considerations: (a) the structure undergoes no degradation process, (b) the area of pre-stressing tendons has already been reduced by 17 %, and (c) the area of pre-stressing tendons has already been reduced by 33 %. The damage degrees of 17 % and 33 % were derived without proof from test data. In addition, these two damage levels serve for the development of the time dependent reliability profile associated with the ultimate strength.

The carrying capacity of the structure could be detected by loosening the equilibrium conditions of the simulation process. Subsequently, the carrying capacity for each of the calculated individual samples (30 non-linear FE models) was collected to obtain a statistical response. This response is interpreted as the resistance *R*, fitted by a normal distribution. The derived resistance *R* compared with the existing traffic load *S*, expressed by a normal PDF, allowed the computation of the performance index $\beta$.

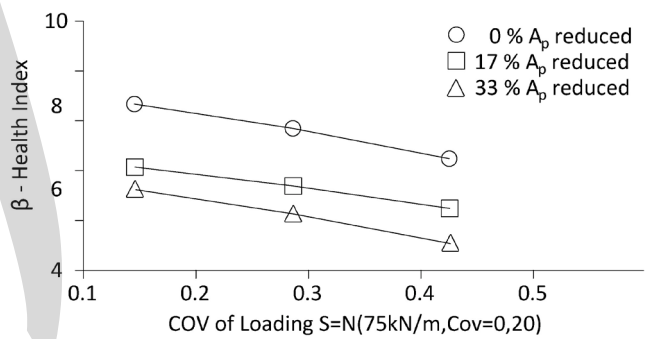


Fig. 10-6 Performance Index vs. variable COV of line load

This document is the intellectual property of the fib – International Federation for Structural Concrete. All rights reserved.
This PDF of fib Bulletin 86 is intended for use and/or distribution solely within fib National Member Groups.

Fig. 10-6 shows the performance index vs. the traffic load $S = N$ (75 kN/m, 75 kN/m · COV), associated with different COVs and the three previously mentioned damage scenarios according to the cross section of the pre-stress steel. More details about the modelling and local and global damage scenarios are given in[672, 738].

### 10.2.4 Time dependent degradation considerations

The probabilistic simulations presented provide tools for degradation considerations. A first approximation according to a degradation process can be a linear reduction of the pre-stressing tendon area (scenario 1, see Fig. 10-7). This model is based on tests carried out by[673] and defines a constant reduction of the reinforcement area as a function of the environmental conditions. The Colle Isarco Viaduct is located in a mean environmental condition, which caused an annual reduction of 40 µm of the reinforcement diameter. Combining this time-dependent area reduction with the probabilistic consideration results in the reliability profile "scenario 1" shown in Fig. 10-7. Model uncertainties were not included in those computations.

Scenario 2 assumes that after 30 and after 40 years a 17 % and a 33 % reduction of the cross-section of the pre-stressed steel will be detected, the probabilistic simulations yield to the reliability indexes as shown in Fig. 10-7 for "Scenario 2". The Weibull function can be used to extrapolate from those obtained reliability indexes the remaining lifetime, assuming no intervention will be performed.

Finally Scenario 3 is based on the assumption that a discrete inspection for the already 50 years existing structure gives a 33 % reduction of the cross-section of the pre-stressed steel. The associated computed and Weibull extrapolated reliability indexes are presented in Fig. 10-7. The Weibull function used for the prediction of the remaining lifetime allows a simple update of the parameters by new existing inspection information.

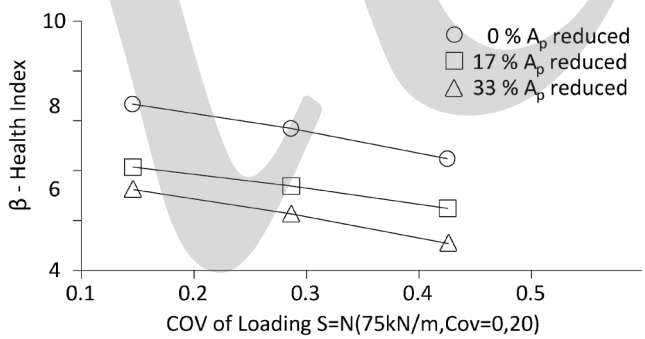


Fig. 10-7 Degradation models / health index vs. lifetime

### 10.2.5 Strengthening measures

The computed reliability index $\beta = 5.6$ (including model uncertainties $\beta = 4.6$) for a cross section reduction of the pre-stressing tendons = 17 % at 30 years is a crucial reason for an intervention or intervention planning. One of interventions could be the strengthening of the structure by raising the reliability to the initial reliability level without influencing the degradation process. Such an increase can be obtained by an external pre-stressing system. An optimization of the number of necessary tendons, the location of them and the required material properties with respect to the constraint of the initial

This document is the intellectual property of the fib – International Federation for Structural Concrete. All rights reserved.
This PDF of fib Bulletin 86 is intended for use and/or distribution solely within fib National Member Groups.

reliability index $\beta = 6.9$ leads to an external pre-stressing system of 8 tendons 1570/1770 0.6′. For a constant degradation rate the systems guaranteed not to violate the reliability level of 4.95 in the next 25 years. More details regarding the optimization of the location and size of tendons are given in[674].

#### 10.2.5.1 Conclusion

A complex methodology including nonlinearities in material, uncertainties and degradation phenomena is proposed for advanced life-cycle reliability analysis of reinforced concrete structures. The methodology described is compiled into the software tool SARA for instantaneous practical application. It represents an innovative decision-making tool for the maintenance of structures, which can be very powerful especially in combination with an existing health monitoring system.

The examples presented demonstrate the feasibility of the proposed procedure and developed program system. Based on selective inspection data, permanent monitoring and degradation models, the phenomenon of degradation and the decrease of the reliability index of bridges in time can be modelled. The concept is powerful too; to support inverse material detection algorithm to deviate time-dependent material conditions from monitored deflection lines.

#### 10.2.5.2 Acknowledgements

This research was conducted with the financial support of the Autobrennero Motor Highway A22, Italy, within the project “SARA” and “SARA M”.

The investigations are performed with the Technical University Bruno, Prof. Drahomir Novák, Prof. Bertislav Teply and Dr. David Lehký, Cervenka Consulting, Dr. Vladimir Cervenka and Dr. Radomir Pukl and the Autobrennero Motor Highway Dr. Ulrich Santa. The opinions and conclusions presented are those of the authors and do not necessarily reflect the views of the sponsoring organizations.

## 10.3 Reliability based structural and durability analysis of a prestressed-precast V-beam bridge - Italy

The preservation of an adequate safety level in concrete bridges subject to gradual degradation due to the in-service effects of traffic and environmental actions is commonly an expensive, and sometimes problematic, task. Chloride ion ingress is an important factor influencing both durability design and maintenance issues, especially in regions where winter de-icing salt application for traffic safety reasons is common, e.g. for highway structures. The following example introduces a feasible approach for the analysis of potential chloride induced corrosion and associated deterioration. It is presented in the context of an actual highway bridge application. Although the concrete bridge in question, the Neumarkt Bridge over the A22 motorway in northern Italy, was demolished after 38 years’ service, samples were extracted from the structure and the necessary chemical analyses were undertaken to establish chloride ion concentration profiles in the concrete. The chloride ion content values at the surface of the concrete were estimated by means of a numerical 1D model which performed an inverse analysis procedure. Subsequently a simulation was carried out using the cellular automata (CA) technique which enabled the laboratory results to be compared with those from a 2D numerical chloride ion ingress model. This work

This document is the intellectual property of the fib – International Federation for Structural Concrete. All rights reserved.
This PDF of fib Bulletin 86 is intended for use and/or distribution solely within fib National Member Groups.

was used to identify regions of the structure where the chloride ion content would reach a critical value (i.e. above the threshold level expected to cause corrosion of embedded steel reinforcement or prestressing). In addition to numerical and experimental investigations of chloride ingress and the corrosion processes, a performance assessment was made for the serviceability and ultimate limit states on the basis of code derived criteria; with the ultimate limit state analysis being performed for various times during the envisaged service life. This allowed circumstances to be identified which would result in the structure reaching the end of its effective service life. These outcomes can be used to inform decisions on the future management of the structure.

### 10.3.1 Introduction

As described earlier, concrete structures are commonly subjected to a variety of ageing processes including those arising from mechanical, environmental and chemical loadings, amongst others. As a result regular inspections need to be made in order to understand and take account of the effects of these processes. Indeed such control and inspection regimes are now common practice for bridge structures in most countries. However, these regimes are mostly based on making a subjective rating of the structural performance of the bridge concerned and they relate only indirectly to the actual mechanical load capacity (strength) of the structures.

As a result the remaining lifetimes of numerous reinforced and pre-stressed concrete structures are not being realistically assessed. This is particularly so for highway structures and bridges exposed to aggressive environmental conditions (e.g. de-icing salts), sometimes in combination with poorly executed interventions or maintenance works, which can result in significant reductions in their expected service lives. Furthermore, maintenance and intervention works programmes which are based on such inspection regimes are not optimised with respect to the actual load capacity or structural reliability of the population of bridges concerned.

However it is also recognised that the length of life that a structure achieves is strongly influenced by the maintenance strategy implemented, the assessment and maintenance planning tools available, and the owner's decisions on investments in interventions and remedial works needed to extend service life. Accordingly the objective of this case study is to illustrate the improvement that can be made to through-life care and management of concrete structures by effective inspection, degradation modelling and the numerical recalculation of structural performance. This approach should allow optimisation of the inspection, maintenance and repair periods and the associated scope of these activities, whilst allowing extension of the lifetime of the structure where this can be shown to be justified.

In general the applied tools involve advanced methodologies comprising non-linear finite element modelling, stochastic modelling and degradation simulation utilising a combination of software packages. Both theory and software are available for practical use, but they are rarely employed in current practice. This case study illustrates the application of these strategies and tools to the investigation and structural assessment of the three-span prestressed precast Neumarkt Bridge over the A22 motorway in northern Italy. The case study also examines several alternative bridge management strategies involving various types of potential remedial intervention works.

This document is the intellectual property of the fib – International Federation for Structural Concrete. All rights reserved.
This PDF of fib Bulletin 86 is intended for use and/or distribution solely within fib National Member Groups.

### 10.3.2 Neumarkt Bridge

The Neumarkt Bridge was a three-span prestressed precast bridge constructed over the A22 motorway in northern Italy in about 1970. It was demolished in 2008. Some details of the bridge are given in Fig. 10-8. Fig. 10-8 shows the geometrical form and dimensions of the longitudinal side elevation and Fig. 10-9 those of the cross-section of the bridge. The main span of 27.00 m was flanked by two side spans of 9.14 m.

The deck of the Neumarkt Bridge consisted of four precast pre-stressed V-girders with a cast in-situ concrete deck overlay; which is representative of the typical construction of high-way overpass bridges in the region. Each main span precast V-girder was pin and roller supported in the longitudinal direction and pin supported in the transversal direction. The top flanges of the V-girders were attached to the cast in-situ concrete slab, which had a thickness of 0.14 m. Accordingly, the bridge deck system was treated as an orthotropic concrete structure with the V-girders acting as the main structural elements. The bridge was divided into two traffic lanes, each 3.75 m wide, and two sidewalks, each 1.00 m wide – as it is shown in Fig. 10-9.

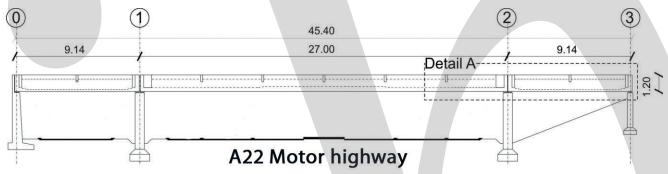


Fig. 10-8 Neumarkt Bridge over the A22 motorway, South Tyrol, northern Italy. Side elevation of Neumarkt Bridge. For Detail A see Fig 10-13

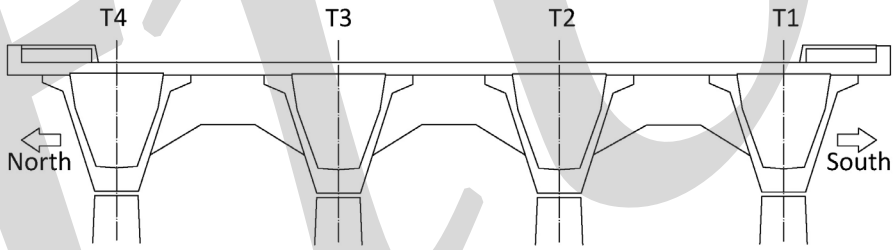


Fig. 10-9 Neumarkt Bridge over the A22 motorway, South Tyrol, northern Italy

### 10.3.3 Inspection

After being in service for 38 years the bridge was highly contaminated by chlorides from de-icing salts. The inspections noted severe water penetration problems through the deck slab movement joint between the main span and the side spans, which was located above the supporting columns. This was due to the failure of the sealing of the road deck slab joint. As a result the head of the supporting columns and the end zones of the main V-girders had experienced significant deterioration of the concrete surface and embedded reinforcement, which was associated with the chloride contamination of the concrete.

The following outlines the inspection and degradation timeline recorded for the Neumarkt Bridge: Inspections made in 1990 noted severe water penetration problems through the deck slab movement joint associated with the failure of the sealing of the

*This document is the intellectual property of the fib – International Federation for Structural Concrete. All rights reserved.*
*This PDF of fib Bulletin 86 is intended for use and/or distribution solely within fib National Member Groups.*

joint between the main span and the side spans. In 1996 the presence of longitudinal cracks on the inner face of the main V-girders and the immediate danger of massive concrete spalling led to the strengthening of the column heads in order to extend their service life -refer Fig. 10-11 and Fig. 10-12.

Demolition and reconstruction of the bridge was suggested on the basis of the 1999 inspection results.

The structure was demolished in spring 2008, after a final inspection by a combined research group from the Institute of Structural Engineering, Department of Civil Engineering and Natural Hazards, University of Natural Resources and Life Sciences, Vienna and of the Faculty of Civil Engineering, Technical University Brno, Czech Republic. At that time concrete cores and drilled powder samples were taken at various locations on the V-bridge girders and from the bridge deck slab. Fig. 10-13 shows the sampling locations. Unfortunately, it was not practical for physical loading tests to be performed prior to the demolition of the structure.

Fig. 10-10 Soffit of the Neumarkt Bridge showing the four columns between the main and side spans

Fig. 10-11 Strengthening of the column heads and the corrosion problems caused by severe water penetration through the deck slab movement joint due to the failure of the sealing of this joint

This document is the intellectual property of the fib – International Federation for Structural Concrete. All rights reserved.
This PDF of fib Bulletin 86 is intended for use and/or distribution solely within fib National Member Groups.

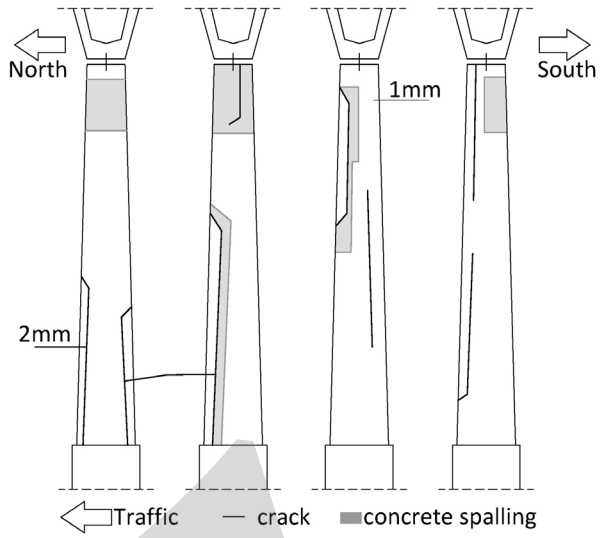


Fig. 10-12 Degradation of the four columns between the main and side spans as recorded in 1999

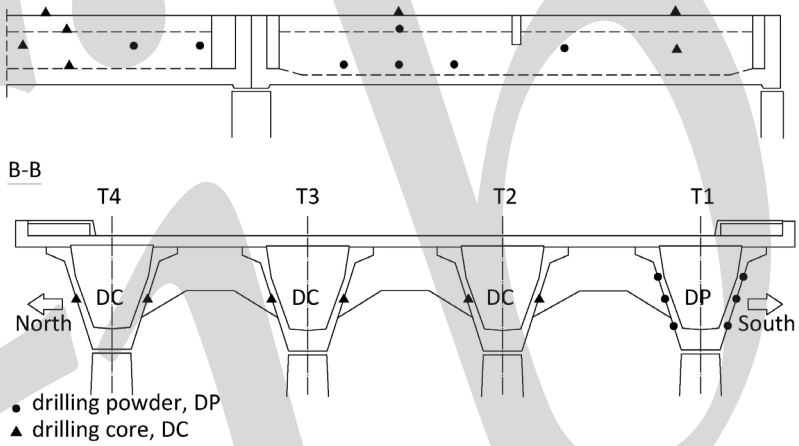


Fig. 10-13 Sampling scheme showing locations where drilled powder samples (DP) and drilled cores (DC) were extracted in 2008. (NB. Refer to Figure 10-8 for the location of Detail A)

## 10.3.4 Performance assessment activities

### 10.3.4.1 Introduction

Prior to the demolition of the bridge the following investigations were performed not only to verify the demolition decision, but also to obtain information to allow a structural assessment to be undertaken on the basis proposed in this case study. This work also allowed the theoretical examination of various possibilities for an extension of the service life of the bridge by considering several alternative bridge strengthening concepts.

Prior to demolition samples were taken at various locations on the V-girders and the bridge deck slab to give chloride ion profiles content with depth into the concrete. Chemical analysis performed in the laboratory allowed comparison with numerical chloride ingress simulations based on Fick's second law. Information was also obtained on the concrete pH-values, indicating that no significant depth of carbonation had occurred during the 38 year service life. Unfortunately no direct measurements were made of the chloride concentration at the surface of the concrete because of access limitations and time restrictions imposed during the bridge inspection.

*This document is the intellectual property of the fib – International Federation for Structural Concrete. All rights reserved.*
*This PDF of fib Bulletin 86 is intended for use and/or distribution solely within fib National Member Groups.*

The surface chloride concentration was estimated at various locations by means of an inverse analysis based on a numerical 1D-model of chloride ingress[611], which was used in combination with the results from the laboratory analysis.

A cellular automata (CA) technique was used to identify those regions in the V-girders where the level of chloride contamination of the concrete at the level of the reinforcing / prestressing steel was likely to be above the threshold deemed to initiate corrosion of embedded steel (taken to be 0.065 % by mass of concrete).

The FREET-D software provides a probabilistic prognosis of the steel corrosion process. Previously determined chloride concentrations on the surface of the V-girders, in the concrete itself and at the depth of the reinforcement served as input parameters that were determined as an antecedent step by the CA technique.

A non-linear finite element analysis (e.g. undertaken using the ATENA software[675] permitted a realistic evaluation of the structural response in the virgin condition and also in the deteriorated state (e.g. with a reduction of the effective reinforcement cross-sectional area due to corrosion). However, input data had to be assumed for the structure in the deteriorated state.

In consequence, uncertainties in input data were incorporated in the analysis of the structural behaviour by statistically-based probabilistic assessment methods provided in the software package SARA[314, 676, 557] classifies these techniques as Level Two assessment tools, which provide information on structural performance by estimating the failure probability $p_f$ and the reliability index $\beta$, respectively.

In addition, to perform a comprehensive structural performance assessment the values for numerous limit states were taken to be those given in EN 1990[557]. Values established in this way included those associated with the maximum allowable concrete stress, along with stress values for mild and prestressing steels under static and dynamic loading.

Finally, the remaining lifetime of the structure was determined on the basis of the corrosion associated time dependent failure probabilities $p_f$. These failure probabilities were obtained from the previously mentioned discrete time-based probabilistic analyses which took account of the effective reduction in the cross-sectional area of the reinforcement due to corrosion. The following Sections give more detail of the matters described in outline above.

#### 10.3.4.2 The cellular automata technique

A cellular automaton is a special class of evolutionary algorithms, a mathematical idealisation of physical systems in which space and time are treated as being discrete. In principle, any physical system which can be defined in terms of differential equations may be approximated as a cellular automaton by introducing discrete coordinates and variables, as well as discrete time steps. A practical application is the modelling of the chloride ion diffusion process in concrete[617, 618, 619] Models for chloride penetration based on the conventional diffusion theory at the macroscopic level are often used (i.e. employing Fick´s second law and the law of mass conservation). Consequently, this can be used to represent the ingress of chlorides into concrete, which can vary significantly both in terms of space (i.e. location) and time.

The cellular automaton technique is very effective at representing variations in the time and location of a salt solution (i.e. involving the application of 2D modelling techniques). In addition the random nature of this process can be modelled. A cellular automaton

*This document is the intellectual property of the fib – International Federation for Structural Concrete. All rights reserved.*
*This PDF of fib Bulletin 86 is intended for use and/or distribution solely within fib National Member Groups.*

consists of a collection of cells (often regular uniform cells) on a grid of specified shape that evolves through a number of discrete time steps according to a set of local rules based on the states of the neighbouring cells. The rules are then applied iteratively for as many time steps as desired. The simulated overall time interval is then the sum of all time steps. Each cell has its own state value, which represents the current component concentration (e.g. chloride ions). The process of chloride ingress is governed by a local rule in which the evolutionary coefficients, the diffusion coefficient, cell size and time step are all involved.

#### 10.3.4.3 Chloride ion concentration on the surface of the V-girders

On the basis of the results of the inspections and some preliminary simulations, it was evident that not all parts of the V-girders had been equally exposed to chlorides. As noted previously, it was not possible to measure the external supply of chloride during the inspection of the Neumarkt Bridge (i.e. as would be represented by the chloride ion concentration on the surface of the concrete). However, as the chloride ion supply is the key input information for the simulation of degradation, considerable effort was put into evaluating this parameter.

The starting point was recognition that the Neumarkt Bridge crossed over a highway with heavy two-lane traffic which both (1) lifted the de-icing salt solution (i.e. the chloride ions) from the highway surface in the form of a spray and (2) created air turbulence between the V-girders which distributed the spray unevenly over the soffit of the bridge deck. It was decided to consider this effect as the main hazard to the lower part of the V-girders. Fig. 10-14 shows the uneven distribution of chloride ion over the lower part of the V-girders. The following methodology was used to estimate the chloride ion concentration on the surface of the V-girders.

The values of chloride concentrations estimated from the laboratory testing for different locations and depths into the concrete were substituted into the relatively simple formula of the 1D model[611] which allowed the back calculation of the chloride ion concentration on the surface of the concrete. The 1D model was used to obtain estimates of the surface chloride ion values for every drilled location.

Using the results from V-girder T1, which was the only fully sampled cross-section (refer Figure 10-6), the effect of air turbulence on the distribution of chloride ion content in the concrete of the lower part of the V-girders was investigated. This revealed that the lower part of the T1 V-girder surface facing the oncoming traffic and the soffit zone had appreciably higher chloride ion content values than the T1 V-girder surface facing the departing traffic. The effect is depicted in Fig. 10-14 (A).

After certain averaging and simplification, the surface chloride ion concentration values were determined. It was assumed that turbulence effect was similar for the zones between all the V-girders. As a result only one V-girder was analysed (the T1 Vgirder), with the results being presented in Fig. 10-14 (B).

This document is the intellectual property of the fib – International Federation for Structural Concrete. All rights reserved.
This PDF of fib Bulletin 86 is intended for use and/or distribution solely within fib National Member Groups.

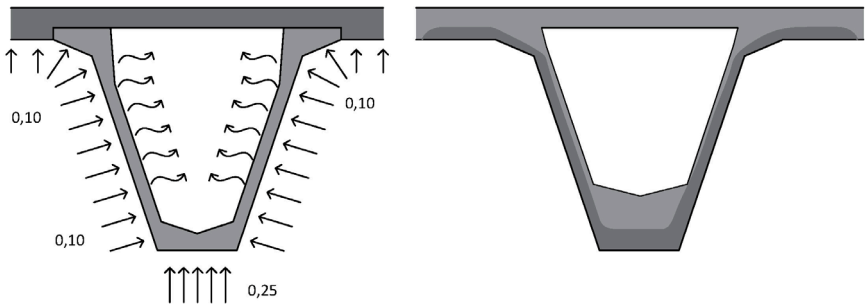


Fig. 10-14 A: Estimated chloride ion concentrations on the lower surfaces of the V-girder T1. B: chloride ion concentrations after 38 years in service – as simulated by the CA technique

### 10.3.3.4 Summarising

Evaluation of the laboratory results established that:

In most cases the chloride ion content $T_F/T_R$ ratio was larger than 1.0; where: $T_F$ = traffic facing; that is the chloride ion content on the V-girder surface facing the oncoming traffic (i.e. the front of the oncoming vehicles), and $T_R$ = traffic reverse; that is the chloride ion content on the V-girder surface facing the departing traffic (i.e. the rear of the departing vehicles). This outcome verified the assumption made regarding the effect of air turbulence produced by the traffic and the influence of traffic direction upon the chloride ion concentration on the various surfaces of the V-girders. The effect is depicted in Figure Fig. 10-14 (A). This shows that the lower part of the traffic facing surface and the soffit had appreciably higher chloride ion content values than the (traffic) reverse surface.

In the majority of samples the chloride ion content decreased and pH values increased with depth into the concrete. This was as expected and was taken to provide a general verification of this aspect of the investigation. The laboratory results were subsequently used as follows.

The data on chloride ion concentration values (obtained for different locations and depths into the concrete) were used for the back calculation of chloride ion concentrations on the concrete surface to make a more detailed assessment of regions where the critical chloride ion concentration had been reached (i.e. the chloride threshold value deemed to initiate corrosion of embedded steel).

The data about pH values was used in the later modelling of reinforcement corrosion.

### 10.3.4.5 Chloride ion concentration at the depth of the reinforcing steel

Using the estimated chloride ion surface concentrations presented in Fig. 10-14 (A), simulations of chloride ingress were performed by the cellular automaton technique as follows. For the present example the diffusion coefficient was kept constant over the simulation period and over the cross-section. The size of a cell was 7 mm and the time step duration was 35 days. Fig. 10-14 (B) shows the pattern of the estimated chloride ion concentration after 38 years in service. The critical chloride ion concentration (i.e. the chloride threshold value deemed to initiate corrosion of embedded steel) is represented by the black area in Fig. 10-14 (B). In this case the chloride threshold value ($C_{cr}$) was taken to be a chloride ion concentration of 0.065 % by mass of concrete.

This document is the intellectual property of the fib – International Federation for Structural Concrete. All rights reserved.
This PDF of fib Bulletin 86 is intended for use and/or distribution solely within fib National Member Groups.

#### 10.3.4.6 Prognosis of the steel corrosion process

Due to the presence of chloride ions, the assessment of the reinforcement degradation during the propagation period had to consider the potential effect of stress corrosion cracking (SCC) and / or pitting corrosion. The prestressing steel used for the Neumarkt Bridge was, due to its production protocols, unlikely to suffer from SCC. Accordingly, pitting corrosion was considered to be the deterioration mechanism most likely to influence the performance of the Neumarkt Bridge. A statistical analysis was performed using a model for pitting corrosion developed by[677] to provide statistical characterisation of the effective decrease in steel cross-sectional area due to the effects of corrosion. The corresponding simulations were carried out using the FREET-D probabilistic calculation tool[595].

#### 10.3.4.7 Nonlinear finite element analysis

Efficient techniques for undertaking both nonlinear numerical and stochastic methods of analysis of engineering structures were combined in the "SARA" research project[676]. This offered an advanced tool for reliability based assessment of the realistic behaviour of concrete structures. Within the framework of this complex approach, attention is paid to modelling of degradation phenomena in the manner described above. The deterioration mechanisms considered included carbonation of concrete, corrosion of reinforcement, chloride induced corrosion, etc. All elements of the analysis (structural analysis, reliability assessment, inverse analysis and degradation modelling) are contained within the SARA (safety and reliability assessment) software system.

The structure of the SARA software package and the interactions between the different program modules is shown schematically in Figure 10-15. The overall software package includes the following modules:

- SARA: A software shell which controls the communication between the individual programs listed below[676].
- ATENA: This performs nonlinear FEM analysis of concrete structures[675].
- FREET: This is the probabilistic engine of the software system, it utilises the Latin Hypercube Simulation (LHS) technique[678, 168].
- DLNNET: Artificial neural network software[399].
- FREET-D: The concrete degradation module based on FREET[595].
- CATES: This is the cellular automata degradation simulation module[618].

This document is the intellectual property of the fib – International Federation for Structural Concrete. All rights reserved.
This PDF of fib Bulletin 86 is intended for use and/or distribution solely within fib National Member Groups.

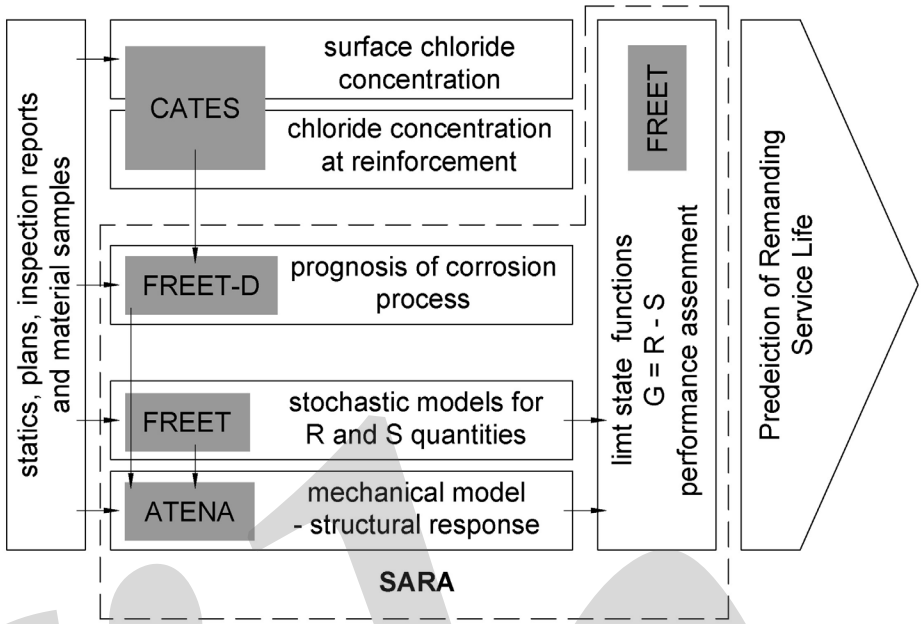


Fig. 10-15 Elements of the SARA (safety and reliability assessment) software system

In order to be able to accurately assess the reliability level of a structure, structural response needs to be calculated for defined load situations based on realistic material models. In this study made using the SARA software shell, structural response is calculated by the ATENA module[675]. The constitutive concrete model SBETA[159] was chosen from several other available material models. Cracking and distributed reinforcement can both be addressed by the 'smeared' approach. This means that certain material properties that are defined / determined for points of the structure are not localised, but always valid for the entire finite element. In addition reinforcement can be represented by discrete elements, if required.

The material model SBETA is able to represent the most relevant characteristics of concrete[679]. These are: non-linear behaviour in compression, including hardening and softening, fracture in tension determined by a fracture-mechanics approach, and a biaxial strength failure criterion. Changes in material strength due to a cracking like reduction of compressive strength, reduction of shear stiffness (variable shear retention) and the tension stiffening effect are also accounted for. The smeared approach implies perfect bond between the distributed reinforcement and concrete; whereas different multi-linear bond models are available when modelling the reinforcement as discrete reinforcing bars. Cracking itself is described by either fixed crack direction (where the orientation of the initiated cracks are kept fixed during the whole analysis and loading process; with shear forces acting on the crack interfaces) or rotated crack direction (where the orientation of the cracks follow the principal stresses; with no shear forces acting on the crack surfaces)[671].

### 10.3.4.8 Probabilistic performance assessment

In general the determination of the safety level of a structure involves the formulation of: Limit state equations for serviceability conditions and ultimate state load bearing capacity; Stochastic models for relevant scattering input variables; A mechanical model, which can be formulated in either an analytical or a numerical format, describing the relation between

*This document is the intellectual property of the fib – International Federation for Structural Concrete. All rights reserved.*
*This PDF of fib Bulletin 86 is intended for use and/or distribution solely within fib National Member Groups.*

input variables and structural response. Although theoretically the safety level can be obtained by direct integration of an analytical formulation, in practice only the application of approximation or simulation techniques is feasible. The former approach includes FORM (first order reliability method) and SORM (second order reliability method)[77]. The latter approach includes Monte-Carlo type sampling techniques, where a limited number of samples is generated and evaluated with respect to the formulated limit state conditions. Since the determination of reliability levels for classical Monte-Carlo simulations needs large numbers of samples, which is not feasible considering the computational demand for nonlinear finite element models, the number of simulations has to be reduced. FREET, the probabilistic engine of the SARA software system, includes Latin Hypercube Sampling (LHS)[388, 680]. This has demonstrated that it allows the satisfactory estimation of the structural reliability level using a relatively low number of analyses.

Note: LHS is a special type of numerical probabilistic simulation where the range of the cumulative distribution function of each random variable is divided into N intervals of equal probability. The regularity of sampling over the range of cumulative distribution functions ensures efficient sampling of the random variables.

The calibration of the non-linear finite element model included the following steps: The geometrical and reinforcement properties were taken from construction drawings. The material properties were extracted from the original design and inspection protocols, as well as from associated literature sources.

The documented prestressing procedure of the V-girders was checked to ensure compliance with the allowable maximum and minimum concrete stress during the different construction stages in order to avoid cracking and thus ensure a suitable calibration of the non-linear finite element model. In particular, the critical situations during the initial prestressing without dead weight, during the removal of the formwork and the final maximum loading situation according to the original design ensure a highly adapted non-linear static model.

This procedure, together with the default values of the material models defined in ATENA[671] and stochastic model parameters extracted from literature[177], gave an estimated confidence level of over 80 % for the structural response (ATENA + FREET = SARA). Nevertheless, there is still a need for measurements and the investigation of actual material properties to get a more accurate determination of the confidence level.

#### 10.3.4.9 Structural performance associated limit states

As previously mentioned a stratified Monte Carlo based analysis was performed for the bearing capacity and the serviceability performance of the structure. This was done in order to capture the dispersion of material-resistance and of load model properties. In particular, the Latin Hypercube Sampling based software FREET[168] reduced the number of analyses required to 30.

The required inputs such as stochastic models for concrete, for mild steel (e.g. used as smeared reinforcement in the numerical model) and for prestressing steel were derived on the basis of laboratory tests and inspection reports. Included are the respective literature sources[671] that, on one hand, served to fill in for missing data and, on the other hand, for the verification of the derived stochastic models.

The gradual increased load model LM1 given in EN1991-2 (Clause 4.3.2), together with the variability in the material characteristics, cause scatter in the structural response

This document is the intellectual property of the fib – International Federation for Structural Concrete. All rights reserved.
This PDF of fib Bulletin 86 is intended for use and/or distribution solely within fib National Member Groups.

which is presented in terms of deflection, concrete stress and steel stress values. These responses serve in the following as actions, $S$, and with respect to the EN 1992[681] defined limits, $R$, to create limit state functions in the form of Equation 10.3-1. For instance, the limit state function $G_0$ addresses the load capacity of the whole structure and is formulated as follows:

$$G_0 = R - S_{LM1,100\%} = 0 \tag{10-3}$$

where $R$ = loading capacity of the cross-section derived from EN1992, and SLM1,100% = the loading arising from the completely applied load model LM1.

The limit state functions $G_1$ and $G_2$ relate to the concrete compressive strength, which EN 1992-1-1 (Clause 7.2) indicates is formulated for quasi-permanent load combination as

$$G_1 = k_1 \cdot f_{ck} - \sigma_c = 0 \tag{10-4}$$

or

$$G_2 = k_2 \cdot f_{ck} - \sigma_c = 0 \tag{10-5}$$

for the characteristic load combination, where $k_1$ and $k_2$ are code based proportional factors equal to 0.45 and 0.6; $f_{ck}$ = characteristic concrete strength; and $\sigma_c$ = computed concrete stress (i.e. a load action). The mild steel strength associated limit state function $G_3$ can be formulated as

$$G_3 = k_3 \cdot f_{yk} - \sigma_a = 0 \tag{10-6}$$

and in particular for indirect forces as

$$G_4 = k_4 \cdot f_{yk} - \sigma_a = 0 \tag{10-7}$$

where $k_3$ and $k_4$ = code defined proportional factors equal to 0.8 and 1.0; $f_{yk}$ = characteristic code based yield strength; and $\sigma_a$ is the computed mild steel stress. In consequence, the prestressing steel associated limit state is characterised by

$$G_5 = k_5 \cdot f_{pk} - \sigma_p = 0 \tag{10-8}$$

with $k_5$ = code defined proportional factor equal to 0.75; $f_{yk}$ = characteristic code based yield strength; and $\sigma_p$ = the computed stress of prestressing steel. Beyond the material associated limit states there are the deformation based limit states, such as the maximum vertical deflection permitted by EN 1992-1-1, Clause 7.2. These limit states are defined for the quasi permanent load combination by

$$G_6 = l/500 - u = 0 \tag{10-9}$$

or for the frequent load combination by

$$G_7 = l/250 - u = 0 \tag{10-10}$$

where $l$ = span width and $u$ = deflection. The crack width w based limit state can be formulated for the quasi permanent load-combination and a severe environmental exposure class[681] as follows

$$G_8 = 0.2 - w = 0 \tag{10-11}$$

and for a characteristic load-combination by

$$G_9 = 0.3 - w = 0 \tag{10-12}$$

*This document is the intellectual property of the fib – International Federation for Structural Concrete. All rights reserved.*
*This PDF of fib Bulletin 86 is intended for use and/or distribution solely within fib National Member Groups.*

In summary, the limit state functions $G_1$ to $G_9$ are characterised by the: Quantities $f_{yk}$, $f_{ck}$, and $f_{pk}$; the properties can be extracted from tests of material specific samples or in case of missing samples from, say, documented conformity tests. Factors $k_1$ to $k_5$, that are specified in the EN1992 standard (CEN 2004) according to the loading format and the structure specific details, representing the barriers R. Computed quantities $\sigma_c$, $\sigma_a$, $\sigma_p$, $u$, $w$, SLM1,100 % stand for actions, $S$.

The objectives of the following discussed probabilistic analyses were the assessment of the ultimate limit state G0 and the serviceability limit states $G_1$ to $G_9$ with respect to the gradually increased load model LM1 for the virgin and for the degraded structure states. The previously described corrosion scenarios serve for the definition of the degradation processes.

### 10.3.4.10 Loading and finite element discretisation

A two-dimensional finite element analysis was able to provide a reasonable representation of the structural system of the Neumarkt Bridge. Fig. 10-16 portrays:

- The subdivision of the main V-girders into 87 macro elements.
- The discretisation of V-girder T2 by means of 6467 quadrilateral elements with a medium element size of 0.05 m and total of 29,689 nodes.
- The course of the prestressing cables in V-girder T2.
- The horizontal projection of the V-girder next to the bridge bearing.
- The idealised V-girder section used for the ATENA 2D model.

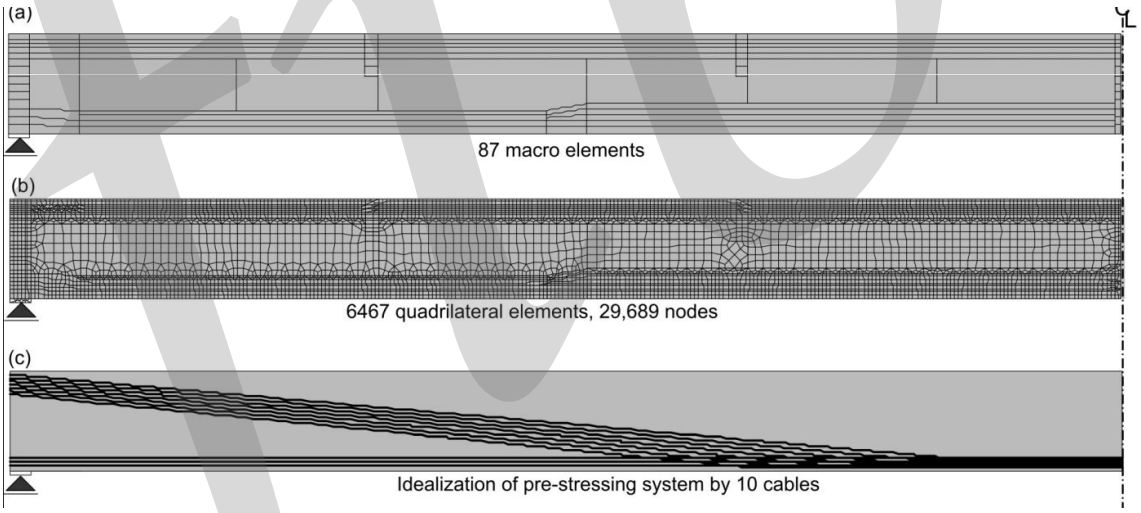


Fig. 10-16 Computational model for V-girder T2 located in the main span of the Neumarkt Bridge; Part A: Subdivision of the V-girder into macro elements; Part B: Finite element meshing for the V-girder; Part C: Prestress cables within the V-girder

The high number of macro elements employed was required to capture the mild steel reinforcement, in both the horizontal and the vertical (stirrups) orientations, by means of smeared reinforcement models[671]. More details of the smeared reinforcement ratio used are given below. The use of a 0.05 m element size also allowed the development of a well-conditioned finite element net which provided satisfactory definition of the mechanical characteristics of the cross-member and of the bottom slab, the thickness of which varied along the length of V-girder T2, as is shown in Fig. 10-16(A).

*This document is the intellectual property of the fib – International Federation for Structural Concrete. All rights reserved.*
*This PDF of fib Bulletin 86 is intended for use and/or distribution solely within fib National Member Groups.*

These model properties have been derived from the original design and construction documentation, as well as from inspection reports, and accordingly serve as a satisfactory basis for determining time-varying reliability levels. The mechanical characteristics of the previously mentioned pre-stressing system, which can be severely and adversely effected by corrosion processes, were obtained from the original design documents which identified these as 0.5 " diameter strands with a yield strength of 1540 MPa and a tensile strength of 1770 MPa. In addition, the V-girders are factory pre-loaded by the prestressing system. Bond between the strands and the concrete was assumed to be perfect.

Fig. 10-16 (C) shows the idealised pre-stressing system used in the ATENA 2D analysis. In particular, the loading associated with the prestressing procedure was applied in load steps according to the original design in the following way:

The V-girders were loaded to 20 % of their own weight.

The first out of three increments of the required prestressing force were applied to the V-girder; this situation was load case 5.

The V-girders were loaded to 40 % of their own weight.

The second out of three increments of the required prestressing force was applied to the V-girder; this situation was load case 6 -refer Fig. 10-17(E). The V-girders were loaded to 40 % of their own weight. The final increment of the required prestressing force was applied to the V-girder; this situation was load case 7 -refer Fig. 10-17 (E).

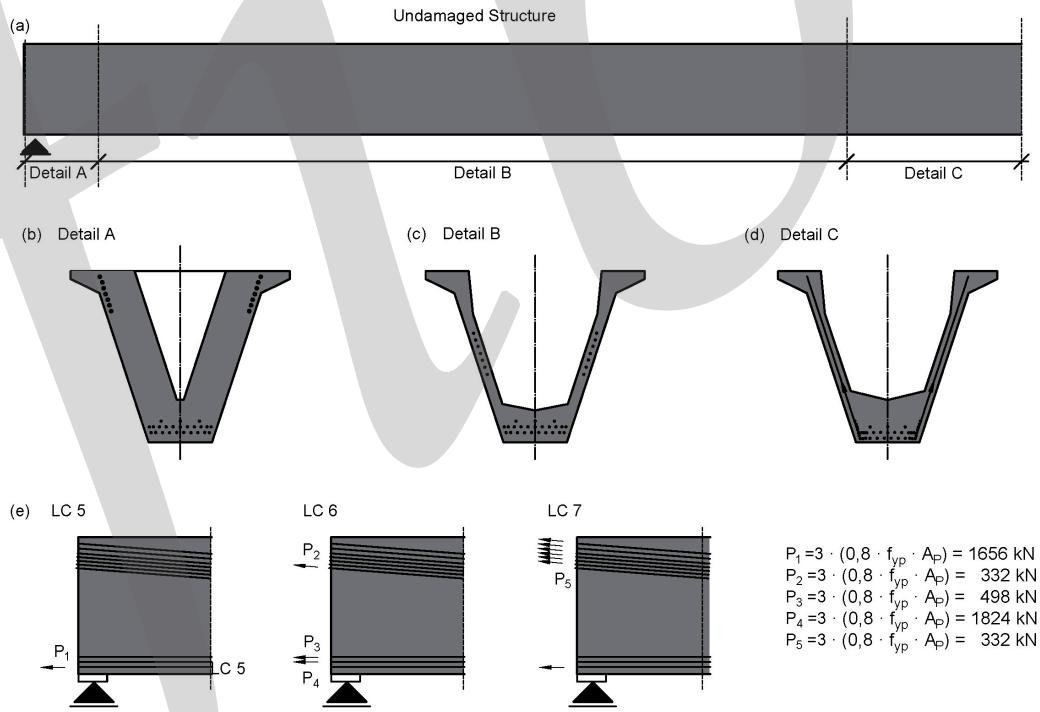


Fig. 10-17 Prestressing of the undamaged V-girder T2 located in the main span of the Neumarkt Bridge

Part A: Side elevation view – showing Zones A – C (Details A -C).

Part B: End cross-section in Zone A (Detail A).

Part C: Cross-section in Zone B (Detail B).

*This document is the intellectual property of the fib – International Federation for Structural Concrete. All rights reserved.*
*This PDF of fib Bulletin 86 is intended for use and/or distribution solely within fib National Member Groups.*

Part D: Cross-section in Zone C (Detail C).

Part E: Prestressing forces applied for load cases 5 to 7.

The prestressing load cases are grouped according to the topology of the strands: the horizontal strands are considered in load case 5 and the inclined strands in load cases 6 and 7, see Fig. 10-17(E). Of particular interest was the extent to which the LM1 traffic load model within EN1991 (CEN 2002 – 2006), as shown in Fig. 10-18, could be applied to a bridge structure designed in the 1960's. Therefore, the first steps of LM1 were applied in 20 % increments, later steps in 5 % increments and the remaining steps in 2 % increments until 120 % of the defined LM1 value was reached. In total 29 monitoring points were placed on the bottom and top surface of V-girder T2 (see Fig. 10-19) in order to monitor the V-girder's response throughout the entire simulated loading process.

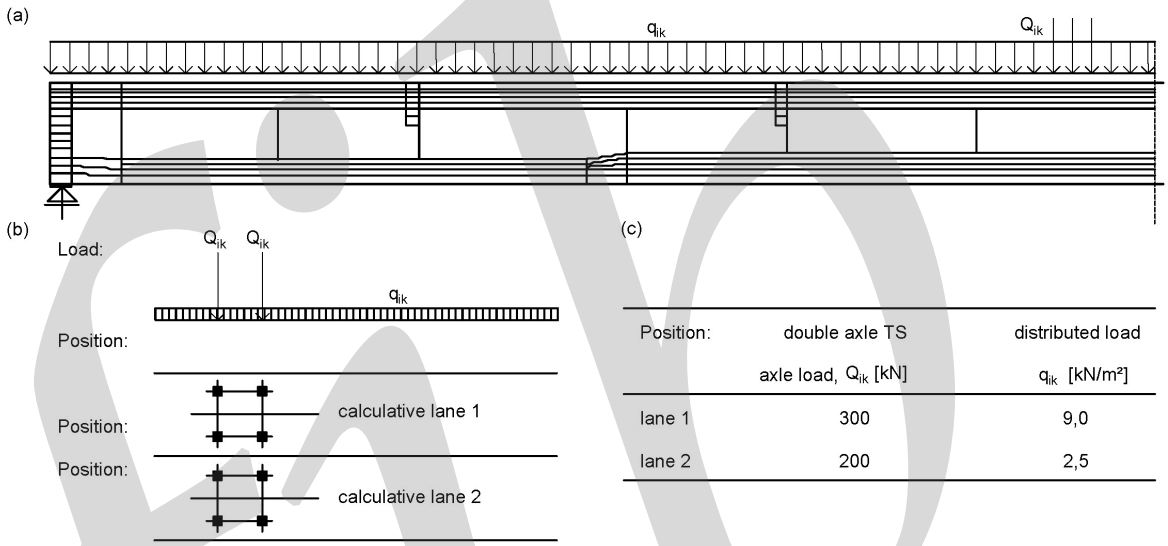


| Position: | double axle TS axle load, $Q_{ik}$ [kN] | distributed load $q_{ik}$ [kN/m²] |
|---|---|---|
| lane 1 | 300 | 9,0 |
| lane 2 | 200 | 2,5 |

Fig. 10-18 Load model, LM1, defined by EN1991-2 Clause 4.3.2 applied to V-girder T2

Part A: Loading scheme.

Part B: Definition of distributed loads and axle loads for the LM1 load model.

Part C: Table of loads according to the LM1 load model.

Unfortunately, as already noted, it was not possible to convince the bridge owner to undertake a proof loading test. This would have allowed the collection of data to perform an additional calibration of the non-linear finite element model before the bridge was demolished. In particular, in most of the monitoring points the deflection, the longitudinal stress, the longitudinal strain and the crack width were recorded. Fig. 10-19 shows the topographical and the measurement quantities of the monitoring points used in the numerical analysis.

Performance assessment of undamaged V-girders Fig. 10-20 portrays the computed serviceability versus ultimate limit state quantities for the undamaged structure for the gradually increasing load model LM1. The lower horizontal axes of the graphs show the probability density function (PDF) of the ultimate limit of the bearing capacity *R*, and the upper horizontal axes show the degree of the deterministically applied load model LM1 indicated by *S*.

*This document is the intellectual property of the fib – International Federation for Structural Concrete. All rights reserved.*
*This PDF of fib Bulletin 86 is intended for use and/or distribution solely within fib National Member Groups.*

The vertical axes of Fig. 10-20 present the simulated serviceability quantities of:

Part A: The vertical displacement, $u$, at monitoring point m7.

Part B: The upper surface concrete stress of the V-girder, $\sigma_{co}$, at monitoring point m3.

Part C: The crack width, $w$, for the lower surface of the V-girder at monitoring point m8.

Part D: The lower surface concrete stress of the V-girder, $\sigma_{cu}$, at monitoring point m9.

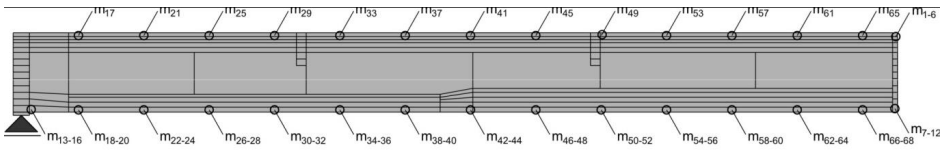


| Mon. Point | x [m] | y [m] | Characteristic | Mon. Point | x [m] | y [m] | Characteristic |
|---|---|---|---|---|---|---|---|
| $m_{7\text{-}12}$ | 13.50 | 0.01 | w, $w_d$, $\sigma_{xx}$ | $m_{1\text{-}6}$ | 13.50 | 1.20 | w, $w_d$, $\sigma_{xx}$ |
| $m_{18\text{-}20}$ | 1.00 | 0.02 | w, $w_d$, $\sigma_{xx}$ | $m_{17}$ | 1.00 | 1.20 | $\sigma_{xx}$ |
| $m_{22\text{-}24}$ | 2.00 | 0.03 | w, $w_d$, $\sigma_{xx}$ | $m_{21}$ | 2.00 | 1.20 | $\sigma_{xx}$ |
| $m_{26\text{-}28}$ | 3.00 | 0.01 | w, $w_d$, $\sigma_{xx}$ | $m_{25}$ | 3.00 | 1.20 | $\sigma_{xx}$ |
| $m_{30\text{-}32}$ | 4.00 | 0.01 | w, $w_d$, $\sigma_{xx}$ | $m_{29}$ | 4.00 | 1.20 | $\sigma_{xx}$ |
| $m_{34\text{-}36}$ | 5.00 | 0.01 | w, $w_d$, $\sigma_{xx}$ | $m_{33}$ | 5.00 | 1.20 | $\sigma_{xx}$ |
| $m_{38\text{-}40}$ | 6.00 | 0.01 | w, $w_d$, $\sigma_{xx}$ | $m_{37}$ | 6.00 | 1.20 | $\sigma_{xx}$ |
| $m_{42\text{-}44}$ | 7.00 | 0.03 | w, $w_d$, $\sigma_{xx}$ | $m_{41}$ | 7.00 | 1.20 | $\sigma_{xx}$ |
| $m_{46\text{-}48}$ | 8.00 | 0.01 | w, $w_d$, $\sigma_{xx}$ | $m_{45}$ | 8.00 | 1.20 | $\sigma_{xx}$ |
| $m_{50\text{-}52}$ | 9.00 | 0.01 | w, $w_d$, $\sigma_{xx}$ | $m_{49}$ | 9.00 | 1.20 | $\sigma_{xx}$ |
| $m_{54\text{-}56}$ | 10.00 | 0.01 | w, $w_d$, $\sigma_{xx}$ | $m_{53}$ | 10.00 | 1.20 | $\sigma_{xx}$ |
| $m_{58\text{-}60}$ | 11.00 | 0.01 | w, $w_d$, $\sigma_{xx}$ | $m_{57}$ | 11.00 | 1.20 | $\sigma_{xx}$ |
| $m_{62\text{-}64}$ | 12.00 | 0.01 | w, $w_d$, $\sigma_{xx}$ | $m_{61}$ | 12.00 | 1.20 | $\sigma_{xx}$ |
| $m_{66\text{-}68}$ | 13.00 | 0.01 | w, $w_d$, $\sigma_{xx}$ | $m_{65}$ | 13.00 | 1.20 | $\sigma_{xx}$ |

Fig. 10-19 Monitoring layout for the numerical simulation of V-girderT2

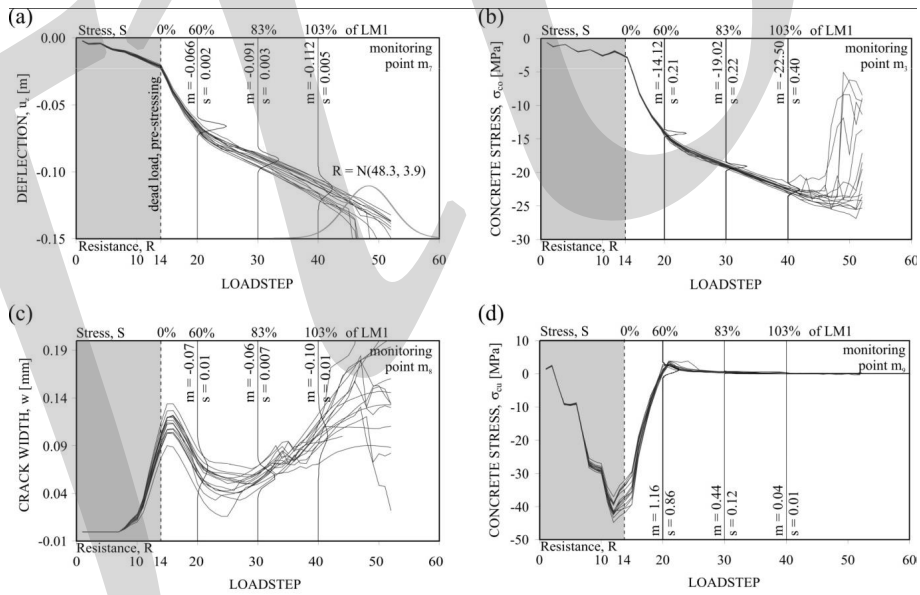


Fig. 10-20 Statistical response of the undamaged structure for gradual increase in load model LM1 Part A: Vertical deflection in the vertical centre line (vCL): monitoring point "m7". Part B: Concrete stress on the top of the V-girder next to the vCL: monitoring point "m3". Part C: Crack width on the bottom of the V-girder next to the vCL: monitoring point "m8". Part D: Concrete stress on the bottom of the V-girder next to the vCL: monitoring point "m9"

This document is the intellectual property of the fib – International Federation for Structural Concrete. All rights reserved.
This PDF of fib Bulletin 86 is intended for use and/or distribution solely within fib National Member Groups.

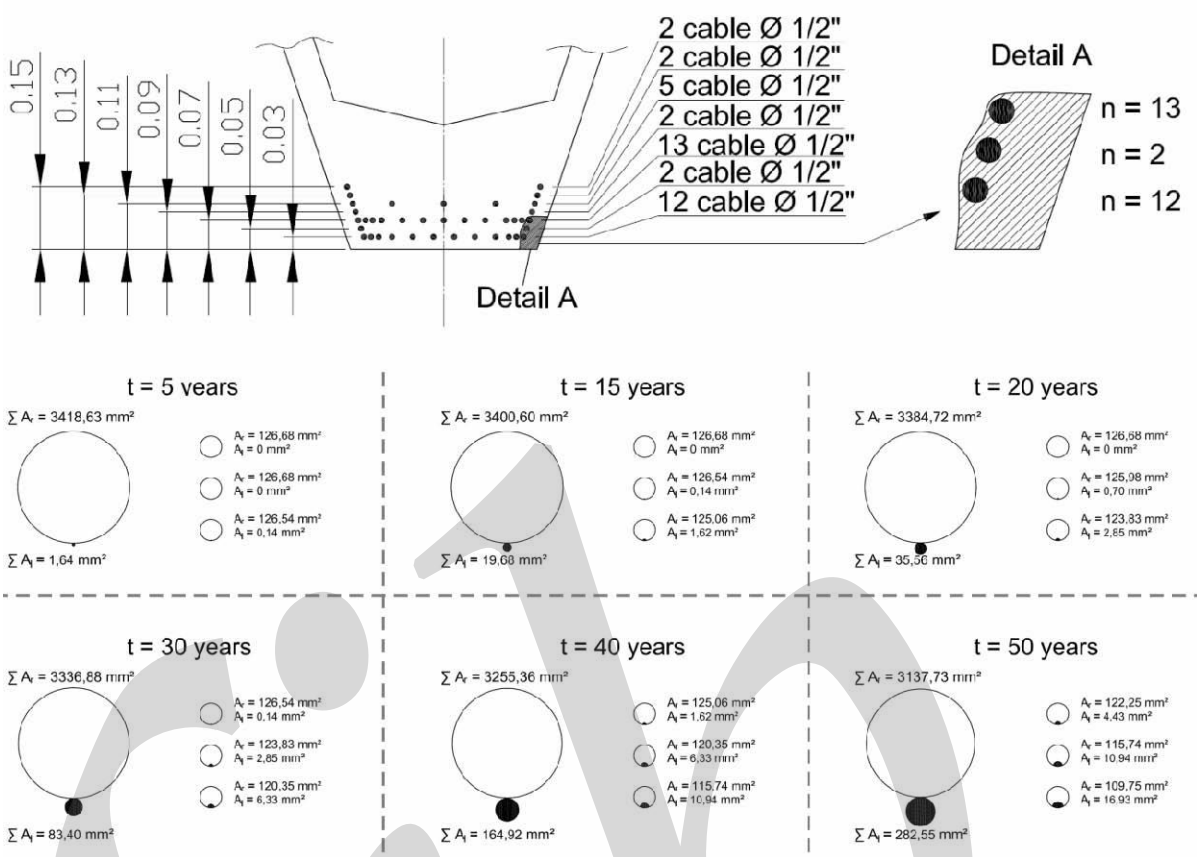


Fig. 10-21 The reduction in the cross-sectional area of the prestressing strands of the 1st, 2nd and 3rd layers for discrete durations of pitting corrosion, $t = x$ years NB. The black circles represent the mechanically inactive cross-section – lost due to corrosion

### 10.3.4.11 Performance assessment of damaged V-girders

The time variable reduction of the cross-sectional area of the prestressing steel due to the effects of corrosion was taken as the most significant damage scenario for the V–girders. The corrosion initiation time of 8 years had been computed using the cellular automata (CA) technique, based on the measured chloride ion concentrations in the drilled concrete powder samples taken from the structure. Fig. 10-21 presents the CA computed loss in cross-sectional area in the prestressing strands in the lower levels of the V-girders for pitting corrosion propagation periods of $t = 5, 15, 20, \ldots 50$ years. The black cross-section areas indicate the proportion of the prestressing strand which is mechanically inactive / lost in the simulated corrosion state.

The load capacity of the whole structure in a deteriorated state was established by means of limit state $G_0$ taking account of the reduction in the cross-sectional area of the prestressing strands due to pitting corrosion at the mid-span position. For example, with an acting load of 60 % of the LM1 load model value and using the numerically derived PDF of the reduced resistance $R$; the following reliability index values were obtained[682]:

For a corrosion propagation period (t) of 30 years: $\beta_0 > 10$

For a corrosion propagation period (t) of 50 years: $\beta_0 > 7.8$

For an acting load of 103 % of the LM1 load model value; the following reliability index values were obtained:

*This document is the intellectual property of the fib – International Federation for Structural Concrete. All rights reserved.*
*This PDF of fib Bulletin 86 is intended for use and/or distribution solely within fib National Member Groups.*

For no corrosion induced deterioration of the prestressing strands: $\beta_0$ = 2.47 [design]

For a corrosion propagation period (t) of 30 years: $\beta_0$ = 1.37

For a corrosion propagation period (t) of 50 years: $\beta_0$ = 0.14

Fig. 10-22(A) and Fig. 10-22 (D) portray the bundle of simulated structural responses of the Vgirder after a corrosion propagation time of 30 years. The overall outcome was that the bearing capacity of the V-girder with respect to the LM1 load model was inadequate due to the effects of corrosion, indicated by the small reliability index value of $\beta_0$ = 1.37.

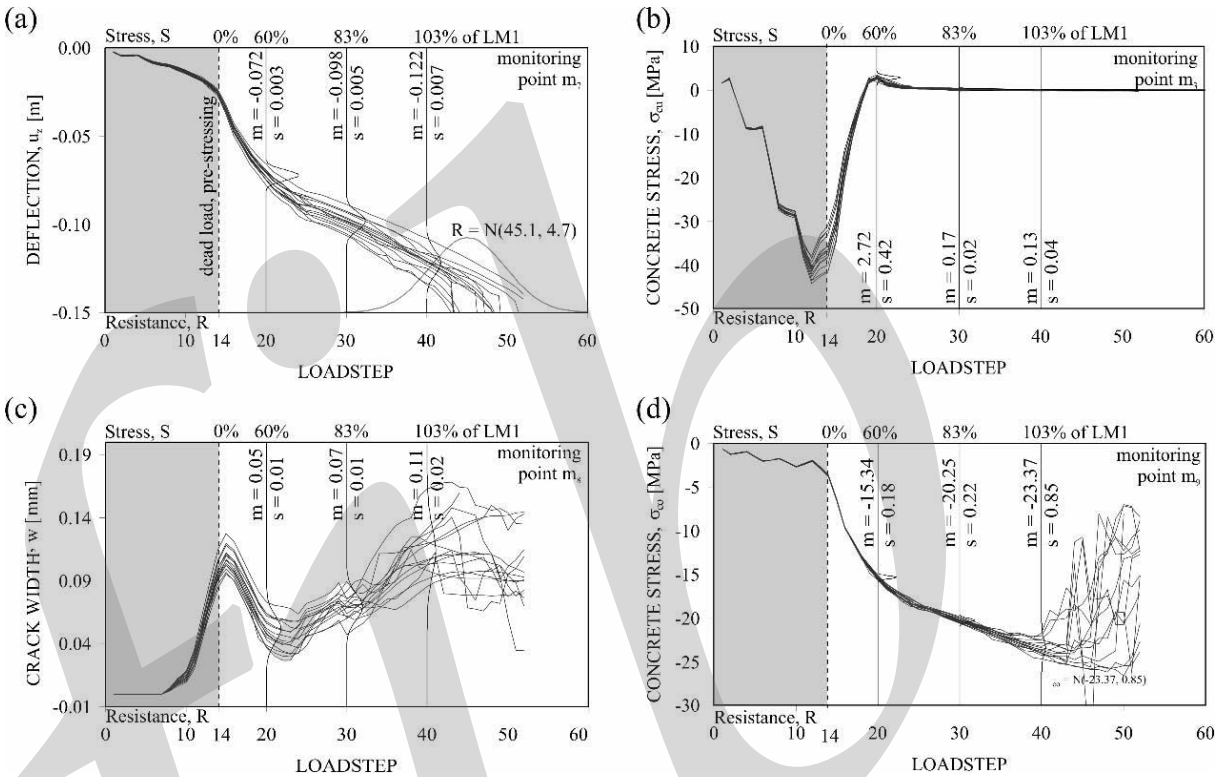


Fig. 10-22 Statistical response of the structure damaged by 30 years pitting corrosion for the gradual increase in load model LM1

### 10.3.4.12 Bridge management – Some possible scenarios

Use of the numerical analysis procedures described above would have justified an extension in the service life of the V-girders by at least 20 years beyond the date of demolition in 2008. If the information from these analyses had been available, the following alternative scenarios could have been considered with respect to the management and maintenance strategy for the Neumarkt Bridge, possibly resulting in overall cost savings. It should be noted that the available inspection reports were used as the basis for developing scenarios for lifetime management of the bridge without interventions being made.

If the severe water penetration problems through the deck slab movement joint between the main span and the side spans detected in 1990 had been resolved at that time, a remaining lifetime of some 18 years could have been justified. The anticipated lifetime was estimated assuming that the V-girders and columns were still subject to ongoing chloride induced deterioration. Fig. 10-23 shows the estimated change in bridge condition rating with time for this scenario and anticipated remaining lifetime of 18 years, giving the estimated end of service for the Neumarkt Bridge as 2008. Note this scenario did not

This document is the intellectual property of the fib – International Federation for Structural Concrete. All rights reserved.
This PDF of fib Bulletin 86 is intended for use and/or distribution solely within fib National Member Groups.

involve the strengthening of the concrete columns. Thus, a critical condition rating would be reached after only 38 years' service, which is considerably less than the structural life of 80 years assumed in design.

In 1996 a further inspection showed substantial damage of the columns due to the leaking water. As a result the heads of the columns were strengthened by applying confinement to the concrete at the head of the columns – as shown in Fig. 10-10. In spite of the strengthening, the remaining lifetime was only some 12 years, as a result of the faster deterioration rate. The end of service for the Neumarkt Bridge was 2008, when the bridge was demolished. Thus a service of only 38 years is achieved, which is considerably less than the structural life of 80 years assumed in design

If instead of strengthening the degraded concrete columns, they had been replaced in 1996; then the V-girders would have become the critical structural elements which would have determined the overall lifetime of the bridge. On this basis the Neumarkt Bridge could have remained in service for about another 32 years, giving an estimated end of service of 2028 as shown in Fig. 10-23.

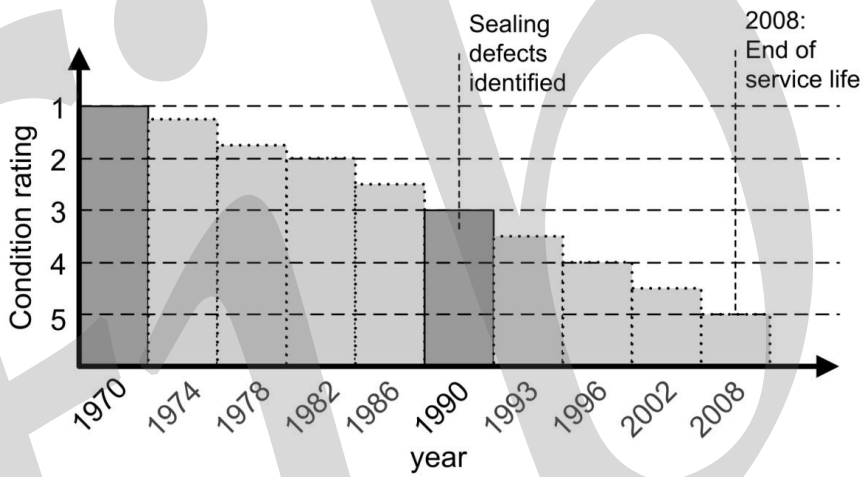


Fig. 10-23 Condition rating assessment and anticipated remaining lifetime of the Neumarkt Bridge assuming the deck slab movement joint was re-sealed in 1990, with no further leakage after that time.[Note. No provisional strengthening of the concrete columns]

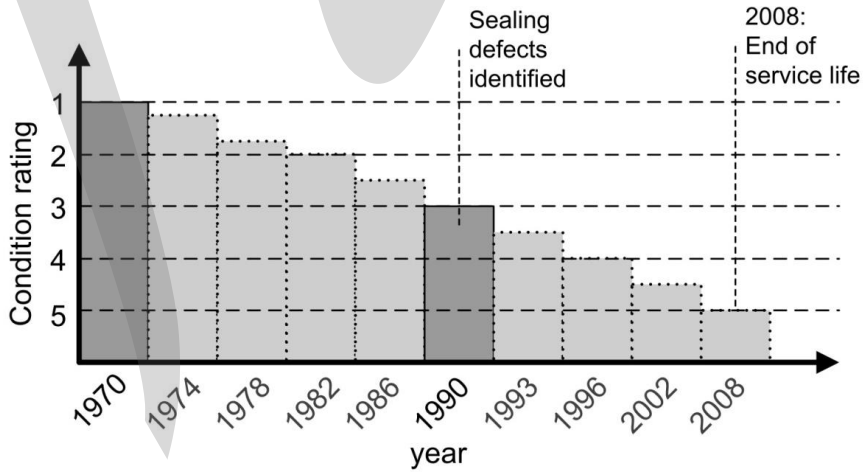


Fig. 10-24 Condition rating assessment and actual remaining lifetime of the Neumarkt Bridge following the provisional strengthening of the columns in 1996

This document is the intellectual property of the fib – International Federation for Structural Concrete. All rights reserved.
This PDF of fib Bulletin 86 is intended for use and/or distribution solely within fib National Member Groups.

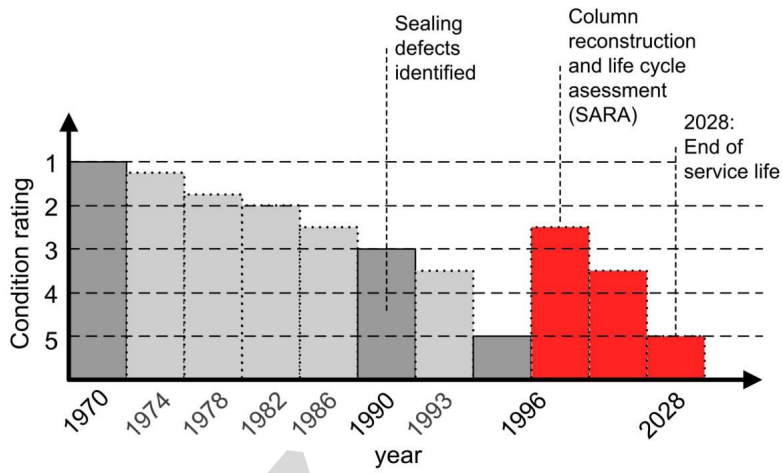


Fig. 10-25 Condition rating assessment and estimated remaining lifetime of the Neumarkt Bridge after column replacement

Fig. 10-23 to Fig. 10-25 show the estimated change in the condition rating (safety level) of Neumarkt Bridge with and without the benefit of the information provided by the previously described numerical analyses. These considered different maintenance and intervention strategies. The levels shown represent the estimated condition rating with respect to the virgin state right after construction and are derived from available inspection reports based on traditional condition rating methodologies as specified in international guidelines such as RVS (1995) or DIN (1999). Light grey areas denote the anticipated change in the condition rating between the available inspection information (shown as a darker grey).

Fig. 10-24 depicts the evolution of the bridge condition rating (safety level) with time for an alternative maintenance strategy – the replacement of the columns in 1996. Since the structural elements most affected by degradation are removed in this scenario, the V-girders become the critical elements for the overall reliability level. Thus this remedial action, in combination with the proposed numerical methodology consisting of the cellular automata approach for chloride ingress prognosis, corrosion simulation and nonlinear mechanical analysis of the structure, allows for an extension of the service life for at least a further 30 years (calculated as a prognosis from 1996) for the then acting loads.

Thus the proposed approach for the remaining lifetime assessment of existing structures under chloride attack can provide a basis for objective decision making that would permit a degree of optimisation of the maintenance strategy of a particular structure. In general, starting after the completion of construction works a regular inspection schedule including mainly visual inspection would be followed as detailed in codes and guidelines. In the case where critical damage is encountered, e.g. a sealing defect, the proposed structure management methodology could kick in, see Fig. 10-25. Basically it would be possible to increase the level of confidence in the condition of the structure by any of the following approaches:

- Evaluating the effects of damage by means of nonlinear mechanical analyses.
- Predicting corrosion initiation and propagation by cellular automata simulations.

The proposed combined approach, as described in this case study.

This document is the intellectual property of the fib – International Federation for Structural Concrete. All rights reserved.
This PDF of fib Bulletin 86 is intended for use and/or distribution solely within fib National Member Groups.

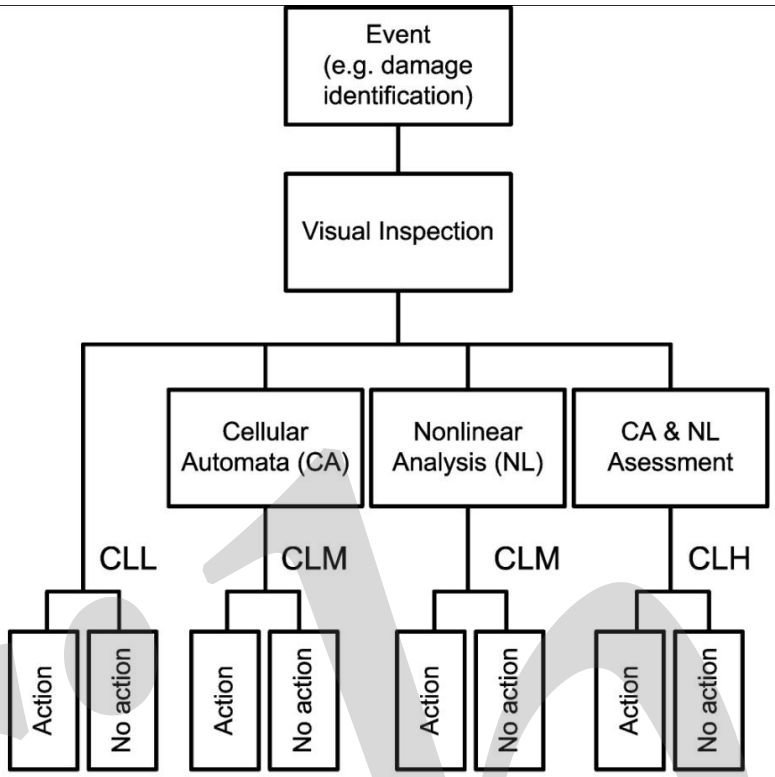


Fig. 10-26 Decision tree after an event (e.g. identification of damage). The use of the presented tools would improve the confidence level in a decision from low (CLL) to medium (CLM) to high (CLH). Note: An "action" could be some form of intervention such as strengthening or possibly reconstruction of a part of the structure

### 10.3.4.13 Concluding comments

There is growing interest in the justification of the extension of the remaining lifetime of structures through the application of advanced methodologies comprising non-linear finite element modelling, stochastic modelling and degradation simulation utilising a combination of software packages. Both theory and software are available for practical use, but they are rarely employed in current practice.

This case study has illustrated the application of these strategies and tools to the investigation and structural assessment of the three-span prestressed precast Neumarkt Bridge over the A22 motorway in northern Italy. The case study has also examined several alternative bridge management strategies involving various types of potential remedial intervention works.

In the case of the Neumarkt Bridge an extension of the service life of some 20 to 30 years would have been possible based on the mechanical performance of the bridge and associated assumptions about the aggressivity of the environment (i.e. the chloride burden) and there being no significant changes in the volume of traffic or in its composition.

Consequently, the application of such numerical analysis techniques, which are able to quantify the degree of damage to the structure and the reduction in lifetime expectancy, can provide decision-maker with objective data allowing different maintenance and intervention strategy options to be explored. Fig. 10-26 shows a decision tree which allows evaluation of the influence of different assessment strategies on the level of confidence associated with structure management decisions.

This document is the intellectual property of the fib – International Federation for Structural Concrete. All rights reserved.
This PDF of fib Bulletin 86 is intended for use and/or distribution solely within fib National Member Groups.

As would be expected, extended analyses will make the assessment process more expensive. However, the outcomes may permit an extended service life or alternative maintenance strategies which save money in the long run. Such considerations are covered by established risk assessment tools such as the terminal analysis (TA) approach, which is a combined fault tree and cost analysis approach. Details are given in[46].

## 10.4 Monitoring and analysis for the evaluation of fatigue resistance in existing post-tensioned concrete bridges

In Germany before 1970, thermal stresses were neglected in the design of post-tensioned continuous concrete bridges. This could cause problems in cross-sections with low permanent load. For example, the points of zero moment are effected, where the tendon coupler assemblies are normally positioned. The lower fatigue resistance of these structural members may lead to fatigue of the post-tensioning steel and as a consequence to a cross-section failure later on. Therefore refined structural analysis needs to be used to estimate the risk of a fatigue failure in these areas. Because of the non-linear behaviour of post-tensioned concrete structures the results strongly depend on the distribution of the permanent internal forces, which are uncertain due to time dependent losses and redistributions. To achieve more realistic results two methods for the evaluation of the risk of a fatigue failure at coupling joints have been developed at the department of concrete structures (Technische Universität München). The first uses probabilistic investigations[683] and the second is based on long term measurements in combination with analysis[684] and is presented in this chapter.

### 10.4.1 Background – Behaviour of prestressed concrete bridges subject to fatigue loading

One of the basic principles to evaluate fatigue relevant stresses in reinforced concrete and prestressed concrete design is to neglect the flexural tensile strength of concrete. Hence the reinforcement stress amplitudes in reinforced concrete members are approximately linear dependent on the variations in traffic loads. In contrast to this in prestressed concrete bridges the stress amplitudes $\Delta\sigma_s$ (referring to reinforcing steel) and $\Delta\sigma_p$ (referring to prestressing steel) do not only depend on the traffic loads but are significantly influenced by the basic loads acting at the same time, i.e. load due to the basic combination of non-cyclic actions, e.g. permanent loads as well as temperature effects. In Fig. 10-27a the relationship between the total acting bending moment $M$ and the prestressing steel stress $\sigma_p$ as well as the relationship between the actual basic moment $M_0$, i.e. the bending moment due to the basic combination of non-cyclic actions, and the stress amplitude $\Delta\sigma_p$ are shown. To compute the latter relation a constant variation of the bending moment $\Delta M_q$ = const. resulting from traffic loads was assumed. Due to the nonlinear cross-sectional behaviour the stress amplitude increases significantly if the moment $M_D$ referring to the decompression of the section is exceeded.

Assuming a continuous prestressed beam, the basic moment $M_0$ consists of the permanent bending moment $M_{\text{perm}}$ and the moment $M_{\Delta t}$ which results from the temperature difference $\Delta T_v$, Eq.(10-13). $M_{\text{perm}}$ is caused by dead loads $M_g$ including redistributions due to creep and shrinkage in bridges constructed span-by-span, the permanent indirect actions $M_{\Delta s}$, e.g. imposed deformations and the statically indetermined effects of prestressing $M_{p,ind}$, (10-14).

This document is the intellectual property of the fib – International Federation for Structural Concrete. All rights reserved.
This PDF of fib Bulletin 86 is intended for use and/or distribution solely within fib National Member Groups.

$$M_0 = M_{perm} + M_{\Delta T} \tag{10-13}$$

$$M_{perm} = M_g + M_{\Delta s} + M_{p,ind} \tag{10-14}$$

As the temperature effects change during the day, also the basic bending moment $M_0$ and hence the reinforcement stress amplitudes $\Delta\sigma$ vary (Fig. 10-27b). Additional long-term influences are affecting $M_0$ and the moment of decompression $M_D$ besides the daily varying thermal effects. Geometrical inaccuracies and variations in creep and shrinkage – especially considering the redistribution of permanent loads in a structure built span-by-span - lead to variations in dead load forces ($\Delta M_g$). In addition to the overall effects related to the basic moment $M_0$ deviations in the actual prestressing force, e.g. due to local prestressing losses, have an important impact on the decompression moment $M_D$ hence on stress amplitudes and fatigue damage.

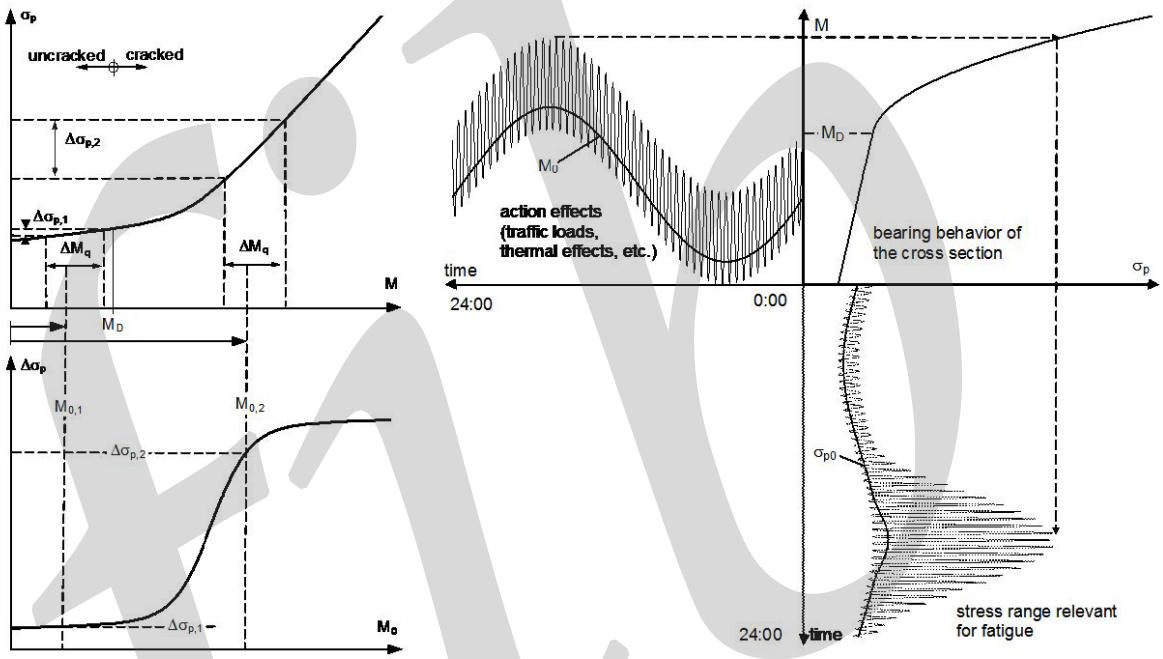


Fig. 10-27 a) relationship between bending moment and reinforcement stresses versus relationship between basic bending moment and stress amplitudes (schematic); b) variation of stress amplitudes during the day due to the changing basic bending moment (schematic)

## 10.4.2 Monitoring

Long term measurement has been performed to detect the moment of decompression $M_D$ of the cracked coupling joint cross-section. Therefore, the influence of the temperature load on the crack width amplitudes under dynamic traffic load was observed. For most of the measurements the point of decompression could clearly be identified in the measurement[685, 686]. The risk of a fatigue failure could then be analysed (see Fig. 10-28) by using the permanent moment, including an exact value for the additive moment $\Delta M$ resulting from the monitoring instead of a value on the safe side given by codes or regulations.

This document is the intellectual property of the fib – International Federation for Structural Concrete. All rights reserved.
This PDF of fib Bulletin 86 is intended for use and/or distribution solely within fib National Member Groups.

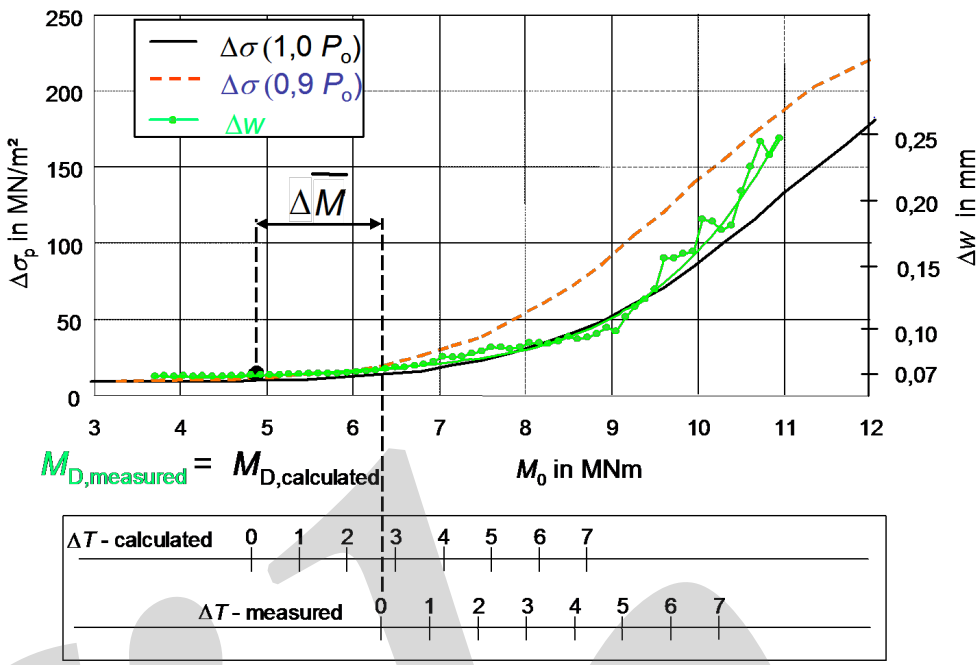


Fig. 10-28 Calculated basic bending moment $M_0$ – stress amplitudes $\Delta\sigma_p$ - relation in comparison to measured crack width to determine the additive moment $\Delta M$

But for the bridge, which is shown in the following, a more extensive analysis was necessary, because the crack was in an open state for all measured temperature loads. The results of this monitoring are shown in[684]. They are used to calibrate a finite element model. With this simulation more realistic stress ranges are determined and afterwards the risk of a fatigue failure is estimated with a service strength evaluation. The procedure is shown in detail in[684] for two bridges. Here a short overview for one monitoring is given.

## 10.4.3 Measuring set-up

The behaviour of the cross-section is detected by measuring concrete strains and crack width changes. Because of the non-destructive installation used it could be guaranteed, that the bond stress-slip relationship is unchanged, whereby no redistributions of stresses could occur.

Fig. 10-29 shows the arangement of the measuring devices at the cross-section of the coupling joint. The crack width sensors (R1 to R4) are positioned directly over the crack. The bridge has two traffic lanes. Both lanes are used by trucks. The crack propagation has a height of 0.2 m on the left web and on the right web 2.0 m. This is why the measurment has primarily been performed on the right side of the bridge.

The concrete strains are measured on the right web on both sides of the coupling joint with the sensors D1 and D2 and on the left side at only one side of the joint with Sensor D3. These cross-sections are uncracked, so the occuring strain amplitudes are nearly independent from the existing basic bending moment $M_0$. They only depend on the traffic load in the considered time interval. Additionally the temperature load of the bridge is determined with 8 temperature sensors, which are distributed over the cross-section according to previous investigations.

This document is the intellectual property of the fib – International Federation for Structural Concrete. All rights reserved.
This PDF of fib Bulletin 86 is intended for use and/or distribution solely within fib National Member Groups.

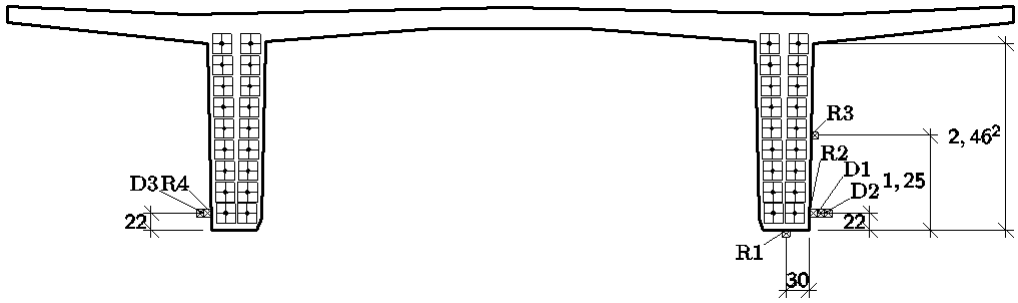


Fig. 10-29 Cross-section with measuring set-up

To monitor the dynamic changes caused by the traffic loads the measurement is performed with a rate of 100 Hz. Due to the temperature dependency they are carried out for a period of about three months, which should include hot weather conditions. The large amount of collected data is minimized by partial analysis on site. Afterwards this data is automatically transmitted with a GSM modem and used as a basis to investigate the relations between temperature changes, dynamic traffic loads and development of crack widths.

#### 10.4.3.1 Analysis of the thermal load

The vertical temperature difference $\Delta T_v$ and the superstructure temperature $T$ are calculated by using the values of the 8 temperature measurement points. Therefore a post-processor was developed, which allows converting the temperatures of the measurement points into constant and linear cross-section temperature values[684].

### 10.4.4 Analysis of the concrete strains and the crack width

The traffic load of the bridge is obtained by the evaluation of the amplitudes of the strain sensors D1 to D3. The simultaneous measurement of the crack width changes caused by the traffic load provides conclusions about the bearing behaviour of the cracked coupling joint cross-section under the existing traffic and temperature loads.

#### 10.4.4.1 Finite element simulation

The finite element simulation is performed with the general-purpose-program MARC. MENTAT. With this program it is possible to include special material properties in user subroutines. This is used to simulate the long term bearing behaviour of cross-sections with coupling joints. The concrete is simulated with plane stress elements, the tendons and couplers with truss elements and the bond with non-linear springs. In the model the following characteristics are taken into account.

#### 10.4.4.2 Long term effects

The effects of creep and shrinkage of concrete and relaxation of prestressing steel are included by defining hypoelastic materials:

$$\Delta\sigma = D \cdot \Delta\varepsilon + \Delta G \tag{10-15}$$

where $D$ = modified elastic material tensor; $\Delta_G$ = tensor of substracted incremental relaxation stresses caused by creep and shrinkage (concrete) or relaxation (prestressing steel).

This document is the intellectual property of the fib – International Federation for Structural Concrete. All rights reserved.
This PDF of fib Bulletin 86 is intended for use and/or distribution solely within fib National Member Groups.

Shrinkage is implemented with the model of the CEB-FIP Model Code 90[140].

$$\varepsilon_{cs}\left(t-t_s\right)=\varepsilon_{cs0}\cdot\beta_s\left(t-t_s\right) \tag{10-16}$$

where $\varepsilon_{cs0}$ = notional shrinkage coefficient; $\beta_s$ = coefficient to describe the development with time; $t$ = age of concrete (days); $t_s$ = age of concrete (days) at the beginning of shrinkage.

To include the shrinkage effects in Eq. (10-15) the uni-axial strains are transformed in bi-axial relaxation stresses.

$$\Delta G_{cs}=D\cdot\Delta\varepsilon_{cs} \tag{10-17}$$

For the implementation of the creep effects and the development of the modulus of elasticity a 7 branch Maxwell Model with the parameters given by[687] is used. This model is almost perfectly equivalent to the creep model given in CEB-FIP Model Code 90:

$$E_{ci}(t)=\beta_E(t)\cdot E_{ci} \tag{10-18}$$

$$\varepsilon_{cc}\left(t,t_0\right)=\varphi\left(t,t_0\right)\frac{\sigma_c\left(t_0\right)}{E_{ci}} \tag{10-19}$$

where $\beta_E(t)$ = age dependent coefficient; $\varphi(t,t_0)$ = creep coefficient; $E_{ci}$ = modulus of elasticity at the age of 28 days.

To include the model in Eq.(10-15) the viscous part is considered in the elastic material stiffness tensor $D$ and the relaxation stresses of the Maxwell Chains are integrated in the tensor $\Delta G$:

$$D=\sum_{i=1}^{7}\frac{\alpha_i\left(t+\Delta t\right)}{1+\dfrac{\Delta t}{\tau_i}}D_{el}\quad \Delta G_{cc}=-\sum_{i=1}^{7}\frac{\Delta t}{\tau_i+\Delta t}\sigma_i(t) \tag{10-20}$$

The increase of the plastic strains $\varepsilon_p$ and the reduction of the modulus of elasticity caused by the dynamic loads are implimented with a model created by[688]. This is a simplifed damage model, which assums that $\varepsilon_p$ inceases monotonic and only depends on the stiffness at the beginning $E_{c0}$, the cracking strain $\varepsilon_0$, the high and low stresses and the number of the load cycles $N$.

$$D\frac{1}{1+\dfrac{2\varepsilon_p}{\varepsilon_0}}D_{el}\quad \Delta G_{cz}=D\cdot\Delta\varepsilon_p \tag{10-21}$$

The long term effects of the prestressing reinforcement are described by the model of[689].

$$\sigma_p(t)=\sigma_p^I\left[1-\frac{\log t}{k}\left(\frac{\sigma_p^I}{f_{p0.1k}}-0.55\right)\right] \tag{10-22}$$

where $\sigma_p^I$ = initial stress at t = 0.

This document is the intellectual property of the fib – International Federation for Structural Concrete. All rights reserved.
This PDF of fib Bulletin 86 is intended for use and/or distribution solely within fib National Member Groups.

#### 10.4.4.3 Bond stress-slip relationship

The bond stress between the concrete and the reinforcing bars and the tendons is calculated with the nonlinear model given in CEB-FIP Model Code 90.

#### 10.4.4.4 Results of the simulation

The measured crack amplitudes for a fixed traffic load range, determined with sensor D2, are taken and mean values for classes of the temperature difference $\Delta T_v$ were calculated. The classes of the temperature load $\Delta T_v$ have been converted into basic bending moments $M_0$ with a linear elastic calculation. The results are shown in Fig. 10-30. Because of the crack opening behaviour over the height of the web it was possible to calibrate the FE simulation by comparing the measured and calculated crack amplitudes, caused by traffic load. Fig. 10-30 shows the results for 70 % of the calculated direct prestressing force $P_{dir,0}$ and for a permanent moment $M_{perm,existing}$, which is 2.2 MNm larger than the calculated moment.

$$P_{dir,0,existing} = 0.7 P_{dir,0} \tag{10-23}$$

$$M_{perm,existing} = M_{perm} + 2.2 MNm \tag{10-24}$$

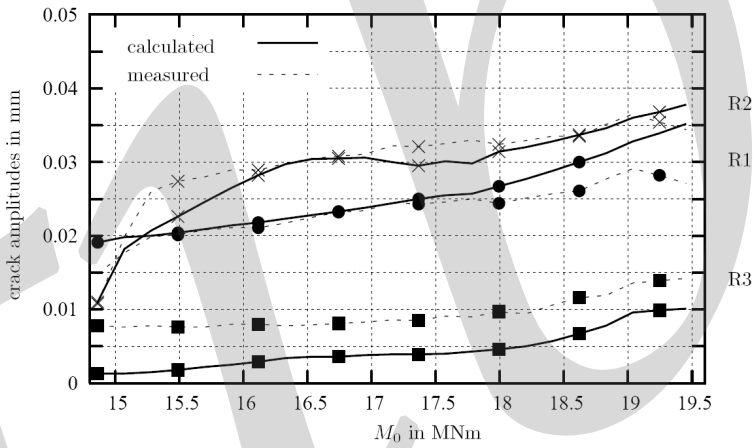


Fig. 10-30 Comparison between the calculated and measured crack amplitudes

### 10.4.5 Verification of the service stress range of the tendon coupler assemblies

The service stress range verification for the bottom tendon layer of this cross-section is performed with the measured temperature and traffic loads. The values for the existing prestressing force and the permanent load are taken from the FE simulation. The used S-N-curve is the standard curve for couplers in DIN-Fachbericht 102[690]. With this the fatigue damage $D$ is calculated using Palmgren-Miner summation for a service life of 100 years. It can be shown that the damage is acceptable for this bridge and strengthening measures concerning fatigue are not necessary.

$$D = \sum_{i=1}^{24} \sum_{k=1}^{6} \frac{n_{E,ik}}{N_{R,ik}} = 0.45 = 45\% \tag{10-25}$$

This document is the intellectual property of the fib – International Federation for Structural Concrete. All rights reserved.
This PDF of fib Bulletin 86 is intended for use and/or distribution solely within fib National Member Groups.

where $n_{E,ik}$ = number of acting stress cycles for class $i$ of the basic bending moment $M_0$ resp. temperature difference $\Delta T_v$ and class $k$ of the traffic load based on measured strain amplitudes; $N_{R,ik}$ = number of resisting stress cycles of class $ik$.

### 10.4.6 Conclusions

The results presented demonstrate the capabilities of the approaches given to evaluate the potential risk of fatigue failure of existing prestressed concrete bridges.

The service life evaluation based on monitoring and FE simulation is an extensive method to detect the risk of a fatigue failure at coupling joints. For bridges with uncertainties due to the construction procedure and long-term effects it allows the determination of a realistic stress range distribution for the tendon coupler assemblies, whereby unnecessary strengthening measures could be avoided quite often.

## 10.5 Monitoring and reliability assessment of a jointless bridge structure – Austria

In structural bridge engineering maintenance strategies and thus budgetary demands are highly influenced by construction type and quality of design. Nowadays bridge owners and planners tend to include life-cycle cost analyses in their decision processes regarding the overall design trying to optimize structural reliability and durability within financial constraints. However efforts to reduce maintenance costs over the expected lifetime by adopting well established design principles leads to unknown risks concerning for instance boundary conditions. Monitoring solutions can reduce the associated risk of new design concepts by constant observation of the performance of structural components during prescribed time periods. In this section an integrative monitoring concept is presented and applied to an existing bridge, with emphasis on time dependent processes including creep, shrinkage and temperature.

### 10.5.1 Introduction

In recent years there have been numerous developments in structural design, in design formats of bridges[691] and in associated material technologies[692, 693, 694]. These developments do have a direct and indirect influence on maintenance and maintenance planning[695, 696]. In addition, there is an increased awareness of structural owners with respect to the quality of design and the appropriate selection of structures in order to reduce maintenance and life cycle costs[296, 237]. The effects of the optimized performance of design and design details on maintenance and life cycle cost of engineering structures can be verified by well-established risk assessment tools, which incorporate e.g. elements of the hazard identification, hazard analysis and the cause analysis[697]. Monitoring systems can support the objectification and can compensate the lack of experience[698, 699] since they can keep pace with the speed of innovation and provide the necessary data basis for (a) early detection of structural failure and (b) verification of existing analytical and numerical models.

There is the tendency to replace structural details that are expensive in maintenance (e.g. bearings and expansion joints) by jointless bridge structures since they are considered as cheap robust solutions considering the total life cycle costs. It must be mentioned, that this approach causes changes in the short term and long term static

This document is the intellectual property of the fib – International Federation for Structural Concrete. All rights reserved.
This PDF of fib Bulletin 86 is intended for use and/or distribution solely within fib National Member Groups.

performance of a multispan bridge system and in the soil structure interaction with respect to traditional solutions.

Practitioners already developed numerous more or less effective solutions for the demands of this type of new frame structure e.g. with respect to the constraints due to temperature and due to the soil structure interaction. Nevertheless, there is a lack of experience regarding the short and long term mechanical behaviour and the required maintenance effort. For this reason, an extensive monitoring program had been commissioned by the structural owner of the Marktwasser Bridge, S33.24.

The objectives of this section are the discussion of monitoring systems applied on the Marktwasser Bridge S33.24 and its recorded quantities, and the verification of its ability to make up for the lack of experience in the design phase.

## 10.5.2 General aspects of the Marktwasser Bridge, S33.24

The Marktwasser Bridge S33.24 is a three span foreland bridge of a newly erected Danube crossing in Lower-Austria, Austria, with 19.50 m, 28.05 m and 19.50 m span width, see Fig. 10-31. The bridge is designed for the five lane highway S33 according to the associated national standard B-EN19xx for reinforced concrete bridges. Its abutments are inclined by 74 degrees to the road axis. The deck width ranges from 19.40 m to 22.70 m excluding two cantilevers of 2.50 m length each. The entire structure is founded on four lines of drilling piles with lengths between 12.00 m and 19.50 m. More details of the geometrical quantities are for example available in[700, 701].

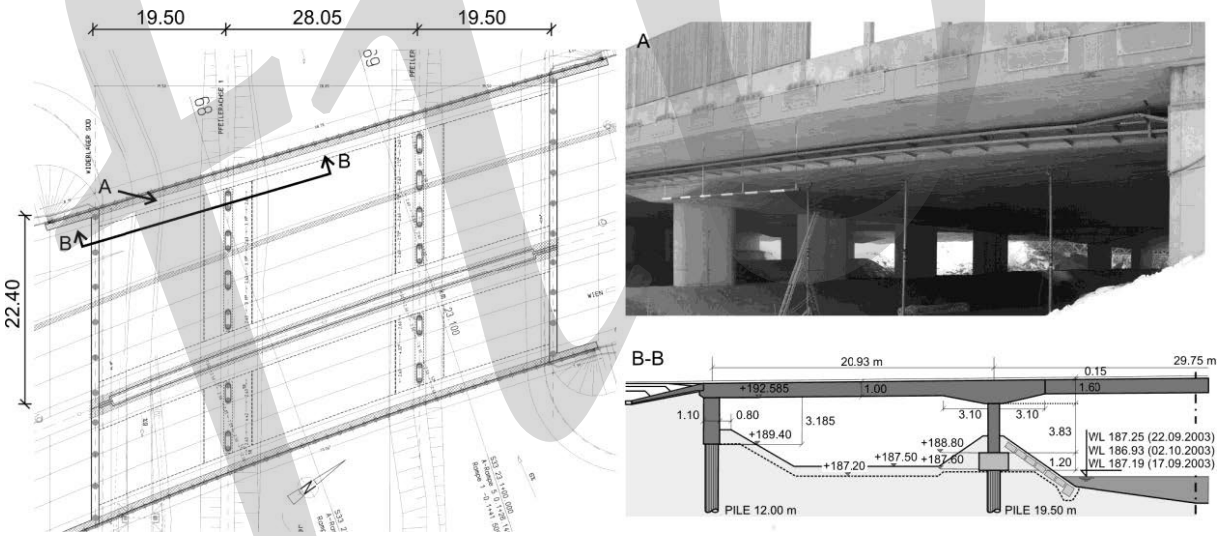


Fig. 10-31 Marktwasser bridge S33.24

The original design of the foreland bridge was drafted by Fritsch, Chiari & Partner ZT GmbH and was based on the computations from Josef Mayer ZT – GmbH in 2007. In order to reduce construction and maintenance cost, the Austrian Highway Financing Company (ASFINAG) instructed the engineering offices to convert the original design to a jointless bridge structure by omitting expansion joints and bearings, which had significant effects on the construction and maintenance costs.

Despite these regulatory design criteria and accurately detailed engineering design, ASFINAG and the Austrian Government commissioned Bernard ZT GmbH together

This document is the intellectual property of the fib – International Federation for Structural Concrete. All rights reserved.
This PDF of fib Bulletin 86 is intended for use and/or distribution solely within fib National Member Groups.

with the University of Natural Resources and Life Sciences to monitor and analyse the behaviour of critical details of the structure (e.g. the soil structure interaction, the temperature affects, and the approach slab solutions) within the research project "Monitoring basierte Analyse einer Integralen Brücke", and to determine generally valid formulations associated with jointless bridges for the developing national application document "RVS - Integrale Brücken".

In addition to the monitoring campaign discussed in the following section, numerous concrete samples had been extracted during the casting procedures in January 2009. These samples served for the determination of the concrete strength and its associated fracture mechanical properties and provided essential information for later interpretation of the monitoring data and a first inverse analysis of the static system, which had been performed by[702]. The inversely updated static system of the bridge was the basis for the initial reliability assessment. Structural response was calculated by the nonlinear finite element fracture mechanics software ATENA. As many uncertainties are involved in the problem, a statistical approach was used to assess the influence of uncertainties on structural response (load-carrying capacity). It is based on a randomization of nonlinear finite element analysis of concrete structures[703]. The scatter of ultimate load capacity was obtained using a Monte Carlo type simulation called Latin hypercube sampling, implemented in the reliability software FREET[168]. Statistical correlation was also considered. Details of the initial reliability assessment are documented in[704].

Jointless bridges are significantly affected by the boundary conditions of the abutment and the approach-slab to the soil body. In order to capture this interaction, a soil monitoring network had been installed in the soil next to the abutment and approach slab in autumn 2009. The monitoring outcomes will be used for the continuous updating of the previously mentioned inverse analysis and reliability assessment procedures and in consequence for the time variable assessment of the lifetime performance.

### 10.5.3 Monitoring systems applied on the Marktwasser Bridge, S33.24

The design of an adequate monitoring system for a particular task is governed by (a) calculation of structural response due to certain loads, (b) the definition of physical monitoring properties according to the monitoring goal, (c) the selection of suitable sensors and (d) the optimisation of the sensor placement. Sensors applied within a permanent monitoring system need to be reliable, show long term stability, and surpass the requirements of resolution and accuracy. Sensors of similar measurement principle in general are to be preferred as they simplify installation and reduce costs. However in cases of high potential damage or the absence of a possibility to repeat a certain measurement it is advised to ensure redundancy within the installation in order to increase robustness with the additional advantage of increasing data density. Critical load cases for the design of statically indeterminate frame structures such as jointless bridges are earth pressure against the abutments, temperature loads as well as creep and shrinkage[705, 706]. For the construction of jointless bridges such as Marktwasser Bridge, a permanently crack-free pavement and the lack of vertical deformations in the dilatation area and thus a smooth riding comfort are, apart from structural considerations, the critical elements which influence the acceptance of the entire design. Consequently many considerations are placed on the design of the transition area between structure and approach. Fig. 10-32 shows the final design of this structural detail mainly consisting of an inclined slab with

This document is the intellectual property of the fib – International Federation for Structural Concrete. All rights reserved.
This PDF of fib Bulletin 86 is intended for use and/or distribution solely within fib National Member Groups.

monolithic connection to the deck. In order to reduce the amount of earth pressure on the abutment wall from full passive earth pressure to active earth pressure, the soil body directly behind the abutment was reinforced with geotextiles and mechanically detached from the abutment wall by means of a soft gap element, as was the top 1.0 m of the drilling piles. The earth body above the slab was reinforced as well based on the design assumption that most of the strain field will develop in between two sliding surfaces originating at the tip of the slab. The reinforcement of this soil body should therefore ensure a more equal distribution of the strains over a longer distance thus reducing the amount of stress on the pavement and consequently the likelihood of cracking.

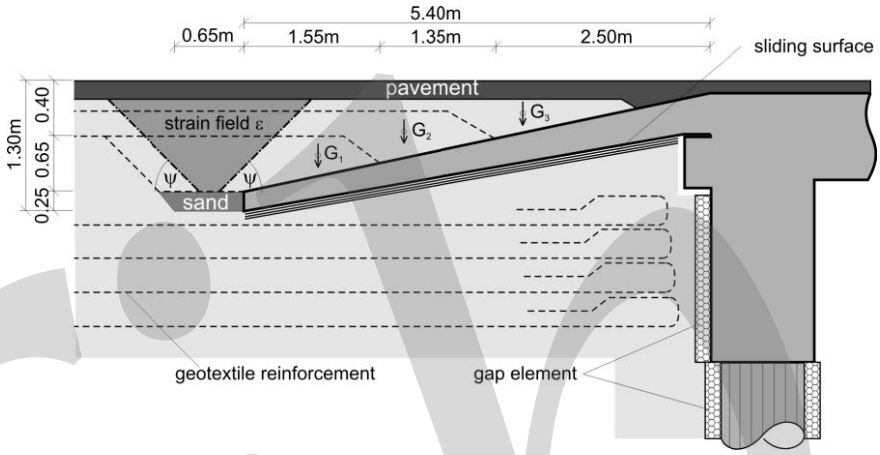


Fig. 10-32 Approach slab design for the transition area between the bridge and the soil

For monitoring and analysing critical details of the bridge structure an integrative monitoring concept was developed with a special focus (a) on the structural behaviour of the first lateral south/west field of the bridge, and (b) on the deformation–strain field performance of the pavement and the soil next to the approach slab and the abutment. In order to capture all structurally relevant properties, both of the deck and the dilatation area, in total five different sensor systems with a total number of 54 sensors were installed in the Marktwasser Bridge and integrated into a permanent monitoring system operating at a sampling frequency of 1 Hz[707, 700, 701, 708].In particular fibre optic sensors had been installed in the deck of the southern lateral part. Furthermore, the sensor network incorporates geotextile embedded fibre optical sensors, electrical strain gauges, inclinometers and extensometers.

### 10.5.3.1 Deck slab

The placement of sensors that have been installed in the deck slab of the first south western part of the bridge were optimized in order to capture the effects due to (a) the consecutive casting of the bridge fields, (b) the removal of the formworks, (c) the pavement loading, (d) the variability in the environmental temperature, (e) the creep and shrinkage processes in the first three years, and (f) a proof loading procedure which was executed in spring 2010. The design of the monitoring network consisted of the selection of suitable sensors as well as the definition of an appropriate number of sensors and their locations. Suggestions by[709] regarding the proper instrumentation of concrete structures in combination with optimization strategies for monitoring networks proposed by[228] influenced the decision process.

This document is the intellectual property of the fib – International Federation for Structural Concrete. All rights reserved.
This PDF of fib Bulletin 86 is intended for use and/or distribution solely within fib National Member Groups.

Due to the many advantages of fibre optic sensor (FOS) systems such as less cabling, stability against electromagnetic interference and corrosion Inaudi[710] the engineering company designing the monitoring system opted for a solution consisting of two independent FOS strands divided between top and bottom reinforcement layer and consisting of six strain and four temperature sensors each. Details about the measurement principle, the selected sensor type and alternative optical sensing methods are given in[711].

The detailed layout of the sensor network with respect to the geometry and the expected moment distribution during construction as well as after completion are given in figure 3. As every measurement is influenced by temperature effects a number of temperature sensors were divided between both concrete surfaces able to accurately capture the temperature field and deduce constant temperature loads and temperature gradient. Local differences in temperature may result from solar radiation, wind effects and the development of cold air pockets below the deck during winter time.

The fibre optic sensing principle of fibre brag gratings (FBGs) serial alignment of sensors in strands thus reducing cabling efforts. The choice for two separate strands was mainly determined by the sequence of installation matching the installation of the bottom and followed by the top reinforcement layers but also ensures a higher degree of redundancy. All sensors were loosely fixed to the rebars by cable restrainers, as shown in Fig. 10-33, which limited installation costs. The dumbbell shaped strain sensors have a length of approximately 10 cm and can directly measure the mean concrete strain via bond, see Fig. 10-33(c). In the compressive zone this principle works perfectly. However, the measurements in the tensile zone need to be interpreted carefully considering the effects of crack development and localisation.

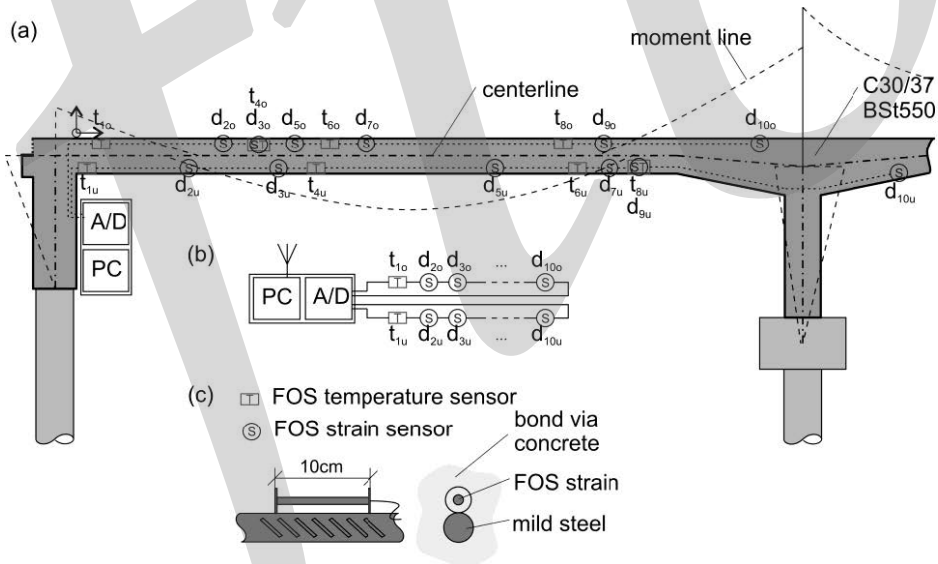


| Id | Pos [m] | Id | Pos [m] |
|---|---|---|---|
| $t_{1o}$ | 0.70 | $t_{1u}$ | 0.30 |
| $d_{2o}$ | 4.10 | $d_{2u}$ | 3.15 |
| $d_{3o}$ | 5.10 | $d_{3u}$ | 5.65 |
| $t_{4o}$ | 5.10 | $t_{4u}$ | 6.70 |
| $d_{5o}$ | 6.10 | $f_{5u}$ | 11.70 |
| $t_{6o}$ | 7.10 | $t_{6u}$ | 14.00 |
| $d_{7o}$ | 8.10 | $d_{7u}$ | 14.90 |
| $t_{8o}$ | 13.60 | $t_{8u}$ | 15.70 |
| $d_{9o}$ | 14.70 | $d_{9u}$ | 15.70 |
| $d_{10o}$ | 19.10 | $d_{10u}$ | 23.00 |

Fig. 10-33 Instrumentation of concrete deck slab; (a) sensor location, (b) cabling principle, (c) FOS-temperature, (d) FOS strain

Strain sensors $d_{2o}$ up to $d_{7o}$ and their counterparts $d_{2u}$, $d_{7u}$ provide information about the strain contribution from dead load, creep shrinkage and temperature gradient. The placement of $d_{10o}$ and $d_{10u}$ was governed by the goal to determine the moment near the pier whereas $d_{7u}$, $d_{9u}$ and $d_{9o}$ should be able to capture the approximate location of the zero-crossings of the moment distribution. The pairing of sensors between bottom and

This document is the intellectual property of the fib – International Federation for Structural Concrete. All rights reserved.
This PDF of fib Bulletin 86 is intended for use and/or distribution solely within fib National Member Groups.

top layer allows for the determination of a two-dimensional strain field thus being able to differentiate between axial and curvature loading.

### 10.5.3.2 Soil-structure interaction

The soil-structure interaction influences two main design aspects. Firstly the performance of bridge structure itself is significantly influenced by the build-up of constraint loads due to temperature effects, creep and shrinkage processes, changes in supports and the activation of earth pressure against the abutment walls. Secondly the limitation of tensile strain and vertical deformations in the dilation area which might influence serviceability.

In order to capture the soil-structure interaction as accurately and completely as possible four different sensor systems were installed in the critical area behind the structure's southern abutment[707, 708]. Fig. 10-34 gives an overview about the location of the different sensors with respect to the geometry. Two extensometers were included to capture the relative movement between abutment and earth dam. For the continuous observation of the strain field above the slab ten fibre-optic strain sensors divided between two geotextile reinforcement layers in combination with 20 electrical strain gauges fixed to two additional reinforcement layers were used. Additionally three vertical inclinometers allowing for a time discrete measurement of absolute deformations were placed in the earth body above the approach slab. Finally one PT100 temperature sensor which provides information about the temperature within the earth approach was included too. More details regarding the sensor systems in the area behind the structures abutment are documented in[712, 713].

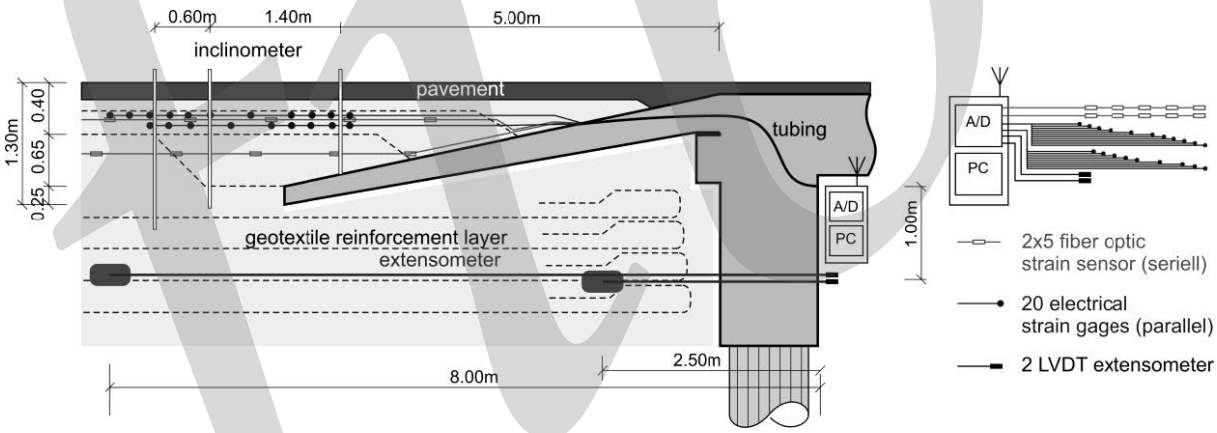


Fig. 10-34 Sensor installation scheme for capturing the soil-structure-interaction

As mentioned earlier, the earth pressure considered during design has high influence on the overall structural performance. Since the build-up of the full earth pressure at rest or even the passive earth pressure could be excluded by structural detailing, see Fig. 10-32, only the active earth pressure was accounted for during the design thus ensuring an efficient design. However, the build-up of a higher earth pressure than accounted for cannot be completely ruled out and would significantly endanger structural safety. In consequence two extensometers were installed; one anchored approximately 8.5 m behind the abutment – outside the expected area of displacement – and one just 2.5 m long. Absolute movements of the abutments are captured by the longer extensometer whereas the shorter one directly measures the relative movement between abutment and earth, see Figure 10-34. Both displacements are measured by LVDT displacement sensors and recorded

*This document is the intellectual property of the fib – International Federation for Structural Concrete. All rights reserved.*
*This PDF of fib Bulletin 86 is intended for use and/or distribution solely within fib National Member Groups.*

every 60 seconds. As the extensometers are installed 1.5 m below the centreline of the concrete deck slab, sensor readings are influenced by translation and rotation of the abutment wall due to the changes in the length of the deck slab caused for instance by temperature or creep/shrinkage. These effects need to be accounted for during data evaluation and interpretation.

The second target of the monitoring campaign aims at the buried slab detail. Although this structural detail does not directly concern structural safety it is of high importance due to its effect on serviceability and traffic safety. The design of the transition area between concrete deck and earth approach should allow for (a) a permanently crack-free pavement, and (b) limit vertical deformations in the dilatation area due to changes in length of the concrete deck.

According to design hypothesis the reinforced earth body above the slab can be assumed to move with the structure resulting in the development of a strain field between two potential sliding surfaces which originate at the end of the slab and whose inclination is among others determined by the shearing angle of the earth material. Consequently the design parameters include (a) the length of the slab, (b) its inclination, (c) the composition and the soil body, and (d) the degree and stiffness of the reinforcement material. For the current design most of the above mentioned questions were decided based on engineering judgement and preliminary models. However, the successful application of this construction type necessitates clear and reproducible instructions/ recommendations for instance included in a currently developing guideline. Apart from solving the problem of the dilatation area locally by an appropriate structural detail, it can be addressed by two opposing global design principles – stiff design and kinematic design. The first strives for a combination of very stiff abutments and foundations which results in high constraint moments in the structure but little dilatations that can easily be absorbed by a traditional slab solution. On the other side a kinematic design ensure a flexible foundation and superstructure. Constraint loads for instance caused by temperature loads can be dissipated by deformation resulting in low internal forces and in consequence reinforcement. However, displacements behind the abutment are comparably large and need to be taken care of. Marktwasser Bridge was designed following generally the second approach.

Detailed knowledge regarding the real strain field in the dilatation area is very important because it not only allows the verification of the chosen design but more importantly provides the necessary input information for the calibration of finite element models which can serve for parameter studies and ultimately the optimization of the entire design with respect to construction and total life cycle costs. The main modelling parameters needing calibration are the correct formulation of boundary conditions for the structural model, the material properties for the earth body as well as the characteristics of interfaces and bond models concerning the geotextile reinforcement, the gap elements and the sliding surface below the slab, see Fig. 10-32. The material properties of the superstructure have already been inversely identified[702].

Motivated by redundancy and the possibility for cross-verification, two independent sensor systems have been installed to capture the strain field and its development over time – one based on the fibre-bragg grating principle[710] and one based on traditional electrical strain gauges. One particular challenge during instrumentation of the earth body is the coarse-grained material that consists of gravel and large crushed stone and endangers the survival of the sensors and cabling.

This document is the intellectual property of the fib – International Federation for Structural Concrete. All rights reserved.
This PDF of fib Bulletin 86 is intended for use and/or distribution solely within fib National Member Groups.

The fibre optic sensor system consists of two layers of five strain sensors each, which are placed in depths of approximately 30 cm and 60 cm with a sensor spacing of 1 m as shown in figure 4. The actual sensors work based on the fibre bragg grating principle[714] and have a technical resolution of 1 µe with a strain range of 1 %. All sensors within a layer work as serial system, where each sensor reflects light at a predefined wavelength. Mechanical loads result in strains which affect the optical properties of the sensors and result in a wave length shift $\Delta\lambda$ that is directly proportional to the strain shift $\Delta\varepsilon$. The optical fibre is woven into a geotextile for protection and bond with the earth material. In order to reduce the effects of the additional stiffness provided by the base material, the geotextile was weakened around the sensors, as shown in Fig. 10-35a and Fig. 10-35b. Consequently every strain reading provided by the individual sensors represents the mean strain in the surrounding area with a base length ranging between approximately 30 cm to 1 m depending on the developing bond.

The installation of the sensor layers consisted of the following steps: (a) the construction of a ditch, (b) the placement of the geotextile onto a thin layer of sand thus further improving protection and bond, (c) slightly covering the sensor layer with sand followed by (d) a careful but adequate compaction of the material and (e) filling the ditch with coarse material up to the next sensor layer. The entire procedure was repeated for all four layers. In Fig. 10-35a the installation of the top geotextile sensor layer is shown.

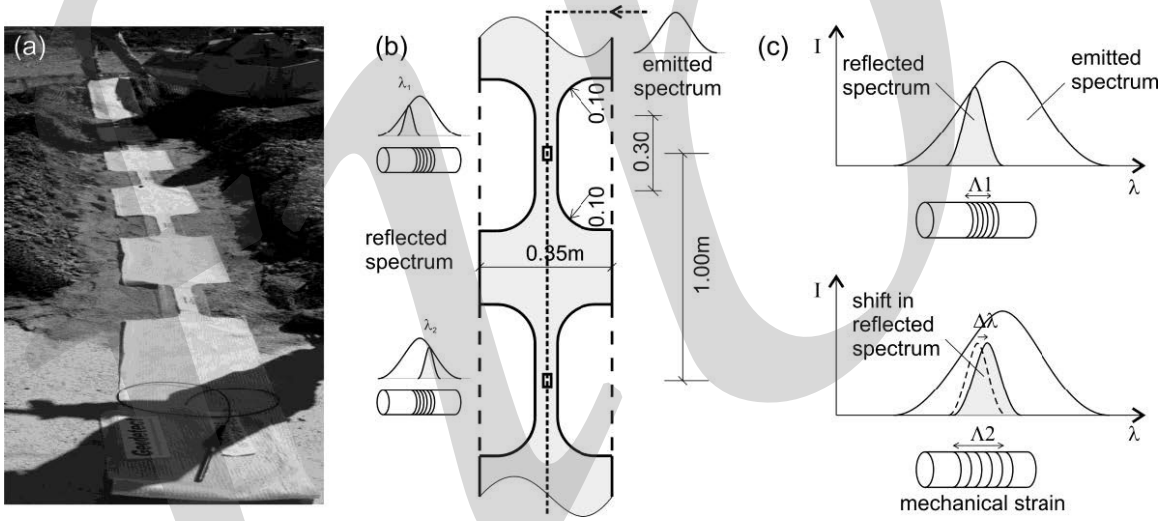


Fig. 10-35 Installation of (a) top fibre-optic sensor layer in sand bed, (b) sensor principle, and geometry of geotextile layer, and (c) principle of fibre-bragg-gratings (FBGs)

Sensor layers 2 and 4 were instrumented with additional 20 electrical strain gauges of three different types – with a base length of 3 mm, 50 mm and 150 mm. The sensor placement was determined by the assumed deformation mechanism and in consequence were placed at areas where high strains were expected[715], see Fig. 10-32 and Fig. 10-34.

Similarly to the FOS system, electrical strain gauges need to be fixed onto a solid surface in order to work. Hence the strain gauges were fixed to some of the geotextile material made from glass fibres covered in PVC that is used for the reinforcement of the earth approach material. Every strain gauge was fixed to a piece of geotextile of approximately 20 cm by 40 cm right at the centre of the middle longitudinal strand. All strands parallel to the instrumented one were cut in order to ensure a representative measurement of mean strains $\varepsilon_{mean}$ between both contact areas according to Fig. 10-36.

This document is the intellectual property of the fib – International Federation for Structural Concrete. All rights reserved.
This PDF of fib Bulletin 86 is intended for use and/or distribution solely within fib National Member Groups.

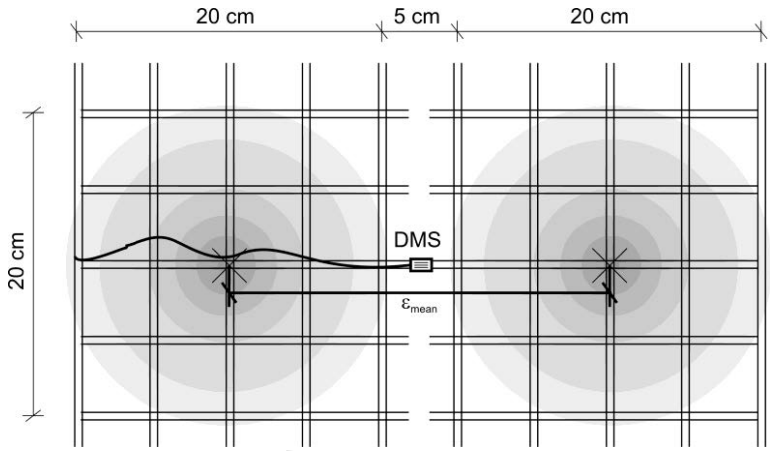


Fig. 10-36 Installation of 5 mm base length strain gauge to geotextile

Fig. 10-37a and Fig. 10-37b show the installation of two different types of strain gauges (50 mm and 150 mm base length), whereas in Fig. 10-37c the prepared top layer placed onto a sand bed is shown.

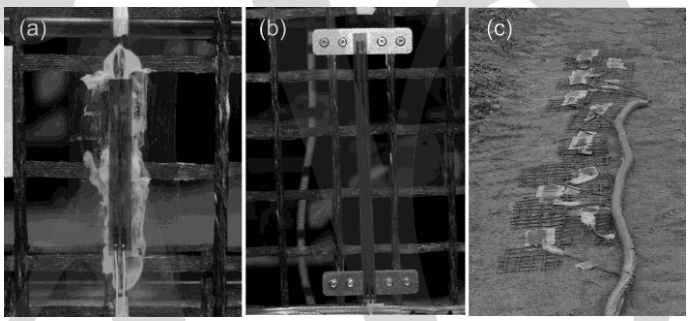


Fig. 10-37 50 mm strain gauge after installation (b) 150 mm strain gauge after installation, (c) top strain gauge layer in sand bed

In general every strain measurement provides only localized information about deformations depending on the sensor base length and necessary distance for the build-up of the full bond stress. The instrumentation of the soil body is furthermore highly affected by the heterogeneous nature of the earth material.

The three vertical inclinometers provide the necessary global verification of the strain measurement and assumed deformation mechanism by means of incremental inclination measurement at discrete points in time. The inclinometers with lengths of 1.6 m, 1.4 m and 1.0 m were placed within the expected area of deformation as well as shortly behind the second potential sliding surface in order to (a) capture the development of both assumed sliding surfaces and (b) determine the length of the earth body which is influenced by the abutment's movements.

The combination of both strain measurement systems should allow for a fairly accurate estimation of the deformation state which will serve for (a) the direct verification of the chosen design and (b) the calibration of advanced finite element models. In consequence these numerical models can be used to numerically optimize the different design aspects associated with the geometry of the slab and the composition of the soil body as well as its reinforcement.

This document is the intellectual property of the fib – International Federation for Structural Concrete. All rights reserved.
This PDF of fib Bulletin 86 is intended for use and/or distribution solely within fib National Member Groups.

In conclusion, 5 different sensor systems with 54 sensors were installed and combined into one permanent monitoring network with the goal of finding answers to the following questions which are crucial in the assessment of the overall performance of indeterminate joint less bridges[407]: (a) the effects of time dependent processes such as creep and shrinkage and associated cracking on structural performance, (b) the development of strain fields and cracks caused by temperature loading, (c) the variability in the earth pressure acting on different structural elements, e.g. on the abutments and the approach slab, (d) the relative settlements of the structure, and (e) the risk of cracks or of a depression behind the abutment.

### 10.5.3.3 Data analysis

The operation of the monitoring network presented consisting of 54 sensors and operating at a sampling rate of 1 Hz results in a huge amount of data. After a first plausibility check the recorded data needs to be properly prepared and analysed with respect to the defined monitoring goals[700].

In general, the observed and recorded raw data first needs to be transformed from the sensor characteristic monitoring quantities to the respective physical monitoring quantities. Fibre-bragg gratings (FBGs) for instance initially provide only information about reflected peak wavelength[710], in case of electrical systems resistance, voltage or current are recorded. Additionally temperature effects on the monitoring property always need to be accounted for during data preparation in order to be able to obtain useful information.

In Fig. 10-38 the data management concept associated with the monitoring system of the Marktwasser Bridge is presented. The chart gives an overview of necessary steps during data evaluation focusing especially on the applied fibre optic sensing system. The subsequent steps comprise (a) data transformation, (b) data reduction depending on the type of analysis, (c) the application of different data analysis techniques such as extreme value statistics or simple trend analysis, and finally (d) data interpretation. Based on the obtained results, predictions for the monitored quantities can be made, for example applying Bayesian updating. Additionally the data can be used for the inverse identification of unknown or uncertain structural characteristics as well as loads by applying suitable analytical and numerical models.

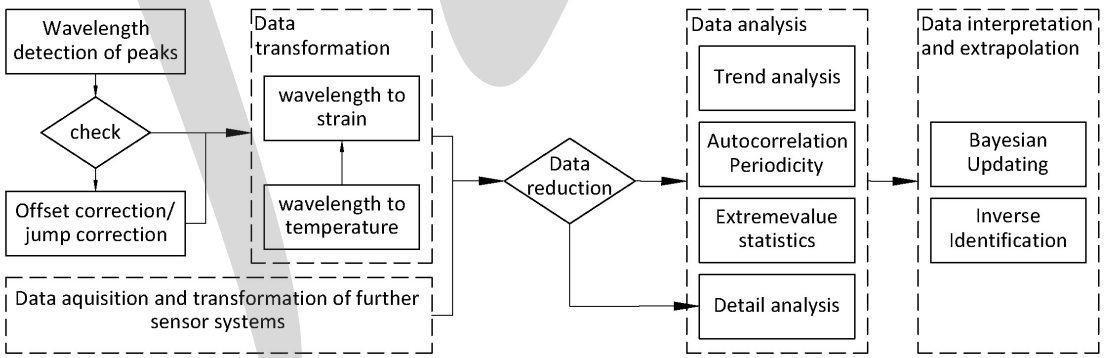


Fig. 10-38 Flow chart for the data management for the monitored data of the Marktwasser Bridge

### 10.5.3.4 Data transformation and correction

Fibre bragg grating (FBGs) sensors use the fact that mechanical strains acting on an optical fibre influence the optical characteristics of the fibre strand[710]. A small grating imposed on

This document is the intellectual property of the fib – International Federation for Structural Concrete. All rights reserved.
This PDF of fib Bulletin 86 is intended for use and/or distribution solely within fib National Member Groups.

an optical fibre reflects light at a certain wavelength depending on the spacing of the grating. This spacing may change with acting mechanical strains or temperature load which results in a shift in the reflected wavelength $\Delta\nu$ that is directly proportional to the acting strain variation $\Delta_\varepsilon$, see also Figure 5(c). Consequently FBGs allow for a localized measurement of certain measurement properties (mainly strain and temperature) depending on the size of the grating and its influence length that is determined by the construction of the sensor. Every sensor reflects light at a unique and predefined wavelength depending on the imposed grating, which allows the direct spatial allocation of the measured property within a serial system. The wavelength shift $\Delta\upsilon(t)$ is calculated as difference between currently reflected wavelength $\upsilon(t)$ and a reference wavelength $\upsilon_0(T_0)$ at a known temperature $T_0$ (1).

$$\Delta\upsilon(t) = \upsilon(t) - \upsilon_0\left(T_0\right) \tag{10-26}$$

Taking into account the actual temperature $T(t)$ at time t and the respective effects on the measurement total strains can be obtained by Equation 2, where $s_\varepsilon$ represents the strain sensitivity of the sensor, which typically amounts to values about 1.2pm/με. The temperature influence on the wavelength shift is specified by a thermal response factor $S_T$ with values around 10 pm/°C. Reference wavelength $\upsilon_0(T_0)$ and reference temperature $T_0$ are ordinarily specified in a calibration sheet or can be determined at site at the start of the measurement campaign in case only relative values are of interest.

$$\varepsilon(t) = \frac{\upsilon(t) - \upsilon_0\left(T_0\right) - \left(T(t) - T_0\right)s_T}{s_\varepsilon} \tag{10-27}$$

Data transformation for fibre-optic temperature sensors works similarly. In this case the sensor needs to be unaffected by mechanical loading. Unlike mechanical strains temperature and wavelength shift show a slightly non-linear relation which can be described by a polynomial equation of the order 2. The coefficients $a_1$ to $a_3$ are again specified in the calibration chart which also specifies the reference wavelength $\upsilon_0$.

$$T(t) = a_1 \cdot \Delta\upsilon(t)^2 + a_2 \cdot \Delta\upsilon(t) + a_3 \tag{10-28}$$

Since every measurement is influenced by temperature effects at least one closely located temperature sensor is necessary for all types of monitoring systems. Although the transformation between wavelength and physical property ordinarily is automatically calculated at site, it is recommended to save the wavelength data for later corrections.

#### 10.5.3.5 Extreme value statistics and strain decomposition

The main goals of the monitoring campaign regarding the superstructure are the determination of the long term development in the monitored quantities and the analyses of acting time dependent processes. Therefore after obtaining a realistic but scattering time series of the physical properties by basic data correction and transformation the full data set resulting from the initially chosen sampling frequency had to be suitably reduced without losing relevant information. For this purpose the statistical properties of the monitoring signal are determined for short time spans such as 10-minute mean, minimum, maximum and standard deviation which not only reduce the amount of data by a factor of 150 but remove some of the scattering in the data and even allow its quantification.

The temperature evolution over time for the four temperature sensors $t_{1o}$, $t_{4o}$, $t_{6o}$ and $t_{8o}$ of the top reinforcement layer after data correction and reduction to 10-minute mean values are shown in Fig. 10-39. The readings present a good agreement among each

*This document is the intellectual property of the fib – International Federation for Structural Concrete. All rights reserved.*
*This PDF of fib Bulletin 86 is intended for use and/or distribution solely within fib National Member Groups.*

other and with respect to the expected variable temperature field next to the asphalt pavement for the time period between March and May.

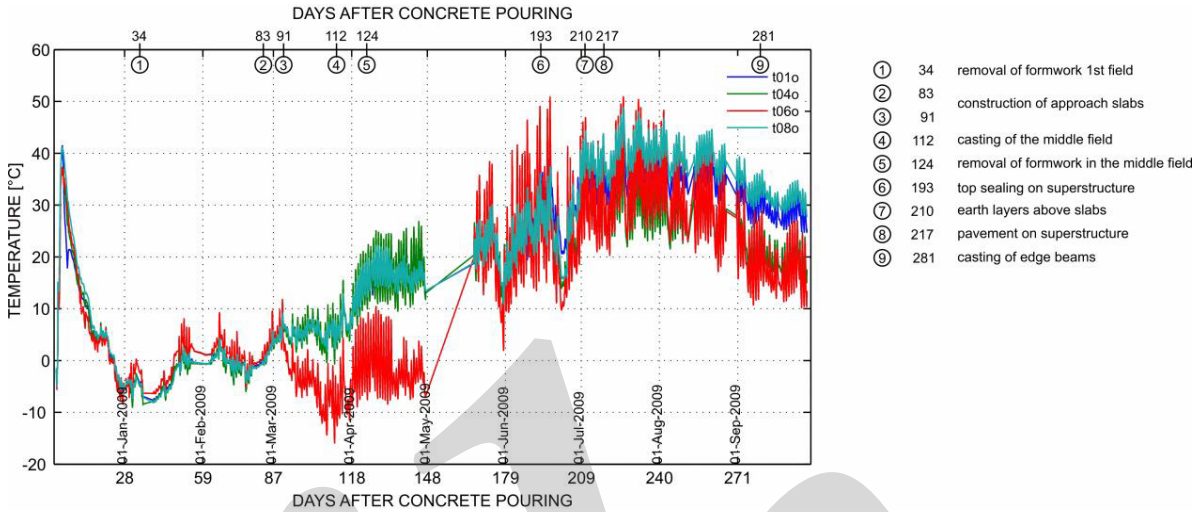


Fig. 10-39 Average temperature per ten minutes vs. time at top reinforcement layer

In Fig. 10-40 the temperature compensated ten minute mean strain readings of the upper reinforcement layer over time are plotted. These transformed readings revealed discontinuities, which are mainly caused by construction stages and the respective redistribution of internal forces. The Time Markers (TM) which are printed on the top horizontal axis indicate significant events over time. TM(1) for instance marks the removal of the formwork in the first southern lateral field on January 7$^{th}$ 2009, whereas TM(2) and TM(3) represent the construction of the approach slabs at the beginning of March (83–91 days after casting (AC)). The casting of the middle part on March 27$^{th}$ (112 days AC) is labelled TM(4), the removal of the formwork in the middle part on April 8$^{th}$ (124 days AC) TM(5) and the application of the top sealing on the structure (193 days AC) TM(6). TM(7) marks the construction of the earth layers above the approach slab (210 days AC), TM(8) the application of the pavement on July 9$^{th}$, and finally TM(9) the concrete pouring of the pedestrian pavements (281 days AC). It must be noted that the mechanical effects due to these events are superimposed by concrete aging, creep and shrinkage. Especially TM(6) caused a significant decrease in strains.

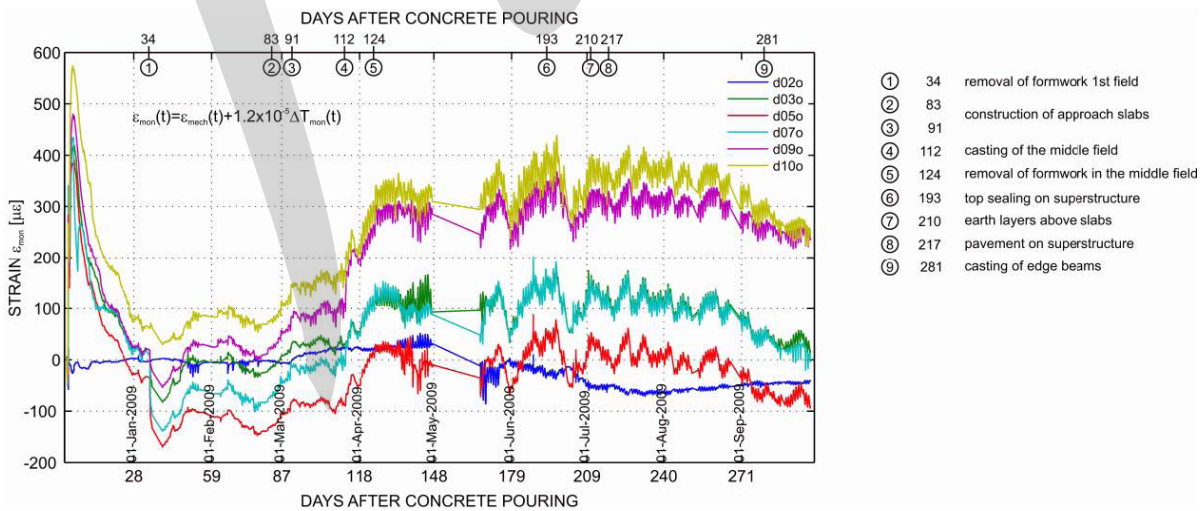


Fig. 10-40 Average temperature per ten minutes vs. time at top reinforcement layer

*This document is the intellectual property of the fib – International Federation for Structural Concrete. All rights reserved.*
*This PDF of fib Bulletin 86 is intended for use and/or distribution solely within fib National Member Groups.*

In addition to the constant observation of the structural performance, there is a high interest in the identification of trends (e.g. increase in strain due to creep), periodic effects (e.g. daily variations in temperature/ strain or yearly cycle in elongation) or correlations (e.g. due to temperature effects or changes in the static system) based on the recorded data (see Fig. 10-38).

Fig. 10-41 shows the seven day mean mechanical strain values for the top reinforcement layer which have been derived based on the extreme value distributions of 10-minute-maximum-strain values compensated by the 10-minute-mean temperatures. Temperature compensation comprises the compensation of the sensor readings as well as the subtraction of those strain contributions that are caused by the mean temperature field. The sensor readings have been evaluated exemplarily for sensor $d_{7o}$ applying extreme value statistics. The dark grey area denotes a deviation of less than one standard deviation from the mean values, whereas the light grey area represents the limit of two standard deviations. On the right hand side the extreme value distributions of $d_{7o}$ that are based on 10-minute-maxima are plotted for time periods of 7 to 14 days. According to the monitoring data structural response during the first 150 days after concrete pouring is affected by three significantly different processes.

The first 34 days until the removal of the formwork can be considered as time phase A which is essentially influenced by temperature effects and curing. Time phase B between TM(1) and TM(3) is characterized by the first construction stage – fully acting dead load in the south lateral part only and a fixed rotation of the deck plate above the first column axis. The fixed rotation was required due to the consecutive casting of the lateral and middle parts. Due to the stationary loading and boundary conditions the temporal development can mainly be assigned to acting creep and shrinkage processes. Time phase C between TM(3) and TM(4) is characterized by the formwork removal in the middle part and the casting of the approach slab next to the southern lateral part and shows a significant change in the structural bearing characteristics. Apart from afore mentioned effects all three time phases are affected by temperature. For instance until TMs (4) and (5), strain sensors $d_{2o}$ and $d_{7o}$ indicate, as expected, compression for an increase in temperature whereas $d_{7o}$ shows tension.

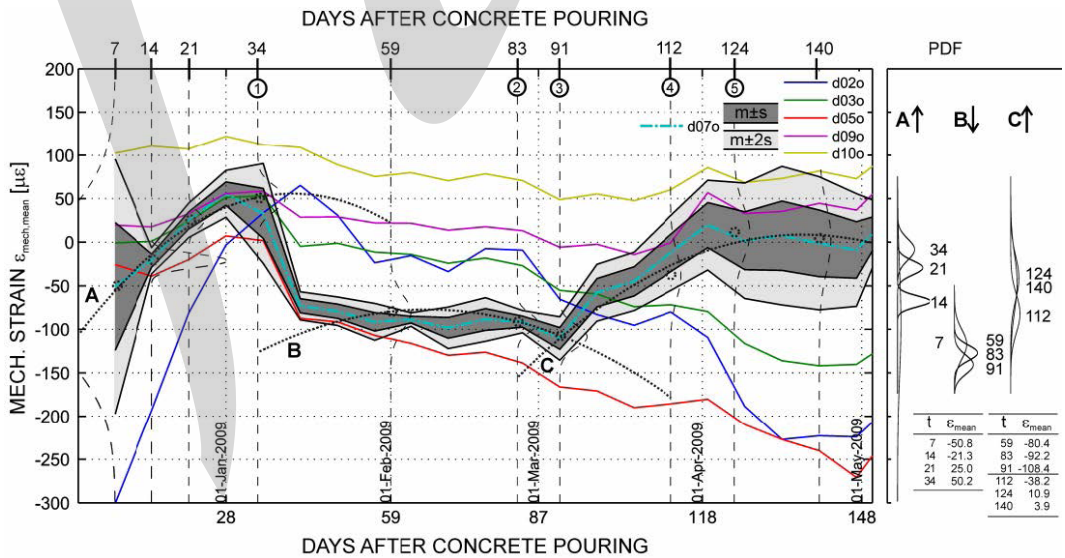


Fig. 10-41 Decomposition of monitored strain data for the extraction of creep & shrinkage effects

This document is the intellectual property of the fib – International Federation for Structural Concrete. All rights reserved.
This PDF of fib Bulletin 86 is intended for use and/or distribution solely within fib National Member Groups.

Fig. 10-41 illustrates the temporal changes in structural response. In particular, the extreme value distributions for sensor $d_{7o}$ are shown for the time frames defined on the top horizontal axis. On the right hand side the fitted probability density functions (PDFs) for all profiles grouped according to the three time phases A, B, C can be found including a list of derived mean strains for the respective time frames. Similar results can be obtained for the strain sensors of the bottom reinforcement layer.

### 10.5.4 Verification of an analytical creep shrinkage model

Since Marktwasser Bridge is highly influenced by creep & shrinkage (CS) processes it is of particular interest to study the agreement between the real monitored development of creep and shrinkage and the theoretically predicted one. Due to the static weight loading, existing CS processes can be extracted from extreme value distributions as presented in Fig. 10-41. The incremental changes in the means of the extreme value distributions for every time frame have been used to derive the creep and shrinkage associated strains $\Delta\varepsilon_{cs}$. The CS- strains $\Delta\varepsilon_{cs}$ and quasi-stresses $\Delta\sigma_{cs}$ of the reinforcement are presented for sensor $d_{2u}$ in Table 10-7, where the transformation from $\Delta\varepsilon_{cs}$ to $\Delta\sigma_{cs}$ is based on a Young's modulus of 210,000 N/mm².

Table 10-7 Identified increases in mean values of extreme value distribution for sensor $d_{2u}$

| Timestep [days] | Strain $\Delta\varepsilon$ [με] | Stress $\Delta\sigma$ [N/mm²] |
|---|---|---|
| 0-7 | 167.7 | 35.0 |
| 7-14 | 57.1 | 12.0 |
| 14-21 | 38.1 | 8.0 |
| 21-28 | 38.1 | 8.0 |
| 28-36 | 57.1 | 12.0 |
| 36-78 | -28.6 | -6.0 |

The extracted CS-strains are the basis for the verification of creep-shrinkage models as proposed in EN1992-1-1 6.7.3.[681]. According to Eurocode the CS related strains are calculated as sum of the load dependent creep $\varepsilon_{cc}(t)$, the autogenous shrinkage $\varepsilon_{ca}(t)$ and the shrinkage caused by drying $\varepsilon_{cd}(t)$[407] at defined points in time $t$ by Eq. (4). The most important input parameters are the type of cement, the mean $f_{cm}$ and characteristic $f_{ck}$ concrete compressive strength as well as the mean Young's modulus $E_{cm}$.

$$\varepsilon_{cs}(t) = \varepsilon_{cc}(t) + \varepsilon_{ca}(t) + \varepsilon_{cd}(t) \tag{10-29}$$

The geometrical properties are included by the calculation of an effective member thickness $h_0$ as shown in Eq. (10-30). This formulation is based on the cross-section area $A_c$ of the concrete member and its circumference $u_c$ as follows:

$$h_0 = \frac{A_c}{2u_c} \tag{10-30}$$

The time evolution of CS is governed by (a) the concrete age at the time of loading $t_{0c}$, (b) the concrete age at the time the shrinkage process is initiated, and (c) the environments relative humidity RH driving shrinkage, and (d) normal stress $\sigma_c$ driving creep. Strain resulting from creep can be estimated by[407]:

This document is the intellectual property of the fib – International Federation for Structural Concrete. All rights reserved.
This PDF of fib Bulletin 86 is intended for use and/or distribution solely within fib National Member Groups.

$$\varepsilon_{cc}(t) = \Phi(t) + \frac{\sigma_c}{E_{c0}} \tag{10-31}$$

where $\Phi(t)$ is the time dependent creep ratio and $E_{c0}$ the Young's modulus at the time $t_0$. The time dependent creep ratio is defined by[407]

$$\Phi(t) = \Phi_0 \cdot \beta_c(t) \tag{10-32}$$

with the basic value $\Phi_0$ of creep

$$\Phi_0 = \Phi_{RH} \cdot \beta_{fcm} \cdot \beta_{t0} \tag{10-33}$$

and the time dependent factor

$$\beta_c(t) = \left( \frac{t - t_{0c}}{\beta_H + t - t_{0c}} \right)^{0.3} \tag{10-34}$$

where, $\Phi_{RH}$, $\beta_{fcm}$, $\beta_{t0}$ are creep specific parameters mainly as function of the concrete strength and the humidity conditions. $t_{0c}$ denotes the concrete age at the time loading starts and $\beta_H$ includes the effects of relative humidity, effective member thickness and mean concrete compressive strength.

Shrinkage caused by drying $\varepsilon_{cd}(t)$ is determined by a time dependent factor $\beta_{ds}$ that is only influenced by the concrete age at time $t_s$ when shrinkage begins and the effective member thickness $h_0$; $k_h$ describing the effects of geometry and $\varepsilon_{cd0}$ including relative humidity and concrete material properties by means of compressive strength. This leads to:

$$\varepsilon_{cd}(t) = \beta_{ds}(t) \cdot k_h \cdot \varepsilon_{cd0} \tag{10-35}$$

with

$$\beta_{ds}(t) = \frac{t - t_s}{\left(t - t_s\right) + 0.04\sqrt{h_0^3}} \tag{10-36}$$

$$\varepsilon_{cd0} = \left(220 + 110\alpha_{ds1}\right) e^{-\alpha_{ds2}\frac{fcm}{fcm0}} 10^6 \beta_{RH} \tag{10-37}$$

where $\alpha_{ds1}$ and $\alpha_{ds2}$ describe the influence of the cement type on shrinkage, $\beta_{RH}$ includes the environments relative humidity, which drives shrinkage, and $f_{cm0}$ = 10 N/mm$^2$ represents the reference compressive strength.

$$\beta_{RH} = 1.55\left(1 - \left(\frac{RH}{100\%}\right)^3\right) \tag{10-38}$$

The autogenous shrinkage, as indicated in Eq.(4) can be computed by the product of the time dependent coefficient:

$$\beta_{as}(t) = 1 - e^{-0.2t^{0.5}} \tag{10-39}$$

and the fully developed shrinkage state

$$\varepsilon_{ca,end} = 2.5\left(f_{ck} - 10\right)10^6 \tag{10-40}$$

as follows

$$\varepsilon_{ca}(t) = \beta_{as}(t) \cdot \varepsilon_{ca,end} \tag{10-41}$$

This document is the intellectual property of the fib – International Federation for Structural Concrete. All rights reserved.
This PDF of fib Bulletin 86 is intended for use and/or distribution solely within fib National Member Groups.

The monitored CS-process can only on a probabilistic basis be verified with respect to the previously summarized analytical CS-model, as most of the input parameters of the analytical models are derived from laboratory test series that do not capture the uncertainties and variability of the environment. In particular, the random variables indicated in Table 10-8 served as inputs for the analytical model described in Eqs (10-30) to (10-41).

Table 10-8 Stochastic models for the analysis of creep. and shrinkage processes

| Quantity | UNIT | mean | COV | PDF |
|---|---|---|---|---|
| $t_0$ | days | 3 | 0.20 | N |
| $t_s$ | days | 1 | 0.20 | N |
| $f_{cm}$ | N/mm² | 40 | 0.08 | LN |
| $f_{ck}$ | N/mm² | 30 | 0.08 | LN |
| $E_{cm}$ | N/mm² | 33,000 | 0.07 | LN |
| RH | % | 60 | 0.20 | N |
| $A_c$ | m² | 10.8 | 0.05 | N |
| $u$ | m | 25.7 | 0.05 | N |
| $\sigma_c$ | N/mm² | 8 | 0.20 | N |

In Fig. 10-42 the measured creep-shrinkage strains $\Delta\varepsilon_{cs}$, as documented in Table 10-7, are plotted with respect to the computed statistical response for the analytical model according to Eurocode 2 using the random variables listed in Table 10-8. The graph shows (a) a good agreement of the strains in the first period of concrete hardening until the removal of the formwork, and (b) a relatively small deviation from the theoretical mean value in the second period until an age of 78 days[716, 700].

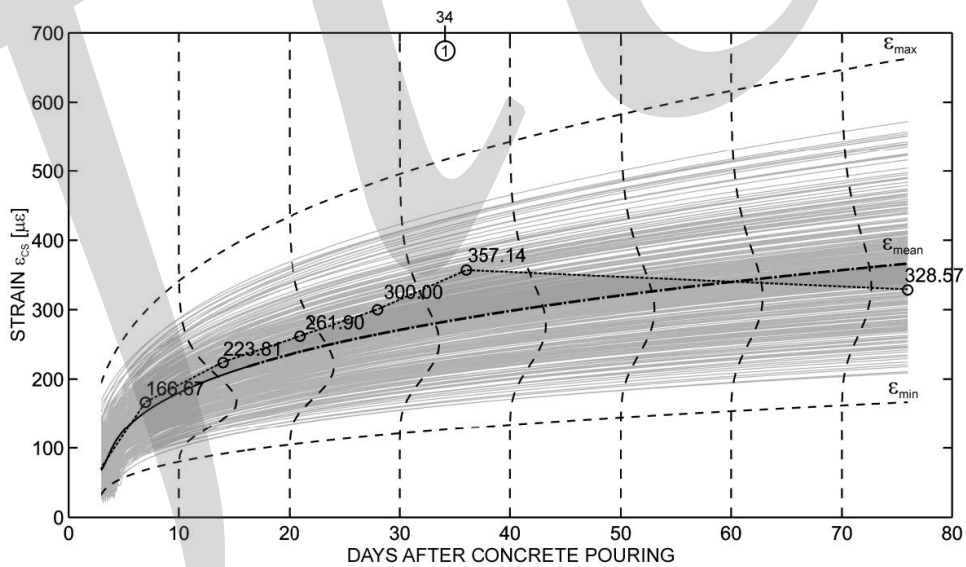


Fig. 10-42 Analytical vs. identified creep shrinkage development of the Marktwasser Bridge

## 10.5.5 Analysis of the slab detail

Apart from the performance of the superstructure and the identification of corresponding relevant time dependent processes the Marktwasser Bridge monitoring campaign is also

*This document is the intellectual property of the fib – International Federation for Structural Concrete. All rights reserved.*
*This PDF of fib Bulletin 86 is intended for use and/or distribution solely within fib National Member Groups.*

aiming at the verification and if necessary optimization of the slab detail, especially with respect to traffic safety and driving comfort. To that end fibre optic strain sensors as well as electrical strain gauges have been installed for the continuous observation of the strain field. Additionally three vertical inclinometers were placed in the vicinity of the southern approach slab.

Considering the placement of the individual strain sensors of every sensor layer, see Fig. 10-34, the time dependent strain field can be derived. In Fig. 10-43 exemplarily the strain field of the bottom fibre optic sensor strand is plotted. The right horizontal axis describes the distance from the outer surface of the abutment wall whereas the time after concrete pouring is plotted on the vertical axis. On the left hand side the mean temperature of the superstructure (orange line) and the temperature of the soil body (blue line) are included for comparison purposes. For the short time span between day 270 and 300 after concrete pouring an obvious increase in strains can be noted that is not directly correlated to a significant decrease in temperature. The strain maximum of 200 µm/m can be located approximately 5.4 m behind the abutment wall – in the area of the predicted sliding surface – between day 285 and 290. Similar results were obtained for the other sensor layers. A more thorough analysis of the strain field in the dilatation area for the entire time period between autumn 2009 and spring 2010 is expected to reveal interesting information regarding the soil-structure interaction and the performance of the approach slab. The analyses again will be based on statistical concepts as discussed for the superstructure. The evaluation of time discrete inclinometer measurements will furthermore allow an absolute confirmation the determined strain field and deformation mechanism.

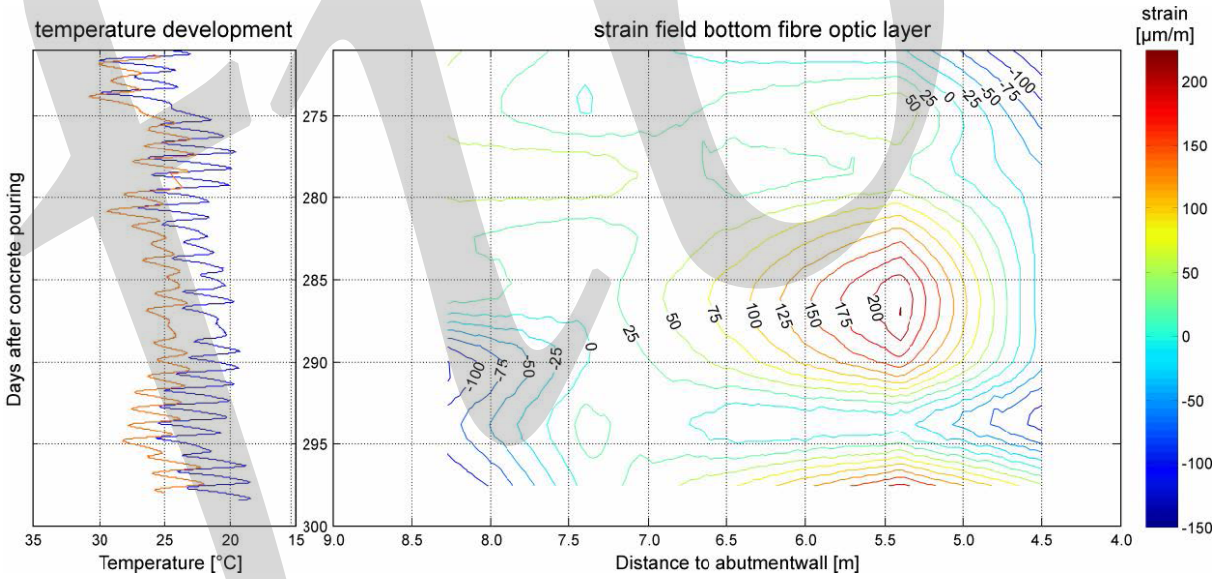


Fig. 10-43 Strain field of lower fibre optic sensor strand in the transition area between Marktwasser Bridge and approach

Parallel to the design and installation of the monitoring system, a nonlinear finite element model of the slab detail defining the soil structure interaction was set up based on all available specification for material properties, composition of the soil material used as well as the initial design considerations. However, many input parameters are highly uncertain, especially the bond law between geotextile reinforcement and soil. In consequence this model needs to be calibrated applying the monitoring results regarding (a) the derived strain field and its statistical characteristics, (b) absolute deformations and

This document is the intellectual property of the fib – International Federation for Structural Concrete. All rights reserved.
This PDF of fib Bulletin 86 is intended for use and/or distribution solely within fib National Member Groups.

movements determined by the inclinometer measurements as well as the extensometer data and (c) identified response of the superstructure with respect to temperature loads and creep shrinkage processes.

After model calibration using the available monitoring data and derived statistical properties, in a next step the updated model can serve for parameter studies concerning different geometrical and material properties as well as an optimization of this design concept – both for this particular structure and as a general approach.

### 10.5.6 Conclusion

A permanent monitoring system consisting of several different sensor types was installed in the newly erected jointless Marktwasser Bridge allowing the observation of time dependent processes and the constant observation of structural response under varying conditions. The obtained data provides the necessary input for the verification of current design assumptions and numerical models and thus increases robustness and reliability of future construction work. Further research in this area will include the application of the methodology to the evaluation of the soil structure interaction, and the calibration of finite element models.

### 10.5.7 Acknowledgement

This research was conducted with the financial support of ASFINAG and BMVIT within the research project "Monitoring and analysis of integral bridge structures" and with the financial support of the Austrian research funding agency FFG within the EUREKA Eurostar research project "Risk Lifetime Assessment of Concrete Structures". The opinions and conclusions presented are those of the authors and do not necessarily reflect the views of the sponsoring organizations.

## 10.6 Egnatia motorway, Northern Greece: Monitoring based risk assessment of bridges

Egnatia Odos SA, Thessaloniki, Greece, has developed and established a bridge maintenance management system based on international experience in cooperation with research institutes and academic laboratories in Greece and Europe. The target was to manage the safety and the serviceability of the about 800 bridges and other reinforced concrete structures of the Egnatia Motorway (with a total length of about 1000 km) in Northern Greece, through the inspection and the monitoring based assessment of their structural and functional sufficiency. This report presents briefly the developed Bridge Maintenance Management System (E_BMS), which is consisted of a Computerized Data Base, the Visual Inspection (for evaluating and rating the structural and functional condition of bridges), the Bridge Health Monitoring (for experimentally checking the structural integrity of bridges and structures), and the Bridge Maintenance Software (for the optimal programming of the required capital maintenance activities).

This document is the intellectual property of the fib – International Federation for Structural Concrete. All rights reserved.
This PDF of fib Bulletin 86 is intended for use and/or distribution solely within fib National Member Groups.

### 10.6.1 Introduction

Egnatia Motorway is a 670 km long highway in Northern Greece, stretching from the Ionian/Adriatic port of Igoumenitsa in the west to the Greek/Turkish border in the East (see Fig. 10-44). It constitutes part of the European Transport Network providing access to the East for the industrial centres of the European Union with no border crossings. "Vertical axes" of about 300 km connect the Egnatia motorway to Pan–European north-south corridors in the Balkan countries. This makes the main axis to be the "horizontal" backbone of an Integrated Transportation Network of high geo-strategic importance for the greater area of South-East Europe. The motorway consists of a dual carriageway with a central reserve and two traffic lanes in each carriageway plus emergency lanes. It comprises a high number of 674 reinforced concrete bridges with a total length of more than 40 km.

Egnatia Odos S.A. (EOAE) is a Greek state-owned company, established by law in 1996, responsible for the design, construction and operation of the Egnatia Motorway and its vertical axes. The construction of the motorway main axis has been completed within 2009. Now, the main activities of the Egnatia Odos S.A. company with respect to the motorway are geared to its operation and maintenance. These activities aim to provide a safe and efficient road network and include, among others, the preparation of a complete inventory of all assets, the continuous collection of data reflecting the condition of the assets and their evaluation, the identification of critical areas and vulnerable points and long-term planning with respect to maintenance and operation.

The above activities belong to a risk management process. Given the plethora of major infrastructure works that the road encompasses, this risk process has to be clearly defined and systematically carried out so that a safe and smooth traffic flow is ensured with the minimum possible cost and environmental impact. Moreover, the risk management approach has to cover various domains involved in the operation and maintenance of the motorway, e.g. transit of dangerous goods through tunnels. This section focuses on one of them, that exhibits a particular interest for the Egnatia Odos S.A. company: reinforced concrete bridges. More specifically, the processes followed by the company EOAE in the risk assessment of bridges and landslides, based on in-house performed monitoring, follows.

### 10.6.2 Risk assessment of bridges

Egnatia Odos SA has developed and established a bridge maintenance management system based on international experience, in cooperation with research institutes and academic laboratories in Greece and Europe. The target is to manage the safety and the serviceability of the about 680 bridges and other structures of the Egnatia Motorway through the inspection and the monitoring based assessment of their structural and functional sufficiency. The Bridge Maintenance Management System (E_BMS) consists of:

- A Computerized Data Base in ORACLETM, for recording and coding the structural and functional characteristics of Egnatia Motorway bridges as well as the findings and the condition ratings from their periodic inspections.
- Visual Inspection, for evaluating and rating the structural and functional condition of bridges and structures using an inspection and an element based evaluation manual.

This document is the intellectual property of the fib – International Federation for Structural Concrete. All rights reserved.
This PDF of fib Bulletin 86 is intended for use and/or distribution solely within fib National Member Groups.

- Structural Health monitoring, for checking the structural integrity of bridges and structures through the experimental identification of their dynamic/static characteristics. Based on the identified modal data the as built models of the bridges are updated to represent the actual mass and stiffness.
- Bridge Maintenance Software, for the optimal programming of the required capital maintenance activities to be conducted within the period of analysis.

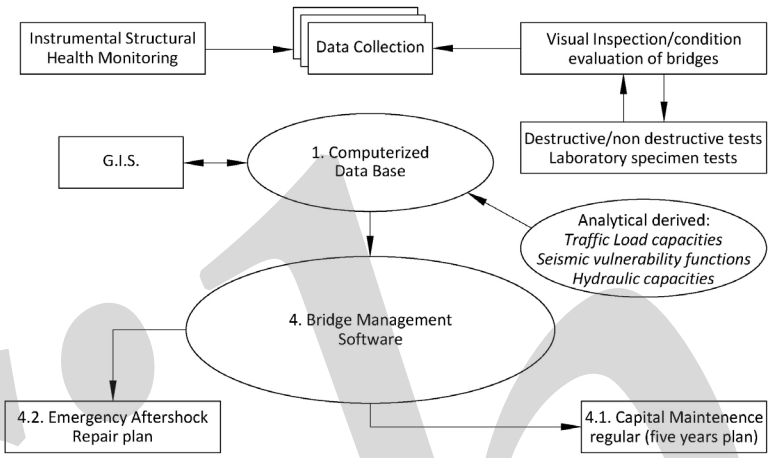


Fig. 10-44 Structure of the Egnatia Bridge Management System.

## 10.6.3 Major risks for Egnatia bridges

The major risks, that affect the serviceability and the integrity of the bridges and the concrete structures of the Egnatia Motorway in general, are the following:

### 10.6.3.1 Seismic risk

All the bridges of the Egnatia motorway are built in seismic prone areas. Although the Egnatia bridges are designed and built according to the latest national seismic code[717, 718], and in some cases according to more unfavourable site specific earthquake spectra, a catastrophic seismic event, that could lead to major damage on some of the more vulnerable bridges, cannot be excluded.

This document is the intellectual property of the fib – International Federation for Structural Concrete. All rights reserved.
This PDF of fib Bulletin 86 is intended for use and/or distribution solely within fib National Member Groups.

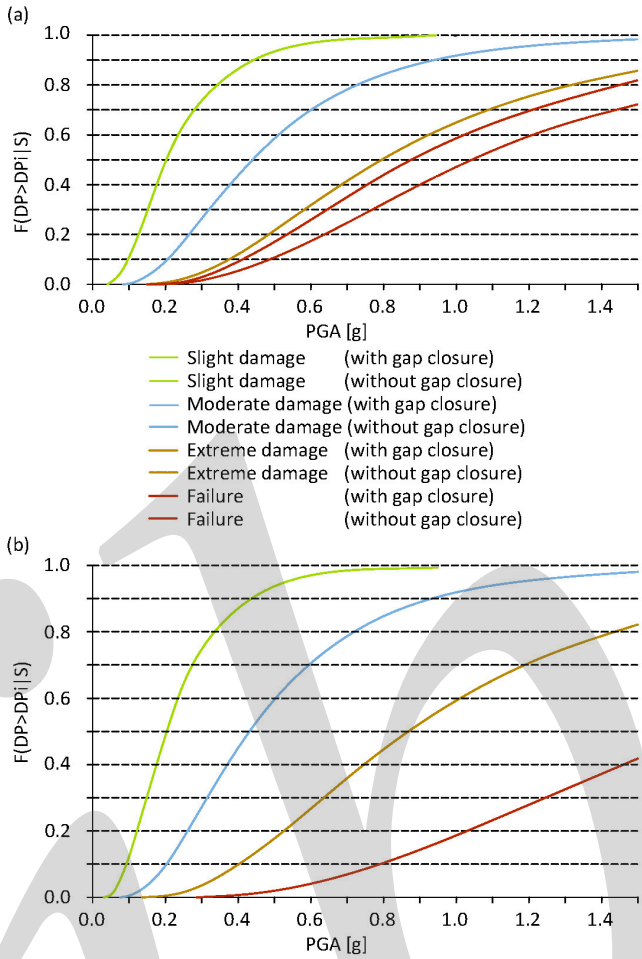


Fig. 10-45 Fragility curve of G9 bridge: (a) Longitudinal, (b) Transverse direction

Therefore Egnatia bridges were classified to 11 structurally representative categories depending on the structural type of the superstructure (box beam, slab, beams), the substructure (hollow piers, walls, frames or single massive columns) and their interconnection (monolithic or with bearings). For these 11 classes their seismic fragility curves were analytically derived[717, 719, 720, 718, 721]. As well known – see[720] – a fragility curve provides the probability of an damage parameter *DP* being at, or exceeding, the value $DP_i$ for the i-th damage state for a given seismic intensity level defined by an earthquake parameter. An example of such a fragility curve is shown in Fig. 10-45.

Next Fig. 10-46 shows main characteristics of some bridges, for which the fragility curves were determined.

*This document is the intellectual property of the fib – International Federation for Structural Concrete. All rights reserved.*
*This PDF of fib Bulletin 86 is intended for use and/or distribution solely within fib National Member Groups.*

| Structural configuration | Bridge name and class | No. of spans | Span length [m] | Total length [m] | Pier-to-deck connection | Curvature | Foundation |
|---|---|---|---|---|---|---|---|
| | Pedini Bridge 111 | 3 | 19.0 + 32.0 + 19.0 | 70.0 | monolithic | in height | pile groups |
| | Siatista Bridge 311 | 3 | 16.25 + 30.5 + 16.25 | 63.0 | monolithic | minor curvature in plan | pile groups |
| | T7 (section 14.1.2) Bridge 121 | 3 | 27.0 + 45.0 + 27.0 | 99.0 | monolithic | no | footings |
| | G11 Bridge (right branch) 221 | 3 | 64.3 + 118.6 + 64.3 | 247.2 | monolithic | in plan | caissons |
| | G9 (section 5.1) Bridge 421 | 2 | 85.0 | 170.0 | monolithic | in plan | caissons |
| | Eirini Bridge 122 | 4 | 45.0 | 180.0 | through bearings | no | pile groups |
| | Lissoss River Bridge 422 | 11 | 1× 29.56 + 3× 37.05 + 6× 44.35 + 1× 26.50 | 433.31 | through bearings | no | pile groups |
| | 2nd Kavala Ravine Bridge 232 | 4 | 42.0 + 2× 43.5 + 42.0 | 180.0 | through bearings | no | caissons |
| | G2 (section 1.1.6) Bridge 332 | 3 | 30.7 + 31.7 + 30.7 | 93.1 | through bearings | no | pile groups |
| | Kossynthos River Bridge 432 | 5 | 35.0 + 3× 36.0 + 35.0 | 178.0 | through bearings | no | pile groups |
| | Krystallopigi Bridge 223 | 12 | 44.17 + 10× 54.98 + 44.17 | 638.19 | monolithic/ through bearings | in plan | pile groups |

Fig. 10-46 Main characteristics of the bridges whose the fragility curves were determined

Using the above fragility curves, the seismic risk assessment of the newly established bridges is supported through relevant software[717]. This combines the seismic hazard model of the area along the motorway and the vulnerability analytically determined for all the representative bridges.

### 10.6.3.2 Concrete & steel deterioration risk

Many of the bridges of the motorway are built in high mountainous areas where freeze-thaw cycles and continuous use of de-icing salts increase the risk of chloride induced corrosion of the reinforcement steel. Other bridges of the Motorway are close to the sea front and for the same reason are in a highly corrosive environment as well. For the assessment of this risk, periodical visual inspection is combined with non-destructive and intrusive tests in order to determine the actual extent and to experimentally detect the rhythm of chloride contamination and the carbonation in Egnatia bridges.

The target is to gather enough data to validate the initial considerations done inside the Bridge Management Software tool. So, the Indiana State Markov deterioration tables (see an example in Fig. 10-47) were adopted for predicting the rhythm and the extent of the bridge component deterioration. The analysis of these data will also enable the calibration of the initial maintenance life cycles as well as the decision trees adopted for the Egnatia Software.

*This document is the intellectual property of the fib – International Federation for Structural Concrete. All rights reserved.*
*This PDF of fib Bulletin 86 is intended for use and/or distribution solely within fib National Member Groups.*

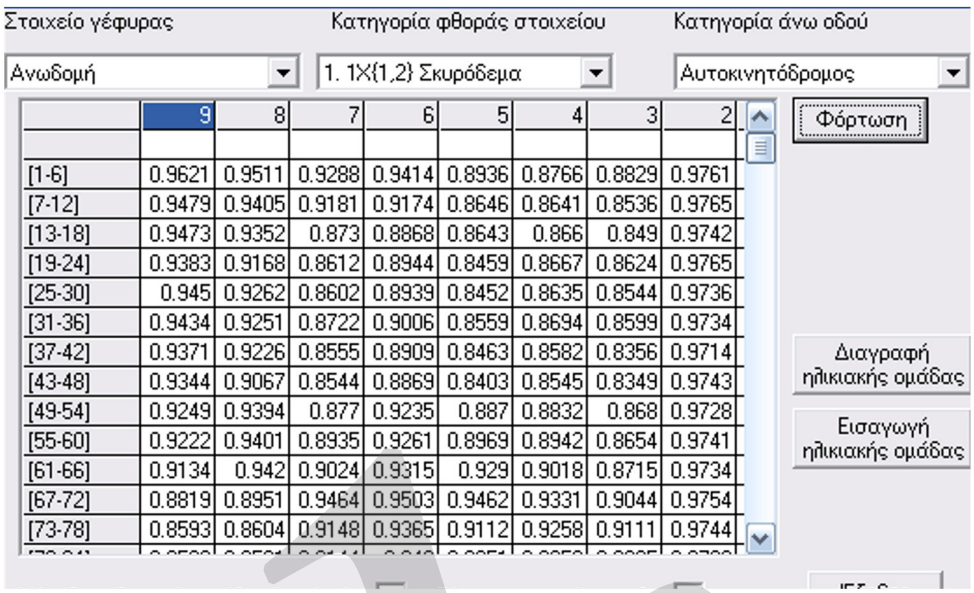


| | 9 | 8 | 7 | 6 | 5 | 4 | 3 | 2 |
|---|---|---|---|---|---|---|---|---|
| [1-6] | 0.9621 | 0.9511 | 0.9288 | 0.9414 | 0.8936 | 0.8766 | 0.8829 | 0.9761 |
| [7-12] | 0.9479 | 0.9405 | 0.9181 | 0.9174 | 0.8646 | 0.8641 | 0.8536 | 0.9765 |
| [13-18] | 0.9473 | 0.9352 | 0.873 | 0.8868 | 0.8643 | 0.866 | 0.849 | 0.9742 |
| [19-24] | 0.9383 | 0.9168 | 0.8612 | 0.8944 | 0.8459 | 0.8667 | 0.8624 | 0.9765 |
| [25-30] | 0.945 | 0.9262 | 0.8602 | 0.8939 | 0.8452 | 0.8635 | 0.8544 | 0.9736 |
| [31-36] | 0.9434 | 0.9251 | 0.8722 | 0.9006 | 0.8559 | 0.8694 | 0.8599 | 0.9734 |
| [37-42] | 0.9371 | 0.9226 | 0.8555 | 0.8909 | 0.8463 | 0.8582 | 0.8356 | 0.9714 |
| [43-48] | 0.9344 | 0.9067 | 0.8544 | 0.8869 | 0.8403 | 0.8545 | 0.8349 | 0.9743 |
| [49-54] | 0.9249 | 0.9394 | 0.877 | 0.9235 | 0.887 | 0.8832 | 0.868 | 0.9728 |
| [55-60] | 0.9222 | 0.9401 | 0.8935 | 0.9261 | 0.8969 | 0.8942 | 0.8654 | 0.9741 |
| [61-66] | 0.9134 | 0.942 | 0.9024 | 0.9315 | 0.929 | 0.9018 | 0.8715 | 0.9734 |
| [67-72] | 0.8819 | 0.8951 | 0.9464 | 0.9503 | 0.9462 | 0.9331 | 0.9044 | 0.9754 |
| [73-78] | 0.8593 | 0.8604 | 0.9148 | 0.9365 | 0.9112 | 0.9258 | 0.9111 | 0.9744 |

Fig. 10-47 Markov Probabilities, adopted in Egnatia Software, for degradation of bridge superstructure

### 10.6.3.3 Risk induced by geotechnical failures

Many of the Egnatia reinforced concrete bridges were built by the balanced cantilevering method of construction and therefore have rigid superstructures, monolithically connected to the piers. For this type of bridges, the risk of serious damage due to extensive settlements and rotations induced by geotechnical failures, as e.g. landslides, liquefaction, high soil creep on their foundations, is very high. This risk will be assessed in the frame of a special developed software called IRIS and similar to European IRIS project (IRIS: Integrated European Industrial Risk Reduction System). An enhancement of the already derived or the analytical determination of new fragility curves considering the geotechnically induced hazard will be carried out by Egnatia research team in this research project. This analytical work will be based on monitoring the bridge and the adjacent foundation soil.

Other major risks affecting the Egnatia river bridges are the scouring of their foundations due to the expected flood events, as well as the erosion of the approach embankments of the road and the bank river slopes. Scouring is a risk significantly decreased due to the fact that all the river and stream bridges of the Egnatia Motorway are founded on deep piles.

## 10.6.4 Bridge visual inspection and data base recording

Egnatia Motorway bridges are visually inspected periodically by the skilled inspection teams of the Structures Maintenance Unit. This is carried out every 2 years for the major bridges and every 5 years for underpasses and culverts. The visual inspections are carried out following the guidelines of the Egnatia Inspection Manual[722]. The typical inspector's reports are noted on site with all the visual findings (e.g. cracks in concrete, rotation of abutments, scour of foundations, steel corrosion indications). The inspectors prepare a report on the condition of the bridge and rate its characteristics. This is realized according to a predetermined nine-point scale, which is similar to the one used by the FHWA and the Federal State of California. Fig. 10-48 shows an example.

The main scope of the periodic visual inspection is the continuous monitoring, recording and rating of the bridge condition. Usually the visual inspections are combined with fast

*This document is the intellectual property of the fib – International Federation for Structural Concrete. All rights reserved.*
*This PDF of fib Bulletin 86 is intended for use and/or distribution solely within fib National Member Groups.*

non-destructive tests including Schmidt hammer, pulse velocity, half-cell and carbonation test measurements. So, over the recent five years visual inspection, combined with non-destructive and invasive tests, has been carried out on the old and seriously deteriorated bridge network of the existing national and regional roads in Thessaly, West and Central Macedonia counties. Hundreds of reinforced and prestressed concrete bridges are included and classified in two main age categories (30 and 50 years old). The results were comprehensive in terms of identified structural damage, such as extensive cracks, scouring, settlements/rotations of foundations, and advanced steel corrosion. Therefore the inspection data help to validate the accuracy of the condition evaluation ranking system of Egnatia, as well as the representativeness of the initial considerations for the rhythm of the deterioration of the Egnatia bridges.

**1.2 Πίνακας Κ1: Δομικά στοιχεία από Οπλισμένο /Προεντεταμένο Σκυρόδεμα***

| Κατάσταση | Περιγραφή | Ενδεικτικές προτεινόμενες ενέργειες |
|---|---|---|
| 9 | Για σκυρόδεμα δομικού στοιχείου που δεν παρουσιάζει ρωγμές, εξάνθηση, αποχρωματισμό και δεν έχει φθαρεί η προστατευτική βαφή του. | 0- Καμία ενέργεια |
| 8 | Για σκυρόδεμα δομικού στοιχείου που παρουσιάζει περιορισμένη εξάνθηση ή/και αποχρωματισμό και έχει φθαρεί η προστατευτική βαφή του. | 0- Καμία ενέργεια<br>1- Προστατευτική Βαφή |
| 7 | Για σκυρόδεμα δομικού στοιχείου με **μη δομικές** ρωγμές εύρους μικρότερου ή ίσου με 0,3 mm. Τοπικά περιορισμένη αποφλοίωση (αποκάλυψη αδρανών), έντονη εξάνθηση σε περιοχές διαβροχής (κορεσμένες επιφάνειες), έντονος αποχρωματισμός, εκτεθειμένοι δευτερεύοντες οπλισμοί (αποστατήρες), ίχνη/ ενδείξεις έναρξης οξείδωσης οπλισμού. | 0- Καμία ενέργεια<br>1- Προστατευτική Βαφή<br>2-Ξεφράγιση των ρηγματώσεων και επισκευή αποφλοιώσεων |
| 6 | Για σκυρόδεμα δομικού στοιχείου με **δομικές** ρωγμές, καμπτικές ή/και διατμητικές εύρους μικρότερου ή ίσου με 0,5mm. Έντονη επιφανειακή αποφλοίωση, ρηγμάτωση και ίχνη σκουριάς από σημαντική οξείδωση οπλισμού. | 0- Καμία ενέργεια<br>1- Προστατευτική Βαφή<br>2-Ξεφράγιση των ρηγματώσεων<br>3- Παρακολούθηση εξέλιξης ρωγμών με ρωγμόμετρα |
| 5 | Για σκυρόδεμα με καμπτικές ή/και διατμητικές ρωγμές εύρους μικρότερου από αυτό που αντιστοιχεί στη διαρροή του οπλισμού (αναλόγως της απόστασης των ρωγμών, του εύρους, του ποσοστού και της κατηγορίας χάλυβα του οπλισμού), γενικά μικρότερες των 2,0mm. Έντονη επιφανειακή αποφλοίωση, μικρή απώλεια διατομής σκυροδέματος, μικρή απώλεια διατομής οπλισμού λόγω προχωρημένης οξείδωσης. Απαιτούνται ειδικοί μη καταστροφικοί/καταστροφικοί επιτόπιοι έλεγχοι και ειδική ανάλυση για ερμηνεία της αιτίας ρηγμάτωσης εφ'όσον μετά από παρακολούθηση προκύπτει ότι οι ρωγμές εξελίσσονται (διευρύνονται). | 0- Καμία ενέργεια<br>1- Προστατευτική Βαφή<br>2- Τσιμεντενέσεις ή ρητινενέσεις σφράγισης των ρηγματώσεων<br>3- Παρακολούθηση εξέλιξης ρωγμών με ρωγμόμετρα<br>4-Αφαίρεση/καθαρισμός διαβρωμένου σκυροδέματος<br>5- Καθαρισμός/βαφή οπλισμού<br>6- Εποξειδικά/θιξοτροπικά κονιάματα επισκευής |
| 4 | Για σκυρόδεμα με καμπτικές ρωγμές ή/και διατμητικές ρωγμές μεγάλου εύρους που αντιστοιχούν σε διαρροή του οπλισμού (αναλόγως της απόστασης των ρωγμών, του εύρους, του ποσοστού και της κατηγορίας χάλυβα οπλισμού), γενικά μεγαλύτερες των 2,0mm. Οι ρωγμές δεν διευρύνονται όπως προκύπτει μετά από παρακολούθηση της εξέλιξής των ρωγμών με ρωγμόμετρα. Ρωγμές λόγω ανακατανομής δεν έχουν παρατηρηθεί. Απαιτούνται ειδικοί μη καταστροφικοί/καταστροφικοί επιτόπιοι έλεγχοι και ειδική ανάλυση για ερμηνεία του μηχανισμού βλάβης. Η απώλεια σκυροδέματος και η οξείδωση του οπλισμού επηρεάζουν την αντοχή και λειτουργικότητα του δομικού στοιχείου. | 0- Καμία ενέργεια<br>4-Αφαίρεση/καθαρισμός διαβρωμένου σκυροδέματος<br>5- Καθαρισμός/βαφή οπλισμού<br>7- Προσθήκη οπλισμού (αποκατάσταση ή ενίσχυση διατομής)<br>6- Εποξειδικά/θιξοτροπικά κονιάματα επισκευής<br>1- Προστατευτική Βαφή |
| 3 | Για σκυρόδεμα με καμπτικές ρωγμές ή/και διατμητικές ρωγμές μεγάλου εύρους που αντιστοιχούν σε διαρροή του οπλισμού (αναλόγως της απόστασης των ρωγμών, του εύρους, του ποσοστού και της κατηγορίας χάλυβα οπλισμού), γενικά μεγαλύτερες των 2,0mm. Οι ρωγμές διευρύνονται όπως προκύπτει μετά από παρακολούθηση της εξέλιξής των ρωγμών με ρωγμόμετρα. Ρωγμές έχουν ανοίξει λόγω στατικής ανακατανομής. Απαιτούνται ειδικοί μη καταστροφικοί/καταστροφικοί επιτόπιοι έλεγχοι και ειδική ανάλυση για ερμηνεία του μηχανισμού βλάβης. Προχωρημένη οξείδωση του οπλισμού και απώλεια διατομής οπλισμού/σκυροδέματος που επηρεάζει σημαντικά την αντοχή του επιμέρους δομικού στοιχείου. | 4-Αφαίρεση/καθαρισμός διαβρωμένου σκυροδέματος<br>5- Καθαρισμός/βαφή οπλισμού<br>7- Προσθήκη οπλισμού (αποκατάσταση ή ενίσχυση διατομής)<br>6- Εποξειδικά/θιξοτροπικά κονιάματα επισκευής<br>1- Προστατευτική Βαφή<br>8- Αντικατάσταση δομικού στοιχείου |
| 2 | Μεγάλες καμπτικές ή/και διατμητικές ρωγμές και προχωρημένη διάβρωση του οπλισμού και απώλεια διατομής οπλισμού/σκυροδέματος που επηρεάζουν σημαντικά την αντοχή του επιμέρους δομικού στοιχείου αλλά και του δομικού τμήματος στο οποίο ανήκει. | 4-Αφαίρεση/καθαρισμός διαβρωμένου σκυροδέματος<br>5- Καθαρισμός/βαφή οπλισμού<br>7- Προσθήκη οπλισμού (αποκατάσταση ή ενίσχυση διατομής)<br>6- Εποξειδικά/θιξοτροπικά κονιάματα επισκευής<br>1- Προστατευτική Βαφή<br>8- Αντικατάσταση δομικού στοιχείου |
| 1 -0 | Η βαθμολογία αυτή δίνεται μόνον στη γέφυρα που έχει απαγορευθεί η κυκλοφορία λόγω σαφούς υποβάθμισης της δομικής ακεραιότητας (κατακόρυφες και οριζόντιες παραμένουσες μετακινήσεις) ή λόγω τμηματικής αστοχίας ή αστοχίας δομικών στοιχείων. | Αντικατάσταση Γέφυρας. |

Fig. 10-48 Concrete nine-point condition ranking (Egnatia Inspection Manual[722])

*This document is the intellectual property of the fib – International Federation for Structural Concrete. All rights reserved.*
*This PDF of fib Bulletin 86 is intended for use and/or distribution solely within fib National Member Groups.*

Fig. 10-49 Characteristic damage findings of the completed visual inspection of old Greek bridges (no Egnatia bridges)

Fig. 10-49 shows some critical deterioration data (e.g. concrete section loss/ advanced steel corrosion) obtained from the visual inspection and condition evaluation of old Greek bridges. Such data support the empirical validation of life cycle predictions (see Fig. 10-50) adopted in Egnatia Bridge Management Software, as well as for risk assessment on bridges in the frame of the ongoing research activities[723].

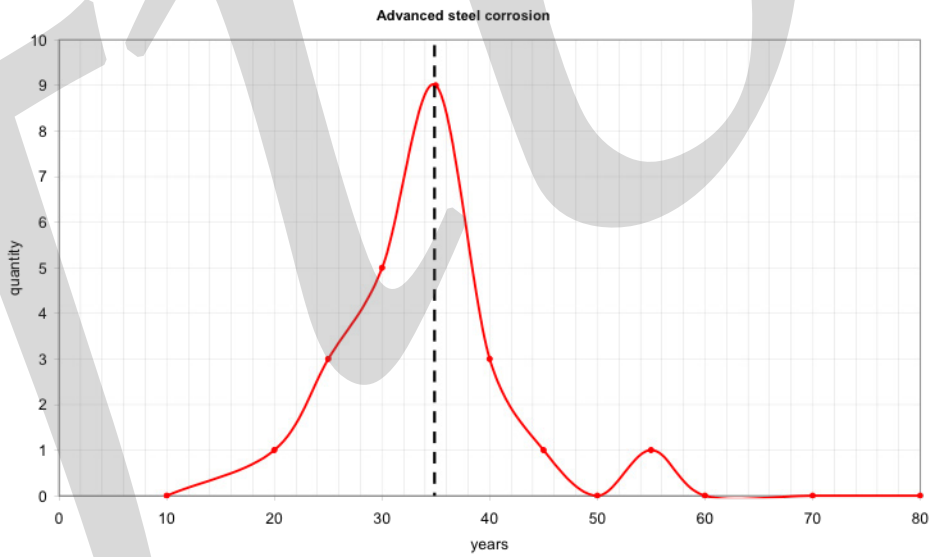


Fig. 10-50 Concrete nine-point condition ranking (Egnatia Inspection Manual[722])

This document is the intellectual property of the fib – International Federation for Structural Concrete. All rights reserved.
This PDF of fib Bulletin 86 is intended for use and/or distribution solely within fib National Member Groups.

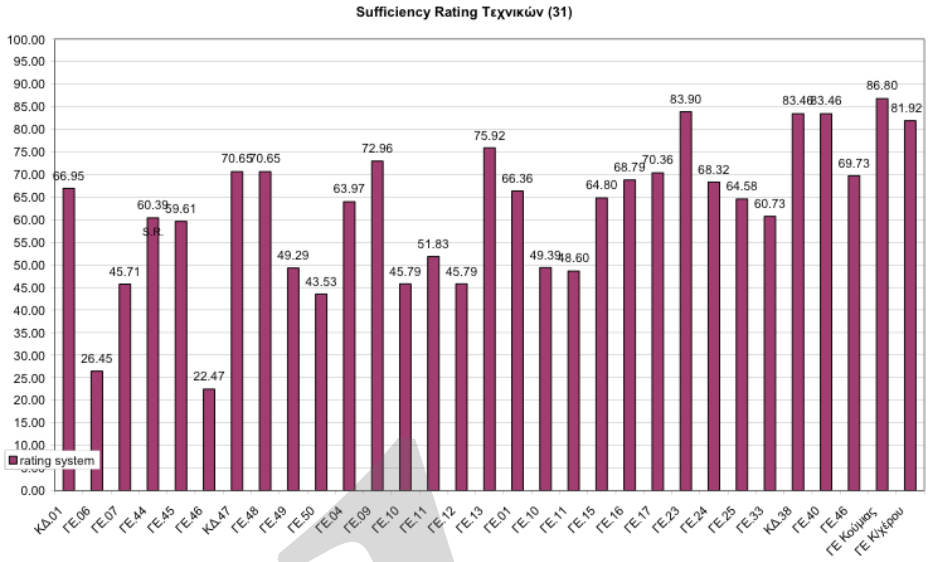


Fig. 10-51 Sufficiency rating of the inspected old Greek concrete bridges

The sufficiency rating of the already inspected bridges – see Fig. 10-51 – was carried out using the Egnatia sufficiency rating system[724, 725]. This system considers the condition rating of the basic structural elements of the bridges, the detour length during their repair actions, the geometry of the deck to carry the traffic, the approach road alignment, the scouring and the vehicle collision, the hydraulic adequacy, etc.

After October 2008 all the bridges of Egnatia Motorway, whose construction was completed and set on service, were inspected and their condition was evaluated. Although these bridges are newly established, some of them are built on active landslides (bridges T9/T11, Panagia G1 bridge) or on liquefiable soil (Nestos bridge) or in the vicinity of active seismic faults (Bridges G2, G4, G7 in Krystallopigi – Paramythia motorway section). Therefore their structural safety risk assessment, considering externally induced risks, is of high priority to be done.

The visual inspection findings as well as the condition evaluation of these bridges are recorded in the Egnatia Bridge Data Base[724].

## 10.6.5 Bridge health monitoring activities

Visual inspection is difficult and time-consuming. It requires skilled staff, special access equipment and is limited in its accuracy. To provide a more robust system, Egnatia Odos S.A. has developed a new type of inspection. This uses instruments installed on the major bridges to monitor their dynamic response (accelerations) from ambient excitations (wind, traffic, etc.) or seismic action[726, 727, 728, 729, 730, 731, 732, 733, 734, 735].

The instrumentation of bridges with accelerometer arrays for measuring their dynamic response (acceleration) is widely used worldwide. In Greece it was first applied on the Evripos bridge and on smaller bridges for research purposes.

### 10.6.5.1 Instrumentation and telemetric monitoring of bridge response.

Ten Egnatia Motorway bridges have been instrumented, selected for their structural representativeness of the majority of Egnatia Bridges and for their high seismicity, and are shown in Fig. 10-52.

*This document is the intellectual property of the fib – International Federation for Structural Concrete. All rights reserved.*
*This PDF of fib Bulletin 86 is intended for use and/or distribution solely within fib National Member Groups.*

Fig. 10-52 Bridges instrumented/monitored by moveable or permanent sensor arrays

Cabled networks of uniaxial or triaxial forced balanced accelerometers, strain-gauges and joint-meters are installed (Fig. 10-53) either on the decks or inside the box beam of the superstructure, on the pier head crossbeams and on the bases of the piers. These networks are connected to multi-channel accelerographs. In the case of two or more accelerographs, these are connected to each other in order to ensure synchronous data acquisition. They are equipped with external wireless GSM/GPRS modems or are connected directly on the fibre optic network, so providing online continuous monitoring. Type, number and cost of sensors installed on the ten Egnatia Bridges are shown in Fig. 10-54.

Fig. 10-53 (a) Accelerometers, (b) Strain-gauges, (c) joint-meters, installed

*This document is the intellectual property of the fib – International Federation for Structural Concrete. All rights reserved.*
*This PDF of fib Bulletin 86 is intended for use and/or distribution solely within fib National Member Groups.*

**BRIDGES INSTRUMENTED WITH SENSORS (CONTINUOUS SH MONITORING)**

| Bridge Name | Section | Accelerometers | Strain guages/ thermometers | Jointmeters | Anemo meters | Structural type |
|---|---|---|---|---|---|---|
| Kristallopigi Bridge | 1.1.6 | 20 | 22 | 2 | - | Box beam/bearings/ Hollow piers |
| G4 | 1.1.6 | 12 | 20 | 2 | - | Composite beam/ bearings/ Hollow piers |
| G7 | 1.1.6 | 12 | 14 | 2 | - | TPC Beams/ Bearings/ Hollow piers |
| Metsovo Bridge | 3.2 | 12 | 14 | 2 | 1 | Box beam/bearings/ Hollow piers |
| G1 | 3.5.1 | 6 | 8 | 2 | - | Box beam/bearings/ Hollow piers |
| G7 | 3.5.1 | 9 | 14 | 2 | - | Box beam/bearings/ Hollow piers |
| G8 | 3.5.2 | 9 | 14 | 2 | - | Box beam/bearings/ Hollow piers |
| G9 | 5.1 | 48 | 8 | 1 | 1 | Box beam/monolithical/ Hollow piers |
| T2 | 9.1 | - | 8 | - | - | TPC Beams/ Bearings/ Multicolumn piers |
| G2 | 13.5 | 48 | - | 1 | 1 | TPC Beams/ Bearings/ Hollow piers |
| TOTAL | | 176 | 122 | 16 | 3 | |
| COST | | 600.000 € | 150.000 € | 30.000 € | 20.000 € | 800.000 € (1,5 %) |

11/11/2010 Bridges Instrumented before October 2008 (Euro Funded Research Project "Seismic Protection of Bridges") 15

Fig. 10-54 Type, number and cost of sensors installed on the ten Egnatia Bridges

### 10.6.5.2 Development and use of user-friendly modal identification software

Traffic-induced acceleration data, the so-called ambient vibrations, are the only easily acquired data apart from seismic data, which can be continuously acquired by the sensor networks installed on the ten Egnatia bridges. These data are processed to obtain the actual dynamic characteristics of the monitored bridges – see Fig. 10-55. Then, the measured characteristics can be compared with the Finite Element Model (FEM) predictions for the purpose of validating design considerations and of assessing the actual bridge condition.

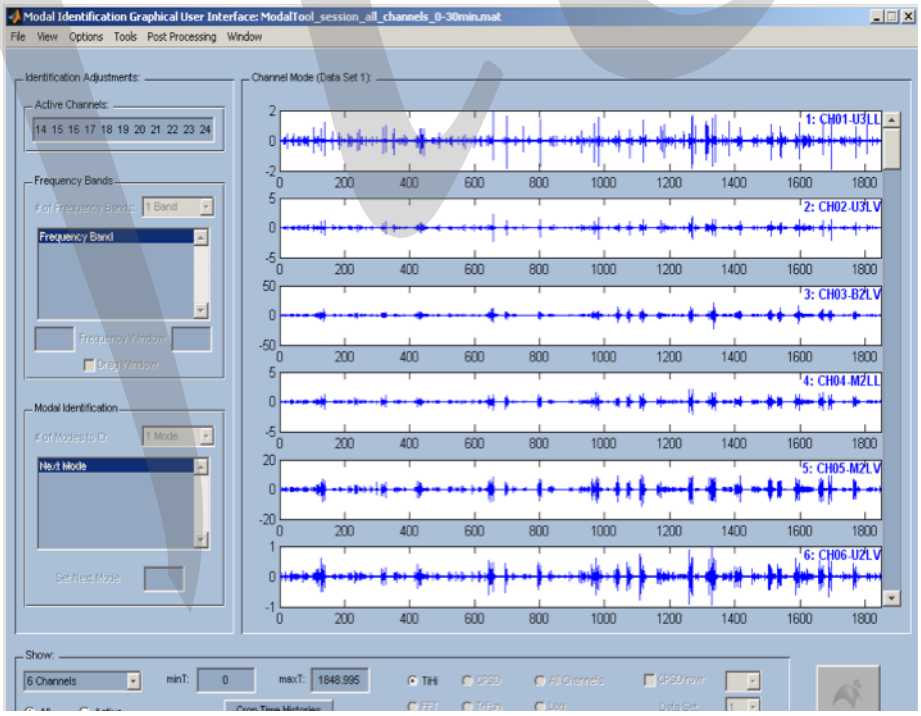

*This document is the intellectual property of the fib – International Federation for Structural Concrete. All rights reserved.*
*This PDF of fib Bulletin 86 is intended for use and/or distribution solely within fib National Member Groups.*

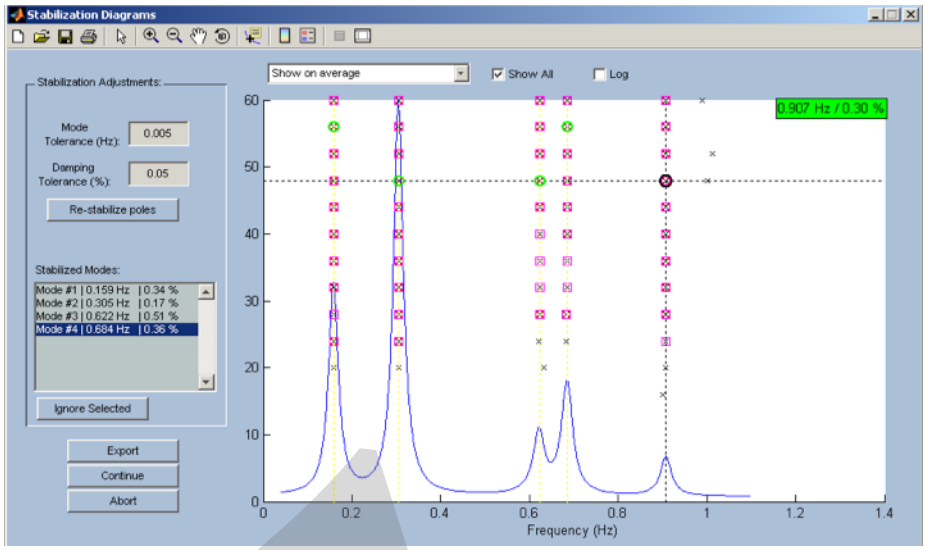


Fig. 10-55 a) Ambient accelerations, b) Identification of eigen frequencies

The ten instrumented Egnatia Motorway bridges – see Fig. 10-52 – were opened to traffic after 2002. Therefore, it is considered unlikely that any significant deterioration, of a magnitude that may have affected their dynamic characteristics, will be diagnosed. The validation of the design considerations for the ten structurally representative bridges and the initial experimental identification of their mass/stiffness/damping properties are very important regarding the monitoring of the structural deterioration process and the timely and accurate prediction of future damage.

User friendly Matlab-based modal identification software enabling the processing of ambient data has been developed in cooperation with university of Thessaly[726, 727, 728, 729]. Once the Power Spectral Densities (PSD) of measured multiple channel responses are computed, it becomes possible to identify all the basic frequencies/mode shapes of the bridge that optimize the fitting of the modal models to the computed ones, using genetic algorithms or other optimization algorithms available in Matlab.

The software tool developed is used for processing the ambient data acquired from monitoring the Egnatia instrumented bridges, as well as some selected old deteriorated bridges, visually inspected as already mentioned in previous section 4. The most important frequencies and damping ratios of the bridges were successfully identified. An example is given in Fig. 10-56.

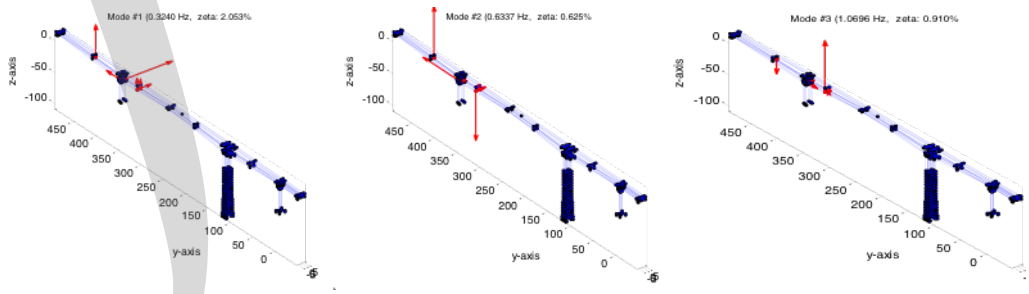


Fig. 10-55 The first three identified eigen modes of Metsovo ravine bridge during operation

This document is the intellectual property of the fib – International Federation for Structural Concrete. All rights reserved.
This PDF of fib Bulletin 86 is intended for use and/or distribution solely within fib National Member Groups.

#### 10.6.5.3 Updating the dynamic models and detecting the damage of the monitored bridges

Sophisticated methods of modal identification, fitting the information measured by sensor arrays to the theoretical predicted by the finite element bridge models (simulating the mechanical performance and the deterioration/damage of the bridge structural system), have been developed in cooperation with the University of Thessaly[729, 733]. The purpose was to check the structural integrity and to detect the location, extent and type of damage.

Damage detection is based on modal parameters identified from measured ambient data of the bridges under normal conditions of operation. When the modal parameters are recognised using the methodology of the previous section, the identified modes and mode shapes are used as input data in order to update linear dynamic models of instrumented bridges. The methodology used is a computationally efficient methodology which has been developed by Egnatia Odos S.A. The physical properties of the structure, such as mass and stiffness, are updated. According to this methodology, the finite element model is parameterized by a parameter set which can represent mass and stiffness properties at an element or substructure level. Such finite element properties to be parameterized could be the elasticity modulus multiplied by the moment of inertia for the superstructure and piers ($E*I$), spring constants simulating elastomeric bearings (GA/h), and others.

Computationally suitable algorithms were developed to update the parametrical values defined by the user. The aim of an update methodology based on a modal model is to find, for the parameters defined by the user, such values that will achieve the convergence of the dynamic characteristics of the finite element model with the ones recognised experimentally. The methodology used looks for the optimum values of the natural properties, which minimize a measure of fit between the modes and modal frequencies of the model and the actual modes and modal frequencies measured.

The abovementioned methodologies were incorporated into suitable software in a user-friendly graphic context developed by Egnatia Odos to recognise finite element models and assess the abovementioned properties of stiffness and mass at the level of a structural element or an entire substructure. The models are updated and the damage is diagnosed through efficient optimization methods. The software has been applied in updating the finite element models of the ten instrumented bridges as well as of the old Greek deteriorated bridges, already mentioned.

The model updating of selected bridges both of Egnatia and of other old national roads are updated on the basis of the ambient vibration experimentally identified modal data.

Some representative results of the application of the above procedure are given in Table 10-9 to Table 10-12:

Table 10-9 Identified eigenfrequencies for 2 old deteriorated concrete bridges

| Eigen mode | Axios river bridge | | Strymonas River bridge | |
|---|---|---|---|---|
| | Eigen Frequencies (Hz) | Damping ratios (%) | Eigen Frequencies (Hz) | Damping ratios (%) |
| 1st bending | 3.97 | 3.87 | 4.03 | 2.89 |
| 1st torsional | 4.09 | 2.30 | 4.42 | 0.86 |

*This document is the intellectual property of the fib – International Federation for Structural Concrete. All rights reserved.*
*This PDF of fib Bulletin 86 is intended for use and/or distribution solely within fib National Member Groups.*

| | | | | |
|---|---|---|---|---|
| 2nd torsional | 12.80 | 1.97 | 13.04 | 0.31 |
| 2nd bending | 13.75 | 1,75 | 13.18 | 0.51 |
| 3rd bending | 14.63 | 1.85 | - | - |

Table 10-10 Identified eigen frequencies for five Egnatia bridges

| Eigen mode | Left Branch Metsovo Const. phase | Right Branch Metsovo Const. phase | Left Branch Metsovo Operation phase | G10 Polymylos Bridge | G2 Kavala Bridge | G9 Operat. vibrations | Polymylos Bridge Seismic vibrations |
|---|---|---|---|---|---|---|---|
| 1st Transverse | 0.16 | 0.16 | 0.28 | 0.89 | 0.81 | 1.13 | 1.29 |
| 2nd Transverse | 0.62 | 0.62 | 0.44 | 1.87 | 1.61 | 1.20 | 1.30 |
| 3rd Transverse | 1.31 | 1.30 | 0.57 | 3.57 | | 2.22 | 2.56 |
| 4th Transverse | 1.72 | 1.47 | 0.64 | 6.04 | | 4.10 | 4.23 |
| 5th Transverse | 2.23 | 2.59 | 0.71 | | | 6.78 | 7.24 |
| 6th Transverse | - | - | 1.03 | | | | |
| 1st Bending | 0.30 | 0.30 | 0.66 | 1.43 | 3.40 | 2.13 | 2.20 |
| 2nd Bending | 0.69 | 0.69 | 1.09 | 2.72 | 3.46 | 3.07 | 3.20 |
| 3rd Bending | 0.91 | 0.91 | 1.48 | 3.47 | 3.47 | 6.66 | 6.89 |
| 4th Transverse | 2.41 | 2.29 | 1.86 | 4.51 | 3.51 | | |
| 5th Bending | 3.17 | 3.24 | 2.08 | 6.79 | | | |
| 6th Bending | | | 2.83 | 7.67 | | | |
| 1st Longitudinal | - | | | | 1.29 | | |
| 1st Torsional | 4.89 | 4.91 | | 5.85 | | | |

Table 10-11 Updated stiffness parameter coefficients of 3 Egnatia bridges

| Parameter | G9 Polymylos bridge | | G2 Kavala bridge | G10 Polymylos bridge | |
|---|---|---|---|---|---|
| Superstructure stiffness | Operational vibrations | Seismic vibrations | 1.57 | bending modes | transverse and bending |
| | 1.00-1.10 | 104 | | 1.45-1.60 | 1.15-1.20 |
| Piers stiffness | Operational vibrations | Seismic vibrations | 1.63 | bending modes | transverse and bending |
| | 0.69-0.82 | 1.55 | | 0.75-1.10 | 0.84-0.92 |
| Bearings stiffness | Operational vibrations | Seismic vibrations | 9.07 | - | |
| | 3.35 - 3.55 | 3.74 | | | |

This document is the intellectual property of the fib – International Federation for Structural Concrete. All rights reserved.
This PDF of fib Bulletin 86 is intended for use and/or distribution solely within fib National Member Groups.

Table 10-12 Updated stiffness parameter coefficients of Metsovo Bridge

| Parameter | Cantilever of pier M3 | | | |
|---|---|---|---|---|
| | Left branch of Metsovo bridge-Construction phase | | Right branch of Metsovo bridge-Construction phase | Left branch of Metsovo bridge-Operation phase |
| | 1st bending 1η torsional | 5 lower eigen modes | | |
| Superstructure stiffness | 1.57 | 0.85-0.92 | 0.85-0.91 | 0.96 – 1.00 |
| Piers stiffness | 1.20 | 1.09-1.15 | 1.09-1.15 | 1.00 – 1.29 |

### 10.6.6 Conclusions

The development of the Egnatia Odos Bridge Management System presented was based on well documented similar experience. The system includes innovations which seem to differentiate it from existing systems regarding its elements both separately and in combination. More specifically, it includes:

1. A sophisticated extensive digital database connected to the EOAE GIS as required to enhance its utility and capability as a strategic tool.
2. Optional autonomous use of the bridge database for condition rating. This makes it a first-class tool for the management of a group of bridges.
3. A manual for bridge visual inspection and condition rating. This manual has already been applied to Egnatia motorway bridges that are in service.
4. Integration of instrumented monitoring of the structural integrity of bridges as an aid to visual inspection.
5. A dual approach to the management of capital maintenance that includes both preventive and emergency maintenance following a catastrophic event. Decision making is supported by special software that assesses seismic risk and aftershock management requirements which is updated with representative vulnerability data in combination with instrumented inspection.
6. Incorporation of seismic considerations into capital maintenance management which has been only been attempted over the past five years in new generation management systems.
7. Consideration of earthquake and seismic vulnerability in the management software algorithms.
8. Models for the analysis and optimization of bridge management software, modal identification software and modal model updating, based on genetic algorithms in combination with other optimisation algorithms (Decision trees, Life cycle analysis, Prioritization of capital maintenance actions).
9. Special considerations, such as extending management software decision trees to cover actions for particular structural elements (e.g. joints and bearings) or structural representativeness in deterioration models which improve the intermediate level of analysis.

*This document is the intellectual property of the fib – International Federation for Structural Concrete. All rights reserved.*
*This PDF of fib Bulletin 86 is intended for use and/or distribution solely within fib National Member Groups.*

Finally, the fact that the system has been developed by the organization that has designed and constructed the project, i.e. Egnatia Odos S.A., before the completion of the project, can be also considered as a novelty.

#### 10.6.6.1 Acknowledgements

The research done for the development of Egnatia Bridge Risk Assessment methodologies and software tools was funded by the Greek General Secretariat of Research and Technology.

Two authors of this section have participated in the Research Project ASPROGE (ASeismic PROtection of BRidges), funded by the General Secretariat of Research and Technology of Greece and by EGNATIA ODOS S.A., Thessaloniki, Greece.

This document is the intellectual property of the fib – International Federation for Structural Concrete. All rights reserved.
This PDF of fib Bulletin 86 is intended for use and/or distribution solely within fib National Member Groups.

# 11 References

[1] Ellingwood, B. R. (2001). "Acceptable risk bases for design of structures." *Progress in Structural Engineering and Materials* 3: 170–179.

[2] Zdenek P. Bazant and Li, G.-H. (2008). Comprehensive Database on Concrete Creep and Shrinkage *Structural Engineering Report No. 08-3/A210c*.

[3] Griffis, L. G. (1993). "Serviceability Limit States under Wind Load." *Engineering Journal AISC*: 1-16.

[4] Podrouzek, J. (2012). "Importance Sampling Strategy for Oscillatory Stochastic Processes." *Journal of Mechanics Engineering and Automation* 2: 663-670.

[5] Björnsson, Í. (2010). Robust design of Bridges - Robustness analysis of Sjölundaviadukt Bridge. *Report TVBK* – 5179.

[6] Karamchandani, A. and Cornell, C. (1992). "Reliability Analysis of Truss Structures with Multistate Elements. II." *Journal of Structural Engineering* 118: 910-925.

[7] Crampton, D., McGormley, J. and Hill, H. (2007). "Improving Redundancy of Two-Girder Bridges." *Transportation Research Record: Journal of the Transportation Research Board* 2028(-1): 59-66.

[8] Frangopol, D. M. and Nakib, R. (1991). "Effects of Damage and Redundancy on the Safety of Existing Bridges." *Third Bridge Engineering Conference*, TRR(1290).

[9] Frangopol, D. M. and Curley, J. P. (1987). "Effects of Damage and Redundancy on Structural Reliability." *Journal of Structural Engineering-Asce* 113(7): 1533-1549.

[10] Paliou, C., Shinozuka, M. and Chen, Y.-N. (1990). "Reliability and Redundancy of Offshore Structures." *J. Engrg. Mech* 116: 359-378.

[11] Hendawi, S. and Frangopol, D. M. (1994). "System reliability and redundancy in structural design and evaluation." *Structural Safety* 16: 47-71.

[12] Chen, K. and Zhang, S. (1996). "Semi-probabilistic Method for Evaluating System Redundancy of Existing Offshore Structures." *Ocean Engineering* 23: 455-464.

[13] Biondini, F., Frangopol, D. M. and Restelli, S. (2008). *On structural robustness, redundancy and static indeterminacy*. Structural Congress 2008, ASCE.

[14] Biondini, F. (2009). *A measure of lifetime structural robustness*. Structural Congress 2009, ASCE.

[15] Ghosn, M. and Moses, F. (1998). *NCHRP Report 406, Redundancy in Highway Bridge Superstructures*. Washington. DC, Transportation Research Board–National Research Council, National Academy Press.

[16] Liu, W. D., National Cooperative Highway Research, P., National Research Council . Transportation Research, B., American Association of State, H., Transportation, O., Imbsen and Associates, I. (2001). *Redundancy in highway bridge substructures*. Washington, D.C., National Academy Press.

[17] Giuliani, L. (2009). Structural integrity: robustness assessment and progressive collapse susceptibility, University of Rome La SapienzaThesis.

[18] Straub, D. and Faber, M. H. (2006). "Computational Aspects of Risk Based Inspection Planning." *Computer-Aided Civil and Infrastructure Engineering* 21: 179-192.

[19] Agarwal, J., Blockley, D. and Woodman, N. (2003). "Vulnerability of structural systems." *Structural Safety* 25(3): 263-286.

*This document is the intellectual property of the fib – International Federation for Structural Concrete. All rights reserved.*
*This PDF of fib Bulletin 86 is intended for use and/or distribution solely within fib National Member Groups.*

[20] Starossek, U. and Haberland, M. (2010). "Approaches to measures of structural robustness." *Structure and Infrastructure Engineering* 7(7-8): 625-631.

[21] Yan, D. and Chang, C. C. (2006). *Vulnerability of long-span cable-stayed bridges under terrorist event*. International Conference on Bridge Engineering- Challenges in the 21st Century.

[22] Gkoumas, F. B. L. G. K. (2007). *Handling the exceptions: robustness assessment of a complex structural system*. 3rd International Conference on Structural Engineering, Mechanics and Computation(SEMC).

[23] ., D. N. (1967). *Straßen- und Wegbrücken: Lastannahmen* : DIN 1072, Beuth.

[24] European Cooperation in the Field of, S., Technical, R. and Coopération Européenne dans le Domaine de la Recherche Scientifique et, T. (2008). *Robustness of structures: proceedings of the 1st Workshop of COST Action TU0601, ETH Zurich, 4-5 February 2008*. [Brussels], COST.

[25] Sørensen, J. D., Rizzuto, E. and Faber, M. H. (2009). Robustness – theoretical framework Proc. Joint Workshop of COST Actions TU0601 and E55. Ljubljana, ETH Zurich, Switzerland: 27-34.

[26] ALA. (2012, 2012). "American Lifelines Alliance." link visited on.

[27] Kim, Y. S. (2007). *Seismic loss assessment and mitigation of critical urban infrastructure systems*, ProQuest.

[28] Chang, S. E. and Nojima, N. (2001). "Measuring post-disaster transportation system performance: the 1995 Kobe earthquake in comparative perspective." *Transportation Research Part A: Policy and Practice* 35(6): 475-494.

[29] Shinozuka, M., Feng, M. Q., Lee, J. and Naganuma, T. (2000). "Statistical analysis of fragility curves." *Journal of Engineering Mechanics* 126: 1224-1231.

[30] General principles on reliability for structures (1998). *ISO 2394*.

[31] (ISO), I. O. f. S. (2012). ISO 16732: Fire safety engineering.

[32] Risk management – Vocabulary – Guidelines for use in standards (2002). *ISO/IEC Guide 73*.

[33] (ISO), I. O. f. S. (2009). ISO/IEC 31010: Risk management – Risk assessment techniques.

[34] Bases for Design of Structures - Assessment of Existing Structures (2001). *ISO 13822*.

[35] Safety aspects – Guidelines for their inclusion in standards (1999). *ISO/IEC Guide 51*.

[36] ISO (2012). ISO 16204:2012-09 Durability — Service life design of concrete structures. Switzerland.

[37] (ISO), I. O. f. S. (2008). General principles on the Design of Structures for Durability, ISO. ISO 13823.

[38] Winkler, R. L., Hora, S. C. and Baca, R. G. (1992). The Quality of Experts' Probabilities Obtained Through Formal Elicitation Techniques. NRC-02-88-005. N. R. Commission. Washington, DC.

[39] Ayyub, B. M. (2001). *Elicitation of Expert Opinions for Uncertainties and Risks*. Boca Raton, Florida, CRC Press.

[40] Paté-Cornell, E. (2002). "Risk and Uncertainty Analysis in Government Safety Decisions." *Risk Analysis* 22: 633-646.

This document is the intellectual property of the fib – International Federation for Structural Concrete. All rights reserved.
This PDF of fib Bulletin 86 is intended for use and/or distribution solely within fib National Member Groups.

[41] Braml, T. and Keuser, M. (2008). *Structural Reliability Assessment for existing bridges with in situ gained structural data only – Proceeding and assessment of damaged bridges*. 6th International Probabilistic Workshop, Darmstadt.

[42] Chhibber, S., Apostolakis, G. and Okrent, D. (1992). A Taxonomy of Issues Related to the Use of Expert Judgements in Probabilistic Safety Studies. *Reliability Engineering and System Safety*. 38: 27-45.

[43] Frangopol, D. M. and Maute, K. (2003). "Life-Cycle reliability-based optimization of civil and aerospace structures." *Computers and Structures* 81: 397-409.

[44] Augusti, G., Baratta, A. and Casciati, F. (1984). *Probabilistic Methods in Structural Engineering*. New York.

[45] Madsen, H. O., Krenk, S. and Lind, N. C. (1986). "Methods of Structural Safety."

[46] Ang, A. H.-S. and Tang, W. H. (2007). *Probability concepts in engineering planning and design, basic principles*, Wiley & Son.

[47] Bucher, C. (2009). *Computational Analysis of Randomness in Structural Mechanics*. London, CRC Press.

[48] Nataf, A. (1962). "Détermination des distributions de probabilités dont les marges sont données." *Comptes Rendus de l'Académie des Sciences* 255: 42.

[49] Der Kiureghian, A. and Liu, P.-L. (1986). "Structural Reliability under Incomplete Probability Information." *Journal of Engineering Mechanics* 112: 85-104.

[50] Safety, J. C. o. S. (2001). JCSS Probabilistic Model Code Part 1: Basis of Design.

[51] Bucher, C. (1988). "Adaptive Sampling – an iterative fast Monte Carlo procedure." *Structural Safety* 5: 119-126.

[52] ECO (2004). H. Handbuch Eurocode 0 – Erläuterungen zur OENORM 1990 und zu OENORM B 1990-1 Wien, Österreichisches Normungsinstitut.

[53] Thoft-Christensen, P. (1996). *Bridge Management Systems: Present and Future*. Bridge Management Systems, Barcelona.

[54] Faber, M. H. (2000). "Reliability based assessment of existing structures." *Progress in Structural Engineering and Materials* 2(2): 247-253.

[55] Division, O. H. E. (1983). *Ontario highway bridge design code*, Ontario Ministry of Transportation and Communications, Highway Engineering Division.

[56] Canada, N. R. C. o. (1977). National Building Code of Canada. Ontario, Canada, National Research Council of Canada.

[57] Officials, A. o. S. H. a. T. (1994). AASHTO-LRFD. Bridge design specifications. Washington DC.

[58] ENV (1991(1) 1994). Eurocode 1: Basis of Design and Actions on Structures, Part 1: Basis of design. Brussels.

[59] Safety, J. C. o. S. (1996). JCSS. Background documentation, Eurocode 1 (ENV 1991) Part 1: basis of design.

[60] Safety, J. C. o. S. (2000). JCSS. Guideline for reliability based assessment of existing structures. JCSS.

[61] Ditlevsen, O. and Madsen, H. O. (1996). Structural Reliability Methods.

[62] Schneider, J. (1997). Introduction to Safety and Reliability of Structures. *Structural engineering Documents*. IABSE.

This document is the intellectual property of the fib – International Federation for Structural Concrete. All rights reserved.
This PDF of fib Bulletin 86 is intended for use and/or distribution solely within fib National Member Groups.

[63] Raiffa, H. and Schlaifer, R. (1961). *Applied Statistical Decision Theory*, Cambridge University Press.

[64] Benjamin, J. R. and Cornell, C. A. (1970). *Probability, statistics and decision for civil engineers*, McGraw-Hill.

[65] Ang, A. H. and Tang, W. H. (1975). *Probability concepts in engineering planning and design*. New York, John Wiley & Sons.

[66] Turkstra, K. (1970). Applications of Bayesian decision theory. *Study No. 3 structural reliability and codified design*. Canada, University of Waterloo.

[67] Sexsmith (1996). Criteria development for serviceability limit states. *IABSE Congress*. Copenhagen, Denmark: 16-20.

[68] Mendoza, E. and Rosenblueth, E. (1971). "Reliability optimization in isostatic structures." *ASCE J Eng Mech Div* 97: 1625-1642.

[69] Faber, M. H., Kroon, I. B. and Sørensen, J. D. (1992). *Decision theory in structural engineering*.

[70] Kroon, I. B. (1994). Decision theory applied to structural engineering problems. Aalborg, Instituttet for Bygningsteknik, Aalborg UniversitetThesis.

[71] Box, G. E. and Tiao, G. C. (1973). *Bayesion inference in statistical analysis*. University of Michigan, Addison-Wesley Pub. Co.

[72] Faber, M. H. (2000). "Reliability based assessment of existing structures." *Progress in Structural Engineering and Materials* 2: 247-253.

[73] Lindley, D. (1976). *Introduction to probability and statistics from a Bayesian viewpoint*. Cambridge, Cambridge University Press.

[74] Aitchison, J. and Dunsmore, I. R. (1975). *Statistical prediction analysis*. Cambridge [Eng.]; New York, Cambridge University Press.

[75] Bolotin, V. V. (1969). *Statistical methods in structural mechanics*. San Francisco, Holden-Day.

[76] Veneziano (1978). Random processes for engineering applications. Massachussetts, Massachussetts Institute of Technology.

[77] Melchers, R. E. (1999). *Structural reliability analysis und prediction*. Chichester - New York - Brisbane - Toronto, Wiley.

[78] *Der Ingenieurbau [8], Tragwerkszuverlässigkeit, Einwirkungen* (1997). Berlin, Ernst und Sohn.

[79] Safety, T. J. C. o. S. (2000). Basic Notes on Resistance Models.

[80] Safety, T. J. C. o. S. (2000). Basic Notes on Load Models.

[81] Box, G. E. P. and Draper, N. R. (1987). *Empirical model-building and response surfaces*. New York, Wiley.

[82] Von Neumann, J. and Morgenstern, O. (1944). *Theory of games and economic behavior / by John Von Neumann and Oskar Morgenstern*, Princeton University Press.

[83] Symposium on Quantitative Nondestructive, E., Chimenti, D. E. and Thompson, D. O. *Review of progress in quantitative nondestructive evaluation*.

[84] Rudlin, J. (1992). Probability of detection during MPI. IOCE. Aberdeen.

[85] Sørensen, J. D., Faber, M. H. and Kroon, I. B. (1995). Optimal reliability-based planning of experiments for POD curves. *The 5th International Offshore and Polar Engineering Conference (ISOPE-95)*. The Hague. IV: 339 - 345.

This document is the intellectual property of the fib – International Federation for Structural Concrete. All rights reserved.
This PDF of fib Bulletin 86 is intended for use and/or distribution solely within fib National Member Groups.

[86] Madsen, H. O. (1985). *Model updating in first order reliabilty theory with application to fatique crack growth*. Second International Workshop on Stochastic Methods in Structural Mechanics., University of Pavia.

[87] Madsen, H. O. (1987). *Model updating in reliability theory*. ICASP.

[88] Rackwitz, R. and Schrupp, K. (1985). "Quality control, proof testing and structural reliability." *Structural Safety Structural Safety* 2: 239-244.

[89] (!!! INVALID CITATION !!!).

[90] Diamantidis, D. (2001). Assessment of existing structures, Joint Committee of Structural Safety JCSS: 161-166.

[91] Mori, Y. and Nonaka, M. (2001). "LRFD for assessment of deteriorating existing structures." *Structural Safety* 23: 297–313.

[92] Mori, Y. and Kato, T. (2003). Practical method of reliability-based condition assessment of existing structures. *Applications of Statistics and Probability in Civil Engineering*. A. Der Kiureghian, S. Madanat and J. M. Pestana. Rotterdam, Millpress: 613-620.

[93] Schueremans, L. and Van Gemert, D. (2001). *Assessment of existing masonry structures using probabilistic methods - state of the art and new approaches*. STRUMAS2001, Fifth International Symposium on Computer Methods in Structural Masonry.

[94] Sadovský, Z. (2002). Reliability based design codes in Slovakia – Historical development and new challenges. *JCSS Workshop on Reliability Based Code Calibration*. Zürich, Switzerland.

[95] Žnidarič, A. and Moses, F. (1997). Structural Safety of Existing Road Bridges. *7th International Conference on Structural Safety and Reliability (ICOSSAR 97)*. Kyoto, Japan: 1843-1850.

[96] Czechowski, A. (2001). Structural Reliability Assurance – A Process Approach. *Safety, Risk, Reliability - Trends in Engineering, Malta*. D. Proske and P. Gelder, Springer Heidelberg Dordrecht London: 11.

[97] Melchers, R. E. and Faber, M. H. (2001). "Aspects of Safety in Design and Assessment of Deteriorating Structures." *Safety, Risk, Reliability - Trends in Engineering*.

[98] ONORM (2006). ONR 24008 Bewertung der Tragfähigkeit bestehender Eisenbahn- und Straßenbrucken. Wien, Osterreichisches Normungsinstitut.

[99] Ahrens, M. A. (2010). Ein stochastisches Simulationskonzept zur Lebensdauerermittlung von Stahlbeton- und Spannbetontragwerken und seine Umsetzung an einer Referenzbrücke. *Lehrstuhl für Massivbau*, Ruhr-Universität Bochum. Dissertation Thesis.

[100] Stangenberg, F. and Lenzen, A. (2006). *Zur uberprufung des Degradationszustandes bei Bauwerken im Hinblick auf die Restlebensdauer*. 29. Darmstadter Massivbauseminar „Sicherheitsgewinn durch Monitoring".

[101] Stangenberg, F., Breitenbücher, R., Bruhns, O. T., Hartmann, D., Höffer, R., Kuhl, D. and Meschke, G. (2009). *Lifetime-Oriented Structural Design Concepts*, Springer.

[102] Fingerloos, F. and Schnell, J. (2009). Tragwerksplanung im Bestand. *Betonkalender 2009*. Berlin, Ernst & Sohn Verlag. 2: 2-51.

[103] Braml, T., Fischer, A., Keuser, M. and Schnell, J. (2009). Beurteilung der Zuverlässigkeit von Bestandstragwerken hinsichtlich einer Querkraftbeanspruchung. *Beton- und Stahlbetonbau*, Ernst & Sohn. 104: 798-812.

This document is the intellectual property of the fib – International Federation for Structural Concrete. All rights reserved.
This PDF of fib Bulletin 86 is intended for use and/or distribution solely within fib National Member Groups.

[104] Shigley, J. E. and Mischke, C. R. (2001). *Mechanical Engineering Design*. New York, McGraw Hill. Inc. 6th.

[105] Schleicher, F. (1949). *Taschenbuch für Bauingenieure*, Springer-Verlag.

[106] Mann, W. (1987). Überlegungen zur Sicherheit im Mauerwerksbau. *Mauerwerks-Kalender 1987*. Berlin, Ernst & Sohn: 1-5.

[107] Busch, P. and Zumpe, G. (1995). *Tragfähigkeit, Tragsicherheit und Tragreserven von Bogenbrücken*. 5. Dresdner Brückenbausymposium.

[108] Wenzel, F. (1997). Mauerwerk – Untersuchen und Instandsetzen durch Injizieren, Vernadeln und Vorspannen. Erhalten historisch bedeutsamer Bauwerke. *Empfehlungen für die Praxis. Sonderforschungsbereich 315*. Karlsruhe, Germany, Universität Karlsruhe.

[109] Tonon, F. and Tonon, L. (2006). "Renovation of the 17th-Century Ponte Lungo Bridge in Chioggia, Italy." *Journal of Bridge Engineering* 11: 13-20.

[110] Visodic, J. P. (1948). Design Stress Factors. *ASME International*. New York. 55.

[111] Norton, R. L. (1996). *Machine Design – An Integrated Approach*. New York, Prentice-Hall 3rd.

[112] Mayer, M. (1926). *Die Sicherheit der Bauwerke und ihre Berechnung nach Grenzkräften anstatt nach zulässigen Spannungen*. Berlin, Verlag von Julius Springer.

[113] Murzewski, J. (1974). *Sicherheit der Baukonstruktionen*. Berlin, DDR, VEB Verlag für Bauwesen.

[114] Tichý, M. (1976). Probleme der Zuverlässigkeit in der Theorie von Tragwerken. *Zuverlässigkeit tragender Konstruktionen*. Dresden, Germany, Weiterbildungszentrum Festkörpermechanik, Konstruktion und rationeller Werkstoffeinsatz Technische Universität Dresden – Sektion Grundlagen des Maschinenwesens.

[115] Freudenthal, A. M. (1947). Safety of Structures. *Transactions ASCE*. 112: 125-180.

[116] Beeby, A. W. (1994). $\gamma$-factors: A second look." *The Structural Engineer* 72(2).

[117] Pugsley, A. G. (1951). "Concepts of safety in structural engineering." *Journal of the Institution of Civil Engineers* 36: 5-30.

[118] Östlund, L. (1991). An Estimation of gamma-Values. An application of a probabilistic method. In: Reliability of Concrete Structures. *Final report of Permanent Commission I*, CEB Bulletin d' Information: 37-51.

[119] Spaethe, G. (1992). *Die Sicherheit tragender Baukonstruktionen*. Wien, Springer.

[120] Tragwerke aus Beton, Stahlbeton und Spannbeton - Teil 1: Bemessung und Konstruktion (Aug 2008). DIN 1045-1.

[121] Richtlinie für Betonbau beim Umgang mit wassergefährdenden Stoffen (1996). *Deutscher Ausschuß für Stahlbeton Berlin*, Beuth-Verlag.

[122] Eurocode 4: Desing of Composite Steel and Concrete Structures, Part 1-2: General rules - Structural fire design (2001). *EN 1994-1-2* European Committee for Standardization.

[123] CENITC250, T. C. (2008). Eurocode 5: Design of timber structures. *EN 1995. E*. C. f. Standardization.

[124] Mann, W. (1999). "Mauerwerk in Europa." *Der Prüfingenieur*: 7.

*This document is the intellectual property of the fib – International Federation for Structural Concrete. All rights reserved.*
*This PDF of fib Bulletin 86 is intended for use and/or distribution solely within fib National Member Groups.*

[125] Bergmeister, K. (2003). *Kohlenstofffasern im Konstruktiven Ingenieurbau*, Verlag Ernst und Sohn.

[126] EVN (2005). Eurocode 6 - Design of masonry structures *ICS 91.010.30*. E. C. f. Standardization.

[127] e.V.), A. G. d. B.-Ü. B. (2001). "Empfehlung für die Bemessung und Konstruktion von Glas im Bauwesen." *Der Prüfingenieur* 18: 55-69.

[128] Onken, P., vom Berg, W. and Neubauer, U. (1997). Verstärkung der West Gate Bridge, Melbourne. *Beton- und Stahlbetonbau*, Ernst & Sohn. 2: 94-104.

[129] Cladding for external walls, ventilated at rear (2010). *DIN 18516:2010*.

[130] CEN/TC250, T. C. Eurocode 9: Design of aluminium structures. *EN 1999*. E. C. f. Standardization, European Committee for Standardization.

[131] Bamboo Scaffolds in Building Construction - Design Guide - Design of Bamboo Scaffolds (2005).

[132] Curbach, M., Günther, L. and Proske, D. (2004). "Sicherheitskonzept für Brücken aus Granitsteindeckern." *Mauerwerksbau* 8: 138-141.

[133] Curbach, M., Hampel, T., Speck, K., Scheerer, S. and Proske, D. (2001). *Determination for Design Values of High Performance Concrete under Bi- and Triaxial Loading*. 8th International Conference on Structural Safety and Reliability ICOSSAR '01, A. A. Balkema, Tokyo.

[134] Empfehlungen für die Bewertung des Tragvermögens bestehender Gewölbebrücken aus Mauerwerk und Beton (1995). *UIC-Kodex: Internationaler Eisenbahnverband*.

[135] Bothe, E., Henning, J., Curbach, M., Bösche, T. and Proske, D. (2004). Nichtlineare Berechnung alter Bogenbrücken auf der Grundlage neuer Vorschriften. *Beton- und Stahlbetonbau*, Ernst & Sohn. 99.

[136] "ZfPBau-Kompendium ". (2004). Link visited on, 2011,www.bam.de/microsites/zfp_kompendium/welcome.html.

[137] Grundlagen der Tragwerksplanung, Sicherheitskonzept und Bemessungsregeln, Einwirkungen auf Tragwerke - Teil 100 (2001). *DIN 1055-100*, Deutsches Institut für Normung DIN 1055-100.

[138] Schäfer, H. G. and a., u. (1996). "Verstärken von Betonbauteilen, Sachstandsbericht." *Deutscher Ausschuss für Stahlbeton* (DAfStb) 467.

[139] Richtlinie Belastungsversuche an Massivbauwerken (Sept 2000). Deutscher Ausschuss für Stahlbeton.

[140] - (1993). CEB-FIP MODEL CODE 1990, Comitte Euro-International du Beton. Bulletin d'information No. 195.

[141] Ellingwood, B., Galambos, T. V., MacGregor, J. C. and Cornell, A. C. (1980). Development of a probability based load criteria for american national standard A 58. Washington, DC, National Bureau of Standards, US Department of Commerce.

[142] Joint Committee on Structural Safety (2001). JCSS Probabilistic Model Code 12th Draft, Joint Committee on Structural Safety.

[143] Allen, D. E. (1991). "Limit states criteria for structural evaluation of existing buildings." *Canadian Journal of Civil Engineering* 18: 995-1004.

*This document is the intellectual property of the fib – International Federation for Structural Concrete. All rights reserved.*
*This PDF of fib Bulletin 86 is intended for use and/or distribution solely within fib National Member Groups.*

[144] Fischer, A. M. (2010). Bestimmung modifizierter Teilsicherheitsbeiwerte zur semiprobabilistischen Bemessung von Stahlbetonkonstruktionen im Bestand Determination of modified partial safety-factors for semiprobabilistic design of existing reinforced concrete structuresThesis.

[145] Reid, S. G. (1999). Load–testing for design of structures with Weibull–distributed strengths. Application of Statistics and Probability (ICASP 8). Sydney. 2: 705-712.

[146] Val, D. V. and Stewart, M. G. (2002). "Safety Factors for Assessment of Existing Structures." *Journal of Structural Engineering* 128(2): 258-265.

[147] Eibl, J. (1992). Nichtlineare Traglastermittlung/Bemessung. *Beton- und Stahlbetonbau*, Ernst & Sohn. 87: 137-139.

[148] Eibl, J. and Schmidt-Hurtienne, B. (1995). "Grundlagen für ein neues Sicherheitskonzept." *Bautechnik* 72(8): 501-506.

[149] Pfeiffer, U. and Quast, U. (2003). Nichtlineares Berechnen stabförmiger Bauteile. *Beton- und Stahlbetonbau*, Ernst & Sohn. 98: 529-538.

[150] Allaix, D. L., Carbone, V. I. and Mancini, G. (2007). Global Safety Factors for Reinforced Concrete Beams. *5th International Probabilistic Workshop*. L. Taerwe and D. Proske. Ghent, Belgium.

[151] Cervenka, V. (2007). Global Safety Format fpr Nonlinear Calculatoin of Reinforced Concrete. *5th International Probabilistic Workshop*. L. Taerwe and D. Proske. Ghent, Belgium.

[152] Holicky, M. (2007 ). *Probabilistic Approach to the Global Resistance Factor for Reinforced Concrete Members*. 5th International Probabilistic Workshop, Ghent, Belgium.

[153] Novák, D., Vořechovský, M., Lehký, D., Rusina, R., Pukl, R. and Červenka, V. (2005). *Stochastic nonlinear fracture mechanics finite element analysis of concrete structures*. 9th Int. conf. on Structural Safety and Reliability Icossar, Rome, Italy.

[154] Eurocode 2: Design of concrete structures – Concrete bridges – Design and detailing rules (2005). *EN 1992-2*.

[155] Holicky, M. (2006). Global resistance factors for reinforced concrete members. *ACTA POLYTECHNICA 2006*. CTU in Prague.

[156] Bertagnoli, G., L., G. and Mancini, G. (2004). Safety format for the nonlinear analysis of concrete structures. *Studies and Researches*. Milano, Italy, Politechnico di Milano.

[157] Červenka, V. (2008). "Global Safety Format for Nonlinear Calculation of Reinforced Concrete structures." *Beton und Stahlbetonbau* 103(6): 37-42.

[158] Cervenka, V. (1998). Simulation of shear failure modes of R/C structures. *Computational Modeling of Concrete Structures (Euro-C 98)*. R. de Borst, N. Bicanic, H. Mang, G. Meschke and A. A. Balkema. Rotterdam, The Netherlands: 833-838.

[159] Cervenka, V. (2002). *Computer simulation of failure of concrete structures for practice*. 1st *fib* Congress 2002: Concrete Structures in 21 Century.

[160] Asin, M. (1999). The Behaviour of Reinforced Concrete Continuous Deep Beam. Delft, The Netherlands, Delft University Press. PhD Thesis.

[161] Yoshida, Y. (2000). Shear Reinforcement for Large Lightly Reinforced Concrete Members. Toronto, University of Toronto. PhD Thesis.

This document is the intellectual property of the fib – International Federation for Structural Concrete. All rights reserved.
This PDF of fib Bulletin 86 is intended for use and/or distribution solely within fib National Member Groups.

[162] Cervenka, V., Dolezel, J. and Novák, D. (2010). *Safety Assessment of Shear Resistance of Large Lightly Reinforced Concrete Beams*. The Third International *fib* Congress.

[163] Schneider, J. and Schlatter, H. P. (1996). Sicherheit und Zuverlässigkeit im Bauwesen. Grundwissen für Ingenieure. Stuttgart, Teubner. 2. überarbeitete Auflage.

[164] Vrouwenvelder, A. C. W. M. and Siemens, T. (1985). Durability – A Probabilistic Approach. *IABSE Periodica*. Zürich, IABSE. P-85/85.

[165] Safety, J. C. o. S. (2001). JCSS Probabilistic Model Code Part 3: Resistance Models.

[166] Safety, J. C. o. S. (2001). JCSS Probabilistic Model Code Part 2: Load Models.

[167] Petschacher, M. VAP 1.5Switzerland.

[168] Novák, D., Vořechovský, M. and Rusina, R. (2008).FReET v.1.5 – program documentation, User's and Theory Guides, Červenka Consulting. Prague, Czech Republic.

[169] Der Kiureghian, A. and Liu, P. L. "CALREL", NISEE/Computer Applications, Earthquake Engineering Research Centre. 379 Davis Hall, University of California, Berkeley, CA 94720 USA.

[170] Routil, L., Lehky, D., Simonova, H., Kucharczykova, B., Kersner, Z., Novak, D., Zimmermann, T. and Strauss, A. (2014). Experimental-computational determination of mechanical fracturre parameters of concrete for probabilistic life-cycle assessment *Life-Cycle Performance of Deteriorating Structures*. H. F. D. M. F. M. Akiyama. London, CRC Press.

[171] Koenig, G., Soukhov, D. and Jungwirth, F. (1998). "Sichere Betonproduktion fuer Stahlbetontragwerke - Schlussbericht - (DBV-Nummer 199)." *KURZBER BAUFORSCH* 39(5): 339-51.

[172] Tue, N. V. (2007). *Statistische Auswertung der Betonqualität - Folgerungen für die Bauwerkssicherheit*. 51. Beton Tage, Neu-Ulm.

[173] Rüsch, H., Sell, R. and Rackwitz, R. (1969). "Statistische Analyse der Betonfestigkeit." *Deutscher Ausschuss für Stahlbeton* (DAfStb) Heft 206.

[174] Hansen, M. (2004). Zur Auswirkung von Überwachungsmaßnahmen auf die Zuverlässigkeit von Betonbauteilen. *Institut für Massivbau*. Hannover, Univ. HannoverThesis.

[175] Brehm, E., Schmidt, H. and Graubner, C. (2008). *Model Uncertainties for Shear Capacity Prediction of Reinforced Concrete Members*. 6th International Probabilistic Workshop, Technische Universität Darmstadt.

[176] Kautsch, R. (2010). About the verification of reinforced and prestressed concrete cross-sections stressed by a combination of bending and shear based on an extension of the classical bending theory. Kaiserslautern, Technische Universität KaiserslauternThesis.

[177] Strauss, A. (2003). Stochastische Modellierung und Zuverlässigkeit von Betonkonstruktionen. Vienna, University BOKU. PhD Thesis.

[178] Santa, U. (2004). Bauwerksinspektion und -überwachung. *Institut für Konstruktiven Ingenieurbau*. Wien, Universität für Bodenkultur. PhD Thesis.

[179] (FSV), F. S.-S.-V. (1992). "Richtlinie für die Überwachung und Prüfung von Straßenbrücken." RVS 13.10.61: Technical Report 800.040/19-VI/A/7-92.

*This document is the intellectual property of the fib – International Federation for Structural Concrete. All rights reserved.*
*This PDF of fib Bulletin 86 is intended for use and/or distribution solely within fib National Member Groups.*

[180] "DotNet Framework 2.0." (2007, 2007). link visited on.

[181] PEC 2006. BAUT 5.5 - Handbuch (2006). Petschacher Consulting.

[182] Bergmeister, K., Mark, P., Österreicher, M., Sanio, D., Heek, P., Krawtschuk, A., Strauss, A. and Ahrens, M. A. (2015). Innovative Monitoringstrategien für Bestandsbauwerke. *Beton-Kalender 2015*, Wiley-VCH Verlag GmbH: 315-458.

[183] Bergmeister, K. and Santa, U. (2001). "Global monitoring concepts for bridges." *Structural concrete* 2(1): 29-39.

[184] Santa, U. B., K. (2001). "Instrumentation and Data Acquisition techniques in Structural Health Monitoring." *International Journal for Restoration of Buildings and Monuments* 3(IJR 7): 321.

[185] Bergmeister, K. and Wendner, R. (2010). Monitoring und Strukturidentifikation von Betonbrücken. *Betonkalender 2010*. K. Bergmeister and J. D. Wörner. Berlin, Ernst & Sohn. 1: 245-290.

[186] Santa, U., Bergmeister, K. and Strauss, A. (2004). "Bauwerksüberwachung der Autobahnbrücke Gossensaß." *Beton- und Stahlbetonbau* 99(12): 975-984.

[187] Bergmeister, K. (2003). *Monitoring and Safety Evaluation of Existing Concrete Structures*: State-of-art Report, *fib* Fédération internationale du béton.

[188] Marsh, P. S. and Frangopol, D. M. (2007). "Reinforced Concrete Bridge Deck Reliability Model Incorporating Temporal and Spatial Variations of Probabilistic Corrosion Rate Sensor Data." *Reliability Engineering & System Safety*.

[189] Alt, D. G. and Meggers, D. A. (1996). "Determination of bridge deck subsurface anomalies by infrared thermography and ground penetrating radar; Polk-Quincy Viaduct I-70, Topeka, Kansas." Link visited on 11.2.2007,http://ntl.bts.gov/lib/9000/9400/9472/KS-96-2.pdf.

[190] Marshall, S. J. (1996). Evaluation of Instrumented-Based Non-Destructive Inspection Methods for Bridges. *Department of Civil, Environmental and Architectural Engineering*. Boulder, Colorado, University of Colorado. Master Thesis.

[191] Millard, S. G., Al-Qadi, I. L., Shaw, M. R., Riad, S. M., Shaari, A. and Bungey, J. H. (2001). "Coaxial Transmission Lines: Development of Test Procedures for Concrete." *Journal of Materials in Civil Engineering* 13(3): 202-208.

[192] Shaw, R. E. (2002). "Ultrasonic Testing Procedures, Technician Skills, and Qualifications." *Journal of Materials in Civil Engineering* 14(1): 62-67.

[193] Iken, H. W., Lackner, R. R., Zimmer, U. P. and Wöhnl, U. (2003). *Handbuch der Betonprüfung. Anleitungen und Beispiele*, Verlag Bau+Technik.

[194] Bungey, J., S Millard, S. and Grantham, G. (2006). *Testing of Concrete in Structures*, Taylor & Francis.

[195] Washer, G., Fuchs, P., Rezai, A. and Ghasemi, H. (2006 ). Ultrasonic Testing for Quality Control of Ultra-High Performance Concrete. *Structures Congress*. St. Louis, Missouri, USA.

[196] Yehia, S., Abudayyeh, O., Nabulsi, S. and Abdelqader, I. (2007). "Detection of Common Defects in Concrete Bridge Decks Using Nondestructive Evaluation Techniques." *Journal of Bridge Engineering* 12(2): 215-225.

[197] Rohrbach, C. (1989). *Handbuch für experimentelle Spannungsanalyse*. Düsseldorf, VDI-Verlag.

This document is the intellectual property of the fib – International Federation for Structural Concrete. All rights reserved.
This PDF of fib Bulletin 86 is intended for use and/or distribution solely within fib National Member Groups.

[198] Murray, W. M. and Miller, W. R. (1992). *The Bonded Electrical Resistance Strain Gauge*. USA, Oxford University Press Inc.

[199] Keil, S. (1995). *Beanspruchungsermittlung mit Dehnmeßstreifen*. Zwingenberg, Cuneus-Verlag.

[200] Wheeler, A. N. and Ganji, A. R. (1996). *Introduction to Engineering Experimentation*. Englewood Cliffs, New Jersey, Prentice Hall Inc.

[201] "DMS-Katalog." (2007). Link visited on 10.2.2007,http://www.hbm.com.

[202] Inaudi, D., Posenato, D. and Glisic, B. (2007, 2007). "Demodulating interferometric and FBG sensors in the spectral domain." Link visited on.

[203] Frangopol, D. M. and Curley, J. P. (1987). "Effects of Damage and Redundancy on Structural Reliability." *Journal of Structural Engineering* 113(7): 1533-1549.

[204] Bayer, V. (1999). Zur Zuverlässigkeitsbeurteilung von Baukonstruktionen unter dynamischen Einwirkungen. *Fakultät Bauingenieurwesen*. Weimar, Bauhaus-Universität Weimar. Dissertation Thesis.

[205] Burdet, O., Muttoni, A., Strassen, S. B. f., Brückenforschung, S. A. and béton, E. p. f. d. L. L. d. c. e. (2006). *Beurteilung bestehender Messsysteme für die Langzeiterfassung der Verformungen von Brücken*, Département fédéral de l'environnement, des transports, de l'énergie et de la communication DETEC, Office fédéral des routes.

[206] Schneider, J. (1997). *Introduction to Safety and Reliability of Structures*. Zürich, International Association for Bridge and Structural Engineering.

[207] Goulet, J. A. (2012). Probabilistic Model Falsification for Infrastructure Diagnosis. Suisse, École Polytechnique Fédérale de Lausanne Thesis.

[208] Mang, H. and Hofstetter, G. (2004). *Festigkeitslehre*. Wien, Springer. 2. Auflage.

[209] Errors due to Misalignment of Strain Gauges (2007). Vishay - Micro Measurements. Tech Note TN-511.

[210] Klarer, A. (2007). Long time response and faults of ESG systems, Product Manager of Hottinger Baldwin Messtechnik: Personal discussion, contacted by phone on February 12,2007.

[211] Bäumel, A. (2006). Messen mit DMS - Grundlagen; Measuring with electrical strain gauges. *Seminar Unterlagen Hottinger Baldwin Messtechnik*. Vienna, Austria.

[212] "Macro Sensors, Division of Howard A. Schaevitz Technologies, Inc.". (2007). Link visited on 7.2.2007,www.macrosensors.com.

[213] Nöther, N. (2010). Distributed Fiber Sensors in River Embankments: Advancing and Implementing the Brillouin Optical Frequency Domain Analysis. Berlin, Bundesanstalt für Materialforschung und -prüfung (BAM)Thesis: 1-157.

[214] Inaudi, D., Posenato, D. and Glisic, B. (2007). "Demodulating interferometric and FBG sensors in the spectral domain." Link visited on 8.2.2007,http://www.smartec.ch.

[215] "Kistler Instrument Corporation." (2007). Link visited on 6.2.2007,www.intertechnology.com/Kistler/.

[216] Qian, S. (2005). *Testing Steel Corrosion in Reinforced Concrete. Inspection and Monitoring Techniques for Bridges and Civil Structures*. Cambridge, England, Woodhead Publishing Ltd.

This document is the intellectual property of the fib – International Federation for Structural Concrete. All rights reserved.
This PDF of fib Bulletin 86 is intended for use and/or distribution solely within fib National Member Groups.

[217] Ahmad, S. (2002). "Reinforcement Corrosion in Concrete Structures. Its Monitoring and Service Life Prediction – A review." *Cement and Concrete Composites* 25: 459-471.

[218] Hodgson, I. (2007). Costs for monitoring systems on 12.2.2007.

[219] Maser, K. and Vandre, B. (2006). Network-Level Pavement Structure Assessment Using Automated Processing of Ground Penetrating Radar (GPR) Data. *ASCE Conference*. 191: 719-728.

[220] "Radar survey." (2007, 2007). *Geomodel*. Link visited on.

[221] "Ultrasonic flow." (2007). *Omega*. Link visited on 11.2.2007,www.omega.com/prodinfo/ultrasonicflowmeters.html.

[222] Hodgson, I. (2007). Costs for monitoring systems. Bethlehem, PA, Ian Hodgson Researcher at the Lehigh University's Center for Advanced Technology for Large Structural Systems: Face-to-face interview.on 12.2.2007.

[223] (FSV), F. S.-S.-V. (2011). Qualitätssicherung bauliche Erhaltung, Überwachung, Kontrolle und Prüfung von Kunstbauten, Straßenbrücken Vienna, FSV. RVS 13.03.11.

[224] Österreicher, M. (2013). Monitoringbasierte Performanceanalyse von Ingenieurstrukturen. *Institut für Konstruktiver Ingenieurbau (IKI)*. Vienna, BOKU-Universität für Bodenkultur. Dissertation Thesis: 274.

[225] Äkerman, H. (2008). *Die Bedeutung objektiver Prüfergebnisse für das Bauwerksmanagement*. Lehrgangs Bauwerksprüfingenieure, Feuchtwangen.

[226] Braml, T. (2010). Zur Beurteilung der Zuverlässigkeit von Massivbrücken auf der Grundlage der Ergebnisse von Überprüfungen am Bauwerk, Univ. der Bundeswehr MünchenThesis.

[227] Braml, T., Keuser, M. and Bergmeister, K. (2011). "Entwicklung eines baupraktischen Näherungsverfahrens zur Beurteilung der Zuverlässigkeit von Massivbrücken auf der Grundlage der Ergebnisse von Bauwerksüberprüfungen." *Beton- und Stahlbetonbau* 106(3): 178-186.

[228] Strauss, A., Frangopol, D. M. and Kim, S. (2008). "Statistical, Probabilistic and Decision Analysis Aspects Related to the Efficient Use of Structural Monitoring Systems." *Beton- und Stahlbetonbau* 103(S1): 23-28.

[229] Hald, A. (1952). *Statistical Theory with Engineering Applications*. New York, J. Wiley and Sons.

[230] Ang, A. H.-S. and Tang, W. H. (1984). *Probability concepts in engineering planning and design*. New York, John Wiley & Sons, II.

[231] Gumbel, E. J. (1954). *Statistical theory of extreme values and some practical applications: a series of lectures*, U. S. Govt. Print. Office.

[232] Frangopol, D. M., Strauss, A. and Kim, S. (2008). "Use of monitoring extreme data for the performance prediction of structures: General approach." *Engineering Structures* 30: 3644-3653.

[233] Estes, A. C. and Frangopol, D. M. (1998). "RELSYS: A computer program for structural systems reliability." *Structural Engineering and Mechanics* 6(8): 18.

[234] Frangopol, D. M., Strauss, A. and Kim, S. (2008). "Bridge Reliability Assessment Based on Monitoring." *Journal of Bridge Engineering* 13: 258-270.

This document is the intellectual property of the fib – International Federation for Structural Concrete. All rights reserved.
This PDF of fib Bulletin 86 is intended for use and/or distribution solely within fib National Member Groups.

[235] Officials, A. A. o. S. H. T. (2002). Standard Specifications for Highway Bridges. Washington, DC, American Association of State Highway and Transportation Officials. HB-17.

[236] *fib* (2012). *Model Code 2010* – Vol. 1 & 2. Bulletins. Lausanne, International Federation for Structural Concrete (*fib*).

[237] Frangopol, D. M. and Messervey, T. B. (2009). Life-cycle Cost and Performance Prediction: Role of Structural Health Monitoring. *Frontier Technologies for Infrastructures Engineering*. G. C. Chen and A. H.-S. Ang. Leiden, The Netherlands, CRC Press-Balkema-Taylor & Francis Group: 361-381.

[238] Okasha, N. M. and Frangopol, D. M. (2010). "Redundancy of structural systems with and without maintenance: An approach based on lifetime functions." *Reliability Engineering & System* Safety 95(5): 520-533.

[239] Akgül, F. and Frangopol, D. (2004). "Lifetime Performance Analysis of Existing Steel Girder Bridge Superstructures." *Journal of Structural Engineering* 130(12): 1875-1888.

[240] Okasha, N. M. and Frangopol, D. M. (2010). "Time-variant redundancy of structural systems." *Structure and Infrastructure Engineering* 6(1-2): 279-301.

[241] Tang, W. H. (1973). "Probabilistic Updating of Flaw Information." *Journal of Testing and Evaluation* 1: 459-467.

[242] Yang, J. N. and Trapp, W. J. (1974). "Reliability Analysis of Aircraft Structures under Random Loading and Periodic Inspection." *AIAA journal* 12(12): 1623-1630.

[243] Yang, J. N. and Trapp, W. J. (1975). "Inspection frequency optimization for aircraft structures based on reliability analysis." *Journal of Aircraft*, AIAA 12(5): 494-496.

[244] Thoft-Christensen, P. and Sørensen, J. D. (1987). "Optimal strategy for inspection and repair of structural systems." *Civil Engineering Systems* 4: 94-100.

[245] Fujita, M., Schall, G. and Rackwitz, R. (1989). *Adaptive Reliability-Based Inspection Strategies for Structures Subject to Fatigue*. *5th ICOSSAR*, San Francisco.

[246] Madsen, H. O., Sørensen, J. D. and Olesen, R. (1989). Optimal Inspection Planning for Fatigue Damage of Offshore Structures. *5th ICOSSAR*. San Francisco. 3: 2099-2106.

[247] Pedersen, C., Nielsen, J. A., Riber, J. P. and et.al. (1992). Reliability Based Inspection Planning for the Tyra Field. *11th Offshore Mechanics and Arctic Engineering Conference*. 2: 255-263.

[248] Sorensen, J. D., Faber, M. H., Rackwitz, R. and et.al. (1992). Reliability Analysis of an Offshore Structure: A Case Study. *11th Offshore Mechanics and Arctic Engineering Conference*. Calgary. 2: 457-463.

[249] Goyet, J., Faber, M. H., Paygnard, J. C. and Maroini, A. (1994). Optimal Inspection and Repair Planning: Case Studies using IMREL software. *13th Offshore Mechanics and Arctic Engineering Conference*. 2: 325-333.

[250] Moan, T., Vårdal, O. T. and Johannesen, J. M. (2000). Probabilistic inspection planning of fixed offshore structures. ICASP8. Sydney: 191-200.

[251] Faber, M. H., Engelund, S., Sørensen, J. D. and Bloch, A. (2000). Simplified and Generic Risk Based Inspection Planning. *19th Offshore Mechanics and Arctic Engineering Conference*. New Orleans.

[252] Straub, D. and Faber, M. H. (2006). "Computational Aspects of Risk Based Inspection Planning." *Computer-Aided Civil and Infrastructure Engineering* 21(3): 179-192.

*This document is the intellectual property of the fib – International Federation for Structural Concrete. All rights reserved.*
*This PDF of fib Bulletin 86 is intended for use and/or distribution solely within fib National Member Groups.*

[253] Chakrabarti, P., Mukkamala, A. and Abu-Odeh, I. (2005). An Overview of the Reassessment Studies of Fixed Offshore Platforms in the Bay of Campeche , Mexico. *24th Offshore Mechanics and Arctic Engineering Conference*. Halkidiki, Greece.

[254] Faber, M. H., Sørensen, J. D., Tychsen, J. and Straub, D. (2005). "Field Implementation of RBI for Jacket Structures." *Journal of Offshore Mechanics and Arctic Engineering* 127(3): 220-226.

[255] Straub, D. (2004). Generic Approaches to Risk Based Inspection Planning for Steel Structures. Zürich, Swiss Federal Institute of Technology. PhD Thesis.

[256] Streicher, H. and Rackwitz, R. (2004). "Time-variant reliability-oriented structural optimization and a renewal model for life-cycle costing." *Probabilistic Engineering Mechanics* 19(1-2): 171-183.

[257] Straub, D. and Faber, M. H. (2005). "Risk Based Acceptance Criteria for Joints Subject to Fatigue Deterioration." *Journal of Offshore Mechanics and Arctic Engineering, Trans. ASME* 127(2): 150-157.

[258] Lassen, T. (1997). Experimental Investigation and Stochastic Modelling of the Fatigue Behaviour of Welded Steel Joints. *Dept. of Building Technology and Structural Engineering*. Aalborg, University of Aalborg, Denmark PhD Thesis.

[259] Newman, J. C. and Raju, I. S. (1981). "An empirical stress intensity factor equation for surface cracks." *Engineering Fracture Mechanics*(15): 185-192.

[260] Straub, D. and Faber, M. H. (2003). Modeling Dependency in Inspection Performance. *11th International Conference on Applications of Statistics and Probability in Civil Engineering*. D. Kiureghian, Madanat and Pestana. San Francisco, California, Millpress: 1123 – 1130.

[261] Hong, H. P. (1997). "Reliability analysis with nondestructive inspection." *Structural Safety* 19(4): 383-395.

[262] Moan, T. and Song, R. (1998). Implication of Inspection Updating on System Fatigue Reliability of Offshore Structures. *17th Offshore Mechanics and Arctic Engineering Conference*: Paper S&R-1214.

[263] Lotsberg, I., Sigurdsson, G. and Wold, P. T. (1999). Probabilistic Inspection Planning of the Åsgard A FPSO Hull Structure with Respect to Fatigue. *18th Offshore Mechanics and Arctic Engineering Conference*. New Foundland, Canada: 259-266.

[264] Straub, D. and Der Kiureghian, A. (2008). "Acceptance Criteria for Deteriorating Elements of Structural Systems." *Journal of Structural Engineering*.

[265] Straub, D. and Faber, M. H. (2005). "Risk Based Inspection Planning for Structural Systems." *Structural Safety* 27(4): 335-355.

[266] Baker, M. J. and Descamps, B. (1999). "Reliability-based methods in the inspection planning of fixed offshore steel structures." *Journal of Constructional Steel Research* 52(1): 117-131.

[267] Frangopol, D. M. and Okasha, N. M. (2008). *Life-cycle performance and redundancy of structures*. 6th Int. Probabilistic Workshop.

[268] Frangopol, D. M. and Estes, A. C. (1997). "Lifetime bridge maintenance strategies based on system reliability." *Structural engineering international* 7: 193-198.

[269] Frangopol, D. M., Lin, K.-Y. and Estes, A. C. (1997). "Life-Cycle Cost Design of Deteriorating Structures." *Journal of Structural Engineering* 123(10): 1390-1401.

This document is the intellectual property of the fib – International Federation for Structural Concrete. All rights reserved.
This PDF of fib Bulletin 86 is intended for use and/or distribution solely within fib National Member Groups.

[270] Estes, A. C. and Frangopol, D. M. (1999). "Repair optimization of highway bridges using system reliability approach." *Journal of Structural Engineering* 125(7): 766-775.

[271] Akgül, F. and Frangopol, D. (2004). "Computational Platform for Predicting Lifetime System Reliability Profiles for Different Structure Types in a Network." *Journal of Computing in Civil Engineering* 18(2): 92-104.

[272] Akgül, F. F., D.M. (2005). *Reliability-based prediction of the lifetime performance of existing bridges*. 9th International Conference on Structural Safety and Reliability, ICOSSAR'05, Rome, Italy.

[273] Mori, Y. and Ellingwood, B. R. (1993). "Reliability-Based Service-Life Assessment of Aging Concrete Structures." *Journal of Structural Engineering* 119(5): 1600-1621.

[274] Mori, Y. and Ellingwood, B. R. (1994). "Maintaining reliability of concrete structures. I: Role of inspection/repair." *Journal of Structural Engineering* 120(3): 824-845.

[275] Mori, Y. and Ellingwood, B. R. (1994). "Maintaining reliability of concrete structures. II: Optimum inspection/repair." *Journal of Structural Engineering* 120(3): 846-862.

[276] Enright, M. P. and Frangopol, D. M. (1998). "Failure time prediction of deteriorating fail-safe structures." *Journal of Structural Engineering* 124(12): 1448-1457.

[277] Enright, M. P. and Frangopol, D. M. (1999). "Maintenance planning for deteriorating concrete bridges." *Journal of Structural Engineering* 125(12): 1407-1414.

[278] Yang, S.-I., Frangopol, D. M. and Neves, L. C. (2004). "Service life prediction of structural systems using lifetime functions with emphasis on bridges." *Reliability Engineering & System Safety* 86(1): 39-51.

[279] Yang, S.-I., Frangopol, D. M., Kawakami, Y. and Neves, L. C. (2006). "The use of lifetime functions in the optimization of interventions on existing bridges considering maintenance and failure costs." *Reliability Engineering & System Safety* 91: 698-705.

[280] Yang, S.-I., Frangopol, D. M. and Neves, L. C. (2006). "Optimum maintenance strategy for deteriorating bridge structures based on lifetime functions." *Engineering Structures* 28: 196-206.

[281] Okasha, N. M. and Frangopol, D. M. (2009). "Lifetime-oriented multi-objective optimization of structural maintenance considering system reliability, redundancy and life-cycle cost using GA." *Structural Safety* 31(6): 460-474.

[282] Neves, L. A., Frangopol, D. M. and Cruz, P. J. (2006). "Probabilistic lifetime-oriented multiobjective optimization of bridge maintenance: Single maintenance type." *Journal of Structural Engineering* 132(6): 991-1005.

[283] Liu, M. and Frangopol, D. (2004). *Probabilistic maintenance prioritization for deteriorating bridges using a multiobjective genetic algorithm*. Proceedings of the Ninth ASCE Joint Specialty Conference on Probabilistic Mechanics and Structural Reliability, Hosted by Sandia National Laboratories, Omnipress, Albuquerque, New Mexico, July 26-28, 6 pages on CD-ROM.

[284] Liu, M. and Frangopol, D. M. (2005). "Bridge annual maintenance prioritization under uncertainty by multiobjective combinatorial optimization." *Computer-Aided Civil and Infrastructure Engineering* 20(5): 343-353.

This document is the intellectual property of the fib – International Federation for Structural Concrete. All rights reserved.
This PDF of fib Bulletin 86 is intended for use and/or distribution solely within fib National Member Groups.

[285] Liu, M. and Frangopol, D. M. (2005). "Multiobjective maintenance planning optimization for deteriorating bridges considering condition, safety, and life-cycle cost." *Journal of Structural Engineering* 131(5): 833-842.

[286] Frangopol, D. M. and Liu, M. (2007). "Maintenance and management of civil infrastructure based on condition, safety, optimization, and life-cycle cost." *Structure and Infrastructure Engineering* 3(1): 29-41.

[287] Liu, C., Hammad, A. and Itoh, Y. (1997). "Multiobjective optimization of bridge deck rehabilitation using a genetic algorithm." *Computer-Aided Civil and Infrastructure Engineering* 12(6): 431-443.

[288] Frangopol, D. M. N., L.A.C. (2008). Optimization of Life-Cycle Maintenance Strategies under Uncertainties: Role of Inspections. *Trends in Computational Structures Technology* B. H. V. Topping and M. Papadrakakis. Stirling, Scotland, Saxe-Coburg Publications: 55-74.

[289] Frangopol, D. M. (2011). "Life-cycle performance, management, and optimisation of structural systems under uncertainty: accomplishments and challenges 1." *Structure and Infrastructure Engineering* 7(6): 389-413.

[290] Frangopol, D. M. and Bocchini, P. (2012). "Bridge network performance, maintenance and optimisation under uncertainty: accomplishments and challenges." *Structure and Infrastructure Engineering* 8(4): 341-356.

[291] Liu, M. and Frangopol, D. M. (2006). "Probability-based bridge network performance evaluation." *Journal of Bridge Engineering* ASCE(11): 5.

[292] Orcesi, A. D., Frangopol, D. M. and Kim, S. (2010). "Optimization of bridge maintenance strategies based on multiple limit states and monitoring." *Engineering Structures* 32(3): 627-640.

[293] Orcesi, A. D. and Frangopol, D. M. (2011). "Optimization of bridge maintenance strategies based on structural health monitoring information." *Structural Safety* 33(1): 26-41.

[294] Orcesi, A. D. and Frangopol, D. M. (2011). "Probability-based multiple-criteria optimization of bridge maintenance using monitoring and expected error in the decision process." *Structural and Multidisciplinary Optimization* 44(1): 137-148.

[295] Zhu, B. and Frangopol, D. (2012). "Risk-Based Approach for Optimum Maintenance of Bridges under Traffic and Earthquake Loads." *Journal of Structural Engineering* 139(3): 422-434.

[296] Frangopol, D. M. and Messervey, T. B. (2009). Maintenance Principles for Civil Structures. *Encyclopedia of Structural Health Monitoring*. C. Boller, F.-K. Chang and Y. Fujino. Chicester, UK, John Willey & Sons Ltd. 4: 1533-1562.

[297] Frangopol, D. M. K., S. (2011). Service Life, Reliability and Maintenance of Civil Structures. *Service Life Estimation and Extension of Civil Engineering Structures*. L. S. Lee and M. Karbhari. Cambridge, U.K, Woodhead Publishing Ltd: 145-178.

[298] Liu, P. L. and Der Kiureghian, A. (1989). Finite-element reliability methods for geometrically nonlinear stochastic structures. *Technischer Bericht*. Berkeley, Structural Engineering, Mechanics, and Materials, Department of Civil Engineering, Department of Civil Engineering, University of California.

[299] Frangopol, D. M. and Okasha, N. M. (2009). *Redundancy of structural systems based on survivor functions*, ASCE.

This document is the intellectual property of the fib – International Federation for Structural Concrete. All rights reserved.
This PDF of fib Bulletin 86 is intended for use and/or distribution solely within fib National Member Groups.

[300] Hoyland, A. and Rausand, M. (1994). *System Reliability Theory: Models and Statistical Methods*. New York, John Wiley and Sons.

[301] Arora, J. (2004). *Introduction to Optimum Design*, Elsevier Science.

[302] Deb, K., Pratap, A., Agarwal, S. and Meyarivan, T. (2002). "A fast and elitist multiobjective genetic algorithm: NSGA-II." *Evolutionary Computation, IEEE Transactions on* 6(2): 182-197.

[303] Kong, J. S. and Frangopol, D. M. (2003). "Life-cycle reliability-based maintenance cost optimization of deteriorating structures with emphasis on bridges." *Journal of Structural Engineering* 129(6): 818-828.

[304] Kong, J. S. and Frangopol, D. M. (2004). "Prediction of reliability and cost profiles of deteriorating bridges under time-and performance-controlled maintenance." *Journal of Structural Engineering* 130(12): 1865-1874.

[305] Kong, J. S. and Frangopol, D. M. (2005). "Probabilistic optimization of aging structures considering maintenance and failure costs." *Journal of Structural Engineering* 131(4): 600-616.

[306] van Noortwijk, J. M. and Frangopol, D. M. (2004). "Two probabilistic life-cycle maintenance models for deteriorating civil infrastructures." *Probabilistic Engineering Mechanics* 19(4): 345-359.

[307] Neves, L. A. C., Frangopol, D. M. and Petcherdchoo, A. (2006). "Probabilistic lifetime-oriented multi-objective optimization of bridge maintenance: Combination of maintenance types." *Journal of Structural Engineering* ASCE(132): 11.

[308] Miyamoto, A., Kawamura, K. and Nakamura, H. (2000). "Bridge management system and maintenance optimization for existing bridges." *Computer-Aided Civil and Infrastructure Engineering* 15(1): 45-55.

[309] Furuta, H., Kameda, T., Fukuda, Y. and Frangopol, D. M. (2004). "Life-cycle cost analysis for infrastructure systems: Life cycle cost vs. safety level vs. service life." *Life-cycle performance of deteriorating structures: Assessment, design and management*: 19-25.

[310] Estes, A. C. (1997). A system reliability approach to the lifetime optimization of inspection and repair of highway bridges, DTIC Document.

[311] Ltd, M. (1999). Serviceable life of highway structures and their components. Final report. Birmingham, Highways Agency, London, UK.

[312] Alampalli, S., Fu, G. and Dillon, E. W. (1997). "Signal versus Noise in Damage Detection by Experimental Modal Analysis." *Journal of Structural Engineering* 123(2): 237-245.

[313] Rytter, A. (1993). Vibration based inspection of civil engineering structures. *Department of Building Technology and Structural Engineering*. Aalborg, Denmark, University of Aalborg. PhD Thesis.

[314] Bergmeister, K., Strauss, A., D., N. and Pukl, R. (2007). *Structural analysis and reliability assessment: SARA part I*. Structural Health Monitoring & Intelligent Infrastructure, SHMII-3, Vancouver, Canada.

[315] Spencer Jr., B. F., Gao, Y. and Yang, G. (2005). Distributed computing strategy for damage monitoring employing smart sensors. *Structural Health Monitoring and Intelligent Infrastructure*. Ou, Li and Duan. Shenzhen, China, Taylor & Francis Group, London: 35-47.

This document is the intellectual property of the fib – International Federation for Structural Concrete. All rights reserved.
This PDF of fib Bulletin 86 is intended for use and/or distribution solely within fib National Member Groups.

[316] Feltrin, G. (2002). Temperature and damage effects on modal parameters of a reinforced concrete bridge. *5th European Conference on Structural Dynamics – EURODYN 2002*. Munich, Germany.

[317] Teughels, A., de Roeck, G. and Suykens, J. A. K. (2002). *CLM, a global optimisation method applied to FEM updating*. 5th European Conference on Structural Dynamics: Eurodyn 2002.

[318] Huth, O., Feltrin, G., Maeck, J., Kilic, N. and Motavalli, M. (2005). "Damage Identification using modal data: Experiences on a prestressed concrete bridge." *Journal of Structural Engineering* 131(12): 1898-1910.

[319] Lehký, D. and Novák, D. (2009). Artificial Intelligence: New Research. *ANN Inverse Analysis in Stochastic Computational Mechanics*. B. R. B. and W. N. Curtis. Hauppauge NY, USA, Nova Science Publishers.

[320] Strauss, A., Bergmeister, K., Wendner, R., D., N. and Lehký, D. (2007). *Sensitivity Factor Based Dynamic Damage Identification SARA - Part III*. Structural Health Monitoring & Intelligent Infrastructure, SHMII-3, Vancouver, Canada.

[321] Doebling, S. W., Farrar, C. R. and Prime, M. B. (1998). "A summary review of vibration-based damage identification methods." *The Shock and Vibration Digest* 30(2): 91-105.

[322] Doebling, S. W., Farrar, C. R., Prime, M. B. and D.W., S. (1996). Damage identification and health monitoring of structural and mechanical systems from changes in their vibration characteristics: a literature review, Los Alamos National Laboratory. Report LA-13070-MS.

[323] Farrar, C. R., Doebling, S. W. and Duffey, T. A. (1999). *Vibration-based damage detection*. SD 2000 Structural Dynamics Forum.

[324] Doebling, S. W., Farrar, C. R., Prime, M. B. and D.W., S. (1996). Damage identification and health monitoring of structural and mechanical systems from changes in their vibration characteristics: a literature review, Los Alamos National Laboratory.

[325] Cawley, P. and Adams, R. W. (1979). "The locations of defects in structures from measurements of natural frequencies." *Journal of Strain Analysis* 14(2): 49-57.

[326] Stubbs, N. and Osegueda, R. (1990). "Global non-destructive damage evaluation in solids." *The International Journal of Analytical and Experimental Modal Analysis* 5: 67-79.

[327] Stubbs, N. and Osegueda, R. (1990). "Global non-destructive damage evaluation in solids." *The International Journal of Analytical and Experimental Modal Analysis* 5(2): 67-79.

[328] Stubbs, N. and Osegueda, R. (1990). "Global damage detection in solids: Experimental verification." *The International Journal of Analytical and Experimental Modal Analysis* 5(2): 81-97.

[329] Armon, D., Ben-Haim, Y. and Braun, S. (1994). "Crack detection in beams by rank-ordering of eigenfrequency shifts." *Mechanical Systems and Signal Processing* 8(1): 81-91.

[330] Choy, F. K., Liang, R. and Xu, P. (1995). "Fault identification of beams on elastic foundation." *Computers and Geotechnics* 17: 157-176.

[331] Messina, A., Williams, E. J. and Contursi, T. (1998). "Structural damage detection by a sensitivity and statistical based method." *Journal of Sound and Vibration* 216(5): 791-808.

This document is the intellectual property of the fib – International Federation for Structural Concrete. All rights reserved.
This PDF of fib Bulletin 86 is intended for use and/or distribution solely within fib National Member Groups.

[332] Morassi, A. (2001). "Identification of a crack in a rod based on changes in a pair of natural frequencies." *Journal of Sound and Vibration* 242: 577-596.

[333] Salawu, O. S. (1997). "Detection of structural damage through changes in frequency: A review." *Engineering Structures* 19: 718-723.

[334] L, P., K, A., S, D. and K, P. (1993). Damage Detection Using Experimentally Measured Mass And Stiffness Matrices. *34th Structures, Structural Dynamics and Materials Conference*, American Institute of Aeronautics and Astronautics.

[335] Rizos, P. F., Aspragathos, N. and Dimarogonas, A. D. (1990). "Identification of crack location and magnitude in a cantilever beam from the vibration modes." *Journal of Sound and Vibration* 138(3): 381-388.

[336] Allemang, R. J. (2002). *The modal assurance criterion (MAC): Twenty years of use and abuse*. 20th International Modal Analysis Conference.

[337] Ho, Y. K. and Ewins, D. J. (2000). *On structural damage identification with mode shapes*. European COST F3 Conference on System Identification & Structural Health Monitoring.

[338] Williams, C. and Salawu, O. S. (1997). *Damping as a damage indication parameter*. 15th International Modal Analysis Conference.

[339] Ndambi Mulambula, J. M. (2002). Damage assessment in reinforced concrete beams by damping analysis. *Mechanics of Materials and Constructions*. Brussel, Belgium, Vrije Universität. PhD Thesis.

[340] Modena, C., Sonda, D. and Zonta, D. (1999). *Damage localization in reinforced concrete structures by using damping measurements*. DAMAS 99 International Conference of Damage Assessment of Structures.

[341] Casas, J. R. and Aparicio, A. C. (1994). "Structural damage identification from dynamic test data." *Journal of Structural Engineering* 120(8): 2437-2450.

[342] Salane, H. J. and J. W. Baldwin, J. (1990). "Identification of Modal Properties of Bridges." *Journal of Structural Engineering* 116(7): 2008-2021.

[343] Farrar, C. R. and Jauregui, D. A. (1998). "Comparative study of damage identification algorithms applied to a bridge: II. Numerical study." *Smart Materials and Structures* 7(5): 720-731.

[344] Salawu, O. S. and Williams, C. (1995). "Bridge assessment using forced-vibration testing." *Journal of Structural Engineering* 121(2): 161-173.

[345] Stubbs, N., Kim, J. T. and Topole, K. (1992). *An efficient and robust algorithm for damage localization in offshore platforms*. ASCE 10th Structures Congress.

[346] Stubbs, N., Kim, J. and Topole, K. (1992). *An efficient and robust algorithm for damage localization in offshore platforms*. Proceedings of the ASCE tenth structures congress.

[347] Shi, Z. H., Law, S. S. and Zang, L. M. (2002). "Structural damage detection from modal strain energy change." *Journal of Engineering Mechanics* 126: 1216-1223.

[348] Carrasco, C. J., Osegueda, R. A., Ferregut, C. M. and Grygier, M. (1997). *Damage localization in a space truss model using modal strain energy*. Proceedings-SPIE the international society for optical engineering, SPIE INTERNATIONAL SOCIETY FOR OPTICAL.

[349] Cornwell, P., Doebling, S. W. and Farrar, C. R. (1997). *Application of the strain energy damage detection method to plate-like structures*. 15th International Modal Analysis Conference.

This document is the intellectual property of the fib – International Federation for Structural Concrete. All rights reserved.
This PDF of fib Bulletin 86 is intended for use and/or distribution solely within fib National Member Groups.

[350] Pandey, A. K., Biswas, M. and Samman, M. M. (1991). "Damage detection from changes in curvature mode shapes." *Journal of Sound and Vibration* 145(2): 321-332.

[351] Ratcliffe, C. P. (1997). "Damage detection using a modified laplacian operator on mode shape data." *Journal of Sound and Vibration* 204(3): 505-517.

[352] Vanlanduit, S., Parloo, E., Guillaume, P. and de Vos, W. (2002). *Validation of on-line linear and nonlinear fatigue crack detection techniques*. Proceedings of 1st European Workshop on Structural Health Monitoring.

[353] Deweer, J., Dierckx, B., Hermans, L., Van der Auweraer, H. and Keppens, T. (1999). Industrial Applicability of Modal Analysis on Operating Data, 1999, SAE Technical Paper.

[354] Pandey, A. K. and Biswas, M. (1994). "Damage detection in structures using changes in flexibility." *Journal of Sound and Vibration* 169(1): 3-17.

[355] Pandey, A. K. and Biswas, M. (1995). "Experimental verification of flexibility difference method for locating damage in structures." *Journal of Sound and Vibration* 184: 311-328.

[356] Raghavendrachar, M. and Aktan, A. E. (1992). "Flexibility by multireference impact testing for bridge diagnostics." *Journal of Structural Engineering* 118(8): 2186-2203.

[357] Bernal, K. (2002). "Load vectors for damage localization." *Journal of Engineering Mechanics* 128(1): 7-14.

[358] Friswell, M. J. and Mothershead, J. E. (1995). *Finite element model updating in structural dynamics*. Dordrecht, The Netherlands, Kluwer Academic Publishers.

[359] Maia, N. M. M., Silva, J. M. M. and He, J. (1997). *Theoretical and experimental modal analysis*. Somerset, England, Research Studies Press Ltd.

[360] Hassiotis, S. and Jeong, G. D. (1986). "Identification of stiffness reductions using natural frequencies." *Journal of Engineering Mechanics* 112(7): 1692-1703.

[361] Casas, J. R. and Aparicio, A. C. (1994). "Structural Damage Identification from Dynamic-Test Data." *Journal of Structural Engineering* 120(8): 2437-2450.

[362] Ruotolo, R. and Surace, C. (1997). "Damage assessment of multiple cracked beams: Numerical results and experimental validation." *Journal of Sound and Vibration* 2006(4): 567-588.

[363] Suykens, J. A. K., Vandewalle, J. and de Moor, B. (2001). "Intelligence and cooperative search by coupled local minimizers." *International Journal of Bifurcation and Chaos* 11: 2133-2144.

[364] Fritzen, C. P. and Bohle, K. (1999). *Model-based health monitoring of structures - Application to the I40 highway bridge*. Identification in Engineering Systems IES99.

[365] Fritzen, C. P. and Bohle, K. (2001). *Vibration based global damage identification - A tool for rapid evaluation of structural safety*. 3rd International Workshop Structural Health Monitoring: The Demands and Challenges.

[366] Thyagarajan, S. K., Schulz, M. J., Pai, P. F. and Chung, J. (1998). "Detecting structural damage using frequency response functions." *Journal of Sound and Vibration* 210(1): 162-170.

[367] Pereira, J. A., Heylen, S., Lammens, S. and Sas, P. (1995). *Influence of the number of frequency points and resonant frequencies on model updating techniques for*

This document is the intellectual property of the fib – International Federation for Structural Concrete. All rights reserved.
This PDF of fib Bulletin 86 is intended for use and/or distribution solely within fib National Member Groups.

*health condition monitoring and damage detection of flexible structure*. 15th International Modal Analysis Conference.

[368] Maia, N., Silva, J., Almas, E. and Sampaio, R. (2003). "Damage detection in structures: from mode shape to frequency response function methods." *Mechanical systems and signal processing* 17(3): 489-498.

[369] Mothershead, J. E. and Friswell, M. J. (1993). "Model updating in structural dynamics: A survey." *Journal of Sound and Vibration* 167(2): 347-375.

[370] Friswell, M. J. and Mothershead, J. E. (2001). *Physical understanding of structures by model updating*. COST F3 International Conference on Structural System Identification.

[371] Ljung, L. (1999). *System Identification – Theory For the User*. Upper Saddle River, N.J., PTR Prentice Hall. 2nd.

[372] Maincon, P. (2004). Inverse FEM I: Load and response estimates from measurements. *Progress in Structural Engineering, Mechanics and Computation*. Zingoni. Capetown, Taylor & Francis Group, London: 967-971.

[373] Maincon, P. (2004). Inverse FEM II: Dynamic and non-linear problems. *Progress in Structural Engineering, Mechanics and Computation*. Zingoni. Capetown, Taylor & Francis Group, London: 991-995.

[374] Fang, X., Luo, H. and Tang, J. (2005). "Structural damage detection using neural network with learning rate improvement." *Computers and Structures* 83: 2150-2161.

[375] Deix, S. and Geier, R. (2004). Updating FE-models using experimental modal analysis for damage detection and system identification in civil structures. *Third European Conference on Structural Control, 3ECSC*. Vienna University of Technology, Vienna, Austria.

[376] Link, M. (1999). *Updating of analytical models – basic procedures and extensions-Modal Analysis and Testing*. NATO Science Series, Kluwer Academic Publishers.

[377] Planas, J., Guinea, G. V. and Elices, M. (1999). "Size effect and inverse analysis in concrete fracture." *International Journal of Fracture* 95: 367-378.

[378] Fairban, E. M. R., Paz, C. N. M., Ebecken, N. F. F. and Ulm, F. J. (1999). "Use of neural networks for fitting of FE probabilistic scaling model parameters." *International Journal of Fracture* 95: 315-324.

[379] Iacono, C., Sluys, L. J. and van Mier, J. G. M. (2003). Development of an inverse procedure for parameters estimates of numerical models. *Euro-C conference*. St. Johann im Pongau, Austria: 259-268.

[380] Novák, D., Keršner, Z., Lehký, D., Řoutil, L., Vořechovský, M., Knězek, J. and Pukl, R. (2005). Virtual stochastic simulation of fiber reinforced concrete experiments. *1st Central European Congress on Concrete Engineering 2005*. Graz, Austria: 35-38.

[381] Novák, D. and Lehký, D. (2004). "Neural network based identification of material model parameters to capture experimental load-deflection curve." *ACTA POLYTECHNICA 2006* 44(5-6/2004): 110-116.

[382] Novák, D. and Lehký, D. (2005). Inverse analysis based on small-sample stochastic training of neural network. *9th International Conference on Engineering Applications of Neural Networks*, EAAN2005. Lille, France: 155-162.

*This document is the intellectual property of the fib – International Federation for Structural Concrete. All rights reserved.*
*This PDF of fib Bulletin 86 is intended for use and/or distribution solely within fib National Member Groups.*

[383] Kučerová, A., Lepš, M. and Zeman, J. (2004). Soft computing methods for estimation of microplane model parameters. *Computational Mechanics Conference, WCCM VI in conjuction with APCOM'04*. Beijing, China, Tsinghua University Press & Springer-Verlag.

[384] Červenka, V., Novák, D., Lehký, D. and Pukl, R. (2005). Identification of shear wall failure mode. *11th International Conference on Fracture, ICF XI*. Torino, Italy: 209pp.

[385] Strauss, A., Bergmeister, K., Novák, D. and Lehkỳ, D. (2004). "Stochastische Parameteridentifikation bei Konstruktionsbeton für die Betonerhaltung." *Beton- und Stahlbetonbau* 99(12): 967-975.

[386] Strauss, A., Lehký, D., Novák, D., Bergmeister, K. and Santa, U. (2004). Probabilistic Response Identification and Monitoring of Concrete Structures. *Third European Conference on Structural Control*, 3ECSC. Vienna, Austria, Vienna University of Technology.

[387] Lehký, D. and Novák, D. (2005). Probabilistic inverse analysis: Random material parameters of reinforced concrete frame. *9th International Conference on Engineering Applications of Neural Networks, EAAN2005*. Lille, France: 147-154.

[388] McKay, M. D., Conover, W. J. and Beckman, R. J. (1979). "A comparison of three methods for selecting values of input variables in the analysis of output from a computer code." *Technometrics* 21: 239-245.

[389] Novák, D., Teplý, B. and Keršner, Z. (1998). The role of Latin Hypercube Sampling method in reliability engineering. *ICOSSAR-97*. Kyoto, Japan: 403-409.

[390] Novák, D., Vorechovský, M. and Rusina, R. (2005). *Small-sample simulation methods for statistical, sensitivity and reliability analyses*. 3rd probabilistic workshop on technical systems and natural hazards, Vienna.

[391] Keramat, M. and Kielbasa, R. (1997). Efficient Average Quality Index of Estimation of Integrated Circuits by Modified Latin Hypercube Sampling Monte Carlo (MLHSMC). *IEEE Symp. on Circuits and Systems*. Hong Kong.

[392] Iman, R. C. and Conover, W. J. (1982). "A distribution free approach to inducing rank correlation among input variables." *Communications in Statistics Theory and Methods* B11: 311-334.

[393] Vořechovský, M. and Novák, D. (2003). Statistical correlation in stratified sampling. *9th Int. Conf. on Applications of Statistics and Probability in Civil Engineering – ICASP 9*. San Francisco, USA, Rotterdam Millpress: 119-124.

[394] Dreyfus, G. (2005). Model and variable selection for nonlinear model design: some developments and methodology (keynote lecture). *9th International Conference on Engineering Applications of Neural Networks, EAAN2005*. Lille, France: 3-16.

[395] Iman, R. C. and Conover, W. J. (1980). "Small Sample Sensitivity Analysis Techniques for Computer Models with an Application to Risk Assessment." *Communications in Statistics Theory and Methods* A9(17): 1749-1842.

[396] Cichocki, A. and Unbehauen, R. (1993). *Neural networks for optimization and signal processing*. Stuttgart, John Wiley & Sons Ltd. & B.G. Teubner.

[397] Novákk, D., Vořechovský, M. and Teplý, B. (2014). "FReET – Software for the statistical and reliability analysis of engineering problems and FReET-D: Degradation Module." *Advances in Engineering Software* 72: 179-192.

This document is the intellectual property of the fib – International Federation for Structural Concrete. All rights reserved.
This PDF of fib Bulletin 86 is intended for use and/or distribution solely within fib National Member Groups.

[398] Novák, D., Vořechovský, M. and Rusina, R. (2013). *FREET version 1.6 – program documentation, User´s and Theory Guides*. Prague, Červenka Consulting.

[399] Lehký, D. (2008).DLNNET - program documentation, Theory and User's Guides, CTU Brno. Brno, Czech Republic.

[400] Hoffmann, S., Bergmeister, K., Strauss, A. and Preslmayr, M. (2007). *Identifying stiffness distributions by direct influence measurements*. 10th international conference on Applications of Statistics and Probability in Civil Engineering, Taylor & Francis Group,.

[401] Taferner, J. (2008). Fugenlose Tragwerke im Hochbau. *Institut für Konstruktiven Ingenieurbau*. Wien, Universität für Bodenkultur BOKU. PhD Thesis: 283.

[402] Wendner, R. (2009). Modale Steifigkeitsidentifikation zur Zustandsbewertung von Strukturen aus Konstruktionsbeton. *Institut für Konstruktiven Ingenieurbau*. Wien, Universität für BodenkulturThesis.

[403] Hoffmann, S. (2008). System identification by directly measured influence lines - A user orientated approach for global damage identification at reinforced concrete bridges. Wien, Universität für Bodenkultur. PhD Thesis: 149.

[404] Teughels, A. (2003). Inverse modelling of civil engineering structures based on operational modal data. *Faculteit Toegepaste Wetenschappen*, Katholieke Universiteit Leuven. PhD Thesis.

[405] Wendner, R., Hoffmann, S., Strauss, A. and Bergmeister, K. (2008). *AIFIT - user orientated identification for infrastructure, theory*. Fourth international conference on bridge maintenance, safety and management, IAMAS'08, Seoul, Korea, Taylor & Francis Group.

[406] Eilbracht, G. (1997). Identifikation von Rissbereichen in Stahlbetonbalken mit Hilfe von Schwingungstestdaten. *Fortschritt Berichte VDI, Reihe 18 Mechanik/ Bruchmechanik*. Düsseldorf, Germany. PhD Thesis.

[407] Zilch, K. and Zehetmaier, G. (2006). *Bemessung im Konstruktiven Ingenieurbau*. Berlin, Springer Verlag.

[408] Strauss, A., Bergmeister, K., Wendner, R. and Hoffmann, S. (2009). System- und Schadensidentifikation von Betonstrukturen. *Betonkalender 2009*. K. Bergmeister and J. D. Wörner. Berlin, Ernst und Sohn. 2: 55-125.

[409] *fib* (2003). *Monitoring and safety evaluation of existing concrete structures*. Task Group 5.1. Lausanne, *fib* - fédération internationale du béton. State of the art report Bulletin 22.

[410] Sohn, H., Farrar, C. R., Hemz, F. and al., e. (2003). A Review of Structural Health Monitoring Literature: 1996-2001. *Los Alamos National Laboratory Report*, Los Alamos National Laboratory. LA-13976-MS.

[411] Phares, B., Wipf, T., Greimann, L. and Lee, Y. S. (2005). Health monitoring of bridge structures and components using smart structure Technology. I. S. University. Madison, Center for Transportation Research and Education.

[412] Wenzel, H. and Pichler, D. (2005). *Ambient vibration monitoring*. England, John Wiley & Sons Ltd.

[413] Introduction to Finite Element Methods (2007). *ASEN 5007*, Department of Aerospace Engineering Sciences, University of Colorado at Boulder.

*This document is the intellectual property of the fib – International Federation for Structural Concrete. All rights reserved.*
*This PDF of fib Bulletin 86 is intended for use and/or distribution solely within fib National Member Groups.*

[414] Luenberger, D. G. (1989). *Linear and Nonlinear Programming*, Addison-Wesley Publishing Company. 2nd Edition.

[415] Optimization Toolbox™ 4, User's Guide (2008). The MathWorks, Inc.

[416] Holland, J. (1975). *Adaptation in natural and artificial systems*. Ann Arbor, University of Michigan Press.

[417] Kirkpatrick, S., Gelatt, C. and Vecchi, M. (1983). "Optimization by simulated annealing." *Science* 220: 671-680.

[418] Suykens, J. A. K., Vandewalle, J. and de Moor, B. (2001). "Intelligence and cooperative search by coupled local minimizers." *International Journal of Bifurcation and Chaos* 11(8): 2133-2144.

[419] Alotto, P., Gaggero, M., Molinari, G. and Nervi, M. (1997). "A design of experiment and statistical approach to enhance the generalised response surface method in the optimisation of multiminima problems." *IEEE transactions on magnetics* 33(2): 1896-1899.

[420] Maeck, J. (2003). Damage assessment of civil engineering structures by vibration monitoring. *Faculteit Toegepaste Wetenschappen*, Katholieke Universiteit Leuven. PhD Thesis.

[421] Clough, R. and Penzien, J. (1993). *Dynamics of structures*. New York, McGraw-Hill.

[422] Peeters, B. (2000). System Identification and Damage Detection in Civil Engineering. *Faculteit Toegepaste Wetenschappen*, Katholieke Universiteit Leuven. PhD Thesis.

[423] Coleman, T. F. and Li, Y. (1996). "An Interior, Trust Region Approach for Nonlinear Minimization Subject to Bounds." *SIAM Journal on Optimization* 6: 418-445.

[424] Coleman, T. F. and Verma, A. (2001). "A Preconditioned Conjugate Gradient Approach to Linear Equality Constrained Minimization." *Computational Optimization and Applications* 20(1).

[425] Kyung, C. and Kuang-Hua, C. (1991). Shape design sensitivity analysis and what-if workstation for elastic solids. *32nd Structures, Structural Dynamics, and Materials Conference*, American Institute of Aeronautics and Astronautics.

[426] Weston Jr, M. (1974). *Variational Methods in Nuclear Reactor Physics*, Academic Press.

[427] Gallagher, R. H. (1973). *Optimum Structural Design: Theory and Applications*, John Wiley & Sons Ltd.

[428] Haug, E. J. and S., A. J. (1979). *Applied Optimal Design*. New York, John Wiley and Sons.

[429] Kirsch, U. (1981). *Optimum structural design: concepts, methods, and applications*, McGraw-Hill.

[430] Komkov, V., Choi, K. K. and Haug, E. J. (1986). *Design Sensitivity Analysis of Structural Systems*, Elsevier Science.

[431] Haslinger, J. and Neittaanmäki, P. (1988). *Finite element approximation for optimal shape design: theory and applications*, Wiley.

[432] Banichuk, N. V. (1990). *Introduction to optimization of structures*, Springer-Verlag

[433] Haftka, R. T. and Gürdal, Z. (1991). *Elements of Structural Optimization*, Springer Netherlands.

This document is the intellectual property of the fib – International Federation for Structural Concrete. All rights reserved.
This PDF of fib Bulletin 86 is intended for use and/or distribution solely within fib National Member Groups.

[434] (1989 - today). *Structural and Multidisciplinary Optimization*.

[435] *Optimization of distributed parameter structures* (1981). Netherlands, Springer, Sijthoff & Noordhoff Internatonal Publishers B.V. 1

[436] *Computer aided optimal design - structural and mechanical systems* (1987). Berlin, Springer

[437] Rozvany, G. I. (1993). *Optimization of large structural systems* Netherlands, Springer. 1

[438] Prager, W. and Shield, R. T. (1968). "Optimal design of multi-purpose structures." *International Journal of Solids and Structures* 4(4): 469-475.

[439] Prager, W. and Taylor, J. E. (1968). "Problems of Optimal Structural Design." *Journal of Applied Mechanics* 35(1): 102-106.

[440] Shield, R. T. and Prager, W. (1970). "Optimal structural design for given deflection." *Zeitschrift für angewandte Mathematik und Physik ZAMP* 21(4): 513-523.

[441] Shield, R. T. (1973). Optimum design of structures through variational principles. *Optimization and Stability Problems in Continuum Mechanics: Lectures Presented at the Symposium on Optimization and Stability Problems in Continuum Mechanics Los Angeles, California*, August 24, 1971. P. K. C. Wang. Berlin, Heidelberg, Springer Berlin Heidelberg: 13-37.

[442] I., R. G. (1981). Variational Methods and Optimality Criteria. *Optimization of distributed parameter structures*. E. J. Haug and J. Céa. Netherlands, Sijthoff & Noordhoff. II: 82-111.

[443] Zienkiewicz, O. C. and Campbell, J. S. (1973). Shape optimization and sequential linear programming. *Optimum structural design Theory and applications*. R. H. Gallagher. New York, NY, John Wiley & Sons: 109-126.

[444] Ramakrishnan, C. V. and Francavilla, A. (1974). "Structural Shape Optimization Using Penalty Functions." *Journal of Structural Mechanics* 3(4): 403-422.

[445] Cea, J. (1981). Problems of Shape Optimal Design. *Optimization of distributed parameter structures*. E. J. Haug and J. Céa. Netherlands, Sijthoff & Noordhoff, NATO ASI. II: 1005-1048.

[446] Cea, J. (1981). Numerical Methods in Shape Optimal Design. *Optimization of distributed parameter structures*. E. J. Haug and J. Céa. Netherlands, Sijthoff & Noordhoff; NATO ASI: 1049–1087.

[447] Choi, K. K. and Haug, E. J. (1983). "Shape Design Sensitivity Analysis of Elastic Structures." *Journal of Structural Mechanics* 11(2): 231-269.

[448] Dems, K. and Mróz, Z. (1983). "Variational approach by means of adjoint systems to structural optimization and sensitivity analysis—I: Variation of material parameters within fixed domain." *International Journal of Solids and Structures* 19(8): 677-692.

[449] Dems, K. and Mróz, Z. (1984). "Variational approach by means of adjoint systems to structural optimization and sensitivity analysis—II." *International Journal of Solids and Structures* 20(6): 527-552.

[450] Mota Soares, C. A., Rodrigues, H. C., Oliveira Faria, L. M. and Haug, E. J. (1984). "Optimization of the Geometry of Shafts Using Boundary Elements." *Journal of Mechanisms, Transmissions, and Automation in Design* 106(2): 199-202.

This document is the intellectual property of the fib – International Federation for Structural Concrete. All rights reserved.
This PDF of fib Bulletin 86 is intended for use and/or distribution solely within fib National Member Groups.

[451] Mota Soares, C. A., Rodrigues, H. C. and Choi, K. K. (1984). "Shape Optimal Structural Design Using Boundary Elements and Minimum Compliance Techniques." *Journal of Mechanisms, Transmissions, and Automation in Design* 106(4): 518-523.

[452] Shu-Yu, W., Yanbing, S. and Gallagher, R. (1985). "Sensitivity analysis in shape optimization of continuum structures." *Computers & structures* 20(5): 855-867.

[453] Seong, H.-G. and Choi, K. K. (1987). "Boundary-Layer Approach to Shape Design Sensitivity Analysis." *Mechanics of Structures and Machines* 15(2): 241-263.

[454] Barone, M. and Yang, R. (1988). "Boundary integral equations for recovery of design sensitivities in shape optimization." *AIAA Journal* 26(5): 589-594.

[455] Kane, J. and Saigai, S. (1988). "Design-sensitivity analysis of solids using BEM." *Journal of Engineering Mechanics* 114(10): 1703-1722.

[456] Cheu, T.-C. (1989). "Sensitivity analysis and shape optimization of axisymmetric structures." *International Journal for Numerical Methods in Engineering* 28(1): 95-108.

[457] Saigal, S., Borggaard, J. and Kane, J. (1989). "Boundary element implicit differentiation equations for design sensitivities of axisymmetric structures." *International Journal of Solids and Structures* 25(5): 527-538.

[458] Ho Choi, J. and Man Kwak, B. (1990). "A unified approach for adjoint and direct method in shape design sensitivity analysis using boundary integral formulation." *Engineering Analysis with Boundary Elements* 7(1): 39-45.

[459] Rice, J. S. and Mukherjee, S. (1990). "Design sensitivity coefficients for axisymmetric elasticity problems by boundary element methods." *Engineering Analysis with Boundary Elements* 7(1): 13-20.

[460] Pedersen, P. (1969). "On the Minimum Mass Layout of Trusses." *Advisory Group for Aerospace Research & Development*, NATO: 1–15.

[461] Haug, E. J. and Rousselet, B. (1980). "Design Sensitivity Analysis in Structural Mechanics. I. Static Response Variations." *Journal of Structural Mechanics* 8(1): 17-41.

[462] Olhoff, N., Lurie, K. A., Cherkaev, A. V. and Fedorov, A. V. (1981). "Sliding regimes and anisotropy in optimal design of vibrating axisymmetric plates." *International Journal of Solids and Structures* 17(10): 931-948.

[463] Cheng, K.-T. and Olhoff, N. (1981). "An investigation concerning optimal design of solid elastic plates." *International Journal of Solids and Structures* 17(3): 305-323.

[464] Cheng, K.-T. and Olhoff, N. (1982). "Regularized formulation for optimal design of axisymmetric plates." *International Journal of Solids and Structures* 18(2): 153-169.

[465] Dems, K. and Mróz, Z. (1987). "A Variational Approach to Sensitivity Analysis and Structural Optimization of Plane Arches." *Mechanics of Structures and Machines* 15(3): 297-321.

[466] Pedersen, P. (1987). "On Sensitivity Analysis and Optimal Design of Specially Orthotropic Laminates." *Engineering Optimization* 11(3-4): 305-316.

[467] Chenais, D., Rousselet, B. and Benedict, R. (1988). "Design sensitivity for arch structures with respect to midsurface shape under static loading." *Journal of Optimization Theory and Applications* 58(2): 225-239.

This document is the intellectual property of the fib – International Federation for Structural Concrete. All rights reserved.
This PDF of fib Bulletin 86 is intended for use and/or distribution solely within fib National Member Groups.

[468] Brockman, R. A. and Lung, F. Y. (1988). "Sensitivity analysis with plate and shell finite elements." *International Journal for Numerical Methods in Engineering* 26(5): 1129-1143.

[469] Dopker, B., Choi, K. K. and Benedict, R. L. (1988). "Shape design sensitivity analysis of structures containing arches." *Computers & Structures* 28(1): 1-13.

[470] Dems, K., Mróz, Z. and Szelag, D. (1989). "Optimal design of rib-stiffeners in disks and plates." *International Journal of Solids and Structures* 25(9): 973-998.

[471] Thomsen, J. and Olhoff, N. (1990). "Optimization of Fiber Orientation and Concentration in Composites." *Control and Cybernetics* 19(3-4): 327-341.

[472] Pedersen, P. (1993). Concurrent Engineering Design with and of Advanced Materials. *Concurrent Engineering: Tools and Technologies for Mechanical System Design*. E. J. Haug. Berlin, Heidelberg, Springer Berlin Heidelberg: 627-670.

[473] Twu, S. L. and Choi, K. K. (1992). "Configuration design sensitivity analysis of built-up structures part I: Theory." *International Journal for Numerical Methods in Engineering* 35(5): 1127-1150.

[474] Dems, K. and Mróz, Z. (1984). "Variational approach by means of adjoint systems to structural optimization and sensitivity analysis — II: Structure shape variation." *International Journal of Solids and Structures* 20(6): 527-552.

[475] Soares, C. M., Rodrigues, H. and Choi, K. (1984). *Shape optimal structural design using boundary elements and minimum compliance techniques*, ASME.

[476] Barone, M. R. and Yang, R. J. (1989). "A boundary element approach for recovery of shape sensitivities in three-dimensional elastic solids." *Computer Methods in Applied Mechanics and Engineering* 74(1): 69-82.

[477] Mróz, Z., Kamat, M. P. and Plaut, R. H. (1985). "Sensitivity Analysis and Optimal Design of Nonlinear Beams and Plates." *Journal of Structural Mechanics* 13(3-4): 245-266.

[478] Haftka, R. T. and Mroz, Z. (1986). "First- and second-order sensitivity analysis of linear and nonlinearstructures." *AIAA Journal* 24(7): 1187-1192.

[479] Szefer, G., Mróz, Z. and Dembowicz, L. (1987). "Variational Approach to Sensitivity Analysis in Nonlinear Elasticity." *Archives of Mechanics* 39(9): 247-259.

[480] Choi, K. K. and Santos, J. L. T. (1987). "Design sensitivity analysis of non-linear structural systems part I: Theory." *International Journal for Numerical Methods in Engineering* 24(11): 2039-2055.

[481] Santos, J. L. T. and Choi, K. K. (1988). "Sizing design sensitivity analysis of non-linear structural systems. Part II: Numerical method." *International Journal for Numerical Methods in Engineering* 26(9): 2097-2114.

[482] Cardoso, J. B. and Arora, J. S. (1988). "Variational method for design sensitivity analysis in nonlinear structural mechanics." *AIAA Journal* 26(5): 595-603.

[483] Phelan, D. G., Vidal, C. and Haber, R. B. (1991). "An adjoint variable method for sensitivity analysis of non-linear elastic systems." *International journal for numerical methods in engineering* 31: 1649-1667.

[484] Tortorelli, D. A. (1992). "Sensitivity analysis for non-linear constrained elastostatic systems." *International journal for numerical methods in engineering* 33: 1643-1660.

[485] Lekszycki, T. and Mróz, Z. (1983). "On optimal support reaction in viscoelastic vibrating structures." *Journal of structural mechanics* 11: 67-79.

*This document is the intellectual property of the fib – International Federation for Structural Concrete. All rights reserved.*
*This PDF of fib Bulletin 86 is intended for use and/or distribution solely within fib National Member Groups.*

[486] Lekszycki, T. (1991). "Application of Variational Methods in Analysis and Synthesis of Viscoelastic Continuous Systems*." *Journal of Structural Mechanics* 19: 163-192.

[487] Lekszycki, T., Olhoff, N. and Pedersen, J. J. (1992). "Modelling and identification of viscoelastic properties of vibrating sandwich beams." *Composite structures* 22: 15-31.

[488] Bendsøe, M. P. and Sokolowski, J. (1987). "Sensitivity analysis and optimization of elastic-plastic structures." *Engineering Optimization* 11(1-2): 31-38.

[489] Bendsøe, M. P. and Sokolowski, J. (1988). "Design Sensitivity Analysis of Elastic-Plastic Analysis Problems." *Mechanics of Structures and Machines* 16(1): 81-102.

[490] Tsay, J. and Arora, J. (1990). "Nonlinear structural design sensivitity analysis for path dependent problems. Part 1: General theory." *Computer Methods in Applied Mechanics and Engineering* 81: 183-208.

[491] Tsay, J. J., Cardoso, J. B. and Arora, J. S. (1990). "Nonlinear structural design sensitivity analysis for path dependent problems. Part 2: Analytical examples." *Computer Methods in Applied Mechanics and Engineering* 81: 209-228.

[492] Zhang, Q. and Mukherjee, S. (1992). "Design Sensitivity Coefficients for Elastic-Viscoplastic Problems by Boundary Element Methods." *International Journal for Numerical Methods in Engineering* 34: 947-966.

[493] Vidal, C., Lee, H.-S. and Haber, R. (1991). "The consistent tangent operator for design sensitivity analysis of history-dependent response." *Computing Systems in Engineering* 2: 509-523.

[494] Vidal, C. A. and Haber, R. B. (1993). "Design sensitivity analysis for rate-independent elastoplasticity." *Computer Methods in Applied Mechanics and Engineering* 107: 393-431.

[495] Haber, R. B., Tortorelli, D. A., Vidal, C. and Phelan, D. G. (1993). Design Sensitivity Analysis Of Nonlinear Structures I: Large-Deformation Hyperelasticity And History-Dependent Material Response. *Structural Optimization: Status And Promise*. M. P. Kamat, American Institute of Aeronautics and Astronautics: 369-405.

[496] Nelson, R. B. (1976). "Simplified calculation of eigenvector derivatives." *AIAA Journal* 14: 1201-1205.

[497] Felix, J. and Vanderplaats, G. (1987). *Configuration optimization of trusses subject to strength, displacement and frequency constraints*, ASME.

[498] Ojalvo, I. (1987). "Efficient computation of mode-shape derivatives for large dynamic systems." *AIAA Journal* 25: 1386-1390.

[499] Haftka, R. T., Cohen, G. A. and Mróz, Z. (1990). "Derivatives of buckling loads and vibration frequencies with respect to stiffness and initial strain parameters." *Journal of applied mechanics* 57: 18-24.

[500] Burczynski, T. and Fedelinski, P. (1991). "Boundary Elements In Shape Analysis And Optimal Design of Vibrating Structures." *Engineering Analysis with Boundary Elements* 8: 294-300.

[501] Meric, R. (1988). "Shape design sensitivity analysis of dynamic structures." *AIAA Journal* 26: 206-212.

[502] Wang, S. and Choi, K. K. (1992). "Continuum design sensitivity of transient responses using Ritz and mode acceleration methods." *AIAA Journal* 30: 1099-1109.

[503] Tortorelli, D. A., Lu, S. C. and Haber, R. B. (1990). "Design Sensitivity Analysis for Elastodynamic Systems." *Journal of Structural Mechanics* 18: 77-106.

This document is the intellectual property of the fib – International Federation for Structural Concrete. All rights reserved.
This PDF of fib Bulletin 86 is intended for use and/or distribution solely within fib National Member Groups.

[504] Tortorelli, D. A. (1993). "Sensitivity analysis for the steady-state response of damped linear elastodynamic systems subject to periodic loads." *Journal of Mechanical Design* 115: 822.

[505] Benedict, R. L. and E., T. J. (1981). Optimal Design of Elastic Bodies in Contact. *Optimization of distributed parameter structures*. E. J. Haug and J. Céa. Netherlands, Sijthoff & Noordhoff: 1553–1599.

[506] Haslinger, J., Neittaanmäki, P. and Salmenjoki, K. (1992). "Sensitivity analysis for discretized unilateral plane elasticity problem." *Finite Elements in Analysis and Design* 12(1): 13-25.

[507] Meric, R. (1979). "Finite element and conjugate gradient methods for a nonlinear optimal heat transfer control problem." *International Journal for Numerical Methods in Engineering* 14: 1851-1863.

[508] Haftka, R. T. (1981). "Techniques for thermal sensitivity analysis." *International Journal for Numerical Methods in Engineering* 17: 71-80.

[509] Dems, K. (1986). "Sensitivity analysis in thermal problems—I: Variation of material parameters within a fixed domain." *Journal of Thermal Stresses* 9: 303-324.

[510] Dems, K. (1987). "Sensitivity analysis in thermal problems—II: structure shape variation." *Journal of Thermal Stresses* 10: 1-16.

[511] Meric, R. (1988). "Shape optimization and identification of solid geometries considering discontinuities." *ASME Transactions Journal of Heat Transfer* 110: 544-550.

[512] Meric, R. (1988). "Shape design sensitivity analysis for non-linear anisotropic heat conducting solids and shape optimization by the BEM." *International Journal for Numerical Methods in Engineering* 26: 109-120.

[513] Tortorelli, D. A. and Haber, R. B. (1989). "First-order design sensitivities for transient conduction problems by an adjoint method." *International Journal for Numerical Methods in Engineering* 28: 733-752.

[514] Tortorelli, D. A., Haber, R. B. and Lu, S. C. (1989). "Design sensitivity analysis for nonlinear thermal systems." *Computer Methods in Applied Mechanics and Engineering* 77: 61-77.

[515] Dems, K. and Mróz, Z. (1987). "Variational approach to sensitivity analysis in thermoelasticity." *Journal of Thermal Stresses* 10(4): 283-306.

[516] Meric, R. (1988). "Sensitivity analysis of functionals with respect to shape for dynamically loaded nonlocal thermoelastic solids." *International Journal of Engineering Science* 26(7): 703-711.

[517] Tortorelli, D. A., Subramani, G., Lu, S. C. and Haber, R. B. (1991). "Sensitivity analysis for coupled thermoelastic systems." *International Journal of Solids and Structures* 27: 1477-1497.

[518] Tortorelli, D. A., Haber, R. B. and Lu, S. C.-Y. (1991). "Adjoint sensitivity analysis for nonlinear dynamic thermoelastic systems." *AIAA Journal* 29: 253-263.

[519] Yang, R. (1993). "Shape design sensitivity analysis of thermoelasticity problems." *Computer Methods in Applied Mechanics and Engineering* 102: 41-60.

[520] Haug, E. J. and Ehle, P. E. (1982). "Second-order design sensitivity analysis of mechanical system dynamics." *International Journal for Numerical Methods in Engineering* 18: 1699-1717.

This document is the intellectual property of the fib – International Federation for Structural Concrete. All rights reserved.
This PDF of fib Bulletin 86 is intended for use and/or distribution solely within fib National Member Groups.

[521] *Computer aided analysis and optimization of mechanical system dynamics* (1984). Springer-Verlag Berlin Heidelberg.

[522] Hsieh, C. and Arora, J. (1985). "Structural design sensitivity analysis with general boundary conditions: dynamic problem." *International Journal for Numerical Methods in Engineering* 21: 267-283.

[523] Paeng, J. and Arora, J. (1989). *Dynamic response optimization of mechanical systems with multiplier methods*, ASME.

[524] (2002). 9th AIAA/ISSMO Symposium on Multidisciplinary Analysis and Optimization, Atlanta, Georgia, American Institute of Aeronautics and Astronautics.

[525] Beck, J. V., Blackwell, B. and Clair, C. R. S. (1985). *Inverse Heat Conduction: Ill-Posed Problems*, Wiley.

[526] Beck, J. (1988). "Combined parameter and function estimation in heat transfer with application to contact conductance." *ASME Transactions Journal of Heat Transfer* 110: 1046-1058.

[527] Zabaras, N. (1990). "Inverse finite element techniques for the analysis of solidification processes." *International Journal for Numerical Methods in Engineering* 29: 1569-1587.

[528] Jarny, Y., Ozisik, M. and Bardon, J. (1991). "A general optimization method using adjoint equation for solving multidimensional inverse heat conduction." *International Journal of Heat and Mass Transfer* 34: 2911-2919.

[529] Huang, C. and Özisik, M. (1992). "Inverse problem of determining unknown wall heat flux in laminar flow through a parallel plate duct." *Numerical Heat Transfer* 21: 55-70.

[530] Maniatty, A., Zabaras, N. and Stelson, K. (1989). "Finite element analysis of some inverse elasticity problems." *Journal of Engineering Mechanics* 115: 1303-1317.

[531] Schnur, D. and Zabaras, N. (1990). "Finite element solution of two-dimensional inverse elastic problems using spatial smoothing." *International Journal for Numerical Methods in Engineering* 30: 57-75.

[532] Nishimura, N. and Kobayashi, S. (1991). "A boundary integral equation method for an inverse problem related to crack detection." *International Journal for Numerical Methods in Engineering* 32(7): 1371-1387.

[533] Zeng, X. and Saigal, S. (1992). "An inverse formulation with boundary elements." *ASME Transactions Series E Journal of Applied Mechanics* 59: 835-840.

[534] Flanigan, C. C. (1987). *Test/analysis correlation of the STS Centaur using design sensitivity and optimization method*. International Modal Analysis Conference, 5th, London, England, Proceedings.

[535] Brandon, J. A. (1990). *Strategies for structural dynamic modification*, Research Studies Press.

[536] Daniel, T. and Alexander, V. (1992). The prediction of the onset of chaos with sensitivity analysis. *33rd Structures, Structural Dynamics and Materials Conference*, American Institute of Aeronautics and Astronautics.

[537] Fiacco, A. V. (1983). *Introduction to sensitivity and stability analysis in nonlinear programming*, Academic press New York.

[538] Vanderplaats, G. N. (1984). *Numerical optimization techniques for engineering design: with applications*, McGraw-Hill New York.

This document is the intellectual property of the fib – International Federation for Structural Concrete. All rights reserved.
This PDF of fib Bulletin 86 is intended for use and/or distribution solely within fib National Member Groups.

[539] Gill, P. E., Murray, W. and Wright, M. H. (1981). *Practical optimization*, Academic Press.

[540] Ang, A. H. and Tang, W. H. (1984). *Probability Concepts in Engineering Planning and Design - Basic Principles*. New York, John Wiley & Sons.

[541] Eschenauer, H., Kneppe, G. and Stenvers, K. H. (1986). "Deterministic and Stochastic Multiobjective Optimization of Beam and Shell Structures." *Journal of Mechanisms, Transmissions, and Automation in Design* 108(1): 31-37.

[542] Cruse, T., Unruh, J., Wu, Y.-T. and Harren, S. (1990). "Probabilistic structural analysis for advanced space propulsion systems." *Journal of Engineering for Gas Turbines and Power* 112: 251.

[543] Cruse, T., Rajagopal, K. and Dias, J. (1990). "Probabilistic structural analysis methodology and applications to advanced space propulsion system components." *Computing Systems in Engineering* 1: 365-372.

[544] Wu, Y. T., Millwater, H. R. and Cruse, T. A. (1990). "Advanced probabilistic structural analysis method for implicit performance functions." *AIAA journal* 28: 1663-1669 (1653-1664).

[545] Hien, T. and Kleiber, M. (1991). "Stochastic design sensitivity in structural dynamics." *International Journal for Numerical Methods in Engineering* 32: 1247-1265.

[546] Ingenieurbauwerke im Zuge von Straßen und Wegen. Überwachung und Prüfung (1999). *DIN 1076*.

[547] Richtlinie zur einheitlichen Erfassung, Bewertung, Aufzeichnung und Auswertung von Ergebnissen der Bauwerksprüfungen nach DIN 1076 (2004). *RI-EBW-PRÜF*, Bundesministerium für Verkehr, Bau- und Wohnungswesen - Abteilung Straßenbau, Straßenverkehr.

[548] RVS (1995). Überwachung, Kontrolle und Prüfung von Kunstbauten - Straßenbrücken. Richtlinien und Vorschriften für den Straßenbau, BmfwA. RVS 13.71.

[549] Phares, B. M., Rolander, D. D., Graybeal, B. A. and Washer, G. A. (2001). "Reliability of Visual Bridge Inspection." *Public Roads Magazine* 65(5).

[550] Frangopol, D. M., Kallen, M. J. and van Noortwijk, J. M. (2004). "Probabilistic models for life-cycle performance of deteriorating structures: review and future directions." *Progress in Structural Engineering and Materials* 6(4): 197-212.

[551] Van Noortwijk, J. M. (2009). "A survey of the application of gamma processes in maintenance." *Reliability Engineering & System Safety* 94(1): 2-21.

[552] Mori, Y. and Ellingwood, B. R. (1993). "Reliability-based service-life assessment of aging concrete structures." *Journal of Structural Engineering* 119(5): 1600-1621.

[553] van Noortwijk, J. (2004). *Gamma process model for time-dependent structural reliability analysis*. Numerical Modelling of Discrete Materials in Geotechnical Engineering, Civil Engineering and Earth Sciences: Proceedings of the First International UDEC/3DEC Symposium, Bochum, Germany, 29 September-1 October 2004, CRC Press.

[554] Frangopol, D. M., Kallen, M.-J. and Noortwijk, J. M. v. (2004). "Probabilistic models for life-cycle performance of deteriorating structures: review and future directions." *Progress in Structural Engineering and Materials* 6(4): 197-212.

[555] General principles on the Design of Structures for Durability (2008). *ISO 13823*.

*This document is the intellectual property of the fib – International Federation for Structural Concrete. All rights reserved.*
*This PDF of fib Bulletin 86 is intended for use and/or distribution solely within fib National Member Groups.*

[556] *Service life design* – Part of the future *fib* Model Code 2008 (2006). *fib* Bulletin N°34.

[557] Eurocodes, C. T.-S. (2002). EN 1990:2002 Eurocode - Basis of structural design.

[558] Izquierdo, D., Andrade, C. and Tanner, P. (2001). *Reliability analysis of corrosion in post-tensional tendons: Case study*. Int. Conf. Safety, Risk, Reliability Trend in Engineering.

[559] Darmawan, M. S. and Stewart, M. G. (2007). "Effect of pitting corrosion on capacity of prestressing wires." *Mag. Concr. Res.* 59(2): 131-139.

[560] Wang, X. and Liu, X. (2004). "Modeling bond strength of corroded reinforcement without stirrups." *Cement and Concrete Research* 34(8): 1331-1339.

[561] Vogel, M., Bohner, E., Guenter, M. and Mueller, H. (2006). *Modeling of carbonation-induced corrosion of concrete facades*. European Symposium on Service Life and Serviceability of Concrete Structures, ESCS-2006, Espoo, Finland.

[562] Maes, M. A., S., T. and Fritzons, K. E. (2006). *Contrasting different reliability-based design formats for the durability of concrete structures*. International RILEM-JCI Seminar on Concrete Durability and Service Life Planning ConcreteLife´06, Israel.

[563] Papadakis, V. G., Roumeliotis, A. P., Fardis, C. G. and Vagenas, C. G. (1996). *Mathematical modeling of chloride effect on concrete durability and protection measures*. International Conference on Concrete in the Service of Mankind (Concrete Repair, Rehabilitation and Protection).

[564] Hunkeler, F., et al. (2005). Corrosion in reinforced concrete: processes and mechanisms. *Corrosion in reinforced concrete structures*. H. Bőhni. Cambridge, UK, Woodhead Publishing Limited.

[565] Ann, K. Y. and Song, H.-W. (2007). "Chloride threshold level for corrosion of steel in concrete." *Corrosion Science* 49(11): 4113-4133.

[566] Glass, G. K. and Buenfeld, N. R. (1995). Chloride threshold levels for corrosion induced deterioration of steel in concrete. *International Workshop Chloride penetration into concrete*, RILEM Publications. 1: 429-439.

[567] Duprat, F. (2007). "Reliability of RC beams under chloride-ingress." *Construction and Building Materials* 21: 1605-1616.

[568] CEN (2010). DIN EN 206: Concrete - Specification, performance, production and conformity.

[569] Rodriguez, J., Ortega, L. M., Casal, J. and Diez, J. M. (1996). *Corrosion of reinforcement and service life of concrete structures*. International Conference on Durability of Building Materials and Components, Stockholm.

[570] Val, D. and Melchers, R. E. (1998). *Reliability analysis of deteriorating reinforced concrete frame structures*. Structural Safety and Reliability.

[571] Bager, D. H. and Jacobsen, S. (1999). *A conceptual model for the freez-thaw damage in concrete*. 3rd Nordic Research seminar.

[572] Fagerlund, G. (1999). *Modified procedure for determination of internal frost resistance by the critical degree of saturation method*. 3rd Nordic Research seminar Lund.

[573] Penttala, V. (2006). "Surface and internal deterioration of concrete due to saline and non-saline freeze-thaw loads." *Cement and Concrete Research* 36(5): 921-928.

This document is the intellectual property of the fib – International Federation for Structural Concrete. All rights reserved.
This PDF of fib Bulletin 86 is intended for use and/or distribution solely within fib National Member Groups.

[574] Contecvet (2001). *Manual for assessing concrete structures affected by frost*. Lund, Sweden, Lund Institute of Technology

[575] Haberland, C., Rath, A. and Dietze, R. (2005). *PP-fibre concrete for a watertight interior shell of a tunnel tube*. The 1st central European congress on concrete engineering.

[576] Morth, W. (2005). *Behavior of optimized tunnel concrete with special aggregates at high temperatures*. The 1st central European congress on concrete engineering, Graz, Austria.

[577] Waltner, R., Kari, H., Kusterle, W. and Lindlbauer, W. (2005). *Analysis of the load-bearing capacity od fibre reinforced concrete during fire*. The 1st central European congress on concrete engineering.

[578] Hironaka, M. C. and Malvar, L. J. (1998). "Jet exhaust-damaged concrete." *Concrete International* 20(10): 32-35.

[579] Noumowe, A. (1995). Effet des hautes températures (20 °C– 600 °C) sur le béton. *Institut National des Sciences Appliquées*. PhD Thesis.

[580] Platret, G. (2002). Suivi de l'hydratation du ciment et de l'évolution des phases solides dans les bétons par analyse thermique. Charactéristiques microstructurales et proprétés relatives à la durabilité des bétons. Méthodes de mesure et d'essai de laboratoire. Février, Laboratoire Central des Ponts et Chaussées. Méthodes d'essai No. 58.

[581] Zhou, Q. and Glasser, F. P. (2001). "Thermal stability and decomposition mechanisms of ettringite at < 120 °C." *Cement and Concrete Research* 31(9): 1333-1339.

[582] Nonnet, E., Lequeux, N. and Boch, P. (1999). "Elastic properties of high alumina cement castables from room temperature to 1600 °C." *Journal of the European Ceramic Society* 19: 1575-1583.

[583] Khoury, G. A. (1992). "Compressive strength of concrete at high temperatures: A reassessment." *Mag. Concr. Res.* 44(161): 291-309.

[584] Richard, N. (1999). Structure et propriétés élastiques des phases cimentières à base de monoaluminate de calcium, Univ. Paris. PhD Thesis.

[585] Grattan-Bellew, P. E. (1996). "Microstructural investigation of deteriorated portland cement concretes." *Construction Building Materials* 10(1): 3-16.

[586] Bickley, J., Hooton, R. D. and Hover, K. C. (2006). Preparation of a Performance-based Specification for Cast-in-Place Concrete: Phase I. P2P Initiative. Silver Spring, USA, RMC Research & Education Foundation.

[587] Bickley, J., Hooton, R. D. and Hover, K. C. (2008). Preparation of a Performance-based Specification for Cast-in-Place Concrete: Phase II. *P2P Initiative*. Silver Spring, USA, RMC Research & Education Foundation.

[588] Stewart, M. G. and Faber, M. H. (2003). Probabilistic modelling of deterioration mechanism for concrete structures. *ICOSSAR*. San Francisco, California: 645-651.

[589] Straub, D., Malioka, V. and Faber, M. H. (2009). "A framework for the asset integrity management of large deteriorating concrete structures." *Structure and Infrastructure Engineering* 5(3): 199-213.

[590] Scholten, C., Enevoldsen, I., Anbjerg-Nielsen, T., Randrup-Thomsen, S., Sloth, M., Engelund, S. and Faber, M. H. (2004). Reliability-Based Clasification of

This document is the intellectual property of the fib – International Federation for Structural Concrete. All rights reserved.
This PDF of fib Bulletin 86 is intended for use and/or distribution solely within fib National Member Groups.

the Load Carrying Capacity of Existing bridges. Danemark, Road Directorate. Report 291: 48.

[591] Publications on Durability of Reinforced Concrete Structures under Combined Mechanical Loads and Environmental Actions: An Annotated Bibliography (2013). Y. Y. W. L. W. F. H., RILEM, The International Union of Laboratories and Experts in Construction Materials, Systems and Structures. Report rep043 175.

[592] Tang, S. W., Yao, Y., Andrade, C. and Li, Z. J. (2015). "Recent durability studies on concrete structure." *Cement and Concrete Research* 78, Part A: 143-154.

[593] ŠOMODÍKOVÁ, M., TEPLÝ, B. and VOŘECHOVSKÁ, D. L., D (2015). Modelling of the service life of concrete structures under combined mechanical and environmental actions. *Safety and Reliability of Complex Engineered Systems*, CRC Press: 4219-4224.

[594] Parrott, L. J. (1987). A review of carbonation in reinforced concrete. Wexham Springs, Cement and Concrete Association.

[595] Teplý, B., Chromá, M., Matesová, D. and Rovnaník, P. (2006).FReET-D, Program Documentation Part I + Part II, Červenka Consulting.

[596] Papadakis, V. G., Fardis, M. N. and Vayenas, C. G. (1992). "Effect of composition, environmental factors and cement-lime mortar coating on concrete carbonation." *Materials and Structures* 25: 293-304.

[597] Papadakis, V. G., Fardis, M. N. and Vayenas, C. G. (1992). "Effect of composition, environmental factors and cement-lime mortar coating on concrete carbonation." *Materials and Structures* 25(149): 293-304.

[598] Morinaga, S. (1988). Prediction of service lives of reinforced concrete buildings based on the corrosion rate of reinforcing steel. Tokyo, Japan, Institute of Technology, Shimizu Corporation. Report No. 23.

[599] Papadakis, V. G. (2000). *Efficiency factors (k-values) for supplementary cementing materials regarding carbonation and chloride penetration*. 5th CANMET/ACI International Conference, CANMET/ACI.

[600] Matoušek, M. (1976). *Carbonation of cellular concrete under the conditions in exposed structures*. RILEM International Symposium, Wexham Springs.

[601] Roy, S. K. and Poh (1999). "K.B. and Northwood Durability of concrete – accelerated carbonation and weathering studies." *Building and Environment* 34: 557-606.

[602] Chromá, M. (2007). Accelerated carbonation studies. Brno, Department of Chemistry, Faculty of Civil Engineering, BUT: (unpublished).

[603] Keršner, Z., Novák, D., Teplý, B. and Bohdanecký, V. (1996). "Concrete carbonation, reinforcement corrosion and service life of a cooling tower (Karbonatace betonu, koroze výztuže a životnost chladící věže)." *Sanace* 4: 21-23.

[604] Keršner, Z., Rovnaníková, P., Teplý, B. and Novák, D. (2004). *Design for durability: An interactive tool for RC structures*. International Conference on Life cycle assessment, behavior and properties of concrete structures (LC 2004).

[605] Papadakis, V. G. (2000). *Efficiency factors (k-values) for supplementary cementing materials regarding carbonation and chloride penetration*. 5th CANMET/ACI International Conference CANMET/ACI. Vol. I, Barcelona, Spain.

[606] Concrete - Part 1: Specification, performance, production and conformity (2000). *EN 206–1*.

This document is the intellectual property of the fib – International Federation for Structural Concrete. All rights reserved.
This PDF of fib Bulletin 86 is intended for use and/or distribution solely within fib National Member Groups.

[607] Teplý, B., Chromá, M. and Rovnaník, P. (2008). "Durability assessment of concrete structures: Reinforcement depassivation due to carbonation." *Structure and Infrastructure Engineering* in press.

[608] Papadakis, V. G. (2000). "Effect of supplementary cementing materials on concrete resistance against carbonation and chloride ingress." *Cement and Concrete Research* 30(2): 291-299.

[609] Collepardi, M., Marcialis, A. and Turrizuani, R. (1972). "Penetration of chloride ions into cement pastes and concrete.." *Journal of the American Ceramic Society* 55(10): 534-535.

[610] Crank, J. (1975). *The mathematics of diffusion*. Bristol, Clarendon Press

[611] Tikalsky, P. J. (2005). *Monte Carlo simulation of chloride diffusion in concrete exposed to de-icing salts*. 6th International Congress Global Construction: Ultimate Concrete Opportunities (Concrete for Transportation Infrastructure).

[612] Nilsson, L. O. and Carcasses, M. (2004). Models for chloride ingress into concrete: A critical analysis. Report of Task 4.1 in EU-Project G6RD-CT-2002-00855, ChlorTest.

[613] Tang, L. and Gulikers, J. (2007). "On the mathematics of time-dependent apparent chloride diffusion coefficient in concrete." *Cement and Concrete Research* 37: 589-595.

[614] Tang, L. (2007). *Service-life prediction based on the rapid migration test and the ClinConc model*. International RILEM Workshop on Performance Based Evaluation and Indicators for Concrete Durability 2006, Madrid, Spain.

[615] Thomas, M. D. A. and Bamforth, P. B. (1999). "Modeling chloride diffusion in concrete: Effect of fly ash and slag." *Cement and Concrete Research* 29: 487-495.

[616] Nilsson, L. O. and Carcasses, M. (2004). Models for chloride ingress into concrete: A critical analysis.

[617] Biondini, F., Bontempi, F., Frangopol, D. M. and Malerba, P. G. (2004). "Cellular Automata Approach to Durability Analysis of Concrete Structures in Aggressive Environments." *Journal of Structural Engineering* 24: 446-458.

[618] Podroužek, J. and Teplý, B. (2008). "Modelling of chloride transport in concrete by cellular automata." *Engineering Mechanics* 15(3): 1-10.

[619] Vořechovska, D., Podroužek, J., Chromá, M., Rovnaníková, P. and Teplý, B. (2009). "Modelling of chloride concentration effect on reinforcement corrosion." *Computer-Aided Civil and Infrastructure Engineering* 24: 446-458.

[620] Živica, V. (1994). "Mathematical modeling of concrete reinforcement corrosion rate and the possibilities of service life prediction of reinforced concrete, Part I - Influence of environmental relative humidity and time." *Building Research Journal* 42(3): 185-198.

[621] Escalante, E. and Satoshi, I. (1990). "Measuring the rate of corrosion of steel in concrete. Corrosion rates of steel in concrete." *ASTM STP* 1065: 86-102.

[622] Živica, V. (1994). "Mathematical modeling of concrete reinforcement corrosion rate and the possibilities of service life prediction of reinforced concrete, Part II - Influence of chloride concentration in reinforced concrete." *Building Research Journal* 42(3): 199-205.

This document is the intellectual property of the fib – International Federation for Structural Concrete. All rights reserved.
This PDF of fib Bulletin 86 is intended for use and/or distribution solely within fib National Member Groups.

[623] Matsushima, M., Tsutsumi, T., H., S. and Matsui, K. (1996). *Corrosion rate of reinforcement in concrete due to chloride attack*. Concrete Repair, Rehabilitation and Protection.

[624] Vu, K. A. T. and Stewart, M. G. (2000). "Structural reliability of concrete bridges including improved chloride-induced corrosion models." *Structural Safety* 22: 313-333.

[625] Schiessel, P. and Raupach, M. (1997). "Laboratory studies and calculations on the influence of crack width on chloride-induced corrosion of steel in concrete." *ACI Material Journal* 94(1): 56-62.

[626] Alonso, C., Andrade, C. and Gonzáles, J. A. (1988). "Relation between resistivity and corrosion rate of reinforcements in carbonated mortar made with several cement types." *Cement and Concrete Research* 8(5): 687-698.

[627] Duracrete (1998). Modeling of degradation.

[628] Langford, P. and Broomfield, J. P. (1987). "Monitoring the corrosion of reinforcing steel." *Construction Repair* 1(2): 32-36.

[629] Broomfield, J. P., Rodriguez, J., Ortega, L. M. and Garcia, A. M. (1993). *GEOCISA Corrosion rate and life prediction for reinforced concrete structures*. Structural Faults and Repairs Symposium.

[630] Andrade, C., Sarria, J. and Alonso, C. (1996). *Corrosion rate field monitoring of post-tensioned tendons in contact with chlorides*. Int. Conf. on Durability of Building Materials and Components 7.

[631] Gonzales, J. A., Andrade, C., Alonso, C. and Feliu, S. (1995). "Comparison of rates of general corrosion and maximum pitting penetration on concrete embedded steel reinforcement." *Cement and Concrete Research* 25(2): 257-264.

[632] Tuutti, K. (1982). Corrosion of steel in concrete. Stockholm, Swedish Cement and Concrete Research Institute.

[633] Bazant, Z. P. (1979). "Physical model for steel corrosion in concrete sea structures-theory." *ASCE Journal of the structural division* 105 (ST6): 1137–1153.

[634] Liu, Y. and Weyers, R. E. (1998). "Modeling the time-to-corrosion cracking in chloride contamined reinforced concrete structures." *ACI Material Journal* 95(6): 675-681.

[635] Maaddawy, T. and Soudki, K. A. (2007). "A model for prediction of time from corrosion initiation to corrosion cracking." *Cement and Concrete Composites* 29(3): 675-681.

[636] Bhargava, K., Ghosh, A. K., Mori, Y. and Ramanujam, S. (2005). "Modeling of time to corrosion induced cover cracking in reinforced concrete structures." *Cement and Concrete Research* 35(11): 2203-2218.

[637] Li, C. Q., Melchers, R. E. and Zheng, J. J. (2006). "An analytical model for corrosion induced crack width in reinforced concrete structures." *ACI Structural Journal* 103(4): 479-482.

[638] Bažant, Z. P. and Planas, J. (1998). *Fracture and Size Effect in Concrete and other Quasibrittle Materials*. Bo-ca Raton, Florida, CRC Press

[639] Tada, H., Paris, P. C. and Irwin, G. R. (2000). *The stress analysis of cracks handbook*. New York, ASME. 3rd.

[640] Andrade, C., Martinez, I., Rebolledo, N. and Castillo, A. (2007). *Development of an engineering approach for modelling corrosion attack*. Int RILEM

This document is the intellectual property of the fib – International Federation for Structural Concrete. All rights reserved.
This PDF of fib Bulletin 86 is intended for use and/or distribution solely within fib National Member Groups.

Workshop on Integral Service Life Modelling of Concrete Structures. 2007, Guimaraes, Portugal.

[641] Osterminski, K. and Schießl, P. (2012). "Design model for reinforcement corrosion." *Structural Concrete* 13(3): 156-165.

[642] Matesová, D. (2005). Fracture/mechanical parameters of quasibrittle materials at high temperatures for numerical modeling. *Fakulty of Civil Engineering, Institute of Structural Mechanics*. Brno, University of Technology. PhD Thesis.

[643] Abrams, M. S. (1971). Compressive strength of concrete at temperatures to 1600F, Temperature and Concrete *ACI SP* 25. A. C. Institute. Detroit, Michigan, American Concrete Institute.

[644] Harmathy, T. Z. and Berndt, J. E. (1966). "Hydrated portland cement and lightweight concrete at high temperatures." *ACI Journal* 63(1): 93-112.

[645] Cruz, C. R. (1966). "Elastic properties of concrete at high temperatures." *PCA Research and Development Laboratories*, 8(1): 37-45.

[646] Philleo, R. (1958). "Some physical properties of concrete at high temperatures." *ACI Journal* 54(10): 857-864.

[647] Kordina, K. and Schneider, U. (1975). "Zum mechanischem Verhalten von Normalbeton unter instantionarer Warmebeanspruchung." *Beton Herstellung und Verwendung* 25(1): 19-25.

[648] Design of concrete structures, Part 1-2: General rules - Structural fire design (2003). *EN 1992-1-2*.

[649] High strength concrete supplementary rules and fire design (1991). *RakMK B4*.

[650] Khoury, G. A., Grainger, B. N. and Sullivan, P. J. E. (1985). "Transient thermal strain of concrete: Literature review, conditions within specimen and behavior of individual constituents." *Materials and Structures* 37(132): 131-144.

[651] Kristensen, L. and Hansen, T. C. (1994). "Cracks in concrete core due to fire or thermal heating shock." *ACI Material Journal* 91(5): 453-459.

[652] Zhang, B., Bicanic, N. and Pearce Balabanic, G. (2001). "Residual fracture properties of normal and high strength concrete subjected to elevated temperatures." *Concrete Research* 53(3): 221-224.

[653] Sullivan, P. J. E. (2004). "A probabilistic method of testing for the assessment of deterioration and explosive spalling of high strength concrete beams in flexure at high temperature." *Cement and Concrete Composites* 26: 155-162.

[654] Zhang, B., Bicanic, N., Pearce and Balabanic, G. (2000). "Assessment of toughness of concrete subjected to elevated temperatures from complete load-displacement curve - Part II: Experimental investigations." *ACI Material Journal* 97(5): 556-566.

[655] Malhotra, H. L. (1956). "The effect of temperature on the compressive strength of concrete." *Materials and Structures* 8(22): 85-94.

[656] Matesová, D., Bonen, D. and Shah, S. P. (2006). "Factors affecting the resistance of cementitious materials at high temperatures and medium heating rates." *Materials and Structures* 39(4): 455-469.

[657] Charlwood, R. G., Solymar, S. V. and Curtis, D. D. (1992). A review of alkali aggregate reactions in hydroelectric plants and dams. *International conference of alkali-aggregate reactions in hydroelectric plants and dams*. Fredericton, Canada: 129.

This document is the intellectual property of the fib – International Federation for Structural Concrete. All rights reserved.
This PDF of fib Bulletin 86 is intended for use and/or distribution solely within fib National Member Groups.

[658] Thompson, G., Charlwood, R., Steele, R. and Curtis, D. (1994). Mactaquac generating station intake and spillway remedial measures. *The eighteenth international congress on large dams*. Durban, South Africa: 347–368.

[659] Bournazel, J. and Moranville, M. (1997). "Durability of concrete: The crossroad between chemistry and mechanics." *Cement and Concrete Research* 2(10): 1543-1552.

[660] Capra, B. and Bournazel, J. (1998). "Modeling of induced mechanical effects of alkali aggregate reactions." *Cement and Concrete Research* 28(2): 251-260.

[661] Capra, B. and Sellier, A. (2003). "Orthotropic modeling of alkali-aggregate reaction in concrete structures: Numerical simulations." *Mechanics of materials* 35(8): 817-830.

[662] Li, K. and Coussy, O. (2002). "Concrete ASR degradation: From material modeling to structure assessment." *Journal of concrete science and engineering* 4: 35-36.

[663] Ulm, F., Coussy, O., Kefei, L. and Larive, C. (2000). "Thermo-chemo-mechanics of ASR expansion in concrete structures." *Journal of Engineering Mechanics* 126(3): 233-242.

[664] Bangert, F. D. and Meschken, G. (2004). "Chemo-hygro-mechanical modeling and numerical simulation of concrete deterioration caused by alkali silica reaction." *International Journal of Numerical Analytical Methods and Geomechanics* 28(7-8): 689-717.

[665] Saouma, V. (2006). "Constitutive Model for Alkali-Aggregate Reactions." *ACI Material Journal* 103(3): 194-202.

[666] Farage, M., Alves, J. and Fairbairn, E. (2004). "Macroscopic model of concrete subjected to alkali aggregate reaction." *Cement and Concrete Research* 34(3): 495-505.

[667] Papadakis, V. G. and Efstathiou, M. P. (2005). *Computer modelling of concrete service life*. International Conference on Cement Combinations for Durable Concrete.

[668] Novák, D., Rusina, R. and Vořechovský, M. (2003). Small-sample statistical analysis - software FREET. *9th International Conference on Applications of Statistics and Probability in Civil Engineering, (ICASP9)*. San Francisco, USA, Rotterdam Millpress: 91-96.

[669] Teplý, B., Matesová, D., Chromá, M. and Rovnaník, P. (2007). *Stochastic degradation models for durability limit state evaluation: SARA part VI*. Structural Health Monitoring & Intelligent Infrastructure, SHMII-3.

[670] Vořechovský, M. and Novák, D. (2009). "Correlation control in small sample Monte Carlo type simulations." *A Simulated Annealing approach. Probabilistic Engineering Mechanics* 24(3): 452-462.

[671] Červenka, V., Jendele, L. and Červenka, J. (2007).ATENA Program Documentation, Part I, Theorie, Cervenka Consulting. Prague, Czech Republic

[672] Strauss, A., Bergmeister, K., Lehký, D. and Novák, D. (2006). Inverse statistical nonlinear FEM analysis of concrete structures. EURO-C 2006. Mayrhofen, Austria.

[673] Rußwurm, D. and Martin, H. (1992). Betonstähle für den Stahlbetonbau: Eigenschaften und Verwendung. Wiesbaden, Deutschland, Bauverlag: 239-270.

[674] Strauss, A., Bergmeister, K. and Maerz, S. (2007). "Reliability assessment of eccentric loaded columns." *Beton- Und Stahlbetonbau* 102(4): 223-230.

This document is the intellectual property of the fib – International Federation for Structural Concrete. All rights reserved.
This PDF of fib Bulletin 86 is intended for use and/or distribution solely within fib National Member Groups.

[675] Cervenka, V., Cervenka, J. and Pukl, R. (2002). "ATENA – A tool for engineering analysis of fracture in concrete." *Sadhana* 27(4): 485-492.

[676] Pukl, R., Červenka, V. and Červenka, J. (2007). *Virtual reliability assessment of structures with damage, SARA - part II*. Structural Health Monitoring & Intelligent Infrastructure, SHMII-3.

[677] Stewart, M. G. and Rosowsky, D. V. (1998). "Time dependent reliability of deteriorating reinforced concrete bridge decks." *Structural Safety* 20(1): 129-139.

[678] Novák, D., Vořechovský, M. and Rusina, R. (2003). *Small-sample probabilistic assessment: FREET software*. International Conference on Applications of Statistics and Probability in Civil Engineering (ICASP 9).

[679] Strauss, A., Wendner, R., Bergmeister, K. and Costa, C. (2012). "Numerically and experimentally based reliability assessment of a concrete bridge subjected to chloride induced deterioration." *Journal of Infrastructure Systems* 19(2): 166-175.

[680] McKay, M. D. (1992). *Latin hypercube sampling as a tool in uncertainty analysis of computer models*. 24th Winter Simulation conference.

[681] - (2004). Eurocode 2: Design of concrete structures - Part 1-1: General rules and rules for buildings. *EN 1992-1-1*. Brussels.

[682] Strauss, A., Frangopol, D. M. and Bergmeister, K. (2010). "Assessment of Existing Structures Based on Identification." *J Struct Eng-ASCE* 136: 86-97.

[683] Buba, R. (2003). Zur stochastischen Zuverlässigkeit bestehender Spannbetonbrücken gegen Ermüdung, Technische Universität München. PhD Thesis.

[684] Penka, E. (2005). Beurteilung der Ermüdungssicherheit von Koppelfugenquerschnitten bestehender Spannbetonbrücken durch Langzeitmessungen. München, Technische Universität. PhD Thesis.

[685] Penka, E. (2002). "Fatigue resistance evaluations for tendon-coupler assemblies of existing post-tensioned concrete bridges using long term measurements." *Bauingenieur* (Sonderpublikation - 4th International Ph.D. Symposium in Civil Engineering).

[686] Zilch, K., Zehetmaier, G., Penka, E. and Buba, R. (2003). *Fatigue and service life of existing PC -bridges – Long term measurements and probabilistic investigation*. The fifth Japanese-German Joint Symposium on Steel and Composite Bridges, Osaka, Japan.

[687] Lacidogna, G. and Napoli, P. (1993). Analytic modeling of relaxation in concrete in accordance with the CEB MC 90 creep formulation. Creep and Shrinkage of Concrete. *RILEM Proceedings*: 665-671.

[688] Park, Y. J. (1990). "Fatigue of concrete under random loadings." *Journal of Structural Engineering* 116: 3228-3235.

[689] Magura, D. D., Sozen, M. A. and Siess, C. P. (1964). "A study of stress relaxation in prestressing reinforcement." *PCI Journal* 9(2).

[690] Betonbrücken (Concrete Bridges) (2003). Berlin, Deutsches Institut für Normung, Beuth. DIN-Fachbericht 102.

[691] Nowak, A. S., Park, C.-H. and Casas, J. R. (2001). " Reliability analysis of prestressed concrete bridge girders: comparison of Eurocode, Spanish Norma IAP and AASHTO LRFD." Structural Safety 23(4): 331-344.

[692] Dallard, P. (2001). "The London Millenium Footbridge." *The Structural Engineer* 79(22): 17-33.

*This document is the intellectual property of the fib – International Federation for Structural Concrete. All rights reserved.*
*This PDF of fib Bulletin 86 is intended for use and/or distribution solely within fib National Member Groups.*

[693] Billington, D. P. (2003). *The Art of Structural Design: A Swiss Legacy*. New Haven, Yale University Press

[694] Brown, J. L. (2004). "Cable-stayed pedestrian crossing doubles as sundial." *Civil Engineering* 74(3): 26-32.

[695] Wiśniewski, D. F. (2007). Safety formats for the assessment of concrete bridges : with special focus on precast concrete, University of PortoThesis.

[696] RVS (2010). Technical Report des Arbeitsausschusses „Überwachung, Kontrolle und Prüfung von Brücken und anderen Ingenieurbauwerken". *Arbeitsgruppe „Brückenbau"*. Wien, Austria, RVS.

[697] Pham, H. (2003). *Handbook of Reliability Engineering*, Springer.

[698] Frangopol, D. M., Strauss, A. and Kim, S. (2008). "Use of monitoring extreme data for the performance prediction of structures: General approach." *Engineering Structures* 30(12): 3644-3653.

[699] Strauss, A., Frangopol, D. M. and Kim, S. (2008). "Use of monitoring extreme data for the performance prediction of structures: Bayesian updating." *Engineering Structures* 30(12): 3654-3666.

[700] Strauss, A., Wendner, R., Bergmeister, K. and Frangopol, D. M. (2010). Monitoring based analysis of an concrete frame bridge "Marktwasser bridge". *Third International fib Congress*. Washington, DC, USA: 11.

[701] Strauss, A., Wendner, R., Bergmeister, K. and Reiterer, M. (2010). Monitoringbasierte Analyse von Integralen Brücken am Beispiel der Marktwasserbrücke. *Schriftenreihe des Departments*. K. Bergmeister. Vienna, Department für Bautechnik und Naturgefahren, Universität für Bodenkultur.

[702] Lehký, D., Keršner, Z. and Novák, D. (2010). Jointless Bridge: Determination of Fracture Mechanical Parameters Values for Nonlinear Analysis. *IABMAS 2010*. Philadelphia, Pennsylvania, USA: (in review).

[703] Bergmeister, K., Novák, D. and Pukl, R. (2004). An advanced engineering tool for reliability assessment of concrete structures. *Progress in Structural Engineering, Mechanics and Computation*. Zingoni. Cape Town, South Africa, Taylor&Francis Group: 899-904.

[704] Podroužek, J. (2010). Jointless Bridge: Reliability Assessment. *IABMAS 2010*. Philadelphia, Pennsylvania, USA: (in review).

[705] Holst, K. H. and Holst, R. (2004). *Brücken aus Stahlbeton und Spannbeton - Entwurf, Konstruktion und Berechnung*. Berlin, Ernst & Sohn. 5th revised edition.

[706] Taferner, J., Keuser, M. and Bergmeister, K. (2009). Integrale Konstruktionen aus Beton. *Betonkalender 2009*. K. Bergmeister, F. Fingerloos and J. D. Wörner. Berlin, Ernst & Sohn. 2: 231-370.

[707] Reiterer, M., Wendner, R. and Strauss, A. (2009). Fibre-Optic Monitoring Systems: Installation strategy on a 3-span Jointless Bridge. *SHMII-4*. Zürich.

[708] Wendner, R., Strauss, A., Bergmeister, K. and Reiterer, M. (2010). Sensor based assessment of soil-structure interaction. *Third International fib Congress*. Washington, DC, USA: 9.

[709] Zilch, K., Weiher, H. and Gläser, C. (2009). Monitoring im Betonbau. *Betonkalender 2009*. K. Bergmeister, F. Fingerloos and J. D. Wörner. Berlin, Ernst und Sohn. 2.

This document is the intellectual property of the fib – International Federation for Structural Concrete. All rights reserved.
This PDF of fib Bulletin 86 is intended for use and/or distribution solely within fib National Member Groups.

[710] Inaudi, D. (1997). Fiber Optic Sensor Network for the Monitoring of Civil Engineering Structures. Lausanne, École Polytechnique Fédérale de Lausanne. PhD Thesis: 262.

[711] Glisic, B. and Inaudi, D. (2007). *Fibre Optic Methods for Structural Health Monitoring*. Southern Gate, Chichester, West Sussex, England, John Wiley & Sons Ltd.

[712] Kampel, I. and Kehrer, K. (2009). Analyse von Messsystemen für die Erfassung von Erdkörperbewegungen im Schleppplattenbereich integraler Brücken. *Project Report*, Institute of Structural Engineering, BOKU Vienna.

[713] Wendner, R., Strauss, A. and Bergmeister, K. (2010). Monitoring based verification of the soil structure interaction of the Markwasser Bridge S33.24. *IABMAS 2010*. D. M. Frangopol, Sause and Kusko. Philadelphia, Pennsylvania, USA, Taylor & Francis, London: 540-547.

[714] Murray, H., Nancey, A. and Herold, A. (2008). Geodetect - Geokunststoff mit Faseroptik-Sensoren: Von der Entwicklung bis zur Anwendung - 4 Jahre Erfahrung. *Bautex 2008*. Chemnitz, Deutschland: 17.

[715] Wendner, R., Strauss, A., Frangopol, D. M., Novák, D., Reiterer, M. and Bergmeister, K. (2009). Probabilistic Design Aspects of Jointless Structures associated with Monitoring *SHMII-4*. Zürich.

[716] Strauss, A., Wendner, R., Bergmeister, K. and Frangopol, D. M. (2010). Monitoring based performance checking of the joint less Marktwasserbrücke, S33.24. *IABMAS 2010*. D. M. Frangopol, Sause and Kusko. Philadelphia, Pennsylvania, USA, Taylor & Francis, London: 534-539.

[717] ASPROGE - Research Project for the ASeismic PROtection of Bridges (2007). *Egnatia Odos S.A*. Thessaloniki, Greece.

[718] Kappos, A. J., Ed. (2010). *Aseismic design and constructions in EGNATIA ODOS, the highway connecting Epirus through Macedonia to Thrace and eastern border of Greece*. Thessaloniki, Greece, Hellenic Society for Earthquake Engineering.

[719] Liolios, A., Panetsos, P. and Makarios, T. (2007). Seismic fragility functions for a bridge of Egnatia motorway in northern Greece. *6th German-Greek-Polish Symposium "Recent Advances in Mechanics"*. Alexandroupolis, Greece.

[720] Moschonas, I. F., Kappos, A. J., Panetsos, P., Papadopoulos, V., Makarios, T. and Thanopoulos, P. (2009). "Seismic fragility curves for greek bridges: Methodology and case studies." *Bulletin of Earthquake Engineering* 7(2): 439-468.

[721] Panetsos, P. and Liolios, A. (2010). Seismic vulnerability functions for a bridge case of Egnatia motorway. *Aseismic design and constructions in EGNATIA ODOS, the highway connecting Epirus through Macedonia to Thrace and eastern border of Greece*. A. J. Kappos. Thessaloniki, Greece, Hellenic Society for Earthquake Engineering.

[722] Panetsos, P. and Barba, Z. (2005). Egnatia Odos Bridge Visual Inspection Manual. *EGNATIA ODOS S.A*. Thessaloniki, Greece. 1st Deliverable of Research Contract 2458, 2459, 2460/ A01/ΔM/EOAE,Box.No. S-330.

[723] Kepaptsoglou, K., Karlaftis, M., Bitsikas, T., Lambropoulos, S. and Panetsos, P. (2006). A Methodology and Decision Support System for scheduling Inspections in a Bridge Network following a Natural Disaster. *3rd. Int. Conf. on Bridge Maint. Safety and Management*.

*This document is the intellectual property of the fib – International Federation for Structural Concrete. All rights reserved.*
*This PDF of fib Bulletin 86 is intended for use and/or distribution solely within fib National Member Groups.*

[724] Bitsikas, T. and Panetsos, P. (2005). Completion of Comp. Data Base of EOAE bridges. *EGNATIA ODOS S.A*. Thessaloniki, Greece. Final Deliverable of Research Contract 2160/A01/ΔM/EOAE, Box.No S-323.

[725] Kepaptsoglou, K., Karlaftis, M. and Panetsos, P. (2005). Development of Algorithms to be implemented in to the BMS Software of EOAE. *EGNATIA ODOS S.A*. Thessaloniki, Greece. 1st Deliv. of Research Contract 2255/A01/ΔM/EOAE, Box No. S-322.

[726] Papadimitriou, C. (2004). "Pareto Optimal Sensor Locations for Structural Identification." *Computer Methods in Applied Mechanics and Engineering* 196(12-16): 1655-1673.

[727] Papadimitriou, C. (2004). "Optimal Sensor Placement Methodology for Parametric Identification of Structural Systems." *Journal of Sound and Vibration* 278(4): 923-947.

[728] Papadimitriou, C. (2004). Bayesian Inference Applied to Structural Damage Detection. *2nd European Workshop on Structural Health Monitoring*. C. Boller and W. J. Staszewski, DEStech Publications: 575-582.

[729] Christodoulou, K. and Papadimitriou, C. (2007). "Structural identification based on optimally weighted modal residuals." *Mechanical Systems and Signal Processing* 21: 4-23.

[730] Strauss, A., Bergmeister, K., Hoffmann, S., Pukl, R. and Novák, D. (2008). "Advanced life-cycle analysis of existing concrete bridges." *Journal of Materials in Civil Engineering* 20(1): 9-19.

[731] Bergmeister, K., Novák, D., Pukl, R. and Červenka, V. (2009). "Structural assessment and reliability analysis for existing engineering structures, theoretical background." *Struct Infrastruct Eng* 5(4): 267-275.

[732] Ntotsios, E., Karakostas, C., Lekidis, V., Panetsos, P., Nikolaou, G., Papadimitriou, C. and Salonikios, T. (2009). "Structural Identification of Egnatia Odos Bridges based on Ambient and Earthquake Induced Vibrations." *Bulletin of Earthquake Engineering* 7(2): 485-501.

[733] Ntotsios, E., Papadimitriou, C., Panetsos, P., Karaiskos, G., Perros, K. and Perdikaris, P. C. (2009). "Bridge Health Monitoring System based on Vibration Measurements." *Bulletin of Earthquake Engineering* 7(2): 469-483.

[734] Strauss, A. and Bergmeister, K. (2010). Integrative Design and Assessment of Concrete Structures based on Inspection- and Monitoring Information. *3rd fib International Congress* - 2010. Washington, The International Federation for Structural Concrete (*fib* - fédération internationale du béton).

[735] Strauss, A., Frangopol, D. M. and Bergmeister, K. (2010). "Assessment of Existing Structures Based on Identification." *J Struct Eng-ASCE* 136(1): 86-97.

[736] Novák, D., Vořechovský, M., Lehký, D., Bergmeister, K., Pukl, R., Červenka, V.; Stochastic nonlinear analysis of concrete structures - Part I: From simulation of experiment and parameter identification to reliability assessment (2007) Applications of Statistics and Probability in Civil Engineering - Proceedings of the 10th International Conference on Applications of Statistics and Probability, ICASP10, pp. 325-326.

[737] Hordijk, D. (1991). Local approach to fatigue of concrete (Unpublished PhD thesis). DelftUniversity of Technology, Delft

[738] Strauss, A; Hoffmann, S; Wendner, R; Bergmeister, K; Structural assessment and reliability analysis for existing engineering structures, applications for real structures; STRUCT INFRASTRUCT ENG. 2009; 5(4): 277-286.

*This document is the intellectual property of the fib – International Federation for Structural Concrete. All rights reserved.*
*This PDF of fib Bulletin 86 is intended for use and/or distribution solely within fib National Member Groups.*

The *fib* (International Federation for Structural Concrete - Fédération internationale du béton) is grateful for the invaluable support of the following national member groups and sponsoring members, which contributes to the publication of *fib* technical bulletins, the *Structural Concrete* journal and *fib*-news.

**National member groups**

AAHES - Asociación Argentina del Hormigón Estructural, Argentina
CIA - Concrete Institute of Australia
ÖBV - Österreichische Bautechnik Vereinigung, Austria
GBB-BBG - Groupement Belge du Béton, Belgium
ABCIC - Associação Brasileira da Construção Industrializada de Concreto, Brazil
ABECE - Associação Brasileira de Engenharia e Consultoria Estrutural, Brazil
IBRACON,Instituto Brasileiro do Concreto, Brazil
*fib* Group of Canada, Canada
CCES - China Civil Engineering Society, China
Cyprus University of Technology, Cyprus
Cyprus Association of Civil Engineers, Cyprus
Česká Betonářská Společnost, Czech Republic
DBF - Dansk Betonforening, Denmark
SB - Suomen Betoniyhdistys, Finland
AFGC - Association Française de Génie Civil, France
DAfStb - Deutscher Ausschuss für Stahlbeton, Germany
Technical Chamber of Greece
University of Patras, Department of Civil Engineering, Greece
Hungarian Group of the *fib*, Hungary
The Institution of Engineers, India
*fib*-Indonesia, Indonesia
University of Amirkabir, Iran
IACIE - Israeli Association of Construction and Infrastructure Engineers, Israel
AICAP - Associazione Italiana Calcestruzzo, Armato e Precompresso, Italy
CTE - Collegio dei tecnici della industrializzazione edilizia, Italy
ITC - CNR, Istituto per le Tecnologie della Costruzione, Italy
ReLUIS, Italy
JCI - Japan Concrete Institute, Japan
JPCI - Japan Prestressed Concrete Institute, Japan
LCS - Lebanese Concrete Society, Lebanon
Administration des Ponts et Chaussées, Luxemburg
*fib* Netherlands, Netherlands
NZCS - New Zealand Concrete Society, New Zealand
NB - Norsk Betongforening / Norwegian Concrete Association, Norway
Polish Academy of Sciences, Committee for Civil Engineering, Poland
GPBE - Grupo Português de Betão Estrutural, Portugal
Polytechnic University of Timisoara, Romania
Technical University of Civil Engineering, Romania
University of Transylvania Brasov, Faculty of Civil Engineering, Romania
Association for Structural Concrete, Russia
Association of Structural Engineers, Serbia
SNK *fib*, Slovakia

*This document is the intellectual property of the fib – International Federation for Structural Concrete. All rights reserved.*
*This PDF of fib Bulletin 86 is intended for use and/or distribution solely within fib National Member Groups.*

Slovenian Society of Structural Engineers, Slovenia
University of Cape Town, Department of Civil Engineering, South Africa
KCI - Korean Concrete Institute, South Korea
ACHE - Asociación Cientifico-Técnica del Hormigon Estructural, Spain
SB - Svenska Betongföreningen, Sweden
Délégation nationale suisse de la *fib*, Switzerland
TCA - Thailand Concrete Association, Thailand
Laboratoire de Génie Civil (LGC), Université de Tunis El Manar, Tunisia
ITU - Istanbul Technical University, Turkey
NIISK - Research Institute of Building Constructions, Ukraine
Society of Engineers, United Arab Emirates
*fib* UK, United Kingdom
ASBI - American Segmental Bridge Institute, United States of America
PCI - Precast/Prestressed Concrete Institute, United States of America
PTI - Post-Tensioning Institute, United States of America
PCA – Portland Cement Association, United States of America

**Sponsoring members**

Liuzhou OVM Machinery Company, China
Peikko Group Corp., Finland
Consolis, France
ECS - European Engineered Construction Systems Association (formerly VBBF), Germany
FBF - Betondienst, Germany
ISB - Institut für Stahlbetonbewehrung, Germany
MKT - Metall-Kunststoff-Technik, Germany
Progress Group GmbH, Germany
Larsen & Toubro Ltd, ECC Division, India
KEF Infrastructure India, India
FUJI P. S. Corporation, Japan
IHI Construction Service Company, Japan
Oriental Shiraishi Corporation, Japan
P. S. Mitsubishi Construction Company, Japan
SE Corporation, Japan
Sumitomo Mitsui Construction Company, Civil Engineering Division, Japan
Hilti, Liechtenstein
BBR VT International, Switzerland
Sika Schweiz, Switzerland
VSL International, Switzerland
PBL Group, Thailand
CCL Stressing Systems, United Kingdom
CEG – The Consulting Engineers Group, United States of America

*This document is the intellectual property of the fib – International Federation for Structural Concrete. All rights reserved.*
*This PDF of fib Bulletin 86 is intended for use and/or distribution solely within fib National Member Groups.*

# *fib* Bulletins published since 1998

1 *Structural Concrete – Textbook on Behaviour, Design and Performance*; Vol. 1: *Introduction, Design Process, Materials*
Manual - textbook (244 pages, ISBN 978-2-88394-041-3, July 1999)

2 *Structural Concrete – Textbook on Behaviour, Design and Performance*; Vol. 2: *Basis of Design*
Manual - textbook (324 pages, ISBN 978-2-88394-042-0, July 1999)

3 *Structural Concrete – Textbook on Behaviour, Design and Performance*; Vol. 3: *Durability, Design for Fire Resistance; Member Design, Maintenance; Assessment and Repair, Practical aspects*
Manual - textbook (292 pages, ISBN 978-2-88394-043-7, December 1999)

4 *Lightweight aggregate concrete: Extracts from codes and standards*
State-of-the-art report (46 pages, ISBN 978-2-88394-044-4, August 1999)

5 *Protective systems against hazards: Nature and extent of the problem*
Technical report (64 pages, ISBN 978-2-88394-045-1, October 1999)

6 *Special design considerations for precast prestressed hollow core floors*
Guide to good practice (180 pages, ISBN 978-2-88394-046-8, January 2000)

7 *Corrugated plastic ducts for internal bonded post-tensioning*
Technical report (50 pages, ISBN 978-2-88394-047-5, January 2000)

8 *Lightweight aggregate concrete*: Part 1 (guide) – *Recommended extensions to Model Code 90*; Part 2 (technical report) – *Identification of research needs*; Part 3 (state-of-art report) – *Application of lightweight aggregate concrete* (118 pages, ISBN 978-2-88394-048-2, May 2000)

9 *Guidance for good bridge design*: Part 1 – Introduction, Part 2 – *Design and construction aspects*
Guide to good practice (190 pages, ISBN 978-2-88394-049-9, July 2000)

10 *Bond of reinforcement in concrete*
State-of-art report (434 pages, ISBN 978-2-88394-050-5, August 2000)

11 *Factory applied corrosion protection of prestressing steel*
State-of-art report (20 pages, ISBN 978-2-88394-051-2, January 2001)

12 *Punching of structural concrete slabs*
Technical report (314 pages, ISBN 978-2-88394-052-9, August 2001)

13 *Nuclear containments*
State-of-art report (130 pages, 1 CD, ISBN 978-2-88394-053-6, September 2001)

14 *Externally bonded FRP reinforcement for RC structures*
Technical report (138 pages, ISBN 978-2-88394-054-3, October 2001)

15 *Durability of post-tensioning tendons*
Technical report (284 pages, ISBN 978-2-88394-055-0, November 2001)

16 *Design Examples for the 1996 FIP recommendations Practical design of structural concrete*
Technical report (198 pages, ISBN 978-2-88394-056-7, January 2002)

17 *Management, maintenance and strengthening of concrete structures*
Technical report (180 pages, ISBN 978-2-88394-057-4, April 2002)

18 *Recycling of offshore concrete structures*
State-of-art report (33 pages, ISBN 978-2-88394-058-1, April 2002)

19 *Precast concrete in mixed construction*
State-of-art report (68 pages, ISBN 978-2-88394-059-8, April 2002)

20 *Grouting of tendons in prestressed concrete*
Guide to good practice (52 pages, ISBN 978-2-88394-060-4, July 2002)

*This document is the intellectual property of the fib – International Federation for Structural Concrete. All rights reserved.*
*This PDF of fib Bulletin 86 is intended for use and/or distribution solely within fib National Member Groups.*

21 *Environmental issues in prefabrication*
State-of-art report (56 pages, ISBN 978-2-88394-061-1, March 2003)

22 *Monitoring and safety evaluation of existing concrete structures*
State-of-art report (304 pages, ISBN 978-2-88394-062-8, May 2003)

23 *Environmental effects of concrete*
State-of-art report (68 pages, ISBN 978-2-88394-063-5, June 2003)

24 *Seismic assessment and retrofit of reinforced concrete buildings*
State-of-art report (312 pages, ISBN 978-2-88394-064-2, August 2003)

25 *Displacement-based seismic design of reinforced concrete buildings*
State-of-art report (196 pages, ISBN 978-2-88394-065-9, August 2003)

26 *Influence of material and processing on stress corrosion cracking of prestressing steel – case studies*
Technical report (44 pages, ISBN 978-2-88394-066-6, October 2003)

27 *Seismic design of precast concrete building structures*
State-of-art report (262 pages, ISBN 978-2-88394-067-3, October 2003)

28 *Environmental design*
State-of-art report (86 pages, ISBN 978-2-88394-068-0, February 2004)

29 *Precast concrete bridges*
State-of-art report (83 pages, ISBN 978-2-88394-069-7, November 2004)

30 *Acceptance of stay cable systems using prestressing steels*
Recommendation (80 pages, ISBN 978-2-88394-070-3, January 2005)

31 *Post-tensioning in buildings*
Technical report (116 pages, ISBN 978-2-88394-071-0, February 2005)

32 *Guidelines for the design of footbridges*
Guide to good practice (160 pages, ISBN 978-2-88394-072-7, November 2005)

33 *Durability of post-tensioning tendons*
Recommendation (74 pages, ISBN 978-2-88394-073-4, December 2005)

34 *Model Code for Service Life Design*
Model Code (116 pages, ISBN 978-2-88394-074-1, February 2006)

35 *Retrofitting of concrete structures by externally bonded FRPs*
Technical Report (224 pages, ISBN 978-2-88394-075-8, April 2006)

36 *2006 fib Awards for Outstanding Concrete Structures*
Bulletin (40 pages, ISBN 978-2-88394-076-5, May 2006)

37 *Precast concrete railway track systems*
State-of-art report (38 pages, ISBN 978-2-88394-077-2, September 2006)

38 *Fire design of concrete structures – materials, structures and modelling*
State-of-art report (106 pages, ISBN 978-2-88394-078-9, April 2007)

39 *Seismic bridge design and retrofit – structural solutions*
State-of-art report (300 pages, ISBN 978-2-88394-079-6, May 2007)

40 *FRP reinforcement in RC structures*
Technical report (160 pages, ISBN 978-2-88394-080-2, September 2007)

41 *Treatment of imperfections in precast structural elements*
State-of-art report (74 pages, ISBN 978-2-88394-081-9, November 2007)

42 *Constitutive modelling of high strength / high performance concrete*
State-of-art report (130 pages, ISBN 978-2-88394-082-6, January 2008)

43 *Structural connections for precast concrete buildings*
Guide to good practice (370 pages, ISBN 978-2-88394-083-3, February 2008)

44 *Concrete structure management: Guide to ownership and good practice*
Guide to good practice (208 pages, ISBN 978-2-88394-084-0, February 2008)

*This document is the intellectual property of the fib – International Federation for Structural Concrete. All rights reserved.*
*This PDF of fib Bulletin 86 is intended for use and/or distribution solely within fib National Member Groups.*

45 *Practitioners' guide to finite element modelling of reinforced concrete structures*
State-of-art report (344 pages, ISBN 978-2-88394-085-7, June 2008)

46 *Fire design of concrete structures —structural behaviour and assessment*
State-of-art report (214 pages, ISBN 978-2-88394-086-4, July 2008)

47 *Environmental design of concrete structures – general principles*
Technical report (48 pages, ISBN 978-2-88394-087-1, August 2008)

48 *Formwork and falsework for heavy construction*
Guide to good practice (96 pages, ISBN 978-2-88394-088-8, January 2009)

49 *Corrosion protection for reinforcing steels*
Technical report (122 pages, ISBN 978-2-88394-089-5, February 2009)

50 *Concrete structures for oil and gas fields in hostile marine environments*
State-of-art report (36 pages, IBSN 978-2-88394-090-1, October 2009)

51 *Structural Concrete – Textbook on behaviour, design and performance*, Vol. 1
Manual – textbook (304 pages, ISBN 978-2-88394-091-8, November 2009)

52 *Structural Concrete – Textbook on behaviour, design and performance*, Vol. 2
Manual – textbook (350 pages, ISBN 978-2-88394-092-5, January 2010)

53 *Structural Concrete – Textbook on behaviour, design and performance*, Vol. 3
Manual – textbook (390 pages, ISBN 978-2-88394-093-2, December 2009)

54 *Structural Concrete – Textbook on behaviour, design and performance*, Vol. 4
Manual – textbook (196 pages, ISBN 978-2-88394-094-9, October 2010)

55 *fib Model Code 2010, First complete draft* – Volume 1
Draft Model Code (318 pages, ISBN 978-2-88394-095-6, March 2010)

56 *fib Model Code 2010, First complete draft* – Volume 2
Draft Model Code (312 pages, ISBN 978-2-88394-096-3, April 2010)

57 *Shear and punching shear in RC and FRC elements - Workshop proceedings*
Technical report (268 pages, ISBN 978-2-88394-097-0, October 2010)

58 *Design of anchorages in concrete*
Guide to good practice (282 pages, ISBN 978-2-88394-098-7, July 2011)

59 *Condition control and assessment of reinforced concrete structures exposed to corrosive environments (carbonation/chlorides)*
State-of-art report (80 pages, ISBN 978-2-88394-099-4, May 2011)

60 *Prefabrication for affordable housing*
State-of-art report (130 pages, ISBN 978-2-88394-100-7, August 2011)

61 *Design examples for strut-and-tie models*
Technical report (220 pages, ISBN 978-2-88394-101-4, September 2011)

62 *Structural Concrete – Textbook on behaviour, design and performance*, Vol. 5
Manual – textbook (476 pages, ISBN 978-2-88394-102-1, January 2012)

63 *Design of precast concrete structures against accidental actions*
Guide to good practice (78 pages, ISBN 978-2-88394-103-8, January 2012)

64 *Effect of zinc on prestressing steel*
Technical report (22 pages, ISBN 978-2-88394-104-5, February 2012)

65 *fib Model Code 2010*, Final draft – Volume 1
Model Code (350 pages, ISBN 978-2-88394-105-2, March 2012)

66 *fib Model Code 2010*, Final draft – Volume 2
Model Code (370 pages, ISBN 978-2-88394-106-9, April 2012)

67 *Guidelines for green concrete structures*
Guide to good practice (56 pages, ISBN 978-2-88394-107-6, May 2012)

68 *Probabilistic performance-based seismic design*
Technical report (118 pages, ISBN 978-2-88394-108-3, July 2012)

*This document is the intellectual property of the fib – International Federation for Structural Concrete. All rights reserved.*
*This PDF of fib Bulletin 86 is intended for use and/or distribution solely within fib National Member Groups.*

69 *Critical comparison of major seismic codes for buildings*
Technical report (216 pages, ISBN 978-2-88394-109-0, August 2013)

70 *Code-type models for structural behaviour of concrete*
State-of-art report (196 pages, ISBN 978-2-88394-110-6, November 2013)

71 *Integrated life cycle assessment of concrete structures*
State-of-art report (62 pages, ISBN 978-2-88394-111-3, December 2013)

72 *Bond and anchorage of embedded reinforcement: Background to the fib Model Code for Concrete Structures 2010*
Technical report (170 pages, ISBN 978-2-88394-112-0, May 2014)

73 *Tall buildings: Structural design of concrete buildings up to 300m tall*
State-of-the-art report (158) pages, ISBN 978-2-88394-113-7, August 2014)

74 *Planning and design handbook on precast building structures*
Manual – textbook (313 pages, ISBN 978-2-88394-114-4, September 2014)

75 *Polymer-duct systems for internal bonded post-tensioning*
Recommendation (172 pages, ISBN 978-2-88394-115-1, December 2014)

76 *Benchmarking of deemed-to-satisfy provisions in standards: Durability of Reinforced Concrete Structures Exposed to Chlorides*
State-of-the-art-report (191 pages, ISBN 978-2-88394-116-8, May 2015)

77 *Corrugated-steel-web bridges*
State-of-the-art-report (110 pages, ISBN 978-2-88394-117-5, December 2015)

78 *Precast-concrete buildings in seismic areas*
State-of-the-art-report (273 pages, ISBN 978-2-88394-118-2, March 2016)

79 *Fibre-reinforced concrete - From design to structural applications*
ACI-*fib* workshop proceedings (480 pages, ISBN 978-2-88394-119-9, May 2016)

80 *Partial factor methods for existing concrete structures*
Recommendation (129 pages, ISBN 978-2-88394-120-5, December 2016)

81 *Punching of structural concrete slabs: Honoring Neil M. Hawkins*
ACI SP-315, ACI-*fib* symposium proceedings (378 pages, ISBN 978-2-88394-121-2, April 2017)

82 *Precast segmental bridges*
Guide to good practice (183 pages, ISBN 978-2-88394-122-9, August 2017)

83 *Precast Tunnel Segments in Fibre-Reinforced Concrete*
State-of-the-art report (162 pages, ISBN 978-2-88394-123-6, November 2017)

84 *Precast insulated sandwich panels*
State-of-the-art report (129 pages, ISBN 978-2-88394-124-3, December 2017)

85 *Towards a rational understanding of shear in beams and slabs*
Technical Report (338 pages, ISBN 978-2-88394-125-0, May 2018)

Abstracts for *fib* Bulletins and lists of available CEB Bulletins and FIP Reports are available on the *fib* website at www.fib-international.org/publications.

*This document is the intellectual property of the fib – International Federation for Structural Concrete. All rights reserved.*
*This PDF of fib Bulletin 86 is intended for use and/or distribution solely within fib National Member Groups.*

fib
CEB-FIP

# Safety and performance concepts

## Contents

1 Performance-based design requirements ensuring the life-cycle
2 Risk issues
3 Methods of structural reliability
4 Safety concepts for design
5 Testing for assessment and design
6 Inspection and monitoring
7 Life cycle performance
8 Structural identification and prediction methods
9 Probabilistic based models for material degradation processes
10 Case studies applications
11 References

International Federation for Structural Concrete
Fédération internationale du béton
www.fib-international.org

ISSN 1562-3610
ISBN 978-2-88394-126-7